ANNUAL REPORT 2002

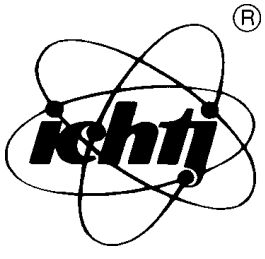

INSTITUTE
OF NUCLEAR CHEMISTRY
AND TECHNOLOGY

EDITORS

Wiktor Smułek, Ph.D.
Ewa Godlewska-Para, M.Sc.

PRINTING

Sylwester Wojtas

CONTENTS

GENERAL INFORMATION

The Institute of Nuclear Chemistry and Technology (INCT) is one of the successors of the Institute of Nuclear Research (INR) which was established in 1955. The latter Institute, once the biggest Institute in Poland, has exerted a great influence on the scientific and intelectual life in this country. The INCT came into being as one of the independent units established after the dissolution of the INR in 1983.

At present, the Institute research activity is focused on:

- radiation chemistry and technology,
- radiochemistry and coordination chemistry,
- radiobiology,
- application of nuclear methods in material and process engineering,
- design of instruments based on nuclear techniques,
- trace analysis and radioanalytical techniques,
- environmental research.

In the above fields we offer research programmes for Ph.D. and D.Sc studies.

At this moment, with its nine electron accelerators in operation and with the staff experienced in the field of electron beam (EB) applications, the Institute is one of the most advanced centres of radiation research and EB processing. The accelerators are installed in the following Institute units:

- pilot plant for radiation sterilization of medical devices and transplants,
- pilot plant for radiation modification of polymers,
- experimental pilot plant for food irradiation,
- pilot plant for removal of SO_2 and NO_x from flue gases,
- pulse radiolysis laboratory, in which the nanosecond set-up was put into operation in 2001. A new 10 MeV accelerator was constructed in the INCT for this purpose.

Based on the technology elaborated in our Institute, an industrial installation for electron beam flue gas treatment has been implemented at the EPS "Pomorzany" (Dolna Odra PS Group). This is the second full scale industrial EB installation for SO_2 and NO_x removal all over the world.

***

In 2002 the INCT scientists published 149 papers in scientific journals registered in the Philadelphia list, among them 24 papers in journals with an impact factor (IF) higher than 1.0. Ellis Horwood Publishers published a book "Concise Chemistry of the Elements" by prof. **S. Siekierski** (INCT) and J. Burgess.

The international journal for nuclear research – NUKLEONIKA published by the INCT was for the first time mentioned on the SCI Journal Citation List with an impact factor equal to 0.37.

Annual rewards of the INCT Director-General for the best publications in the period 2000-2001 were granted to the following research teams:

- First award to prof. **K. Bobrowski**, dr. **D. Pogocki**, dr. **J. Sadło**, dr. **G. Strzelczak**, dr. **P. Wiśniowski** for a series of papers on radiation-induced radical processes in aminoacids and peptides with thioether group.
- Second award to prof. **J. Ostyk-Narbutt** and dr. **J. Krejzler** for the paper explaining the differences in coordination chemistry of cations in the 3rd and 13th groups.

- Third award to prof. **A. Wójcik** and prof. **I. Szumiel** for the publication on the analysis of correlation between cellular radiosensitivity and telomer length.

In 2002, **J. Ostyk-Narbutt**, Ph.D., D.Sc. obtained a professor title conferred by the President of Polish Republic.

W. Łada (INCT) was awarded with the World Intellectual Property Organization Certificate of Merit on the occasion of the 2th Competition – Plebiscite for "Woman Inventor" – 2001, organized by the Association of Polish Inventors and Rationalizers (SPWIR), in cooperation with the "Przegląd Techniczny" magazine and the Society for Technical Culture in Poland

In the autumn 2002, eight new persons were admitted to the Ph.D. studies in the INCT based on the results of entrance examinations. Thereby, the total number of Ph.D. students in the INCT increased to 24 persons.

Four scientific meetings have been organized by the INCT in 2002:

- National Symposium on Nuclear Techniques in Industry, Medicine, Agriculture and Environmental Protection (Chairman of organizing comittee: dr. **G. Zakrzewska-Trznadel** – INCT);
- Accelerators for Radiation Processing – Technical Meeting (Organizing committee: prof. **A.G. Chmielewski**, dr. **Z. Zimek** and **S. Bułka**);
- The Final Regional Workshop of IAEA TC Project "Quality assurance and quality control of nuclear analytical techniques" (Organizer: dr. **H. Polkowska-Motrenko** – INCT);
- A Conference on Incineration Problems with Municipal Wastes (Organizing committee: dr. M. Obrębska – Warsaw University of Technology and **A. Ostapczuk** – INCT).

Two European Commission research projects were run in the INCT in 2002:

- Electron beam for processing of flue gases, emitted in metallurgical processes, for volatile organic compounds removal (project coordinated by prof. **A.G. Chmielewski** – INCT);
- Sulphur radical chemistry of biological significance: the protective and damaging roles of the thiol and thioether radicals (principal investigator: prof. **K. Bobrowski** – INCT).

Prof. **Z.P. Zagórski** (INCT) participated in the programme "Actinide chemistry and repository science" sponsored by the Los Alamos National Laboratory (USA).

MANAGEMENT OF THE INSTITUTE

MANAGING STAFF OF THE INSTITUTE

Director
Assoc. Prof. **Lech Waliś**, Ph.D.

Deputy Director for Research and Development
Prof. **Jacek Michalik**, Ph.D., D.Sc.

Deputy Director for Administration
Roman Janusz, M.Sc.

Accountant General
Barbara Kaźmirska

HEADS OF THE INCT DEPARTMENTS

- Department of Nuclear Methods of Material Engineering
  Assoc. Prof. **Lech Waliś**, Ph.D.
- Department of Structural Research
  Wojciech Starosta, M.Sc.
- Department of Radioisotope Instruments and Methods
  Prof. **Piotr Urbański**, Ph.D., D.Sc.
- Department of Radiochemistry
  Prof. **Jerzy Narbutt**, Ph.D., D.Sc.
- Department of Nuclear Methods of Process Engineering
  Prof. **Andrzej G. Chmielewski**, Ph.D., D.Sc.
- Department of Radiation Chemistry and Technology
  Zbigniew Zimek, Ph.D.
- Department of Analytical Chemistry
  Prof. **Rajmund Dybczyński**, Ph.D., D.Sc.
- Department of Radiobiology and Health Protection
  Prof. **Irena Szumiel**, Ph.D., D.Sc.
- Experimental Plant for Food Irradiation
  Assoc. Prof. **Wojciech Migdał**, Ph.D., D.Sc.
- Laboratory for Detection of Irradiated Foods
  Wacław Stachowicz, Ph.D.
- Laboratory for Measurements of Technological Doses
  Zofia Stuglik, Ph.D.

SCIENTIFIC COUNCIL (1999-2003)

1. Assoc. Prof. **Aleksander Bilewicz**, Ph.D., D.Sc.
   Institute of Nuclear Chemistry and Technology
   • radiochemistry, inorganic chemistry
2. Prof. **Krzysztof Bobrowski**, Ph.D., D.Sc.
   Institute of Nuclear Chemistry and Technology
   • radiation chemistry, photochemistry, biophysics
3. Prof. **Andrzej G. Chmielewski**, Ph.D., D.Sc.
   Institute of Nuclear Chemistry and Technology
   • chemical and process engineering, nuclear chemical engineering, isotope chemistry
4. Prof. **Jadwiga Chwastowska**, Ph.D., D.Sc.
   Institute of Nuclear Chemistry and Technology
   • analytical chemistry

5. **Jakub Dudek**, Ph.D.
   Institute of Nuclear Chemistry and Technology
   • analytical chemistry
6. Prof. **Rajmund Dybczyński**, Ph.D., D.Sc.
   Institute of Nuclear Chemistry and Technology
   • analytical chemistry
7. Prof. **Zbigniew Florjańczyk**, Ph.D., D.Sc.
   Warsaw University of Technology
   • chemical technology
8. **Zyta Głębowicz**
   Institute of Nuclear Chemistry and Technology
   • staff representative
9. Assoc. Prof. **Edward Iller**, Ph.D., D.Sc.
   Radioisotope Centre POLATOM
   • chemical and process engineering, physical chemistry
10. Prof. **Janusz Jurczak**, Ph.D., D.Sc.
    Polish Academy of Sciences, Institute of Organic Chemistry; Warsaw University
    • organic chemistry, stereochemistry
11. **Iwona Kałuska**, M.Sc.
    Institute of Nuclear Chemistry and Technology
    • radiation chemistry
12. **Barbara Kaźmirska**
    Institute of Nuclear Chemistry and Technology
    • staff representative
13. Assoc. Prof. **Marcin Kruszewski**, Ph.D., D.Sc.
    Institute of Nuclear Chemistry and Technology
    • radiobiology
14. **Gabriel Kuc**, M.Sc.
    Institute of Nuclear Chemistry and Technology
    • radiation chemistry
15. Prof. **Janusz Lipkowski**, Ph.D., D.Sc.
    Polish Academy of Sciences, Institute of Physical Chemistry
    • physico-chemical methods of analysis
16. Prof. **Andrzej Łukasiewicz**, Ph.D., D.Sc.
    Institute of Nuclear Chemistry and Technology
    • material science
17. **Kazimiera Malec-Czechowska**, M.Sc.
    Institute of Nuclear Chemistry and Technology
    • radiation chemistry
18. Prof. **Bronisław Marciniak**, Ph.D., D.Sc.
    Adam Mickiewicz University in Poznań
    • physical chemistry
19. Prof. **Józef Mayer**, Ph.D., D.Sc.
    Technical University of Łódź
    • physical and radiation chemistry
20. Prof. **Jacek Michalik**, Ph.D., D.Sc.
    (Co-chairman)
    Institute of Nuclear Chemistry and Technology
    • radiation chemistry, surface chemistry, radical chemistry
21. Prof. **Jerzy Narbutt**, Ph.D., D.Sc.
    Institute of Nuclear Chemistry and Technology
    • radiochemistry
22. **Ewa Pańczyk**, M.Sc.
    Institute of Nuclear Chemistry and Technology
    • nuclear physics
23. **Jan Paweł Pieńkos**, Eng.
    Institute of Nuclear Chemistry and Technology
    • electronics
24. Prof. **Leon Pszonicki**, Ph.D., D.Sc.
    (Chairman)
    Institute of Nuclear Chemistry and Technology
    • analytical chemistry
25. **Zbigniew Samczyński**, Ph.D.
    Institute of Nuclear Chemistry and Technology
    • analytical chemistry
26. Prof. **Sławomir Siekierski**, Ph.D.
    Institute of Nuclear Chemistry and Technology
    • physical chemistry, inorganic chemistry
27. Prof. **Irena Szumiel**, Ph.D., D.Sc.
    (Co-chairman)
    Institute of Nuclear Chemistry and Technology
    • cellular radiobiology
28. Prof. **Jan Tacikowski**, Ph.D.
    (Co-chairman)
    Institute of Precision Mechanics
    • physical metallurgy and heat treatment of metals
29. Prof. **Marek Trojanowicz**, Ph.D., D.Sc.
    Institute of Nuclear Chemistry and Technology
    • analytical chemistry
30. Prof. **Piotr Urbański**, Ph.D., D.Sc.
    Institute of Nuclear Chemistry and Technology
    • radiometric methods, industrial measurement equipment, metrology
31. Assoc. Prof. **Lech Waliś**, Ph.D.
    Institute of Nuclear Chemistry and Technology
    • material science, material engineering
32. **Paweł Wiśniowski**, Ph.D.
    Institute of Nuclear Chemistry and Technology
    • radiation chemistry, photochemistry, biophysics
33. Prof. **Stanisław Wroński**, Ph.D., D.Sc.
    Warsaw University of Technology
    • chemical engineering

34. Prof. **Zbigniew Zagórski**, Ph.D., D.Sc.
    Institute of Nuclear Chemistry and Technology
    • physical chemistry, radiation chemistry, electrochemistry

35. **Wiesław Zieliński**, M.Sc.
    Institute of Nuclear Chemistry and Technology
    • staff representative

36. **Zbigniew Zimek**, Ph.D.
    Institute of Nuclear Chemistry and Technology
    • electronics, accelerator techniques, radiation processing

HONORARY MEMBERS OF THE INCT SCIENTIFIC COUNCIL (1999-2003)

1. Prof. **Antoni Dancewicz**, Ph.D., D.Sc.
   Institute of Nuclear Chemistry and Technology
   • biochemistry, radiobiology

SCIENTIFIC STAFF

PROFESSORS

1. **Ambroż Hanna B.**
   physical and radiation chemistry, biological chemistry, photochemistry
2. **Bobrowski Krzysztof**
   radiation chemistry, photochemistry, biophysics
3. **Chmielewski Andrzej G.**
   chemical and process engineering, nuclear chemical engineering, isotope chemistry
4. **Chwastowska Jadwiga**
   analytical chemistry
5. **Dancewicz Antoni**
   biochemistry, radiobiology
6. **Dybczyński Rajmund**
   analytical chemistry
7. **Leciejewicz Janusz**
   crystallography, solid state physics, material science
8. **Łukasiewicz Andrzej**
   material science
9. **Michalik Jacek**
   radiation chemistry, surface chemistry, radical chemistry
10. **Narbutt Jerzy**
    radiochemistry
11. **Piekoszewski Jerzy**
    solid state physics
12. **Pszonicki Leon**
    analytical chemistry
13. **Rzewuski Henryk**
    solid state physics
14. **Siekierski Sławomir**
    physical chemistry, inorganic chemistry
15. **Szot Zbigniew**
    radiobiology
16. **Szumiel Irena**
    cellular radiobiology
17. **Trojanowicz Marek**
    analytical chemistry
18. **Urbański Piotr**
    radiometric methods, industrial measurement equipment, metrology
19. **Zagórski Zbigniew**
    physical chemistry, radiation chemistry, electrochemistry

ASSOCIATE PROFESSORS

1. **Bilewicz Aleksander**
   radiochemistry, inorganic chemistry
2. **Grigoriew Helena**
   solid state physics, diffraction research of non-crystalline matter
3. **Iller Edward**
   chemical and process engineering, physical chemistry
4. **Kruszewski Marcin**
   radiobiology
5. **Legocka Izabella**
   polymer technology
6. **Migdał Wojciech**
   chemistry
7. **Waliś Lech**
   material science, material engineering
8. **Wójcik Andrzej**
   cytogenetics
9. **Żółtowski Tadeusz**
   nuclear physics

SENIOR SCIENTISTS (Ph.D.)

1. **Bartłomiejczyk Teresa**
   biology
2. **Borkowski Marian**
   chemistry
3. **Bryl-Sandelewska Teresa**
   radiation chemistry
4. **Buczkowski Marek**
   physics
5. **Cieśla Krystyna**
   physical chemistry
6. **Danko Bożena**
   analytical chemistry
7. **Dembiński Wojciech**
   chemistry
8. **Deptuła Andrzej**
   chemistry
9. **Dobrowolski Andrzej**
   chemistry
10. **Do-Hoang Cuong**
    nuclear physics
11. **Dudek Jakub**
    chemistry
12. **Dźwigalski Zygmunt**
    high voltage electronics, electron injectors, gas lasers
13. **Fuks Leon**
    chemistry
14. **Gniazdowska Ewa**
    chemistry
15. **Grądzka Iwona**
    biology
16. **Grodkowski Jan**
    radiation chemistry
17. **Harasimowicz Marian**
    technical nuclear physics, theory of elementary particles
18. **Jaworska Alicja**
    biology
19. **Kierzek Joachim**
    physics
20. **Kleczkowska Hanna**
    biology
21. **Krejzler Jadwiga**
    chemistry
22. **Krynicki Janusz**
    solid state physics
23. **Kunicki-Goldfinger Jerzy**
    conservator/restorer of art
24. **Machaj Bronisław**
    electricity
25. **Mirkowski Jacek**
    nuclear and medical electronics
26. **Nowicki Andrzej**
    organic chemistry and technology, high-temperature technology
27. **Owczarczyk Andrzej**
    chemistry
28. **Owczarczyk Hanna B.**
    biology
29. **Palige Jacek**
    metallurgy
30. **Panta Przemysław**
    nuclear chemistry
31. **Pawelec Andrzej**
    chemical engineering
32. **Pawlukojć Andrzej**
    physics
33. **Pogocki Dariusz**
    radiation chemistry, pulse radiolysis
34. **Polkowska-Motrenko Halina**
    analytical chemistry
35. **Przybytniak Grażyna**
    radiation chemistry
36. **Ptasiewicz-Bąk Halina**
    physics
37. **Rafalski Andrzej**
    radiation chemistry
38. **Sadło Jarosław**
    chemistry
39. **Samczyński Zbigniew**
    analytical chemistry
40. **Skwara Witold**
    analytical chemistry
41. **Sochanowicz Barbara**
    biology
42. **Stachowicz Wacław**
    radiation chemistry, EPR spectroscopy
43. **Strzelczak Grażyna**
    radiation chemistry
44. **Stuglik Zofia**
    radiation chemistry

45. **Szpilowski Stanisław**
chemistry

46. **Świderska Małgorzata**
physics

47. **Tymiński Bogdan**
chemistry

48. **Walicka Małgorzata**
biology

49. **Warchoł Stanisław**
solid state physics

50. **Wąsowicz Tomasz**
radiation chemistry, surface chemistry, radical chemistry

51. **Wierzchnicki Ryszard**
chemical engineering

52. **Wiśniowski Paweł**
radiation chemistry, photochemistry, biophysics

53. **Wojewódzka Maria**
radiobiology

54. **Wrońska Teresa**
chemistry

55. **Zakrzewska-Trznadel Grażyna**
process and chemical engineering

56. **Zimek Zbigniew**
electronics, accelerator techniques, radiation processing

RADIATION CHEMISTRY
AND PHYSICS,
RADIATION TECHNOLOGIES

MULTIFREQUENCY EPR STUDY OF SOME NATURAL DOSIMETRIC MATERIALS

Grażyna Strzelczak, Jarosław Sadło, Wacław Stachowicz, Marek Danilczuk, Jacek Michalik, Freddy Callens[1/], Etienne Goovaerts[2/]

[1/] Ghent University, Belgium
[2/] University of Antwerp, Belgium

Electron paramagnetic resonance spectroscopy (EPR) has been advanced as a rapid, sensitive and accurate method for the control of irradiated food [1], and among other applications as dating, accidental dose measurements and medical studies. This method is also employed for radiation dosimetry [2-5]. The most successful results of the EPR method in those areas have been achieved with minerals of bone and shell of molluscs [6]. The specific EPR signal observed after irradiation of mineralized tissues is derived from crystalline hydroxyapatite fraction and was shown to be stable during several years of storage. Paramagnetic species produced by irradiation at room temperature in mineral part of bone as well as in shell of molluscs are mainly CO_2^- ion radicals [7]. The measurements of CO_2^- signal amplitude generated by irradiation in bone or shell can be used to estimate the absorbed dose.

In this study we present the analysis of X-, Q- and W-band EPR spectra of irradiated bone powder and shell mollusc *Arcidae.* The aim of analysis is to differenciate between paramagnetic centres contributing to the complex EPR spectra of these materials.

As model samples a deproteinized human bone and a shell of *Arcidae* sea mollusc were used. The samples, 100 mg each, were irradiated with a dose of 7 kGy of γ-rays. The EPR measurements of irradiated samples were performed at room temperature in X-, Q- and W-band. In the Institute of Nuclear Chemistry and Technology (INCT), a Bruker ESP-300 spectrometer was applied to perform the measurements in X-band (9.5 GHz), while the Q-band measurements were carried out with a Bruker ELEXSYS E-500 spectrometer of the Ghent University at a frequency of 34 GHz. The Bruker ELEXSYS E-600 spectrometer in University of Antwerp, in turn, was used for the measurements on shell and bone samples in W-band (95 GHz).

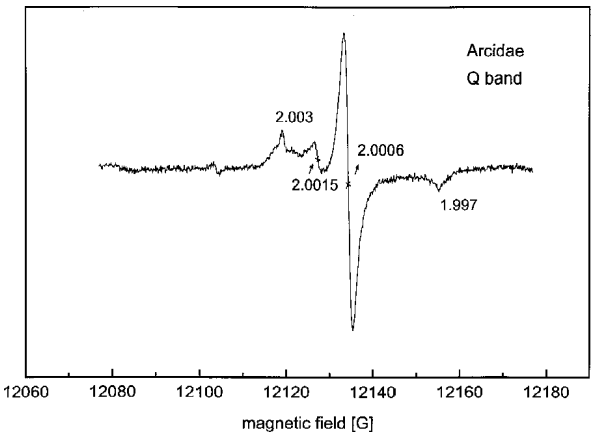

Fig.1. Experimental EPR spectrum recorded in *Arcidae* shell, Q-band measurement.

After the action of ionizing radiation several paramagnetic species are stabilized in the samples of bones and shells, and can be studied by EPR techniques at room temperature. The EPR spectra of natural samples recorded in X-band are complex and it is not easy to interpret them because signals of different centers are overlapped. The spectra recorded in Q- or W-bands are usually better resolved and the assignments of individual paramagnetic species in complex spectra become easier.

The most stable, long-lived paramagnetic center identified in *Arcidae* shell and deproteinized human bone is radical anion CO_2^-, with orthorhombic g tensor.

The X-band spectrum of bone sample is composed of only one unresolved EPR signal. A*rcidae* shell, in contrast to the bone powder, reveals some spectral resolution, suggesting its composite structure. Typical spectrum recorded at Q-band for *Arcidae* shell sample is shown in Fig.1. It clearly shows two reasonably well-resolved signals: CO_2^- orthorhombic radical anion, with $g_x=2.0030$, $g_y=1.9970$, $g_z=2.0015$ and $\Delta H=0.25$ mT as well as another type of CO_2^- entity with isotropic $g_{av}=2.0006$ and $\Delta H=0.3$ mT.

Orthorhombic CO_2^- radical ion is located inside the apatite structure, whereas isotropic CO_2^-

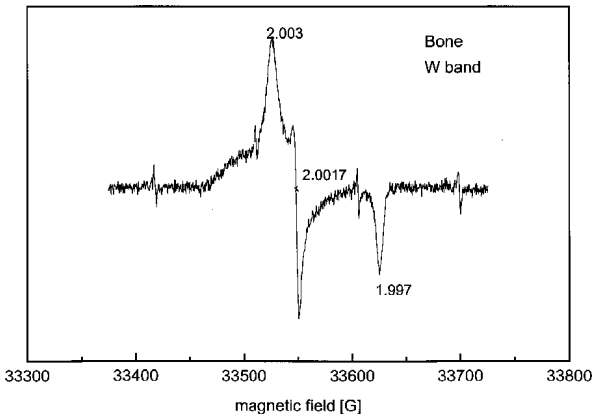

Fig.2. Experimental EPR spectrum recorded in bone powder, W-band measurement.

(freely rotating) is stabilized in the presence of water in carbonate containing apatities [7].

In bone powder sample, in contrast to *Arcidae* shell, at Q-band only one type of CO_2^- radical anion (orthorhombic) has been observed. The spectrum of the same bone recorded at W-band reveals an anisotropic singlet of CO_2^- radical with three well-resolved g components: $g_x=2.0030$, $g_y=1.9970$, $g_z=2.0017$ and $\Delta H=0.25$ mT (Fig.2).

The overlapping of isotropic CO_2^- and orthorhombic CO_2^- signals in *Arcidae* shell may cause inaccurate dose estimates based on EPR measurements at X-band and confound the quantification procedure. The identification of only one type of CO_2^- radical in the deproteinized bone powder confirmed by Q- and W-band measurements, proved univocally that this type of samples can be routinely used for dosimetry of ionizing radiation.

References

[1]. Desrosiers M.F.: J. Agric. Food Chem., 37, 96-100 (1989).

[2]. Stachowicz W., Burlińska G., Michalik J., Dziedzic-Gocławska A., Ostrowski K.: Nukleonika, 38, 67-82 (1993).

[3]. Stachowicz W., Sadło J., Strzelczak G., Michalik J., Bandiera P., Mazzarello V., Montella A., Wojtowicz A., Kaminski A., Ostrowski K.: It. J. Anat. Embryol., 104, 19-31 (1999).

[4]. Ziaie F., Stachowicz W., Strzelczak G., Osaimi S.-Al.: Nukleonika, 44, 603-608 (1999).

[5]. Dziedzic-Gocławska A., Stachowicz W.: Advances in Tissue Banking. 1. Sterilization of Tissue Allografts. Eds. G.O. Phillips *et al*. World Scientific Publishing Co Pte Ltd., Singapore 1997, pp.251-311.

[6]. Ikeya M.: New Applications of Electron Spin Resonance Dating, Dosimetry and Microscopy. In: Phosphates: Bioapatite for Anthropology. Eds. M.R. Zimmerman, N. Whitehead. World Scientific, Singapore, N. Jersey, London, Hong Kong 1993, pp.237-265.

[7]. Callens F., Vanhaelewyn G., Matthys P., Boesman E.: Appl. Magn. Reson., 14, 235-254 (1998).

RADICALS IN AROMATIC CARBOXYLIC ACIDS CONTAINING THIOETHER GROUP. EPR STUDY

Grażyna Strzelczak, Anna Korzeniowska-Sobczuk, Krzysztof Bobrowski

Radicals and ion radicals derived from aromatic thioethers play an important role in many chemical processes as: organic synthesis, radical photo-induced polymerization, environmental and biological systems.

The aim of our study was identification of radicals induced by gamma irradiation in polycrystalline aromatic carboxylic acids containing thioether groups. The samples of phenylthioacetic acid and benzylthioacetic acids were irradiated in a gamma source ^{60}Co in liquid nitrogen. The electron paramagnetic resonance (EPR) measurements were performed using a Bruker ESP-300 spectrometer operating in X-band equipped with a cryostat and variable temperature unit. The measurements were performed in vacuum over the temperature range 77-293 K.

The main component of the EPR signals recorded at 95 K for both the samples was an anisotropic singlet with g-values: $g_1=2.018$, $g_2=2.01$ and $g_3=2.000$. This spectrum was attributed to the monomeric sulfur radical cations ($PhS^{+\bullet}$-CH_2-COO^-) and (Ph-CH_2-$S^{+\bullet}$-CH_2-COO^-). Another EPR signal recorded at 95 K was a singlet with g=2.0068 and $\Delta H=7$ G – anion radical formed by addition of an electron to the carboxyl group.

Warming the samples to 180 K, EPR spectra indicated a new anisotropic singlet with g-values: $g_1=2.052$, $g_2=2.021$ and $g_3=1.997$ which we assigned to the thiyl radicals $PhS^\bullet$ obtained after fragmentation of monomeric radical cations. As the temperature increased to 250 K the spectra indicated the presence of two spectral components. The multiline spectrum of phenylthioacetic acid (Fig.1) can be simulated as a dublet with g=2.003 and

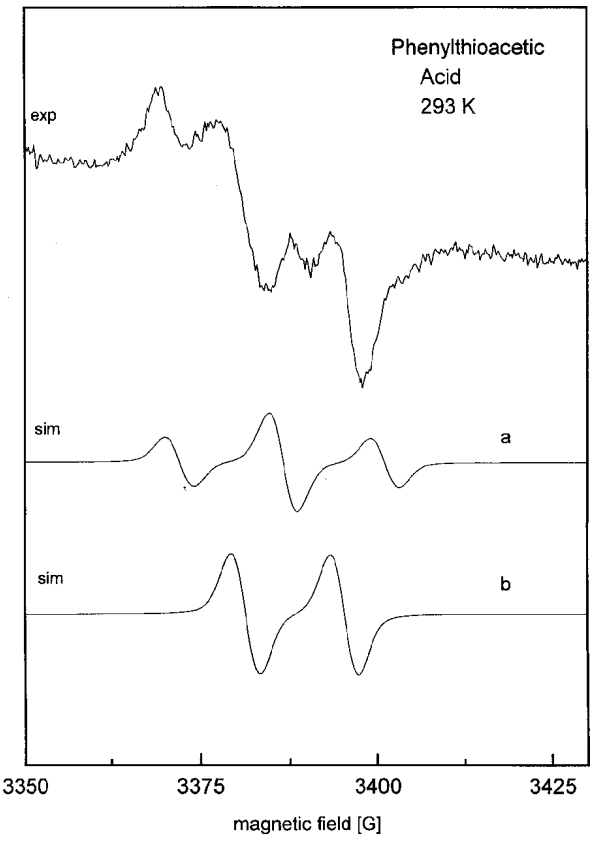

Fig.1. Multicomponent EPR spectra of phenylthioacetic acid: a – decarboxylation radicals, b – α(alkylthio)alkyl radicals.

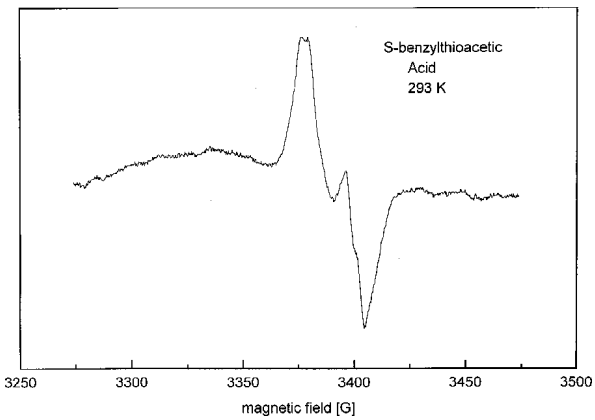

Fig.2. EPR spectrum of benzylthioacetic acid, α(alkylthio)alkyl radicals.

hyperfine splitting a_H=14 G and triplet with a_H=16 G. The dublet component can be attributed to the α(alkylthio)alkyl radicals (PhS-$^{\bullet}$CH-COOH) that might result from deprotonation of the monomeric sulfur radical cation. Triplet component we can assign to the decarboxylation radicals PhS-C$^{\bullet}H_2$. Similar type of radicals we have observed in benzylthioacetic acid.

Additionally, carbon dioxide (CO_2) was identified by a GC technique in both samples studied and exposed to gamma radiation. The yield of decarboxylation is higher in benzylthioacetic acid.

At room temperature the most stable radicals observed in benzylthioacetic acid (Fig.2) can be attributed to the α(alkylthio)alkyl radicals (Ph-CH_2-S-$^{\bullet}$CH-COO^-) obtained after deprotonation of monomeric sulfur radical cation, dublet with g=2.003 and hyperfine splitting a_H=14.5 G. We suppose, based on a captodative stabilization effect, that H abstraction takes place from the methyl group adjacent to the carboxyl group.

This work was supported by the Polish State Committee for Scientific Research (KBN) – grant No. 3 T09A 037 19.

ESR STUDY OF SILVER CLUSTERS IN SAPO-17 AND SAPO-35 MOLECULAR SIEVES

Jacek Michalik, Jarosław Sadło, Larry Kevan[1/]

[1/] University of Houston, USA

Silicoaluminophosphate (SAPO-n) molecular sieves, where n denotes a particular structure type, form a new class of microporous crystalline materials comparable to zeolites. Zeolites have cages or channels formed by alumina and silica tetrahedra linked by oxygen bridge. Substitution of other elements for Si and/or Al in the molecular sieve framework can yield a various kind of new materials. In the early eighties, the synthesis of aluminophosphate (AlPO) molecular sieves was reported [1]. Replacement of some phosphorus by silicon in neutral framework AlPO materials leads to SAPO materials with a negative framework charge, which is balanced by H^+ cations after template removal by calcination. The protons can be exchanged to some extent by metal cations. The structures of AlPO and SAPO molecular sieves can be the same as certain zeolites or they are unique with no zeolite analogues.

Up to now, only limited number of electron spin resonance (ESR) studies was undertaken to investigate the silver agglomeration processes and the interaction of silver clusters with molecular adsorbates in SAPO molecular sieves: AgH-SAPO-42, AgH-SAPO-5 and AgH-SAPO-11. The aim of this work was to study the silver agglomeration processes in AgH-SAPO-17 and AgH-SAPO-35 molecular sieves. The cluster structures and the location of trapping site in the lattice will be also discussed.

SAPO-17 and SAPO-35 molecular sieves were synthesized by the hydrothermal method under autogenous pressure without agitation using cyclohexylamine and hexamethylamine as organic template, respectively. Protonized forms of SAPOs were obtained by heating as-synthesized SAPO-17 at 550°C (600°C for SAPO-35) in O_2 for removal the organic templates. After synthesis, powders were examined by X-ray diffraction to check their crystalline structure. Silver forms of SAPOs were obtained by ion-exchange overnight with 1 M $AgNO_3$ solution at room temperature in the darkness. The exchanged samples were washed with deionized water to remove Ag^+ from external surface and dried in air at room temperature. For ESR measurements samples were placed into Suprasil quartz tubes and evacuated to a final pressure of 10^{-2} Pa. All sample were gamma-irradiated at 77 K in a ^{60}Co source with a dose of 4 kGy. ESR spectra were recorded on a Bruker ESP-300E X-band spectrometer at various temperatures in the range 110-300 K by using a variable-temperature Bruker unit.

The SAPO-17 molecular sieve structurally analogous to the commercially important zeolite, erionite is composed of erionite cages (supercages), cancrinite cages and hexagonal prisms (Fig.1a). SAPO-35 molecular sieve consists of hexagonal prisms and levyne cages (Fig.1b).

Ag-SAPO-17 irradiated after dehydration shows at 110 K only sharp lines of silver atoms: $^{107}Ag^0$: A_{iso}=57.3 mT, g_{iso}=2.0023 and $^{109}Ag^0$: A_{iso}=66.5 mT, g_{iso}=2.0023 which decay above 200 K and then Ag_2^+ signal appears. In dehydrated Ag-SAPO-35 similar spectra are recorded. At room temperature in both molecular sieves Ag_2^+ clusters are stabilized.

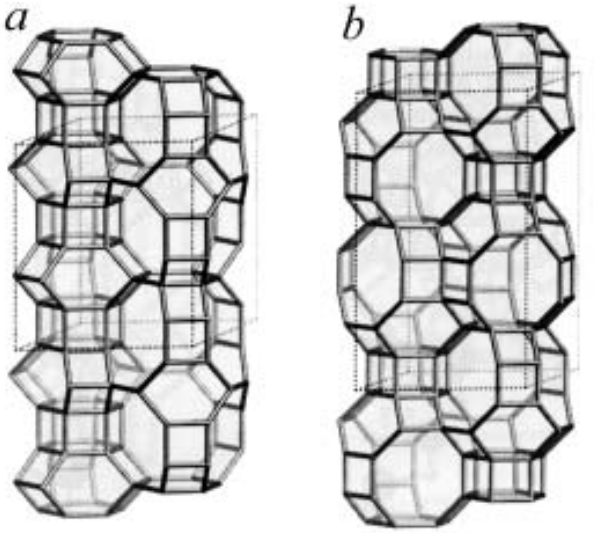

Fig.1. Structural model of SAPO-17 (a) and SAPO-35 (b) molecular sieves.

In hydrated SAPO-17 at 110 K (Fig.2) four signals representing silver species are observed: isotropic doublets A with narrow lines (H_{pp}=1.3 mT)

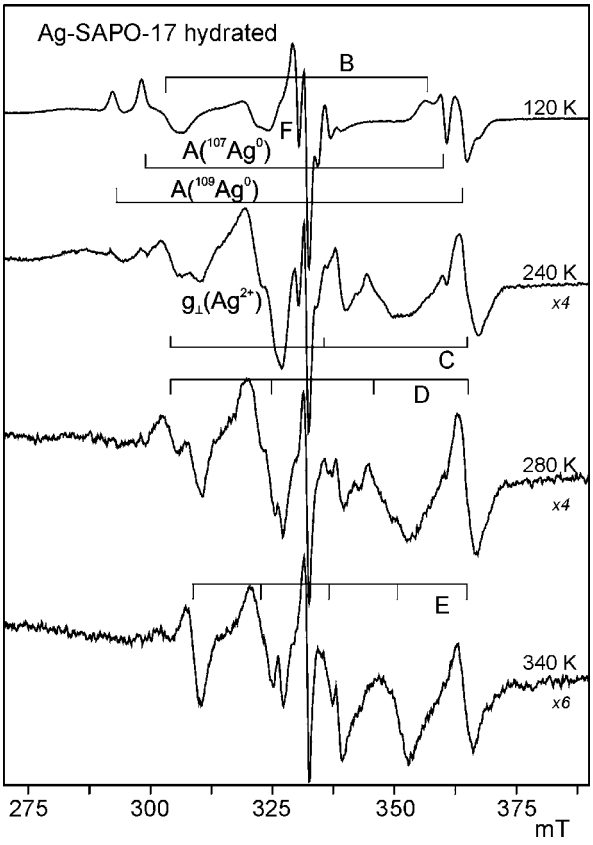

Fig.2. ESR spectra of hydrated Ag-SAPO-17 molecular sieve, irradiated at 77 K and recorded at 120, 240, 280 and 340 K.

of silver atoms: $^{107}Ag^0$: A_{iso}=61.3 mT, g_{iso}=2.0023 and $^{109}Ag^0$: A_{iso}=70.7 mT, g_{iso}=2.0025, doublet B with distinctly broader lines (H_{pp}=5.2 mT) and lower hyperfine splitting A_{iso}=55.4 mT of silver atoms in different site and anisotropic doublet of Ag^{2+} cations ($g_{\perp}$=2.750, $g_{||}$=2.345). The most intense signal recorded at 110 K is, however, a singlet F at g=2.006. Because it is also observed in gamma-irradiated Na-SAPO-17 samples, we assigned it to the radiation-induced paramagnetic centers in silicaalumina framework.

After annealing at 200 K, the doublets of Ag^0 atoms decay and the spectrum observed at 240 K is composed of a triplet C: A_{iso}=30.5 mT, g_{iso}=1.985 of clusters and quartet D: A_{iso}=20.5 mT, g_{iso}=1.975 of Ag_3^{2+} trimers. For further annealing at 280 K Ag_2^+ triplet becomes less intense and a new signal builds up. Its appearance is seen in the most clear way at low field around 310 mT. On thermal annealing above room temperature the Ag_3^{2+} quartet decays quickly and then the features of new signal are more visible. It is a pentet E with A_{iso}=13.9 mT and g_{iso}=1.975, which we assigned to Ag_4^{3+} cluster. Tetrameric silver was earlier stabilized in AgCs-rho zeolite and its ESR parameters are well known [2].

In hydrated Ag-SAPO-35 at 110 K only doublet: A_{iso}=59.7 mT, g_{iso}=1.978 of silver atoms is seen. The narrow doublets of $^{107}Ag^0$ and $^{109}Ag^0$ are not observed at all. On thermal annealing at 200 K the Ag^0 doublet transforms into a triplet: A_{iso}=30.6 mT, g_{iso}=1.990 of Ag_2^+ dimer. The central line of triplet is superimposed by a strong singlet of framework paramagnetic centers but outer lines show additional splittings to three lines with intensity ratio 1:2:1 – the pattern characteristic of dimer isotopomers $^{107}Ag_2^+$, $(^{107}Ag^{109}Ag)^+$ and $^{109}Ag_2^+$. The Ag_2^+ spectrum is observed also at room temperature with slowly decreasing intensity.

When Ag-SAPO-35 is exposed to D_2O vapour before irradiation, the ESR spectra recorded at 110 and 290 K are similar to the spectra observed for hydrated Ag-SAPO-35. Only silver dimers are stabilized at room temperature. In Ag-SAPO-17 exposed to D_2O, the spectrum recorded after thermal annealing at 340 K is the same as in hydrated Ag-SAPO-17 indicating stabilization of Ag_4^{3+} clusters.

Taking into account the preference location sites of cations in both molecular sieves [3, 4] we tentatively assume that in dehydrated sieves silver atoms are located in hexagonal prisms, connected erionite and levyne cages, respectively in SAPO-17 and SAPO-35. During thermal annealing silver atoms are able to migrate close to hexagonal windows and react with Ag^+ cations located in bigger cages (erionite or levyne) forming Ag_2^+ dimer.

It is interesting that in SAPO-17 clusters of bigger nuclearity are stabilized in presence of water molecules although bigger void space is available in the cages after dehydration. In our opinion this is caused by the blocking effect of water molecules which make difficult the migration of Ag^0 atoms from small to bigger cages. This suggests that Ag_4^{3+} cluster could be located in cancrinite cages and should coordinate H_2O molecules from nearby erionite cages. In the nearest future we intend to carry out ESEEM studies for Ag-SAPO-17 samples exposed to D_2O, CH_3OD and CD_3OH to prove this hypothesis.

In Ag-SAPO-35 in hydrated and dehydrated form, cationic silver cluster bigger than dimmers are not stabilized at all. Similar results were reported earlier for AgNa-X and AgNa-Y zeolites in which open framework structure makes easier the migration of atoms and small clusters from small cages to the bigger ones. SAPO-35 molecular sieve has no suitable cages to trap small silver clusters, therefore they can easily migrate through octagonal windows from one levyne cage to another until they reach the surface of polycrystallite where bigger metal particles are formed.

A comparison of silver agglomeration processes in SAPO-17 and SAPO-35 univocally indicates that small structural cages with small openings are indispensable for stabilization of cationic silver clusters in molecular sieves.

References

[1]. Wilson S.T., Lok B.M., Messina C.A., Cannan E.R., Flanigen E.M.: J. Am. Chem. Soc., 104, 1146 (1982).
[2]. Michalik J., Sadło J., Yu J.-S., Kevan L.: Colloids and Surfaces A: Physicochem. Eng. Aspects, 115, 239-247 (1996).
[3]. Prakash A.M., Kevan L.: Langmuir, 13, 5341 (1997).
[4]. Prakash A.M., Hartmann M., Kevan L.: Chem. Mater., 10, 932 (1998).

REACTIVE OXYGEN SPECIES FROM ALZHEIMER'S β-AMYLOID PEPTIDE: MECHANISM AND PROOF OF CONCEPT

Christian Schöneich[1/], Dariusz Pogocki, Jarosław Kański[1/], Maria Aksenova[2/], Allan Butterfield[2/]

[1/] Department of Pharmaceutical Chemistry, University of Kansas, Lawrence, USA
[2/] University of Kentucky, Lexington, USA

The formation and deposition of cytotoxic β-amyloid (βAP) peptide is a major hallmark of Alzheimer's disease. This peptide shows a high tendency to complex redox-active transition metals such as Cu(II), and metal-metal catalyzed formation of reactive oxygen species has been linked to the cytotoxic action of βAP [1]. In two simultaneously issued papers we have shown theoretical [2] and experimental [3] evidence that the pronounced ability of βAP to reduce C(II) may be connected to conformational and dynamic properties of its C-terminal domain containing Met^{35}. Surprisingly, this Met residue is essential for the redox activity of βAP, although the peptide contains a Tyr residue in its N-terminal metal-binding domain. However, the Met^{35} sulfur is located in close contact to the peptide bond carbonyl function of Ile^{31}, suggesting that electron transfer is facilitated by sulfur-oxygen bond formation [4], in reaction (1), of βAP methionine radical cations.

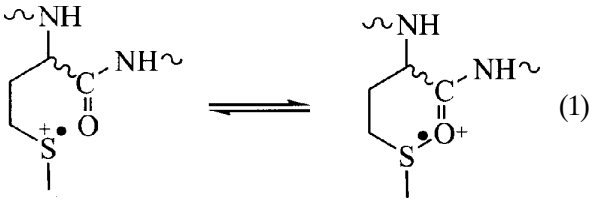

(1)

That sulfur-oxygen interaction significantly lowers the peak reduction potential of MetS/Met($S^{\bullet+}$) pair, making Met^{35} a better one-electron donor [5]. The molecular modeling results (Table) suggest that such sulfur-oxygen bond formation can be avoided if Ile^{31} is substituted by Pro^{31}.

Table. Relative rate constants of reaction (1) obtained in the Langevin dynamics modeling [2].

$k\times10^{-9}$ [s^{-1}]		
	"water"	"lipid"
βAP	7.0±2.0	17.8±2
βAP(Ile^{31}Pro)	1.5±0.5	0.9±0.15

Indeed, the βAP(Ile^{31}Pro) mutant is not cytotoxic and shows a significantly lower ability to reduce Cu(II) though the peptide still contains Met^{35} and an intact metal-binding site [3]. These results point to the importance of peptide and protein dynamics in initiating oxidative stress, and similar phenomena may play a role in related neurodegenerative diseases.

This material has been presented at the 9th Annual Meeting of the Oxygen Society, 20-24 November 2002, San Antonio, USA.

References

[1]. Pogocki, D., Serdiuk K.: Wiad. Chem., in press.
[2]. Pogocki D., Schöneich C.: Chem. Res. Toxicol., 15, 408-418 (2002).
[3]. Kanski J., Aksenova M., Schöneich C., Butterfield D.A.: Free Radical. Biol. Med., 32, 1205-1211 (2002).
[4]. Pogocki D., Schöneich C.: J. Org. Chem., 67, 1526-1535 (2002).
[5]. Pogocki, D., Serdiuk K.: unpublished results (2002).

SPECTRAL AND CONDUCTOMETRIC PULSE RADIOLYSIS STUDIES OF RADICAL CATIONS DERIVED FROM *N*-ACETYL-METHIONINE AMIDE

Krzysztof Bobrowski, Dariusz Pogocki, Gordon L. Hug[1/], Christian Schöneich[2/]

[1/] Radiation Laboratory, University of Notre Dame, USA
[2/] Department of Pharmaceutical Chemistry, University of Kansas, Lawrence, USA

N-Acetyl-methionine amide (*N*-Ac-Met-NH_2) represents a simple chemical model compound for the amino acid, methionine (Met) incorporated within a peptide. The $^{\bullet}$OH-induced reaction pathways in *N*-acetyl-methionine amide have been characterized by the complementary pulse radiolysis measurements coupled to time-resolved UV-VIS spectroscopy and conductivity [1]. The reaction of $^{\bullet}$OH radicals with the thioether function of N-acetyl-methionine amide leads at pH 4.0 to the formation of four UV-VIS-detectable intermediates: hydroxysulfuranyl radical (**1**), the two-α-(alkylthio)alkyl radicals (**2a** and **2b**), the intermolecularly sulfur-sulfur three-electron bonded dimeric radical cation (**3**), and the intramolecular sulfur-oxygen bonded radical cation (**4**) (Chart 1). The equality in the radiation chemical yields of the intermolecularly sulfur-sulfur three-electron bonded dimeric radical cation (**3**) and the intramolecular sulfur-oxygen bonded radical cation (**4**) (calculated from deconvoluted absorption spectra) and the total yields of the sulfide radical cations (calculated from the conductivity signal) has been accounted for by the formation of the sulfide radical cation containing sulfur-amide oxygen bond.

We extended our previous optical and conductivity pulse radiolysis studies at pH 4 to the higher pH region (up to 5.4) and probed additionally a couple of intermediate pH's: 4.6 and 5.0. In agreement with our earlier data for pH 4.0 the experimental spectrum recorded at 2 μs after pulse irradiation was deconvoluted into contributions from the four components: (**1**), (**2a**/**2b**), (**3**), and (**4**) (Fig.1a). The sum over all component spectra yields

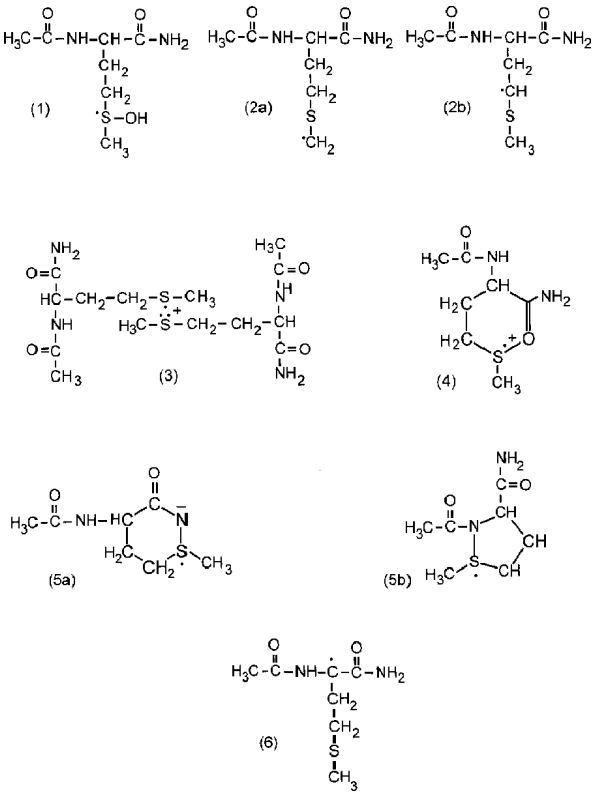

Chart 1.

an excellent fit of the experimental spectra. Radical cations (**3**) and (**4**) are present with yields of G_3=1.5 and G_4=1.2, i.e G_{3+4}=2.7. The simultaneous formation of radical cations (**3**) and (**4**) with the yield = 2.7 was confirmed by time-resolved conductivity experiments (Fig.2a). A careful examination of radiation chemical yields of radical cations (**3**) and (**4**) obtained from deconvolution of the absorption recorded at 4 μs after the pulse shows a significant discrepancy with the radiation chemical yields of radical cations obtained by time-resolved conductivity measurements. While the sum over all component spectra (**1**, **2a**/**2b**, **3**, and **4**) yields an excellent fit of the experimental spectrum at 4 μs (with G_3=2.2 and G_4=0.6), i.e G_{3+4}=2.8 (Fig.1b), the total yields of G_{3+4}=2.4 measured in the conductivity experiments (Fig.2a) do not match the G-values of radical cations (**3** and **4**) measured in optical experiments.

Our new data obtained by the time-resolved conductivity experiments extended to pH 4.6, 5.0, and 5.4, show significant differences in the amplitude of negative conductivity signals for each particular pH (Fig.2b-d). Moreover, they reveal a significant trend, for higher pH the lower amplitude of a negative signal. The different maximum loss of equivalent conductivity indicates a pH-dependent change in the yields of radical cations (**3** and **4**), and yields G-values = 2.1, 1.6 and 1.4 of sulfide radical cations (**3** and/or **4**) for pH 4.6, 5.0 and 5.4, respectively. Time-resolved UV-VIS-spectroscopic analysis at the same pH's reveals information about identity and quantity of specific radical cations and other-short-lived intermediates. For better clarity we will only discuss the data for the highest pH, i.e. 5.4. An excellent spectral deconvolution of the original UV-VIS spectrum recorded at 10 μs after pulse irradiation gives the total yield of sulfur radical cations, G_{3+4}=2.6. However, in contrast to the earlier data for pH 4.0, the total yields of sulfur radical cations (G_{3+4}) do not match the G-value of radical cations (G_{ions}=1.4) measured at the maximum loss of equivalent conductivity in the time-resolved conductivity experiments (*vide supra*) (Fig.2d). Similar picture is obtained at 15 μs after the pulse, where the total yields of G_{3+4}=2.4 differ significantly from the G_{ions}=1.4 measured in the conductivity experiments (Fig.2d). Consequently, the sulfur-oxygen bonded species (**4**) cannot be responsible for the absorption in the 390-400-nm region and indicates the presence of an additional species with similar absorbance characteristics. Sulfur-nitrogen bonded species have been observed for radical cations of a variety of amino-substituted organic sulfides [2] including *N*-methionyl peptides [3, 4]. A representative spectrum taken from the pulse radiolysis data of methionine amide (Met-NH_2) [5] shows a broad absorption with λ_{max} ca. 390 nm and ε_{390}=4500 $M^{-1}cm^{-1}$. Therefore, we hypothesized that the absorption around 390-400 nm at ≥ 10 μs

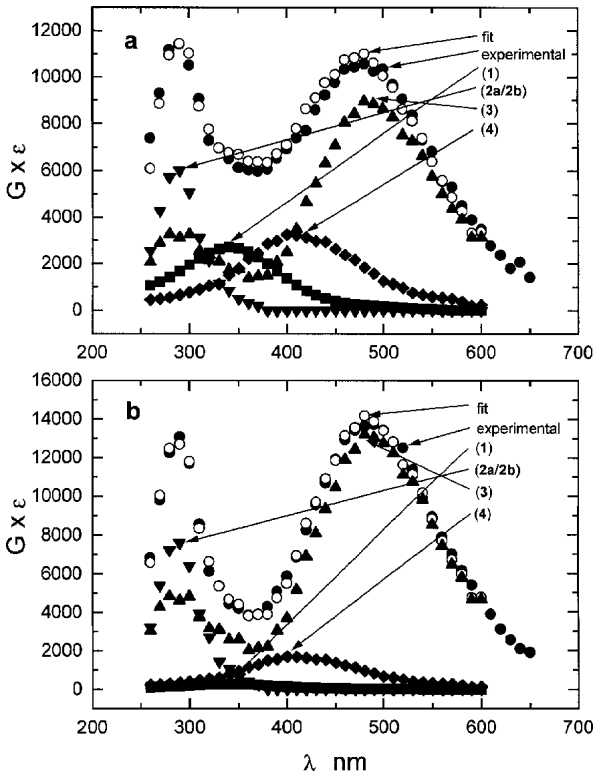

Fig.1. Resolution of the spectral components in the transient absorption spectra following the •OH-induced oxidation of *N*-acetyl-methionine amide (0.2 mM) in N_2O saturated aqueous solutions at pH 4.0 taken (a) 2 μs, (b) 4 μs after the pulse.

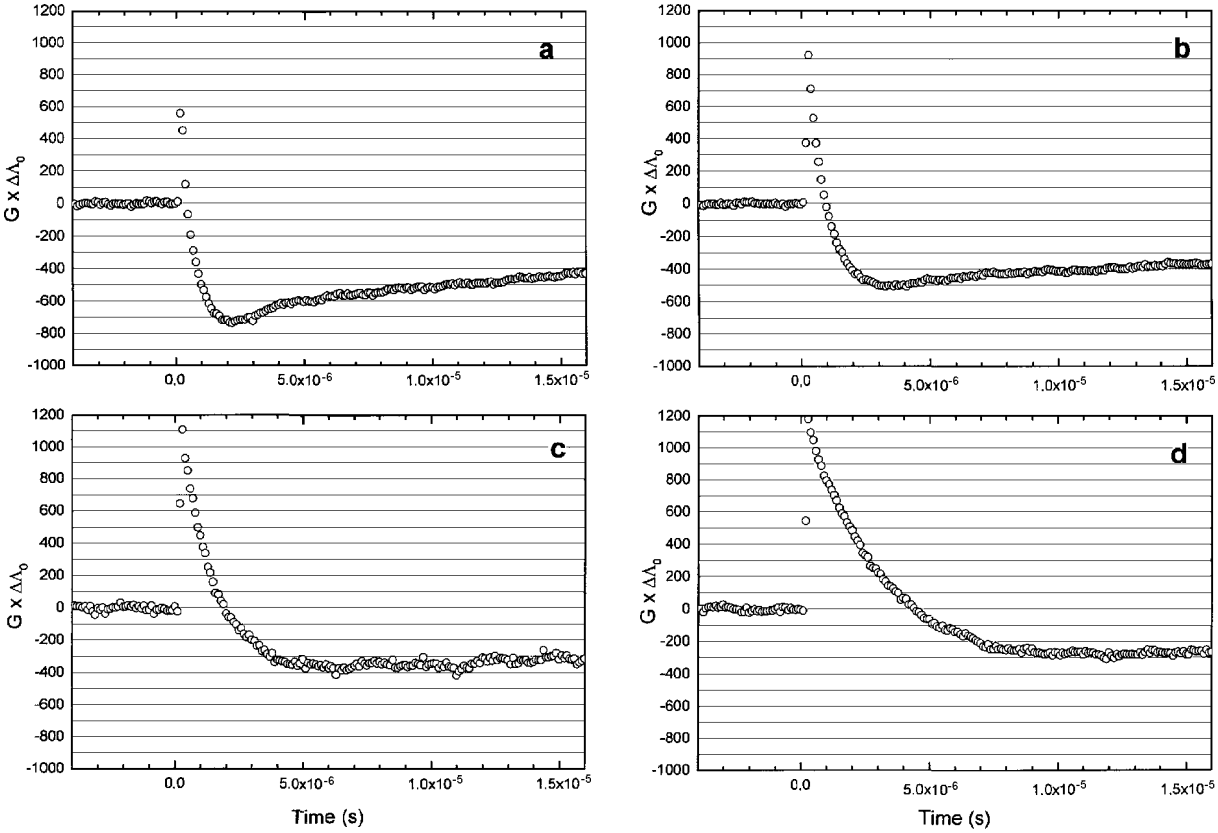

Fig.2. The equivalent conductivity changes represented as ($G \times \Delta\lambda_0$) *vs.* time profile following the $^{\bullet}OH$-induced oxidation of *N*-acetyl-methionine amide (0.2 mM) in N_2O saturated aqueous solutions at pH (a) 4.0, (b) 4.6, (c) 5.0, and (d) 5.4.

after pulse irradiation may indicate the formation of a new, sulfur-nitrogen intermediate. Moreover, the sulfur-nitrogen bonded species cannot be a radical cation and we conclude tentatively that it would have either the structure **5a** or **5b** (Chart 1). An excellent spectral deconvolution is achieved when sulfur-oxygen bonded intermediate (**4**) is replaced by a sulfur-nitrogen bonded intermediate (**5a**/**5b**). At 10 μs after the pulse, deconvoluted experimental spectrum contains the following components: **2a**/**2b** (G=2.2), **3** (G=1.4), **5a**/**5b** (G=0.9) and (**6**) (G=0.5). The yield of **3** obtained from the spectral deconvolution corresponds very well with the yield of ions (G=1.4) measured in the time-resolved conductivity experiments. This is also consistent with the neutral character of **5a**/**5b** species, being not a radical cation (*vide supra*).

In this report, by applying complementary time-resolved conductivity and UV-VIS spectrophotometric measurements in *N*-acetyl-methionine amide, we provide evidence for sulfur radical cation interactions that involve either the carbonyl oxygen or nitrogen functionality.

References

[1]. Schöneich C., Pogocki D., Wiśniowski P., Hug G.L., Bobrowski K.: J. Am. Chem. Soc., 122, 10224-10225 (2000).
[2]. Asmus K.-D., Göbl M., Hiller K.-O., Mahling S., Mönig J.: J. Chem. Soc. Perkin Trans. II, 1641-1646 (1985).
[3]. Bobrowski K., Holcman J.: Int. J. Radiat. Biol., 52, 139-144 (1987).
[4]. Bobrowski K., Holcman J.: J. Phys. Chem, 93, 6381-6387 (1989).
[5]. Bobrowski K., Hug G.L.: unpublished results.

RADICAL CATIONS, RADICALS AND FINAL PRODUCTS DERIVED FROM AROMATIC CARBOXYLIC ACIDS CONTAINING THIOETHER GROUP

Anna Korzeniowska-Sobczuk, Gordon L. Hug[1/], Jacek Mirkowski, Krzysztof Bobrowski

[1/] Radiation Laboratory, University of Notre Dame, USA

Introduction

Sulfur-centred radicals and radical cations derived from aromatic thioethers play an important role in many chemical processes including those of organic synthesis [1], environmental [2], photo-induced polymerization [3] and biological significance [4, 5] including xenobiotic-glutathione conjugates [6, 7]. Therefore, it is of interest to examine the spectral and kinetic properties of intermediate species and to identify final products formed dur-

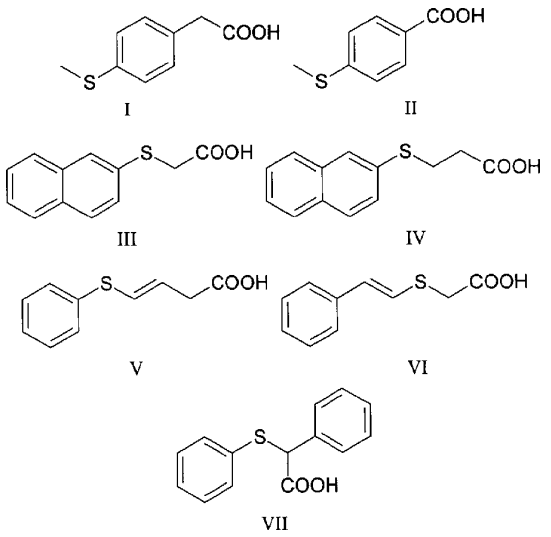

Chart 1.

ing the oxidation of aromatic thioethers containing carboxylic functionality in various position in relation to the aromatic ring and to the thioether function.

In previous report [8] we presented the results of pulse- and γ-radiolysis studies of phenylthioacetic acid and benzylthioacetic acid, in N_2O-saturated aqueous solutions at various pH's. Particular emphasis was placed on the $^{\bullet}OH$-radical induced oxidation since it allowed a detailed quantification of the relative contribution of the $^{\bullet}OH$ addition to aromatic ring and to the thioether functionality [9]. In this presentation we report the results of pulse radiolysis studies of the following carboxylic acids: 4-(methylthio)phenylacetic acid – 4-MTPA (**I**), 4-(methylthio)benzoic acid (**II**), 2-(naphtylthio)acetic acid – 2-NphTA (**III**), 3-(2-naphtylthio)propionic acid (**IV**), 3-(phenylthio)acrylic acid (**V**), and Z-(styrylthio)acetic acid (**VI**), and α-(phenylthio)phenylacetic acid – α-PTPA (**VII**), (Chart 1). We have focused on the spectral and kinetic characterization of radical cations and the qualitative identification of final products derived from these acids.

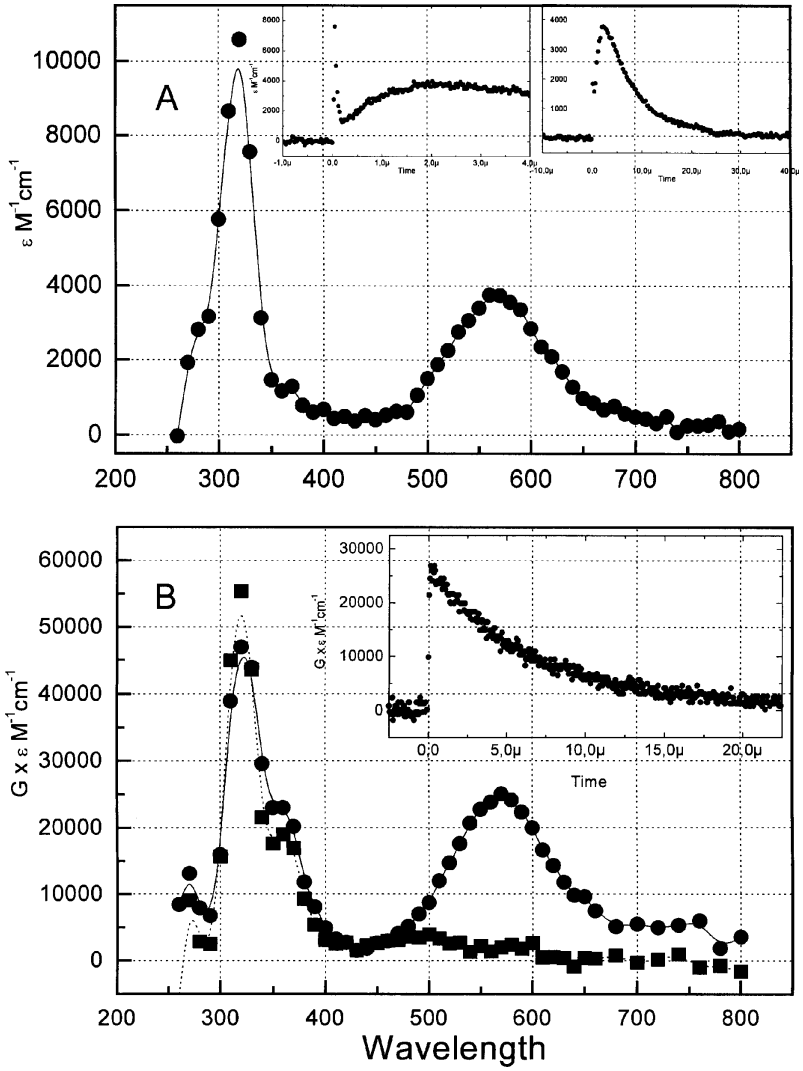

Fig.1. A – Transient absorption spectrum recorded after pulse irradiation of an Ar-saturated aqueous solution containing 0.2 mM 4-(methylthio)phenylacetic acid, 2 mM $K_2S_2O_8$, and 0.1 M *tert*-butyl alcohol 2.25 μs after the pulse at pH 5.4. Insets: (left) experimental trace for the formation of $H_3C\text{-}S^{+\bullet}\text{-}Ph\text{-}CH_2\text{-}COO^-$ at λ_{max}=570 nm; (right) experimental trace for the decay of $H_3C\text{-}S^{+\bullet}\text{-}Ph\text{-}CH_2\text{-}COO^-$ at λ_{max}=570 nm. B – Transient absorption spectra recorded after pulse irradiation of an N_2O-saturated aqueous solution containing 2 mM 4-(methylthio)phenylacetic acid (●) 275 ns and (■) 20.5 μs after the pulse at pH 6.0. Inset: experimental trace for the decay of the $CH_3\text{-}S^{+\bullet}\text{-}Ph\text{-}CH_2\text{-}COO^-$ radical cation at λ_{max}=570 nm.

Spectral and kinetic properties of sulfur monomeric radical cations by applying reaction of with carboxylic acids

The radical anion is known to react with aromatic thioether compounds through one-electron oxidation, forming the corresponding monomeric sulfur-centered radical cation (1):

+Ph-S-R +Ph-$S^{+\bullet}$-R (1)

A strong transient absorption spectrum with λ_{max}=320- and 570-nm was seen 2.25 μs after the radiolytic pulsing of an aqueous, Ar-saturated solution containing 0.2 mM 4-(methylthio)phenylacetic acid, 2 mM $K_2S_2O_8$, and 0.1 M *tert*-butyl alcohol at pH 5.4 (Fig.1A). The 320- and 570-nm absorption bands were attributed accordingly to the monomeric sulfur radical cation H_3C-$S^{+\bullet}$-Ph-CH_2-COO^-. The monomeric sulfur radical cation derived from 4-(methylthio)phenylacetic acid is characterised by a relatively long lifetime (Fig.1A, right inset) longer than for analogous monomeric sulfur radical cations derived from phenylthioacetic acid and benzylthioacetic acid. The spectral and kinetic parameters of the monomeric sulfur-centered radical cations derived from carboxylic acids under study are given in Table 1.

Table 1. Selected spectral and kinetic parameters of sulfur monomeric radical cations derived from carboxylic acids containing thioether functionality.

Compound	$\lambda^{a)}$ [nm]	$\lambda^{b)}$ [nm]	$k^{b)}$ [s^{-1}]	$\lambda^{c)}$ [nm]	$k^{c)}$ [s^{-1}]
H_3C-S-Ph-CH_2-COOH	320 570	320 540	7.3×10^2	320 570	7.3×10^4
H_3C-S-Ph-COOH	320 560	330 550	1.8×10^4	320 560	2.1×10^4
Nph-S-CH_2-COOH	330 650	330 640	4.7×10^4	330 650	1.8×10^5
Nph-S-CH_2-CH_2-COOH	330 630	d)	d)	d)	d)
Ph-S-CH=CH_2-COOH	325 670	e) 650	1.6×10^4	330 670	2.6×10^4
Ph-CH=CH_2-S-CH_2-COOH	e) 640	e) 640	1.7×10^4	e) 640	7.3×10^4
Ph-S-CH(COOH)-Ph	f)	f)	f)	f)	f)

a) generated *via* reaction with .
b) generated *via* reaction with $^\bullet$OH at pH 1.
c) generated *via* reaction with $^\bullet$OH at pH~6.
d) not measured yet.
e) not measured because of a strong absorption of the parent compound.
f) not measured because of a very short life time of the monomeric sulfur radical cation.

Reaction of $^\bullet$OH radicals with carboxylic acids containing thioether functionality

The pulse irradiation of an N_2O-saturated aqueous solutions, pH~6.0-6.5, containing 2 mM carboxylic acids under study (Chart 1) yields complex spectra of transients with absorption maxima that can be assigned to the monomeric sulfur radical cations (by comparison to the spectra of the species formed from carboxylic acids by electron transfer to $SO_4^{\bullet-}$), OH- and H-adducts to the aromatic ring, and C-centred radicals produced either from decarboxylation or fragmentation of the respective monomeric sulfur radical cations. Because the second absorption band of the monomeric sulfur radical cations does not overlap with the absorption bands of the other species, one can calculate the rate constants for the decay of the respective radical cations at two pH's: 1 and 6 (Table 1), where the carboxyl group exists in protonated and deprotonated state, respectively.

In the case of 4-(methylthio)phenylacetic acid (Fig.1B), the transient spectrum at pH 6.0 observed 275 ns after the pulse consists of two distinct bands with λ_{max}=320- and 570-nm bands which are assigned accordingly to the monomeric sulfur radical cation (H_3C-$S^{+\bullet}$-Ph-CH_2-COO^-). Because addition to the aromatic ring is one of the likely reaction pathways for $^\bullet$OH radicals and $^\bullet$H atoms, we have attributed the distinct 360-nm shoulder, both to hydroxycyclohexadienyl-type, H_3C-S-Ph$^\bullet$(OH)-CH_2-COO^- and cyclohexadienyl-type radicals, H_3C-S-Ph$^\bullet$(H)-CH_2-COO^-, respectively. After decay of H_3C-$S^{+\bullet}$-Ph-CH_2-COO^- radical cation (Fig.1B, inset), the spectrum observed 20.5 μs after the pulse is dominated by an absorption maximum at λ_{max}=320 nm (Fig.1B). The appearance of the 320-nm band is an indication that substituted benzyl-type H_3C-S-Ph-$^\bullet CH_2$ are formed. These radicals are produced from the decarboxylation of H_3C-$S^{+\bullet}$-Ph-CH_2-COO^- radical cations, which is, in turn, indicated by the formation of CO_2 and 4-methylthioanisole (*vide infra*).

The decay of the monomeric sulfur radical cations both *via* the decarboxylation and fragmentation pathway is illustrated for 2-(naphtylthio)acetic acid in aqueous solution at pH 6.5. The pulse irradiation of an N_2O-saturated aqueous solutions, containing 2 mM leads to the spectrum shown in Fig.2A, observed 200 ns after the pulse. It consists of the distinct band with λ_{max}=640 nm, which can be assigned to the monomeric sulfur radical cation (2-Nph-$S^{+\bullet}$-CH_2-COO^-) by comparison to the spectrum of the species formed from 2-(naphtylthio)acetic acid by electron transfer to . The

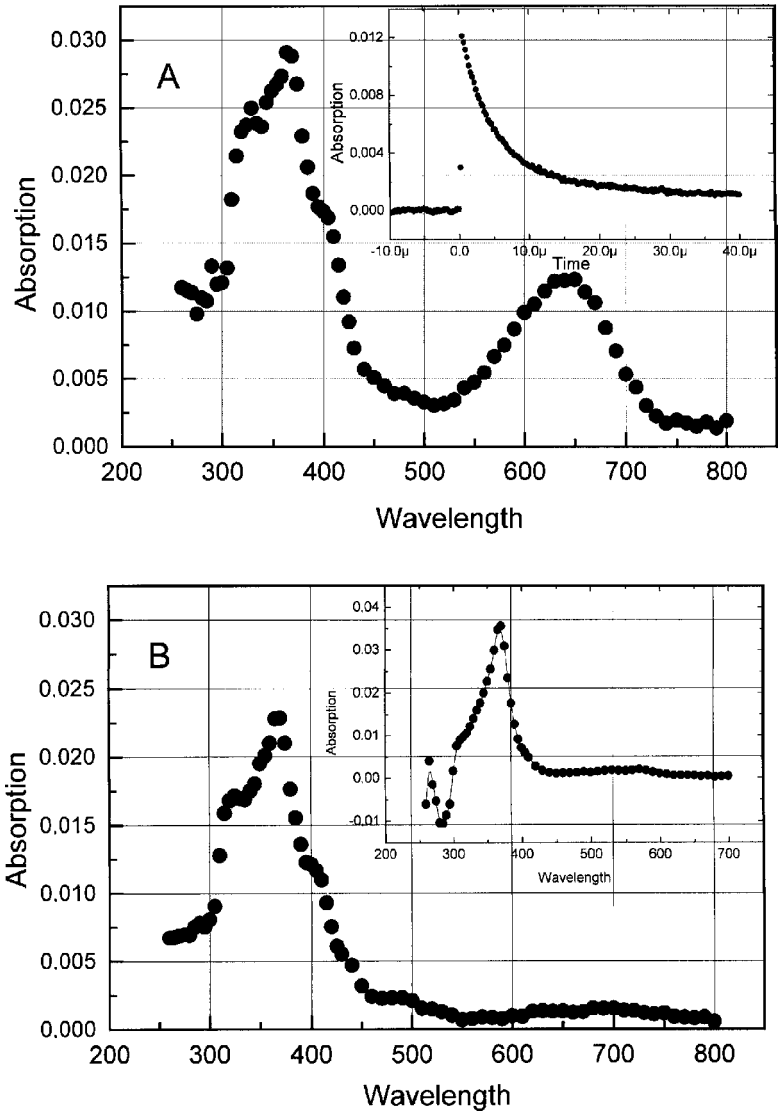

Fig.2. A – Transient absorption spectrum recorded after pulse irradiation of an N_2O-saturated aqueous solution containing 2 mM 2-(naphtylthio)acetic acid 200 ns after the pulse at pH 6.5. Inset: experimental trace for the decay of Nph-$S^{+\bullet}$-CH_2-COO^- radical cation at λ_{max}=640 nm. B – Transient absorption spectrum recorded after pulse irradiation of an N_2O-saturated aqueous solution containing 2 mM 2-(naphtylthio)acetic acid 30 μs after the pulse at pH 6.5. Inset: transient absorption spectrum recorded after pulse irradiation of an N_2O-saturated aqueous solution containing 0.2 mM 2-(naphtylthyl)methyl sulfide and 0.5 M. KOH at 50 μs after the pulse.

appearance of the 320-nm band is an indication of formation of OH-adducts to the napthalene aromatic ring [10]. Following the decay of the 2-Nph-$S^{\bullet+}$-CH_2-COO^- radical cation (Fig.2, inset), the spectrum is dominated by an absorption spectrum at λ_{max}=370 nm (Fig.2B). The appearance of the 370-nm band is an indication that
are formed, by analogy to the absorption spectrum of the product of the dehydrogenation of 2-Nph-S-CH_3 by $O^{\bullet-}$ (Fig.2B, inset). Two shoulders located at λ∼390 nm and λ∼490 nm can be assigned as belonging to the 2-napthalenylthio radical (2-Nph$S^\bullet$) [11]. This radical is produced by fragmentation of 2-Nph-$S^{\bullet+}$-CH_2-COO^- radical cation, which is, in turn, indicated by the formation 2-napthalene thiol (*vide infra*).

The decay of the monomeric sulfur radical cations *via* the fragmentation pathway is illustrated for α-(phenylthio)phenylacetic acid. Following the very fast decay of the Ph-$S^{\bullet+}$-CH(Ph)-COOH radical cation, the spectrum consists of the absorption band with λ_{max}∼460 nm (Fig.3), which is assigned to the thiyl-type radical Ph$S^\bullet$ [12].

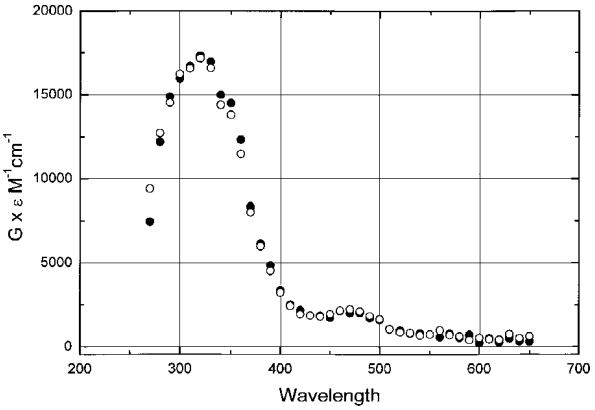

Fig.3. Transient absorption spectra recorded after pulse irradiation of an N_2O-saturated aqueous solution containing 2 mM α-(phenylthio)phenylacetic acid at pH 6 (●) 2.8 μs after the pulse and (o) 22 μs after the pulse.

Final products of the •OH radicals induced oxidation of carboxylic acids containing thioether functionality

Identification of stable products is of great help to support the reaction pathway of the monomeric sulfur radical cations established upon identification of transient species using pulse radiolysis. Moreover, an appearance of the specific stable products can also show an occurence of the additional reaction pathways that were not possible for determination based only on the time-resolved UV-VIS spectroscopy. The stable products formed after γ-radiolysis of N_2O-saturated aqueous solutions of carboxylic acids under study (Chart 1) were identified using GC, GC-MS, and HPLC methods. The selected stable products identified in the γ-irradiated solutions of carboxylic acids with thioether functionality are shown in Table 2. The presence of 4-methylthioanisole and benzylphenyl sulfide confirms decarboxylation pathway in 4-(methylthio)phenyl acetic and (phenylthio)phenylacetic acids, respectively. On the other hand, the presence of diphenyl sulfide, diphenyldisulfide, and diphenyl in α-(phenylthio)phenylacetic acid, napthalene and napthalene thiol in 2-(napthylthio)acetic acid and dimethyl sulfide in 4-(methylthio)phenylacetic acid confirms fragmentation pathway in decay of the respective sulfur radical cations (Table 2).

Table 2. Selected stable products identified after γ-radiolysis in carboxylic acids containing thioether group using GC-MS.

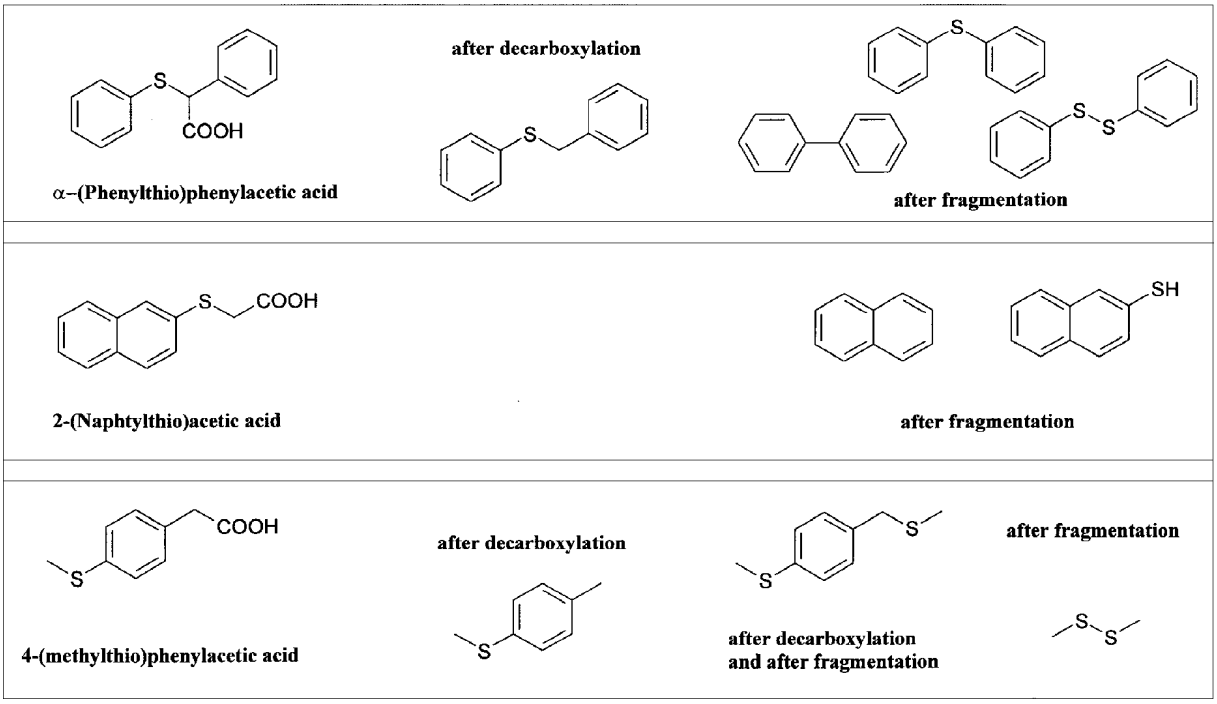

Conclusion

The •OH-radical induced oxidation of aromatic carboxylic acids containing thioether group results in a primary formation of monomeric sulphur radical cations and •OH-adducts to the aromatic ring. The mutual location of the thioether and carboxyl functionalities in relation to the aromatic ring, separation of the thioether functionality from either the carboxyl group or the aromatic ring by the double bond affects the life-time of the monomeric sulfur radical cations. The monomeric sulfur radical cations decay *via* three competitive reaction pathways: decarboxylation, deprotonation and fragmentation.

This work was supported by the Polish State Committee for Scientific Research (KBN) – grant No. 3 T09A 037 19.

References

[1]. Chatgilialoglu C., Bertrand M.P., Ferreri C.: In: S-centered radicals. Ed. Z.B. Alfassi. John Wiley & Sons Ltd., Chichester 1999, pp.311-354.
[2]. Tobien T., Cooper W.J., Nickelesen M.G., Pernas E., O'Shea K.E., Asmus K-D.: Env. Sci. Technol., 34, 1286-1291 (2000).
[3]. Wrzyszczynski A., Filipiak P., Hug G.L., Marciniak B., Paczkowski J.: Macromolecules, 33, 1577-1582 (2000).
[4]. Ozaki S., de Montelano O.: J. Am. Chem. Soc., 117, 7056-7064 (1995).
[5]. Stubbe J.A., van der Donk W.A.: Chem. Rev., 98, 705-762 (1998).
[6]. Seńczuk W.: Toksykologia. PZWL, 2002, pp.149-152.
[7]. Monks T.J., Lau S.S.: Chem. Res. Toxicol., 10, 1296-1313 (1997).
[8]. Korzeniowska-Sobczuk A., Hug G.L., Bobrowski K.: In: INCT Annual Report 2001. Institute of Nuclear Chemistry and Technology, Warszawa 2002, pp.19-21.
[9]. Korzeniowska-Sobczuk A., Hug G.L., Carmichael I., Bobrowski K.: J. Phys. Chem. A, 106, 9251-9260 (2002).
[10]. Zevos N., Sehested K.: J. Phys. Chem., 82, 138-141 (1976).
[11]. Yoshikawa Y., Watanabe A., Ito O.: J. Photochem. Photobiol. A, 89, 209-214 (1995).
[12]. Ito O.: In: S-centered radicals. Ed. Z.B. Alfassi. John Wiley & Sons Ltd., Chichester 1999, pp.193-224.

CHEMICAL AND RADIATION MODIFICATION OF DIPEPTIDES MODELLING ENKEPHALIN FRAGMENTS

Gabriel Kciuk, Cecille Roselli[1/], Chantal Houeé-Levin[1/], Krzysztof Bobrowski

[1/] Laboratoire de Chimie Physique, University Paris XI, Orsay, France

There is a growing interest in the mechanistic characterization of the oxidation of biological molecules such as peptides and proteins by various forms of reactive oxygen species (ROS), in particular hydroxyl radicals [1]. Such reaction pathways are of general importance for biological systems exposed to conditions of oxidative stress [2]. The oxidative modifications caused by ROS are actually acknowledged as important contributors to ageing and neurodegenerative diseases, such as Parkinson's [3] and Alzheimer's syndromes [4].

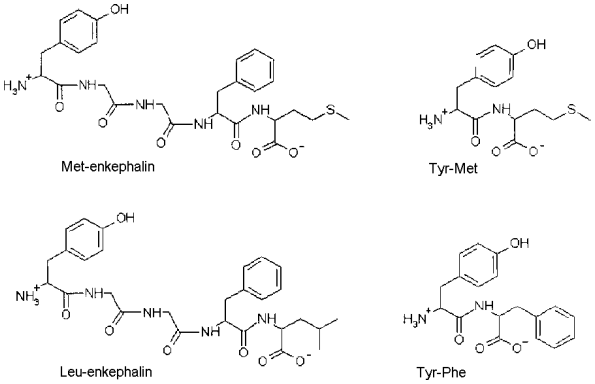

Chart 1.

Enkephalins (Chart 1), the class of opioid peptides, that bind to opiate receptors are of great interest because of their role as neurotransmitters or neuromodulators [5]. The aromatic amino acids and methionine (Met) residues are especially susceptible to oxidation in these peptides. Functional changes upon oxidation might appear to be connected with activity in the case of enkephalins, and to be of pathophysiological significance.

The main objective of our studies is to investigate the potential protective function of Met residues in enkephalins against oxidative attack, studying enkephalins with and without Met and leucine (Leu) residues. In previous report [6] we presented preliminary results of pulse radiolysis studies of Leu- and Met-enkephalins, in N_2O-saturated aqueous solutions using $^{\bullet}OH$ and $^{\bullet}N_3$ radicals as oxidants.

In this presentation we report the results of oxidation of two dipeptides (Chart 1): tyrosyl-phenylalanine (Tyr-Phe) and tyrosyl-methionine (Tyr-Met) modelling enkephalin fragments. It was of particular interest to study whether the $^{\bullet}OH$- or $^{\bullet}N_3$-induced processes would also occur during metal-catalysed oxidation by hydrogen peroxide. The study was divided into two sections. First, Tyr-Phe and Tyr-Met dipeptides were subjected to oxidation *via* a "Fenton-like" reaction [7] by hydrogen peroxide, catalysed by $[(Fe^{II})EDTA]^{2-}$ (reactions 1 and 2):

$$[(Fe^{II})EDTA]^{2-} + H_2O_2 \rightarrow [(Fe^{III})EDTA]^{-} + {}^{\bullet}OH + OH^{-} \quad (1)$$

$$^{\bullet}OH + \text{dipeptide} \rightarrow \text{oxidation products} \quad (2)$$

Subsequently, oxidation processes were induced by radiolytically produced $^{\bullet}OH$ (reactions 3-4 and 2) and $^{\bullet}N_3$ radicals (reactions 3-6):

$$H_2O \rightarrow {}^{\bullet}OH, \ , {}^{\bullet}H \quad (3)$$

$$+ N_2O + H_2O \rightarrow {}^{\bullet}OH + OH^{-} + N_2 \quad (4)$$

$$^{\bullet}OH + \rightarrow OH^{-} + {}^{\bullet} \quad (5)$$

$$^{\bullet}N_3 + \text{dipeptide} \rightarrow \text{oxidation products} \quad (6)$$

Oxidation of Tyr-Phe dipeptide by a "Fenton-like" system

Hydroxyl radicals were generated in the two "Fenton-like" systems that differ in concentration

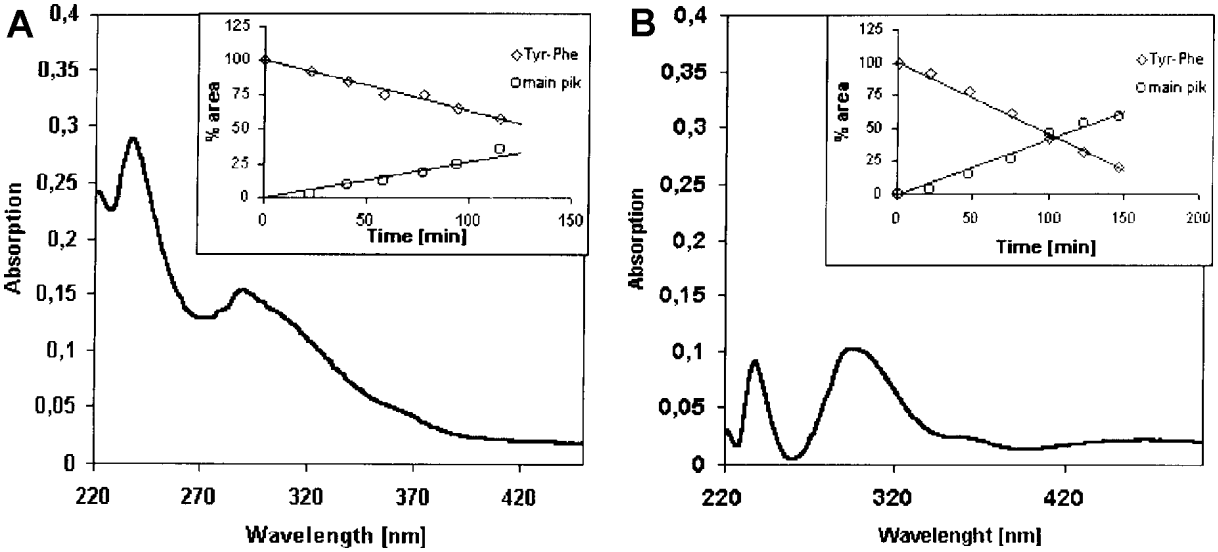

Fig.1. Absorption spectra recorded during oxidation of Tyr-Phe (0.05 mM) by a "Fenton-like" systems containing 10 mM K-phosphate (pH 7.0) and: (A) 0.1 mM $(NH_4)_2Fe^{II}(SO_4)_2$, 0.1 mM EDTA and 2.5 mM H_2O_2 after 210 min of incubation; (B) 0.25 mM $(NH_4)_2Fe^{II}(SO_4)_2$, 0.25 mM EDTA and 2.5 mM H_2O_2 after 60 min of incubation. Blank cuvettes contained all reagents except H_2O_2. Insets: Concentration *vs.* time profiles for the decay of Tyr-Phe and for the formation of the main product obtained by capillary electrophoresis.

ratio of $[(Fe^{II})EDTA]^{2-}$ complex and H_2O_2. In the first system concentrations of $[(Fe^{II})EDTA]^{2-}$ complex and H_2O_2 were equal to 0.1 and 2.5 mM, respectively, in the second system concentrations of $[(Fe^{II})EDTA]^{2-}$ complex and H_2O_2 were equal to 0.25 mM. Differences in the concentration ratios were reflected in the rate of H_2O_2 consumption: 0.0015 mM s^{-1} in the first system *vs.* 0.002 mM s^{-1} in the second system. In order to determine the oxidation products, a course of the reaction of Tyr-Phe with hydroxyl radicals was monitored spectrophotometrically. The absorption spectra observed after 210 min (Fig.1A) and 60 min (Fig.1B) of incubation are characterised by a distinct absorption band with λ_{max}=235 nm, a broader band with λ_{max}=290 nm, and a shoulder around 360-370 nm. In both systems containing 0.05 mM Tyr-Phe increase in the absorbance around 235 and 290 nm *vs.* incubation time was observed. The consumption of Tyr-Phe dipeptide and the formation of one of the oxidation products was monitored by capillary electrophoresis based on the peak area (insets in Figs.1A and B). Formation of dityrosine (excitation at λ=325 nm, emission at λ_{max}=418 nm) (Fig.2) and an unidentified oxidation product (excitation at λ=400 nm, emission at λ_{max}=490 nm) was observed employing fluorescence detection. In both "Fenton-like" systems the intensity of fluorescence monitored at λ=418 nm increases with incubation time, however, with different rate and characteristics pattern (inset in Fig.2).

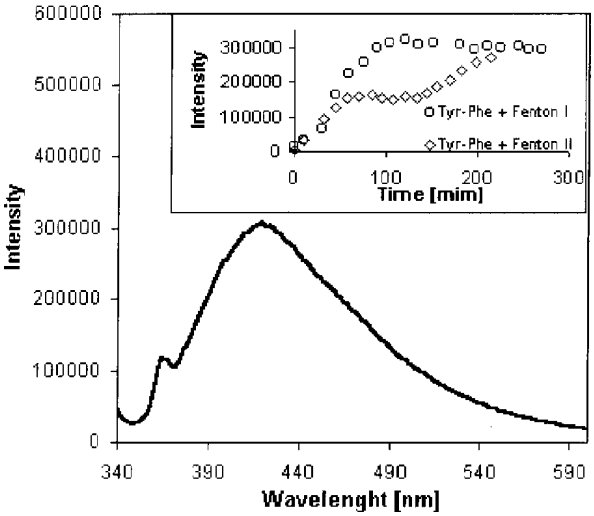

Fig.2. Fluorescent spectrum (excitation at λ=325 nm) recorded after 210 min of incubation in Tyr-Phe by a "Fenton-like" system containing 0.1 mM $(NH_4)_2Fe^{II}(SO_4)_2$, 0.1 mM EDTA, 2.5 mM H_2O_2, and 10 mM K-phosphate (pH 7.0). Blank cuvettes contained all reagents except H_2O_2. Inset: intensity of fluorescence *vs.* time profile measured at λ=418 nm in two "Fenton-like" systems (see text).

Oxidation of Tyr-Phe dipeptide by radiolytically produced $^{\bullet}OH$ and $^{\bullet}N_3$ radicals

There are no significant differences between the absorption spectra observed in the "Fenton-like" systems (Fig.1) and in the system-containing radiolytically produced $^{\bullet}OH$ radicals (Fig.3A). This becomes particularly evident from the comparison of the location of the respective absorption maxima. Absorption spectrum recorded in the solution containing 0.5 mM Tyr-Phe after irradiation with the dose of 81 Gy is characterized by two bands with λ_{max}=235 and 290 nm and two broad shoulders around 320 and 360 nm. The intensities of these bands depend linearly on the dose (inset in Fig.3A). A piece of evidence for the formation of dityrosine and the same unidentified product observed previously in the "Fenton-like" system was obtained: fluorescence detection shows the same emission spectra (λ_{max}=418 and 490 nm), applying the same excitation wavelengths, 325 and 400 nm, respectively.

For comparison, the UV-VIS spectrum observed in the system-containing radiolytically produced $^{\bullet}N_3$ radicals is presented (Fig.3B). It shows much more distinct absorption bands with λ_{max}=235 and 290 nm and a more distinct shoulder around 320 nm. However, it does not show a broad shoulder around 360 nm. This may indicate that certain amounts of OH-adducts to the aromatic rings of tyrosine and phenylalanine participate in the oxidation process.

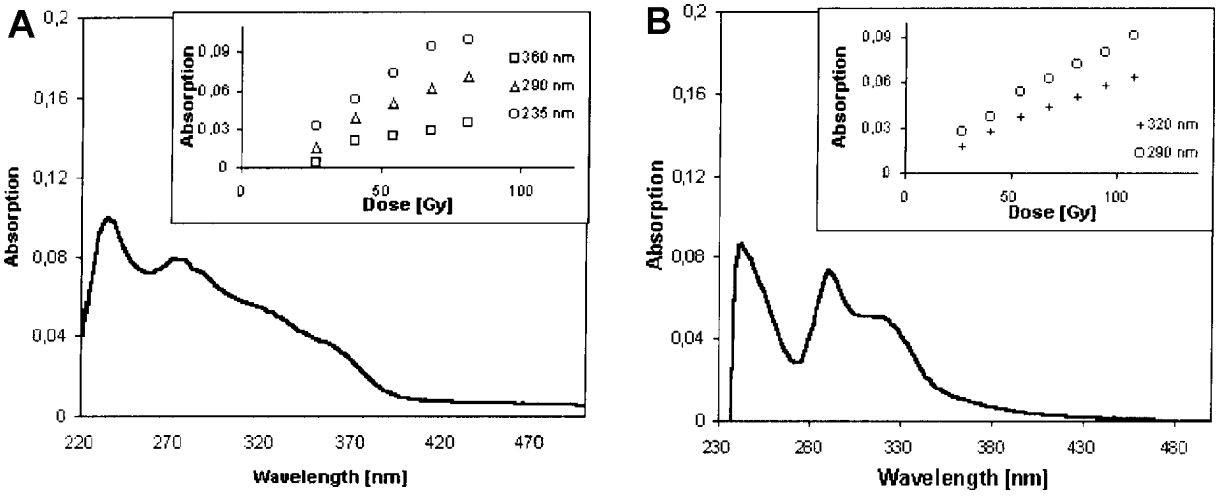

Fig.3. Absorption spectra recorded after γ-irradiation with a dose of 81 Gy in N_2O-saturated aqueous solutions containing 10 mM K-phosphate (pH 7.0) and: (A) Tyr-Phe, 0.5 mM; (B) Tyr-Phe, 0.5 mM, and NaN_3, 10 mM. Insets: Absorption *vs.* dose profiles measured at selected wavelenghts: (A) (o) 235 nm, (Δ) 290 nm, and (□) 360 nm; (B) (Δ) 290 nm, and (+) 360 nm. Blank cuvettes were not irradiated.

Oxidation of Tyr-Met dipeptide by a "Fenton-like" system

When the C-terminal Phe residue is substituted by Met, the absorption spectrum of the solution observed after 400 min of incubation does not change drastically. It shows again two absorption bands with λ_{max}=235 and 290 nm, however, does not show a shoulder in the region 360-370 nm (Fig.4A). This difference observed for the oxidation of Tyr-Phe and Tyr-Met might be caused by the contribution of the oxidation product of the phenylalanine residue in the Tyr-Phe system. An increase in the absorbance around 235 and 290 nm *vs.* incubation time was observed in the Tyr-Met system (inset in Fig.4A), however slower than analogous increase observed in the similar "Fenton-like" system containing Tyr-Phe. Fluorescent spectra using excitation at two wavelengths (325 and 400 nm) confirms again a presence of dityrosine (Fig.4B) and the same unidentified product that was observed in Tyr-Phe system. This implies that the formation of the product involves the primary oxidation of the tyrosine residue. The intensity of fluorescence monitored at λ=418 nm increases with incubation time, however, with different rate and characteristics pattern (inset in Fig.4B) in comparison to the Tyr-Phe systems (inset in Fig.2).

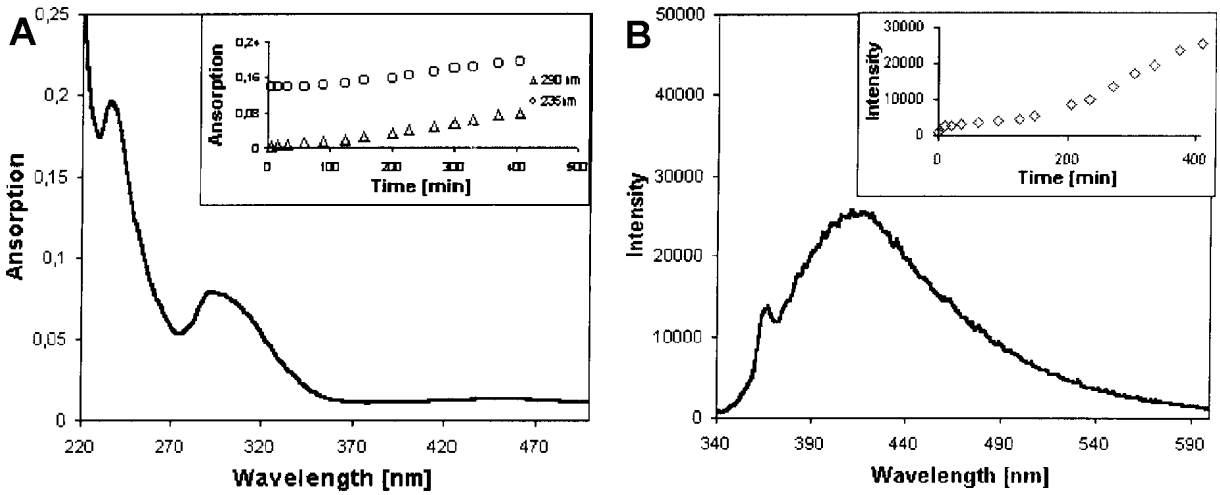

Fig.4. (A) Absorption spectrum recorded during oxidation of Tyr-Met (0.05 mM) by a "Fenton-like" systems containing 0.1 mM $(NH_4)_2Fe^{II}(SO_4)_2$, 0.1 mM EDTA, 2.5 mM H_2O_2, and 10 mM K-phosphate (pH 7.0) after 400 min of incubation. (B) Fluorescent spectrum (excitation at λ=325 nm) recorded after 400 min of incubation in Tyr-Met (0.05 mM) by a "Fenton-like" system containing 0.1 mM $(NH_4)_2Fe^{II}(SO_4)_2$, 0.1 mM EDTA, 2.5 mM H_2O_2, and 10 mM K-phosphate (pH 7.0). Blank cuvettes contained all reagents except H_2O_2. Inset: intensity of fluorescence *vs.* time profile measured at λ=418 nm.

Oxidation of Tyr-Met dipeptide by radiolytically produced $^{\bullet}OH$ and $^{\bullet}N_3$ radicals

There are no significant differences between the absorption spectra observed in the "Fenton-like" system (Fig.4A) and in the system-containing radiolytically produced $^{\bullet}OH$ radicals (Fig.5A). It is apparent, that the location of the respective absorption maxima are the same. Absorption spectrum recorded in the solution containing 0.5 mM Tyr-Met after irradiation with the dose of 81 Gy is characterized by two bands with λ_{max}=235 and 290 nm and a distinct shoulder around 320 nm. The

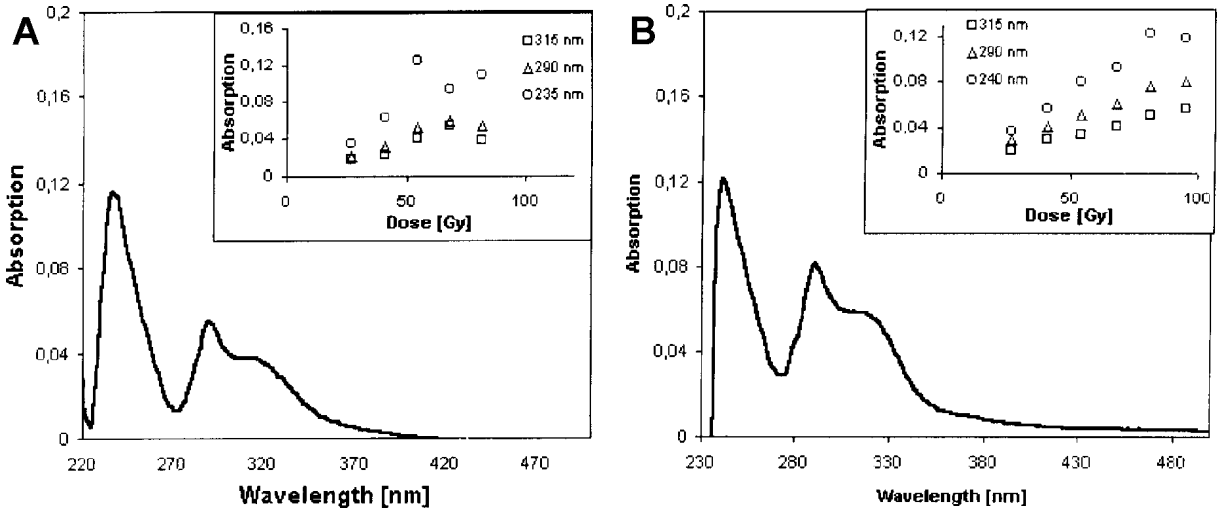

Fig.5. Absorption spectra recorded after γ-irradiation with a dose of 81 Gy in N_2O-saturated aqueous solutions containing 10 mM K-phosphate (pH 7.0) and: (A) Tyr-Met, 0.5 mM; (B) Tyr-Met, 0.5 mM, and NaN_3, 10 mM. Insets: Absorption *vs.* dose profiles measured at selected wavelenghts: (A) (o) 240 nm, (Δ) 290 nm, and (□) 315 nm; (B) (o) 235 nm, (Δ) 290 nm, and (□) 315 nm. Blank cuvettes were not irradiated.

intensities of the absorption measured at the maxima of these bands depend again linearly on the dose (inset in Fig.5A)

For comparison, the UV-VIS spectrum observed in the system-containing radiolytically produced $^{\bullet}N_3$ radicals after irradiation with the dose of 81 Gy is presented (Fig.5B). It shows two absorption bands with λ_{max}=235 and 290 nm and a distinct shoulder around 320 nm, albeit the intensity of the absorption measured in the region 260 and 350 nm is lower, in comparison to the system-containing radiolytically produced $^{\bullet}OH$ radicals (Fig.5A).

Further studies are now in progress with model peptides of defined primary structure in order to characterise the influence of amino acid residues on the pattern of transient and final products formed during chemical and radiation-induced oxidation.

This work described herein was partly supported by the European Commission (Marie Curie Host Fellowship HPMT-CT-2000-00023 for G. Kciuk).

References

[1]. Davies M.J., Dean R.T.: Radical-mediated protein oxidation. From Chemistry to Medicine. Oxford University Press, Oxford 1997.
[2]. Stadtman E.: In: Free Radicals, Oxidative Stress, and Antioxidants. Ed. T. Özben. Plenum Press, New York 1998, pp.131-143.
[3]. Adams J.D., Odunze I.N.: Free Radical Biol. Med., 10, 161-169 (1991).
[4]. Markersbery W.R.: Free Radical Biol. Med., 23, 134-147 (1997).
[5]. Enkephalins and Endorphins. Stress and the Immune System. Eds. N.P. Plotnikoff, R.E. Faith, A.J. Murgo, R.A. Good. Plenum Press, New York and London 1986.
[6]. Kciuk G., Mirkowski J., Bobrowski K.: In: INCT Annual Report 2001. Institute of Nuclear Chemistry and Technology, Warszawa 2002, pp.23-24.
[7]. Borg D.C.: In: Oxygen Free Radicals in Tissue Damage. Eds. M. Tarr, F. Samson. Birkhäuser, Boston 1993, pp.12-53.

EFFECT OF Fe(II)/EDTA COMPLEX ON DNA DAMAGE

Hanna B. Ambroż, Ewa M. Kornacka, Grażyna Przybytniak

We present studies of the influence of ferrous ion on DNA damage as examined by gel electrophoresis using plasmid DNA for estimation of single strand breaks (ssb) and double strand breaks (dsb). The plasmid form of DNA is very informative because it allows to separate by electrophoresis undamaged molecules (supercoiled, Form I), singly--damaged molecules together with multi-singly broken (ssb, circular Form II) and doubly broken (dsb, linear Form III). The metal ions are important as they are present in cell nuclei and play crucial roles in the biochemistry of oxygen. Despite the enormous amount of work done in this field, some mechanisms are still considered controversial.

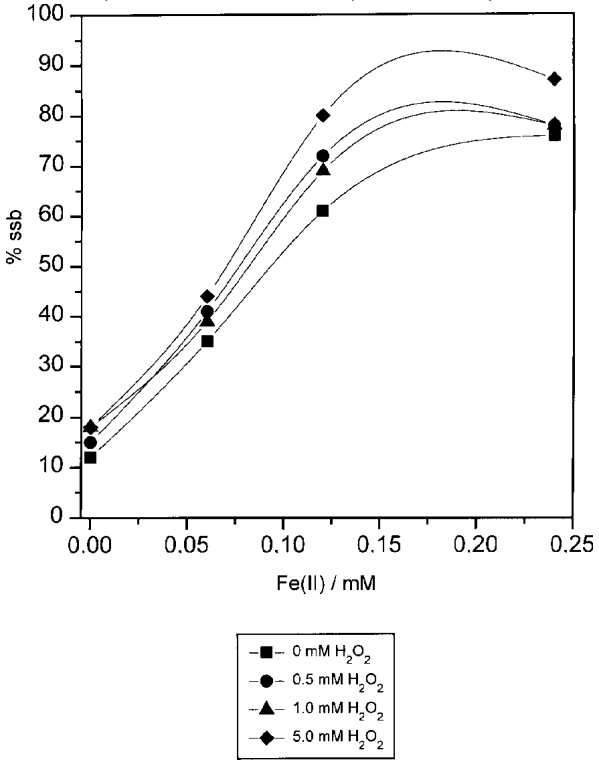

Fig.1. Effect of Fe(II) on strand breakage at various concentrations of H_2O_2 at room temperature.

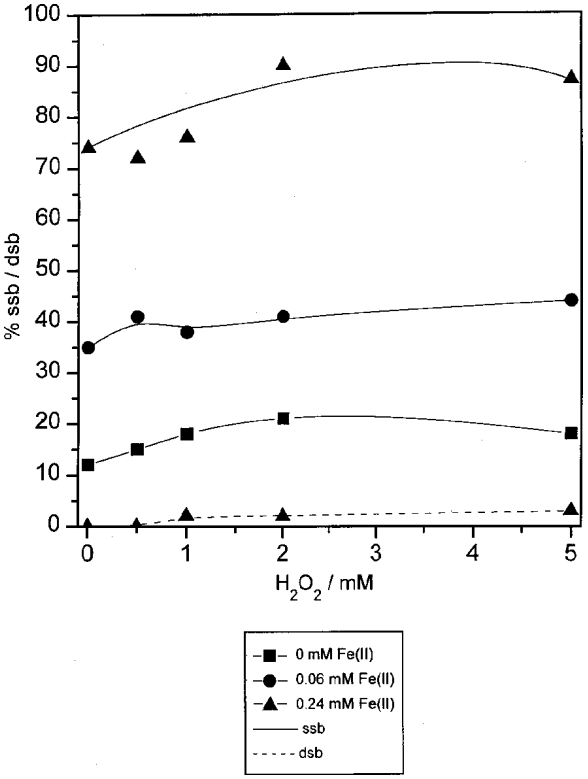

Fig.2. Effect of H_2O_2 on strand breakage at various concentrations of Fe(II) at room temperature.

These experiments were performed to elucidate some aspects of the influence of Fe(II) ions on dam-

age to DNA in the absence of ionising radiation. Low concentrations of iron (up to 0.24 mM) and a large excess of hydrogen peroxide (up to 5 mM) were applied to follow Fenton-type reactions. Under our conditions a very strong influence of Fe(II) in enhancing ssb can be observed and a limited effect of the added hydrogen peroxide even at high concentration (Figs.1 and 2). At ca. 0.15 mM concentration, Fe(II) generates over 50% singly broken form of plasmid under the applied conditions. No dsb was observed even when almost no supercoiled form of the plasmid was left. The effect of an increased amount of H_2O_2 is not very appreciable: it is stronger at low concentration and seems to saturate at 2 mM, indicating an inhibition of the catalytic reaction.

EDTA, which is present in the system as a component of buffer (pH=6.8), coordinates Fe(II) *via* oxygen and nitrogen atoms to form water-soluble complex, preventing precipitation of iron as polynuclear ferric oxidohydroxides. Fe(II)/EDTA inhibits or stimulates oxidation reactions, depending on the molar ratio Fe:EDTA, pH or even on the methods of preparation of the complex [1]. Despite its complex nature, EDTA is considered to promote the aerial oxidation of Fe(II) to Fe(III) at neutral pH [2] with simultaneous formation of reactive oxygen species. Therefore, the mechanism of Fe(II) damage to DNA involves reaction with oxygen dissolved in aqueous solution. Some authors postulate that the reduced iron slowly reacts with oxygen to form a superoxide radical in the reversible process [3]:

Superoxide radical undergoes further fast reactions to form a hydroxyl radical and then the Fenton reaction can proceed:

According to this mechanism, the reactive oxygen species produced are able to break the DNA backbone *via* degradation of, e.g. the sugar moiety. It is generally accepted that ferrous ion can form a complex with EDTA and 1 molecule of H_2O, H_2O_2 or O_2 as EDTA is hexadentate and in the Fe(II)/EDTA complex there is a free coordination site. In such a system the damage to biomolecules can proceeds *via* sequence of reaction in which chelator plays an important role. On the basis of our results we conclude, that the Fe(II)/EDTA/O_2 system facilitates the formation of strand breakage and presence of H_2O_2 is not necessary to initiate damaging processes.

References

[1] Symons M.C.R., Gutteridge J.M.C.: Free radicals and iron: chemistry, biology and medicine. Oxford University Press, 1998.
[2]. Höbel B., von Sonntag C.: J. Chem. Soc., Perkin Trans., 2, 509-513 (1998).
[3]. Harllwell B., Gutteridge J.M.C.: Free radicals in biology and medicine. Oxford University Press, 1989.

INTERACTION BETWEEN FERROUS ION AND DNA AS SEEN BY CD AND LD SPECTROSCOPY

Hanna B. Ambroż, Terence J. Kemp[1/], Grażyna Przybytniak

[1/] University of Warwick, Coventry, Great Britain

The role of the two oxidation states of iron ions in modifying the response of DNA to ionising radiation depends not only on their contrasting redox character but also on their differing abilities to induce major conformational change to the helix. Circular dichroism (CD) and linear dichroism (LD) studies presented here reveal that Fe(II) exercises minor stereochemical effects compared with Fe(III). The effects have significant consequences for the electron transfer pathway.

The CD spectra reveal that the interaction of $FeCl_2$ with DNA is very weak (Fig.1A). The changes in conformation are negligible even at concentrations of 400 μM $FeCl_2$ (i.e. Fe(II): nucleotide = 4:1). At such high concentration of ferrous chloride, the pH of the solution decreases to 5.6. Apparently, the acidity alone does not cause distinct structural perturbation of DNA. For aerated samples containing EDTA (Fig.1B) the Fe(II)/EDTA complex is oxidised to Fe(III)/EDTA in the course of seconds [1]. The intensities of all peaks are lower but much less so than observed in the case when Fe(III) is directly added to the system [2]. Figure 1C shows LD signals of DNA on addition of $FeCl_2$. The gradual loss of the signal reflects progressive reduction in DNA orientation; again the behaviour of the system with ferrous ions is very different from that observed with ferric ions.

The results give evidence that the effect of Fe(II) on the DNA helix is relatively weak. The CD spectra preserve almost the same shape and intensity even at significant concentrations, which suggest that under the applied conditions Fe(II) is bound rather to the phosphate residues. The reduction of the LD peaks confirms this conclusion. The intensity of the LD spectra decreases with increasing ferrous ion concentration, indicating a loss of DNA orientation, but not of local helicity because the CD signals remain unchanged. We believe that the differences between the interactions of Fe(III) and Fe(II) with DNA originate mainly from their different behavior on hydrolysis, i.e. that different species are available in both cases. In neutral solutions $[Fe(H_2O)_6]^{2+}$ barely undergoes deprotonation as the pK of its first stage is probably above 7 (there are big discrepancies among various authors, who mostly place the pK value in the region 7-9.5 [e.g. 3].

EDTA efficiently inhibits the interaction of DNA with Fe(II) due to fast complexation and oxida-

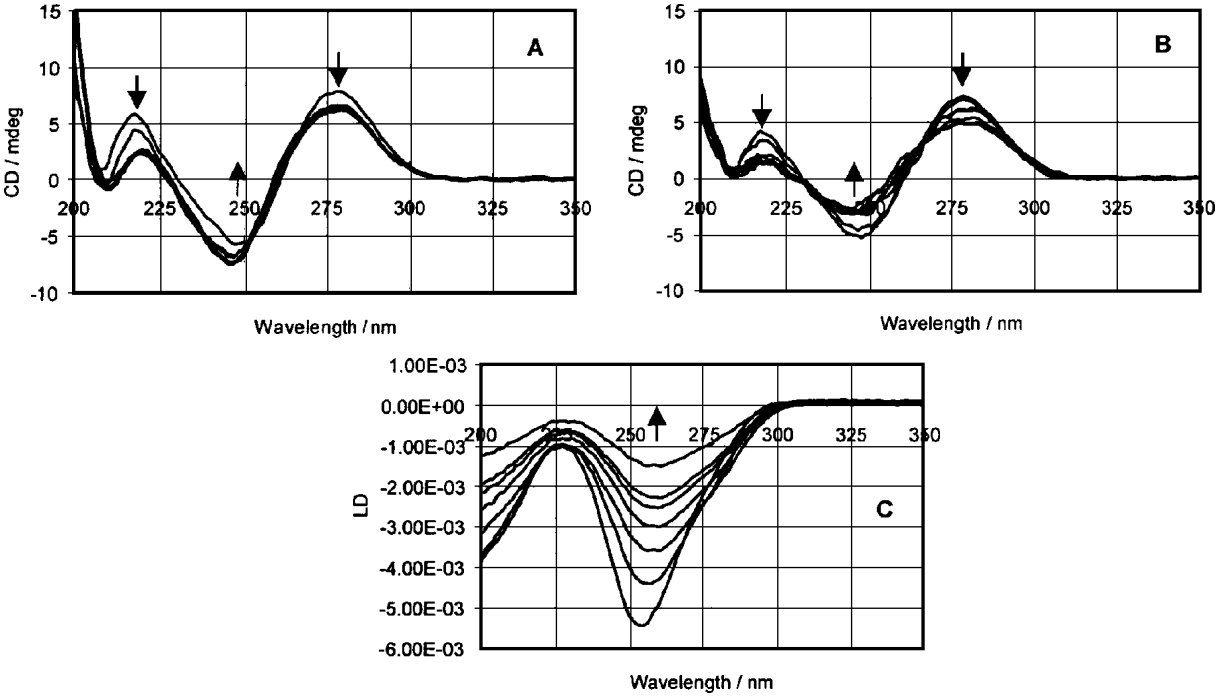

Fig.1. CD spectra of DNA in aqueous solutions (100 μM DNA). Panel A: CD spectra in presence of 0, 50, 100, 200, 400 μM $FeCl_2$. Panel B: as in panel A in presence of 50 μM EDTA. Panel C: LD spectra in presence of 0, 25, 50, 75, 100, 200 and 400 μM $FeCl_2$.

tion of ferrous to ferric ions. The Fe(II)/EDTA complex possesses a relatively low redox potential (+0.12 V) [4]. In addition, the EDTA chelator is insufficiently large to prevent the iron complex from achieving direct access to oxygen. If the ratio of [Fe(II)]:[EDTA] is higher than 1, then "free ferrous ions" are either in bulk solution or bound to DNA electrostatically. Oxidised ferrous ion in the complex with EDTA destabilises the helix, lowering all bands as in the case when ferric ions are added to the DNA and EDTA solution directly. On the other hand, it seems that double helix is stabilised by Fe(II). This is attributed not only to the charge difference but also to the site of binding of the ions: Fe(III) is probably ligated to base nitrogen atoms while Fe(II) is localised at the backbone.

References

[1]. Lambeth D.O., Ericson G.R., Yorek M.A., Ray P.D.: Biochim. Biophys. Acta, 719, 501-508 (1982).
[2]. Ambroż H.B., Kemp T.J., Rodger A., Przybytniak G.: will be published.
[3]. Comprehensive inorganic chemistry. Vol. 3. Eds. J.C. Bailar, H.J. Emeleus, R. Nyholm, A.F. Trotman-Dickenson. Pergamon Press, 1973.
[4]. Basolo F., Johson R.C.: Coordination Chemistry. W.A. Benjamin, INC, 1968.

INTERACTION OF SILVER ATOMS WITH ETHYLENE IN Ag-SAPO-11 MOLECULAR SIEVE

Marek Danilczuk, Dariusz Pogocki, Jacek Michalik

Investigations of the interaction between metal cations or small metal clusters and adsorbed molecules are essential to understand the mechanism of catalytic reactions on metal active sites. Atoms or metal clusters formed by metal sublimation or irradiation of metal cations under vacuum are much more reactive than in bulk forms and can form many complexes with different ligands. The interaction of silver, cooper or nickel with ethylene in a matrix of inert gases under cryogenic conditions has been studied by different techniques for many years. Metals from 1B group have unpaired electron and their complexes show visible adsorption bands. IR and VIS optical studies together with Raman spectroscopy have been successfully used to study the structure of $Ni(C_2H_4)_n$ and $Cu(C_2H_4)_n$ complexes [1-5].

The formation of silver-ethylene complex in inert gas matrixes has been also reported earlier. Based on the electron paramagnetic resonance (EPR) results, Kasai [6-9] proposed the formation of $Ag(C_2H_4)_n$, n=(1,2) complexes in an argon matrix. Howard [10] identified mononuclear-ethylene complexes $Ag(C_2H_4)$ and $Ag(C_2H_4)_2$ and cluster--ethylene complexes $Ag_3(C_2H_4)$ and $Ag_7(C_2H_4)_n$, where $n \geq 1$ in hydrocarbon matrices at 77 K.

Zeolites containing different transition metals have attracted a lot of interest because of their chemical and electronic properties and catalytic activity in many chemical reactions. They have unique properties to stabilize cationic metal clusters and metal nanoparticles produced radiolytically or by hydrogen reduction. Because the clusters are highly dispersed, the product selectivity of cata-

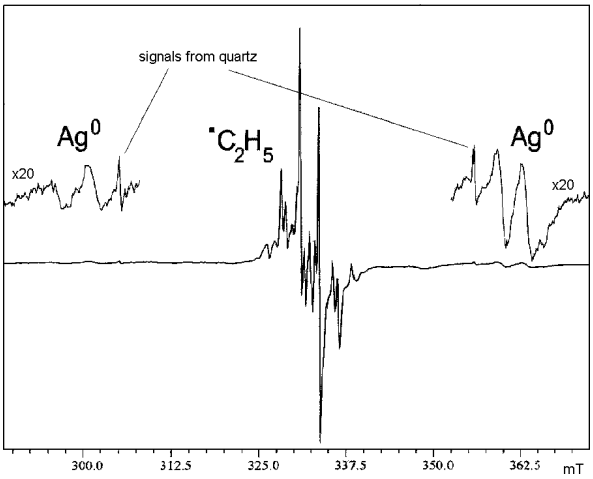

Fig.1. EPR spectrum at 110 K of gamma-irradiated Ag-SAPO-11 exposed to 5 Torr of C_2H_4.

lytic reactions can be better controlled. The chemical properties of silver exchanged zeolites have been studied by numerous experimental techniques.

The SAPO-11 molecular sieve in protonated form was synthesized by the Loke's methods [11] and ion-exchanged with $AgNO_3$ water solution at room temperature for 24 h in the dark. The zeolite powder was then repeatedly washed with distilled water to remove the excess of silver and air--dried subsequently. The ethylene of 99.0% purity was purchased from Aldrich Chemical Co. and was used without further purification.

The Ag-SAPO-11 zeolite placed into Suprasil EPR tubes equipped with stopcocks was gradually

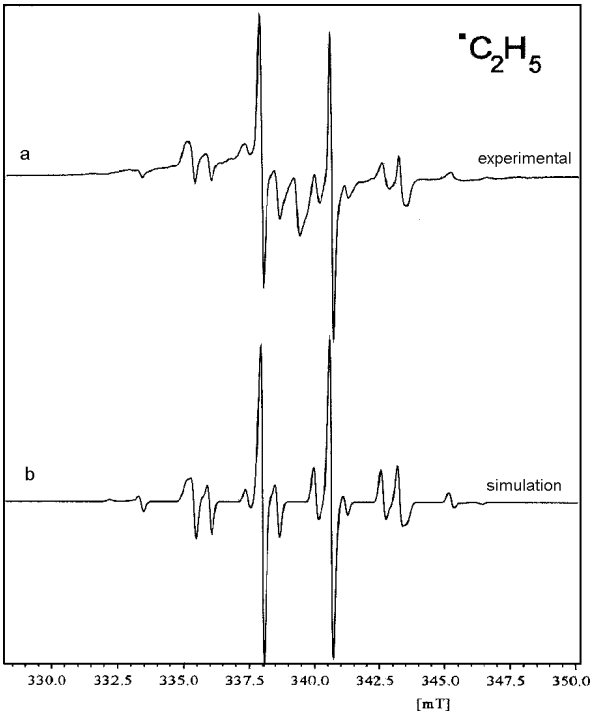

Fig.2. Experimental (a) and simulated (b) EPR spectra of C_2H_5 radical trapped inside SAPO-11 channels. T=210 K.

dehydrated *in vacuo* raising the temperature till 200°C for 2 h. Then, the samples were oxidized under a pressure of 600 Torr at 300°C for 3 h. Thereafter, oxygen was pumped off at the same temperature for 3 h. Ethylene was adsorbed at room temperature under a pressure of 3 Torr for 24 h. Finally, the samples were irradiated in a ^{60}Co-source at the liquid nitrogen temperature (77 K) with a dose of 5 kGy.

The EPR spectra were recorded with an X-band Bruker ESP 300E spectrometer equipped with a liquid nitrogen cryostat. Variable temperature unit controlled the temperature of the sample in the range 100-310 K.

SAPO-11 molecular sieve consists of 4-ring, 6-ring and 10-ring channels. 10-ring channel has elliptical shape with a size of 6.4x4.0 Å. The framework negative charges after calcination are balanced by protons which can be easily exchanged by different cations.

The EPR spectrum of gamma-irradiated Ag-SAPO-11/C_2H_4 molecular sieve recorded at 110 K is shown in Fig.1. It consist of two sets of lines-intensive multiplet at g=2.0023 region representing ethyl radicals and two doublets of silver atoms: ^{107}Ag: A_{iso}=57.9 mT and ^{109}Ag: A_{iso}=66.9 mT. Similar hyperfine splittings were reported for silver atoms trapped in inert gas matrices [12, 13]. On thermal annealing above 210 K, the Ag^0 doublets

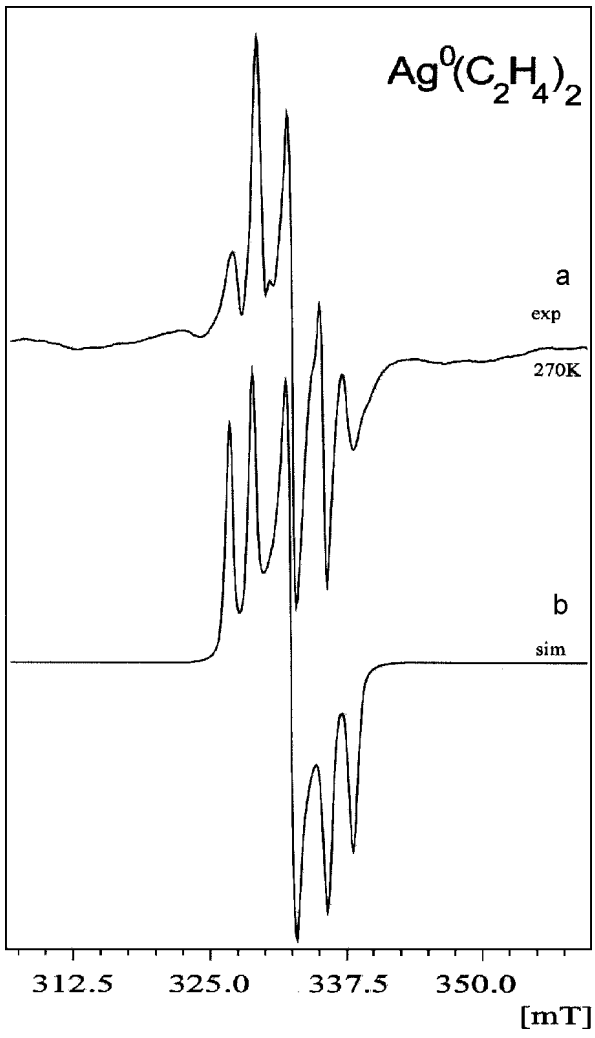

Fig.3. Experimental (a) and simulated (b) EPR spectra of $Ag^0(C_2H_4)_2$ complex formed in SAPO-11 above 230 K.

decay completely without any indication of the formation of EPR signal representing paramagnetic silver clusters.

During radiolysis of liquid ethylene or ethylene adsorbed on solid surface ethyl radicals are formed by hydrogen atoms addition to C_2H_4 molecules. The EPR spectra of $^{\bullet}C_2H_5$ radicals in liquid ethylene as well as of radicals adsorbed on solids are known [13-15]. The experimental spectrum at 210 K of ethyl radical in dehydrated Ag-SAPO-11/C_2H_4 is shown with field expanded scale in Fig.2a. This spectrum was successfully simulated with the following parameters: Ag (α)=2.01 mT, $A_{||}(\alpha)$=2.87 mT for α-protons and Ag (β)=2.68 mT, $A_{||}(\beta)$=2.80 mT for β-protons of methyl group and g=2.0023 (Fig.2b). The singlet in the center of the experimental spectrum represents radiation-induced paramagnetic centers in zeolite framework. The profiles of the outermost lines show the axial symmetry typical for the anisotropy of hyperfine interactions in solids. This indicates that the ethyl radicals being trapped in the molecular sieve channels are unable to rotate freely. It should be stressed that in contrast to radiolysis of liquid ethylene, the EPR spectra of vinyl radicals are not recorded.

At 230 K the $^{\bullet}C_2H_5$ spectrum decays completely and then the EPR signal associated with the $Ag^0(C_2H_4)_2$ complex is clearly seen (Fig.3a). This signal was simulated (Fig.3b) using the following EPR parameters:

1Ag: g_x=2.004, g_y=1.977, g_z=2.033
A_x=0.9 mT, A_y=2.34 mT, A_z=2.19 mT
8H: A_{iso}=0.3 mT

which are similar to the parameters of $Ag^0(C_2H_4)_2$ complexes formed in argon and neon matrices. It was proven based on theoretical calculations [16] that the diligand silver-ethylene complex has a symmetric D_{2n} geometry where the ligands located at the opposite sites of Ag^0 adopt an eclipsed parallel conformation.

In irradiated Ag-SAPO-11 molecular sieve exposed to ethylene, the $Ag^0(C_2H_4)_2$ complex is formed upon annealing above 230 K. The unusual stability of this complex at room temperature is related to the fact that it is trapped inside SAPO-11 channels. Although the stoichiometry of this complex was not unequivocally proved by EPR simulations there is a little doubt that it is a reactive catalytic intermediate which promotes further reactions of ethylene molecules.

References

[1]. Buck A.J., Mille B., Howard J.A.: J. Am. Chem. Soc., 105, 3381-3387 (1983).
[2]. Hubner H., Ozin G.A., Power W.J.: J. Am. Chem. Soc., 98, 6508-6511 (1976).
[3]. Pitzer R.M., Schaefer III H.F.: J. Am. Chem. Soc., 101, 7176-7183 (1979).
[4]. Kasai P.H., McLeod D.: J. Am. Chem. Soc., 100, 625-627 (1978).
[5]. Ozin G.A., Huber H., McIntosh D.: Inorg. Chem., 16, 3070-3078 (1977).
[6]. Kasai P.H., McLeod D., Jr.: J. Am. Chem. Soc., 97, 6602-6603 (1975).
[7]. Kasai P.H.: J. Phys. Chem., 86, 3684-3686 (1982).
[8]. Kasai P.H.: J. Am. Chem. Soc., 106, 3069-3075 (1984).
[9]. Kasai P.H., Mcleod D., Jr., Watanabe T.: J. Am. Chem. Soc., 102, 179-190 (1980).
[10]. Lok B.M., Messina C.A., Patton R.L., Gajek R.T., Cannan T.R., Flanigen E.M.: U.S. Patent 4440 871.
[11]. Howard J.A., Joly H.A., Mile B.: J. Phys. Chem, 94, 1275-1279 (1990).
[12]. Kasai P.H., McLeod D., Jr.: J. Chem. Phys., 55, 1566-1568 (1971).
[13]. Fessenden R.W., Schuler R.H.: J. Chem. Phys., 39, 2147-2195 (1963).
[14]. Fessenden R.W.: J. Phys. Chem., 71, 74-83 (1967).
[15]. Shiga T., Lund A.: J. Phys. Chem., 77, 453-455 (1973).
[16]. Pogocki D., Danilczuk M.: In: INCT Annual Report 2002. Institute of Nuclear Chemistry and Technology, Warszawa 2003, pp.37-39.

SILVER ATOM-ETHYLENE MOLECULAR COMPLEXES. A DENSITY FUNCTIONAL THEORY STUDY

Dariusz Pogocki, Marek Danilczuk

In this report, we communicate the results of density functional theory (DFT) calculations of the structure, electronic composition and electron spin resonance (ESR) coupling constants of Ag atom-ethylene complexes: $Ag(C_2H_4)$, $Ag(C_2H_4)_2$.

The initial conformational space scan of $Ag(C_2H_4)$ and $Ag(C_2H_4)_2$ complexes were carried out in "gas-phase" with B3LYP hybrid functional [1] and the LANL2DZ basis sets with effective core potential (ECP) from the 28-electron Ag core, designed by Hay and Wadt [2]. Then, the structures of complexes were fully optimized in the vicinity of respective C_{2v} and D_{2h} symmetry structures, using the analytical gradient technique with the DZVP all electron basis sets of Godbout and Andzelm [3]. The nature of each located stationary point was checked by evaluating harmonic frequencies. The theoretical estimates of the hyperfine coupling constants were obtained in single point calculations at the B3LYP/DZVP level calculated geometries (from here on referred to as $\Re$-level). Due to the lack of freely available "properties basis sets" [4] adequately describing the spin-spin coupling for Ag, calculating the hyperfine coupling constants we employed basis sets of increased flexibility in the core region. The DGauss A1 DFT Coulomb Fitting basis sets of Godbout and Andzelm [3] (from here on referred to as A1CF) was applied for Ag, while, the EPR-III basis sets of Barone [5] was applied for the organic ligands. The nature of bonding we studied with natural bond orbital analysis (NBO) [6, 7]. All DFT calculations were performed with the Gaussian'98 suite of programs [8], employing computational resources of the University of Linköping, Sweden. The basis sets were obtained from the EMSL Basis Set Library

provided by the Pacific Northwestern Laboratory, USA [9].

Table 1. The ℜ-level calculated bond lengths (r [Å]), bond order (BO), the H-bending angle ([°]).

	Symmetry	$r_{(Ag-C)}$/BO	$r_{(C=C)}$/BO	$r_{(C=H)}$/BO	$\angle_{(H-Et)}$
C_2H_4	D_{2h}	-	1.337/2.148	1.088/0.922	0
$Ag(C_2H_4)$	C_{2v}	3.599/0.103	1.339/2.056	1.088/0.917	0.19
$Ag(C_2H_4)_2$	D_{2h}	2.317/0.326	1.406/1.642	1.088/0.895	9.46

Basic properties of silver-ethylene complexes obtained in the calculations are submitted to Tables 1 and 2. All obtained results seems in line with previous notions [10-14] originated from the model of π-complexation proposed by Dewar [15] to explain the π-coordinated metal-olefin complexes. However, our calculations suggest a slightly different reason of relative instability of $Ag(C_2H_4)$ complex than previously proposed by Kasai and coworkers [10]. Based on EHT (extended Hückel theory) calculation, they implied that Ag is not able to form a *bona fide* complex with one C_2H_4 molecule, since the separation between Ag(5*s*) one-electron donor orbital and the bonding π orbital of ethylene as well as between Ag($4d_{xy}$) the π* orbital is too large to form an effective dative bond. On the other hand, Cu may form a $Cu(C_2H_4)$ complex since the energy separation between Cu($3d_{xy}$) the π* is small enough to permit an effective dative Cu($3d_{xy}$) to π* interaction [10]. Consequently, the formation of the weakly bonded pseudocomplex $Ag\cdots C_2H_4$, that has been observed in the matrix spectroscopic studies [10, 16], they attributed to the van der Waals type interaction prevailing in the low-temperature matrix environment.

Table 2. The Ag^{107} hyperfine coupling constants (A [mT]) calculated on the B3LYP/A1CF//ℜ and B3LYP/(A1CF+EPR-III)//ℜ (given in parenthesis) levels.

	Isotropic Fermi Contact Couplings	Anisotropic Spin Dipole Couplings		
	A_{Iso}	ΔA_{xx}	ΔA_{yy}	ΔA_{zz}
Ag^0	-84.50	-	-	-
$Ag(C_2H_4)$	-82.76 (-79.96)	-0.02 (-0.02)	0.01 (0.01)	0.01 (0.01)
$Ag(C_2H_4)_2$	2.16 (2.24)	0.23 (0.20)	-0.42 (-0.37)	0.19 (0.16)

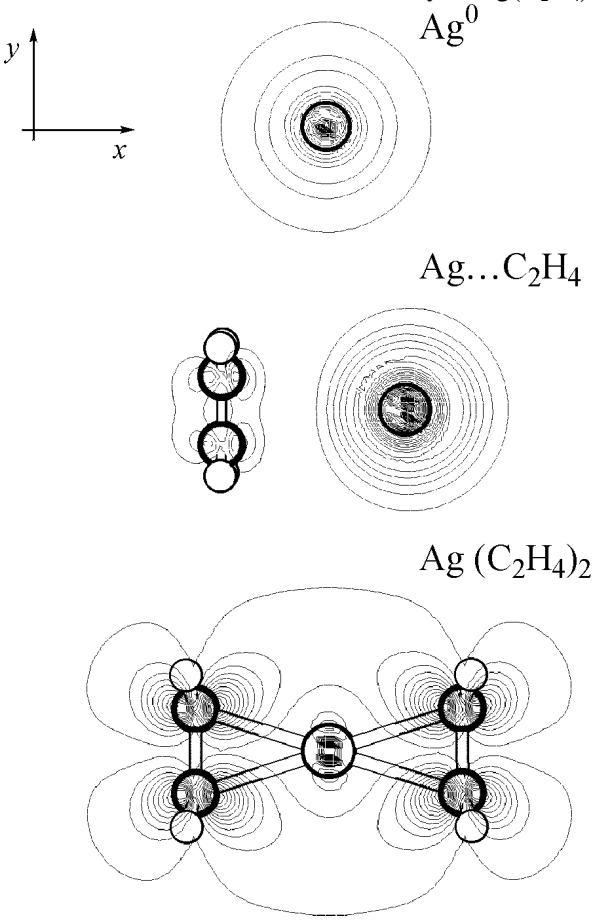

Fig.1. Two-dimensional (2D) contour plot of the B3LYP/A1CF//ℜ-level calculated total spin density in Ag^0, and $Ag(C_2H_4)$ and $Ag(C_2H_4)_2$ silver-ethylene complexes.

While in our study both Cu and Ag have a similar ability to accept the π-electron density on the valence *s* orbital, due to the similar *s* and π levels separation (3.4 and 2.5 eV, respectively). However, we observe a significant separation of Cu($3d_{xy}$) and Ag($4d_{xy}$), and the π* (*ca*. 8 and 17.6 eV, respectively), which particularly in the Ag-case prohibits an effective dative interaction. As expected, the $Ag\cdots C_2H_4$ interaction does not significantly change the geometry of ethylene ligand (Table 1). The NBO analysis shows that in $Ag\cdots C_2H_4$ *ca*. 98% of unpaired spin density remains in the 5*s* orbital on the metal, merely 2% migrates to the *p* orbital on ethylene (Fig.1). Thus, the ESR signal of such a complex should resemble that of the atomic silver (see the coupling constants in Table 2).

$[Ag(C_2H_4)_2]$: The obtained mononuclear diligand complex has a symmetric D_{2h} geometry (Fig.1) with the ligands adopting an eclipsed conformation on either side of the Ag atom. The silver-ethylene bonding occurs because of orbital overlap between the filled ligand π orbitals and sp_x-hybridized orbitals on the metal and the semifilled p_y orbital and the empty ligand π* orbitals. The formation of $Ag(C_2H_4)_2$ implies a decrease of ligands π density, and thus decrease of the order of both unsaturated bonds. The NBO analysis shows unpaired electrons distributed over the $5p_y$ orbitals of the metal (11%)

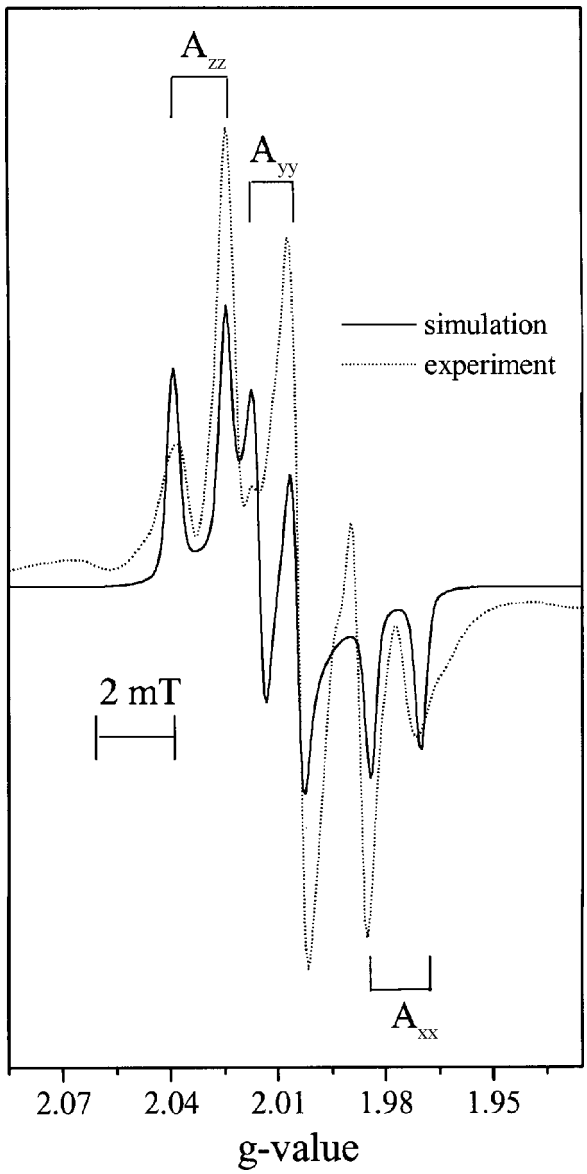

Fig.2. EPR spectrum of $Ag(C_2H_4)_2$ simulated with parameters taken from the gas-phase B3LYP/A1CF//ℜ-level calculation (solid line) compared to the experimental spectrum obtained in the ethylene saturated Ag-SAPO-11 molecular sieve (doted line) [17].

and the π*-ethylene orbitals (84%). The calculated unpaired spin flow out of the Ag atom results in accordingly lower hyperfine coupling constants (Table 2). The obtained values that are in pretty good agreement with results of the ESR experiment carried out in the ethylene saturated Ag-SAPO-11 zeolite [17]. Figure 2 shows our attempt to resolve the experimental EPR spectrum using the anisotropic hyperfine coupling obtained in the calculation.

The DFT calculations, which provide a dipper insight into the nature of paramagnetic complexes, can efficiently supplement usage of modern experimental techniques. Thus, the near future of this project is the calculation of the properties of silver-hydrocarbons complexes "encapsulated" in the molecular sieves framework. Such calculations can provide important information allowing more precise interpretation of the EPR experiment.

References

[1]. Becke A.D.: J. Chem. Phys., 98, 5648-5652 (1993).
[2]. Hay P.J., Wadt W.R.: J. Chem. Phys., 82, 270-283 (1985).
[3]. Godbout N., Salahub D.R., Andzelm J., Wimmer E.: Can. J. Chem., 70, 560-571 (1992).
[4]. Jensen F.: Introduction to Computational Chemistry. John Wiley & Sons Ltd., Chichester 1999, pp.1-429.
[5]. Rega N., Cossi M., Barone V.: J. Chem. Phys., 105, 11060-11067 (1996).
[6]. Foster J.P., Weinhold F.: J. Am. Chem. Soc., 102, 7211-7218 (1980).
[7]. Weinhold F., Landis C.R.: Chem. Educ. Res. Pract. Eur., 2, 91-104 (2001).
[8]. Frisch M.J. *et al.*: Gaussian 98. (Rev.A.7). Gaussian Inc., Pittsburgh 1998.
[9]. Pacific Northwestern Laboratory. EMSL Basis Set Library. 2002.
[10[. Kasai P.H., McLead D., Jr., Watanabe T.: J. Am. Chem. Soc., 179-190 (1980).
[11]. Kasai P.H.: J. Phys. Chem., 86, 3884-3686 (1982).
[12]. Cohen D., Bash H.J.: J. Am. Chem. Soc., 105, 6980-6982 (1983).
[13]. Howard J.A., Joly H.A., Mile B.: J. Phys. Chem., 94, 1275-1279 (1990).
[14]. Howard J.A., Joly H.A., Mile B.: J. Phys. Chem., 94, 6627-6631 (1990).
[15]. Dewar M.S.J.: Bull. Soc. Chim. Fr., 18, C71 (1951).
[16]. McIntosh D.F., Ozin G.A., Messmer R.P.: Inorg. Chem., 19, 3321-3327 (1980).
[17]. Danilczuk M., Pogocki D., Michalik J.: In: INCT Annual Report 2002. Institute of Nuclear Chemistry and Technology, Warszawa 2003, pp.35-37.

REACTION KINETICS IN THE IONIC LIQUID METHYLTRIBUTYLAMMONIUM BIS(TRIFLUOROMETHYLSULFONYL)IMIDE

Jan Grodkowski, Pedatsur Neta[1/]

[1/] Physical and Chemical Properties Division, National Institute of Standards and Technology, Gaithersburg, USA

Room-temperature ionic liquids serve as good solvents for various thermal and electrochemical reactions, are nonvolatile and nonflammable, and have been proposed as "green solvents" for various industrial processes. To understand the effects of these solvents on rates of chemical reactions, we have begun to study the rate constants for several elementary reactions in ionic liquids and to compare them with those in other solvents.

The reactions of trifluoromethyl radicals ($^{\bullet}CF_3$) with pyrene, phenanthrene, crotonic acid, and 2-propanol in the ionic liquid methyltributylammonium

bis(trifluoromethylsulfonyl)imide (R_4NNTf_2) were studied by pulse radiolysis [1]. Radiolysis of R_4NNTf_2 leads to formation of solvated electrons and organic radicals, including $^{\bullet}CF_3$. The solvated electrons do not react rapidly with the solvent and reacted with CF_3Br to produce additional $^{\bullet}CF_3$ radicals. The rate constants for addition of $^{\bullet}CF_3$ radicals to pyrene and phenanthrene are determined to be $(1.1\pm0.1)\times10^7$ and $(2.6\pm0.4)\times10^6$ L mol^{-1} s^{-1}, respectively. By competition kinetics, the rate constant for reaction of $^{\bullet}CF_3$ radicals with crotonic acid is determined to be $(2.7\pm0.4)\times10^6$ L mol^{-1} s^{-1}, and the reaction is predominantly addition to the double bond. Competition kinetics with 2-PrOH in the absence of CF_3Br gives a rate constant of $(4\pm1)\times10^4$ L mol^{-1} s^{-1} for H-abstraction from 2-PrOH, but in the presence of CF_3Br, the rate constant cannot be determined because a chain reaction develops. The rate constants for reactions of $^{\bullet}CF_3$ radicals in acetonitrile solutions are slightly higher, by a factor of 2.3 for pyrene and phenanthrene and by a factor of 1.3 for crotonic acid. The rate constant for pyrene in aqueous acetonitrile (30% water) solutions is 4 times higher than that in the ionic liquid.

More hydrogen-abstraction reactions in R_4NNTf_2 of various radicals have been studied with 4-mercaptobenzoic acid (MB) and compared to aqueous solutions [2]. The rate constants in the ionic liquid are in the range of 10^7-10^8 L mol^{-1} s^{-1} and are essentially controlled by the diffusion rate; variations within this range appear to be due mainly to changes in viscosity. The $^{\bullet}CF_3$ radical reacts slightly more slowly (3.6×10^6 L mol^{-1} s^{-1}) with MB in the ionic liquid, in agreement with the low reactivity in water of radicals bearing electron-withdrawing groups. The rate constants in aqueous solutions are in the range of $(1\text{-}3)\times10^8$ L mol^{-1} s^{-1} for the reactions of MB with several alkyl radicals, are higher with reducing radicals (6.4×10^8 L mol^{-1} s^{-1} for CH_3 HOH and 1.4×10^9 L mol^{-1} s^{-1} for $(CH_3)_2$ OH) and lower with oxidizing radicals (10^7 L mol^{-1} s^{-1} for $^{\bullet}CH_2COCH_3$). Because the bond dissociation energy for the S-H bond is much lower than that for the C-H bonds involved in these reactions, it appears that hydrogen abstraction from mercaptobenzoic acid is not controlled by the relative bond dissociation energies but rather by the electron density at the radical site through a polar transition state. The rate constants for similar reactions in alcohols are slightly lower than those in water, supporting a polar transition state.

As a next challenge, solvent effects on the stability of $Br_2^{\bullet-}$ and the rate constant of oxidation of chlorpromazine by have been examined in R_4NNTf_2 and other solvents [3]. Reaction of solvated electrons with $BrCH_2CH_2Br$ produces Br^- and $^{\bullet}CH_2CH_2Br$, which decomposes rapidly into $CH_2{=}CH_2$ and $Br^{\bullet}$. Reaction of $Br^{\bullet}$ with Br^- forms . The stability of is much greater in the ionic liquid and in acetonitrile than in water or alcohols. The rate constant for oxidation of chlorpromazine by radicals decreases upon changing the solvent from water (6×10^9 L mol^{-1} s^{-1}) to methanol (2.8×10^9 L mol^{-1} s^{-1}), ethanol (1.2×10^9 L mol^{-1} s^{-1}), isopropyl alcohol (1.2×10^9 L mol^{-1} s^{-1}), 1-propanol (7.5×10^8 L mol^{-1} s^{-1}), *tert*-butyl alcohol (3.0×10^8 L mol^{-1} s^{-1}), acetonitrile (2.0×10^7 L mol^{-1} s^{-1}), *N*,*N*-dimethylformamide (5.3×10^6 L mol^{-1}s^{-1}), the ionic liquid R_4NNTf_2 (1.1×10^6 L mol^{-1} s^{-1}), and hexamethylphosphoramide (8×10^4 L mol^{-1} s^{-1}). The rate constants show reasonable correlations with hydrogen bond donor acidity and with anion-solvation tendency parameters. From the good correlation with the free energy of transfer of Br^- ions from water to the various solvents, it is suggested that the change in the energy of solvation of Br^- in the different solvents is the main factor that affects the rate constant of the reaction through its effect on the reduction potential of . The present results show the need for meausurements of reduction potential and solvation energies in ionic liquids as reactivity predictors. The experiments were conducted at the National Institute of Standards and Technology.

References

[1]. Grodkowski J., Neta P.: J. Phys. Chem. A, 106, 22, 5469-5473 (2002).
[2]. Grodkowski J., Neta P.: J. Phys. Chem. A, 106, 39, 9030-9035 (2002).
[3]. Grodkowski J., Neta P.: J. Phys. Chem. A, 106, 46, 11130-11134 (2002).

INFLUENCE OF A NUCLEATING AGENT ON THE MECHANICAL PROPERTIES OF POLYPROPYLENE AND ITS BLENDS

Izabela Legocka, Jerzy Bojarski, Zbigniew Zimek, Krzysztof Mirkowski, Andrzej Nowicki

Isotactic polypropylene (iPP) and propylene copolymers are the commodity polymers, which displayed the fastest growth rate in the recent years. It can be anticipated that this trend will continue in the future. Polypropylene main features are as follows: low price, friendly environmental behavior, easy processing and recycling, rather good performance. It meets requirements suitable for many customers. Polypropylene materials are used often for medical disposable manufacturing. Radiation sterilization of medical devices made of iPP has been actively carried out but with some limitations. The degradation effect is observed at the dose required for product sterility which influences on the properties of products [1].

Generally, the degradation caused by high energy ionizing irradiation [2] is characterized by yellowing, embrittlement and lost of mechanical

properties (Young's modulus, tensile strength). It is guessed that radiation stability of the semicrystalline polymers is greatly effected by the addition of antioxidants, UV absorbers, and mobilizers, nucleating agents, which have influence on distortion of their crystal structure [3]. It is well known that iPP crystallization begins at crystallization site. Addition of nucleating agent increases the number of those sites. Increasing the number of crystallization sites in a polymer increases the overall crystallization rate and decreases spherulite size [4]. Nucleators through intercrystalline links and smaller spherulites improve the tensile strength, Young's modulus and transparency of modified iPP [5]. At the same time nucleating agent, because of the presence of aromatic rings in the main chain, can change not only crystal structure of a polymer but also may have influence on the formation of radicals and their deactivation. That may lead to improvement of material resistance to dose deposited during sterilization process [6].

In the presented study, the iPP and propylene copolymers were modified by the addition of a low content of 1,3:2,4-bis-O-(4-methylbenzylidene) sorbitol (DMDBS). The influence of this nucleating agent containing aromatic rings on mechanical properties of polypropylenes, before and after sterilization process was investigated.

Materials and testing methods

Isotactic polypropylene PP Malen P J601 with a melt flow index of 7 g (230°C/2.16 kg), PKN ORLEN (Poland).

Random copolymer of propylene and ethylene (90:10) Moplen PLZ841, Montell Polyolefines.

The nucleating agent used was DMDBS – Irgaclear DM, Ciba-Geigy (Fig.1).

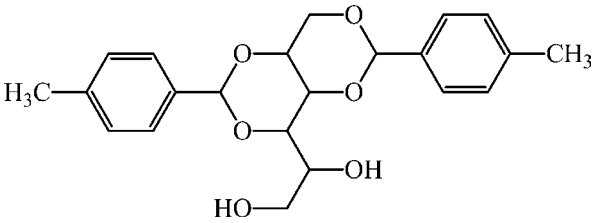

Fig.1. Formula of DMDBS.

Mixing of materials was carried out at 60 rpm and 200°C using a Brabender machine connected with an extruder. The compositions was later compressed into sheets by molding under pressure for 5 min at 210-220°C. The compressed sheets were irradiated in air with electron beam with doses: 35 and 50 kGy.

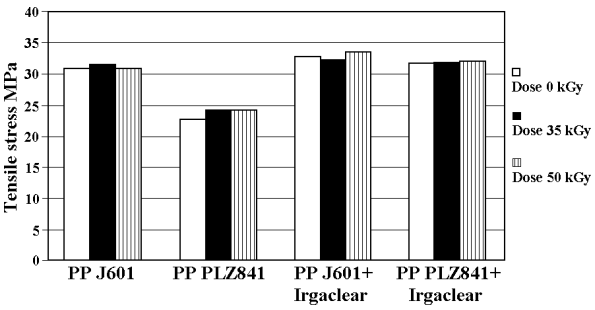

Fig.2. Stress at yield.

The mechanical characteristics was determined from stress-strain curve measurements using an Instron universal machine model 5550 in accordance with standards at ambient temperature (23°C). The impact strength of the some samples was measured in Izod test.

Influence of additive nucleating agent and irradiation on mechanical properties

Mechanical properties such as yield stress presented in Fig.2 and Young's modulus presented in Fig.3 show that addition of DMDBS results in

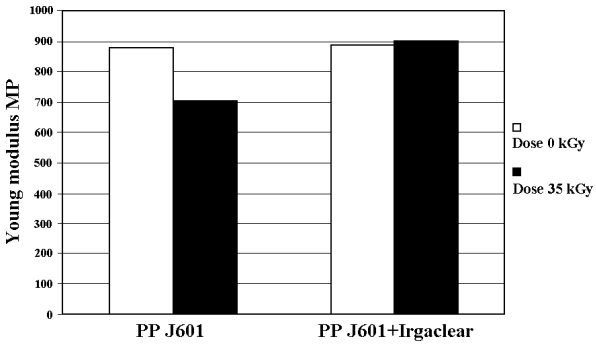

Fig.3. Young's modulus.

an increase of these parameters. In addition, the tensile strain at break for the investigated samples are significantly lower than for the unmodified polypropylenes (Fig.4). Such behavior may be caused by the higher crystallinity compared with the initial material in addition to degradation ef-

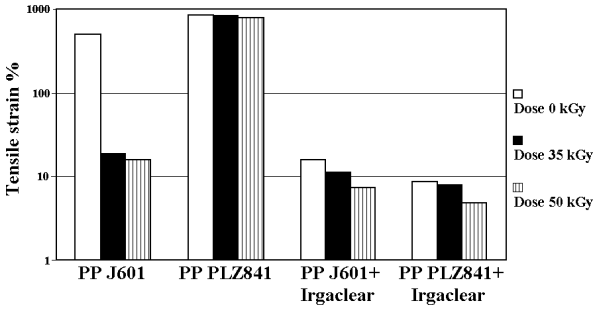

Fig.4. Tensile strain at break.

fect observed in irradiated samples. Results of Izod test shown in Fig.5 can be partly explained by such reasons. The susceptibility of the used polymers depends on its chemical structure. The homopolymer with a nucleating agent, before and

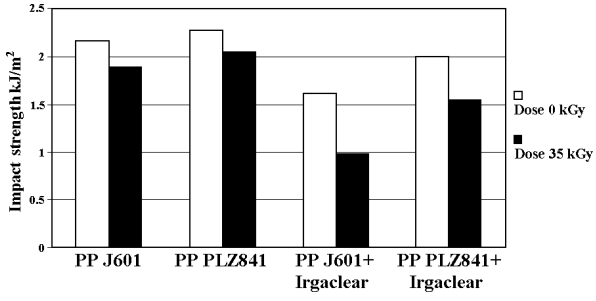

Fig.5. Impact strength (Izod test).

after irradiation process as compared with the copolymer, is characterized by higher Young's modulus and stress at yield. The elongation of both polymers is very low, especially for samples after

irradiation. It can be correlated with the occurrence of radiation induced oxidative degradation (Fig.6).

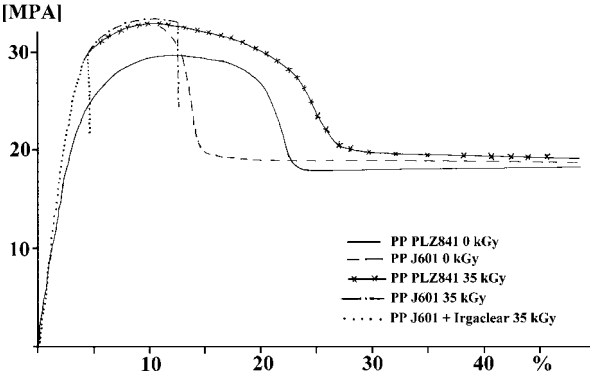

Fig.6. Nominal stress at nominal elongation.

The low elongation at break and lower impact strength (Izod test) of the modified samples after irradiation is caused not only by the higher crystallinity stimulated by the nucleating agent, but also by the destruction of polymer chains initiated by radiation. This means that addition of DMDBS did not influence the formation of radicals and their deactivation. In the future this leads to the addition of some radical scavengers and antioxidants.

Conclusion

The obtained results may lead to the conclusion that the addition of DMDBS leads to improving strength of the samples, but at the same time this increases their stiffness. Addition of the used nucleating agent DMDBS (containing aromatic rings) did not protect the polypropylene against destruction during irradiation process.

References

[1]. Bojarski J., Bułhak Z., Burlińska G., Zimek Z.: Medical quality of the radiation resistant polypropylene. Radiat. Phys. Chem., 46, 801 (1995).
[2]. Thorat H.B., Prabhu C.S.: Stabilization of ethylene-propylene copolymer against γ-ray induced degradation. Radiat. Phys. Chem., 51, 215 (1998).
[3]. Kadir Z.A., Yoshii F., Makuuchi K.: Durability of radiation sterilized polymers (XIII). Die Angew. Makromol. Chem., 174, 31 (1990).
[4]. Maeco C., Gomez M.A., Ellis G., Arribas J.M.: Highly efficient nucleating additive of isotactic polypropylene studied by differential scanning microscopy. J. Appl. Polym. Sci., 84, 1669 (2002).
[5]. Kotek J., Raab M., Baldrian J., Grellmann W.: The effect of specific nucleation on morfology and mechanical behavior of isotactic polypropylene. J. Appl. Polym. Sci., 85, 1174 (2002).
[6]. Shamshad A., Basfar A.: Influence of benzoic acid on thermal crystallization and mechanical properties of isotactic polypropylene under irradiation. Nucl. Instrum. Meth. Phys. Res. B, 151, 169 (1999).

RADIATION CROSSLINKING AND SPURS IN A CHOSEN ELASTOMER

Jacek Bik[1/], Wojciech Głuszewski, Władysław M. Rzymski[1/], Zbigniew P. Zagórski

[1/] Institute of Polymers, Technical University of Łódź, Poland

Radiation induced crosslinking of polyethylene is a routine method, applied also commercially in the Institute of Nuclear Chemistry and Technology (INCT). Now, the radiation crosslinking is proposed as an alternative to conventional chemical methods of crosslinking of elastomers on the example of hydrogenated acrylonitrile-butadiene rubber (HNBR), containing 43% of bound acrylonitryle. The most hydrogenated samples were >99.5 mol. % (H43) and less hydrogenated – 94.5 mol. % (S43) of starting double bonds content. Plates of the rubber of 1 mm thickness were prepared from cold masticated HNBR by press molding under pressure in heated stainless steel forms. Samples of rubber were conditioned, after keeping under vacuum, for weeks in an oxygen atmosphere and another set was left, also for a long period of time in argon. Irradiations have been performed by electron beam (EB), of energy of 10 MeV, bent by 270° downwards and scanned over the conveyor. Bending of the beam causes the reduction of its power from 9 to 6 kW, but produces a monoenergetic beam [1]. The applied doses varied from 20 up to 300 kGy. A split dose technique (20 kGy increments) has been applied to avoid excessive heating of samples [2] caused by the adiabatic character of the process. Dosimetry was typical for radiation processing of polymers in the INCT; it is traced to absolute calorimetric dosimetry, according to the ASTM standards.

Irradiated samples were investigated for the degree of crosslinking and for the properties important to understand the role of spurs. Effects of

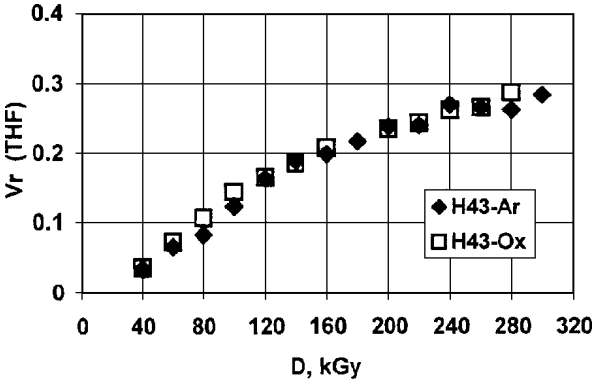

Fig.1. Degree of crosslinking V_r (THF) for Therban A4307 (H43-Ar – samples oxygen-free and H43-Ox – samples saturated with oxygen).

irradiation were determined by standard methods used in previous studies on HNBR [3]. Figures 1

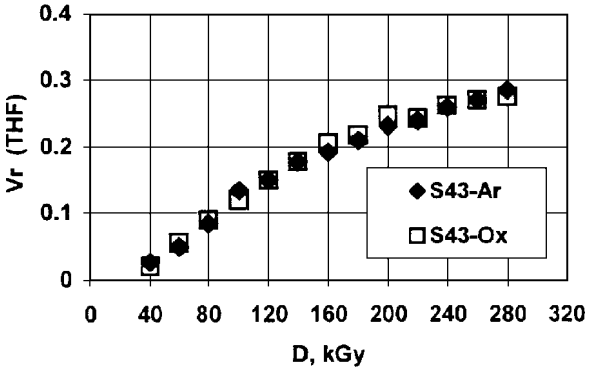

Fig.2. Degree of crosslinking V_r(THF) for Therban C4367 (S43-Ar – samples oxygen-free and S43-Ox – samples saturated with oxygen).

and 2 show the crosslinking of both kinds of rubbers deoxygenated or oxygenated, expressed as extend of crosslinking $V_r=(1+Q_v)^{-1}$ in the function of dose D. Q_v denotes the volume fraction of rubber in swollen gel. Changes of elasticity constants $2C_1$ of Mooney-Rivlin equation of both rubbers, containing oxygen and those oxygen-free, contents of sol fractions in coordinates according to Charlesby--Pinner's equation; elongations at break and tensile strengths in the function of dose are shown in the full version of the paper (to be published).

As in all polymers, 80% of deposited energy of radiation appears in single ionization spurs, located far one from another. The smaller part of the energy is deposited in multi-ionisation spurs, localised in the accidental centers of small volumes. They are caused by electrons reaching the final degradation of their energy, with next generations not able to travel far from this site. Accumulation of >100 eV energy in a small volume leads inevitably to scission of the chain. Single ionization spurs are characterized by much lower deposits of energy, sufficient for ionization and excitation only, without the chain scission [4]. Transfer of primary effects along the chains to energetically favourable sites leads to the crosslinking of macromolecules, if there are no geometrical obstacles, like in the case of polypropylene which does not crosslink, in contrary to the polyethylene. Crosslinks originating by single ionization spurs are of the tetrafunctional X-type. Fragments of molecules formed in the result of multi-ionization spurs can also enter the crosslinking reaction, but the type of structure formed is different in comparison to the crosslinking product of single-ionization spurs. It is of the trifunctional Y-type, because the loose chain ends, with their reactive groups, enter into reaction with the closest macromolecule. Some broken chains cannot find partners for reaction and contribute to the population of degraded macromolecules.

Analysis of diagrams of effects *vs.* dose shows that a certain dose has to be applied before crosslinking can start. Energy deposited at the beginning of irradiation is used in other reactions, probably destroying, or transforming chemical additives present in commercial products. That observation has been published already in the preliminary report [5]. The initial dose was determined from the linear dependence of the sol content S from the dose D in double logarithmic coordinates. Its value is similar for both polymers (29.1 and 24.8 kGy for H43 and S43 rubbers respectively, both oxygen-free) and it is only slightly influenced by the presence of oxygen (21.6 and 25.4 kGy for H43 and S43 rubber, respectively). It is evident that it depends to a small extent only on the remaining double bond content >C=C< in the HNBR studied.

From the basic radiation chemistry point of view, the quantitative determination of participation of crosslinking *vs.* degradation of chosen elastomers is important. These acts relate to the partition of deposited ionizing energy between single- and multi-ionization spurs. We have based the calculation of mer units participating in degradation p, and those participating in crosslinking q, on the fundamental Charlesby-Pinner equation [6] for doses exceeding 80 kGy. From the determined values of p/q one can conclude that for 100 acts of crosslinking there are 6-9 acts of degradation of macromolecules. Radiation yield, calculated as the number of effective crosslinks per 100 eV of absorbed energy is: 2.49, 2.69, 2.68 and 2.77 for H43-Ox, H43-Ar, S43-Ox and S43-Ar respectively. Differences are not statistically significant, and should not be commented; further research is needed for the speciation of X- and Y-types of crosslinks.

The participation of multi-ionization spurs in solids is not very well explored yet. It is only known for the case of comparatively simple case of irradiation of crystalline alanine [7], where the participation of multi-ionization spurs is estimated to be *ca*. 20% of total deposited energy, as in all systems, including even aqueous solutions, irradiated with low linear energy transfer (LET) radiations. Our result of p/q is lower than expected, because in our case a part of the effects of multi-ionization spurs can result in additional crosslinks. They are of different type: loose ends of broken chains react with the closest present unaffected molecule. Methods of the detection and the determination of crosslinking do not distinguish between chains crosslinked in the effect of single-ionization spur (X-type) and crosslinked by the product of multi--ionization spurs (Y-type). Our results of low yield of degradation are lower for several reasons, than results for degradation reported by Zhao *et al*. [8]. However, these authors have studied HNBR filled with carbon black and irradiated by gamma radiation in the presence of air. In such condition of low dose rate, there is always an excess of oxygen in the material and degradation proceeds *via* peroxides and ketones.

Further investigations are concentrating on optical measurements of irradiated HNBR, because the material is sufficiently transparent and conventional spectrophotometry can be applied, also time resolved, not only the diffuse reflection spectrophotometry, useful in investigations on radiation chemistry of polymers [9]. Mechanisms of radiolysis will be described in detail in next publications, also including electron paramagnetic resonance (EPR) measurements, now under progress.

The work is in progress and publications are in continuous preparation. The closest one is [10].

This research is supported by the Polish State Committee for Scientific Research, Project No. 7T08E 016 21 and a statutory grant for the INCT .

References

[1]. Zagórski Z.P.: Dependence of depth-dose curves on the energy spectrum of 5 to 13 MeV electron beams. Radiat. Phys. Chem., 22, 409-418 (1983).
[2]. Zagórski, Z.P.: Thermal and electrostatic aspects of radiation processing of polymers. In: Radiation Processing of Polymers. Eds. A. Singh, A., J. Silverman. Hanser Publishers, Munich, Vienna, New York 1992, pp.271-287.
[3]. Rzymski W. M., Srogosz A.: Studies on curing and properties of hydrogenated nitrile rubbers. Elastomery, 1(1), 11-20 (1996), in Polish.
[4]. Zagórski Z.P.: Modification, degradation and stabilization of polymers in view of the classification of radiation spurs. Radiat. Phys. Chem., 63, 9-19 (2002).
[5]. Zagórski Z.P.: Polymers and radiation. Postępy Techniki Jądrowej, 43, (4) 2-13 (2000), in Polish.
[6]. Charlesby A., Pinner S.H.: Analysis of the solubility behaviour of irradiated polyethylene and other polymers. Proc. Royal. Soc., London, A249, 367-386 (1959).
[7]. Zagórski Z.P.: Solid state radiation chemistry - features important in basic research and applications. Radiat. Phys. Chem., 56, 559-565 (1999).
[8]. Zhao W., You L., Zhong X., Youefang Z., Sun J.: Radiation vulcanization of hydrogenated acrylonitrile butadiene rubber (HNBR). J. Appl. Polym. Sci., 54, 1199-1205 (1994).
[9]. Zagórski Z.P.: Diffuse reflection spectrophotometry (DRS) for recognition of products of radiolysis in polymers. Int. J. Polymer. Mater., 52, 323-333 (2003).
[10]. Bik J., Głuszewski, Rzymski W.M., Zagórski Z.P.: EB radiation crosslinking of elastomers. Radiat. Phys. Chem., in press.

ROLE OF RADIATION CHEMISTRY IN WASTE MANAGEMENT

Jacek Dziewinski[1/], **Zbigniew P. Zagórski**

[1/] Los Alamos National Laboratory, USA

Department of Radiation Chemistry and Technology (Institute of Nuclear Chemistry and Technology – INCT) has entered the wide cooperation with Los Alamos National Laboratory (LANL) on the contribution of radiation chemistry to problems of radioactive waste management. The interface between radiochemistry, which is the scientific background of radioactive waste problems and radiation chemistry is seldom discussed in the literature. Recently Zimbrick [1], in a review paper on the future of radiation chemistry has stressed the importance of that part of chemistry, but specifically only in the case of particularly difficult case of half a century old waste at Hanford. This complex waste dates to the time of first large scale separations of plutonium from the spent nuclear fuel. Nowadays, a more general and universal chemical approach is needed, starting already with the time of creation of the waste. LANL is not fully prepared to experiments in radiation chemistry, mainly because of lack of proper high power sources of ionizing radiation. Theoretical and experimental potential of the INCT is supplementing the LANL activities in radioactive waste management, which does not involve sufficiently the radiation chemical aspects of the field. This paper presents the basic philosophy of connections between waste management and radiation chemistry. The analysis is done from the point of view of materials involved and experimental techniques applied to solve defined problems, like the chemical reactions evolving in different time scale during the lifetime of the waste from generation of it, till to the end of the story which means the acceptable level of activity of the deposit.

Radiation chemistry is fundamentally involved in management of radioactive waste on every time scale: from the zero point of waste generation, through its preliminary storage and processing, transportation, and final storage. The main fragment of radiation chemistry involved is the solid state radiation chemistry, not explored fully as yet, as it is the liquid phase, especially aqueous radiation chemistry. Solid state radiation chemistry occurs in our program as radiation chemistry of inorganic material embedding radioactive waste, like materials of controlled composition as blocks of concrete and silicate glasses, but also as natural salt deposits of uncontrolled composition. Other solid state material undergoing radiolysis are synthetic polymers of very different nature like elastomers used in nuclear industry, and many other polymers of different response to radiation like aromatic polystyrenes, which are rather resistant to radiation, but also polymers which easily degrade under irradiation, like teflon. Natural polymers, like cellulose, lignine can occur in the waste, contaminated with plutonium. Radiation induced degradation is seldom as innocuous as the resulting reduction of average molecular weight, even advantageous in the case of waste. Degradation of poly(vinylchloride) causes releasing of highly corrosive HCl. The danger is even higher in the case of iodine containing polymers, recently proposed as biological shield instead of lead containing composites. Release of hydrogen, which is explosive in mixtures with air, is possible from irradiation of any material which contains chemically bound hydrogen. These examples show that any material in contact, especially long, with radioactive material has to be examined for radiation induced chemical reactions.

Liquid phase radiation chemistry is also involved in the program. The worst case scenario of storage of radioactive waste in salt deposits assumes penetration of water and dissolution of salt. The first reaction is that of irradiated salt (for some aspects of NaCl radiation chemistry c.f. [2]), in which electrons are trapped (F centres), with water. The hypochlorite is formed, entering into reactions

with solutes in penetrating water, e.g. humic acids. The brine formed is irradiated by radiation emitted by still decaying nuclides. Studies of radiation chemistry of aqueous solutions are important in nuclear waste repository science, especially for environmental evaluation of deep underground salt repositories. Although such salt deposits have remained dry for millions of years and the probability of solubilization is remote, possibilities of actinide migration are extensively studied under an unlikely accident scenario of water penetration into a repository. Under such a scenario, radiolytic effects in brines become very important because of the likelihood of radiolytic formation of oxidizing species, such as chlorine species or hydrogen peroxide. Those species raise the Eh and may cause oxidizing the actinides into more soluble forms, e.g. Pu(VI) or Pu(V) and also may cause actinide complexations. Preliminary studies of several brine solutions have been conducted using the 10 MeV linear accelerator of electrons (LAE 13/9) in the INCT and were presented in [3]. Radiolytically produced chlorine species were observed.

The most rigid conditions for the environmental safety require that the final fate of waste is predictable for thousand of years. Prediction of behavior in such long periods of time requires performing of experiments, which would compress the effects from thousands of years to minutes. The modern techniques of radiation chemistry make it possible. Properly adjusted experiments help to assume what will happen to the medium, in which radioactive nuclides are embedded. Radiation induced phenomena in the waste are exceeding by several orders of magnitude of the time scale. Use of high power electron accelerators allows the simulations of chemical changes in any materials absorbing radiation of any linear energy transfer (LET) value, often shortening to minutes the effects occurring during thousands of years of storage. Rules of effective simulations are outlined here under the principles of radiation chemistry.

These experiments must take into account the action of egzogenic reagents, e.g. of air. This may create some problems, where transport of these agents has to be increased to match the increased dose rate of ionizing energy. Some of these problems may be solved by operating with increased concentration of the egzogenic reagents, others may be addressed by the increase of the diffusion rate of these reagents, e.g. by raising the temperature. To reach proper conclusions, two sets of experiments is always made, assuming extreme versions of egzogenic influences. For instance, it is difficult to guess what will be the oxygen content of water sipping into the salt deposit. It will not contain oxygen, most probably, due to the presence of organic reducing species. However, a set of experiments is performed in the presence of air, because the presence or absence of oxygen does influence the final result of radiolysis. Therefore, the results have to account for two versions of the worst scenario. Generally, two techniques may be used for time accelerated study of behavior of nuclear waste: first, the increase of the irradiation dose rate, which can be done easily by high power electron beams, the second, time resolved radiolysis, realized again by electron accelerators coupled with special fast detecting systems (pulse radiolysis, in relation to solid state c.f. [4]).

The question of the LET value of the applied radiation is important while simulating the effects of alpha radiation emitted by actinides, by low LET radiations. Both types of radiation differ in the total deposited energy ratio of single- and multi-ionization spurs. In aqueous solutions this ratio is high in the case of low LET radiations (gammas and electron beams), but low in the case of high LET (alphas). In the case of organics, especially of polymers, these ratios do not differ much, because both kinds of spurs result in production of hydrogen, the main object of interest in the transportation of waste to the site of deposition. There are some difficulties in recalculation of electron beam irradiation results into those obtained, or assumed with alphas. These difficulties are well compensated by the cleanness of the experiments with electron beams, with their long range and depth of penetration, and their easy negotiation of walls of containers with investigated materials.

Specifics of multi-ionization spurs lie in overlapping of the elementary spurs. In case of low LET radiations such overlap takes place with final generations of secondary electrons of energy close to the subexcitation levels. These electrons are not able to move very much further and, therefore, they ionize the next molecule to the previous one, or the next element of the chain of a polymer [5, 6]. In case of high LET radiations, the primary ionizing particles create a high concentration of ionizations already at the beginning of their travel, resulting in enormous overlapping of spurs and formation of columns of ions. Single ionization spurs are formed around these columns, because part of secondary electrons from primary ionizations have sufficient energy to escape from the column and move into the bulk of the material. Here they produce single ionization spurs with the products exactly the same as the products of single ionization spurs generated by low LET radiations.

Because the nature of multi-ionization spurs lies in the overlap of single ionization spurs, the method of simulating alpha irradiations with electron beam is obvious: it is the application of very high dose rates of irradiation. We are accomplishing this with the INCT accelerator LAE 13/9, which can generate straight, not scanned beam of electrons concentrated in the diameter of 1 cm. The main difficulty with a high dose rate irradiation is the temperature effect [7], as most of the energy supplied by ionizing radiation is turned into heat. The columns of alpha tracks are warm, contributing to the radiation damage.

A typical experiment consists of irradiation of a chosen sample (cement sludge, brine, organic debris, polymer etc.), sometimes conditioned in the desired way and analyzed chemically or investigated by special methods. The most useful method of analysis is UV-VIS spectrophotometry, applied for solid, semitransparent samples as DRS (diffuse

reflection spectrophotometry), described in [8]. The latter method has been developed in the INCT with excellent results, especially in the field of radiation chemistry of polymers, which, with few exceptions, are usually opaque. A more refined approach is time resolved radiolysis, i.e. pulse radiolysis with optical or electrochemical detection of transient species. Although performed mostly in liquid state, it may also be applied to solid or rigid state [4]. Such experiments help formulating the mechanisms of radiolysis and are superior over the traditional determination of only the final stable products, which often leads to speculations only. Pulse radiolysis experiments are followed by computer-assisted simulations, which often allow to eliminate some unnecessary experiments. Another kind of computer simulations allow to extrapolate radiation induced phenomena over thousands of years.

Irradiation sources, mainly accelerators of electrons, as well as techniques of high dose irradiations were described earlier, c.f. [9-11].

The present report is an introduction to partial reports under the contract with LANL, No. 45302-001-02-AA. Detailed reports from the experiments will appear in next publications.

References

[1]. Zimbrick J.D.: Radiation chemistry and the Radiation Research Society: A history from the beginning. Radiat. Res., 158, 127-140 (2002).
[2]. Zagórski Z.P., Rafalski A.: A thin, composite sodium chloride dosimeter with diffuse reflected light spectrophotometric read out. J. Radioanal. Nucl. Chem., 245, 233-236 (2000).
[3]. Paviet-Hartmann P., Dziewinski J., Hartmann T., Marczak S., Ninping L., Walthall M., Rafalski A., Zagórski Z.P.: Spectroscopic investigation of the formation of radiolysis products by 13/9 MeV linear accelerator of electrons (LAE) in salt solutions. WM'02 Conference, 24-28 February 2002, Tucson, USA. Proceedings, electronic version only: wm'02.pdf.
[4]. Zagórski Z.P.: Pulse radiolysis of solid and rigid systems4. In: Properties and Reactions of Radiation Induced Transients, Selected Topics. Ed. J. Mayer. PWN, Warszawa 1999, pp.219-233.
[5]. Zagórski Z.P.: Solid state radiation chemistry – features important in basic research and applications. Radiat. Phys. Chem., 56, 559-565 (1999).
[6]. Zagórski Z.P.: Modification, degradation and stabilization of polymers in view of the classification of radiation spurs. Radiat. Phys. Chem., 63, 9-19 (2002).
[7]. Zagórski Z.P.: Thermal and electrostatic aspects of radiation processing of polymers. In: Radiation Processing of Polymers. Eds. A. Singh, J. Silverman. Hanser Publishers, Munich, Vienna, New York 1992, pp.271-287.
[8]. Zagórski Z.P.: Diffuse reflection spectrophotometry (DRS) for recognition of products of radiolysis in polymers. Int. J. Polymer. Mater., 52, 323-333 (2003).
[9]. Zagórski Z.P.: Instrumentation for radiation chemistry research in the Institute of Nuclear Research in Warsaw. Nukleonika, 22, 725-758 (1977).
[10]. Zagórski Z.P.: Dependence of depth-dose curves on the energy spectrum of 5 to 13 MeV electron beams. Radiat. Phys. Chem., 22, 409-418 (1983).
[11]. Zagórski Z.P.: Design and applications of a constant-temperature box for high-energy electron-beam processing at temperatures -20°C to 70°C. Int. J. Appl. Radiat. Isot., 36, 243-245 (1985).

APPLICATION OF IONIZING RADIATION FOR DEGRADATION OF PESTICIDES IN ENVIRONMENTAL SAMPLES

Przemysław Drzewicz, Anna Bojanowska-Czajka, Grzegorz Nałęcz-Jawecki[1/], Józef Sawicki[1/], Stanisław Wołkowicz[2/], Abdurrahman Eswayah[3/], Marek Trojanowicz

[1/] Department of Environmental Health Sciences, Medical University of Warsaw, Poland
[2/] Polish Geological Institute, Warszawa, Poland
[3/] Tajoura Nuclear Research Center, Tripoli, Libya

A broad application of intensive agricultural methods in the last few decades with the use of large amount of agrochemicals results in the presence of increasing amount of pesticides in natural waters. From the sixties large amounts of obsolete and unwanted pesticides are stored in concrete bunkers in various locations. It is estimated that there are about 300 bunkers with above 20 000 tons of agrochemicals in Poland, however, there is limited documentation for most of pesticide dump bunkers and a real amount of dumped pesticide can be higher. Chloroorganic pesticides (DDT group, HCH group), phosphoroorganic pesticides, phenoxyalkanoic acids pesticides are the main chemical groups of biocides present in these dumpsites [1]. In many cases, these bunkers were constructed in flooded areas, water-bearing layer or sand. The influence of rain water, ground water and stored chemicals cause corrosion of concrete and leakage of the content to the environment. The released agrochemicals may pollute ground water and soil even far away from the bunker site, therefore one of the most significant environmental needs is to clean up ground water.

The aim of the present studies was a further investigation of decomposition of selected pesticides and formation of by-products during application of ionizing radiation for the treatment of pesticides in synthetic aqueous solutions and also in real samples of contaminated ground water samples. Earlier obtained results of studies on the application of ionizing radiation for decomposition of pesticides for environmental purposes have been promising [2-6]. Additionally, the recent results of studies on application of ionizing radiation for decontamination reviewed by Gray [7], have shown that the radiation process is economically reasonable and may be efficient also in remediation of contaminated soil.

Irradiation of water and slurry soil samples was performed using a ^{60}Co γ-source "Issledovatel" (2.72 kGy/h) and with an electron beam (EB) accelerator "Elektronika" (10 kW, 10 MeV).

Determination of 2,4-dichlorophenoxyacetic acid (2,4-D), 3,6-dichloro-2-methoxy-benzoic acid (dicamba) and chlorophenols was carried out by reversed-phase HPLC using a Shimadzu Chromatograph with a diode array UV/VIS detector, equipped with a column Luna ODS2, 5 μm and a guard column from Phenomenex. Injected sample volume was 20 μl. As eluent a mixture of 2 g/l citric acid solution in water, methanol and acetonitrile at a ratio of 65:35:5 was used at a flow rate of 1 ml/l.

Chemical Oxygen Demand (COD) was determined according to ISO 6060:1989 method using a setup from Behr-Labor-Technik (Düsseldorf, Germany). Oxygen concentration was measured by a commercially available Clark electrode and Oxymeter model 3000 from WTW (Weilheim, Germany).

Toxicity measurements in irradiated solutions were carried out using a commercial Microtox® test with a setup purchased from Azur Environmental (Wokingham, England). For toxicity measurements of soil, Ostracodtoxkit™ F test from MicroBioTest Inc. (Nazareth, Belgium) was used. Additionally, a 2% sodium chloride water solution extract from soil was tested by toxicity test Protoxkit™ F from MicroBioTest and Microtox®.

Recently, the mechanism of degradation of 2,4-D to mono-chlorohydroxyphenoxy acetic acid and to 2,4-D was reported [3]. It is also shown that decomposition of 2,4-D and its mineralization is more effective in oxygenated solution. The reported studies were performed with distilled water solutions of 2,4-D, however, natural water may contain some potential scavengers of radicals such as carbonate and nitrate, which can affect degradation of 2,4-D. Hydroxyl radicals formed from radiolysis of water are scavenged by nitrates and carbonates or their radicals [8]. Thus, the presence of a scavenger may affect the efficiency of decomposition of organic compounds in solution. A difference in decomposition efficiency of 2,4-D in different ground waters was observed earlier [2], and it was attributed to different concentration of nitrates.

In this study, measurements of oxygen concentration during γ-irradiation of 2,4-D solutions have shown that all oxygen in solution containing 110 ppm of 2,4-D with carbonates or nitrites was consumed at higher doses than it occurs in the absence of a scavenger. These results confirm a scavenging mechanism based on reaction of scavenger with $H^{\bullet}$, e_{aq} and peroxyl radicals [9, 10]. Scavenging of $H^{\bullet}$ and e_{aq} results in low amount of formed and which participate in degradation of organic compounds. On the other hand, , and other peroxyl radicals are scavenged by carbonate and nitrate or their radical. This can be considered as an additional mechanism of scavenging besides the scavenging of $OH^{\bullet}$. Addition of ozone during irradiation may reduce the scavenging effect by delivering an additional amount of radicals to the solution [2].

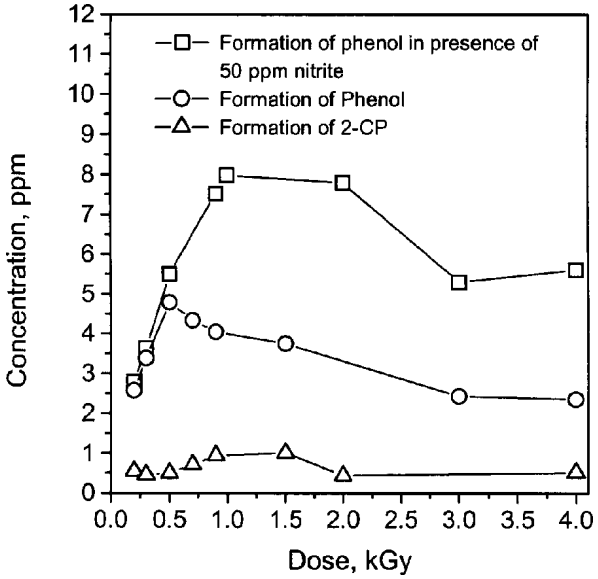

Fig.1. Effect of irradiation dose on formation of phenol and 2-chlorophenol during γ-irradiation of 110 ppm of dicamba solution in the presence and absence of 50 ppm of nitrate.

Our preliminary investigation on radiolytic degradation of another pesticide dicamba has shown that EB irradiation, especially in the presence of ozone, is very effective also in removal of dicamba from aqueous solutions [2], however, the mechanism of dicamba degradation was not examined, as yet. One can expect that this mechanism should be similar to that of other aromatic compounds. It may be assumed that in the presence of oxygen, $OH^{\bullet}$ adducts form hydroxyperoxycyclohexadienyl radicals of dicamba, which then can decay by two competing pathways with the formation of phenol isomers or benzene ring fragmentation (aliphatic acid formation). The presence of COOH and $O\text{-}CH_3$ groups in the benzene ring minimizes the strength of C-Cl bonding due to their electronegative properties. This can lead to formation of hydroxy-monochloroderivatives of dicamba as additional intermediate products of decomposition

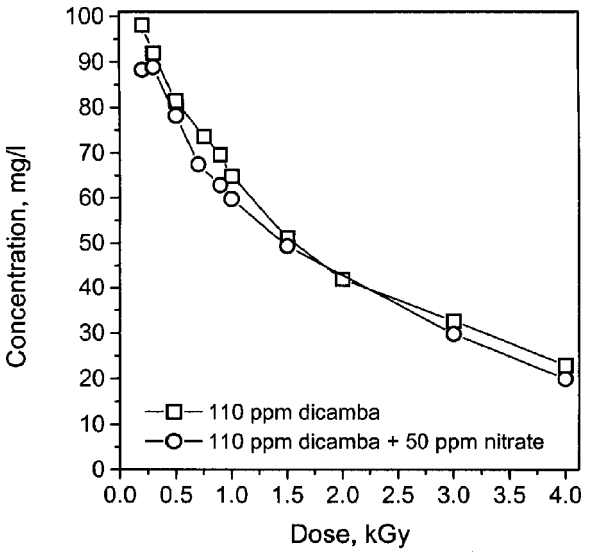

Fig.2. Effect of irradiation dose on decomposition of dicamba during γ-irradiation in the presence and absence of nitrate.

of dicamba. In irradiated 110 ppm aqueous aerated solutions of dicamba with doses up to 4 kGy, phenol and 2-chlorophenol were determined, but also some other non-identified substances were observed on recorded chromatograms. They will be a subject of further investigation. Low yield of ionizing radiation can be applied for the purification of groundwater.

As a complementary approach to reported above preliminary studies on the use of ionizing radiation for treatment of ground waters, similar experiments were carried out on irradiation of

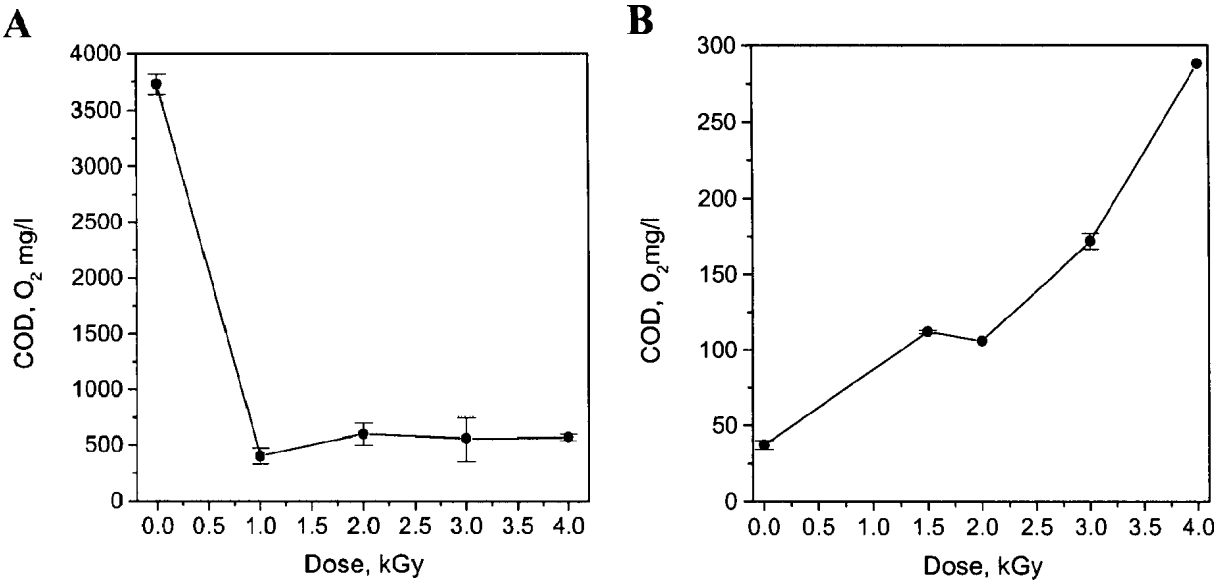

Fig.3. Changes of COD values of ground water from the vicinity of pesticide dumpsites at Przytoń-Brzeźniak (A) and Chrząstowo (B) during γ-irradiation with different doses.

phenolic intermediates (Fig.1) may be attributed to the high reaction rate constants of chlorophenols with hydroxyl radicals (7 to $10x10^9$ $M^{-1}s^{-1}$). The reaction of dicamba with $OH^{\bullet}$ was shown to be diffusion controlled ($4.8x10^{12}$ $M^{-1}h^{-1}$) [11]. In contrary to 2,4-D radiolytic degradation, the presence of 50 ppm of nitrates in irradiated solutions does not affect the decomposition of 110 ppm dicamba (Fig.2).

In preliminary studies of natural samples, the polluted ground waters were collected from the vicinity of two pesticide dumpsites at Chrząstowo and Przytoń-Brzeźniak in Northern Poland. Before irradiation water samples were saturated with air, which did not change COD values of these samples. In case of the sample from Przytoń-Brzeźniak, irradiation with a 1 kGy dose significantly decreases COD value from 3730 to 400 mg O_2/l. whereas in case of sample from Chrząstowo, an increase of COD value was observed (Fig.3). The latter result can be interpreted by incomplete mineralization of some resistant organic compounds during COD measurements. The measurement of COD employed here is based on the standard procedure of oxidation of organic substances using potassium dichromate in concentrated sulfuric acid for 2 h at 150°C. It was already demonstrated that some organic compounds are not oxidized in such conditions [12]. In both samples all dissolved oxygen was consumed at a 1 kGy dose. Both examined samples were not toxic to Microtox® test either before and after irradiation. Certain organic species, however are toxic even at very low concentration level and low COD value does not inform whether these compounds are removed or reduced to a safety level. These preliminary results have shown that aqueous suspensions of soils collected in the vicinity of pesticide dumpsites. In recent publications devoted to application of high energy irradiation for treatment of soils, the authors proposed supercritical fluid extraction [13], washing with solutions containing surfactants [14], or solvent extraction processes [15], as preliminary step before degradation of pollutants using ionizing irradiation.

In this study, as the first attempt, degradation of pollutants in soil suspension with water was examined. The sample of soil was taken from the vicinity of pesticide tomb at Ostrowiec (Northern Poland). The total organic content was very low in the examined soil samples (average 0.1%). Soil was amended

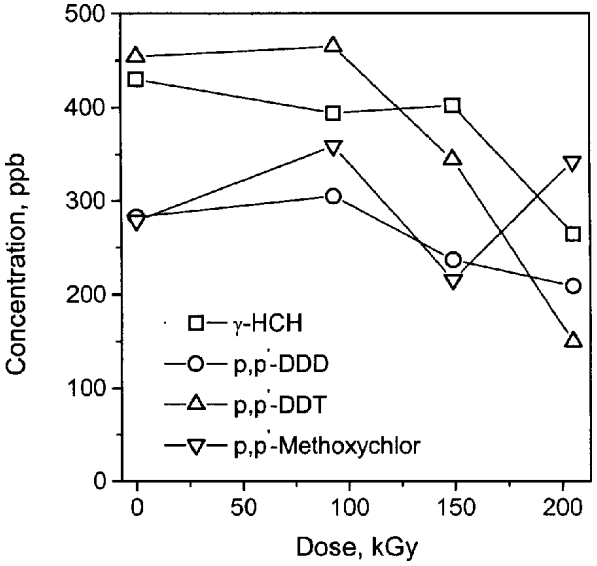

Fig.4. Degradation of chloroorganic pesticides during EB irradiation of soil samples amended with 25% w/w of water determined by GC-MS.

with 25% w/w of water before irradiation. After irradiation, the soil was dried overnight at 105°C and sieved through a 2 mm sieve. In dichloromethane extracts the content of selected chloroorganic pesticides was determined by GC-MS, including metoxychlor, DDT, γ-HCH, and DDD, which is the product of degradation of DDT and methoxychlor. Only about 50% of pesticides was decomposed

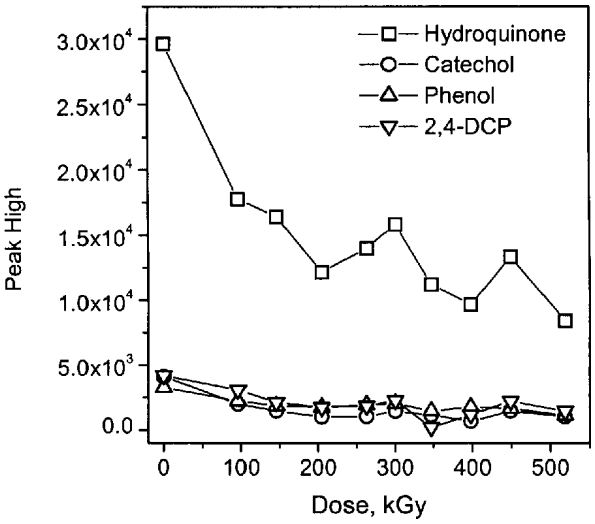

Fig.5. Effect of irradiation dose on the content of phenolics in methanolic extracts from irradiated soil samples.

under EB irradiation in spite of a very large dose used (Fig.4). In methanol extracts of the same soil samples, some possible products of decomposition of pesticides were determined by HPLC such as phenol, hydroquinone, catechol and 2,4-dichlorophenol (Fig.5). The content of these substances has decreased with dose increase. After irradiation, the samples of soil were tested by toxicity tests. It was found that toxicity to Ostracodtoxkit™ F test was decreased only by 30% after a 519 kGy dose, however, it was observed that the toxicity of water extract of soil to Microtox® and Protoxkit™ decreased by 90%.

References

[1]. Pestycydy, występowanie, oznaczanie i unieszkodliwianie. Ed. M. Biziuk. WNT, Warszawa 2001.
[2]. Drzewicz P., Zona R., Gehringer P., Solar S., Trojanowicz M.: in preparation.
[3]. Zona R., Solar S., Gehringer P.: Wat. Res., 36, 1369 (2002).
[4]. de Campas S.X., Vieira E.M.: Quim. Nova, 25, 529 (2002).
[5]. Karpel Vel Laitner N., Berger B., Gehringer P.: Radiat. Phys. Chem., 55, 317-322 (1999).
[6]. Angelini G., Bucci R., Carnevaletti F., Colosim M.: Phys. Chem., 59, 303-307 (2000).
[7]. Gray K.A., Cleland M.R.: J. Adv. Oxid. Technol., 3, 22-36 (1998).
[8]. Buxton G.V., Greenstock C.L, Helman W.P., Ross A.B.: J. Phys. Chem. Ref. Data., 17, 513 (1988).
[9]. Peroxyl Radicals. Ed. Z.B. Alfassi. New York 1997, pp.173-234.
[10]. Neta P., Huie R.E., Ross A.B.: J. Phys. Chem. Ref. Data, 17, 1027-1284 (1988).
[11]. Armbrust K.L.: Environ. Toxicol. Chem., 19, 2175-2180 (2000).
[12]. Baker J.R, Milke M.W., Mihelcic J.R.: Wat. Res., 33(2), 327-334 (1999).
[13]. Yak H.K., Mincher B.J., Chiu K.-H., Wai C.M.: J. Hazard. Mater., 69, 209-216 (1999).
[14]. Curry R.D., Clevenger T., Stancu-Ciolac O., Miller W.H., Farmer J., Mincher B.J., Kapila S.: J. Adv. Oxid. Technol., 3, 55-66 (1998).
[15]. Galav V., Waite T.D., Kurucz C.N., Cooper W.J.: Contam. Soils, 2, 295-304 (1997).

ENLARGEMENT OF ANALYTICAL ABILITIES OF THE LABORATORY FOR DETECTION OF IRRADIATED FOODS DEHYDRATED FRUITS

Katarzyna Lehner, Wacław Stachowicz

In October 2001 a new European Standard has been issued by the Committee for Standardisation (CEN) on the detection of irradiated food containing crystalline sugar by electron paramagnetic resonance (EPR) spectroscopy [1]. Some of the data cited in this document and used for the validation of the method have been obtained with the contribution of the Laboratory for Detection of Irradiated Foods [2]. The usefulness of the EPR spectroscopy for the identification of irradiation in dried figs and dates based on the detection of stable radical produced in crystalline sugar domains has been reported by us elsewhere [3, 4]. In these studies the stability of specific, relatively strong EPR signals derived from sugar-born radiation induced radicals has been proved by prolonged kinetic studies. It has been found that radiation treatment of dried fruits can be detected by this method even after eight months of storage. The subject of the earlier investigations were seeds excised from dried fruits only.

The intention of the present study is to adapt the procedure given in EN 13708 to routine analytical practice of the Laboratory and to extend on this way the list of food products which can be identified as irradiated or non-irradiated. In contrast to earlier studies [4] we focused our attention not on seeds but on pulps of dehydrated fruits only since now-a-day most of commercially available dehydrated fruits is delivered free of seeds. The following fruits were used in the experiments: pineapple, banana, date, fig, papaya, raisin, plum and apricot. The samples of pulps were irradiated with doses between 0.5 and 3.0 kGy in a ^{60}Co source, covering the range of doses recommended for radiation processing of dehydrated fruits. Then the EPR spectra of all samples, both irradiated and non-irradiated, were recorded 7 and 30 days after the irradiation. The analysis of the results allowed to draw conclusions concerning the stability of the signals involved.

The non-irradiated samples of dehydrated fruits give rise in EPR to a weak single line. Sometimes this native signal is not seen at all. The native signal in dehydrated fruits can be easily distinguished from radiation induced one which is more intense and have a complex, hyperfine structure (Fig.). It is believed that EPR signals in dehydrated fruits are mostly derived from radicals produced in crystalline saccharides by irradiation. It has been proved experimentally that crystalline sugar is a pool for the stabilisation of parent radicals of one or more

The EPR examination of plum and apricot was not successful. The EPR signals recorded with irradiated pulps of these fruits although more intense than those of native signals, were not characteristic and did not exhibit clearly complex structure. Therefore, they could not be a proof for the detection of irradiation.

The experiments done on pineapple, banana, date, fig, papaya and raisin were positive. The spectra recorded after irradiation with low and higher doses were specific and intense enough, as shown

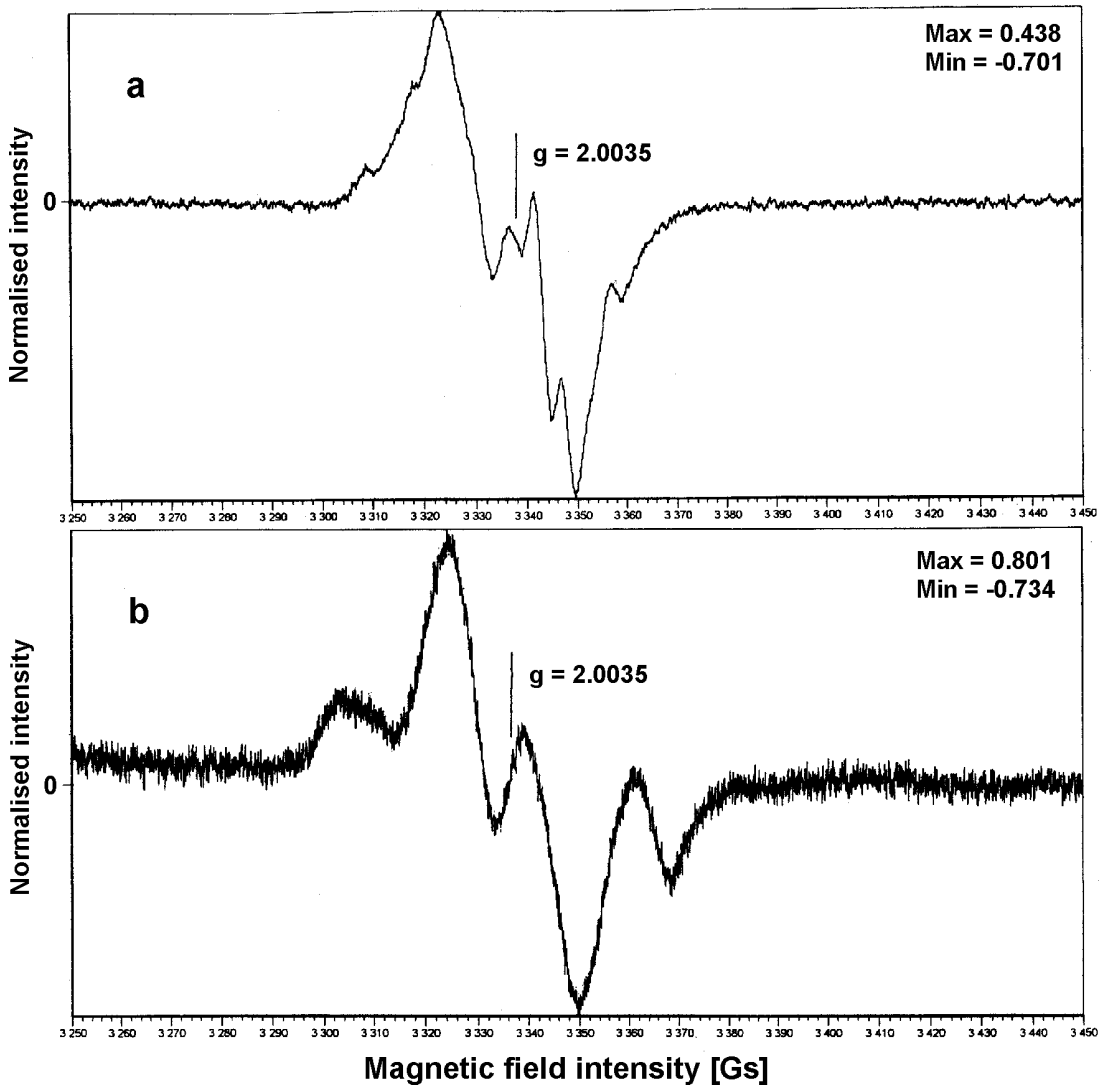

Fig. EPR spectra (first derivative) of dehydrated pulp of papaya (a) and fig (b). Microwave power – 5 mW, dose – 3 kGy.

types. It is because that not only fructose but also some other sugars can be usually found in dried fruits. For this reason the identification of the specific EPR signals in dehydrated fruits exposed to ionising radiation has not yet been achieved. The intensity of the EPR signal and its specific, complex structure is the decisive criterion for the identification of irradiation in dehydrated fruits. Another proof is the measurement of the position of the g-value in the centre of the EPR signal. It should be positioned near to 2.0035, as shown in Fig. The g-value in the EPR spectrum is adjusted by the calculation based on the comparison with g-values of peaks No.3 and No.4 of the well defined Mn^{2+} six line spectrum.

in Fig. In order to evaluate the stability of the EPR signals in irradiated fruits the quantitative measurements of the intensities of the central line belonging to the main EPR spectral component of the complex signal have been done. The results are comprehended in Table.

As seen, the decrease of the intensities after 30 days of storage is not significant. It can be expected, therefore, that after prolonged storage time of several months the irradiation will be still detectable.

The negative result of the experiments done on plums and apricots may indicate that the crystalline sugar domains were probably not present in the pulps of these fruits. The presence of such domains depends on the specificity of fruits but also on the

Table. Peak-to-peak heights (h_{pp}) of the stable EPR signals recorded in the pulp of dehydrated fruits exposed to different of gamma radiation. The numerical data normalised for mass (per 100 mg) and gain (1000). Microwave power – 5 mW.

Absorbed dose [kGy]	Pineapple		Banana		Date		Fig		Papaya		Raisin	
	Storage time after irradiation											
	7 days	30 days	7 days	30 days	7 days	30 days	7 days	30 days	7 days	30 days	7 days	30 days
0	no signal recorded		0.084[a]		no signal recorded		0.010[a]		no signal recorded		0.072[a]	
0.5	0.235[b]	0.235[b]	0.338[b]	0.318[b]	0.048[c]	0.039[c]	0.130[c]	0.106[c]	0.376[b]	0.235[b]	0.187[c]	0.105[c]
1	0.377[b]	0.377[b]	0.361[b]	0.368[b]	0.107[c]	0.108[c]	0.231[c]	0.184[c]	0.384[b]	0.384[b]	0.201[c]	0.200[c]
3	0.628[b]	0.628[b]	0.388[b]	0.376[b]	0.123[c]	0.113[c]	0.292[c]	0.189[c]	0.447[b]	0.420[b]	0.446[c]	0.346[c]

[a] a narrow single EPR line (native EPR signal).
[b] modulation amplitude – 0.2 mT.
[c] modulation amplitude – 1.0 mT.

quality of the drying processing. It seems possible, that in the same kind of dehydrated fruits originated from different sources, one product will be easily recognised as irradiated, while another one will meet difficulties in the identification of irradiation by the EPR method. The prolonged storage of dehydrated fruits which will be not opened to the contact with external humidity should not influence the EPR detection of irradiation in this products.

References

[1]. EN 13708, Foodstuffs – Detection of irradiated food containing crystalline sugar by ESR spectroscopy. European Committee for Standardisation, Brussels, October 2001.

[2]. Raffi J. *et al.*: Establishment of an Eastern Network of Laboratories for Identification of Irradiated Foodstuffs. Final Report of Copernicus Concerted Action CIPA-CT94-0134, CCE, March 1998.

[3]. Stachowicz W., Burlińska G., Michalik J., Dziedzic-Gocławska A., Ostrowski K.: The EPR detection of foods preserved with the use of ionising radiation. Radiat. Phys. Chem., 46, 4-6, 771-777 (1995).

[4]. Stachowicz W., Burlińska G., Michalik J., Dziedzic-Gocławska A., Ostrowski K.: EPR spectroscopy for the detection of foods treated with ionising radiation. In: Detection methods for irradiated foods, current status. Eds. C.H. McMurray *et al.* The Royal Society of Chemistry, Information Service, Special Publication No. 171, pp.23-32.

DETECTION OF IRRADIATED PAPRIKA ADMIXED TO FLAVOUR COMPOSITIES OF NON-IRRADIATED SPICES, HERBS AND SEASONINGS

Kazimiera Malec-Czechowska, Wacław Stachowicz

The regulation on the treatment and trade of irradiated foods in the European Union are defined in two directives numbered 1999/2/EC and 1999/3/EC [1, 2]. According to the Directive 1999/2/EC, the irradiated foodstuffs but also foods produced with an admixture of irradiated component(s) should be labelled.

In order to be able to verify the labelling of irradiated foods, it is necessary to apply reliable detection methods capable to identify various groups of the admixture of irradiated foods and irradiated components should be labelled. According to the document issued by the International Consultative Group for Food Irradiation (ICGFI) spices, medical herbs and seasonings are most frequently irradiated around the world [3]. According to the Directive 1999/3/EC only these products are currently accepted for free distribution in the European Union.

Table 1. Composition of food products used in experiments.

Commercial name of the product	Composition
Herbal composite for salad	Dried parsley, onion leaves (chive), paprika, leek, onion, celery, dill, carrot, lovage
Mixed spices for the filling of cottage cheese	Paprika, salt, onion, parsley, garlic, chive, caraway, black pepper, cayenne pepper, nutmeg, basil
Seasoning for butter	Onion, salt, white pepper, E 620, garlic, powdered mustard, parsley, E 330, dill, chive, lovage, parsnip, paprika
Seasoning for salad	Chive, white mustard, parsley, tarragon, garlic, onion, nutmeg, pepper, paprika

The detection of irradiated spices, medical herbs and seasonings is achieved with the use of several

methods. Some of these methods have the status of European Standards, for example those based on EPR spectroscopy enabling the detection of irradiated foods containing cellulose (EN 1786) and on thermoluminescence (TL) measurements allowing the detection of irradiated foods which contain silicate minerals (EN 1788) [4, 5]. Both methods are routinely used in the Laboratory for Detection of Irradiated Foods (Institute of Nuclear Chemistry and Technology) for the detection of irradiation in foods delivered by the clients for the control.

Recently, in the Laboratory the research work is carried out on the usefulness of the TL method for the detection of the admixtured of irradiated spices, herbs, seasonings as well as dehydrated mushrooms. These products appear in small amounts in non-ir-

Table 2. TL intensities integrated over the temperature range 214-284°C and k_{TL} of silicate minerals isolated from food products enriched in irradiated paprika of different concentration.

Name of the product	The percentage of irradiated paprika [%]	TL intensity		TL glow ratio, k_{TL}
		Glow 1	Glow 2	
Herbal composite for salad	0	152053 39457 16115	53377264 37106329 9817211	0.002 0.001 0.001
	0.05	180816 721449 660058	65667430 66474249 36179951	0.003 0.011 0.018
	0.1	246658 828599 238977	67119553 40700188 50683086	0.004 0.020 0.004
	0.3	333066 42025 499785	19458284 3090589 7300188	0.017 0.013 0.068
	1.0	242069 1412755 207287	2176588 23523210 17510246	0.111 0.060 0.012
	5.0	6269088 219904 7608947	9888509 2085533 22939498	0.634 0.105 0.332
Mixed spices for the filling of cottage cheese	0	3459 9141 3015	988470 1191349 189786	0.003 0.007 0.016
	0.05	141465 17493 120859	14670874 2531100 8574786	0.010 0.007 0.014
	0.1	60818 299909 787742	18396767 18265455 22081453	0.003 0.016 0.036
	0.3	752262 26478 377567	1717930 191880 2949059	0.438 0.138 0.128
	1.0	8946062 4995771 6399180	24985566 5358096 9558935	0.358 0.932 0.669
	5.0	16117694 5662439 21944401	12127504 3593316 14475864	1.329 1.576 1.516

radiated foodstuffs such as: (i) type curd cheese (cottage cheese), (ii) red meat sausages "metka", (iii) flavour mixture of spices used for the preparation of cold sauces and dressings.

The communication presents the results of the work on the TL detection of different amounts of admixture of irradiated paprika to non-irradiated mixtures of spices, herbs and seasonings.

Four kinds of commercially produces flavour mixtures were used in experiments. All four are the composites of spices, herbs, seasonings and other

The minerals isolated from individual samples were placed on stainless steel TL measuring dishes 0.1 mm thick and 10 mm in diameter.

The thermoluminescence has been measured with the use of the computer operated TL reader type TL/OSL, model TL-DA-15, Risoe National Laboratory (Denmark) under the following conditions: initial temperature – 50°C, final temperature – 500°C, heating rate – 6°C/s. Three parallel measures on silicate minerals have been done for each model sample.

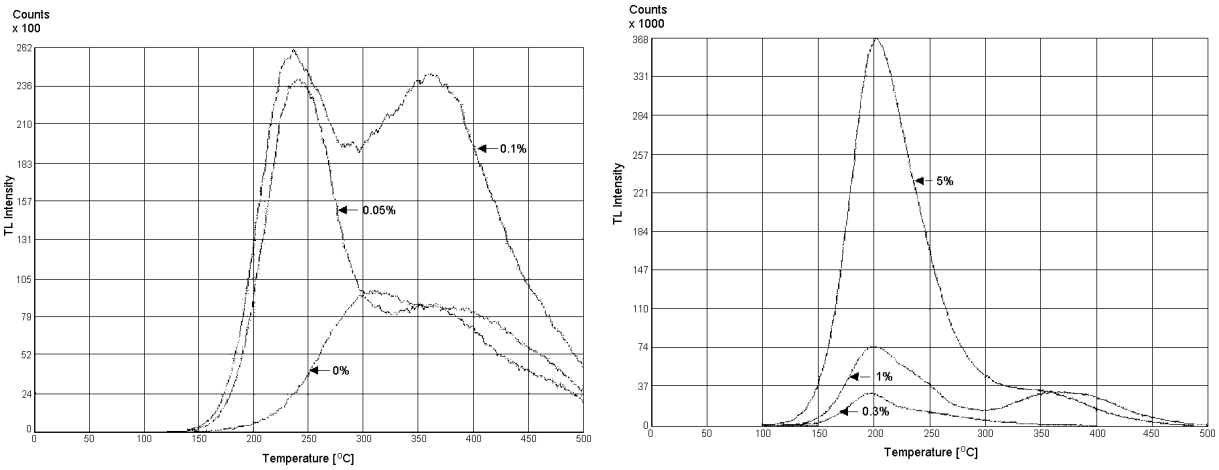

Fig.1. TL glow 1 curves of silicate minerals isolated from herbal composite for salad containing different amounts of irradiated paprika. The percentage of irradiated paprika by weight given in the graph correspond to glow curves marked with arrows.

additives which are allowed to be added to foodstuffs. All contain paprika as one of the components. The products have been purchased in retail trade. The compositions of these products are given in Table 1. They were examined by TL method based on PN-EN-1788 whether irradiated or not. From each kind of the product the model samples were prepared with a known content of powdered paprika irradiated with 7 kGy of gamma rays. The content of irradiated paprika in model samples was as follows: 0.05, 0.10, 0.30, 1.0 and 5.0% by weight. The separation of silicate minerals from the samples was pro-

The glow 1 curves were recorded and then for the purpose of normalization the samples were irradiated with 1 kGy of gamma rays in a ^{60}Co source "Issledovatel". Thereafter, the glow 2 curve was recorded under the same measuring conditions.

It has been proven that the products taken for experiments were not irradiated and hence it was assumed that they do not contain irradiated paprika at all (0%).

TL intensities of silicate minerals integrated over the temperature range 214-284°C (glow 1 and glow 2) as well as the TL glow ratio (k_{TL}) for two

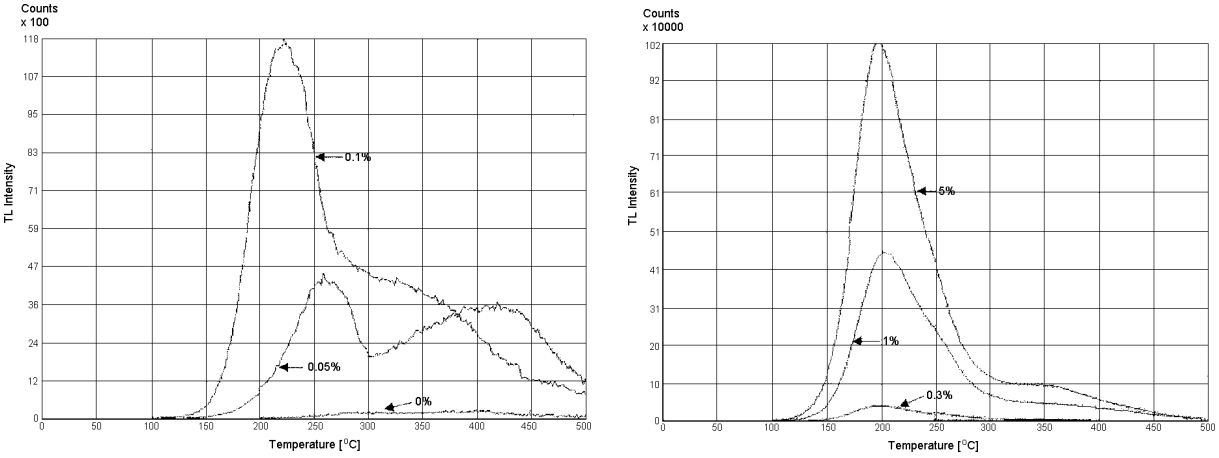

Fig.2. TL glow 1 curves of silicate minerals isolated from mixed spices for the filling cottage cheese containing different amounts of irradiated paprika. The percentage of irradiated paprika by weight given in the graph correspond to glow curves marked with arrows.

ceeded by the procedure given in the standard i.e. by density separation with the use of a water solution of sodium polytungstate of the density 2 g/cm^3.

selected products (mixed spices for salads and mixed spices for filling of cottage cheese) containing different percentage of irradiated paprika are given

in Table 2. The adapted temperature range meets the requirement of PN-EN 1788:2002. The k_{TL} is defined as the ratio of integrated TL intensities of glow 1 to glow 2, evaluated over the adapted temperature range. The glow 1 curves of silicate minerals isolated from the samples are shown in Figs.1 and 2.

The silicate minerals are natural contaminants of spices, herbs and seasonings. They are mainly composed of quartz and feldspar, as proved in earlier works [6-8]. The specific TL of these minerals has its source in the action of earth radioisotopes and cosmic radiation, while the corresponding glow curves have their maxima in the range over 300°C. The presence of irradiated material in the sample influences significantly both TL intensity and the shape of the glow curves of isolated minerals. The content of irradiated components in mineral fraction depends on the content of irradiated paprika in the samples, as seen in Table 2. The glow 1 curves of minerals isolated from the mixtures which contain irradiated paprika are characterised by the TL maximum within the temperature range 235 ±23°C, as shown in Figs.1 and 2. The value of the k_{TL} depends significantly on the content of irradiated paprika in the sample. If this content equals to 0.3% or less (0.05%), k_{TL} becomes much lower than 0.1 while for the contents of irradiated paprika on the level 5.0 and 1.0%, TL glow ratios become higher than 0.1.

The method of the TL measurement on silicate minerals can be successfully used for the detection of irradiation in individual component of multicomponent mixtures of spices, herbs and seasonings.

The criterion decisive for the confirmation of the irradiated component in a multicomponent mixtures of spices, herbs or seasonings is the shape of the glow 1 curve of silicate minerals with a TL maximum within the temperature range 235 ±23°C.

The value of the k_{TL} of the separated mineral fraction is a measure of the content of irradiated component in multicomponent product.

The present work has been done in the frames of the research project No. 6 PO 6T 026 21 financed by the Polish State Committee for Scientific Research (KBN).

References

[1]. Directive 1999/2/EC of the European Parliament and of the Council of 22 February 1999 on the approximation of the Member States concerning foods and food ingredients treated with ionising radiation. Off. J. European Communities L 66/16-23 (13.3.1999).
[2]. Directive 1999/3/EC of the European Parliament and of the Council of 22 February 1999 on the establishment of a Community list of food and food ingredients treated with ionising radiation. Off. J. European Communities L 66/24-25 (13.3.1999).
[3]. Loaharanu P.: IAEA Bulletin, 43, 2, 37-42 (2001).
[4]. European Standard EN 1787:2000. Foodstuffs – Detection of irradiated food containing cellulose – Method by ESR spectroscopy. European Committee for Standardisation, Brussels.
[5]. European Standard EN 1788:2001. Foodstuffs – Thermoluminescence detection of irradiated food from which silicate minerals can be isolated. European Committee for Standardisation, Brussels.
[6]. Pinnioja S., Siitari-Kauppi M., Jernström J., Lindberg A.: Radiat. Phys. Chem., 55, 743-747 (1999).
[7]. Sanderson D.C.W., Slater C., Cairns K.J.: Radiat. Phys. Chem., 34, 915-924 (1989).
[8]. Soika Ch., Delincée H.: Lebensm.-Wiss. u. -Technol., 33, 440-443 (2000).

STUDIES OF THERMAL DECOMPOSITION AND GLASS TRANSITION OCCURRING IN POTATO STARCH, NATIVE AND GAMMA-IRRADIATED

Krystyna Cieśla, Olivier Collart[1/], Etienne F. Vansant[1/]

[1/] Department of Chemistry, University of Antwerp, Belgium

Little is known until now about the processes taking place during heating of dried preparations of biopolymers and the resulting products. Our previous studies carried out by applying thermal analysis methods have shown the differences between thermal decomposition occurring in non-irradiated and gamma-irradiated proteins [1] as well as the differences between thermal decomposition, glass transition, melting and crystallisation behaviour of artificial polymers submitted to heavy ion irradiation.

At present, studies were carried out dealing with the course of the processes taking place during heating of the dried starch preparations in the temperature range from ambient till 1000°C. The studies were carried out applying thermogravimetry (TGA – thermogravimetric analysis, DTGA – differential thermogravimetric analysis), differential thermal analysis (DTA), differential scanning calorimetry (DSC) and Fourier Transform Infrared Spectroscopy (FTIR). The influence of irradiation on the processes of dehydration, glass transition and thermal decompositions was examined.

Several preparations of potato starch were extracted in laboratory applying various conditions. Amylose (A-0512) and amylopectin (A-8515) were Sigma products. The native dried preparations as well as water suspensions were irradiated with ^{60}Co radiation applying various conditions (dose, dose rate). The water suspensions were afterwards dried in vacuum at room temperature. Doses as high as 9, 18, 20, 36 and 440 kGy were used. Irradiations were carried out in a gamma cell "Issledovatel" in the Department of Radiation Chemistry, Institute of Nuclear Chemistry and Technology. The results obtained for the irradiated samples were compared to those obtained for the reference samples, submitted to the same treatment, apart to irradiation.

TGA, DTGA and DSC measurements were carried out using during heating with a rate of 3°C/min in an oxygen and nitrogen stream. The Mettler thermoanalyser and Perkin-Elmer differential scanning calorimeters were used. FTIR spectroscopy was performed at elevated temperature in a nitrogen stream. These instruments are installed in the University of Antwerp, Belgium. Simultaneous TGA, DTGA and DTA measurements were performed in a nitrogen stream applying a Derywatograph Q1500D by MOM, Hungary.

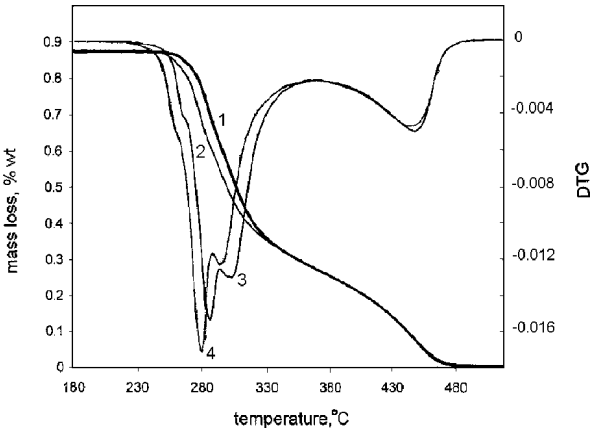

Fig.1. The examples of TGA and DTGA curves recorded for potato starch during heating in oxygen for the reference non-irradiated starch (curves 1, 3) and the solid native sample irradiated with a 20 kGy dose (curves 2, 4). Peak temperature of the first and the second effects recorded on DTGA curves are determined at 287.4 and 305°C in the case of the reference samples and at 280.2 and 296.4°C and the 20 kGy irradiated, respectively. The maximum of the third effect on DTGA was recorded for both samples at *ca*. 450°C.

During heating of potato starch on thermobalance, the mass loss of *ca*. 16% connected to starch dehydration was observed in the temperature range from ambient to *ca*. 130°C. Several stages of thermal decomposition (as concluded on the basis of TG and DTG curves) occur at higher temperature (Fig.1). Three principal stages of decomposition were recorded in the temperature range from *ca*. 220°C till *ca*. 500°C during heating of starch in oxygen. When heated in nitrogen, the process, however, was not finished even at a temperature as high as 1000°C. Two stages decomposition occur during heating of the pure amylose and pure amylopectin preparations.

Two exothermal effects with maxima at *ca*. 302°C and at *ca*. 465°C were observed by DSC in the range up to 500°C during heating in oxygen. These decomposition effects are preceded by a two step increase in heat capacity (Fig.2, detail a). It can be deduced that the increase in heat capacity is caused by glass transition expected for starch in this temperature range [2]. The conclusion was confirmed at present by simultaneous TGA, DTGA and DTA.

FTIR spectra (Fig.3) show on decrease, during heating, of the intensity of the bands corresponding to the absorbed water at *ca*. 1650 nm. Absorbed water disappeared at *ca*. 130°C. The changes in appearance and intensity of the bands corresponding to the O-H and C-H elongation (at 3000-3600

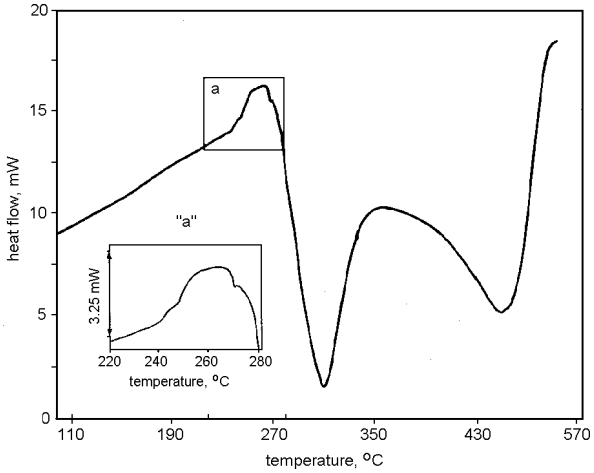

Fig.2. Comparison of DSC curves recorded during heating in oxygen for the initial potato starch irradiated with a 20 kGy dose.

and 2800-3000 nm, respectively) are noticed. At 250°C the intensive bands at *ca*. 1708 and 1620 nm have appeared. Simultaneously, the intensity of the band at 1043 nm, increases and during further heating till 400°C the intensities of the bands at 1135 and 1176 nm increase. It might be concluded, on the basis of the presented data, that some carbonyl groups issued from the rearrangement of the starch chain and that the further thermal treatment leads to a progressive aromatisation of the residue between 250-400°C [3]. Residue contains a meaningful amount of OH groups till 400°C.

Dehydration of the irradiated samples seems to occur in a more narrow range of slightly lower temperature than those of the non-irradiated ones. Differences may be concluded between thermal decomposition processes occurring in the non-irradiated and the irradiated starch on the basis of TGA and DTGA curves. The first stage of thermal decomposition occur after irradiation at lower temperature, while the second and the third stages seems to be inhibited. More material decomposes also during this first stage. The differences were noticed between the influence of the irradiation carried out for dry native starch and starch water suspensions. It results in the more evident separation of effects on the DTGA curves, corresponding to the first and the second stages of thermal decomposition after irra-

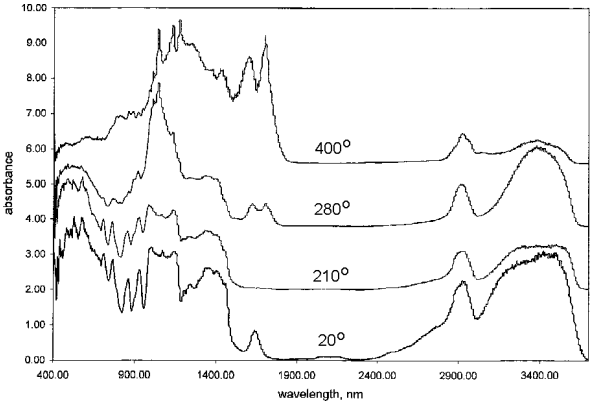

Fig.3. Comparison of FTIR spectra (Kubelka-Munk transformation) recorded for the selected starch sample at 20, 210, 280 and 400°C.

diation of solid dried starch, in comparison to those occurring in the non-irradiated samples. In contrary, the occurrence of those two stages was less evident after irradiation carried out in water suspensions.

No special differences can be observed by DSC in the course of thermal decomposition up to 500°C. Glass transition of the irradiated samples, however, occurs at a lower temperature than glass transition of the appropriate reference non-irradiated samples (Fig.2), due to decreased chain length after irradiation. For example, glass transition temperature was determined (in nitrogen) at 228.5 and 225.0°C for the initial starch and for that irradiated with 20 kGy, respectively.

References

[1]. Cieśla K.: Zastosowanie analizy termicznej w badaniach napromieniowanych białek (Application of thermal analysis in studies of irradiated proteins). Proceedings of the National Symposium on Radiation Techniques in Medicine, Industry, Agriculture and Environmental Protection, Rynia, April 1995, pp.148-152.

[2]. Karel M., Anglea S., Buera P., Karmas R., Levi G., Roos Y.: Thermochim. Acta, 246, 249-269 (1994).

[3]. Marin N., Krzton A., Koch A., Robert D., Weber J.V.: Thermal Anal. Cal., 55, 765-772 (1999).

MODIFICATION OF THE PROPERTIES OF MILK PROTEIN FILMS BY GAMMA IRRADIATION AND POLYSACCHARIDES ADDITION

Krystyna Cieśla, Stephane Salmieri[1/], Monique Lacroix[1/]

[1/] Canadian Irradiation Center, Research Laboratories in Sciences Applied to Food, INRS-Institute Armand Frappier, University of Quebec, Laval, Canada

Edible packaging based on proteins, polysaccharides, lipids or their combination serves as a barrier for water, oxygen and lipid transfer in food system. Using the edible films and coating meets the increased consumer demand for both higher quality and longer shelf-life foods and the necessity for environmental protection. Moreover, the cost of raw material is low. Therefore, during the last years the interest increases in improvement of the properties of such packaging by using the modified composition or applying various chemical and physical treatment. Gamma irradiation was found to be an effective method for improvement of both barrier and mechanical properties of the films and coatings based on calcium and sodium caseinates alone or combined with some globular proteins [1, 2]. It is in regard to the radiation induced crosslinking.

At present, the studies were carried out dealing with influence of gamma irradiation on the properties of the films containing calcium caseinate, whey protein isolate and glycerol (1:1:1). Moreover, the influence was tested of the addition of three polysaccharides to films composition (at a ratio of polysaccharide to total protein amount equal to 0.05:1) [3].

Calcium caseinate (New Zealand Milk Product Inc.), whey protein isolate (by BiPro Davisco) and chemical grade glycerol were used. Sodium alginate, potato starch (insoluble) and potato soluble starch were all Sigma products. The 7.5% solutions containing calcium caseinate were irradiated with gamma rays from ^{60}Co in Canadian Irradiation Centre, applying doses of 0, 8, 16, 32 kGy at a dose rate of 7 Gy s^{-1}. The solutions were dissolved to 5%, heated at 90°C during 30 min and then the films were prepared. Pre-gelatinised polysaccharides were added to the film forming solutions (non-irradiated and irradiated with a 32 kGy dose) before thermal treatment. Sodium alginate was added, however, to the solution before or after irradiation in purpose to test whether the change in preparation method will influence properties of the resulting films.

The films were kept after peeling for 48 h at 56% humidity at ambient temperature. Water vapour permeability (WVP) tests were conducted using a modified ASTM procedure [2] at a temperature of 30°C and relative humidity of 56%. Mechanical tests [2] (tensile strength, deformation, viscoelasticity) were carried out using a Stevens LFRA Texture Analyser Model TA/100 (USA). Analysis of variance and Duncan multiple-range tests with p 0.05 (applying the SAS statistical package) were used to analyse the results statistically. The Student-t test was used and paired-comparison. Differences between means were considered significant when p 0.05.

Improvement of the film strength results from irradiation. The results obtained for composition of calcium caseinate-whey protein isolate-glycerol (1:1:1) are shown in the Table. The values of tensile strength are significantly (p 0.05) higher in the case of the irradiated films than in the case of the reference ones and higher when the irradiation dose is higher. Simultaneously, water vapour permeability decreases when the irradiation dose increases. It is accompanied by creation of the more rigid films, as shown by the lower values of deformation as well as of higher values of the viscoelasticity factor.

Addition of potato starch and sodium alginate induces diminution in films elasticity. For example, viscoelasticity coefficients were equal to 0.555 and 0.553 for the non-irradiated films containing potato starch and sodium alginate, respectively, as compared to 0.524 found for these containing proteins alone.

Addition of insoluble potato starch to the film forming solution do not influence in a really essential way tensile strength of the resulting films (although p 0.05 for both non-irradiated and irradiated films). It causes, however, improvement of the barrier properties, showed by a significantly lower value of WVP. It might be also concluded

Table. Properties of the calcium caseinate-whey protein isolate-glycerol (1:1:1). The groups distinguished using SPSS statistical programme (Duncan test) for all the films (together with those containing polysaccharides) are shown in parantheses. There is no meaningful difference between the mean value in the same column followed by the same letter.

No.	Dose [kGy]	Tensile strength [N·mm^{-1}]	Deformation [mm]	Viscoelasticity	WVP [x10 g·mm/m^2·d·mm Hg]
1	0	53.9 ± 2.6$^{(b)}$	4.46 ± 0.29$^{(f)}$	0.524 ± 0.01$^{(a)}$	168.6 ± 10.1$^{(e)}$
2	8	57.9 ± 3.1$^{(c)}$	4.27 ± 0.37$^{(d, e, f)}$	0.546 ± 0.02$^{(b)}$	151.3 ± 11.9$^{(d)}$
3	16	63.0 ± 2.8$^{(d)}$	4.14 ± 0.44$^{(c, d, e)}$	0.549 ± 0.02$^{(b)}$	135.0 ± 13.2$^{(c)}$
4	32	77.4 ± 3.2$^{(f)}$	4.07 ± 0.35$^{(c, d)}$	0.561 ± 0.01$^{(c, d)}$	114.9 ± 9.6$^{(b)}$

that the barrier properties of the films prepared with starch additive were similar, independently whether the solutions were irradiated or not.

A smaller tensile strength and slightly higher WVP values were detected in the case of films prepared from the non-irradiated solution containing soluble potato starch, as compared to the films prepared from the solution containing proteins alone. Although significant decrease in WVP accompanied by increment in tensile strength takes place after irradiation, the irradiation effect is smaller than in the case of the films prepared using the other compositions (Figs.1 and 2).

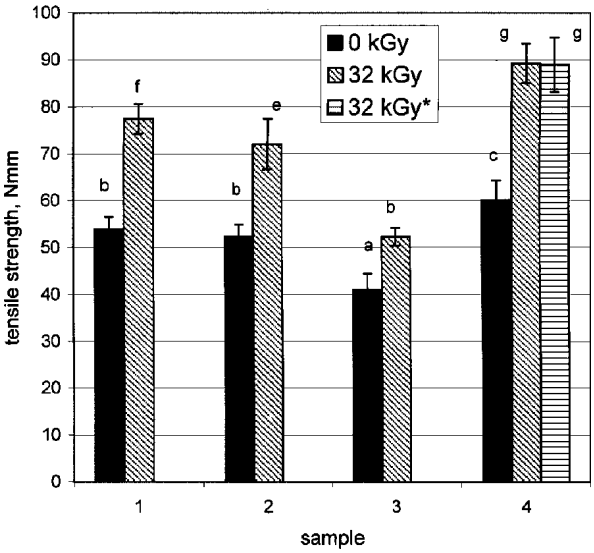

Fig.1. Tensile strength of the films prepared using various compositions, non-irradiated and irradiated with a 32 kGy dose: 1 – calcium caseinate-whey protein isolate-glycerol (1:1:1), 2 – calcium caseinate-whey protein isolate-glycerol-potato starch (1:1:1:0.05), 3 – calcium caseinate-whey protein isolate-glycerol-potato soluble starch (1:1:1:0.05), 4 – calcium caseinate-whey protein isolate-glycerol-sodium alginate (1:1:1:0.05). The groups distinguished using Duncan test are shown by letters. There is no meaningful difference between the mean value followed by the same letter.

The non-irradiated films prepared with addition of sodium alginate have revealed the improved barrier properties and mechanical resistance as compared with the films prepared from protein alone or with addition of both starch polysaccharides. Irradiation induces, moreover, further improvement of the films properties (Figs.1 and 2). In result, the films characterised by the smallest permeability and the largest mechanical resistance were obtained on the way of irradiation of the solution accompanied by addition of sodium alginate. It was stated that the tensile strength and water vapour permeability of the films obtained from the

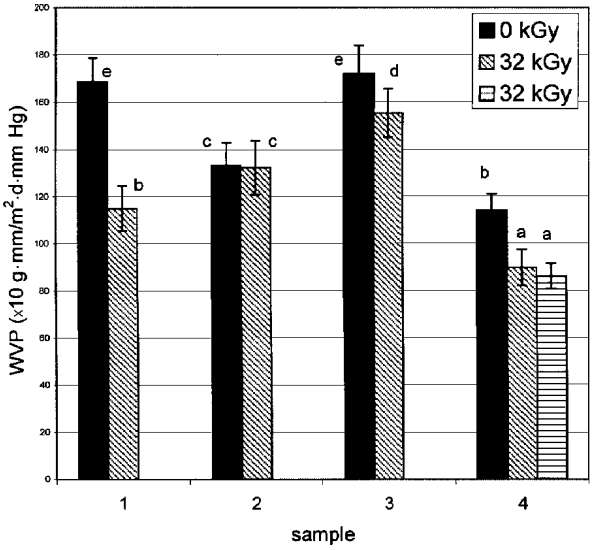

Fig.2. Water vapour permeability of the films prepared using various compositions, non-irradiated and irradiated with a 32 kGy dose: 1 – calcium caseinate-whey protein isolate-glycerol (1:1:1), 2 – calcium caseinate-whey protein isolate-glycerol-potato starch (1:1:1:0.05), 3 – calcium caseinate-whey protein isolate-glycerol-potato soluble starch (1:1:1:0.05), 4 – calcium caseinate-whey protein isolate-glycerol-sodium alginate (1:1:1:0.05). The groups distinguished using Duncan test are shown by letters. There is no meaningful difference between the mean value followed by the same letter.

irradiated solutions containing additive of sodium alginate were similar ($p>0.05$) to those obtained after addition of this polysaccharide to the irradiated solution. The films of this first type seem, however, to be more elastic (as shown by larger deformation and smaller viscoelasticity coefficient) than the films prepared when the compound was introduced to the solution after irradiation.

It arises from our experiments that addition of sodium alginate accompanied by irradiation enable to obtain the films characterised by the best mechanical and barrier properties in relation to the other compositions tested in the present work.

Financial support of the International Atomic Energy Agency (IAEA) enabling to perform the studies (fellowship of K. Cieśla) is appreciated.

References

[1]. Brault D., G'Aprano D., Lacroix M.: J. Agric. Food Chem., 45, 2964-2969 (1997).

[2]. Lacroix M., Le T.C., Ouattara B., Yu H., Letendre M., Sabato S.F., Mateescu M.A., Paterson G.: Radiat. Phys. Chem., 63, 827-832 (2002).

[3]. Cieśla K., Salmieri S., Lacroix M.: Modification of the properties of milk protein films by gamma irradiation and starch polysaccharides addition. Nucl. Instrum. Meth. Phys. Res. B, submitted.

PROGNOSIS OF THE APPLICATION OF SPICES, NON-DECONTAMINATED AND DECONTAMINATED BY IRRADIATION ON THE SANITARY STATE OF FOODSTUFFS

Wojciech Migdał, Hanna B. Owczarczyk

The concept of Hazard Analysis Critical Control Point (HACCP) System ensures food safety and quality through the identification of potential hazards and establishes preventive technological measures to reduce risk probability. Critical Control Point (CCP) is a step in which control can be carried out and is essential to prevent or eliminate food safety hazard or reduce it to an acceptable level. From this point of view the microbial quality of raw materials used for manufacture of food products becomes one of the CCP steps that needs determination of critical limits for microbial contamination and evaluation of corrective action, if required.

The process of radiation pasteurization when applied to spices, together with microbiological prognosis, may serve as an example of preventing action in the HACCP System.

Pathogen Modeling Program ver.4 (PMP) was used to determine risks connected with applying contaminated spices in raw pork-butcher's meat type "metka" [1]. According to the PMP program the main parameters in the "metka" are given in Table 1. The selection of microorganisms for the prognosis is supported by the fact, that *Salmonella sp, Staphylococcus aureus, Enterobacteriaceae family* and *Listeria monocytogenes* are the reason of many alimentary and other diseases [2, 3]. *Coliform bacteria* are also the indicators of hygienic purity in the production. It has been assumed, that microbiological contamination of spices as 40 000 colonies for units (cfu/g) even in conditions of good manufacturing practice, the spices can be contaminated at that level [4]. For that reason, contamination of the final product "metka" by microorganisms will be at a level of 400 cfu/g. It has been assumed, that irradiation at a dose of 10 kGy decreases the primary contamination of spices by 6 logarithmic cycles [5]. In that case, total count of microorganisms in the "metka" will be at a level of 0.0004 cfu/g. The storage time has been predicted as 120 h.

Table 1. The basic parameters and level contamination of the "metka" product.

Parameters	Characteristics
NaCl content [%]	2.7
pH	6.5
Sodium nitrite content [μg/g]	125
Storage temperature	10 and 20°C
Content of spices [%]	1
Critical microorganisms	*Escherichia coli 0157:H7, Salmonella sp, Staphylococcus aureus, Listeria monocytogenes*
Level of contamination	40 000

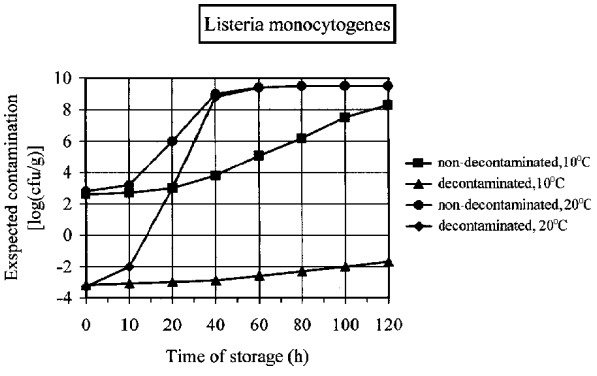

Fig.1. Prognosis of consequence of decontamination of spieces by irradiation in the "metka" product – *Listeria monocytogenes*.

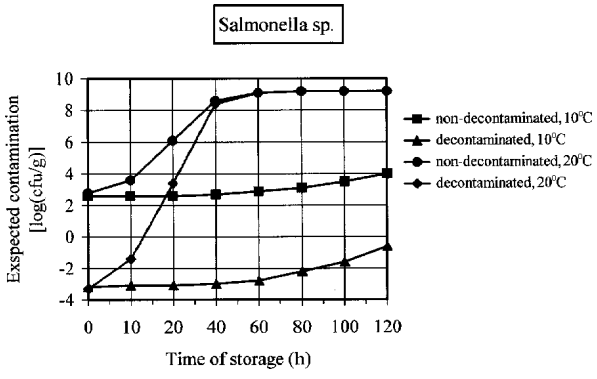

Fig.2. Prognosis of consequence of decontamination of spieces by irradiation in the "metka" product – *Salmonella sp*.

Expected growth of pathogenic bacteria in the "metka" is given in Figs.1-4. In the case of non-decontaminated spices, the growth probability of *Listeria monocytogenes* increases in the "metka" stored at

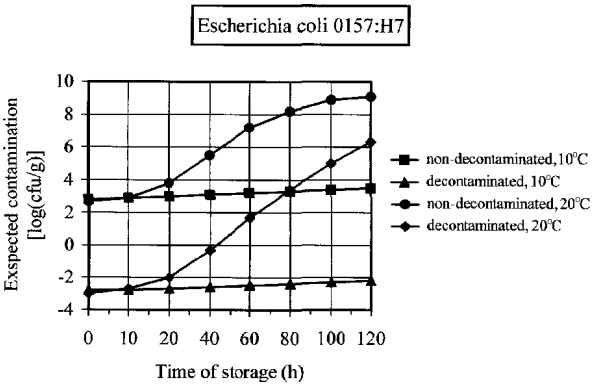

Fig.3. Prognosis of consequence of decontamination of spieces by irradiation in the "metka" product – *Escherichia coli*.

10°C. After 30 h of storage, the growth of that microorganism will be in the lag phase (Fig.1). This results confirm the fact that pathogen is able to grow even at lower temperatures [6]. In the same conditions, the level of contamination by *Salmonella* and *Escherichia* should not be changed (Figs.2 and 3). The growth of *Staphylococcus aureus* is not probable.

The growth of particular pathogens should be changed at a temperature of 20°C. The growth of *Listeria monocytogenes* and *Salmonella* should be very intensive (Figs.1 and 2). The growth of *Staphylococcus aureus* is also probable (Fig.4). So, the temperature is a parameter which influences on the quality and quantity of pathogenic bacteria in the "metka".

The growth curves of pathogenic bacteria in the "metka" with decontaminated spices at 10°C may be described as follows: the contamination level of the "metka" can be assess in categories of survival probability only, but not in the real microorganism presence. It means that practically one cell bacteria will be present in 10 or more grams of the "metka".

Increase of temperature to 20°C causes an increase of microorganism growth. Approximate time of storage at that temperature at which 1 cfu/g will be present is given in Table 2. It can been seen that radiation decontamination of spices causes extension of the storage time of the "metka" at 20°C.

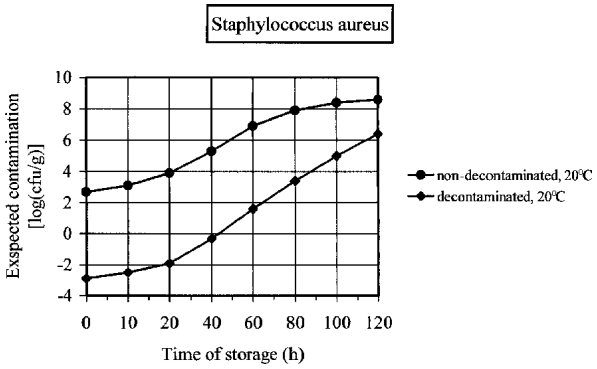

Fig.4. Prognosis of consequence of decontamination of spieces by irradiation in the "metka" product – *Staphylococcus aureus*.

The results of the presented prognosis show that microbiological radiation decontamination of spices assures a good quality of the final "metka" product. That process eliminates a food safety hazard and may be the one of the steps in the HACCP System.

Table 2. Estimation of the storage time of the "metka" needed to be contaminated at a level of 1 cfu/g (h).

Pathogen	Decontaminated spices	Non-decontaminated spices
Escherichia coli	40-45	0
Listeria monocytogenes	10-15	0
Salmonella sp.	12-15	0
Staphylococcus aureus	25-30	-

References

[1]. PMP (Pathogen Modelling Program). Philadelphia, USA 1994.
[2]. Safety and nutritional adequacy if irradiated food. WHO, Geneva 1994.
[3]. Food Irradiation. WHO, Geneva 1988.
[4]. Report of an ICGFI Consultation on Microbiological Criteria of Food to Futher Processed Including by Irradiation. WHO, Geneva 1989.
[5]. Mossel D.D.A., Nadkarni G.B.: Microbiological status and antifungal properties of irradiated spices. J. Agric. Food Chem., 32, 1061 (1985).
[6]. Trojanowska K.: Mikroorganizmy w żywności – sojusznicy czy wrogowie. PTTŻ, Poznań 1995.

RADIATION DECONTAMINATION OF LYOPHILISED VEGETABLES AND FRUITS

Hanna B. Owczarczyk, Wojciech Migdał, Paweł Tomasiński

Lyophilised products are the products which after being sublimated keep theirs natural properties such as vitamins, smell, colour and nutritious value. That food can be stored for a very long period of time (from 1 to 2 years) and is free from preservatives and salt. After being dried, the products are very light as lose 95% of their weight (water). The products can be raw or cooked, crumbled or whole; they only need some water and then return to their natural freshness. This is perfect food supplies. For

Table 1. Microbiological contamination of lyophilised vegetables and fruits before irradiation.

Samples	Aerobic bacteria [cfu/g]	Moulds [cfu/g]	*Enterobacteriaceae* [family in 0.01 g]
Chive	4.8×10^4	1.1×10^2	+
Horseradish	1.5×10^5	10	-
Parsley	1.1×10^6	3.4×10^3	+
Carrot	9.2×10^2	3.0×10^2	+
Dill	4.3×10^5	4.1×10^2	-
Celery	2×10^4	110	-
Leek	1.9×10^5	3.0×10^2	+
Garlic	4.8×10^4	50	-
Beetroot	0.9×10^3	1.0×10^2	+
Corn	6.3×10^4	2.0×10^3	+
Strawberries	5.1×10^3	3.2×10^2	+
Bananas	2.0×10^4	1.3×10^3	+
Blueberries	1.5×10^5	1.2×10^2	-

cfu – colonies for units; (+) – present; (-) – absent.

all of that, the technology of lyophilisation not always ensures high microbiological purity of products as is required. Degree of microbiological decontamination and organoleptic properties of lyophilised vegetables and fruits was investigated after radiation treatment.

Lyophilised raw vegetables and fruits were the research materials. The samples were irradiated at a dose of 5 kGy from an accelerator "Elektronika" 10-10 (10 MeV, 10 kW). Microbiological analysis concerned enumeration of total count of aerobic bacteria, moulds and count of coliform bacteria [1].

Microbiological contamination of lyophilised vegetables and fruits before and after irradiation is given in Tables 1 and 2. Analysis has shown that before irradiation the total count of aerobic bacteria in lyophilised horseradish, dill, leek and blueberries exceeded permissible level ($1x10^5$). In most cases *Enterobacteriaceae* family was present. In some samples the content of moulds was also higher than allowed (Table 1). Decontamination by irradiation at a dose of 5 kGy was sufficient to achieve a high microbiological purity of all the lyophilised vegetables and fruits (Table 2). The lyophilised vegetables and fruits did not change their organoleptic properties such as colour, taste, smell and consistency after irradiation.

Table 2. Microbiological decontamination of lyophilised vegetables and fruits after irradiation at the dose 5 kGy.

Samples	Aerobic bacteria [cfu/g]	Moulds [cfu/g]	*Enterobacteriaceae* [family in 0.01 g]
Chive	6.0×10^2	1.1×10^2	-
Horseradish	1.2×10^3	<10	-
Parsley	2.8×10^3	3.0×10^2	-
Carrot	1.9×10^2	5.1×10^1	-
Dill	2.0×10^2	-	-
Celery	2.1×10^2	-	-
Leek	<10	-	-
Garlic	1.1×10^1	-	-
Beetroot	<10	-	-
Corn	2.1×10^2	-	-
Strawberries	<10	-	-
Bananas	<10	-	-
Blueberries	1.8×10^2	-	-

cfu – colonies for units; (+) – present; (-) – absent.

POLISH-CHINESE INTERCOMPARISON OF HIGH-DOSE GAMMA-RAY DOSIMETRY

Zofia Peimel-Stuglik, Min Lin[1/], Sławomir Fabisiak, Ying Cui[1/], Huazhi Li[1/], Zhenhong Xiao[1/], Yundong Chen[1/]

[1/] Radiometrology Centre of China Institute of Atomic Energy, Beijing, China

High-dose intercomparison between the Laboratory for Measurements of Technological Doses (LMTD) of the Institute of Nuclear Chemistry and Technology (INCT), and the Radiometrology Centre of China Institute of Atomic Energy (RCCIAE, Beijing, China) started in the middle of 2002. The test was aimed at a check of gamma-ray dosimetry procedures used in both participated laboratories and also at the check of transfer dosimeters developed and used in RCCIAE.

During the first part of test, described here, LMTD acted as reference irradiation laboratory and RCCIAE as the transfer dosimeter owner. The results of comparison are presented below. The reference quantity was the absorbed dose in water.

China-produced alanine-PE foil dosimeters were manufactured by extrusion of a mixture of crystalline DL-α-alanine powder with a low-density polyethylene (LDPE) at a ratio of 2:1 in weight. LDPE acts as a binder and does not contribute to the zero signal or irradiation induced signal. Before extrusion, DL-α-alanine and LDPE were mixed in a mill at about 110°C. The mixture was subsequently extruded at 160~165°C by a Bravender plastogragh [1] and finally formed into a strip with 30 mm in width and 180~220 μm in thickness, which was then cut into dosimeters of 30 mm in length and 7.5 mm in width. Because of good resistance to environmental conditions alanine-polymer dosimeters were irradiated without any individual cover.

A calibration curve established in CIAE was based on Fricke dosimeter as a reference standard. The irradiation was performed in a standard water phantom by a ^{60}Co gamma source, whose dose rate was 2.50 kGy/h. Irradiation temperature was controlled within 24 ±2°C.

Chinese transfer dosimeters were measured by a BRUKER EMX/2.7 EPR spectrometer with a high sensitivity cavity in RCCIAE. The operating parameters were set as follows: 350.3 mT for center magnetic field, 2 mT for scan width, 1.0 mT for modulation amplitudes (100 kHz) and 4 mW for microwave power. The dosimeters were set in the gap of flat quartz holder for fixing the dosimeter in the cavity. Stability was checked periodically using an alanine dosimeter irradiated to about 1 kGy and weak pitch (electron paramagnetic resonance – EPR intensity standards). Peak-to-peak amplitude of EPR-signal was used for the absorbed dose measurement. This dosimetric signal has been normalized to the weight of dosimeter, calibrated gain coefficient and EPR intensity alanine standard.

A ^{60}Co gamma source "Issledovatel" (made in the former USSR) is similar in its construction [2] to the well-known Gammacell 220 (Nordion, Canada). Individual ^{60}Co sources are placed at fixed positions around the cylindrical working area. The irradiated samples are lifted automatically (electric motor) into the working area. The stand made from Plexiglas fulfils approximate electronic equilibrium conditions during the INCT calibration irradiation.

The dose absorbed by the sample consists of two parts: (a) dose obtained by the sample at stationary, immobile position and (b) dose obtained during sample moving into and from the radiation field (throw-out or down-up dose). The later one

Table 1. Results of the first run of Polish-Chinese intercomparison. Irradiation date – 2002.08.06 and 2002.08.12.; dose rate – 2.060 and 2.056 kGy/h, respectively; mean irradiation temperature – 24.5°C.

Sample No.	D_{nom} [kGy]	$D_{read-out}$ [kGy]	SD [kGy]	RSD [%]	$(D_{nom} - D_{read-out})/ D_{nom}$ [%]
	Warszawa	Beijing			
1	20.08	19.87	0.04	0.22	+1.05
2	20.08				
3	20.08				
4	0.110	0.124	0.002	1.57	-13
5	0.110				
6	0.110				
7	1.01	1.020	0.001	0.12	-0.99
8	1.01				
9	1.01				
10	5.01	5.047	0.021	0.41	-0.74
11	5.01				
12	5.01				

Table 2. Doses measured by means of Fricke dosimeter. Date of irradiation – 2002.10.01, dose rate – 2.019 kGy/h, mean irradiation temperature – 24.5-24.7°C. Dose obtained in rest, calculated from the dose rate was 50 Gy for dosimeters 1-3 and 100 Gy for dosimeters 4-6.

No.	$A - A_o$ $\lambda = 303$ nm	Dose [Gy]	Mean value [Gy]	SD [Gy]	RSD [%]	Throw-out dose [Gy]
1	0.3001	62.5	62.6	0.43	0.69	12.6
2	0.3018	63.0				
3	0.2987	62.1				
4	0.4755	111.3	112.4	1.15	1.03	12.4
5	0.4838	113.6				
6	0.4794	112.4				

limits from the bottom the dose range offered by "Issledovatel".

The dose rate in stationary conditions, D_t, was established by means of Fricke dosimeter and compared with National Physical Laboratory (NPL, Teddington, United Kingdom) and High Dose Reference Laboratory (HRDL, Risoe, Denmark) during the realization of EU-project IC 15-CT96-0824. Its uncertainty is evaluated to be ±2.1% (k=2). The uncertainty of throw-out dose is higher. Because of that, the combined uncertainty of calibration irradiation in "Issledovatel" is evaluated to be ±2.1% (k=2) only for doses at which the throw-out dose can be omitted (D>1 kGy). For lower doses it grows up and, for instance, for D=0.1 kGy it is estimated to be ±2.3%.

Chinese transfer dosimeters were sent to Poland and irradiated in "Issledovatel". Next, they were sent back to RCCIAE and measured according to the same procedure as that used for calibration curve establishment. The results of measurements had been corrected by irradiation temperature.

At first run of experiment (Table 1), the nominal dose was calculated from the known D_t – value, time of irradiation at rest position and throw-out dose evaluated from repetitive irradiation of Fricke dosimeter.

For higher doses (three dose points) the differences between nominal and measured doses were at a level of 1%, i.e. much lower than the estimated combined uncertainty of gamma irradiation. However, the result for the lowest dose was evidently incorrect and we have to look for the reason of this discrepancy.

Very good results for higher doses evidently confirmed the correct value of the dose rate, D_t. The possibility of wrong time measurements (human error) was rejected. Bad environmental or transport conditions (humidity, water) could lead to read-out a value lower than nominal, instead of experimentally observed – higher one.

In such situation we concentrated on factors peculiar for low doses and decided:

- to check the throw-out dose, i.e. the dose delivered to the dosimeter during sample moving to and out of stationary irradiation position (LMTD);
- to check the calibration curve at the low dose region (RCCIAE).

We also decided to repeat low dose gamma irradiation of alanine-polymer transfer dosimeters together with Fricke dosimeters as direct and the most reliable low dose dosimetry system (run 2).

Table 3. Results of second run of intercomparison. Date of irradiation – 2002.10.01; dose rate – 2.019 kGy/h; mean irradiation temperature – 24.5-24.7°C; the new, improved calibration curve.

Sample No.	D_{nom} [Gy]	$D_{read-out}$ [kGy]	SD [Gy]	RSD [%]	$(D_{nom} - D_{read-out})/ D_{nom}$ [%]
	Warszawa	Beijing			
1	62.6	61.7	1.17	1.89	+1.4
2	62.6				
3	62.6				
4	112.4	111.2	2.6	2.32	+1.1
5	112.4				
6	112.4				

The results of the second run of experiments are shown in Tables 2 and 3.

Throw-out dose used to nominal dose calculation at run 1 was evaluated from 10 repetitive irradiations of Fricke dosimeter and was equal to 10.1 Gy ±10%. New measurements by the same method confirmed this value. However, throw-out dose evaluated from the Fricke dosimeter calibration curve was higher by 20-25%. Similar, higher values of throw-out dose were obtained also from the differences between the doses measured by Fricke system and the doses calculated as a product of dose rate and time of irradiation at rest (Table 2).

We suppose that the lower values obtained before from repeated irradiation can be ascribed to

Table 4. Results of the third run of intercomparison. Date of irradiation – 2002.10.14, dose rate – 2.01 kGy/h, mean irradiation temperature – 23.1°C.

Sample No.	D_{nom} [kGy]	$D_{read-out}$ [kGy]	SD [Gy]	RSD [%]	$(D_{nom} - D_{read-out})/ D_{nom}$ [%]
	Warszawa	Beijing			
1	0.744	0.754	2.6	0.34	-1.3
2	0.744				
3	0.744				
4	6.66	6.754	2.1	0.32	-1.4
5	6.66				
6	6.66				

the higher speed of moving part of the gamma source at repetitive movements than at single irradiation.

Taking into account the corrected throw-out dose equal to 12.5 Gy we calculated a new, corrected value of the dose given to the samples 4-6 (run 1) as 112.5 Gy.

The check on the low-dose part of the calibration curve for the alanine foil dosimeter at RCCIAE gave a new, averaged read-out for samples 4-6: 113.9 Gy (SD=2.1 Gy, RSD=1.89%). So, finally the difference between the nominal and the red-out values diminished to -1.4 Gy i.e. about -1.2%.

To be quite sure of our procedures, we carried out a third run of experiments. Its results are presented in Table 4. A convergence between the nominal and red-out doses was satisfactory.

The intercomparison test oriented on high dose dosimetry of gamma radiation turned out useful for both participated laboratories. Some difficulties observed at the beginning (run 1) that connected with low doses allowed to improve our dosimetric procedures (new calibration curve for alanine-polymer dosimeters in RCCIAE and improved value of throw-out dose in LMTD).

At the moment we can conclude that:

- gamma-ray dosimetry systems used at LMTD and at RCCIAE are compatible with each other within the uncertainty limits of LMTD calibration irradiation facility;
- Chinese production of alanine-polyethylene foil dosimeters and procedures of their use give good transfer dosimetry system for gamma-ray absorbed dose measurement, at least between 60 Gy and 20 kGy.

In the near future we plan to continue comparison tests in the area of electron beam dosimetry.

References

[1]. Kojima T. *et al*.: Appl. Radiat. Isot., 44, 41-45 (1993).
[2]. Stuglik Z.: In: INCT Annual Report 2000. Institute of Nuclear Chemistry and Technology, Warszawa 2001, pp.57-58.

RADIOCHEMISTRY
STABLE ISOTOPES
NUCLEAR ANALYTICAL METHODS
GENERAL CHEMISTRY

EFFECT OF CROWN ETHERS ON THE Sr^{2+}, Ba^{2+} AND Ra^{2+} UPTAKE ON TUNNEL STRUCTURE ION EXCHANGERS

Barbara Bartoś, Aleksander Bilewicz

Radium is an important member of the natural uranium decay series. ^{226,228}Ra released with water from uranium and coal mines causes a significant radioisotope pollution in many regions. Because of the low concentration levels of radium usually encountered in environmental samples, radium determination requires one or more preliminary separation and preconcentration steps, both to free the sample from interfering radioisotopes and to isolate it from relatively large quantities of inactive substances. Typically, this separation and preconcentration includes multiple coprecipitation of Ra^{2+} with $BaSO_4$, subsequent dissolution in EDTA solution and separation on an ion exchange resin. Moreover, the radium levels in many barium reagents are not negligible, sometimes preliminary purification of the reagents is necessary.

The objective of the present work was to separate Ra^{2+} from other Group II cations in a single step utilizing a synergistic effect between crown ethers complexation and ion exchange in α-crystalline polyantimonic acid (PAA) and cryptomelane manganese dioxide (CMD).

The inorganic ion exchangers with tunnel structure like PAA and CMD exhibit a high affinity for heavy alkaline earth cations [1]. Unfortunately, the Ra-Ba separation on these sorbents is rather poor. On other hand, it is known that crown ethers are selective ligands that form stable complexes with alkaline earth cations based on the ionic radius – cavity size compatibility concept [2].

Using the ^{89}Sr, ^{133}Ba and ^{224}Ra radiotracers, distribution coefficients of heavy alkaline earth cations in acidic solutions of crown-5 and crown-6 on the PAA and CMD sorbents were determined. In the case of PAA, selectivity series of $Sr^{2+} > Ra^{2+} > Ba^{2+}$ was found. Crown-5 and crown-6 complexation causes decreasing Ra-Sr selectivity and increasing selectivity for Ra-Ba. CMD has been demonstrated to show excellent ion-exchange selectivity for cations with a crystal ionic radius of 130-150 pm, e.g. Ba and Ra, but selectivity of Ra-Ba is low. As shown in Fig., Ra/Ba selectivity coefficient sharply increases with crown ether concentration, especially with crown-5 which forms much stronger com-

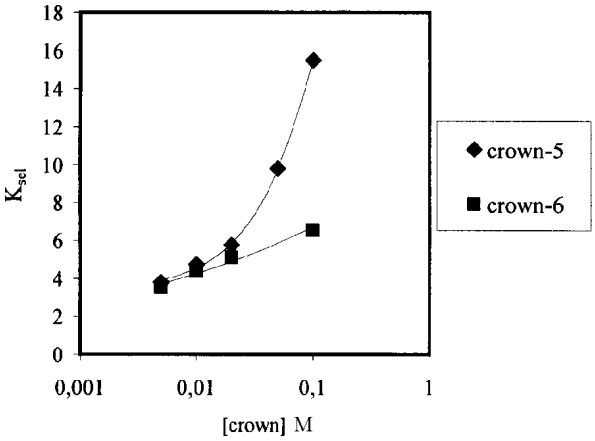

Fig. Influence of crown ether concentration on Ra/Ba selectivity coefficient on CMD.

plexes with Ba^{2+} than with Ra^{2+}. Application of tunnel inorganic sorbents with a crown ether eluent gives a unique possibility to separate Ra^{2+} from other Group II cations in a simple single step procedure.

References

[1]. Bartoś B., Bilewicz A., Delmas R., Neskovic C.: Solv. Extr. Ion Exch., 15, 533 (1997).
[2]. Pedersen C.J.: Science, 242, 536 (1988).

PREPARATION OF THE ^{225}Ac GENERATOR USING A CRYPTOMELANE MANGANESE DIOXIDE SORBENT

Barbara Bartoś, Barbara Włodzimirska, Aleksander Bilewicz

Treatment of cancer by the use of monoclonal antibodies labelled with α-emitting radionuclide is promising and supported by recent clinical reports [1, 2]. The most promising radionuclides are ^{213}Bi ($T_{1/2}$=46 min) and ^{211}At ($T_{1/2}$=7.2 h), and clinical tests employing these two radionuclides are ongoing. Recently, also studies with the longer lived ^{225}Ac ($T_{1/2}$=10 days) are reported [3-5]. The decay process of ^{225}Ac includes four α-emissions and two β^- emissions to a stable ^{209}Bi daughter. As a very large amount of energy (~28 MeV) is released during this process, much lower amounts of activity of the radionuclide are actually required to produce the desired effects, however, this isotope demonstrates extreme cytotoxicity [5].

The ^{225}Ac as a daughter product of ^{225}Ra belongs to the ^{233}U family. The half-life of grandparent, ^{229}Th ($T_{1/2}$=7370 years), is long enough for the generator to be used for a long time.

Numerous methods for milking actinium radionuclides from radium precursors, based on solvent extraction and ion exchange have been described [6, 7]. All these procedures, however, suffer from various limitations e.g. low selectivity, small recoveries and insignificant radiation resistant of the extractans and ion exchange resins. Also ^{225}Ac is eluted with certain organics like citrates [7] or products of radiolytic degradation of extractants and ion exchange resins. To avoid these disadvantages, we have applied an inorganic ion exchanger

– cryptomelane-MnO_2. In the previous paper [8], a simple one-step procedure was used for the separation of ^{228}Ac from ^{228}Ra in the column filled with cryptomelane-MnO_2. This procedure is a basis for the preparation of a ^{225}Ac generator described in the present paper.

Figure presents a scheme of the generator for the production of ^{225}Ac from ^{233}U. The first column was filled with teflon grains impregnated with HDEHP

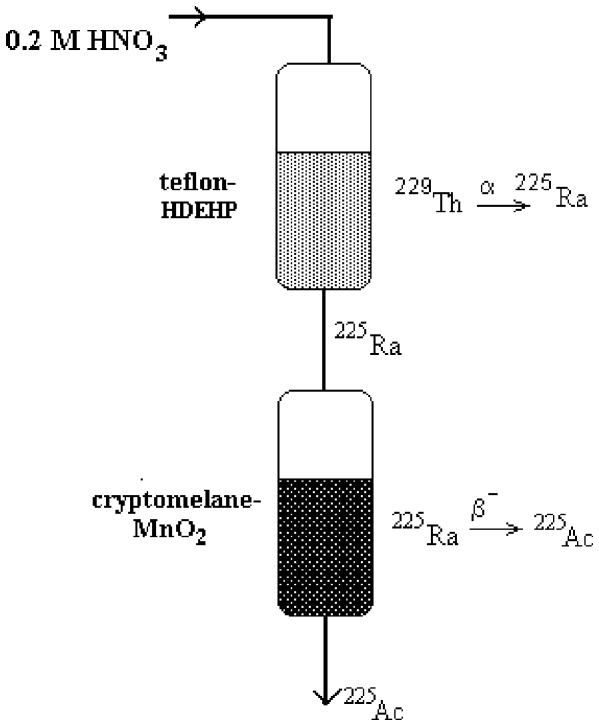

Fig. Scheme of the ^{225}Ac generator system. Columns sizes: HDEHP-teflon – 8x20 mm, cryptomelane-MnO_2 – 3x50 mm.

and the second with the cryptomelane-MnO_2 sorbent. A 30 year old sample of ^{233}U with accumulated decay products dissolved in a 0.2 mol·dm^{-3} HNO_3 solution was loaded onto the first column. In these conditions, only ^{233}U, ^{229}Th and ^{225}Ac were adsorbed by HDEHP, while ^{225}Ra was quantitatively eluted and transported to the second column filled with cryptomelane-MnO_2. After 20 days, which is an optimum time for growing ^{225}Ac in the cryptomelane-MnO_2 column and growing ^{225}Ra in the teflon-HDEHP column, the 0.2 mol·dm^{-3} HNO_3 solution was passed again trough the columns. ^{225}Ra was eluted from the first column and retained on the top of the MnO_2 column and, in the same time, ^{225}Ac was quantitatively eluted from the second (MnO_2) column. As described earlier [8], the cryptomelane-MnO_2 sorbent exhibits an excellent ion-exchange selectivity towards Ra^{2+}. The distribution coefficients of Ac^{3+} are lower by a few orders of magnitudes. The elution-sorption-elution cycles could be repeated many times with no loss of activity.

Very high efficiency of ^{225}Ra-^{225}Ac separation on cryptomelane-MnO_2 allows to produce ^{225}Ac of high radionuclide purity. Combination of ^{225}Ra elution from the HDEHP column, adsorption of ^{225}Ra on cryptomelane-MnO_2, followed by elution of ^{225}Ac makes it possible to produce ^{225}Ac in one cycle. Milking of ^{225}Ac can be repeated many times without breakthrough of the columns. High radiation resistance of the inorganic sorbent makes an additional advantage of this generator system.

References

[1]. Stöklin G., Qaim S.M., Rösch F.: Radiochim. Acta, 70/71, 249 (1995).
[2]. Schubiger A., Alberto R., Smith A.: Bioconjugate Chem., 7, 170 (1976).
[3]. McDevitt M.R. *et al.*: Appl. Radiat. Isot., 57, 841 (2002).
[4]. Deal K.A. *et al.*: J. Med. Chem., 42, 2998 (1999).
[5]. Khalkin V.A., Tsuko-Sitnikov V.V., Zaitseva N.G.: Radiochemistry, 39, 483 (1997).
[6]. Tsuko-Sitnikov V.V., Norseev Y., Khalkin V.A.: J. Radioanal. Nucl. Chem. (Articles), 205, 75 (1996).
[7]. Chuanchu Wu., Brechbiel M.W., Gansow O.A.: Radiochim. Acta, 79, 141 (1997).
[8]. Włodzimirska B., Bilewicz A.: In: INCT Annual Report 2001. Institute of Nuclear Chemistry and Technology, Warszawa 2002, p.59.

IONIC RADII OF HEAVY ACTINIDE(III) CATIONS

Aleksander Bilewicz

Filling of the 4*f* orbitals in the lanthanide series and 5*f* orbitals in the actinide series is accompanied by a significant decrease of the atomic and ionic radii. This effect, called the lanthanide (actinide) contraction, is a consequence of incomplete shielding of outermost *p* orbitals from nuclear charge by the 4*f* and 5*f* electrons, respectively. In addition to the increase of the effective nuclear charge, relativistic effects contribute considerably to the actinide contraction [1]. Relativistic effects influence the contraction of the lanthanide(III) and actinide(III) ionic radii in two ways: by splitting the outermost *p* orbitals and stabilisation of $p_{1/2}$ orbitals, and by expanding the $f_{5/2}$ and $f_{7/2}$ orbitals. The latter results in less effective shielding from the nuclear charge. For the heaviest actinides this may lead to much smaller ionic radii than in the absence of relativistic effects.

For the five heaviest members of the lanthanide series, the spacing between ionic radii of the adjacent elements decreases regularly from 1.3 to 1.0 pm (Table 1). Unexpectedly, in the case of end actinides the spacings between r_i of the neighbouring elements change irregularly. For example, difference in r_i between Es^{3+} and Fm^{3+} is 1.7 pm, whereas that between Md^{3+} and No^{3+} only 0.2 pm.

Ionic radii are usually obtained from X-ray diffraction data for oxides or fluorides. In the case of heavy actinides from Bk^{3+} to Es^{3+}, r_i were determined from lattice parameters of sesquioxides

measured by electron diffraction [4]. Unfortunately, elements heavier than einsteinium are produced in non-weighable amounts, so that the experimental structural data for these elements are

Table 1. Ionic radii of heavy lanthanides and actinides on the Tempelton and Dauben scale.

Ln^{3+} ion	r_i [pm], [2]	An^{3+} ion	r_i [pm]
Ho^{3+}	89.4	Es^{3+}	92.8 [3]
Er^{3+}	88.1	Fm^{3+}	91,1 [4]
Tm^{3+}	86.9	Md^{3+}	89.6 [5]
Yb^{3+}	85.8	No^{3+}	89.4 [5]
Lu^{3+}	84.8	Lr^{3+}	88.1 [6]

not available. For Fm^{3+}, Md^{3+}, No^{3+} and Lr^{3+}, the values of r_i were determined only by the chromatographic method [4-6]. The r_i of Fm^{3+}, Md^{3+} and Lr^{3+} were estimated by comparing their elution position with the position of rare earth tracers and actinides of known ionic radii on a strong acidic cation exchange resin with α-hydroxyisobutyrate solution as eluent [4, 6]. In the case of No, which is unstable in the +3 oxidation state, r_i was also determined chromatographically but on the cryptomelane-MnO_2 – inorganic ion exchanger which shows strong oxidation properties. The HNO_3-H_5IO_6 solution was used both as oxidant and eluent [5].

In order to understand sources of irregularity in the contraction of heavy actinides ionic radii we compared the experimental r_i with radii of the maximum charge density (R_{max}) of the outermost orbital radii of these cations. Linear correlations of r_i on R_{max} and expectation values of orbital radii (<r>) were found for cations of the same charge in many groups of the Periodic Table [7]. These correlations are suitable to predict r_i of ions in case when experimental measurements are difficult or impossible.

Figure 1 presents the dependence of the ionic radius on R_{max} of the outermost shell in the heaviest actinides. The orbital radii have been calculated by V. Pershina using the Dirac-Slater method. As the outermost orbital radii we used the 2j+1 weighted R_{max}. In the case of the heaviest actinides

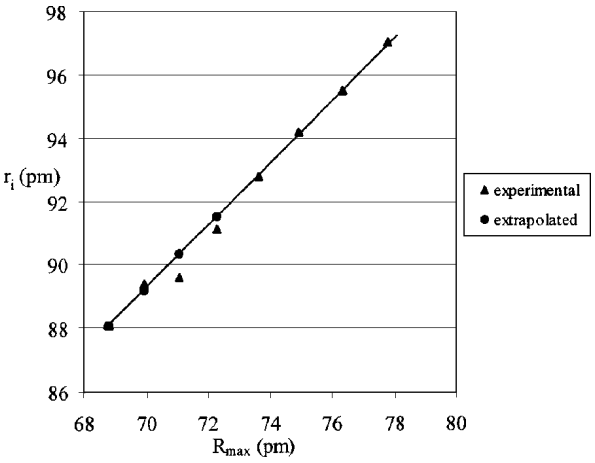

Fig.1 Dependence of the r_i on R_{max} of the outermost shell in the heaviest actinides.

(Bk^{3+}, Cf^{3+}, Es^{3+}, Fm^{3+}, Md^{3+} and Lr^{3+}) all available experimentally ionic radii are given on the Templeton and Dauben scale. In order to make comparison possible, we also used the Templeton and Dauben scale to present the ionic radii of the lanthanide and actinide cations studied. As shown in Fig.1 linear dependence of r_i on R_{max} is observed for +3 actinides from Cm to Es. For these cations the experimental r_i were determined from the electron diffraction on oxides. It is important to notice that r_i of Lr^{3+} and No^{3+} fit the straight-line plot. As shown in Table 2, large differences between the extrapolated and experimental radii are observed for Md^{3+} and Fm^{3+}.

Table 2. Experimental and extrapolated r_i for the heaviest actinides on the Tempelton and Dauben scale.

An^{3+} ion	r_i [pm] experimental	r_i [pm] extrapolated
Fm^{3+}	91.1	91.5
Md^{3+}	89.6	90.3
No^{3+}	89.4	89.2
Lr^{3+}	88.1	88.1

As mentioned earlier, the ionic radii of Fm^{3+}, Md^{3+} and Lr^{3+} were determined only chromatographically. The linear correlation of the logarithm of the distribution coefficients (K_d) with r_i for the tri-positive ions of heavy lanthanides and actinides in α-hydroxyisobutyrate solutions was the basis of the r_i determination for the mentioned cations [4, 6]. Unfortunately, in complexing solutions, when the water molecules in the solvation sphere are exchanged by the ligands, strong deviations from linearity between log K_d and r_i are observed. This effect called the tetrad or double-double effect [8, 9] involves division of the lanthanide and actinide series into two subgroups by f^7 configuration and the further division of each subgroup by the f^3-f^4 and f^{10}-f^{11} pairs. Figure 2 presents the dependence of log separation factor (α) on r_i for the third segments consisting of four Ln^{3+} (Gd^{3+}-Ho^{3+}) and four An^{3+} (Cm^{3+}-Es^{3+}) cations in the α-hydroxyisobutyrate – strong acidic cation exchange resin system. The α_{Ln} are the ratios of K_d of Ln^{3+} divided by K_d of Gd^{3+} and α_{An} are K_d of An^{3+} divided by K_d of Cm^{3+}. As shown in Fig.2, the dependence of log α on r_i for

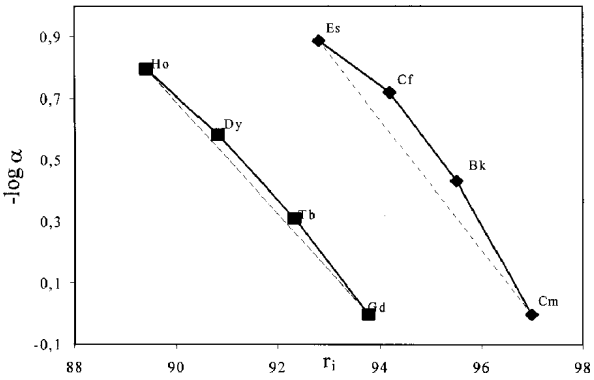

Fig.2. Dependence of log α on r_i for the third segments consisting of four of Ln^{3+} (Gd^{3+}-Ho^{3+}) and four of An^{3+} (Cm^{3+}-Es^{3+}) cations in the α-hydroxyisobutyrate – strong acidic cation exchange resin system.

Ln^{3+} is nearly linear. However, in the case of the third segments of An^{3+} well established tetrad effect and a strong deviation from linearity of this function is observed. This is related to the larger expansion and diffusion of 5*f* orbitals in comparison with 4*f*, which causes a stronger participation of 5*f* orbitals in metal-ligand bonding. Similar effect should take place in the fourth segments of Ln^{3+} (Er^{3+}-Lu^{3+}) and An^{3+} (Fm^{3+}-Lr^{3+}). In the case of Ln^{3+}, a small deviation from linearity is observed, while for Fm^{3+}-Lr^{3+} a strong tetrad effect is expected. As mentioned earlier, crystallographic radii of these cations are not available, therefore, the shape of dependence of log K_d or log α on r_i may be only anticipated. It becomes apparent that the ionic radii of the heaviest An^{3+} cannot be determined using α-hydroxyisobutyrate – cation exchanger experiment, as there is no way of unfolding the tetrad effect from the elution position data. This is the source of the differences between the ionic radii for Fm^{3+} and Md^{3+} determined by this method, and ionic radii calculated from the orbital radii.

References

[1]. Seth M., Dolg M., Fulde P., Schwerdtfeger P.: J. Am. Chem. Soc., 117, 6597 (1994).
[2]. Templeton D.H., Dauben C.H.: J. Am. Chem. Soc., 76, 5237 (1954).
[3]. Haire R.G., Baybarz R.D.: J. Inorg. Nucl. Chem., 35, 489 (1973).
[4]. Chopin G.R., Silva R.J.: J. Inorg. Nucl. Chem., 3, 153 (1956).
[5]. Bilewicz A.: J. Nucl. Radiochem. Sci., 3, 147 (2002).
[6]. Brüchle W. *et al.*: Inorg. Chim. Acta, 146, 267 (1988).
[7]. Siekierski S.: Comments Inorg. Chem., 19, 121 (1997).
[8]. Fidelis I., Siekierski S.: J. Inorg. Nucl. Chem., 28, 185 (1966).
[9]. Peppard D.F., Mason G.W., Lewey S.: J. Inorg. Nucl. Chem., 31, 2271 (1969).

STUDIES OF BISMUTH TRIFLUOROMETHANESULFONATE SOLUTION IN *N,N*-DIMETHYLTHIOFORMAMIDE

Krzysztof Łyczko, Ingmar Persson[1/], Aleksander Bilewicz

[1/] Department of Chemistry, Swedish University of Agricultural Sciences, Uppsala, Sweden

Due to relativistic stabilization of $6p^2_{1/2}$ electron pair bismuth exists in uncommon oxidation state +1, however, the Bi^+ cation is not stable in aqueous solutions [1]. The aim of the present work was to search for stable lower oxidation states of bismuth and towards this goal we investigated solution of bismuth trifluoromethanesulfonate ($Bi(OTf)_3$) in *N,N*-dimethylthioformamide (DMTF). Previously, it was found that the DMTF solvent stabilised lower oxidation states of the metal cations [2, 3]. Dark yellow/red colour is observed upon adding of anhydrous $Bi(OTf)_3$ to the DMTF solvent [4]. DMTF is a monodentate sulfur donor ligand with a high dipole moment (μ=4.44 D) and permittivity (ε=47.5), and is, therefore, a suitable solvent for metal salts.

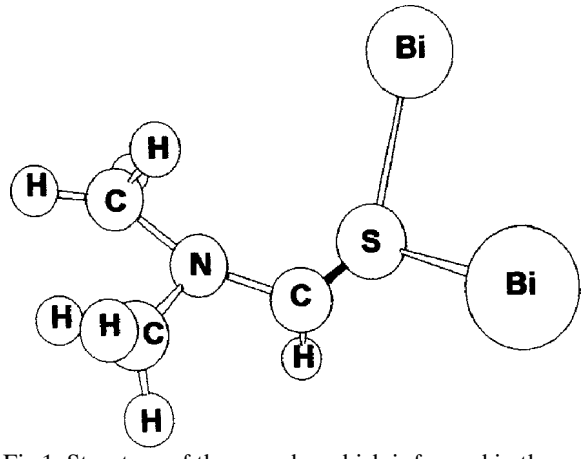

Fig.1. Structure of the complex which is formed in the solution of $Bi(OTf)_3$ in DMTF.

The structure of the solvated bismuth ions in this solution was determined by an EXAFS technique at the Stanford Synchrotron Radiation Laboratory (SSRL), (Fig.1).
It was found that one sulfur atom in the DMTF molecule coordinates two bismuth ions with a mean Bi-S bond distance of 2.54 Å.

To analyze this system, spectroscopic and electrochemical methods were employed. The electron spectroscopy properties of $Bi(OTf)_3$ in DMTF solution have been studied using a GBC Cintra 40 UV-VIS spectrometer. Because of the very high absorption, a thin film of the solution (~0.01 mm) was prepared for the UV-VIS measurements. The maximum of absorption was observed at 457 nm for a wide range of concentrations of the solution (Fig.2).

Far- and mid-infrared spectra of the solution were recorded at room temperature with a Bruker Equinox 55 FT-IR spectrometer and compared

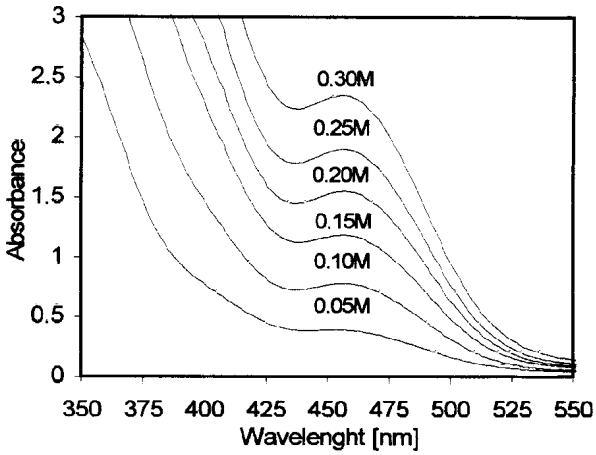

Fig.2. Absorption spectra of the solutions of $Bi(OTf)_3$ in DMTF (thickness of the films about 0.01 mm).

with the spectra of DMTF solvent [5]. The bands observed in the IR spectra can be divided into three groups ascribed to the vibrations of the *N,N*-dimethylthioformamide molecule, the trifluoromethanesulfonate anion and the metal-ligand bond. The bismuth-ligand vibration appears at similar frequencies as for the copper(I) and silver(I) solvates with the same ligand (DMTF) [2]. The bismuth-sulfur stretching contributes strongly to the broad band around 290 cm^{-1}, but probably, also to a weaker band between 380-400 cm^{-1}. The main bands derived from the vibrations of the CF_3SO_3 group are located in the middle part of the infrared spectrum.

In order to confirm the existence of lower than +3 oxidation states of bismuth in Bi-DMTF solvate, a cyclic voltammetry investigation has been carried out. These experiments provided evidence that more than one kind of bismuth ions are present in the solution of $Bi(OTf)_3$ in DMTF. In the reduction half-cycle of the voltammetric curve, we observed two partially overlapping maximas (Fig.3) corresponding to the reduction processes: (1) – Bi(1+) to Bi(0) and (2) – Bi(3+) to Bi(0). The shape of the voltammogram was compared to that recorded for bismuth trifluoromethanesulfonate solution in *N,N*-dimethylformamide (similar ligand but with oxygen atom as donor instead of sulfur). Only a single maximum due to the reduction of Bi(3+) to Bi(0) was found in the latter case.

The intensive colour of $Bi(OTf)_3$ in DMTF solution results probably from the formation of an intervalence charge transfer transition in a dimer containing two bismuth ions connected through a bridging sulfur atom of the solvent molecule. The existence of that dimer was proved by means of EXAFS. The results of the electrochemical studies indicate that in the anhydrous bismuth trifluoromethanesulfonate solution in *N,N*-dimethylthioformamide, bismuth may appear in two different oxidation states: +1 and +3. However, structural studies showed the equivalence of both Bi-S bonds in the dimer suggesting the formation of a resonance structure with both bismuth cations in the oxidation state +2.

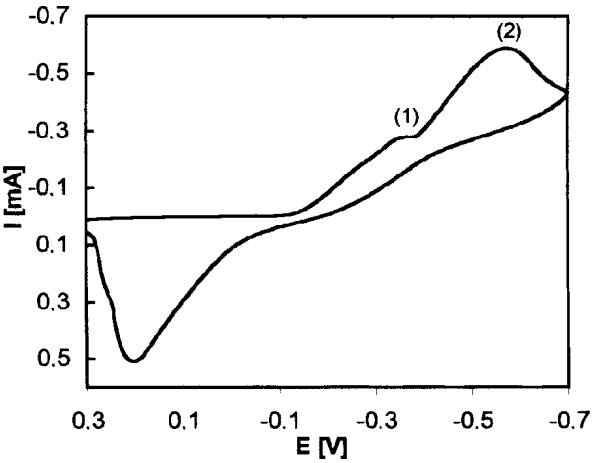

Fig.3. Cyclic voltammogram of the solution of $Bi(OTf)_3$ in DMTF/$Bu_4N(OTf)$; (v=50 mV/s).

References

[1]. Ulvenlund S., Bengtsson L.A.: Acta Chem. Scand., 48, 635-639 (1994).
[2]. Stålhandske C.M.V., Stålhandske C.I., Persson I., Sandström M., Jalilehvand F.: Inorg. Chem., 40, 6684-6693 (2001).
[3]. Persson I., Jalilehvand F., Sandström M.: Inorg. Chem., 41, 192-197 (2002).
[4]. Näslund J., Persson I., Sandström M.: Inorg. Chem., 39, 4012-4021 (2000).
[5]. Stålhandske C.M.V., Mink J., Sandström M., Papai I., Johansson P.: Vib. Spectrosc., 14, 207-227 (1997).

OUTER-SPHERE HYDRATES OF TRIS(PROPANE-1,3-DIONATO)METAL(III) CHELATES: A SUPERMOLECULAR APPROACH

Marian Czerwiński[1/], **Jerzy Narbutt**

[1/] Chemistry Institute, Pedagogical University, Częstochowa, Poland

Interactions between amphiphilic molecules and water play a decisive role in numerous chemical and biochemical processes. Therefore, it is of interest to consider aqueous solutions of metal complexes with organic ligands, containing various hydrophilic and hydrophobic centres, where hydrogen bonding is of primary importance. References cited in [1] are devoted to hydrogen bonding in systems consisting of relatively simple molecules. Less attention was paid to more complex structures, especially those including metal ions. Amphiphilic metal chelates in aqueous solution interact with the solvent on two different ways. Hydrocarbon fragments of ligands promote the local structure of water making it more ordered due to hydrogen bonds formed between the neighbouring water molecules. The negative entropy of the process increases the thermodynamic activity of the chelate molecules in solution. Such a phenomenon is often called hydrophobic hydration. The hydrophilic centres of the metal chelate molecules are specifically hydrated which decreases the thermodynamic activity of the chelates in solution. Apart from inner-sphere hydration of coordinatively unsaturated complexes, where water molecules are bonded *via* their oxygen atoms directly to the central metal ion, increasing its coordination number, other water molecules are hydrogen-bonded to hydrophilic fragments of the ligands, in particular to the electron-donor oxygen atoms which coordinate the central metal ion. In a series of experimental papers [2-5] the second model was studied and called "outer-sphere hydration".

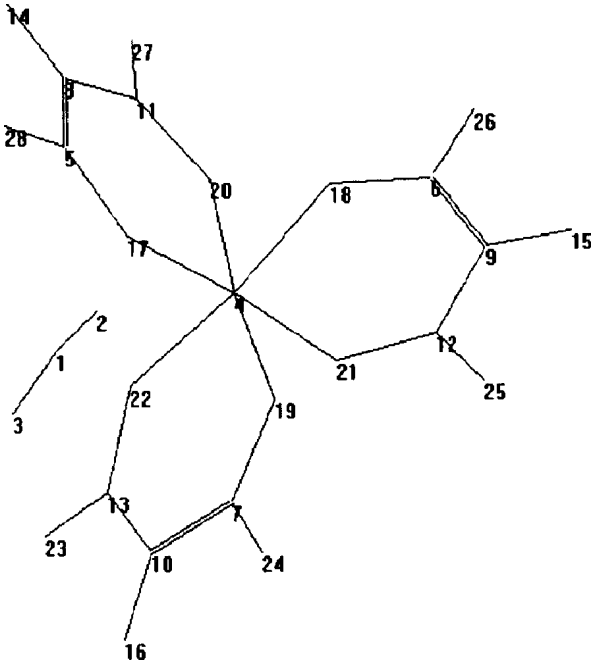

Fig. The optimized geometry of the hydrate $Co(mala)_3 \cdot H_2O$. The metal ion occupies the central position 4, oxygen atoms are situated in sites 1, 17, 18, 19, 20, 21 and 22, while hydrogens are placed in sites 2, 3, 14, 15, 16, 23, 24, 25, 26, 27 and 28. The other sites are occupied by carbon atoms.

Theoretical chemistry well describes simple hydrogen-bonded systems composed of two small molecules [6]. On the other hand, larger hydrogen--bonded systems, especially those containing metal ions, are of interest not only because of their chemical complexity but also due to their practical applications. The aims of this work were: (i) to find quantum chemistry evidence for hydrogen bonding between molecules of water and model compounds, tris(propane-1,3-dionato)metals(III); (ii) to determine the type of hydrogen bond formed; and (iii) finally to find which of the theoretical methods studied most adequately reproduces the properties of these hydrogen-bonded systems.

Two coordinatively saturated metal chelates, further referred to as $M(mala)_3$, were studied: tris(propane-1,3-dionato)scandium(III) and tris(propane-1,3-dionato)cobalt(III), as well as their water adducts, $M(mala)_3 \cdot H_2O$, further referred to as hydrates. The ligand is the deprotonated enol form of malonaldehyde, $[O{=}CH\text{-}CH{=}CH\text{-}O]^-$, further abbreviated $mala^-$, which we assume to be a good model for familiar acetylacetonate. The metal ions, scandium and cobalt(III), have been selected for this study because trisacetylacetonates of these metals had been experimentally characterised by the least (Sc) and the most (Co) negative energies of outer-sphere hydration in aqueous solution of the whole series of 3*d* metal(III) ions, the energy being a function of the metal ion radius [5]. Optimization of the systems: $Sc(mala)_3 + H_2O$ and $Co(mala)_3 + H_2O$ in the gas state leads to hydrates with the water molecule hydrogen-bonded to the oxygen atoms of the coordinated ligands (Fig.).

The calculations by means of the Density Functional Theory (DFT) with the Lanl2dz double-ζ basis set and three-parameter Becke functionals of the B3LYP type have been described in a recent paper [7]. Berny geometry-optimization algorithm was applied to calculate the geometry of the neutral metal chelates, water and their 1:1 adducts. The calculation results have been presented with regard to polarization functions on each atom. The system Hessian with (3*n*-6) eigenvalues confirms that the minimum energies were found for all the compounds. The results were also obtained with corrections for a basis set superposition error (BSSE) and zero-point vibrational energies (ZPVE). All the numerical calculations were carried out using Cray J90 and Cray Y-MP supercomputers, based on the implementation of the GAUSSIAN-94 program [8]. The computational details and equations used (comments to Table 2) to calculate the energy within the supermolecular approach [9] will be presented in a subsequent paper [10].

Table 1 shows some selected geometrical parameters of both hydrates, and the changes in charge distribution on selected atoms due to the hydrate formation. In both hydrates the oxygen atom of water molecule is located at a short distance, of *ca.* 2.8 Å typical for hydrogen bonding, from one of the oxygen atoms (O_{17}) of a $mala^-$ ligand (the numbering of atoms in the hydrates is given in Fig.). Formation of a hydrogen bond ($O_1\text{-}H_2\cdots O_{17}$) between the molecules of water and the chelates studied is, therefore evidenced. The angles α ($O_1\text{-}H_2\text{-}O_{17}$) and β ($O_1\text{-}O_{17}\text{-}C_5$), slightly (below $10^o \div 20^o$) deviated from the expected 180° and 120°, respectively, show that the hydrogen bond is nearly linear and only slightly deviated from the direction of the lone electron pair on the O_{17} atom (sp^2), it is thus the classical hydrogen bond of σ-type (σ-HB). Somewhat shorter $O_1\text{-}O_{17}$ distance in the cobalt than scandium hydrate (Table 1) points to stronger hydrogen bond in the former.

Table 1. DFT-B3LYP optimization of $M(mala)_3 \cdot H_2O$ hydrates: selected geometry parameters, changes of charge distribution on selected atoms in the chelates upon hydrate formation, dipole moments of the hydrates (the numbering of atoms is given in Fig.).

	Distances [Å]		Bond angles[a] [deg]				Charge changes on atoms[b], Δq				μ [debyes]
M	$O_1\text{-}O_{17}$	$O_1\text{-}O_{19}$	α	β	γ	ω	M	O_{17}	H_2	O_1	
Sc	2.806	3.235	171.1	111.5	175.2	110.7	0.012	-0.062	0.074	-0.049	2.76
Co	2.799	3.501	160.1	110.5	170.1	9.0	0.007	-0.080	0.068	-0.042	3.08

[a] Definition of angles: $\alpha = O_1\text{-}H_2\text{-}O_{17}$; $\beta = (O_1\text{-}O_{17}\text{-}C_5)$; $\gamma = C_8\text{-}C_5\text{-}O_{17}\text{-}O_1$; $\omega = M_4\text{-}C_{13}\text{-}H_3\text{-}O_1$.

[b] The charge change, Δq, is the difference between the atom charge in a given chelate and the respective hydrate, calculated using Mulliken population analysis.

A more detailed information of both hydrogen--bonded systems arises from the analysis of dihedral angle ω (M-C_{13}..H_3-O_1) between the direction of the second O-H bond in the water molecule and a line in the plane of another $mala^-$ ligand in the chelate molecule. The great difference between the angles ω in the hydrates of scandium (110.7°) and cobalt (9.0°) chelates clearly suggests that the O_1-H_3 bond is directed towards the plane of another ligand in the scandium chelate, which is not the case for the cobalt system. This different orientation of the water molecule in both hydrates may be interpreted in terms of an additional hydrogen bond formed with the participation of the second proton of the water molecule and π electrons of the other chelate ($mala^-$) ring in $Sc(mala)_3 \cdot H_2O$ but not in $Co(mala)_3 \cdot H_2O$, which is in line with different distances between the water oxygen and the oxygen atom of the other ligand in the hydrates of scandium and cobalt chelates, d(O_1-O_{19}), equal to 3.24 and 3.50 Å, respectively. Because of less usual direction of this hydrogen bond towards the plane of quasi-aromatic chelate ring and of its length significantly greater than classical 2.8 Å (in σ-HB), we assume this additional bond found in $Sc(mala)_3 \cdot H_2O$ hydrate to be of π-type (π-HB).

In both calculation cases, the formation of the $M(mala)_3$-H_2O hydrogen bond has been accompanied by small changes in the geometry of the molecules and in charge distribution on their atoms (Table 1). For example, the M-O_{17} distances increase by about 0.03 Å in the Sc and 0.05 Å in the Co systems. In both systems the O_1-H_2 distances increase by about 0.01 Å. Some electron density displaces from the metal ions to the hydrogen-bonded ligand oxygen atoms. All the results give us the qualitative picture of the hydrogen-bonded systems studied, which is in line with the hypothesis of outer-sphere hydration of metal chelates [2-5].

The next challenge was to characterise the systems quantitatively, i.e. to evaluate the energy of hydrogen bonding in the systems studied, and to explain – at least on the model level – the reason of unexpected [5] stronger hydration, in aqueous solution, of tris(acetylacetonato)cobalt(III) than tris(acetylacetonato)scandium(III). Table 2 shows the values of interaction energy between molecules of water and $M(mala)_3$ calculated by using various models: in the gas phase at 0 K, in gas at room temperature, and in the electrostatic field from the continuum of water molecules at room temperature. The calculations for the gas phase at 0 K show stronger interactions with water of the scandium chelate, even if the energies of σ-HB bonds alone are considered, contrary to the calculated lengths of the hydrogen bonds (σ-HB in both hydrates). Corrections for BSSE and ΔZPVE do not essentially change the picture.

A significant improvement has finally been reached when polarization functions were introduced to the calculation procedure, resulting in the energies of the σ-type hydrogen bonds of -0.0051 and -0.0052 a.u. (-11.5 and -11.7 $kJ \cdot mol^{-1}$) in the Sc and Co systems, respectively, in line with the calculated length of the hydrogen bonds. However, the calculated energy differences for both chelates were still much less than the experimental data [5]. Such a situation is not surprising, because the experiment was carried out at a temperature of 25°C and the chelates were extracted from the liquid phase (in water environment), while the calculations related to isolated systems which may be modelled by the gas phase (vacuum) at a temperature of 0 K. The temperature correction factor accounting for thermal energy of molecules studied, ΔE^T, made the picture even worse pointing to instability ($\Delta G > 0$) of both hydrates in the gas phase at room temperature (Table 2).

The problem arose, how to compare the thermodynamic functions of chelate hydration, calculated for the gas phase, with the experimental data [5] obtained for the two-phase system: dilute aqueous solution where the chelates are hydrated to a different degree and an organic (heptane) solution where both chelates are dehydrated. Because the chelates evenly interact with the organic solvent, only the effect of the aqueous environment may be accounted for. The Self-Consistent Isodensity Polarized Continuum Model (SCI-PCM) [11] has been designed for this purpose. This procedure locates the complex molecule (hydrate) within a cavity in the field modelling water (a continuum of a given dielectric constant), and then determines the electron density which minimises the energy of the system ($E^{SCI\text{-}PCM}$ – Table 2), including the solvation (hydration) energy.

The calculated enthalpies of hydration, $\Delta H^{SCI\text{-}PCM}$, of $Sc(mala)_3$ and $Co(mala)_3$ equal to *ca*. -86 and -91 $kJ \cdot mol^{-1}$ respectively, are about twice as large as the experimental enthalpies of transfer (heptane → water) of the corresponding acetylacetonates [5], the difference in the respective ΔG values being still greater (the effects of van der Waals interactions of the chelates with heptane may be neglected in these considerations). However, the difference between the calculated enthalpy values, +5.2 $kJ \cdot mol^{-1}$, is comparable with the experimental value of +11.3 ±1.9 $kJ \cdot mol^{-1}$. Also the differences between the calculated and experimental ΔG values are comparable (Table 2). This means that the SCI-PCM model does not account for the water structuring effects (hydrophobic hydration), of mainly entropic origin, related to the cavity formation. The effects, presumably of the same value for both chelates, cancel each other when the relative values are considered.

The question arise however, why the aqueous environment makes the cobalt chelate more hydrophilic than the scandium one, while the energies of their hydrogen bonding are practically the same. In our opinion, this effect can be qualitatively explained with the 10% difference between the calculated dipole moments of scandium and cobalt hydrates (2.76 and 3.08 debyes respectively). As a result of electrostatic interactions of the hydrate molecules of significant but different dipole moments with the field created by the continuum of water molecules, the higher decrease in energy is expected for the molecule of higher dipole moment, i.e. the hydrate of cobalt chelate, which can

Table 2. Energies [a.u.][a] of hydrogen bonds in the $M(mala)_3 \cdot H_2O$ molecules, and the related thermodynamic functions, calculated for various models using DFT-B3LYP method.

Model	Function, X	Sc	Co	$\Delta\Delta X_{Sc/Co}$ [b]	Comments
Gas phase 0 K	E_{INT}	-0.0157	-0.0138	-4.3	chelate hydration energy[c]
	E_{INT} – BSSE	-0.0115	-0.0092	-5.2	d:o., corrected for BSSE
	ΔZPVE	-0.0053	-0.0057		correction term[d]
	$E_{\pi HB}$	-0.0016	0		π-type hydrogen bond[e]
	$E_{\sigma HB}$	-0.0088	-0.0081		σ-type hydrogen bond[f]
	$E^{*}_{\sigma HB}$	-0.0051	-0.0052		with polarization functions
Gas phase r.t.	ΔE^{T}	-0.0117	-0.0099		correction term[g]
	$E^{T}_{\sigma HB}$	-0.0197	-0.0180		σ-type hydrogen bond
	ΔH	-0.0128	-0.0110	-4.07	enthalpy of hydration
	ΔG	0.0007	0.0020		free energy of hydration
SCI-PCM Water field r.t.	$\Delta E^{SCI\text{-}PCM}$	-0.0251	-0.0292		correction term[h]
	$\Delta H^{SCI\text{-}PCM}$	-0.0379	-0.0402	5.20	[i]
	$\Delta G^{SCI\text{-}PCM}$	-0.0244	-0.0272	6.33	[j]

[a] 1 a.u. = 2262 kJ·mol^{-1}.

[b] The difference [kJ·mol^{-1}], between the calculated thermodynamic functions of hydration of scandium and cobalt chelates; the differences of the experimental values (under assumption that the difference of the thermodynamic functions of hydration of the chelates is equal to the difference of the respective standard functions of heptane-water partition of scandium and cobalt trisacetylacetonates) are: $\Delta(\Delta H) = 11.3 \pm 1.9$ kJ·mol^{-1} and $\Delta(\Delta G) = 12.2 \pm 0.2$ kJ·mol^{-1} [5].

[c] The difference between the total energies of hydrate, chelate and water molecules, all in the hydrate geometry, calculated in the hydrate basis set [9, 10].

[d] The difference between the zero-point vibrational energies (ZPVE) of the hydrate molecule and those of its components: chelate and water.

[e] Calculated as the difference between the total energy of the scandium hydrate and the total energy of the same hydrate at a different geometry – where the water molecule had been twisted around its primary (σ) hydrogen bond, enough to break the additional (π) bond but keeping all other important interactions unchanged, i.e. the σ-bond length, etc.

[f] Calculated using equation: $E_{INT} = E_{\sigma HB} + E_{\pi HB} + \Delta ZPVE$.

[g] Thermal energy correction term, equal to the sum of the total energy at 0 K, vibrational, rotational and translational energies of the molecule at room temperature calculated using equation: $E^{T} = E + E_{vib} + E_{rot} + E_{trans}$.

[h] Water-field energy correction term: $\Delta E^{SCI\text{-}PCM} = E^{SCI\text{-}PCM} - E(gas)$.

[i] $\Delta H^{SCI\text{-}PCM} = \Delta E^{SCI\text{-}PCM} + \Delta H$; enthalpy of chelate hydration at room temperature.

[j] $\Delta G^{SCI\text{-}PCM} = \Delta E^{SCI\text{-}PCM} + \Delta G$; Gibbs free energy of chelate hydration at room temperature.

be considered as stronger hydration of the cobalt chelate.

We conclude that calculations by the DFT method of complex hydrogen-bonded systems, e.g. outer-sphere hydrates of neutral metal chelates, can result in erroneous correlations between the length and the energy of the hydrogen bond. That is due to low accuracy of the energy calculations in incomplete basis sets and to insufficient definition of the interaction energy. Additional calculations with polarization functions on each atom markedly improve the results, the relationship between the length and energy of hydrogen bond becoming correct. On the other hand, corrections for the zero-point vibrational energy change calculated within the DFT B3LYP method can be neglected.

The geometry of larger molecules may result in formation of an additional hydrogen bond by the same water molecule with participation of its second proton and the electrons from another ligand, as found for the scandium hydrate. This hydrogen bond of π-type, significantly longer and weaker than the usual σ-type hydrogen bonds, contributes to the calculated total energy of the system. However, the calculations of the interaction energy in the gas phase do not correctly reflect the interactions in aqueous solution. Another important effect which must be accounted for is due to electrostatic interactions of polar solute molecules with the water environment. These interactions to a different degree contribute to the energy of solutes with different dipole moments.

A general conclusion can be drawn that the supermolecular model is an adequate tool to describe the interactions between molecules of coordinatively saturated metal chelates and water, which leads to correct understanding and description of the outer-sphere hydration phenomena.

References

[1]. Theoretical Treatment of Hydrogen Bonding. Ed. D. Hadzi. John Wiley, New York 1997.
[2]. Narbutt J.: J. Inorg. Nucl. Chem., 43, 3343 (1981);
[3]. Moore P., Narbutt J.: J. Solut. Chem., 20, 1227 (1991).
[4]. Narbutt J.: J. Phys. Chem., 95, 3432 (1991).
[5]. Narbutt J., Bartoś B., Siekierski S.: Solv. Extr. Ion Exch., 12, 1001 (1994).

[6]. Guo H., Sirois S., Proynov E.I., Salahub D.R.: Chapter 3. In: Theoretical Treatment of Hydrogen Bonding. Ed. D. Hadzi. John Wiley, New York 1997.
[7]. Narbutt J., Czerwiński M., Krejzler J.: Eur. J. Inorg. Chem., 3187 (2001).
[8]. GAUSSIAN 94, Revision D.3, Gaussian, Inc., Pittsburgh PA, 1995.
[9]. Van Duijneveldt-van de Rijdt J.G.C.M., van Duijneveldt F.B.: Chapter 2. In: Theoretical Treatment of Hydrogen Bonding. Ed. D. Hadzi. John Wiley, New York 1997.
[10]. Czerwiński M., Narbutt J.: Outer-sphere hydrates of tris(propane-1,3-dionato)metal(III) chelates: a supermolecular approach, submitted.
[11]. Foresman J.B., Keith T.A., Wiberg K.B., Snoonian J., Frisch M.J.: J. Phys. Chem., 100, 16098 (1996).

PLATINUM(II) AND PALLADIUM(II) COMPLEXES WITH UREA DERIVATIVES: QUANTUM-CHEMICAL CALCULATIONS

Nina Sadlej-Sosnowska[1/], **Leon Fuks**

[1/] National Institute of Public Health, Warszawa, Poland

The long-standing interest in platinum(II) complexes, especially in *cis*-$[PtCl_2(NH_3)_2]$ (clinically known as *cis*platin [1, 2]), originates from the well-established anticancer activity of these compounds. Today, *cis*-platin is commonly used in clinical therapy and is considered as a potent drug in the therapy of the testicular carcinom, ovarian carcinomas and numerous tumor kinds of the head and neck [3, 4]. Although the nephrotoxicity of cisplatin can be effectively inhibited, other severe toxic side effects of the therapy have been found. The latter have stimulated intensive research towards the design of new platinum (and other metals) chemotherapeutic agents e.g. [5-8].

Among others, our group has already synthesized and tested the neutral and cationic platinum(II) and palladium(II) complexes with O-methyl-3,4-diamino-2,3,4,6-tetradeoxy-α-L-lyxo-hexopyranoside – a modified carbohydrate portion of the anticancer antibiotic, daunorubicin [9-12]. Structure of the *cis*platin is illustrated in Scheme.

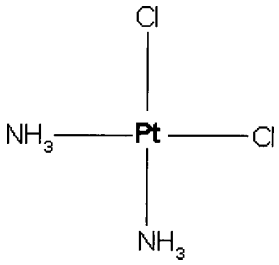

Scheme. Structure of the *cis*-diamminedichloroplatinum(II), *cis*platin.

The discovery of cisplatin has led to numerous experimental and theoretical investigations on the molecular properties and the mechanism of action of this therapeutic compound. The aim of the presented paper is to show our preliminary results obtained as the contribution to the theoretical studies on the structure of novel platinum(II) compounds with potential therapeutical properties. Ligands, which occupy two complexing sites of the platinum(II) or palladium(II) cation are the following: urea, thiourea and selenourea molecules, respectively.

To calculate optimized geometrical structures two consecutive quantum-chemical methods were used: (i) semiempirical PM3 (ii) the *ab initio* Hartree-Fock procedure. The latter was performed using the LanL2DZ numerical basis set. The basis is commonly applied for molecules containing atoms creating the Periodic Table rows greater than third and takes into account the relativistic effects. All calculations were made using (i) SPARTAN Pro 5.0 (PC version) and (ii) Gaussian 98 program on the Silicon Graphics IRIS Indigo workstation with the processor 10 000, respectively.

In the presented studies, structure of the platinum(II) and palladium(II) complexes has been computed for three main cases: (i) 1:1 complex formed by means of the lone electron pairs of two urea nitrogen atoms; (ii) 1:2 complex of the *cis*-structure, formed by lone electron pairs of the urea oxygen (sulfur, selenium) atoms; (iii) *trans*-structured 1:2 complex, formed also by the latter electron pairs. Proposed structures (in the sample case of the platinum(II)-urea complex) are presented in Fig.

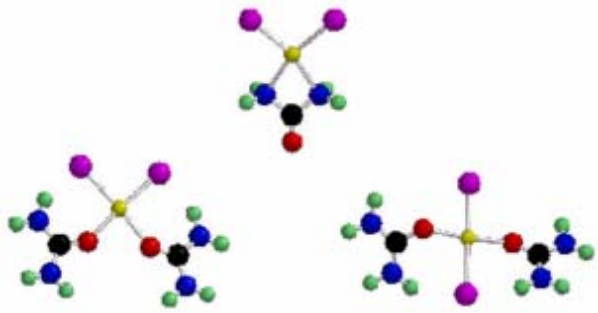

Fig. Schematic structures of the investigated complexes: upper line – complex 1, bottom-left – complex 2 and bottom-right – complex 3.

Optimized molecular structures were initially obtained by the PM3 semiempirical method. To get more accurate results, in the following, structures of all these complexes were refined by the *ab initio* calculations. Appropriate structures obtained using both calculation methods appeared to be close each other. Results presenting main crystallographic data are presented in Tables 1-3. Distance values (d) in the Tables are given in Å, angles (a and A) – in degs, while energy values (E) – in the atomic units (hartree).

In Table 1 one can see that the energy of both *trans*-structures is about 3 kcal·mole^{-1} lower than

at the *cis*-isomers. Simultaneously, it is much more favorable than energy of the hypothetical compounds of the 1 type: small, four members rings, formed with the use of two nitrogen atoms.

Detailed crystallographic and spectroscopic (FT-IR, NMR) studies of the investigated complexes, as well as the biological tests, are in progress. Further calculations are also forseen, because within

Table 1. Platinum(II) and palladium(II) complexes with the urea.

$Pt[O=C(NH_2)_2]_xCl_2$		$Pd[O=C(NH_2)_2]_xCl_2$	
Structure 1			
d(Pt-Cl)	2.373	d(Pd-Cl)	2.335
d(Pt-N)	2.183	d(Pd-N)	2.276
d(C=O)	1.196	d(C=O)	1.203
d(Pt····C)	2.627	d(Pd····C)	2.642
a(Cl-Pt-Cl)	97.55	a(Cl-Pd-Cl)	100.18
a(Cl-Pt-N)	99.11	a(Cl-Pd-N)	100.21
a(N-Pt-N)	64.24	a(N-Pd-N)	61.22
A(Pt-N-N-C)	149.89	A(Pd-N-N-C)	139.31
non-plane structure		non-plane structure	
E	-371.6365179	E	-379.2482106
Structure 2			
d(Pt-Cl)	2.421	d(Pd-Cl)	2.396
d(Pt-O)	2.093	d(Pd-O)	2.102
d(C=O)	1.262	d(C=O)	1.261
d(H····Cl)	2.270	d(Pd····C)	2.270
a(Cl-Pt-Cl)	91.01	a(Cl-Pd-Cl)	91.98
a(Cl-Pt-O)	93.46	a(Cl-Pd-N)	92.30
a(O-Pt-O)	82.08	a(O-Pd-O)	83.40
a(Pt-O-C)	142.43	a(Pd-O-C)	144.21
plane structure		plane structure	
E	-595.6654385	E	-603.2819807
Structure 3			
d(Pt-Cl1)	2.413	d(Pd-Cl)	2.444
d(Pt-Cl2)	2.497	d(Pd-O)	2.050
d(C=O)	1.261	d(C=O)	1.262
d(Pt-O)	2.049	d(H····Cl)	2.291
a(Cl1-Pt-O1); a(Cl1-Pt-O2)	87.85	a(Cl1-Pd-O1); a(Cl1-Pd-O2)	87.51
a(Cl2-Pt-O1); a(Cl2-Pt-O2)	92.15	a(Cl2-Pt-O1); a(Cl2-Pt-O2)	92.48
a(Pt-O-Cl)	139.07	a(Pd-O-Cl)	145.77
A(Cl1-Pt-O-C)	-32.89		
non-plane structure			
E	-595.6701346	E	-603.2874784

Table 2. Platinum(II) and palladium(II) complexes with the thiourea.

$Pt[S=C(NH_2)_2]_xCl_2$		$Pd[S=C(NH_2)_2]_xCl_2$	
Structure 1			
d(Pt-Cl)	2.372	d(Pd-Cl)	2.333
d(Pt-N)	2.192	d(Pd-N)	2.298
d(C=S)	1.639	d(C=S)	1.657
d(Pt····C)	2.608	d(Pd····C)	2.623
a(Cl-Pt-Cl)	97.66	a(Cl-Pd-Cl)	98.14
a(Cl-Pt-N)	99.58	a(Cl-Pd-N)	100.97
a(N-Pt-N)	63.19	a(N-Pd-N)	59.83
A(Pt-N-N-C)	142.73	A(Pd-N-N-C)	132.63
non-plane structure		non-plane structure	
E	-306.655958	E	-314.268843

Table 3. Platinum(II) and palladium(II) complexes with the selenourea.

$Pt[Se=C(NH_2)_2]_xCl_2$		$Pd[Se=C(NH_2)_2]_xCl_2$	
Structure 1			
d(Pt-Cl)	2.374	d(Pd-Cl)	2.333
d(Pt-N)	2.188	d(Pd-N)	2.303
d(C=Se)	1.767	d(C=Se)	1.792
d(Pt····C)	2.601	d(Pd····C)	2.615
a(Cl-Pt-Cl)	97.60	a(Cl-Pd-Cl)	98.19
a(Cl-Pt-N)	99.61	a(Cl-Pd-N)	101.06
a(N-Pt-N)	63.18	a(N-Pd-N)	59.58
A(Pt-N-N-C)	141.55	A(Pd-N-N-C)	130.85
non-plane structure		non-plane structure	
E	-305.7741455	E	-313.3870869
Structure 2			
		d(Pd-Cl)	2.421
		d(Pd-Se)	2.613
		d(C=Se)	1.929
		d(H····Cl)	2.156
		a(Cl-Pd-Cl)	90.01
		a(Cl-Pd-Se)	94.40
		a(Se-Pd-Se)	81.22
		a(Pd-Se-C)	110.34
		A(Cl-Pd-Se-C)	37.76
		non-plane structure	
		E	-471.5725738
Structure 3			
d(Pt-Cl)	2.450		
d(Pt-Se)	2.585		
d(C=Se)	1.926		
d(H····Cl)	2.174		
a(Cl1-Pt-Se)	80.38		
a(Cl2-Pt-Se)	99.62		
a(Pt-Se-C)	114.2		
a(Se-C-N)	125.85		
plane structure			
E	-463.9723345		

the LanL2DZ numerical basis set not all the structures can be optimized.

References

[1]. Rosenberg B., Van Camp L., Krigas T.: Nature, 205, 698 (1965).
[2]. Rosenberg B., Van Camp L., Trosko J.E., Mansour V.H.: Nature, 222, 385 (1969).
[3]. Metal Complexes in Cancer Chemotherapy. Ed. B.K. Keppler. Verlag Chemie, Weinheim 1993.
[4]. Uses of Inorganic Chemistry in Medicine. Ed. N.P. Farell. Royal Soc. Chem., 1999, pp.109-134.
[5]. Reedijk J.: Chem. Rev., 99, 2499 (1999).
[6]. Lippert B.: Coord. Chem. Rev., 182, 263 (1999).
[7]. Wong E., Giandomenico C.M.: Chem. Rev., 99, 2451 (1999).
[8]. Köpf-Maier P.: Eur. J. Clin. Pharmacol., 47, 1 (1994).
[9]. Kruszewski M., Bouzyk E., Ołdak T., Samochocka K., Fuks L., Lewandowski W., Fokt I., Priebe W.: Teratogenesis, Mutagenesis and Carcinogenesis, 11, 1 (2003).
[10]. Samochocka K., Lewandowski W., Priebe W., Fuks L.: J. Mol. Struct., 203, 614 (2002).
[11]. Samochocka K., Fokt I., Anulewicz-Ostrowska R., Przewloka T., Mazurek A.P., Fuks L., Lewandowski W., Kozerski L., Bocian W., Bednarek E., Lewandowska H., Sitkowski J., Priebe W.: J. Chem. Soc., Dalton, in press.
[12]. Fuks L., Samochocka K., Anulewicz-Ostrowska R., Kruszewski M., Priebe W., Lewandowski W.: Eur. J. Med. Chem., in press.

SYNTHESIS OF RHENIUM(VI) COMPLEX WITH 2-AMINOBENZENETHIOL AT CARRIER FREE CONDITIONS

Ewa Gniazdowska, Jerzy Narbutt, Holger Stephan[1/], Hartmut Spies[1/]

[1/] Institute of Bioinorganic and Radiopharmaceutical Chemistry, Forschungszentrum Rossendorf, Dresden, Germany

2-Aminobenzenethiol (H_2abt) is known as a bidentate ligand that forms complexes with technetium and rhenium in oxidation states +V and +VI [1, 2]. Tris-ligand complexes of technetium(VI) and rhenium(VI) were isolated as solid complexes showing a trigonal-prismatic geometry [3, 4] (Fig.1). Besides tris-ligand complexes $[M(abt)_3]^{0,\,1-}$, oxometal(V) bis-ligand complexes $[(MO(abt)_2]^{1-}$ have been described [5, 6].

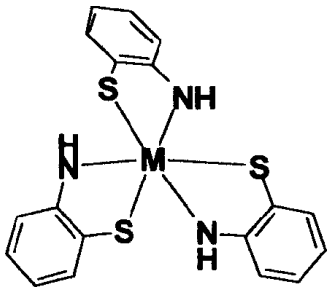

Fig.1. Schematic presentation of complex molecule, M=Tc or Re.

We are interested, whether the technetium and rhenium abt system can be exploited for radiopharmaceutical design, in particular for technetium-99m in view of diagnostic, and rhenium-188 as therapeutic application.

The general aim of our investigations was to find appropriate conditions to carry out the synthesis of carrier free $^{188}Re^{VI}(abt)_3$ complex. In view of previous experience with the preparation of technetium complexes, we performed the reduction of perrhenate ion by stannous chloride in the presence of sodium-gluconate. It is likely that the reaction occurs *via* the $[Re^{V}O(gluconate)_2]^-$ complex which is a suitable precursor to the preparation of rhenium(V) and rhenium(VI) complexes in aqueous solutions [6]. Because of the high lipophilicity of both H_2abt ligand and its rhenium complex, the synthesis has to be carried out in a mixed water-ethanol solution. But there are problems with the solubility of the hydrophilic sodium gluconate as precursor. Hence, it is required to find another auxiliary ligand more suitable than gluconate. In searching for auxiliary ligands which would both stabilize the $(Re^{V}O)^{3+}$ core and homogenize the reaction solution, we tested the following species: sodium tartrate, 2-ethyl-2-hydroxy butyric acid, α-, β-, γ-cyclodextrin and their 2-hydroxylpropyl-derivatives. To a mixture of the auxiliary ligand dissolved in water $^{188}RO_4^-$ eluate, some propylene glycol as modifier, an ethanolic solution of the H_2abt ligand, and finally a solution of $SnCl_2$ in dilute HCl was added. The pH of the reaction mixture was kept constant in the range of 2÷8, depending on the system studied. The reaction progress was checked by thin-layer chromatography (TLC).

Examination of our data suggests that 2-ethyl--2-hydroxy butyric acid is the most suitable auxiliary ligand of the species studied and that the reduction occurs at pH<3. However, the formation of $^{188}Re(abt)_3$ complex is a very slow process. The reaction proceeds slowly. After 4 h only about 33% of perrhenate ions have been converted into the

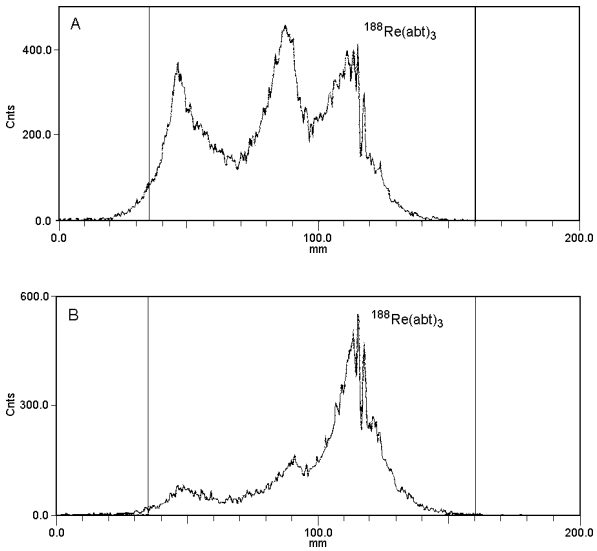

Fig.2. The TLC chromatogram of reaction mixture, after 4 h (A) and 24 h (B), developed in chloroform/ethyl acetate/methanol (9/3/1 v/v) solution.

$^{188}Re^{VI}$ complex, and after 24 h the yield was about 75% (Fig.2). It is worth mentioning that the addition of oxalic acid accelerates the conversion of perrhenate. Under these conditions no free perrhenate was found in the solution after 15 min. The labelling efficiency can be improved with increasing in temperature.

This work is a part of common Polish-German project "Nanoscalic metallodendrimers based on radioactive rhenium aminobenzenethiolate complexes".

References

[1]. Gardner J.K., Pariyadath N., Corbin J.L., Stiefel E.I.: Inorg. Chem., 17, 897-904 (1978).
[2]. Spies H., Pietzsch H., Hoffmann I.: Inorg. Chim. Acta, 161, 17-19 (1989).
[3]. Baldas J., Boas J., Bonnyman J., Mackay M.F., Williams G.A.: Aust. J. Chem., 35, 2413-2422 (1982).
[4]. Danopoulos A.A., Wong A.C.C., Wilkinson G., Hursthouse M.B., Hussain B.: J. Chem. Soc. Dalton Trans., 1, 315-331 (1990).
[5]. Bandoli G., Gerber T.I.A.: Inorg. Chim. Acta, 126, 205-208 (1987).
[6]. Noll B., Kniess T., Friebe M., Spies H., Johannsen B.: Isotopes Environ. Health Stud., 32, 21-29 (1996).

TRICARBONYL TECHNETIUM(I)-99m COMPLEXES WITH LIPOPHILIC BIDENTATE LIGANDS IN SOLUTION

Jerzy Narbutt, Monika Zasępa, Ewa Gniazdowska

Technetium-99m plays an important role in diagnostic nuclear medicine because of its advantageous nuclear properties and rich coordination chemistry. Current development of technetium-99m compounds used as radiopharmaceuticals requires cooperation in many fields of science: organic chemistry, coordination chemistry, radiochemistry, biochemistry, biology and medicine. The main aim of designing such compounds is to combine the radionuclide with suitable ligands or with biologically active molecules.

Triaquatricarbonyltechnetium(I) complex $[^{99m}Tc(CO)_3(H_2O)_3]^+$ is a convenient precursor for obtaining various radionuclides used in nuclear medicine [1]. The suitability for labelling biomolecules arises from the high inertness of the $[^{99m}Tc(CO)_3]^+$ core and its stability in aqueous solutions in a wide pH range. The CO ligands stabilise low oxidation states because electron density is retracted from the metal by back-bonding. This mimics higher oxidation state of the metal what makes it less vulnerable for oxidation.

The precursor $[^{99m}Tc(CO)_3(H_2O)_3]^+$ was prepared following Alberto's method [1]. In this work the complexes $[^{99m}Tc(CO)_3L(H_2O)]$ have been prepared in a simple one-step synthesis between $[^{99m}Tc(CO)_3(H_2O)_3]^+$ and anionic forms L^- of moderately lipophilic, bidentate ligands: HL=tropolone (Htrop), 8-hydroxyquinoline (Hox), monotiodibenzoylomethane (Hsdbm) [2] and neutral *N,N*-diethylpicolinamide. The complexes were obtained at n.c.a. level in aqueous solution and characterised by HPLC and TLC. The TLC analysis was performed using various mobile phases: 85% methanol, phosphate buffer, acetone, CEM (chloroform:ethyl acetate:methanol; 9:3:1 v/v). The main impurity, probably $^{99m}TcO_2$, retained at the origin of the strips in all mobile phases.

The yields of $[^{99m}Tc(CO)_3L(H_2O)]$ determined by TLC were in the range of 70-90%, the yields determined by HPLC were higher (80-95%). The differences between the results of both methods were caused mainly by the retention of the main impurity, $^{99m}TcO_2$, retained on the HPLC pre-column. The yields determined by extraction in the water--heptane system were much lower (4-40%), strongly depending on conditions, particularly on the presence of oxygen in the system.

Distribution coefficients (D) of the complexes $[^{99m}Tc(CO)_3L(H_2O)]$, measured under air as a function of time, decreased with time. The D values remained, however, nearly stable in time if the extraction system had previously been saturated with nitrogen or argon and kept under the inert gas atmosphere during the experiment (Fig.1). Therefore, the low stability of the complexes $[^{99m}Tc(CO)_3L(H_2O)]$ was probably due to the slow oxidation of technetium(I) by air. The other possible reason, e.g. dissociation of the complex at low pH values, or hydrolysis of technetium(I) at higher pH,

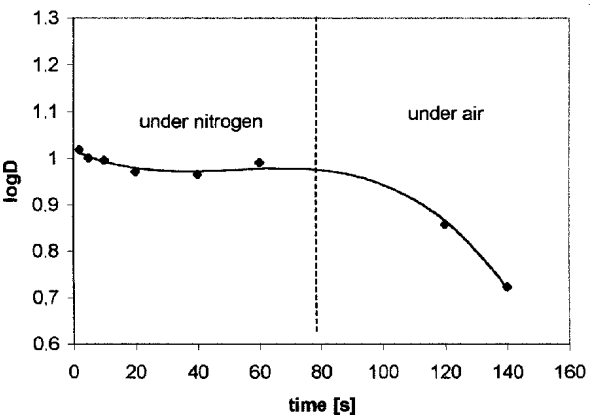

Fig.1. Effect of the gas refluxing the heptane-water extraction system on the distribution coefficient of $[^{99m}Tc(CO)_3(sdbm)(H_2O)]$ complex.

seems to be less important. The observed effect of low stability of the tricarbonyl technetium(I) complexes was rather unexpected in view of the reported stability of other related complexes [1]. The lipohilicity of $[^{99m}Tc(CO)_3L(H_2O)]$ increases in the order: tropolonate 8-hydroxyquinolinate < monotiodibenzoylomethanate.

Besides the stabilization of low oxidation states, the strongly bound CO ligands also labilize the water molecules in the complexes $[^{99m}Tc(CO)_3(H_2O)_3]^+$ and $[^{99m}Tc(CO)_3L(H_2O)]$. The reactivity of the last water molecule remaining in $[^{99m}Tc(CO)_3L(H_2O)]$, important from the point of view of *in vivo* behaviour of these complexes, was also studied. We assumed that this water molecule may be exchanged for plasma components, e.g. glutathione (GSH) [3], which makes the technetium-99m complexes able to react with whole blood or to be retained in leukocytes after crossing the cell membrane. Such labelled leukocytes may be used for imaging inflammable states.

The reaction of complexes $[^{99m}Tc(CO)_3L(H_2O)]$ with GSH was studied by both HPLC and solvent

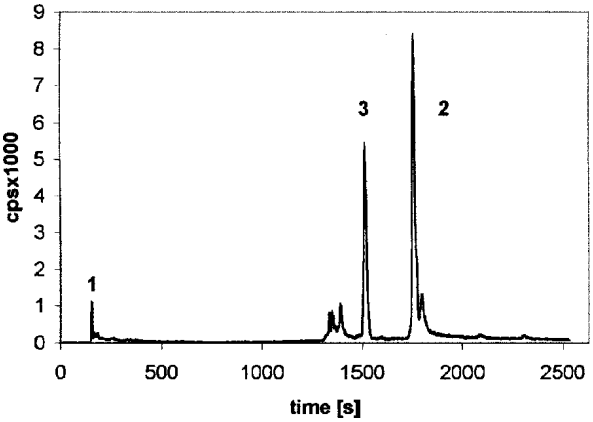

Fig.2. HPLC chromatogram of reaction mixture after adding glutathione (10 mM) to the solution of $[^{99m}Tc(CO)_3(sdbm)(H_2O)]$: 1 – $[^{99m}Tc(CO)_3(H_2O)_3]^+$, 2 – $[^{99m}Tc(CO)_3(sdbm)(H_2O)]$, 3 – $[^{99m}Tc(CO)_3(sbdm)GSH]$.

extraction. HPLC chromatogram brought the evidence for the formation of GSH complex, somewhat more hydrophilic than [^{99m}Tc(CO)$_3$L(H$_2$O)], presumably [^{99m}Tc(CO)$_3$(GSH)L], where L=trop, ox and sdbm (Fig.2). However, the formation of GSH complexes could not be detected by the liquid-liquid distribution method because of the rather small change in D value observed after addition of GSH (10 mM) to the extraction system.

In further studies we will investigate the influence of ligands L on the exchange of the remaining water molecule in [^{99m}Tc(CO)$_3$L(H$_2$O)]. We suppose that this study would allow us to select convenient tricarbonyl technetium(I)-99m complexes to be used as radiopharmaceuticals.

References

[1]. Alberto R., Schibli R., Waibel U., Abram U., Schubiger P.A.: Coord. Chem. Rev., 190-192, 901-919 (1999).
[2]. Narbutt J., Zasępa M., Gniazdowska E.: In: Technetium, Rhenium and Other Metals in Chemistry and Nuclear Medicine 6. Eds. M. Nicolini, U. Mazzi. Padova 2002, pp.147-149.
[3]. Pietzsch H., Gupta A., Reisgys M., Drews A., Seifert S., Syhre R., Spies H., Alberto R., Abram U., Schubiger P.A., Johannsen B.: Bioconjugate Chem., 11, 414-424 (2002).

ELABORATION OF THE METHOD OF GROUP SEPARATION OF REE FROM BIOLOGICAL MATERIALS FOR THEIR DETERMINATION BY RNAA

Bożena Danko, Zbigniew Samczyński, Rajmund Dybczyński

Nowadays, rare earth elements (REEs) are widely used in many applications such as ceramics, semiconductors, magnetic resonance imaging, contrast reagents, fertilizers etc. It has been forecasted that the agricultural usage of REEs and resulting environmental contamination by REEs will continue to grow in the next few decades [1]. There is a need for research, which could provide information for assessment of the help and environmental risk associated with the large-scale application of REE fertilizers. Therefore, it is important to study the distribution of REEs in biological materials, which can help in evaluating the extent of their pollution of the environment.

On the other hand, however, the latest published results indicate that REEs can travel across the bio-membrane into cells of living organism [2]. As a consequence we face the question whether the REE compounds are toxic for humans and animals or not.

Despite of rapid progress in the field of modern analytical techniques, still only very few methods can assure reliable determination of lanthanides on trace and ultra-trace levels of concentration. One of them is neutron activation analysis (NAA), offering very favorable detection limits, for practically all REEs. However, due to interference encountered, and typically low abundance of REEs in biological materials, purely instrumental NAA

Table. Results of the determination of REE in the biological CRMs.

Element	CTA-OTL-1	CTA-VTL-1	CTA-TL-1	CTA-MPH-2
Ce [μg/g]	2.69 ± 0.30 1.80 ± 0.18	1.91 ± 0.29 1.45 ± 0.20	0.790 ± 0.076 0.688 ± 0.058	1.12 ± 0.10 0.976 ± 0.029
Dy [ng/g]	137 ± 9	99 ± 10	149 ± 16	74 ± 16
Eu [ng/g]	38.0 ± 9.0 37.0 ± 12	(33) 41 ± 10	50.0 ± 9.0 73.0 ± 17.0	16.0 ± 2.0 16.0 ± 1.5
La [μg/g]	1.44 ± 0.16 1.46 ± 0.19	1.01 ± 0.10 1.13 ± 0.08	1.00 ± 0.07 1.29 ± 0.16	0.571 ± 0.046 0.664 ± 0.089
Lu [ng/g]	8.8 ± 1.1	7.4 ± 1.0	17 ± 2 15 ± 3	9.0 ± 1.5 4.3 ± 0.8
Nd [μg/g]	0.864 ± 0.190	0.660 ± 0.145	(0.810) 0.835 ± 0.142	0.457 ± 0.091 0.406 ± 0.039
Pr [μg/g]	0.228 ± 0.054	0.196 ± 0.023	0.245	0.145
Sm [μg/g]	0.229 ± 0.052 0.174 ± 0.050	0.157 ± 0.022 0.169 ± 0.030	0.177 ± 0.022 0.183 ± 0.032	0.094 ± 0.008 0.089 ± 0.010
Tb [ng/g]	32 ± 6 24 ± 5	22 ± 5 19 ± 4	26.5 ± 2.4 32 ± 5	13.5 ± 1.1 10.0 ± 2.4
Yb [ng/g]	(130) 87 ± 16	(80) 63 ± 8	118 ± 13 105 ± 14	53 ± 7 39 ± 9

Mean value ± expanded standard uncertainty (k=2).
Certified values with their confidence limits are underlined, information values are in parentheses.

is not enough sensitive [3, 4]. Isolation of the elements of interest from matrix constituents before irradiation enables to overcome the above problems and makes the quantification of the most of lanthanide elements possible.

On the basis of experiments with radiotracers the analytical scheme for quantitative and selective group separation of REEs from biological material was elaborated in 2001 [5]. In this year, attention has been drawn to check the usefulness of the proposed scheme for quantification of REEs in real samples of biological origin by NAA. As among the elements of interest the dominant activity originated from Sc was present in the separated REE fraction, a slight modification of the separation scheme was necessary. The additional elution with 0.5 mol·l^{-1} H_2SO_4 was introduced in order to minimize the presence of Sc. The analyzed material, *ca*. 500 mg, was digested in a microwave oven using a thoroughly tested procedure. Next, ion exchange column chromatography in the systems: Dowex 1-X8 [Cl^-]-8M HCl was employed to separate U and other elements forming strong chloride complexes. This allows us to avoid the well-known interference due to fission products from fossil material present in the sample.

The rest of accompanying elements was removed in the Dowex 50 WX-8 [H^+] cation-exchange chromatography process, applying stepwise elution with: 0.75 mol·l^{-1} HCl/H_2O/0.5 mol·l^{-1} H_2SO_4/H_2O/1 mol·l^{-1} HNO_3. Finally, almost pure fraction of REEs was eluted with 5 mol·l^{-1} HNO_3, transferred into irradiation vessels and evaporated to dryness.

The package of blank, preprocessed samples, standards and neutron flux monitor (La – 50 μg) was irradiated in the nuclear reactor MARIA with a neutron flux of density: $6x10^{13}$ n cm^{-2}s^{-1} for duration of 30 min.

A rapid post-irradiation procedure dividing the whole REEs into two subgroups was introduced in order to examine the potential cross-influence of light and heavy lanthanides.

Three counting series were performed: 2 h after irradiation, for the determination of Dy, Er, Eu and Pr; 24 h after irradiation for the determination of La, Sm, Ho, Yb and Lu, and the third one for the determination of Ce, Nd, Eu, Tb and Yb with cooling time longer than 2 weeks.

As far as we know all sources of systematic errors potentially influencing the uncertainty of REEs determination by NAA were taken into consideration [6, 7].

A test irradiation was made on individual elements in order to provide sufficient information to design the optimum grouping of REEs in standards. Special care was taken to avoid cross-contamination as well as cross-interference phenomenon. As a result of the devised analytical scheme, a selective REEs fraction free from most of the potential interference was obtained. Only small activities of Pa-233 and reduced to a large extend Sc activity were found in the analytes fraction. For verification of our procedure, four certified reference materials (CRMs) of plant origin were used: CTA-OTL-1, CTA-VTL-2, CTA-TL-1 and CTA-MPH-2. (The plant matrices are usually the most complex among the biological materials). The results of the determination of REEs in the CRMs – mean value together with their expanded uncertainty, estimated for k=2 – are illustrated in Table. Almost for all elements determined, the confidence limits overlap with the uncertainty of the certified value. This allows us to conclude that the devised analytical procedure for REEs determination by NAA is reliable.

References

[1]. Volokh A.A., Gorbunov A.V., Gundorina S.F., Revich B.A., Frontasyeva M.V., Pal C.: Sci. Total Environ., 95, 141-148 (1990).
[2]. Wu Y.P., Mi Y., Shen H., Yao H.Y., Cheng Y., Wang X., Zhang J.X.: Nucl. Instrum. Meth. Phys. Res. B, 189, 459-463 (2002).
[3]. Tjioe P.S., Volkers K.J., Kroon J.J., De Goeij J.J.M.: J. Radioanal. Nucl. Chem., 80, 1-2, 129-139 (1983).
[4]. Becker D., Greenberg R.R.: Trans. ANS, 71, 48-50 (1994).
[5]. Danko B., Dybczyński R.: In: INCT Annual Report 2001. Institute of Nuclear Chemistry and Technology, Warszawa 2002, p.67.
[6]. Wasek M., Kulisa K., Dybczyński R.: Chem. Anal., 41, 647 (1996).
[7]. CRC Handbook of Radioanalytical Chemistry. Eds. J. Tolgyessy, E. Bujdoso. Boston 1991.

STUDIES ON POSSIBILITY OF DETERMINATION OF SOME RARE EARTH ELEMENTS BY ION CHROMATOGRAPHY

Krzysztof Kulisa, Halina Polkowska-Motrenko, Rajmund Dybczyński

In previous years, procedures for the determination of chosen transition, alkali and alkaline earth elements in water [1] and biological samples [2, 3] by ion chromatography (IC) have been elaborated using an ion chromatograph Dionex 2000i/SP with an Ion Pac CS5 analytical column and an Ion Pac CG5 guard column. In this year, efforts have been aimed at the elaboration of determination procedure of rare earth elements (REEs) in biological samples with the use of the same ion chromatographic system.

In aqueous solution, REEs are present as trivalent cations. Because of the similarity of ionic properties of the lanthanides they cannot be separated easily by cation exchange as trivalent cations, but the use of strong complexing agents can increase the selectivity of separation of lanthanide metal ions. The use of oxalic acid as a complexing agent

results in the formation of anionic complexes of the lanthanide metals and under these conditions the rare earth metals can be separated by an anion exchange mechanism employing an anion-exchanger with alkanol quaternary ammonium functional groups. The possibility of REE separation and determination has been tested using the Dionex 2000i/SP ion chromatograph equipped with the Ion Pac CS5 analytical column, Ion Pac CG5 guard column and a post-column Ion Pac Membrane Reactor. The following REE cations have been examined: La^{3+}, Ce^{3+}, Pr^{3+}, Nd^{3+}, Sm^{3+}, Eu^{3+}, Gd^{3+}, Tb^{3+}, Dy^{3+}, Ho^{3+}, Er^{3+}, Tm^{3+}, Yb^{3+}, Lu^{3+}.
These cations were separated as anionic complexes using an oxalic acid complexing eluent modified with diglycolic acid. The separation of lanthanide anionic complexes has been achieved with opposing linear gradients of oxalic acid and diglycolic acid eluents obtained applying a gradient pump (Dionex, AGP). Details of this gradient and eluent composition have been established experimentally and are as follows:

- eluent 1 – 100 mM oxalic acid + 190 mM LiOH,
- eluent 2 – 100 mM diglycolic acid + 190 mM LiOH,
- eluent 3 – Millipore superpure water (18 M ·cm).

Gradient program for Dionex, AGP:

- time – 0.0: eluent 1 – 100%, eluent 2 – 0%, eluent 3 – 0%;
- time – 20.0: eluent 1 – 26%, eluent 2 – 23%, eluent 3 – 51%.

The lanthanide compounds in the eluate have been converted into colour complexes with the use of post-column complexing reagent PAR (4-(2-pyridylazo)resorcinol) in the following solution: 0.2 mM PAR + 1 M CH_3COOH + 3 M NH_4OH. The Dionex Ion Pac Membrane Reactor was applied for this purpose. Flow rate of the eluents was 1 ml·min^{-1}. Post-column reagent flow rate was 0.7 ml·min^{-1}. Coloured REE complexes have been detected by photometric detection at 520 nm using Dionex UV/VIS Variable Wavelength Detector VDM II. Because REE are present in real biological samples often in very small amounts, care must be taken to minimize reagent and sample contamination during preparation and handling to obtain possibly low detection limits. All the eluent and standard solutions were prepared with the use of superpure water (18 M ·cm) obtained by a Milli-QRG ultra-pure water system (Millipore Co.) and deoxygenated with nitrogen. 10 mg·l^{-1} standards of all REE were used for analysis. Detection limits of determination of REE have been estimated according to Small definition [4] for separated and determined REE and are as follows (in ppm): La – 0.39, Ce – 0.13, Pr – 0.18, Nd – 0.16, Sm – 0.12, Eu – 0.10, Gd – 0.14, Tb – 0.1, Dy – 0.15, Ho – 0.22, Er – 0.36, Tm – 0.33, Yb – 0.1, Lu – 0.1.

The procedure of ion-chromatographic determination of lanthanides in biological samples consists of sample preparation steps followed by chromatographic separation and quantitation step [5]. Sample preparation procedure of biological matrices has been as follows: The samples of biological material (*ca*. 0.5 g) were weighed into two PTFE vessels and digested in a microwave oven (Plazmatronika Service, Wrocław) with a mixture of 6 ml of concd. HNO_3 + 2 ml HF + 2 ml H_2O_2 according to the 3-stage procedure (5 min – 60%, 5 min – 80%, 15 min – 100% of power). After mineralization, the solutions were transferred quantitatively into PTFE evaporation dishes and triply evaporated with concd. HCl. Then, the residues were dissolved in 3 ml of 8 M HCl. The next stage of sample preparation procedure was the ion-exchange separation of REE as a group with the use of classical column IC. U and Fe have been separated on an ion-exchange column 7 cm x 0.4 cm^2 filled with the resin Dowex 1 x 8 using 30-40 ml of 8 M HCl as an eluent. Then, the eluate was evaporated and dissolved in 3 ml of 0.5 M HCl. It has been followed by the separation of potassium group, Sc and calcium group on an ion-exchange column (10 cm x 0.4 cm^2) filled with the resin Dowex 50W x 4[Cl^-] using as a eluent 30 ml 0.75 M HCl, 25 ml 0.5 M H_2SO_4 and 10 ml 1 M HNO_3, respectively. Finally, the REE fraction was eluted from this column using 25 ml of 5 M HNO_3. The REE fraction has been evaporated, dissolved in 0.5 M HNO_3 and finally evaporated up to the volume of 1 ml. The blank solutions were prepared in the same way.

Table. Results of REE determination in certified reference biological materials.

CRMs	REE contents [mg·kg^{-1}]									
	La		Ce		Sm		Nd		Yb	
	IC $\bar{x} \pm u$	Certified value [6-8]	IC $\bar{x} \pm u$	Certified value [6-8]	IC $\bar{x} \pm u$	Certified value [6-8]	IC $\bar{x} \pm u$	Certified or „information" value [7, 8]	IC $\bar{x} \pm u$	Certified or „information" value [6-8]
CTA-OTL-1	1.33 ±0.13	1.44 ±0.16	2.50 ±0.25	2.69 ±0.30	0.33 ±0.07	0.23 ±0.05	nd	nd	nd	0.13
MPH-2	nd	0.57 ±0.046	nd	1.12 ±0.1	nd	0.094 ±0.008	0.41 ±0.21	0.46 ±0.09	nd	0.053 ±0.006
TL-1	nd	1.00 ±0.07	0.68 ±0.07	0.79 ±0.08	0.23 ±0.05	0.18 ±0.02	nd	0.81	0.23 ±0.11	0.12 ±0.013

± u – mean value ± expanded standard uncertainty with a coverage factor k=2.

The obtained solutions of REE fractions have been analyzed by IC without any dissolving. The reliability of the elaborated procedure has been checked analyzing three reference biological materials with a certified content of a few REE: Oriental Tobacco Leaves (CTA-OTL-1), Mixed Polish Herbs (INCT-MPH-2) and Tea Leaves (INCT-TL-1).

Contents of the majority of lanthanides in all the biological reference materials studied were close to or below the level of detection limits evaluated for the IC method. The obtained results are presented in Table. The uncertainty budget was performed and combined uncertainties have been evaluated. As can be seen from Table for some REE, whose contents are higher than detection limits, quite satisfactory agreement is observed between the determined and certified values of REE concentration (except for Yb in INCT-TL-1). The La and Ce peaks in INCT-MPH-2 as well as the La peak on INCT-TL-1 chromatograms were masked by unidentified peaks originating from sample contamination, so in that case the determinations of La and Ce in INCT-MPH-2 and La in INCT-TL-1 were impossible. On the basis of the obtained results, the presented IC method can be considered as a valuable tool for the determination of REE contents in biological materials. However, taking into account the detection limits, samples of greater mass should be taken for analysis to enable determination of several REEs in one sample.

References

[1]. Kulisa K., Polkowska-Motrenko H., Dybczyński R.: In: INCT Annual Report 1999. Institute of Nuclear Chemistry and Technology, Warszawa 2000, p.74.
[2]. Kulisa K., Polkowska-Motrenko H., Dybczyński R.: In: INCT Annual Report 2000. Institute of Nuclear Chemistry and Technology, Warszawa 2001, p.68.
[3]. Kulisa K., Polkowska-Motrenko H., Dybczyński R.: In: INCT Annual Report 2001. Institute of Nuclear Chemistry and Technology, Warszawa 2002, p.68.
[4]. Small H.: Ion Chromatography. Plenum Press, New York 1989.
[5]. Danko B., Dybczyński R.: In: INCT Annual Report 2001. Institute of Nuclear Chemistry and Technology, Warszawa 2002, p.67.
[6]. Dybczyński R., Polkowska-Motrenko H., Samczyński Z., Szopa Z.: Preparation and certification of the Polish reference material "Oriental Tobacco Leaves" (CTA-OTL-1) for inorganic trace analysis. Institute of Nuclear Chemistry and Technology, Warszawa 1996, Raporty IChTJ. Seria A No. 1/96.
[7]. Dybczyński R., Danko B., Kulisa K., Maleszewska E., Polkowska-Motrenko H., Samczyński Z., Szopa Z.: Preparation and certification of the Polish reference material: Tea Leaves (INCT-TL-1) for inorganic trace analysis. Institute of Nuclear Chemistry and Technology, Warszawa 2002, Raporty IChTJ. Seria A No. 3/2002.
[8]. Dybczyński R., Danko B., Kulisa K., Maleszewska E., Polkowska-Motrenko H., Samczyński Z., Szopa Z.: Preparation and certification of the Polish reference material: Mixed Herbs (INCT-MPH-2) for inorganic trace analysis. Institute of Nuclear Chemistry and Technology, Warszawa 2002, Raporty IChTJ. Seria A No. 4/2002.

BEHAVIOUR OF TRACE CONCENTRATION OF PALLADIUM AND PLATINUM POLLUTANTS IN SOIL AND THEIR LEACHING FOR ANALYTICAL PURPOSES

Jadwiga Chwastowska, Witold Skwara, Elżbieta Sterlińska, Leon Pszonicki

Trace amounts of palladium and platinum, the major noble metals used in the automobile catalysts, are ejected with the exhausted gases and contaminate roads and their surrounding area. Although these metals, particularly platinum, are chemically inert, they are able to form reactive ligand systems. In this form they can be solubilised and enter soils, sediments, waters and plants and, in consequence, they may enter the food chain [1]. The ejected metals are cumulated, at first, in the road dust and in the surface layer of the soil around streets. They can penetrate gradually deep into the ground and then, after transformation with time under the influence of atmospheric, chemical and biological factors in soluble forms, into ground waters and plants. Therefore, the concentration of palladium and platinum in the soil is a good indicator of the contamination of an area.

The particles of metals emitted from the catalysts have a median size of 5-10 μm with an estimated emission rate of 2-40 $ng \cdot km^{-1}$ [2]. Taking into account, however, the high temperature of the catalyst work and the presence of sulphur and nitrogen oxides and hydrocarbons in the stream of exhausted gases it may not be excluded the formation of some compounds of palladium and platinum less chemically resistant than the metals. The aim of the presented work was to study the behaviour of various chemical forms of these metals introduced into the soil samples and the possibility of their leaching by water and 0.1 M hydrochloric acid (acidic rain) into solution for analysis. The soil is of similar type as the geological materials and it is a well known fact that the digestion of the total amount of the noble metals from such samples is very difficult. The best results are achieved by fire assay or chlorination [3]. In this case, however, in the investigation of soil contamination, these metals can be cumulated only on the surface of material grains and, therefore, for the determination of their total contents the digestion by *aqua regia* was applied.

For testing the recovery of the soluble compounds of both the metals they were introduced to the samples of soil, free from these metals, in the form of their nitric acid solution and in the form of water solution of chloroplatinate and chloropalladate salts. To study the behaviour of organic complexes of both the metals their complexes with thio-

urea were chosen. They are very stable and, therefore, it may be assumed that the obtained results will concern also the other less stable complexes.

An appropriate volume of a solution containing 5 μg of platinum and 2 μg of palladium were added to 1 g of soil samples and the samples were air dried and carefully homogenised. Then after the time of zero, 24 or 98 h the samples were digested by water or 0.1 M hydrochloric acid in a ultrasonic bath, centrifuged and palladium and platinum were determined in the solution [4]. In the samples digested directly after their preparation, the recovery for platinum was about 50% and for palladium about 15%. After 24 h these amounts were about 20 and 15%, respectively. After 96 h neither platinum nor palladium were detected after water or 0.1 M hydrochloric acid digestion.

In all type of the samples prepared as above and digested by *aqua regia*, the recovery of platinum and palladium in the solution was always in the range 95-101%. The same results were obtained also when the spiked samples after homogenisation were heated at 400°C. At this temperature, the palladium and platinum compounds are transformed into more chemically resistant forms.

On the basis of the above presented experiments it may be stated that palladium and platinum introduced into the soil even in the form of easily soluble compounds are quickly (24-96 h) completely bound with the soil matrix and cannot be re-extracted by water or dilute acids. This suggests that their infiltration into the ground waters and plants is strongly limited. On the other hand, application of *aqua regia* as the digesting medium enables their complete extraction and the total determination of both the metals.

References

[1]. Balcerzak M.: Analyst, 122, 67R-74R (1997).
[2]. Wei Ch., Morrison G.M.: Anal. Chim. Acta, 284, 587 (1994).
[3]. Rao C.R.M., Reddi G.S.: Trends Anal. Chem., 19, 565-586 (2000).
[4]. Chwastowska J., Skwara W., Sterlińska E., Dąbrowska M.: Application of dithizone sorbent to the separation and preconcentration of platinum from soil samples for its determination by atomic absorption spectrometry. Institute of Nuclear Chemistry and Technology, Warszawa 2001. Raporty IChTJ. Seria A No. 2/2001.

SPECIATION ANALYSIS OF CHROMIUM III AND VI IN MINERAL WATERS BY GF-AAS AFTER SEPARATION

Jadwiga Chwastowska, Witold Skwara, Elżbieta Sterlińska, Leon Pszonicki

Chromium belongs to the elements widely spread. It enters the environment as a result of effluent discharge from steel works, electroplating, tanning industry, oxidative dyeing, chemical industries and cooling water towers. The interest in the speciation analysis of chromium is governed by the fact that its toxicity depends critically on its oxidation state. Chromium III is considered as indispensable for the metabolism of glucose, lipids and proteins in the living organisms. Chromium VI as a strong oxidiser is highly toxic and can affect lungs, liver and kidneys and is mutagenic and carcinogenic.

Usually, the speciation of chromium is carried out by separation of chromium VI followed by the determination of chromium VI and the total chromium content. For the separation of both the forms of chromium various methods were used. From among the classic methods, there should be mentioned co-precipitation [1], solvent extraction [2-4] and ion exchange [5, 6]. In the last decade an HPLC separation technique [7, 8] and solid phase extraction [9, 10] were used most frequently. The separation processes base very often on the lability of chromium III resulting from the difficulty of displacing the water molecules from the strongly hydrated chromium III ions. Atomic absorption spectrometry (AAS) with flame or electrothermal atomization and ICP emission spectrometry are the methods used most frequently for determination of chromium.

In the presented work, the complex with ammonium pyrrolidinedithiocarbamate (APDC) was used for chromium speciation. Under the proper conditions, APDC reacts only with chromium VI. The strongly hydrated chromium III ions require a higher temperature and extended reaction time. The complex Cr(VI)-APDC was adsorbed on the macro-porous resin Diaion HP-2MG (methyl-methacrylic ester polimer) and, then, desorbed by nitric acid and determined by the AAS method.

Optimal conditions for the separation process were found on the basis of the artificially prepared water with the composition similar to the natural river water and spiked with chromium III and VI. They are as follows: pH of solution – 4.0; volume of solution – 100 ml; volume of added phthalic buffer – 5 ml; concentration of APDC – 3%; amount of resin – 1 g; shaking time – 20 min.

All experiments were carried out for two concentration ranges: 0.5 and 5 μg of chromium VI with the determination by flame AAS and 100 and 200 ng of chromium VI with the determination by GF-AAS. The recovery of chromium VI was from 82 to 90% for the higher concentration range and about 70% for the lower one. The described procedure was used for the determination of chromium VI in various natural mineral waters, e.g. in "Buskowianka" in which it was found 500 $ng \cdot L^{-1}$ of chromium VI and in "Nałęczowianka" chromium VI was not detected.

On the basis of the presented experiments it may be stated that the proposed procedure enables the separation and determination of chromium VI on the level from 70 to 90%, dependently on its

concentration in the sample. This decrease of results may be caused by the partial reduction of chromium during the separation process. The literature data indicate that chromium VI is unstable in the complex systems because of its high oxidation potential. In was found that concentration of chromium VI spiked into pond waters in an amount of 1.2 $\mu g \cdot ml^{-1}$ was diminished by of about 10% after 2 h [11]. The other authors obtained also the decreased results [5].

References

[1]. Lan C.R., Tseng C.L., Yang M.H., Alfassi Z.B.: Analyst, 116, 35 (1991).
[2]. Subramanian K.S., Anal. Chem., 60, 11 (1988).
[3]. de Jong G.J., Brinkman U.A.Th.: Anal. Chim. Acta, 98, 243 (1978).
[4]. Gardner M., Comber S.: Analyst, 127, 153 (2002).
[5]. Adria-Cerezo D.M., Llobat-Estelles M., Mauri-Aucejo A.R.: Talanta, 51, 531 (2000).
[6]. Coedo A.G., Dorado T., Padilla I., Alguacil F.J.: J. Anal. At. Spectrom., 15, 1564 (2000).
[7]. Posta J., Berndt H., Luo S., Schaldach G.: Anal. Chem., 63, 2590 (1993).
[8]. Andrle C.M., Broekaert J.A.C.: Fresenius J. Anal. Chem., 346, 653 (1993).
[9]. Rychlovsky O., Krenželok M., Volhejnowa R.: Collect. Czech. Chem. Commun., 63, 2015 (1998).
[10]. Vassileva E., Hadjiivanov K., Stoychev T., Daiev Ch.: Analyst, 125, 693 (2000).
[11]. Syty A., Christensen R.G., Rains T.C.: J. Anal. At. Spectr., 3, 193 (1988).

DETERMINATION OF POTASSIUM CONTENT IN THE B, C AND D CORNING REFERENCE GLASSES USING GAMMA-RAY SPECTROMETRY

Joachim Kierzek, Jerzy J. Kunicki-Goldfinger

Potassium is an important constituent of historical glasses. The determination of potassium concentration frequently plays a basic role in the examination of technology and provenance of glass artefacts. Gamma-ray spectrometry belongs to the group of non-destructive methods of determination of potassium content. Papers [1, 2] present details of the determination of the element concentration in historic glasses. A short description of the analytical procedure presented in those papers is given below.

Potassium contains 0.0119% ^{40}K, which is the only radioactive isotope of this element. The ^{40}K decays with a half-life of 1.28×10^9 years by an electron capture (10.5% yield) and a beta particle emission (89.3% yield). The maximum energy of beta particles is 1314 keV. The gamma-ray energy of 1460.8 keV has a branching ratio of 10.5%.

The radiometric measurements were performed with the use of a gamma-ray spectrometer, which contained an HPGe detector with the resolution of 1.9 keV, and a relative detection efficiency of 92.4% for a 1.33 MeV gamma line. The 10-cm passive lead shield lined with 0.5 cm cadmium and 0.5 cm copper was applied for reducing the natural background radiation.

The full examination consisted of two measurements. The first step included measurement of a silicon mould with the examined glass inside. For the second measurement, the same mould was filled with a powdered material that was used for calibration. High purity K_2SO_4 was used for this purpose. The self-absorption effect was taken into account during the computation of results. The counting time of each measurement was 24 h.

For the validation of the analytical procedure applied, measurements of potassium concentration were made for a group of three reference glasses, Corning B, C and D*. The glasses were prepared for the Corning Museum of Glass, USA [3, 4]. Laboratories in most countries very frequently use these reference glasses as comparison samples for chemical analyses of historical glasses.

Three measurements were made for each sample and for the calibration material. The reference glasses had a shape of rectangular prism; their dimensions were approximately 20x18x13 mm. The relative correction for self-absorption was determined and applied for the calculation of K_2O content [5].

The results obtained and recommended are listed in Table. The results confirm the efficiency of the procedure applied for the determination of potassium concentration as well as the recommended values of potassium concentration in the reference glasses examined [4].

Table. Comparison of K_2O contents obtained by the gamma-ray spectrometry method with the recommended values given in [4].

Reference glass	Weight of glass sample [g]	K_2O [wt.%]	
		Recommended value [4]	Gamma-ray spectrometry
B	15.7	1.00	1.02 ±0.03
C	14.8	2.84	2.84 ±0.06
D	11.8	11.3	11.2 ±0.3

However, we should remember that in case of complicated shapes of historical glass objects, it is difficult to make a correction for the self-absorption effect for the procedure applied. Moreover, there

are additional factors, which can deteriorate the accuracy of analyses carried out using gamma-ray spectrometry. These factors are difficulties in obtaining a uniform distribution of sulphate inside of a complicated mould made of rubber.
For simple shapes, gamma-ray spectrometry provides a very accurate determination of potassium concentration, which is confirmed by the results obtained.

References

[1]. Kunicki-Goldfinger J., Kierzek J.: Glastech. Ber. Glass Sci. Technol., 71, 11, 332-335 (1998).
[2]. Kierzek J., Kunicki-Goldfinger J., Kasprzak A.: Glastech. Ber. Glass Sci. Technol., 73, 11, 351-355 (2000).
[3]. Brill R.H.: A chemical-analytical round-robin on four synthetic ancient glasses. International Congress on Glass, Versailles, September-October 1971, Artistic and Historical Communications, Paris, L'Institut du Verre, 1972, pp.93-110.
[4]. Brill R.H.: Chemical Analyses of Early Glasses. The Corning Museum of Glass, Corning, New York 1999. Vol. 2, Appendices B, C, D, pp.539-544.
[5]. American National Standard Calibration and Use of Germanium Spectrometers for the Measurement of Gamma-Ray Emission Rates of Radionuclides. ANSI, N42.14-1991.

* The glasses were made available for examination thanks to Dr. Robert Brill from the Corning Museum of Glass.

A PROVENANCE STUDY OF BAROQUE GLASS

Jerzy J. Kunicki-Goldfinger, Joachim Kierzek, Aleksandra J. Kasprzak[1/], Bożena Małożewska-Bućko, Piotr Dzierżanowski[2/]

[1/] National Museum in Warsaw, Poland
[2/] Faculty of Geology, Warsaw University, Poland

The goals of the project are the determination of the provenance and dating as well as recognition of technology of the 18th century central European tableware. This interdisciplinary project has begun in 1998 and till now it has covered over 1400 vessels originated from the Polish-Lithuanian Commonwealth, German lands, Bohemia, Silesia and Russia. In its preliminary screening step, it has consisted of inventory works, conservation surveys, historical studies, archive searching and physicochemical examinations by means of the non-destructive tools – observation of glass fluorescence under the ultraviolet radiation (UV) and an energy dispersive X-ray fluorescence analysis (EDXRF). The results obtained allow us to differentiate particular groups of vessels in respect of their technology and origin. Based on single items of certain provenance, entire groups have been attributed to particular glasshouses and periods. The multivariate statistical analyses are used for analysis of large set of data. The second step of the project is conducted by the use of electron probe microanalysis (EPMA) that has been applied for quantitative analyses of samples taken from the selected vessels.

For studying the provenance of baroque glass vessels many elements have to be taken into consideration (like typological and stylistic analysis, archive data, characterisation of glass composition). Differences in the chemical composition of glass made in numerous glass centres as well as differences between glass batches manufactured in one place at the same time must be taken into account. Glass vessels from different places made from similar batches by the use of similar or the same raw materials, often being important from one source, in several cases can disclose more similarities of their chemical composition than glass vessels made in one glasshouse by the use of different recipes. Three main technological kinds of glass were discovered, independently of the place of their origin. These are crystal, white (chalk) and ordinary glass. For almost all of the crystal glasses, it seems possible to differentiate items manufactured in various glasshouses. This is possible for only some of the white glasses, and for ordinary glasses, drawing such distinctions is a very difficult task. One of the most interesting findings was the presence of significant amounts of lead in many glasses manufactured in central Europe since the beginning of the 18th century. Main discriminating features of the distinguished glass formulations concern As/Ca and K/Ca ratios. The ingredients like Pb, B and Cl and their specific ranges of content differ from one glasshouse to another, and concern particular glass formulations, too. The trace elements' concentrations (like Sr, Zr, Rb, Y) often constitute a key parameter for glass production centre and dating determination. Thanks to this multistage procedure, the attribution of numerous vessels has been determined without any need to sample them.

The project is a result of a many years' collaboration among many Polish research centres and museums and has been partly supported by the Polish State Committee for Scientific Research (grant No. 1HO1E 028 18), KARIA (Warszawa), NDT Systems (Warszawa), OSTOYA Auction House (Warszawa).

APPLICATION OF DISCRIMINANT AND CLUSTER ANALYSIS FOR THE PROVENANCE STUDIES OF HISTORIC GLASS BASING OF X-RAY FLUORESCENCE ANALYSIS

Joachim Kierzek, Jerzy J. Kunicki-Goldfinger, Aleksandra J. Kasprzak[1/], Bożena Małożewska-Bućko

[1/] National Museum in Warsaw, Poland

Introduction

Radioisotope X-ray fluorescence (XRF) analysis was used for studying the composition of luxury colourless glassware originating from the selected 18th century glasshouses in the Polish-Lithuanian Commonwealth and Germany. The concentration of minor and trace elements enabled to infer the glass production recipes, the raw materials used and their origin. A number of characteristic chemical elements was selected. Cluster and discriminant analyses with variables, calculated from the measured radiation intensities for individual elements, were used to differentiate the objects manufactured in different glasshouses.

Minor and trace element analysis and multivariate statistical techniques demonstrated a large potential for provenance determination of museum and archaeological objects [1-7]. The presented results refer to objects manufactured in Dresden (Saxony), Potsdam/Zechlin (Brandenburg), Naliboki and Lubaczów (Polish-Lithuanian Commonwealth) in the 18th century.

Among the examined glass objects there was a group of crystal glasses. These central European, 18th century crystal glasses had been characterized in earlier papers [7, 8].

The aim of this study was to demonstrate the possibility of application of discriminant and cluster analysis to provenance determination of 18th century glass objects based on of Ca, Mn, Fe, Cu, Zn, As, Rb, Sr, Y, Zr and Pb contents, determined by XRF analysis.

Experimental

The energy-dispersive X-ray fluorescence (EDXRF) analysis was performed by using a spectrometer equipped with an 80 mm^2 Si(Li) detector with the 180 eV resolution at 5.9 keV, a ^{109}Cd radioisotope annular source (~200 MBq activity), an amplifier, a multichannel analyser and a personal computer. The examined objects were placed directly on the source shield. The analysed area of glass surface was about 2 cm^2. The collected spectra were analysed by the AXIL software [9].

Matrix and measurement geometry were corrected by taking the ratio of element line count, N_{ij}, to the sum of the coherently, $N_{j(\mathrm{coh})}$, and the incoherently, $N_{j(\mathrm{incoh})}$, scattered AgKα source counts, as in equation (1) for element, i, and object, j [7, 10].

$$S_{ij} = \frac{N_{ij}}{N_{j(\mathrm{coh})} + N_{j(\mathrm{incoh})}} \qquad (1)$$

The obtained results of, S_{ij}, were used for classification of glass objects and for futher comparative studies.

Discriminant analysis

Principle

Discriminant analysis is a statistical method for studying differences between two or more groups of objects for which a number of variables is measured. A set of objects must be known to belong to the studied groups [1]. Linear functions (discriminant functions) of the variables are used to describe the differences between groups. The objective of discriminat analysis is to estimate the coefficients of discriminant function (linear combinations) in such a way that the ratio of between-group variance to the within-group variance is maximized [11].

The application of this method consist of the following steps:

- Selection of learning set of objects belonging to well-defined class.
- Selection of a set of variables that best discriminate between groups.
- Testing that the presumed groups are really distinct (discriminant functions).
- Derivation, using the learning set, of the classification functions which can be used to assign future observations into one of selected groups. Observations are assigned to the group with the largest classification score.

Learning and test sets

The learning and test sets were created based on the knowledge of a vessel type and its decoration, the archive sources and the results of XRF measurements published earlier [7, 8].

A set of 76 objects, representative for 4 glass producing centres : Naliboki, Lubaczów, Dresden and Potsdam/Zechlin, was selected.

Table 1. Groups of the learning set (53 objects).

Glass centre	Crystal glass		Non-crystal glass	
	Group symbol	Number of objects	Group symbol	Number of objects
Naliboki	NPb	12	NO	10
Lubaczów	-	-	LO	10
Dresden	SPb	7	SO	7
Potsdam/Zechlin	ZPb	7	-	-

The origin of objects, the technology of their production, the number of objects in the learning set groups and their symbols are given in Table 1.

The test set contained 23 objects and was composed of 12 items belonging to NPb group, of 8 items belonging to NO group and 3 objects belonging to LO group.

The division of the learning set into groups was verified by the use of the cluster analysis [1, 11] of XRF results. A grouping dendrogram of the learning set is shown in Fig.1.

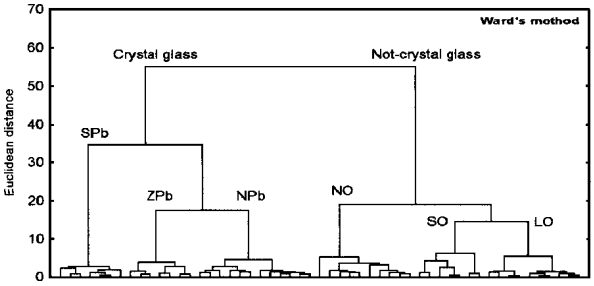

Fig.1. Cluster analysis: dendrogram for the learning set of glass vessels.

The S_{ij} values as defined in equation (1) were calculated for the following elements : Ca, Mn, Fe, Cu, Zn, As, Rb, Sr, Y, Zr and Pb.

The evaluation of results was done using program STATISTICA.

Data processing

The best set of variables for derivation the discriminant and classification functions were selected using a forward stepwise procedure:

- Selection criterion – F-statistic
- Predetermined significance levels of F-statistic:
  - F to-enter = 4.0,
  - F to-remove = 3.9.
- Input variables : S_{ij} for Ca, Mn, Fe, Cu, Zn, As, Rb, Sr, Y, Zr, Pb.

The ellipses drawn are the 95% confidence limit boundaries of the groups.

Results of calculations for the learning set

There is evident division of the glasses into the crystal and non-crystal ones (Fig.2). The basis of

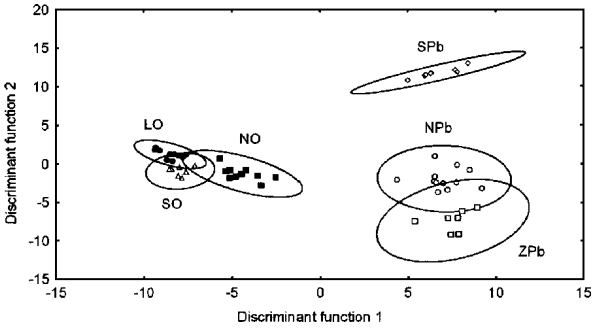

Fig.2. Discriminant analysis for the learning set of 53 glass vessels assumed to belong to 6 different groups. Discriminant function 1 and 2 comprises 54.6 and 29.3% of between – group variance, respectively. Variables: S_{ij} for Pb, Y, Sr, Fe, Zr, Rb in the sequence of decreasing importance. Correct classification rate: 100%.

division is the variable for Pb that reflects the introducing of lead compounds as the raw material. Other variables characterise the impurities of raw materials (first of all, this concerns sand and lime). The discriminant analysis was applied separately to crystal and non-crystal glasses:

a) Results for the crystal glasses are shown in Fig.3. There are 3 well separated groups. Beside the trace elements, being the impurities of raw materials, the S_{ij} coefficients for Ca and Mn were

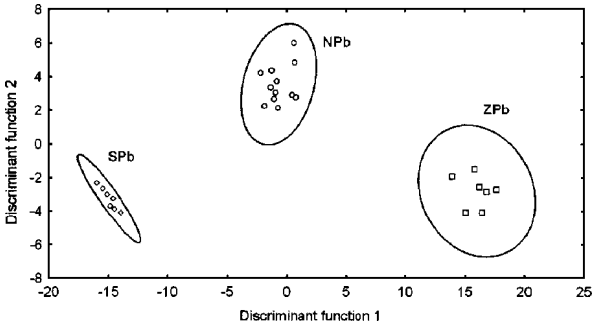

Fig.3. Discriminant analysis of 26 crystal vessels in the learning set. Discriminant function 1 and 2 comprises 92.3 and 7.7% of between – group variance, respectively. Variables: S_{ij} for Zr, Y, Fe, Ca, Rb, Mn in the sequence of decreasing importance. Correct classification rate: 100%.

introduced to the computation model and these 2 elements were the components of recipe. Pb, the most characteristic component of these glasses, was neglected in the calculation model. The 3 groups originated from different glasshouses (Dresden, Naliboki, Potsdam/Zechlin) and were fabricated using the different recipes. This is confirmed by the presence of Ca and Mn taken into account in a set of variables in the model.

b) Results for the non-crystal glasses are shown in Fig.4.

Only the chemical elements representing the raw material impurities were introduced to the computation model. For assignment of these glasses to a particular group important are the raw

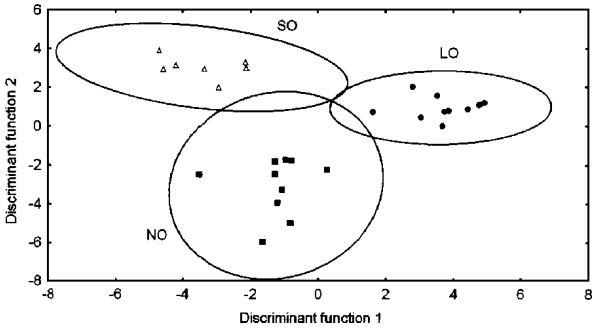

Fig.4. Discriminant analysis of 27 non-crystal vessels in the learning set. Discriminant function 1 and 2 comprises 58.0 and 42.0% of between – group variance, respectively. Variables: S_{ij} for Sr, Fe, Rb, Zr in the sequence of decreasing importance. Correct classification rate: 100%.

material source and their preparation for production, the differences in recipes are less meaningful in distinguishing the not-crystal glasses. Among impurities the Sr and Fe contents play a basic role. The first one constitutes a lime impurity, the second one, first of all-sand impurity.

Table 2. Correct classification and prediction rates using derived classification functions.

Method of validation	Number of items	Correct classification rate
Resubstitution for learning set	53	100%
Test set	23	100%
Cross-validation for some objects of groups SO and ZPb and SPb not present in test set	6	100%

In the presented model for the not-crystal glasses, it is characteristic the omission of Y, a distinctive impurity of the silicate raw materials. This element played an important role in distinguishing the crystal glasses fabricated in the particular glassworks (Fig.3).

Results of validation

To verify that the computed classification models and prediction performances of classification functions are correct, three validation techniques were applied:

- resubstitution of learning set,
- classification of test set,
- cross-validation (leave-one-out) for objects of groups not present in test set.

The results of validation are presented in Table 2.

Conclusions

The results presented confirm the usefulness of the discriminant analysis for determination of the glass provenance and the technology of its production when XRF is used for the glass elemental composition measurement.

When the set of proper groups and variables is used, then the recognition and prediction ability can be very high.

The disadvantage of the discriminant analysis is that a completely unknown object will always be assigned to one of classes in the learning set to which it should not belong.

In this paper, the elements with the atomic number equal and higher than calcium have been considered. The elements with lower atomic numbers present in glass as the main components or impurities were not considered. Taking them into account would further improve or extend the classification of objects. Nevertheless, the variables used presented a sufficient set for correct grouping of the examined glasses.

References

[1]. Baxter M.J.: Exploratory Multivariate Analysis in Archaeology. Edinburgh University, New York 1996.
[2]. Baxter M.J.: Archaeometry, 31, 45-53 (1989).
[3]. Kowalski B.R., Schatzki T.F.: Anal. Chem., 44, 2176-2180 (1972).
[4]. Harbottle G.: Activation analysis in archaeology. In: Radiochemistry. Vol.3. Ed. G.W.A. Newton. Chem. Soc., London 1976, pp.33-72.
[5]. Mommsen H.: J. Radioanal. Nucl. Chem., 247, 657-662 (2001).
[6]. Beier T., Mommsen H.: Archaeometry, 36, 287-306 (1994).
[7]. Kunicki-Goldfinger J., Kierzek J., Kasprzak A., Małożewska-Bućko B.: X-Ray Spectrom., 29, 310-316 (2000).
[8]. Kunicki-Goldfinger J., Kierzek J., Kasprzak A., Małożewska-Bućko B.: XVIII-wieczne naczynia szklane z hut w Nalibokach i Urzeczu. Badania fizykochemiczne. Raporty IChTJ. Seria B nr 2/99. Instytut Chemii i Techniki Jądrowej, Warszawa 1999.
[9]. Van Espen P., Janssens K., Nobels J.: Chemom. Intell. Lab. Syst., 1, 109 (1986).
[10]. Swerts J., Aerts A., De Biscop N., Adams F., Van Espen P.: Chemom. Intell. Lab. Syst., 22, 97 (1994).
[11]. Subhash Sharma: Applied Multivariate Techniques. John Wiley and Sons, Inc., New York 1996.

APPLICATION OF TRACK MEMBRANES FOR MICROFILTRATION OF WATER SAMPLES INFLUENCED BY TEMPERATURE CHANGES

Marek Buczkowski, Danuta Wawszczak, Bożena Sartowska, Wojciech Starosta

Track membranes (TMs) manufactured by means of heavy ions beam accelerated in a cyclotron can be applied for different microfiltration processes. In this work, TMs made of poly(ethylene terephthalate) film, 10 μm in thickness, in the Joint Institute for Nuclear Research (JINR, Dubna, Russia), have been used for microfiltration of water samples after a process of freezing out. Specific features of TMs have been applied: precisely determined pore diameter makes it possible cascade microfiltration in the range from 3 to 0.2 μm and a smooth membrane surface enables convenient observation of microfiltration results by scanning electron microscope (SEM) [1-5].

For experiments two kinds of mineral water commercially available: No. I with high (2530 mg/dm^3), No. II with low (234 mg/dm^3), minerals content and a sample of tap water were used. All samples were treated by introductory filtration (with the end stage by a metallic grid of 50 μm mesh value) and then by microfiltration with 3 kinds of TMs at decreasing pore sizes: 2.3, 1.3, and 0.45 μm. After each stage of microfiltration, the membrane discs were dried and weighed. This made it possible to determine masses of sediments and then to calculate concentration of suspensions. These results are given in the first part of Table (lines: 1, 2, and 3).

Table. Parameters of water samples after the microfiltration processes: 1-3 initial samples, 4-6 samples after freezing out.

	Kind of water	pH of initial sample	pH of sample after microfiltration	TM 2.3 μm, Mass of sediment [mg]	TM 2.3 μm, Concentration of suspensions [mg/dm^3]	TM 1.3 μm, Mass of sediment [mg]	TM 1.3 μm, Concentration of suspensions [mg/dm^3]	TM 0.45 μm, Mass of sediment [mg]	TM 0.45 μm, Concentration of suspensions [mg/dm^3]
1.	Mineral water (I)	6.95	6.79	Non-meas.	-	Non-meas.	-	0.25	0.27
2.	Mineral water (II)	6.90	6.64	0.1	0.066	0.25	0.67	0.1	0.50
3.	Tap water	7.58	7.56	0.25	0.26	0.75	0.79	0.3	0.86
4.	Mineral water (I)	6.98	6.52	62.5	138.89	0.5	1.11	0.3	1.15
5.	Mineral water (II)	7.49	7.20	0.85	1.25	0.15	0.22	0.05	0.10
6.	Tap water	7.54	7.52	0.4	2.23	0.2	1.25	0.1	0.63

In the next part of experiments, other samples of the same kind of water were treated by introductory filtration and then frozen at a temperature of -16°C. After the natural process of melting ice at room temperature, the procedures described above were carried out again. The results are given in the second part of Table (lines: 4, 5, and 6).

TMs appeared to be useful for the determination of distribution of microsuspension sizes occurring in water samples after the process of freezing out. It was concluded that in case of the sample of highly mineralized water, after freezing out an amount of 5.6%, initially dissolved mineral components, were produced as suspensions. The majority of separated components was in the range 50-2.3 μm.

Photographs from SEM allow us to conclude that the sediment on the TMs surface has the form of crystals with an average size of a few micrometers. One can find also conglomerates with a few dozen micrometers of size after joining together many smaller crystals. Such images appear after freezing out the high mineralized water (Figs.1 and 2). In case of tap water the amount of sediments is smaller and they are not so regular (Fig.3). It seems

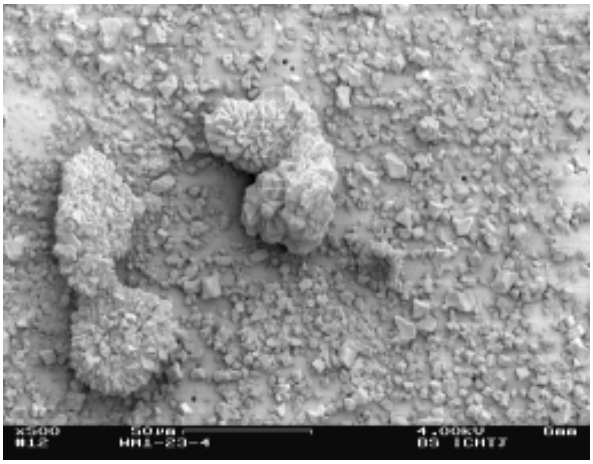

a)

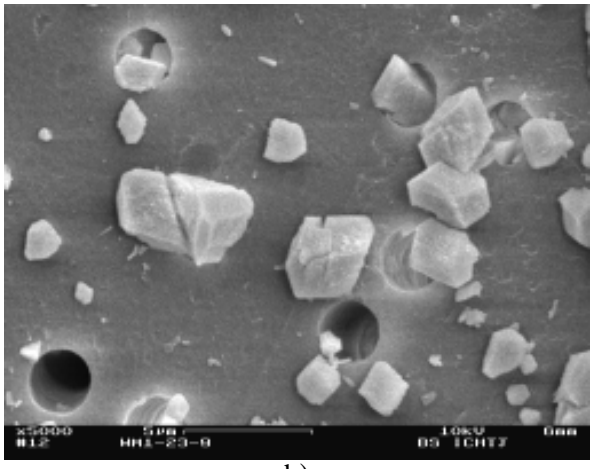

b)

Fig.1. SEM photographs of sediments on the TM surface with pore size 2.3 μm after microfiltration of a freezed out of highly mineralized water sample: a) magnification x500 – single crystals and conglomerates of many crystals are seen, b) magnification x5000 – single crystals are seen.

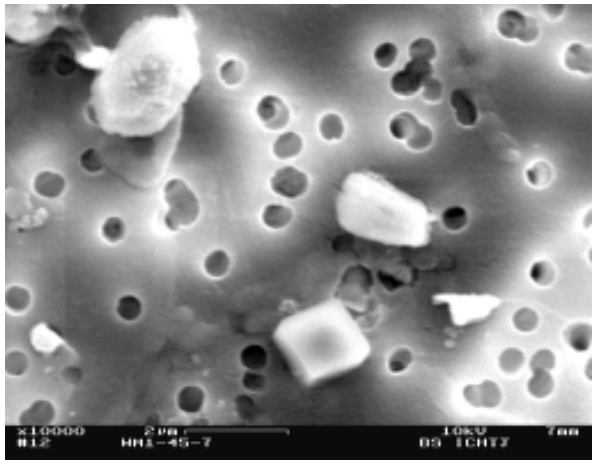

Fig.2. SEM photographs of sediments on the TM surface with pore size 0.45 μm after microfiltration of a freezed out highly mineralized water sample.

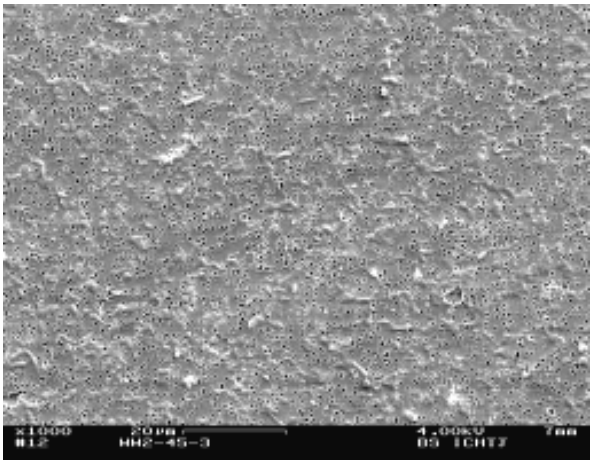

Fig.3. SEM photographs of sediments on the TM surface with pore size 0.45 μm after microfiltration of a freezed out tap water sample.

that more precise observations can explain the mechanism of forming such components.

Extraction of mineral suspensions after freezing out water samples and their observation can be one of the indicators of water quality. This effect should also be taken into account in analysis of technological processes where temperature changes can appear as well as in processes of water cycle in the natural environment.

References

[1]. Spohr R.: Ion Tracks and Microtechnology, Principles and Application. Vieweg, Braunschweig 1990, 272 p.
[2]. Particle track membranes and their applications. Proceedings of the 2nd Meeting, Szczyrk, Poland, 2-6 December 1991. Eds. W. Starosta, M. Buczkowski. Institute of Nuclear Chemistry and Technology, Warszawa 1992, 90 p.
[3]. Bodzek M., Bohdzewicz J., Konieczny K.: Techniki membranowe w ochronie środowiska. Wyd. Pol. Śl., Gliwice 1997, 444 p.
[4]. Granops M., Kaleta J.: Odnowa wody. Laboratorium. Oficyna Wydawnicza Politechniki Rzeszowskiej, 1996, 136 p.
[5]. Sartowska B., Wawszczak D., Buczkowski M.: Particle track membranes – application for filtering out impurities from water samples. SEM Investigations. X Conference on Electron Microscopy of Solids, Warszawa-Serock, Poland, 20-23 September 1999, pp.393-396.

KINETICS OF POLYPYRROLE DEPOSITION INTO ISOPOROUS MEMBRANE TEMPLATES

Danuta Wawszczak, Wojciech Starosta, Bożena Sartowska, Marek Buczkowski

Polypyrrole (PPy) belongs to conducting polymers which are the most stable in typical environmental conditions. For such kinds of polymers that are used as switching devices, catalytic supports and carriers for active ingredients, they must have a high and predictable surface area and controlled morphology. This requires carrying out some investigations concerning the mechanism of forming PPy surface and kinetics of such process [1-4].

Presented results are a continuation of investigations performed earlier. As before, synthesis of PPy was carried out in track membranes (TMs) made of a 10 μm thick poly(ethylene terephthalate) (PET) film (Joint Institute for Nuclear Research – JINR, Dubna, Russia). For the synthesis, aqueous solutions: 0.1 M pyrrole and 0.3 M $FeCl_3$ (III) as oxidant, have been taken [5, 6].

PPy synthesis into TMs with pores size 1.3 and 0.2 μm has been carried out. Observations by SEM (DSM 942 Zeiss-Leo type) allow us to conclude that a buildup process takes place on the TMs surface as well as in the membrane pores. So called microtubules are formed inside the TMs pores and their thickness changes *vs*. polymerization time. Such relation given in Fig.1 allows us to conclude that it is a two-stage process. In the first stage, the speed of buildup PPy layer inside the pores of 0.2 μm diameter is equal to 5.6 nm/min, and inside the pores of 1.3 μm – 12.1 nm/min. In the second stage, such speed is equal to 1.4 and 4.9 nm/min, respectively. Decreasing of buildup speed in the second stage is probably connected with the reduction of diffusion speed of reagents, which is an important factor during the process of PPy forming.

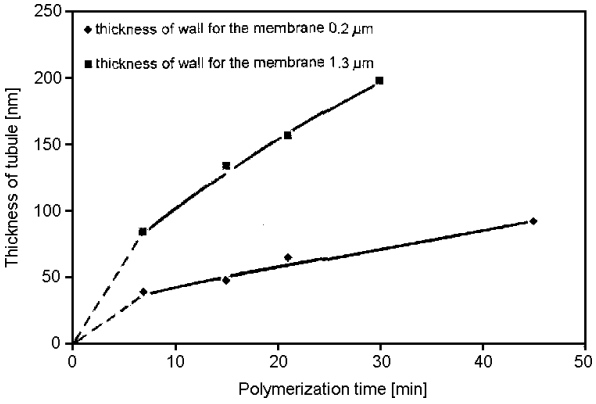

Fig.1. Thickness of tubules *vs*. polymerization time.

SEM photographs (Fig.2) show the buildup process of PPy layer on the TM surface and the process of microtubules forming inside the pores at different intervals of polymerization time (10, 21, and 30 min). Measurements of wall thickness of microtubules and their inside diameter allow to conclude that up to 30 min interval of time the described processes are uniform. Increasing of polymerization time up to 45 min causes closing of the pores on the membrane surface but this does not lead to forming pins inside the pores. The present authors, while continuing these investigations, would like to explain this phenomenon and to dissolve membrane templates in order to get only the PPy structure.

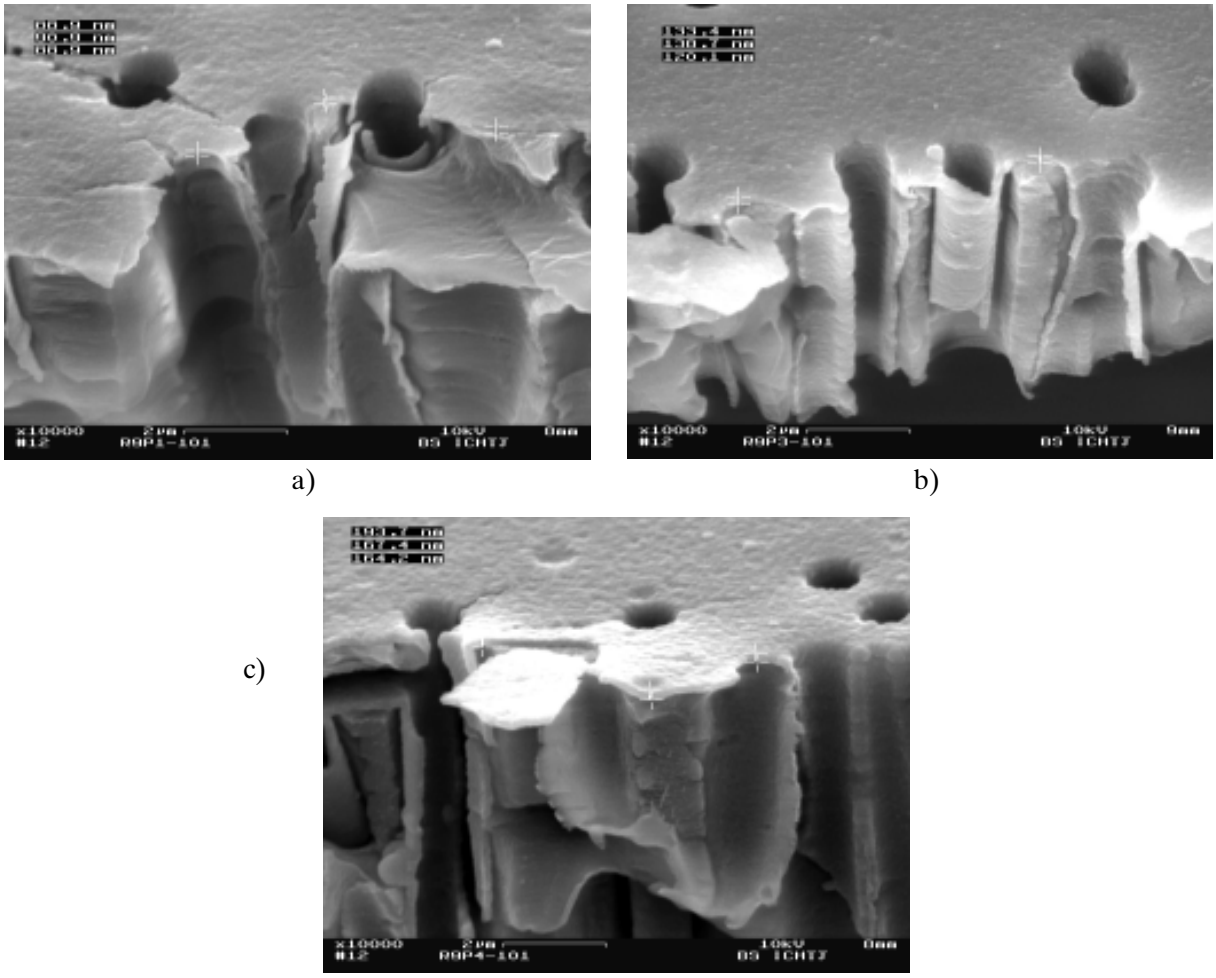

Fig.2. SEM photographs of a PPy deposition on the surface of the track membrane (pore diameter – 1.3 μm) and inside the pores at different intervals of polymerization time: a) 10 min, b) 20 min, c) 30 min.

References

[1]. Nakata M., Kise H.: Polym. J., 25, 91 (1993).
[2]. Huczko A.: Appl. Phys., A 70, 365-376 (2000).
[3]. Panner M., Martin C.R.: J. Electrochem. Soc., 133, 2206 (1986).
[4]. Burford R.P., Tongtam T.J.: J. Mater. Sci., 57, 3766 (1991).
[5]. Martin C.R. *et al*.: Synth. Met., 57, 3766 (1993).
[6]. Zhitariuk N.I., Moel A.Le., Mermilliod N., Trautmann C.: Nucl. Instrum. Meth. Phys. Res. B, 105, 204-207 (1995).

SYNTHESIS OF $LiFePO_4$/Ni,Cu, AND Ag NANOCOMPOSITES FOR ELECTROCHEMICAL APPLICATIONS BY COMPLEX SOL-GEL PROCESS

Andrzej Deptuła, Tadeusz Olczak, Wiesława Łada, Bożena Sartowska, Andrzej G. Chmielewski, Fausto Croce[1/], Josef Hassoun[1/]

[1/] University "La Sapienza", Roma, Italy

Among several materials developed for the use as cathodes in lithium ion batteries, $LiFePO_4$ of the phospho-olivine family appears particularly interesting due to its environmental compatibility. In a paper [1], $LiFePO_4$ was prepared by the solid-state reaction of Li_2CO_3 and $(NH_4)_2HPO_4$ with $Fe(CH_3COO)_2$. The last reagent is very expensive (1 g Fe ≅ 25 DM). We elaborated [2, 3] a new method of the preparation of this compound by Complex Sol-Gel Process (CSGP) using a very cheep iron(III) nitrate (1 g Fe 1.4 DM). In our paper [2] we briefly described a process with the application of inexpensive iron(III) nitrate as iron source for preparation of $LiFePO_4$, also metal doped. The idea of doping was concluded from the proposal of Goodenough and his coworkers [4] who improved iron based cathode material, but by adding of carbon as electronic conductive substance. In our process the reduction of iron(III) to iron(II) was effected by ascorbic acid (ASC) in CSGP, in which a strong complexing agent having reductive properties is used. This proprietary procedure (INCT) has been patented [5] and successfully applied for synthesis of other cathode materials such as $LiMn_2O_4$ [6] and $LiNi_xCo_{1-x}O_2$ [7]. The goal of this work was a continuation of more de-

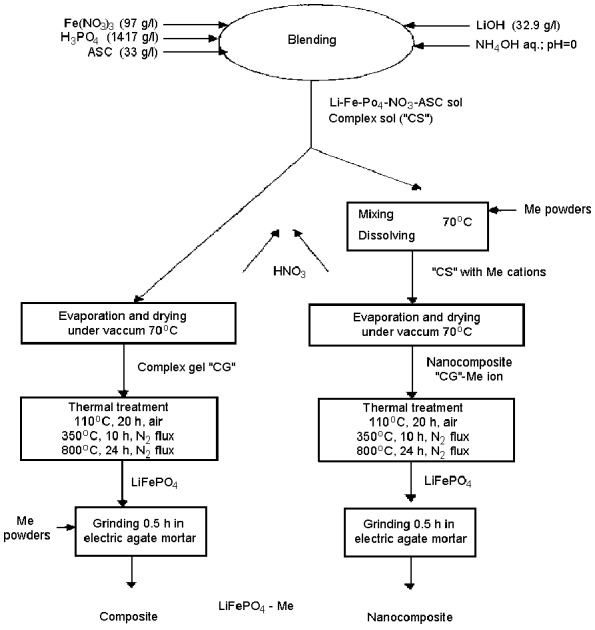

Fig.1. Flowchart for preparation of $LiFePO_4$ with Me nanocomposites (denoted with "-": $LiFePO_4$-Me) and composites (denoted with "+": $LiFePO_4$+Me).

tailed studies on the process. Moreover, we would like to elucidate the influence of Me-doping procedure on the properties of the final materials. We decided to add of metallic powders (Me-powders) to sols (route "PS") or, to the earlier prepared by CSGP olivine powders (route "PP").

A flowchart of the preparation procedures is shown in Fig.1. The first step of the process consists of the addition of concentrated H_3PO_4 to an aqueous solution of $Fe(NO_3)_3$. After reduction of Fe^{3+} to Fe^{2+} by ASC, stoichiometric quantities of LiOH and fine metallic powders (silver, copper or nickel) were dispersed into the sol to form submicronic colloidal particles. This conclusion is confirmed by SEM powder data e.g. for copper (Fig.2). In contrast, in materials obtained by addition of Me-powders to synthesized $LiFePO_4$ (route "PP") these were observed. It is evidently proved for copper powders represented by particles of fern frond shape.

The results of the thermal decomposition of various $LiFePO_4$ gels in air are shown in Fig.3.

Finally, the gels were heated at 800°C for 24 h in a nitrogen flux. XRD patterns indicate that the resulting powders were single phase $LiFePO_4$. High stability of the product at elevated temperatures (also against reoxidation) has been proved by thermal analysis. The cathodes prepared of this material exhibited good electrochemical properties (cyclic voltammetry, charge-discharge curves and cycle life) in a cell prototype.

Goodenough and coworkers [4] were the first researchers who demonstrated the possibility of application of $LiFePO_4$ (trihylit) of the phospho-olivine family for the use as a cathode in lithium ion batteries. Recently, Yamada, Chung and Hinokume [8] underlined that iron based lithium compounds appear particularly interesting due to their environmental compatibility and low cost of constituents. They demonstrated that $LiFePO_4$ is the only good candidate among all known iron phosphates,

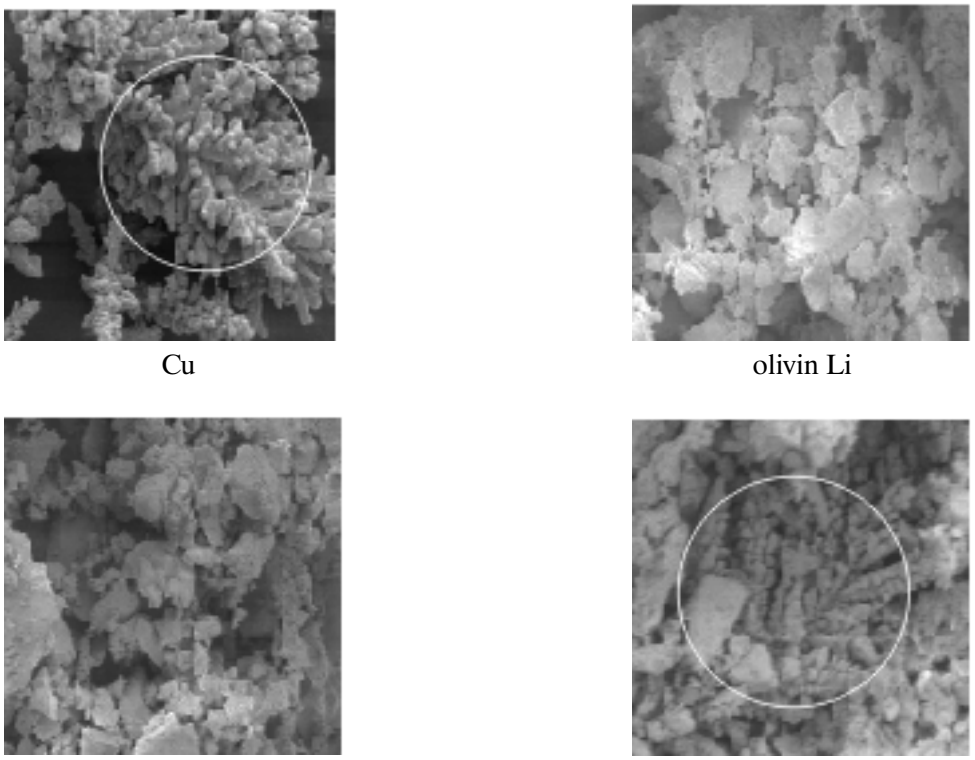

Fig.2. SEM microphotographs of copper powders and composite materials obtained. Metal particles indicated in white rectangle.

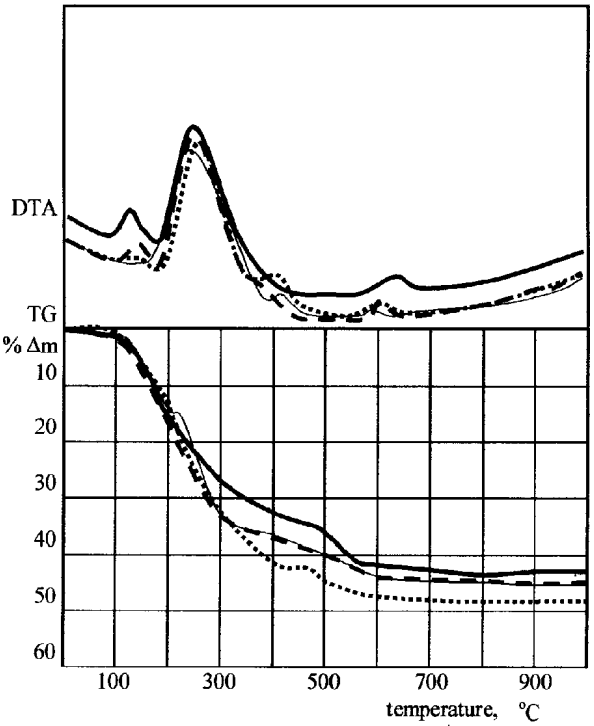

Fig.3. Thermal analyses traces of the $LiFePO_4$-Me gels dried for 20 h at 110°C: $LiFePO_4$ (bold line), $LiFePO_4$-Ag (fine line), $LiFePO_4$-Cu (dashed line) and $LiFePO_4$-Ni (dotted line).

where iron(II) oxalate was applied instead of acetate. We observed [2] that one drawback of this conventional preparation route for these compounds is the necessity of using the expensive Fe^{2+} precursors and inert atmosphere during preparation and final thermal treatment. Calculation shows that 1 g of iron at this valence costs: in acetate = 25 DM and in chloride = 8 DM. The prices are definitely lower for iron(III) salts e.g. for nitrate = 1.4 DM.

The processing procedures are summarized in Fig.1. In the first step "blending", the change of the yellow-brown color of starting $Fe(NO_3)_3$ solution trough a violet-brown after addition of H_3PO_4 and finally intensive dark-brown after addition of ASC appeared. This is an indication of the reduction of iron(III) to (II). No precipitates were observed during this operations as well as after addition of LiOH and aq. ammonia, but in the last case it has been seen only proved at pH<0.3. To the sol prepared as above, metallic powders were added (route "PS"). Particulars are shown in Fig.2.

We observed that during evaporation to dry mass at 70°C for 1 h, nitric acid was nearly completely distilled out. At this step the quantity of metallic powder sediment decreased radically, and finally was completely dissolved. We conducted experiments of dissolving metal powders separately at RT in "broth" obtained in this way that contains all components except iron ion. After 3 h, the major part of powders were dissolved. Initially, transparent broth changed its color to light-brown in the presence of silver, green-brown with nickel and exhibited milky-blue opalescence with copper added. The last observation seems to indicate that metal powders can be dissolved in sols to form colloidal particles not only of ionic form. We noted that all powders remained unchanged even after 2 days when kept in phosphoric acid. This conclusion is confirmed by SEM microphotographs presented in Fig.2. In the nanocomposites $LiFePO_4$-Me synthesized by "PS" route, we never observed the particles of a shape typical for starting metallic powders. In contrast, in materials obtained by addition of Me-powders to synthesized $LiFePO_4$ (route "PP") these were observed. This is evidently proved for copper powders represented by particles of shape fern frond.

Metallic powders dissolved to form Me hydroxides (or salts) are reduced during thermal treatment to submicron metals particles by ASC or, more probably by organics formed from it. Reduction of nickel ion to metallic form, even in air, was observed earlier [7] during the thermal decomposition of $LiNi_xCo_{1-x}O_2$ gels. Therefore, it was also studied by us.

At 250°C a very distinct exothermic effect appeared, which represents the combustion effect of residual organics. Their content is evidently sufficient for the reduction process and also to maintain a reducing atmosphere during thermal treatment in an inert atmosphere.

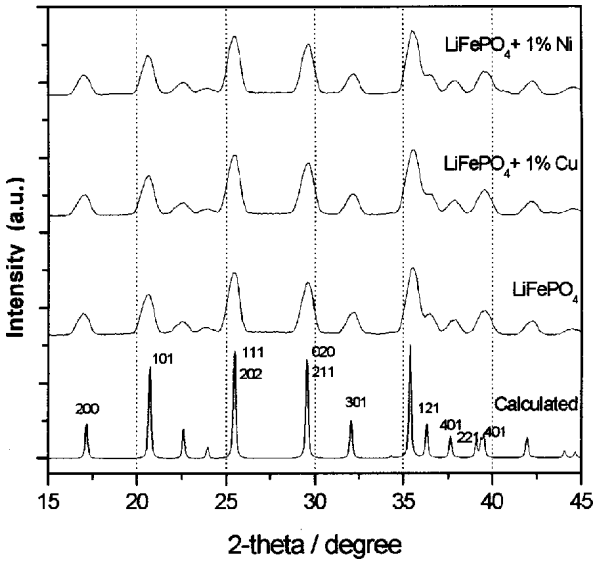

Fig.4. XRD patterns of $LiFePO_4$-Me nanocomposites.

XRD patterns of final nanocomposites are shown in Fig.4. It can be concluded that all synthesized materials have the structure of $LiFePO_4$. The bands attributed to metal additives are not observed, presumably due to the low concentration and these homogeneous distribution.

Thermal resistance of nanocomposite (Fig.5) heated in air has been also studied. The graph completely free of any mark of thermal events (no weight increasing and practically DTA thermal effects) indicates that both $LiFePO_4$ and its nanocomposites are stable. Presumably, the oxidation of Me, if it occurs, cannot be observed in our equipment. Even if all added Me would be subjected to oxidation process, the weight increase should be lower than approximately 0.5%.

In the former paper [2], we describe some electrochemical properties of synthesized nanocom-

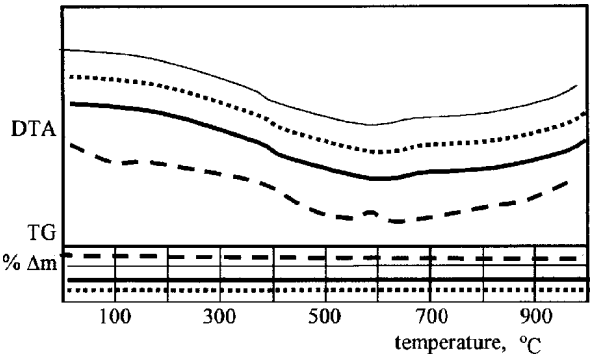

Fig.5. Thermal analyses traces of the $LiFePO_4$-Me nano- and composites obtained at 800°C: $LiFePO_4$ (bold line), $LiFePO_4$-Ag (fine line), $LiFePO_4$-Cu (dotted line), $LiFePO_4$+Cu (dashed line).

posites. The increase in capacity, when passing from the standard to the modified $LiFePO_4$-Cu electrode, was clearly shown: a change from 120 to 145 $mAhg^{-1}$ is observed. This difference is obviously associated with the presence of the metal, and confirms its role in optimizing the morphology of the $LiFePO_4$ electrode material, thus leading to substantial enhancement of the kinetics of its electrochemical process. The capacity and the rate capabilities substantially were improved for nanocomposites too. The beneficial role of the dispersed metal powders may be explained by assuming that these powders act as nucleation sites for the growth of the $LiFePO_4$ compound, thus helping in obtaining samples with low and uniform particle size, as well as in enhancing their overall electronic conductivity. In addition, the dispersion of metal powders is also expected to provide contact bridges between the $LiFePO_4$ particles, reducing the inter-particle resistance and thus, to assure the progress of the electrochemical reaction throughout the electrode mass. Evidently, these advantages cannot be attained by mechanical admixing of metallic powders into $LiFePO_4$ earlier prepared ordinary composites.

References

[1]. Huang H., Yin S.-C., Nazar L.F.: Electrochem. Solid-State Lett., 4, A170 (2001).
[2]. Croce F., D'Epifanio A., Hassoun J., Deptuła A., Olczak T., Scrosati B.: Electrochem. Solid-State Lett., 5, A47 (2002).
[3]. Croce F., Serraino Fiory F., Persi L., Scrosati B.: Electrochem. Solid-State Lett., 4, A121 (2001).
[4]. Ravel N., Goodenough J.B.: private communication, 1998.
[5]. Deptuła A., Łada W., Olczak T., Lanagan M., Dorris S.E., Goretta K.C., Poeppel R.B.: Method of preparing of high temperature superconductors. Polish Patent No. 172618.
[6]. Deptuła A., Olczak T., Łada W., Ciancia A., Giorgi L., Di Bartolomeo A., .Brignocchi A., Croce F.: CIMTEC, Proceedings. Volume L. Innovative Materials in Advanced Energy Technologies. Ed. P. Vincenzini. Techna, Faenza, Italy 1999, p.149.
[7]. Deptuła A., Olczak T., Łada W., Croce F., Giorgi L., Di Bartolomeo A., Brignocchi A.: J. Sol-Gel Sci. Technol., in press.
[8]. Yamada A., Chung S.C., Hinokuma K.: J. Electrochem. Soc., 148, A224 (2001).

THERMAL CONVERSION OF Li^+-Me^{2+}-CH_3COO^--ASCORBIC ACID-OH GELS TO $LiMn_2O_4$ AND $LiNi_xCo_{1-x}O_2$

Andrzej Deptuła, Tadeusz Olczak, Wiesława Łada, Bożena Sartowska, Fausto Croce[1/], Leonardo Giorgi[2/], Angelo Di Bartolomeo[2/], Aldo Brignocchi[2/]

[1/] Department of Chemistry, University "La Sapienza", Roma, Italy

[2/] Italian Agency for the New Technologies, Energy and Environment (ENEA), C.R.E. Casaccia, Rome, Italy

Among the wide family of intercalation compounds the layered oxides and spinels have received considerable attention as positive electrode materials in high-energy density lithium and lithium ion batteries. $LiMn_2O_4$ and $LiNi_xCo_{1-x}O_2$ systems are extensively studied within this frame, as they are the only known materials capable to intercalate reversibly lithium at high cell voltage (3.5-4 V). Usually, these compounds are prepared by high temperature solid state reaction of lithium oxides, carbonates, acetates or nitrates with respective compounds of manganese, nickel or/and cobalt. In previous papers [1-6] we described a new variant of sol-gel process named Complex Sol-Gel Process (CSGP) suitable to synthesize the above mentioned materials. The latter process offers the advantage of lowering both the temperature and the time of formation, but it requires to follow several steps that need to be optimized for the achievement of an overall acceptable yield.

The main feature in CSGP process is the application of a very strong complexing agent (ascorbic acid – ASC) for sol preparation. The procedure has been patented by the Institute of Nuclear Chemistry and Technology (INCT, Poland) and Argonne National Laboratory (ANL, USA) teams [7] and successfully applied to the synthesis of superconductors. In all lithium compounds prepared with ASC we observed that thermal treatment of gels is a very complex process, which involves foaming, self-ignition, and sometimes formation of carbonates too.

In the present study we have pursued the goal of trying to elucidate some aspects of thermal transformation of gels into the final crystalline phases, paying special attention to foaming, self-ignition phenomena and formation of carbonates.

The spinel $LiMn_2O_4$ and layered oxides $LiNi_xCo_{1-x}O_2$ (x=1, 0.75, 0) have been prepared by CSGP. On the basis of our former experience [4]

we selected as a starting solution manganese, nickel and cobalt aq. acetates to which ASC was added. In order to decrease the quantity of organics, we decided to add LiOH instead of lithium acetate. We observed that the content of a sufficient amount of ASC did not involve precipitation. The flow chart of this modified process is shown in Fig.1.

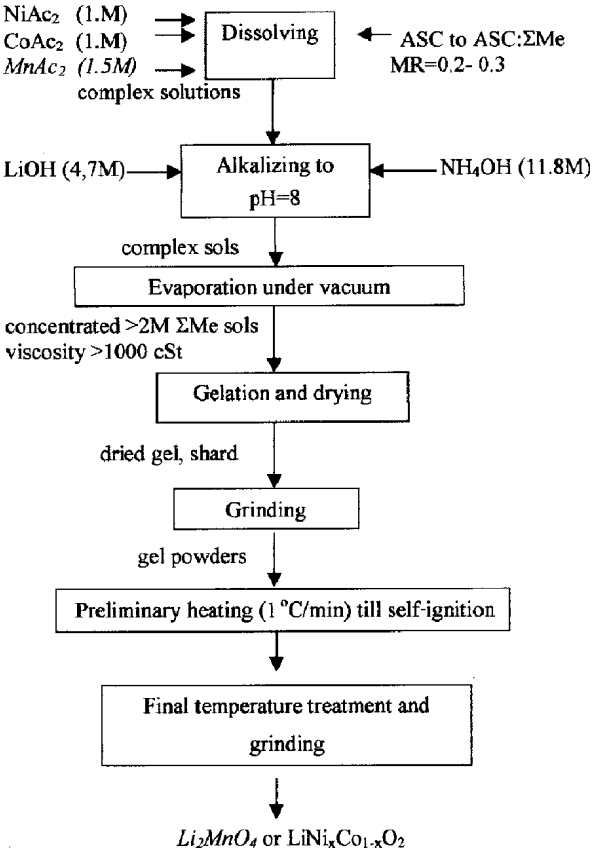

Fig.1. Flow chart for preparation of Li_2MnO_4 or $LiNi_xCo_{1-x}O_2$ by CSGP.

As in our previous works [1-6] we observed intense foaming from concentrated sols during their heating, even if a very slow heating rate (<0.5°C/min) was adapted. The process led to the formation of highly voluminous (2-5 times of starting volume) macroporous structures. This phenomenon is a clear consequence of an intense gas evolution from sols or, more correctly, from melted gels. We have noticed that while sols were fluids in the temperature range 110-160°C, they solidified at room temperature. The foam is formed in this systems by the release of gases produced as a consequence of the thermal decomposition of organic compounds which are present in sols. Subsequently, the decomposition of foam is followed by its simultaneous solidification. However, heating of gels to higher temperatures results in a violent self-ignition. Consequently, we dried generally samples 4 days at 170°C. The homogeneous, but porous "cakes" were

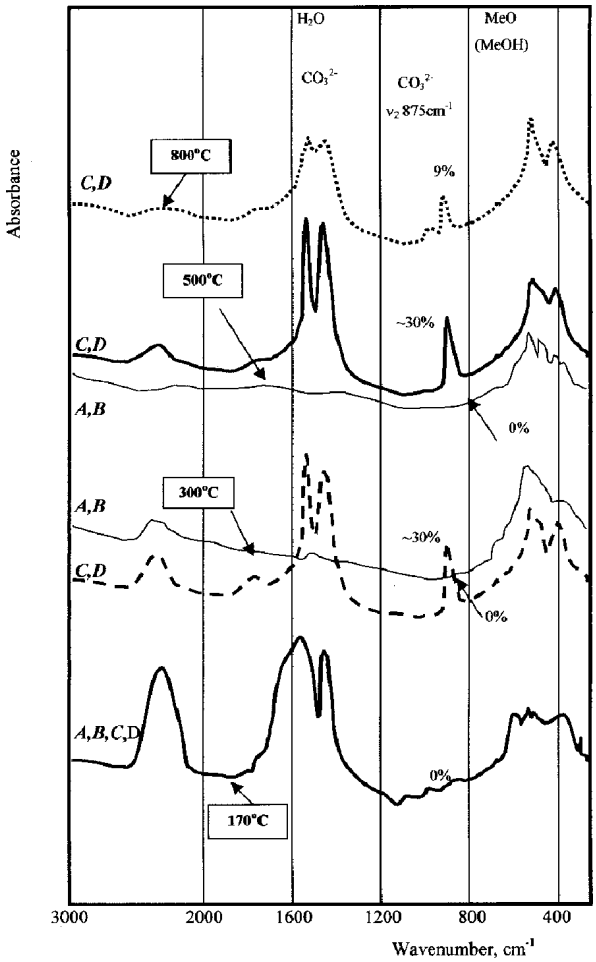

Fig.2. Infrared spectra of (A – $LiMn_2O_4$, B – $LiCoO_2$, C – $LiNi_{0.75}Co_{0.25}O_2$ and D – $LiNiCoO_2$) gels heated at various temperatures.

Table. Chemical analysis, SIT and specific surface area.

Sample and heating	SIT [°C]	% C	% H	% N	S [m^2/g]
"A" $LiMn_2O_4$ – 170°C	320	31.66	3.80	1.56	2.4
"B" $LiMn_2O_4$ – 170°C	438	30.05	3.76	1.30	2.3
"C" $LiMn_2O_4$ – 440°C, 1 h (sample B after self-ignition)		0.5*	0	0.1	9.1
$LiCoO_2$ – 170°C	440	32.89	3.72	2.79	3.3
"D" $LiNi_{0.5}Co_{0.5}O_2$ – 170°C	510	35.90	3.81	5.63	3.2
"E" $LiNi_{0.25}Co_{0.75}O_2$ – 170°C	430	36.01	4.50	6.73	2.8
"F" $LiNi_{0.25}Co_{0.75}O_2$ – 440°C, 1 h (sample E after self-ignition)					3.1
Ascorbic acid (foaming was not observed)	Not observed				

* carbon is not retained as carbonates.

grounded and then analyzed. The results of chemical analyses are comprehended in Table. The self--ignition temperature (SIT) and specific surface area (S) are included. It has to be noted that the results of chemical analysis are roughly similar. The analysis of IR spectra of representative samples shown in Fig.2 prove the absence of carbonates in the sample dried at 170°C. It means consequently that all carbon if present, represents organics only. Evidently, hydrogen belongs only partially to organics while nitrogen is bonded within inorganic species.

Therefore, we confirm in the present study the conclusion drawn in our former work [6] that the SIT does not depend on the content of carbonaceous compound. We suggested in this work, however, that SIT is determined perhaps by specific surface area S of samples. As seen, the results given in Table do not confirm this hypothesis. At present, we believe that SIT depends probably on the structure

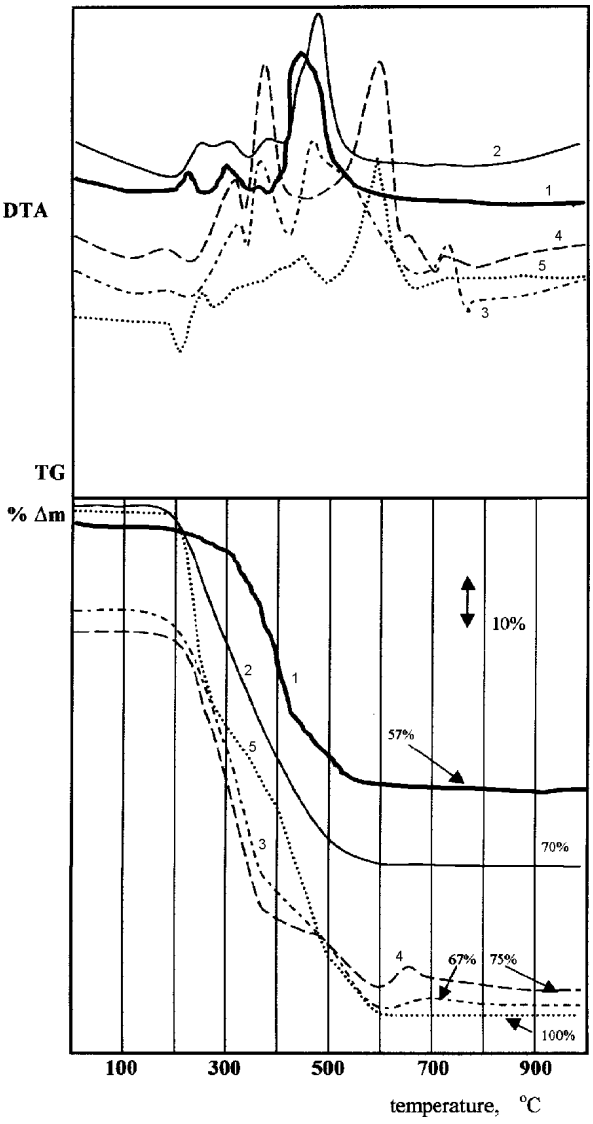

Fig.3. TG and DTG traces of the Li-Ni-Co gels dried at 170°C and pure ASC: 1 – $LiMn_2O_4$, 2 – $LiCoO_2$, 3 – $LiNi_{0.75}Co_{0.25}O_2$, 4 – $LiNiO_2$, 5 – ASC.

and morphology of the carbonaceous materials formed by the decomposition of ASC. Knowing that SIT of Li-Ni-Co compounds now studied is higher than that of $LiMn_2O_4$, as well as that self--ignition do not appear in pure ASC, we suggest now an important role of metallic species in the discussed process.

Further decomposition of the tested samples was studied by thermal analysis. The representative TG and DTA traces of all gels studied are shown in Fig.3.

In both $LiMn_2O_4$ and $LiCoO_2$ gels, the continuous and quite large loss of the weight accompanied by a small thermic effects was observed up to *ca.* 400°C. At this temperature level, a very distinct exothermic effect appears, that represents the combustion effect of residual organics. The above temperature roughly corresponds to the SIT (Table) as observed during the stationary heating of samples. On the basis of recorded the IR spectra (Fig.2), we can conclude now that in both investigated compositions carbonates are not formed. In our previous papers [5, 6], we observed that $LiMn_2O_4$ was completely formed at 400°C. On the other hand,

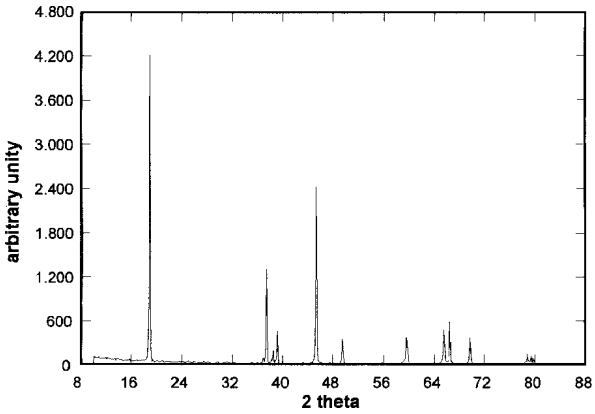

Fig.4. XRD patterns of the $LiCoO_2$ formed at 600°C.

the XRD patterns, shown in Fig.4, indicate that $LiCoO_2$ is formed only at 600°C.

Dramatic changes of the thermal decomposition traces were observed with gels containing nickel. Final exothermic effect, which appeared for the Li-Co gel, is roughly similar and corresponds to SIT level. The effect is accompanied by a strong increase of the specific surface area for carbonate free precursors (Table). However, in nickel containing layered oxides at a lower temperature (about 350°C), another distinct exothermic effect appears. It can be associated with the formation of lithium and nickel carbonates from organics. The carbonate analysis shown in Fig.2, as well as the XRD patterns (Fig.5), indicate that after the heating at 300 and 500°C, quite large quantities of carbonates are still present in the system.

Lack of the increase in specific surface area after self-igniton of those precursors confirms suggestion that the presence of Li_2CO_3 involves sintering. After a long heating at 800°C the CO_3 content decreases. However, according to our earlier work [4] even at 900°C the presence of 1-2% of CO_3 (not observed by XRD) in the samples with x 0.75 is still noted. It means that full removal of carbonates from those type of layered oxides by thermal treatment seems impossible. Evidently, too high final temperatures cannot be used in this kind of

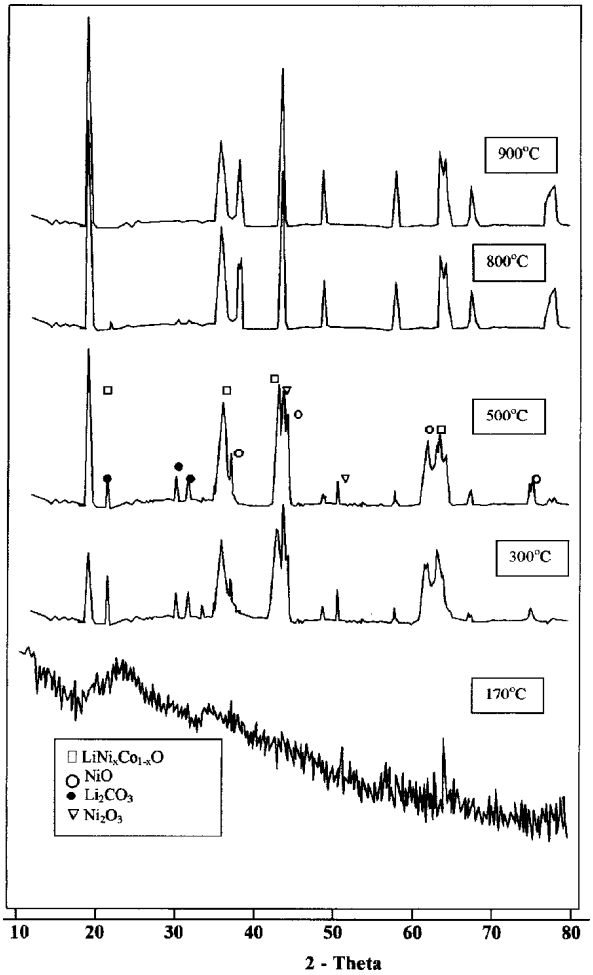

Fig.5. XRD patterns of the $LiNi_{0.75}Co_{0.25}$ gels calcined at various temperatures.

process due to (i) decomposition of the materials which occurs above 850°C according to the reaction:

$$(1\text{-}x)LiNiO_2 \quad Li_{1-x}Ni_{1-x}O_2 + xLi_2O + 0.5O_2$$

and (ii) to the possibility of evaporation of Li_2O.

For both nickel layered oxides a small distinct drop of mass was observed at 600°C, followed by the increase of the weight up to 650°C. This phenomenon is associated with the reduction of Ni^{+3} by the carbonaceous species and subsequent re-oxidation of the metallic nickel, similarly as it was observed in [8] during the decomposition of nickel acetate. This observation seems to be crucial for the interpretation of the retarded formation of pure layered oxide phase in the case of nickel containing compositions. Evidently, the reaction of nickel with other components of precursors is not so effective as in the case of nickel oxides. It is why nickel cathodes, known as very resistant against molten lithium carbonate attack, are commonly used in Molten Carbonate Fuel Cells.

The results of electrochemical test of materials synthesized by CSGP indicated clearly that only $LiMnO_2$ and $LiCoO_2$ species, which are completely carbonate free, exhibit very good electrochemical properties. Because of unsatisfactory results obtained with LiNiCo-layered oxide, evidently the consequence of the presence of carbonates in there, we elaborated a very efficient method for the decarbonization of them by the treatment with nitric acid and hydrogen peroxide [9].

The self-ignition process discussed above seems to be quite similar to the "combustion synthesis" of ceramic materials. However, in this latter case the addition of a fuel (e.g. urea) and of an oxidizer (e.g. nitrates) was necessary to initiate the combustion. On the contrary, no additives were necessary for self-ignition of the ascorbate gels which are examined in this work. In fact, carbonaceous species which are formed during ASC decomposition, are very reactive and even atmospheric oxygen is sufficient to start their ignition. It was observed that self-ignition is especially violent in respect to more massive samples. From technological point of view this phenomenon can be utilized for energy saving during the calcinations process.

References

[1]. Deptuła A., Łada W., Olczak T., Croce F., Ronci F., Ciancia A., Giorgi L., Brignocchi A., Di Bartolomeo A.: Materials for Electrochemical Energy Storage and Conversion II – Batteries, Capacitors and Fuel Cells. Vol. 496. Eds. D.S. Ginley, D.H. Doughty, B. Scrosati. MRS Pittsburg, PA, USA, 1998, p.237.

[2]. Croce F., Deptuła A., Łada W., Marassi R., Olczak T., Ronci F.: Ionics, 3, 390 (1997).

[3]. Croce F., D'Epifanio A., Ronci F., Deptuła A., Łada W., Ciancia A., Di Bartolomeo A., Brignocchi A.: New Materials for Batteries and Fuel Cells. Proceedings. Vol. 575. Eds. D.H. Doughly, L.F. Nazar, M. Arakawa. MRS Pittsburg, PA, USA, 2000, p.97.

[4]. Deptuła A., Łada W., Olczak T. Croce F., D'Epifanio A., Di Bartolomeo A., Brignocchi A.: J. New Mater. Electrochem. Syst., in press.

[5]. Deptuła A., Łada W., Croce F., Appetecchi G.B., Ciancia A., Giorgi L., Brignocchi A., Di Bartolomeo A.: Second International Symposium on New Materials for Fuel Cell and Modern Battery Systems. Eds. O. Savadogo, P.R. Roberge. Montreal, Canada, 1997, p.732.

[6]. Antolini S.: J. Mater. Sci. Lett., 13, 1599 (1994).

[7]. Deptuła A., Łada W., Olczak T., Lanagan M., Dorris S.E., Goretta K.C., Poeppel R.B.: Method of preparing of high temperature superconductors. Polish Patent No. 172618.

[8]. Elmasry A., Gaber A., Khater E.M.H.: J. Therm. Anal., 47, 757 (1996).

[9]. Deptuła A., Olczak T., Łada W., Sartowska B., Croce F., Di Bartolomeo A., Brignocchi A.: Formation of pure $LiNi_xCo_{1-x}O_2$ spinel phase by decarbonization of gels by low-temperature treatment with nitric acid and hydrogen peroxide following by thermal treatment. 11th International Workshop on Glasses, Ceramics, Hybrids and Nanocomposites from Gels, Padova, Italy 15-21 September 2001.

CRYSTAL CHEMISTRY OF COORDINATION COMPOUNDS WITH HETEROCYCLIC CARBOXYLATE LIGANDS. PART XL: THE CRYSTAL AND MOLECULAR STRUCTURES OF TWO CALCIUM(II) COMPLEXES WITH PYRAZINE-2,6-DICARBOXYLATE AND WATER LIGANDS

Wojciech Starosta, Halina Ptasiewicz-Bąk, Janusz Leciejewicz

The structure of {*catena*-[μ-aqua-O]bis[μ-pyrazine-2,6-dicarboxylato-O,N-O']} [diaqua-calcium(II)]} consists of dimeric units composed of two calcium(II) ions, two ligand molecules and six water

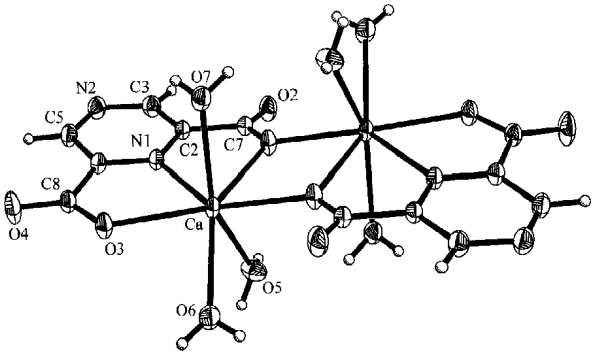

Fig.1. The structural unit observed in both title compounds with atom labelling scheme. Non-hydrogen atoms are shown as 50% probability elipsoids.

molecules. The calcium ions are bridged by two bidentate oxygen atoms, each donated by one carboxylic group of the ligand. The calcium(II) ion is also coordinated by one oxygen atom of the second carboxylate group and the hetero-ring nitro-

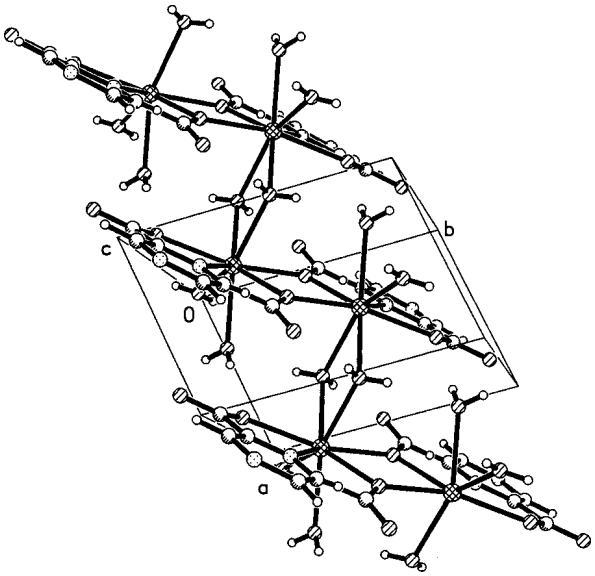

Fig.2. A fragment of a molecular ribbon.

gen atom belonging to the same ligand molecule (Fig.1). Both calcium ions in a dimer are bridged to the calcium(II) ions in adjacent dimers by a pair of water molecules forming infinite molecular ribbons. In addition, each calcium(II) ion is coordinated by three water molecules; one of them is used for bridging the adjacent dimer (Fig.2). The coordination polyhedron around the calcium(II) ion is a pentagonal bipyramid with two apices above and one apex below the equatorial plane. The same molecular pattern is observed in the structure of {*catena*-[μ-aqua-O]bis[μ-pyrazine-2,6-dicarboxylato-O,N-O']}[diaqua-calcium(II)]}dihydrate which, in addition, contains two solvation water molecules per unit cell. In both compounds the molecular ribbons are held together by extended systems of hydrogen bonds.

X-ray diffraction measurements were carried out using the KUMA KM4 four circle diffractomer at the Institute of Nuclear Chemistry and Technology. Data processing and structure refinement was performed using SHELXL programme package.

References

[1]. Part XXXI. Starosta W., Ptasiewicz-Bąk H., Leciejewicz J.: Dimeric molecules in the crystals of a calcium complex with pyridine-3,5-dicarboxylate ligands. J. Coord. Chem., 55, 1 (2002).

[2]. Part XXXII. Starosta W., Ptasiewicz-Bąk H., Leciejewicz J.: Dimeric molecules in the crystals of a calcium(II) complex with pyridine-2,6-dicarboxylate and water ligands. J. Coord. Chem., 55, 469 (2002).

[3]. Part XXXIII. Paluchowska B., Maurin J.K., Leciejewicz J.: The crystal and molecular structures of Pb(II) complexes with furan-2-carboxylate and furan-3-carboxylate ligands. J. Coord. Chem., 55, 771 (2002).

[4]. Part XXXIV. Starosta W., Ptasiewicz-Bąk H., Leciejewicz J.: The crystal structures of two polymorphic forms of a calcium(II) complex with pyridine-2,6-dicarboxylate, water and nitrate ligands. J. Coord. Chem., 55, 873 (2002).

[5]. Part XXXV. Starosta W., Ptasiewicz-Bąk H., Leciejewicz J.: Molecular chains in the crystals of a calcium(II) complex with pyridine-3,5-dicarboxylate (dinicotitate) and water ligands. J. Coord. Chem., 55, 985 (2002).

[6]. Part XXXVI. Starosta W., Ptasiewicz-Bąk H., Leciejewicz J.: The crystal and molecular structure of a new calcium(II) complex with pyridine-2,6-dicarboxylate, water and nitrate ligands. J. Coord. Chem., 55, 1147 (2002).

[7]. Part XXXVII. Starosta W., Ptasiewicz-Bąk H., Leciejewicz J.: The crystal structure of an ionic calcium(II) complex with pyridine-3,5-dicarboxylate and water ligands. J. Coord. Chem., 56, 33 (2003).

[8]. Part XXXVIII. Ptasiewicz-Bąk H., Leciejewicz J.: The crystal structures of pyrazine-2,6-dicarboxylic acid dihydrate and hexaquamagnesium pyrazine-2,6-dicarboxylate. J. Coord. Chem., 56, 173 (2003).

[9]. Part XXXIX. Ptasiewicz-Bąk H., Leciejewicz J.: The crystal structure of a strontium(II) complex with pyrazine-2,6-dicarboxylate and water ligands. J. Coord. Chem., 56, 223 (2003).

CRYSTAL CHEMISTRY OF COORDINATION COMPOUNDS WITH HETEROCYCLIC CARBOXYLATE LIGANDS. PART XLI: THE CRYSTAL AND MOLECULAR STRUCTURE OF A ZINC(II) COMPLEX WITH PYRAZINE-2,6-DICARBOXYLATE AND WATER LIGANDS

Michał Gryz[1/], Wojciech Starosta, Halina Ptasiewicz-Bąk, Janusz Leciejewicz

[1/] National Institute of Public Health, Warszawa, Poland

The structure of the title compound is composed of molecular chains propagating along the b axis of the unit cell (Fig.1). The chain is built up by zinc(II) ions linked through the pyrazine-2,6-dicarboxylate ligand (2,6-PZDC) molecules. The bridging pro-

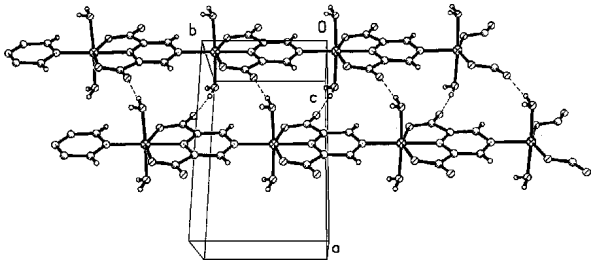

Fig.1. The alignment of molecular chains in the structure of $Zn(2,6\text{-}PZDC)(H_2O)_2$.

ceeds *via* two carboxylate oxygen atoms each donated by a separate carboxylate group and the hetero-ring nitrogen atom located between them (the N,O bonding moiety) on one side and the second hetero-ring nitrogen atom on the other.

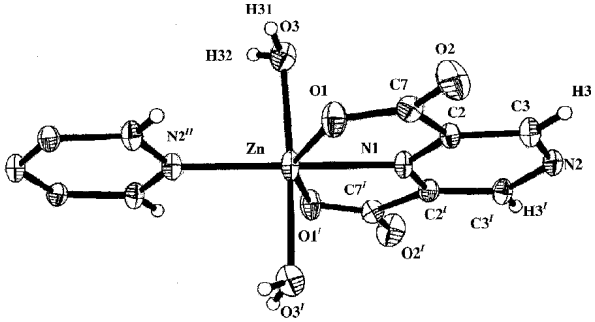

Fig.2. A fragment of the molecular chain in the structure of $Zn(2,6\text{-}PZDC)(H_2O)_2$ with atom labelling scheme. Non-hydrogen atoms are shown as 50% elipsoids.

Figure 2 shows the environment of a zinc(II) ion with the atom labelling scheme. The coordination around the metal ion is distorted octahedral. The zinc(II) ion, two chelating carboxylate oxygen atoms and the two hetero-ring nitrogen atoms are coplanar. The observed Zn-O and Zn-N bond distances are typical for zinc coordination compounds with carboxylate ligands, however, the bond angles within the above plane deviate considerably from 90 deg. indicating a distortion of the coordination polyhedron. Two symmetry related water oxygen atoms, one above and the other below the base form the apices of an octahedron. The O3-Zn-O3^I angle is 176.1(1) deg. also indicating a distortion. The pyridazine ring of the ligand molecule only slightly deviates from planarity, since its carbon atoms are shifted from the mean plane by ±0.021(1) Å. On the other hand, the carboxylate group atoms are shifted by: C7: 0.131(4) Å, O1: 0.170(4) Å and O2: 0.216(5) Å.

The most interesting feature of the structure of the title compound is the use of both hetero-ring nitrogen atoms of the ligand molecule to bridge the zinc ions. The use of both pyrazine ring nitrogen atoms has been up to now observed only in the structure of the strontium complex with pyrazine-2,5-dicarboxylate and water ligands [1], however, in this structure two N,O bonding moieties of the ligand molecule are active in bridging, while in the title compound apart from the N,O,O moiety, only a single hetero-ring N atom acts as bridging.

A simple hydrogen bond scheme which holds together the molecular chains in the structure of the title compound consists of moderately strong bonds of 2.7 Å.

X-ray diffraction measurements were carried out using the KUMA KM4 four circle diffractomer at the Institute of Nuclear Chemistry and Technology. Data processing and structure refinement was performed using SHELXL programme package.

CRYSTAL CHEMISTRY OF COORDINATION COMPOUNDS WITH HETEROCYCLIC CARBOXYLATE LIGANDS. PART XLII: THE CRYSTAL AND MOLECULAR STRUCTURE OF DIAQUABIS(PYRIDAZINE-3-CARBOXYLATE-N,O)ZINC(II) DIHYDRATE

Michał Gryz[1/], Wojciech Starosta, Halina Ptasiewicz-Bąk, Janusz Leciejewicz

[1/] National Institute of Public Health, Warszawa, Poland

In the course of systematic X-ray diffraction structural studies of coordination compounds of divalent metals with diazine carboxylate ligands, the crystal structure of diaquabis(pyridazine-3-carboxylate-N,O)zinc(II) dihydrate was determined. The crystals of the title compound are triclinic (space group P1 bar) and are built of monomeric molecules consisting of a zinc(II) ion coordinated by

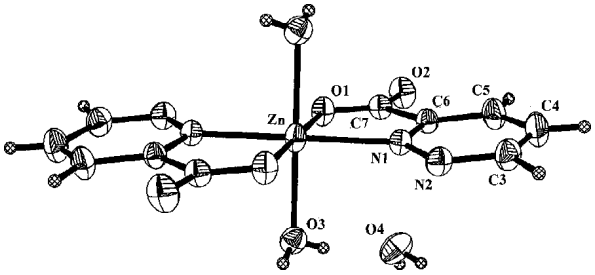

Fig.1. The molecule of diaquabis(pyridazine-3-carboxylato-N,O)zinc(II) dihydrate with atom labellinging scheme.

two pyridazine-3-carboxylate ligands, each through one hetero-ring nitrogen atom and the nearest to it carboxylate oxygen atom forming a N,O bonding moiety. Two oxygen atoms donated by water molecules complete the coordination number to six. Figure 1 shows the coordination mode with atom labelling scheme. The coordinated atoms form an octahedron with typical for zinc(II) complexes bond lengths: Zn-$O_{carboxylate}$ 2.066(1) Å, Zn-O_{water} 2.179(1) Å and Zn-N 2.107(1) Å. The N1-Zn-O1 angle is 78.50(4) deg., the N1-Zn-$O1^{I}$ angle 101.50(4) deg. The solvation water molecules take part in a network of hydrogen bonds. The latter are shown as broken lines on the packing diagram displayed in Fig.2.

X-ray diffraction measurements were carried out using the KUMA KM4 four circle diffractomer at the Institute of Nuclear Chemistry and Technology. Data processing and structure refinement was performed using SHELXL programme package.

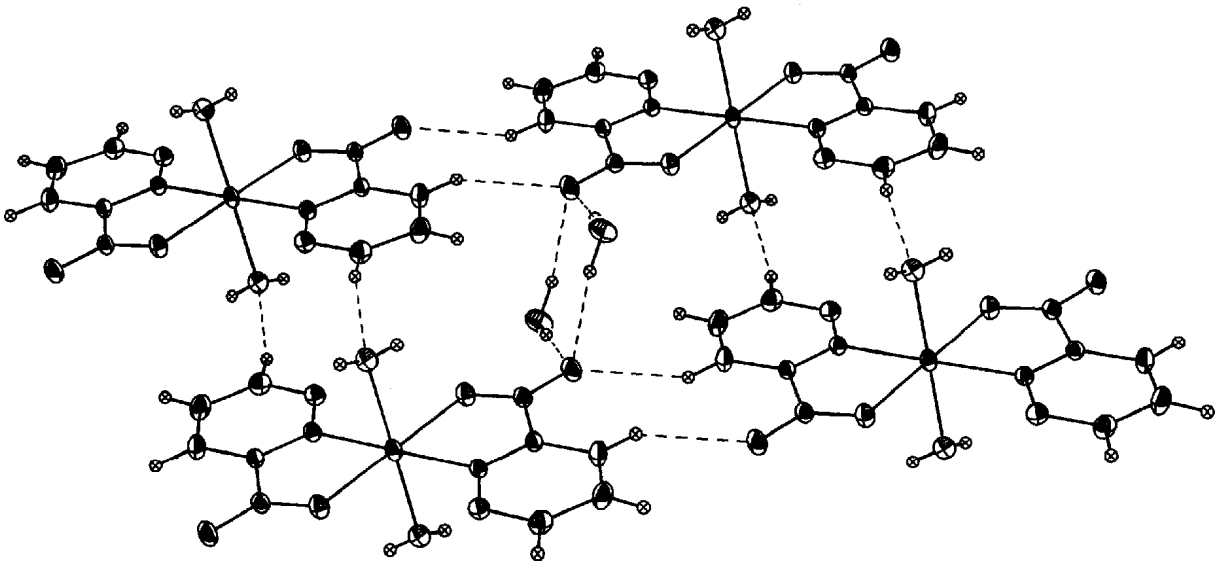

Fig.2. A fragment of the packing diagram of diaquabis(pyridazine-3-carboxylato-N,O)zinc(II) dihydrate.

CRYSTAL CHEMISTRY OF COORDINATION COMPOUNDS WITH HETEROCYCLIC CARBOXYLATE LIGANDS. PART XLIII: THE CRYSTAL AND MOLECULAR STRUCTURE OF A LANTHANUM(III) COMPLEX WITH PYRAZINE-2-CARBOXYLATE AND WATER LIGANDS

Halina Ptasiewicz-Bąk, Janusz Leciejewicz, Thathan Premkumar[1/], Subbiah Govindarajan[1/]

[1/] Department of Chemistry, Bharathiar University, Tamilnadu, India

The structure of *catena*-[(aqua-O)(pyrazine-2-carboxylato-N,O)di(pyrazine-2-carboxylato-N,O-μ-O')]lanthanum(III) trihydrate contains La^{+3} ions, each coordinated by three pyrazine-2-carboxylate (PYR) ligands and a water molecule, forming a $La(PYR)_3(H_2O)$ structural unit shown in Fig.1. The PYR ligand donates one hetero-ring nitrogen atom (N11, N21 and N31) and the nearest to it carboxylate oxygen atom (O11, O21 and O31) forming three coordinating bonding N,O moieties. The second hetero-ring nitrogen atom of each pyrazine ring (N12, N22 and N31) remains unbonded to the metal ion. In addition, the La^{+3} ion is coordinated by two carboxylate oxygen atoms (O22 and O32) belonging to the pyrazinate ligands chelated to adjacent metal ions. In this way the latter are bridged by two carboxylate groups *via* their both oxygen atoms. The observed bridging paths: La-O21-C27-$O22^{III}$-La^{III} and La-O22-$C27^{III}$-La^{III} which link adjacent $La(PYR)_3(H_2O)$ units into pairs and two other: La-O31-C37-$O32^{I}$-La^{I} and La-O32-$C37^{II}$-$O31^{I}$-La^{I} which link the pairs into molecular sheets. A fragment of the packing diagram is shown in Fig.2. The carboxylate group of the third ligand donates to coordination only one carboxylate oxygen atom (O11) leaving the second (O12) unbonded to the

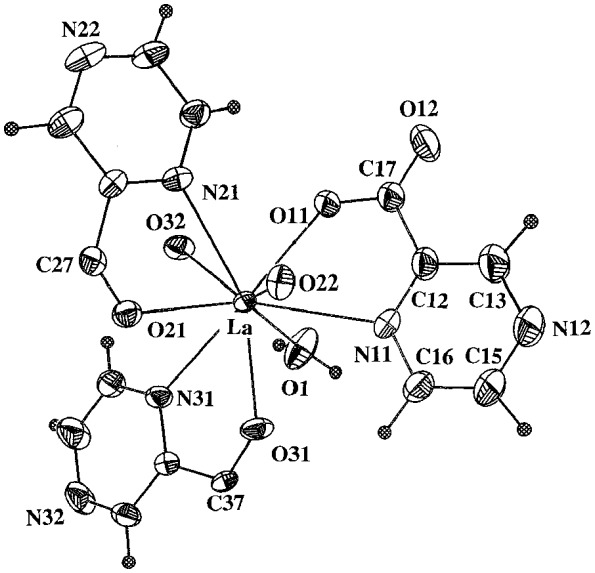

Fig.1. The structural unit $La(PYR)_3(H_2O)$ with atom numbering scheme. Non-hydrogen atoms are displayed as 50% probability elipsoids.

metal ion. Thus the coordination number of La^{+3} ion is nine. The coordination of a lanthanum(III)

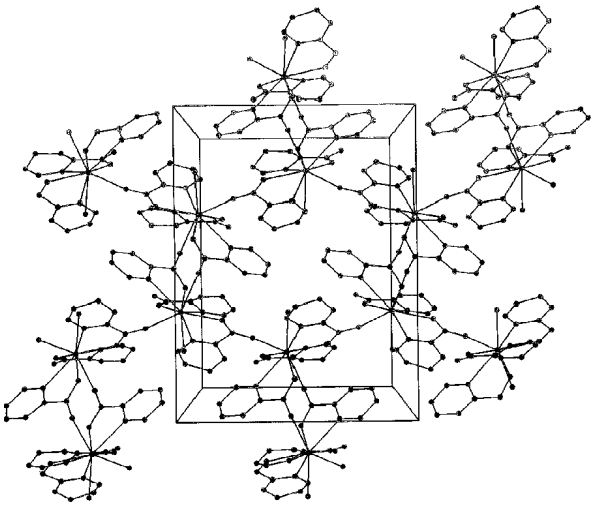

Fig.2. A fragment of the packing diagram of lanthanum(II) pyrazinate.

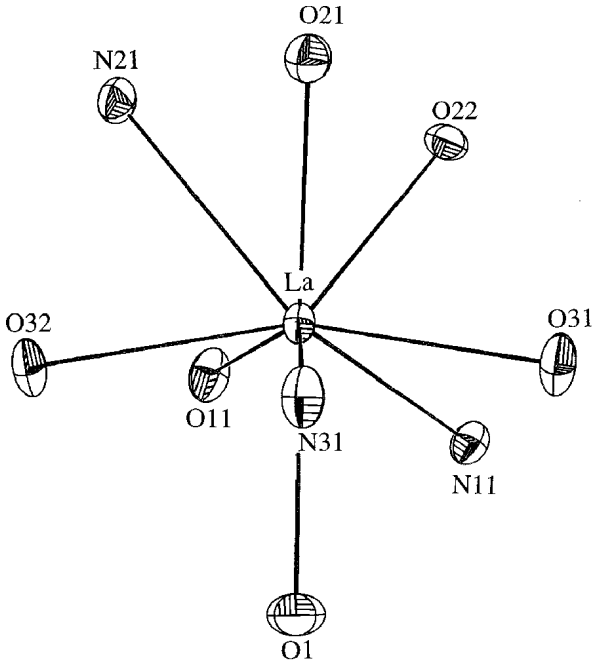

Fig.3. Coordination of a lanthanum(III) ion viewed along the La-N31 bond.

ion is shown in Fig.3. Three solvation water molecules per $La(PYR)_3(H_2O)$ unit participate in a hydrogen bond network which holds together the molecular sheets.

X-ray diffraction measurements were carried out using the KUMA KM4 four circle diffractomer at the Institute of Nuclear Chemistry and Technology. Data processing and structure refinement was performed using SHELXL programme package.

RADIOBIOLOGY

LABILE IRON POOL SIZE IS RELATED TO IRON CONTENT IN NUCLEUS AND INVOLVED IN GENERATION OF OXIDATIVE DNA DAMAGE IN L5178Y CELLS

Marcin Kruszewski, Teresa Iwaneńko

Labile iron pool (LIP) is placed at crossroads of metabolic pathways of iron-containing compounds and is midway between the cellular need of iron, its uptake and storage. In this study we investigated the oxidative DNA damage in relation to the labile iron pool size in a pair of mouse lymphoma L5178Y (LY) sublines (LY-R and LY-S) differing in sensitivity to hydrogen peroxide.

Using the alkaline comet assay, we compared the total DNA breakage in the studied cell lines treated with hydrogen peroxide (25 μM for 30 min at 4°C). More DNA damage was found in LY-R cells than in LY-S cells (Fig.).

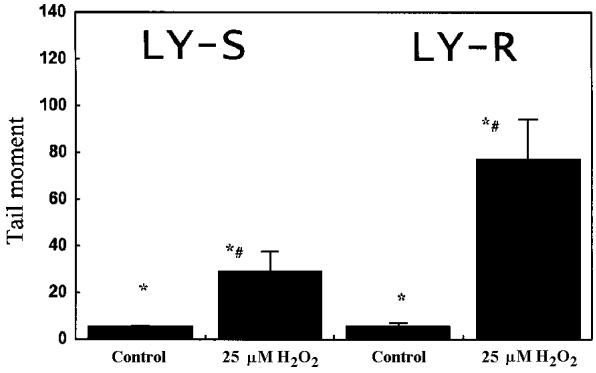

Fig. H_2O_2 induced DNA damage in LY cells: * – statistically significant difference treated *vs*. control, $p<0.05$; # – statistically significant difference LY-R *vs*. LY-S, $p<0.05$.

Measurements of total cellular iron do not reflect actual abundance of iron ions available for redox reactions, as most of cellular iron is bound to heme and non-heme proteins and does not enter Fenton reaction. In contrast, all aspects of intracellular iron homeostasis are mirrored in LIP level, a weakly chelated iron that rapidly passes through the cell. Since fluorometric assay to assess LIP level in intact living cells has recently been available [1], we measured LIP in L5178Y cell lines. LIP level in the LY-R cell is 3.16-times higher than in the LY-S cell (Table). Interestingly, it is fairly proportional to the content of iron in L5178Y cell nuclei, previously measured by flame atomic absorption spectrometry [2].

Table. Labile iron pool and Fe content in the nuclei of L5178Y cell lines.

	L5178Y-R (a)	L5178Y-S (b)	a/b
H_2O_2-sensitivity	High	Low	
Total LIP [μM] ([5])	0.57 ±0.19	0.18 ±0.8	3.16
Total Fe content in the nucleus [ng/10^6 cells] ([2])	7.7 ±1.8	3.1 ±0.9	2.48

The role of LIP in the induction of oxidative DNA damage was unclear, until the demonstration by Petrat *et al*. [3] that a chelatable iron pool is present in the cell nucleus. It is plausible to assume that this nuclear redox-active iron pool may be involved in DNA damage induction by hydrogen peroxide and other oxidizing compounds. Indeed, our data suggest that sensitivity of LY-R cells to H_2O_2 is partially caused by the higher yield of the oxidative DNA damage, as compared to that in LY-S cells. Although other factors, such as differences in antioxidant defence [4], cannot be excluded, the critical factor in the cause-effect relation appears to be the availability and abundance of transition metal ions that take part in the OH radical-generating Fenton reaction (very likely in the form of LIP).

Supported by the Polish State Committee for Scientific Research (KBN) statutory grant for the INCT.

References

[1]. Epsztejn S., Kakhlon O., Glickstein H., Breue W., Cabantchik I.: Anal. Biochem., 248, 31-40 (1997).
[2]. Szumiel I., Kapiszewska M., Kruszewski M., Iwaneńko T., Lange C.S.: Radiat. Environ. Biophys., 34, 113-119 (1995).
[3]. Petrat F., De Groot H., Rauen U.: Biochem. J., 356, 61-69 (2001).
[4]. Boużyk E., Iwaneńko T., Jarocewicz N., Kruszewski M., Sochanowicz B., Szumiel I.: Free Rad. Biol. Med., 22, 697-704 (1997).
[5]. Lipinski P., Drapier J.C., Oliveira L., Retmańska H., Sochanowicz B., Kruszewski M.: Blood, 95, 2960-2966 (2000).

PROTEIN HYDROPEROXIDE FORMATION INDUCED BY IONIZING RADIATION IN VARIOUS BIOLOGICAL SYSTEMS

Marcin Kruszewski, Janusz M. Gebicki[1/], Hanna Lewandowska

[1/] Department of Biological Sciences, Macqaire University, Sydney, Australia

Protein peroxides are among the products formed in biological systems in result of imbalance between their antioxidant capacity and excessive formation of reactive oxygen species, which may be caused by drugs, toxins and radiation. Although peroxides of proteins are relatively stable, in the presence of

biological reductants and metal ions they may further react causing damages in some important cellular structures [1-3]. First reports on formation of amino acid and protein peroxides were published by Latarjet and Laiseleur [4] who examined aqueous solutions of a set of these compounds after irradiation by X-rays. Further research on this subject was performed mostly by Gebicki *et al.* [1, 5-8].

The aim of this work was to compare the level of hydroperoxides induced by ionizing radiation in whole cells and cellular extracts of two closely related murine lymphoma sublines, L5178Y-R (LY-R) and L5178Y-S (LY-S), with differential sensitivity to various DNA damaging agents (UV-C and ionizing radiation, hydrogen peroxide). LY-R cells are radioresistant and hydrogen peroxide-sensitive, whereas LY-S cells are radiosensitive and hydrogen peroxide-resistant [9].

To estimate the level of hydroperoxides of proteins we applied a modified spectrophotometric xylenol orange method (PCA-FOX). This method is based on reduction of hydroperoxides by Fe^{2+} and complexation of the formed Fe^{3+} by xylenol orange (XO) in perchloric acid solution and has earlier been applied for determination of peroxides of proteins by Gay *et al.* [10]. Briefly, in case of bovine serum albumin (BSA) and cellular extracts 0.9 ml samples were prepared in phosphate buffer saline (PBS) and irradiated in a ^{60}Co gamma source. The hydrogen peroxide generated by radiation was removed by 20 min incubation with 0.1 ml of catalase solution (2000 USP/ml). The sample was mixed with 1 ml of solution of ferrous ammonium sulphate (FAS) and XO in perchloric acid. Final concentrations were: 2.5 mM XO, 2.5 mM FAS and 110 mM $HClO_4$. The obtained solutions were incubated at 37°C for 30 min and absorbance was measured at 560 nm in a Beckmann 3600 UV-VIS spectrophotometer.

In the case of the whole cell suspensions, 2 ml samples of PBS containing 10^6 cells were irradiated, then the cells were spun down at 1000 g and resuspended in 2 ml of XO-FAS solution in $HClO_4$ at the final concentrations given above. The samples were incubated at 37°C for 30 min, centrifuged and the supernatant was measured spectrophotometrically. Protein concentration in BSA solutions and cellular extracts was determined spectrophotometrically after reaction with Coomasie blue. Exact perchloric acid concentrations were determined by titration of the diluted acid with a solution of NaOH standard solution.

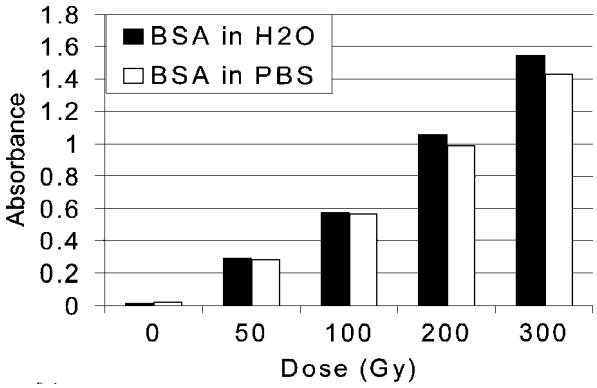

Fig.1. Radiation dose dependent level of protein hydroperoxides in gamma-irradiated BSA.

To assess if the chosen method of protein peroxide determination is suitable for our purposes, we irradiated BSA solutions (450) with 0, 50, 100, 200, 300 Gy of gamma rays. As the samples of biological origin require buffering and often contain molecules with dissociable protons, we evaluated the effect of buffering on the obtained results (Fig.1). As can be seen in the Figure, the level of BSA hydroperoxides is linearly dependent on dose of radiation. Comparison of hydroperoxide levels in phosphate buffer saline and water shows that PBS acts like a scavenger, substantially lowering the level of the formed protein hydroperoxides. Its presence in the studied samples, however, is indispensable, providing the required pH and osmotic pressure in biological samples. Results for BSA are a good reference for the biological material, studies of which are presented in the next report [11].

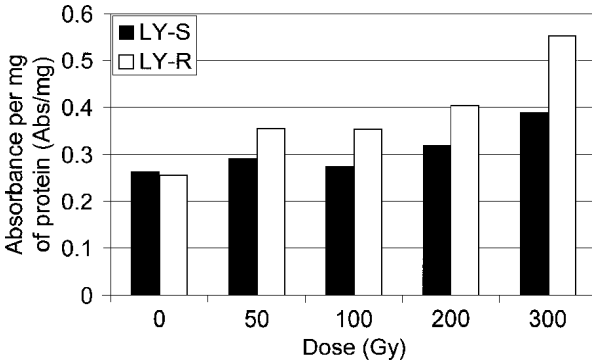

Fig.2. Levels of protein hydroperoxides in LY-R and LY-S cell extracts irradiated with increasing doses of gamma radiation.

We investigated the level of protein peroxides forming after irradiation of cellular extracts of LY-R and LY-S sublines. The results are shown in Fig.2. As one can see, the level of peroxides was higher in LY-R cell extracts. This is in good agreement with the former findings that higher concentration of iron, potentially active in the Fenton reaction, was found in the hydrogen peroxide-sensitive LY-R cells than in the hydrogen peroxide-resistant LY-S cells [12], whereas the antioxidant defence of LY-R cells was weaker [13].

Then, we applied the PCA-FOX method to the whole cell suspensions. The acquired data are shown in Fig.3. In general, the level of hydroperoxides in

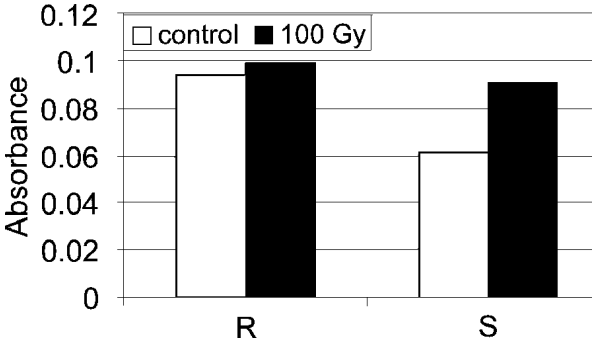

Fig.3. Levels of protein hydroperoxides in LY-R and LY-S cells before and after gamma irradiation.

irradiated cells is higher than in control cells, however, we experienced troubles during the application of PCA-FOX method to the whole cell assay and a good dose response could not be obtained. The level of hydroperoxides in LY-R cells is much higher than in LY-S cells before, as well as after irradiation; this confirms the above presented findings for cellular extracts.

Supported by the Polish State Committee for Scientific Research (KBN) statutory grant for the INCT.

References

[1]. Stadtman E.R.: Ann. Rev. Biochem., 62, 797-821 (1993).
[2]. Giulivi C., Davies K.J.A.: J. Biol. Chem., 268, 8752-8759 (1993).
[3]. Garrison W.M.: Radiat. Res. Rev., 3, 305-326 (1972).
[4]. Latarjet R., Laiseleur J.: Compt. Rend., 136, 60-63 (1942).
[5]. Gebicki S., Gebicki J.M.: Biochem. J., 289, 743-749 (1993).
[6]. Gieseg S., Duggan S., Gebicki J.M.: Biochem. J., 350 Pt 1, 215-218 (2000).
[7]. Fu S., Gebicki S., Jessup W., Gebicki J.M., Dean R.: Biochem. J., 311, 821-827 (1995).
[8]. Gebicki J.M., Du J., Collins J., Tweeddale H.: Acta Biochim. Polon., 47, 901-911 (2000).
[9]. Kruszewski M., Zastawny T.H., Szumiel I.: Acta Biochim. Polon., 48, 525-533 (2001).
[10]. Gay C.A., Gebicki J.M.: Anal. Biochem., 304, 42-46 (2002).
[11]. Kruszewski M., Gebicki J.M., Lewandowska H.: In: INCT Annual Report 2002. Institute of Nuclear Chemistry and Technology, Warszawa 2003, pp.107-108.
[12]. Szumiel I., Kapiszewska M., Kruszewski M., Iwaneńko T., Lange C.S.: Radiat. Environ. Biophys., 34, 113-119 (1995).
[13]. Bouzyk E., Grądzka I., Iwaneńko T., Kruszewski M., Sochanowicz B., Szumiel I.: Acta Biochim. Polon., 47(4), 881-888 (2000).

LEVEL OF PROTEIN HYDROPEROXIDES INDUCED BY DIFFERENT FACTORS IN BIOLOGICAL SYSTEMS

Marcin Kruszewski, Janusz M. Gebicki[1/], Hanna Lewandowska

[1/] Department of Biological Sciences, Macqaire University, Sydney, Australia

Free radicals and other reactive species deriving from oxygen are well known to form during numerous biological redox processes [1, 2]. Additionally, they appear in living organisms in result of the oxygen stress generated by many exogenous agents such as drugs, toxins and radiation. Most of reactive oxygen species (ROS) may oxidize or otherwise damage many important molecular components of the cell. Next to inert water, the most abundant cellular compounds are proteins. Therefore, most likely, they are the first cellular targets of ROS. Results of Gebicki support this hypothesis [3-5]. Peroxides of proteins are relatively stable, but in the presence of biological reductants and metal ions they may further react, causing damages in some important cellular structures [6-8].

Water gamma-radiolysis leads to a selective and quantitative production of radical species, which allows the study of the one-electron oxidation or reduction of several biological systems, especially lipids and proteins. The aim of this work was to compare the level of hydroperoxides induced by ionizing radiation in various biological extracts with that produced during incubation with hydrogen peroxide. Such a comparison gives an important piece of information on the kinetics of peroxide formation in living organisms.

For hydroperoxide determination, 0.9 ml samples of amino acids, bovine serum albumin (BSA) or cellular extracts were prepared in phosphate buffer saline (PBS) and either irradiated in a ^{60}Co gamma source or treated with increasing concentrations of hydrogen peroxide for 30 min. Next, superfluous hydrogen peroxide was removed by 20 min incubation with 0.1 ml of catalase solution (2000 USP/ml). To estimate the level of hydroperoxides of proteins we applied a modified spectrophotometric xylenol orange method. This method is based on reduction of hydroperoxides by Fe^{2+} and complexation of the formed Fe^{3+} by xylenol orange in perchloric acid solution: it has been applied before to determination of peroxides of proteins by Gay *et al.* [9]. The procedure of spectrophotometric detection of protein hydroperoxides has been described in the preceding report [10]. Cellular extracts were prepared from two closely related murine lymphoma sublines, L5178Y-R (LY-R) and L5178Y-S (LY-S), cross-sensitive to hydrogen peroxide and ionizing radiation [11].

Well defined quantities of $^{\bullet}OH$, $HO_2^{\bullet}$ free radicals can be specifically produced by radiolysis of water. Knowledge of radiation efficiency of hydrogen peroxide (G) allows the comparison of the effect induced by radiation with that formed in the presence of H_2O_2. According to Bartosz [12]:

$$G = 7.255 \times 10^{-2}$$

The level of protein peroxides in LY-R and LY-S extracts incubated with H_2O_2 was low and indicated

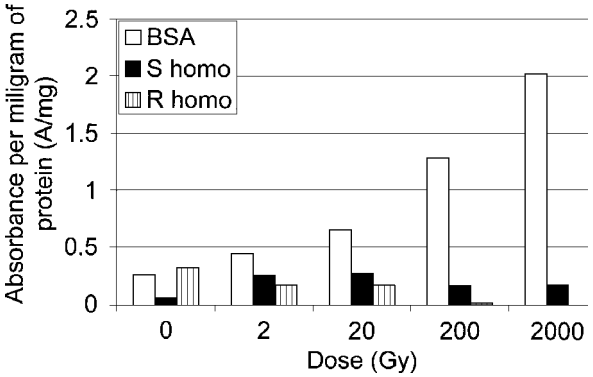

Fig.1. Hydroperoxide levels in LY cell extracts and a BSA solution after treatment with H_2O_2.

no correlation with the hydrogen peroxide concentration (Fig.1). Comparison of these results to those presented in the former report [10], relating gamma irradiation of LY cellular extracts leads to an interesting conclusion: protein peroxide formation seems not to involve hydrogen peroxide, derived from water radiolysis. Unexpectedly, incubation of BSA with H_2O_2 gave a rectilinear hydroperoxide level – radiation dose dependence (Fig.1).

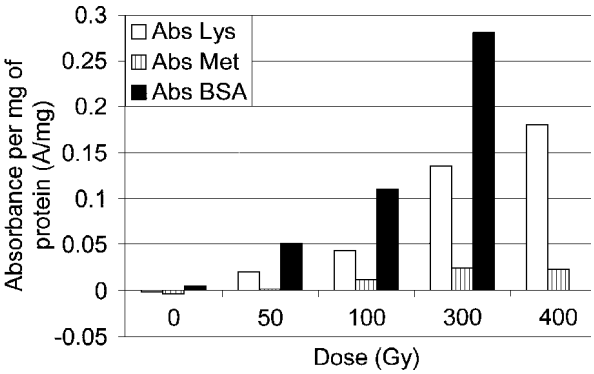

Fig.2. Hydroperoxide levels in lysine and methionine water solutions after gamma irradiation.

To further study the conditions of protein hydroperoxide formation we compared solutions of lysine (Lys) and methionine (Met), either irradiated or incubated with hydrogen peroxide. According to [3] lysine is one of amino acids most susceptible and methionine is the least susceptible to formation of peroxides after gamma irradiation. Our results are in agreement with those mentioned above, as can be seen in Fig.2. However, when subjected to incubation with H_2O_2, Lys and methionine solutions did not produce any hydroperoxides detectable by the chosen method (data not shown). This finding supports the hypothesis that protein peroxide formation does not involve radicals derived from H_2O_2. Hereby presented results warrant further investigation of protein hydroperoxide formation processes.

Supported by the Polish State Committee for Scientific Research (KBN) statutory grant for the INCT.

References

[1]. Halliwell B., Gutteridge J.M.C.: Free Radicals in Biology and Medicine. Clarendon Press, Oxford 1989.
[2]. Sies H.: Eur. J. Biochem., 215, 213-219 (1993).
[3]. Gebicki S., Gebicki J.M.: Biochem. J., 289, 743-749 (1993).
[4]. Gieseg S., Duggan S., Gebicki J.M.: Biochem. J., 350 Pt 1, 215-218 (2000).
[5]. Fu S., Gebicki S., Jessup W., Gebicki J.M., Dean R.: Biochem. J., 311, 821-827 (1995).
[6]. Stadtman E.R.: Ann. Rev. Biochem., 62, 797-821 (1993).
[7]. Giulivi C., Davies K.J.A.: J. Biol. Chem., 268, 8752-8759 (1993).
[8]. Garrison W.M.: Radiat. Res. Rev., 3, 305-326 (1972).
[9]. Gay C.A., Gebicki J.M.: Anal. Biochem., 304(1), 42-46 (2002).
[10]. Kruszewski M., Gebicki J.M., Lewandowska H.: In: INCT Annual Report 2002. Institute of Nuclear Chemistry and Technology, Warszawa 2003, pp.105-107.
[11]. Kruszewski M., Zastawny T.H., Szumiel I.: Acta Biochim. Polon., 48, 525-533 (2001).
[12]. Bartosz G.: Druga twarz tlenu. PWN, Warszawa 1995, 371 p.

NOVEL PLATINUM COMPLEXES RADIOSENSITISE CHO CELLS ACCORDING TO THE MODE OF ACTION ON DNA

Iwona Grądzka, Iwona Buraczewska, Irena Szumiel, Janina Kuduk-Jaworska[1/]

[1/] Department of Chemistry, University of Wrocław, Poland

We have previously examined the anti-proliferative effect of thirteen recently synthesised platinum dicarboxylate complexes, very similar in their chemical, structural and kinetic properties to carboplatin [1, 2]. Complexes with the primary amine (ethylenediamine) (group I complexes, moderate toxicity and moderate to high reactivity with GSH) are more effective than complexes containing the tertiary amine (1-alkylimidazole) (group II complexes, low toxicity and moderate to low reactivity with GSH).

For further examination, we chose from group I ethylenediamine(L-malato)platinum(II), Pt1; from group II – bis(1-ethylimidazole(L-malato)platinum(II), Pt4. As described in the previous report [3], we examined the radiosensitising properties of both complexes, using CHO cells and clonogenic survival as end-point. To learn how Pt1 and Pt4 affect the X-ray generated initial double strand breaks (DSB) and the subsequent DSB rejoining, we used pulse field gel electrophoresis (PFGE).

The electrophoretic method of DSB estimation has an important limitation: it is not reliable in the case of asynchronous cell cultures, as DNA release from S-phase cells diminishes considerably in comparison to interphase cells. We omitted this problem by using human lymphocytes, 20-24 h after stimulation with phytohemagglutinin A. At that time, a synchronous population is obtained of cells in the G1-phase of the cell cycle. The lymphocytes in G1-phase were subjected to Pt complex treatment alone and in combination with 10 Gy of X-rays.

Figure 1A shows the initial damage induced by X-rays alone, Pt complex alone and in combination with X-rays. Pt1 induces very few DSBs during the 20 h incubation with the drug prior to irradiation with 10 Gy X-rays. There is an apparent decrease in DNA fragmentation after combined treatment, which indicates crosslinking by the Pt complex. Interestingly, this crosslinking effect is absent after using Pt4 and an identical treatment schedule (bars first and third are equal). The drug

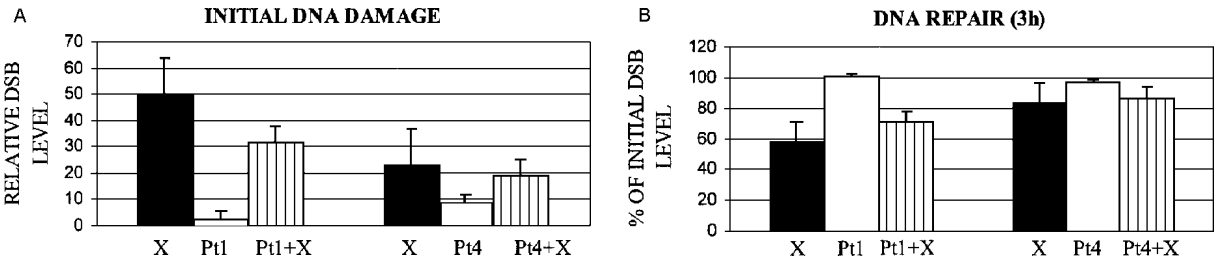

Fig.1. A – Initial and B – residual DSB induced in G1-phase lymphocytes by 10 Gy of X-rays alone, Pt compound alone and in combination with X-rays. The drug (10 or 0.5 μg/ml for Pt1 and Pt4, respectively) was present for 1 h before irradiation as well as during irradiation and the 3 h repair interval.

alone induces relatively more DSB than Pt1. To illustrate this difference in action between Pt1 and Pt4, data obtained for one donor are shown, from the full data set (to be published). The dose-response curve for DSB induction by X-rays for this donor is linear, with the slope of the linear regression curve 0.478 Gy^{-1} (not shown).

As judged from the level of residual damage (Fig.1B), pre-treatment with Pt1 slows down the DSB rejoining (the damage expressed as % of initial DSB level is higher after combined treatment than after X-irradiation alone), whereas Pt4 is without effect (the same % of initial DSB level after combined treatment and after X-irradiation alone).

Pt4 pre-treatment arrests cells in G2-phase and thus, sensitises to X-rays these cells that have a radiosensitive G2-phase (2nd mode of action). This into irreparable one (1st mode of action). The requirements for this mode of sensitisation are functional DNA repair systems (NER and NHEJ), as judged from our earlier work with L5178Y (LY) cells, lacking functional NHEJ (LY-S) or NER (LY-R). This result is in agreement with the previously formulated rule concerning the effects of combined treatment [4]: both damaging agents must inflict sublethal damage in order to interact. This is the case with CHO cells, whereas is not – with LY cells and xrs6 cells (see Table 1 for summary).

Table 1. Differences in response and sensitivity to various damaging agents (applied alone or in combination) and in CHO wild type and mutant cells and a pair of LY sublines.

Damaging agent(s)	CHO	xrs6	LY-R	LY-S
X/gamma radiation	Moderate resistance (NHEJ functional)	High sensitivity (NHEJ impaired)	Moderate sensitivity (NHEJ functional)	High sensitivity (NHEJ impaired)
DNA crosslinking Pt complexes: Cis-PAD, Pt1	Resistance (NER functional)	Not determined (NER 50% functional)	High sensitivity (NER impaired)	Resistance (NER functional)
Cis-PAD +X-rays	More than additive response	Not determined	Additive response	Additive response
Pt1+X-rays	More than additive response	Additive response	Additive response	Additive response

Table 2. Differences in G2-phase radiosensitivity and response to combined treatment with Pt4 and X-rays in CHO cells and a pair of LY sublines.

Cells	High G2-phase radiosensitivity in relation to other cell cycle phases	Pt4 - induced G2 arrest	Effect of combined Pt4 + X-rays
CHO	yes	yes	more than additive
Subline LY-R	no	yes	additive
Subline LY-S	no	yes	additive

So, Pt1 has a DNA crosslinking action and slows down rejoining of X-ray induced DSB. In contrast, Pt4 does neither crosslink DNA nor affect DSB rejoining; it shows a considerable ability to arrest cells in G2-phase. Both compounds exert a more than additive lethal effect on CHO-K1 cells subjected to combined Pt complex treatment and X-irradiation.

We find that, as earlier proposed for other Pt complexes, the radiosensitising effect of Pt1 is connected with converting reparable DNA damage mode of action has been found in CHO cells (see Table 2 for summary).

Supported by the Polish State Committee for Scientific Research (KBN) in the frame of the Research Contract No. 4105F 032 19 and a statutory grant for the INCT.

References

[1]. Buraczewska I., Bożyk E., Kuduk-Jaworska J., Waszkiewicz K., Gasińska A., Szumiel I.: Chem. Biol. Interact., 129, 297-315 (2000).

[2]. Kuduk-Jaworska J., Waszkiewicz K.: Trans. Met. Chem., 250, 443-449 (2000).
[3]. Buraczewska I., Jarocewicz N., Szumiel I., Kuduk-Jaworska J.: In: INCT Annual Report 2001. Institute of Nuclear Chemistry and Technology, Warszawa 2002, pp.110-111.
[4]. Szumiel I.: Int. J. Radiat. Biol., 33, 605-608 (1978).

DNA DOUBLE STRAND BREAK REPAIR DEPENDENCE ON POLY(ADP-RIBOSYLATION) IN L5178Y AND CHO CELLS

Maria Wojewódzka

Two L5178Y (LY) sublines, LY-R and LY-S, differ in radiation sensitivity. The main reason for the high radiation sensitivity of LY-S cells is a deficiency of double strand break (DSB) repair [1] in DNA, apparently caused by impaired non-homologous end-joining (NHEJ) [2], whereas homologous recombination repair is functional [3]. In LY-R cells both repair systems are functional. The cell sublines differ in several features of response to ionising radiation, among them, in response to combined treatment with poly(ADP-ribose) polymerase (PARP) inhibitor, benzamide (Bz) and ionising radiation: 2 mM Bz sensitises LY-S but not LY-R cells [4].

To test a hypothesis that impaired NHEJ is the cause of DNA repair dependence on PARP activity, we compared DNA double strand break repair in LY sublines and a pair of CHO lines: wild type CHO (Chinese hamster ovary) cells and its mutant xrs6, with impaired NHEJ due to mutation in Ku80 subunit of DNA-PK (DNA-dependent protein kinase). The cells were irradiated with an X-ray machine (ANDREX, Holger Andreasen, Denmark, 200 kVp, 5 mA, dose rate 1.2 Gy/min). For the detection of DSB comet assay under neutral conditions was used in a recently introduced and validated modification [5].

Cells were incubated with 2mM Bz at 37°C for 2 h, cooled and X-irradiated on ice with 10 Gy and incubated again at 37°C for DNA repair estimation. The latter was done with the neutral comet assay after 15, 60 and 120 min of incubation. Electrophoresis conditions were: for CHO and xrs6 cells, 18 V, 12 mA, 1 h; for LY cells, 14 V, 7-8 mA, 1 h. Further processing was according to the standard procedure, as recently described [5]. As shown in Figure, only LY-S cells show dependence of DSB repair on Bz presence; the rejoining is considerably slower in the Bz-treated cells. In contrast, xrs6 cells repair at the same rate in the presence or absence of Bz.

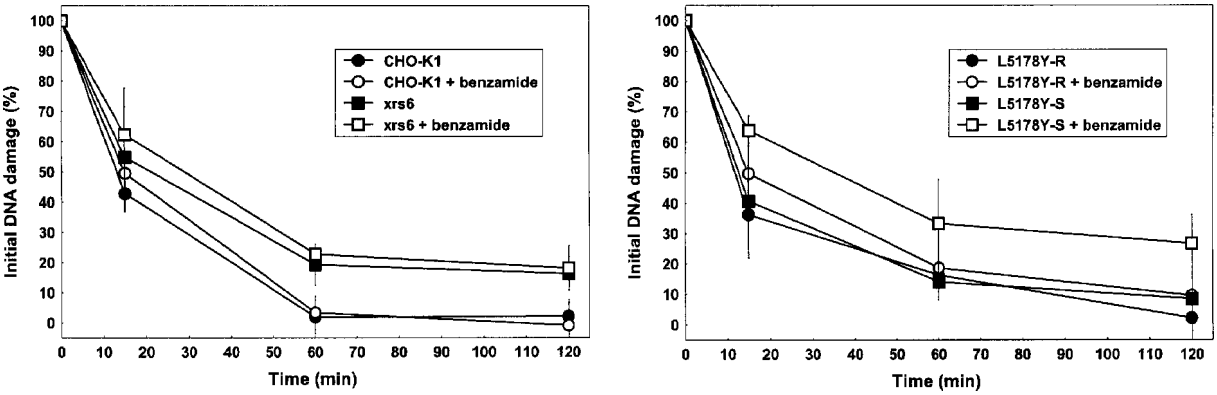

Fig. DSB rejoining as estimated by the neutral comet assay in CHO, xrs6 (left panel), LY-R and LY-S (right panel) cells in the presence or absence of poly(ADP-ribosylation) inhibitor, benzamide. X-irradiation of pre-treated or control cells with 10 Gy at 0°C was followed by incubation at 37°C up to 2 h.

In conclusion, the tested hypothesis has not been confirmed. Apparently, in LY-S cells the DSB repair dependence on poly(ADP-ribosylation) is not connected with impaired DNA-PK function in the NHEJ repair system.

Supported by the Polish State Committee for Scientific Research (KBN) statutory grant for the INCT.

References

[1]. Wlodek D., Hittelman W.N.: Radiat. Res., 115, 566-575 (1988).
[2]. Kruszewski M., Wojewódzka M., Iwaneńko T., Szumiel I., Okuyama A.: Mutat. Res., 409, 31-36 (1998).
[3]. Grądzka I., Skierski J., Szumiel I.: Cell Biochem. Funct., 16, 239-252 (1998).
[4]. Johanson K.J., Sundell-Bergman S., Szumiel I., Wlodek D.: Acta Radiol. Oncol., 24, 451-457 (1985).
[5]. Wojewódzka M., Buraczewska I., Kruszewski M.: Mutat. Res., 518, 9-20 (2002).

BASAL AND X-RAY-MODIFIED EXPRESSION OF DNA-PK GENES IN LY-R AND LY-S CELLS

Iwona Grądzka, Barbara Sochanowicz, Grażyna Woźniak[1/]

[1/] National Institute of Public Health, Warszawa, Poland

DNA-dependent protein kinase (DNA-PK) is an enzyme which stimulates DNA double strand break (DSB) repair by non-homologous end-joining (NHEJ), the mechanism predominating in G1-phase of the cell cycle. DNA-PK complex consists of a catalytic subunit (DNA-PKcs) and a regulatory Ku70/Ku80 heterodimer. It is assumed that, after binding to double-stranded DNA termini, DNA-PK recruits other components of the NHEJ machinery, i.e. XRCC4 protein and ligase IV.

L5178Y-S (LY-S, sensitive) murine lymphoma subline is hypersensitive to ionizing radiation, as compared to its parental L5178Y-R (LY-R, resistant) subline. The defect in LY-S cells is associated with impaired DSB rejoining and expressed most strongly in G1-phase of the cell cycle [1, 2]. Post-irradiation DSB repair in LY-S, but not in LY-R subline, is resistant to a specific DNA-PK inhibitor, OK-1035 [3] which indicates that NHEJ function in LY-S cells is disturbed. Studies carried out on rodent mutant cells [4, 5] showed that a defect or insufficiency of any of the NHEJ component (DNA-PKcs, Ku70, Ku80, XRCC4 or ligase IV) led to an impaired DSB repair. The nature of DSB repair defect in LY-S cells is still unknown. We present preliminary data concerning the expression of genes coding DNA-PK subunits in LY-R and LY-S cells.

LY-R and LY-S cells were growing in suspension in Fisher's medium supplemented with 10% foetal bovine serum. Cell cultures in logarithmic phase of growth (asynchronous populations) were used. X-irradiation was carried out with the use of an ANDREX defectoscope (Holger Andreasen, Denmark), at a dose rate of 1 Gy/min, at 0°C (initial damage) or 37°C (repair).

- DNA-PKcs:
  5' TAC AGC CGA GCT AAC CGT AC
  5' CAT CCA GGG CTC CCA TCC TT (810 bp),
- Ku70:
  5' ACC TTG TTC AGC GCT CTG CT
  5' AGA GTA AGG CAC AGT GAT GT (840 bp),
- Ku80:
  5' CAG TGT CTG CTG CAT AGA GC
  5' TTG TCT GCT AGG ATG ACG TC (840 bp).

PCR was carried out in a Perkin Elmer Gene Amp PCR system 2400 thermocycler. The cycling parameters were: 5 min at 95°C (predenaturation), then 30 cycles of 94°C for 40 s (denaturation), 56°C for 30 s (annealing), 72°C for 45 s (elongation), and final elongation step at 72°C for 7 min. The PCR products were electrophoresed in 1.5% agarose gel in the presence of ethidium bromide and visualised under a UV-transilluminator.

For RT-PCR analysis, total cellular RNA was isolated from 106 cells per sample using the Total RNA Prep Plus kit (A&A Biotechnology, Poland). First strand cDNA synthesis was primed using the Reverse Transcription System with oligo(dT) (Promega, USA). The cDNA was amplified using the same primers and conditions as for the PCR reaction (see above). Additionally, specific primers for mouse β-actin were included for reference of a stable gene expression:

β-actin:
5' GAC TAC CTC ATG AAG GAT CCT
5' ATC GTA CTC CTG CTT GCT GAT (531 bp).

After separation in 1.5% agarose gel, the RT-PCR products stained with ethidium bromide were visualised under UV-light. The image was captured by a CCD camera connected to the PC. Intensities of the bands were quantified using a GelScan im-

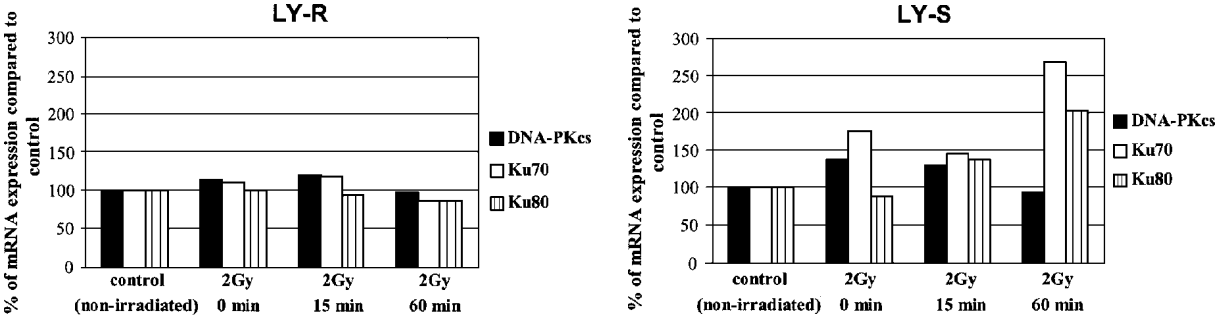

Fig. Changes in DNA-PK genes expression in X-irradiated LY-R and LY-S cells. Quantification of the data from the electrophoretic image intensities of the bands corresponding to DNA-PK components cDNAs were normalized to β-actin cDNA band intensities. Levels of mRNA expression were compared to the non-irradiated control (assumed as 100%). Shown are means of two RT-PCR analyses from single experiment.

For PCR analysis,total cellular DNA was isolated from 10^6 cells per sample using the Genomic DNA Prep Plus kit (A&A Biotechnology, Poland). The genes of DNA-PK complex were amplified using specific primer sets. The primers sequences and the expected fragment sizes of the corresponding PCR products were as follows:

age analysis Software (Kucharczyk electrophoretic techniques, Poland) and normalized to the β-actin band intensities.

PCR analysis showed identical DNA amplification patterns for specific gene fragments of DNA-PK components in both LY sublines. All DNA-PK components were present and there was

no difference in the gene copy numbers between LY sublines.

As shown in the Figure, after X-irradiation, RT-PCR analysis pointed to only a slight transient increase (at 15 min) in DNA-PKcs and Ku70 mRNA in LY-R cells. LY-S cells responded with similar transient expression of DNA-PKcs mRNA, however, they showed a marked, continuous increase in Ku70 and Ku80 mRNA levels until 60 min after irradiation. So, the DSB repair defect in LY-S cells is not related to absence or insufficient expression of genes coding the components of the DNA-PK complex.

Supported by the Polish State Committee for Scientific Research (KBN) statutory grant for the INCT.

References

[1]. Wlodek D., Hittelman W.N.: Radiat. Res., 115, 550-565 (1988).
[2]. Wlodek D., Hittelman W.N.: Radiat. Res., 115, 566-575 (1988).
[3]. Kruszewski M., Wojewódzka M., Iwaneńko T., Szumiel I., Okuyama A.: Mutat. Res., 409, 31-36 (1998).
[4]. Jeggo P.A.: Radiat. Res., 150 (5 Suppl.), S80-S91 (1998).
[5]. Zdzienicka M.Z.: Biochimie, 81, 107-116 (1999).

0.5M NaCl – SENSITIVE SECTOR OF POTENTIALLY LETHAL DAMAGE IN X-IRRADIATED LY-S CELLS DEFECTIVE IN DNA DOUBLE STRAND BREAK REPAIR

Barbara Sochanowicz, Iwona Grądzka, Irena Szumiel

X-irradiation of mammalian cells induces potentially lethal damage (PLD), a sector of which is sensitive to treatment with hypertonic salt solution, usually 0.5M NaCl. Radiosensitisation by such treatment has recently been explained [1]. In rat fibroblasts 80% of the Ku subunits of the DNA-dependent protein kinase (DNA-PK), component of double strand break (DSB) repair system, non-homologous end-joining (NHEJ), are localized in the cytoplasm. Upon irradiation, there is a translocation of these proteins to the nucleus. Altered tonicity of the medium inhibits the translocation, thus impairing the fast DSB repair and, in consequence, diminishing survival. Increase in nuclear Ku subunits was not observed in fibroblasts from a mutant strain of Long-Evans Cinnamon (LEC) rat that has an enhanced radiosensitivity and a reduced level of repair of DSBs after X-irradiation [2] – in contrast, 10 min after irradiation a loss of Ku from the nucleus was observed. This was in spite of the presence of all subunits of DNA-PK identical with the wild type rat cells. Therefore, a defect in maintaining the levels of Ku subunits in the nuclei of LEC rat cells was suggested.

The properties of LEC rat cells are reminiscent of those of LY-S cells, a radiation sensitive subline of L5178Y murine lymphoma. These cells contain DNA-PK activity comparable to that of the parental, radiation resistant LY-R cells, when measured *in vitro* [3], but exhibit a defect in DSB repair, most pronounced in G1-phase of the cell cycle [4], apparently due to impaired NHEJ [5]. We checked, whether hypertonic salt solution affects the response to X-irradiation of LY-S cells, in view of the possibility that a similar defect as in LEC rat cells is the cause of their radiation sensitivity. LY-R cells served as a reference strain. The cells were X-irradiated with 2 Gy at +4°C in cell culture medium and NaCl solution added to the final concentration of 0.5M (identical volume of isotonic salt solution added to the controls). The cells were then placed at 37°C and, after 20 min, bovine serum added to 28% concentration (in order to prevent cell lysis during centrifugation, that

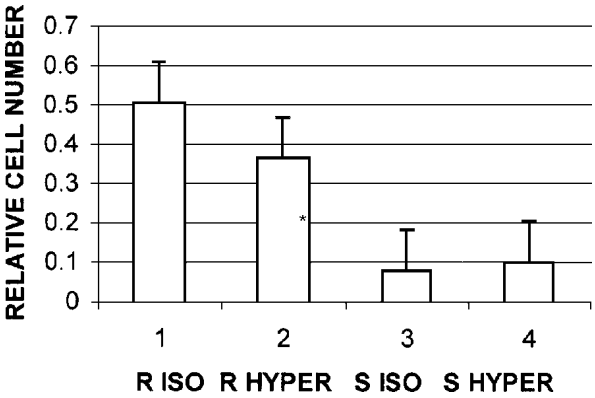

Fig. Relative cell numbers in LY cell cultures treated with isotonic (ISO) or hypertonic i.e. 0.5M (HYPER) sodium chloride for 20 min after irradiation with 2 Gy X-rays. The difference between ISO and HYPER cell samples for LY-R cells is statistically significant (Student's t-test).

is necessary for medium replacement). After 48 h incubation in the full culture medium relative cell numbers were estimated.

The results in Fig. show that LY-R cells are sensitised by the treatment, whereas LY-S cells are not. This indicates that in contrast with LY-S cells, the fast PLD repair in LY-R cells is inhibited in hypertonic medium in a manner comparable to that in wild type rat cells [1]. Thus, the effect of hypertonicity may rely on translocation of Ku subunits, as proposed by Endoh *et al.* [1]. We wanted to confirm these conclusions by comparing the amounts of Ku70 in the cytoplasmic and nuclear extracts in control and X-irradiated cells, with the use of Western blotting. The expected difference was found in LY-R cells (increase in nuclear Ku70, 10 and 60 min after irradiation, with a concomitant decrease in the cytoplasmic Ku70 (not shown). In contrast, in LY-S cells no changes in the levels of nuclear and cytoplasmic Ku70 were found. So, the radiation sensitivity-related defect in LY-S cells is different from that in LEC rat cells.

Supported by the Polish State Committee for Scientific Research (KBN) statutory grant for the INCT.

References

[1]. Endoh D., Okui T., Kon Y., Hayashi M.: Radiat. Res., 155, 320-327 (2001).
[2]. Okui T., Endoh D., Kon Y., Hayashi M.: Radiat. Res., 157, 553-561 (2002).
[3]. Sochanowicz B., Kruszewski M., Szumiel I.: In: INCT Annual Report 1999. Institute of Nuclear Chemistry and Technology, Warszawa 2000, p.99.
[4]. Wlodek D., Hittelman W.N.: Radiat. Res., 112, 146-155 (1987).
[5]. Kruszewski M., Wojewódzka M., Iwaneńko T., Szumiel I., Okuyama A.: Mutat. Res., 409, 31-36 (1998).

A CROSS-PLATFORM PUBLIC DOMAIN PC IMAGE-ANALYSIS PROGRAM FOR THE COMET ASSAY

Krzysztof Końca[1/], Anna Lankoff[2/], Anna Banasik[2/], Halina Lisowska[2/], Tomasz Kuszewski[3/], Stanisław Góźdź[3/], Zbigniew Koza[1/], Andrzej Wójcik[2,4/]

[1/] Institute of Theoretical Physics, University of Wrocław, Poland
[2/] Świętokrzyska Academy, Kielce, Poland
[3/] Holycross Cancer Center, Kielce, Poland
[4/] Institute of Nuclear Chemistry and Technology, Warszawa, Poland

The single-cell gel electrophoresis (SCGE), also known as the comet assay, is a sensitive method to measure genotoxicity and cytotoxicity of chemical and physical agents [1-3]. SCGE has also been used to analyse the capacity of cellular DNA repair [4-6].

Although the methodology of SCGE is straightforward and does not require sophisticated equipment, the analysis of comet images is not so simple. The visual classification of comets on the basis of their morphology and degree of damage is possible, but is not very precise [3]. A better sensitivity is achieved by computer analysis of comet images. Several commercial applications are available, however, they are generally sold as combined soft-

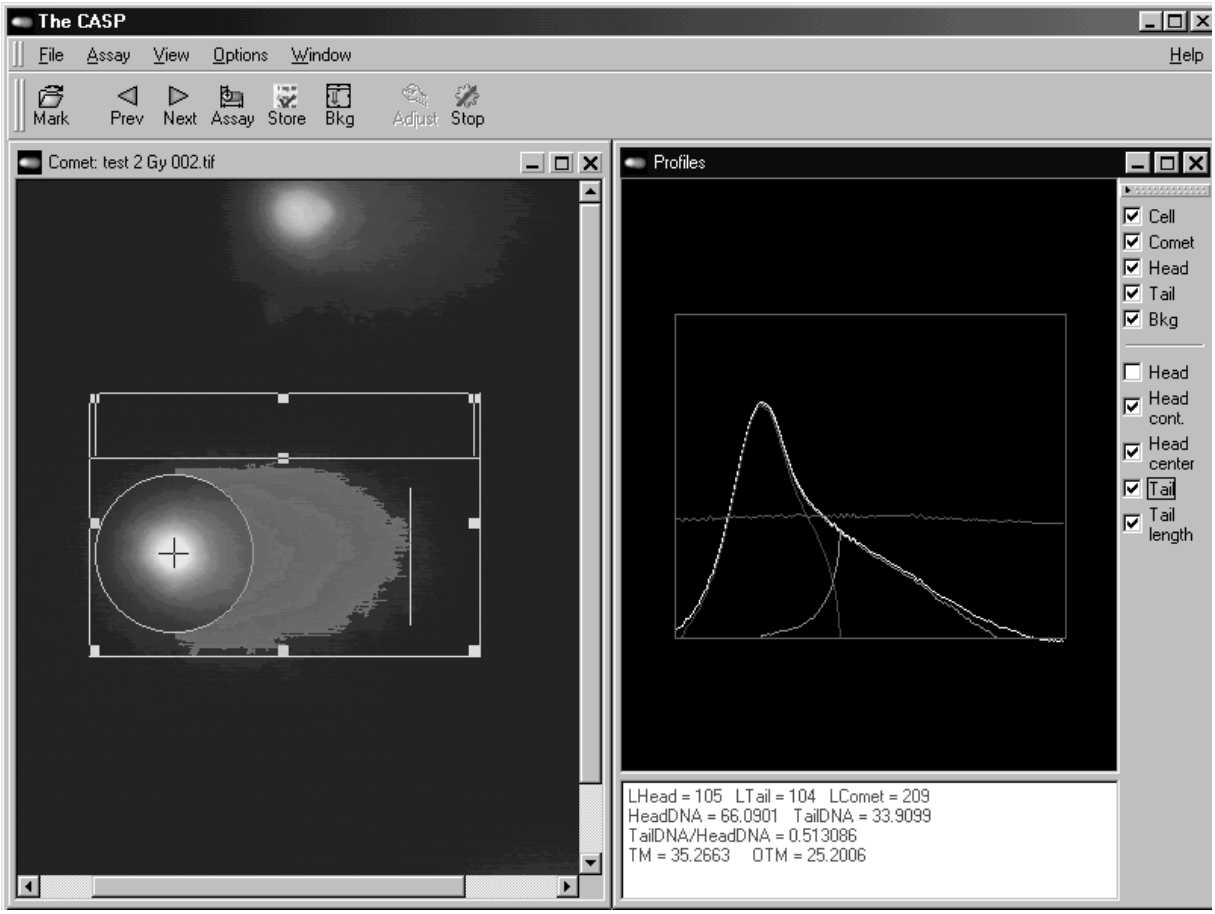

Fig. View of the program windows. In the left-hand window the comet image with the measurement frame is visible, with tail and head marked. The measurement frame is split into two frames: a background and a comet frame. In the right-hand window the intensity profiles are plotted and the checkbox bar is shown with options of profile and image view. Below the profile window selected measurement results are printed.

ware/hardware packages and are rather expensive. In addition they cannot be modified because their source codes are not supplied. Given the rapid development of computer technique, obtaining of comet images through a video camera or by scanning of photographs does not seem to be problematic for most research laboratories. A bigger obstacle is the availability of a specialized software for the analysis of comet images.

A public domain macro is available on the internet for NIH Image, a graphic program running under Macintosh computers [7]. No corresponding, freeware programs exist for the PC platform. We have, therefore, developed a simple and user-friendly public domain program for the analysis of comet images (Fig.). Its graphic user interface is based on a cross-platform library FOX (www.fox-toolkit.org), and so, the whole application can be compiled and run under a variety of operating systems, including MS Windows and Linux. The program, together with the source code is publicly available under the GNU License at www.casp.of.pl.

Supported by the Polish State Committee for Scientific Research (KBN) statutory grant for the INCT.

References

[1]. Singh N.P., Tice R.R., Stephensen R.E., Schneider E.: Mutat. Res., 252, 289-296 (1991).
[2]. Fairbairn D.W., Olive P.L., O'Neil K.L.: Mutat. Res., 339, 37-59 (1995).
[3]. Olive P.L., Frazer G., Banath J.P.: Radiat. Res., 136, 130-136 (1993).
[4]. Wójcik A., Sauer K., Zölzer F., Bauch T., Müller W.-U.: Mutagenesis, 11, 291-297 (1996).
[5]. Müller W.-U., Bauch T., Wójcik A., Böcker W., Streffer C.: Mutagenesis, 11, 57-60 (1996).
[6]. Wojewódzka M., Kruszewski M., Iwaneńko T., Collins A.R., Szumiel I.: Mutat. Res., 416, 21-35 (1998).
[7]. Helma C., Uhl M.: Mutat. Res., 466, 9-15 (2000).

CORRELATION OF CHROMOSOMAL ABERRATIONS AND SISTER CHROMATID EXCHANGES IN INDIVIDUAL CHO CELLS PRE-LABELLED WITH BrdU AND TREATED WITH DNase I OR X-RAYS

Magdy Sayed Aly[1/], Andrzej Wójcik[2,3/], Christian Schunck[4/], Günter Obe[4/]

[1/] Faculty of Science, Cairo University, Egypt
[2/] Institute of Nuclear Chemistry and Technology, Warszawa, Poland
[3/] Świętokrzyska Academy, Kielce, Poland
[4/] Institute of Genetics, University of Essen, Germany

Sister chromatid exchanges (SCE) are regarded as manifestation of repair of DNA damage by homologous recombination [1]. SCE are thought to arise during the S-phase, when the DNA replication apparatus is hindered by a DNA damage [2]. In accordance with this, S-phase dependent agents induce SCE efficiently [3]. In contrast, the S-phase independent agent, ionising radiation, is a poor inducer of SCE and is only effective when cells pre-labelled for one cell cycle with 5'-bromodeoxyuridine (BrdU) are irradiated in G1-phase [4].

In experiments in which cells pre-labelled with BrdU for one cell cycle are irradiated during G1-phase chromosomal rearrangements may be visible as SCE. This led to the suggestion that radiation-induced SCE observed under such experimental scenario are in fact "false" SCE [5]. We could show that X-rays do induce "true" SCE [6] and that these arise as a consequence of radiation damage to BrdU [7]. The nature of DNA lesions induced by damage to BrdU, which lead to SCE, is not known. However, given the fact that following irradiation of cells in G1-phase, which are unifilarily labelled with BrdU, chromatid-type aberrations are observed [8]. It may be speculated that radiation damage to BrdU gives rise to lesions which are S-phase dependent.

Several authors have reported that restriction enzymes (RE) and DNase I efficiently induce SCE when cells unifilarily labelled with BrdU are treated in G1-phase of the cell cycle. RE and DNase I induce mainly DNA double strand breaks (DSB) and are S-phase independent chromosome breaking agents. Treatment of cells with RE and DNase I in G1-phase of the cell cycle leads to very high frequencies of chromosome-type aberrations.

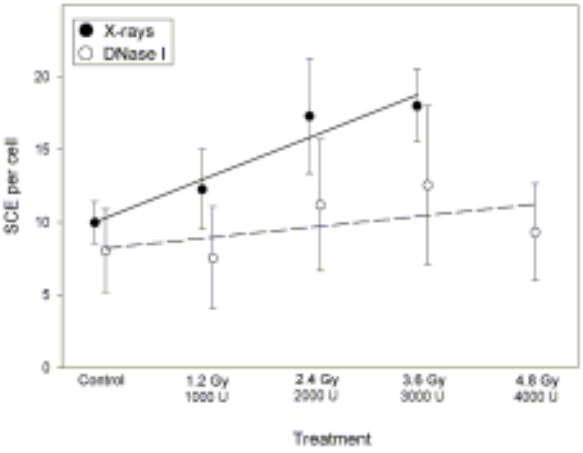

Fig. Frequencies of SCEs in cells without chromosomal aberrations following treatment with X-rays and DNase I. Pooled results of all experiments. Vertical bars represent standard deviations of per cell values.

The mechanisms by which RE and DNase I induce SCE are not known. Ortiz *et al*. [9] have analysed the possibility that the RE-DNA binding complex may be the primary cause of SCE. However, they found that production of DSB is necess-

ary to induce SCE. Because the cellular signalling mechanisms efficiently prevent entering into S-phase of cells with unrepaired DSB [10] it is difficult to imagine that dsb induce SCE in S-phase. How then does treatment of cells with RE or DNase I lead to SCE? A simple explanation would be the assumption that SCE induced by these compounds are in fact "false" SCE, i.e. chromosomal aberrations. In order to test this hypothesis CHO cells were labelled with BrdU for one round of DNA replication and treated with DNase I and X-rays in G1-phase. Using a computer-aided metaphase relocation system mitoses were first analysed for SCE, destained, restained with orcein and reanalysed for chromosomal aberrations. Thus, a precise correlation between the frequencies of aberrations and SCE could be established. The results indicate that X-rays induce more SCE than expected on the basis of aberrations, whereas the frequencies of SCE induced by DNase I can be accounted for by chromosomal aberrations. The conclusion that X-radiation induces "true" SCE and DNase I "false" SCE is substantiated by the observation that in cells without chromosomal aberrations a dose dependent increase in SCE is evident in irradiated cells but not in cells treated with DNase I (Fig.).

Supported by the Polish State Committee for Scientific Research (KBN) statutory grant for the INCT.

References

[1]. Sonoda E., Sasaki M.S., Morrison C., Yamaguchi-Iwai Y., Takat M., Takeda S.: Mol. Cell Biol., 19, 5166-5169 (1999).
[2]. Painter R.B.: Mutat. Res., 70, 337-341 (1980).
[3]. Latt S.: Ann. Rev. Genet., 15, 11-55 (1981).
[4]. Littlefield L.G., Colyer S.P., Joiner E.J., DuFrain R.J.: Radiat. Res., 78, 514-521 (1979).
[5]. Mühlmann-Diaz M.C., Bedford J.S.: Radiat. Res., 143, 175-180 (1995).
[6]. Wójcik A., Opalka B., Obe G.: Mutagenesis, 14, 633-637 (1999).
[7]. Bruckmann E., Wójcik A., Obe G.: Chrom. Res., 7, 277-288 (1999).
[8]. Natarajan A.T., Kihlman B.A., Obe G.: Mutat. Res., 73, 307-317 (1980).
[9]. Ortiz T., Pinero J., Cortes F.: Chrom. Res., 4, 540-544 (1996).
[10]. Szumiel I.: Int. J. Radiat. Biol., 66, 329-341 (1994).

APPLICATION OF THE BIOTIN-dUTP CHROMOSOME LABELLING TECHNIQUE TO STUDY THE ROLE OF 5-BROMO-2'-DEOXYURIDINE IN THE FORMATION OF UV-INDUCED SISTER CHROMATID EXCHANGES IN CHO CELLS

Andrzej Wójcik[1,2/], Clemens von Sonntag[3,4/], Günter Obe[5/]

[1/] Institute of Nuclear Chemistry and Technology, Warszawa, Poland
[2/] Świętokrzyska Academy, Kielce, Poland
[3/] Max-Planck-Institut für Strahlenchemie, Mülheim an der Ruhr, Germany
[4/] Institut für Oberflachenmodifizierung, Leipzig, Germany
[5/] Institute of Genetics, University of Essen, Germany

Although sister chromatid exchanges (SCEs) are observed in cells treated with chemical agents which produce various types of DNA lesions [1], not all types of DNA lesions have the same potency to induce SCEs. It has been shown that the interstrand crosslinks are a major DNA lesion leading to the formation of SCEs [2].

With respect to UV radiation, there are data pointing towards cyclobutane pyrimidine dimers (PDs) and (4-6) photoproducts, typically located at the same strand, as the lesion responsible for SCE formation [3]. In this context, it is interesting to note that some interstrand crosslinks are also formed in UV-irradiated DNA [4].

SCEs can be visualised by growing cells for either two rounds of replication in the presence of 5-bromo-2'-deoxyuridine (BrdU). Incorporation of BrdU into DNA is known to sensitise cells to UV and ionising radiation [5], and it has been shown that the frequencies of both spontaneous and UV-induced SCEs increase with increasing BrdU incorporation into cellular DNA [6]. However, the influence of BrdU on UV radiation-induced formation of SCEs and the degree of sensitisation was difficult to assess for a long time, because no alternative technique existed that allowed differential staining of chromatids with high resolution.

We have recently developed a method to differentially label sister chromatids with biotin-16-2'-deoxyuridine (biotin-dU) [7]. The advantage of biotin-dU over BrdU is that it lacks a halogen atom which dissociates homolytically (or heterolytically) upon exposure to UV (or ionising) radiation thereby generating the highly reactive uracilyl radical in the DNA. SCEs are only induced by ionising radiation, albeit with a low frequency, when the cells were unifilarily labelled with BrdU prior to irradiation [8].

The aim of the present investigation was to analyse the influence of BrdU on the frequency of SCEs induced by UV radiation. Cells unifilarily labelled with either BrdU or biotin-dU were irradiated in the G1-phase of the cell cycle either at 254 or 313 nm. UV radiation at 254 nm is absorbed by all DNA bases including bromouracil (BrU), whereas radiation at 313 nm is predominantly absorbed by BrU. It has been shown that several $J \cdot m^{-2}$ of 254 nm radiation suffice to induce SCEs in cells

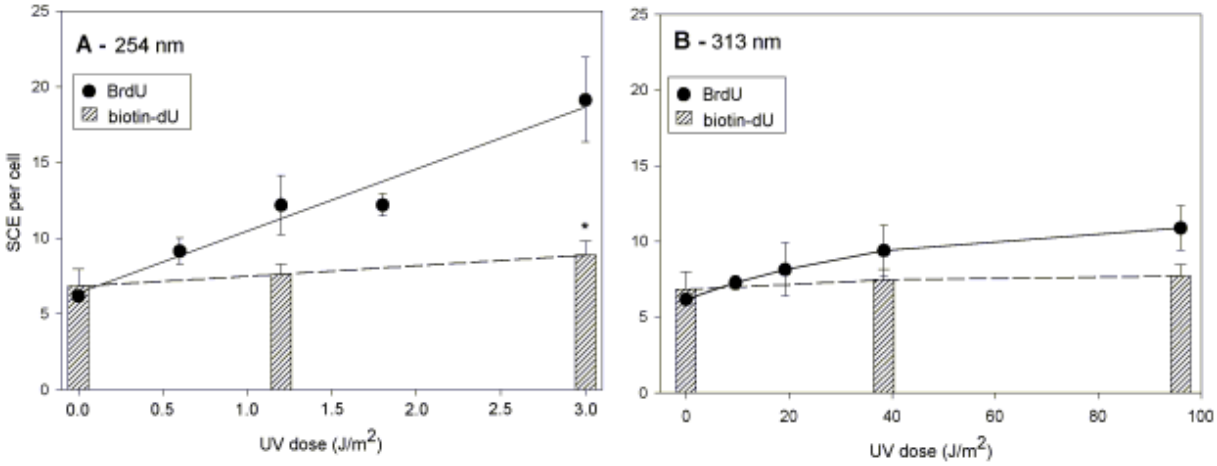

Fig. Dose response curves for SCEs in cells pre-labelled with BrdU (circles) or biotin-dU (bars) and exposed to UV radiation of 254 nm (panel A) or 313 nm (panel B). Error bars represent the standard errors of the mean. * - difference to control significant (only calculated for biotin-dU labelled cells).

irradiated before labelling them with BrdU, while UV radiation at 313 nm requires doses in the range of thousands of $J \cdot m^{-2}$, before an effect is observed. In BrdU-substituted DNA the cross-section for uracilyl radical formation at 254 nm radiation is ~100-fold higher than that at 313 nm [9].

The results shown in the Fig. indicate that following irradiation with 254 nm the SCE frequency is ~6-times higher in BrdU-labelled than in biotin-dU-labelled cells. As expected, the dose required to induce similar frequencies of SCEs by radiation at 313 nm as compared to 254 nm was 50-80 times higher. Based on theoretical considerations and the fact that chemical agents, which form DNA interstrand crosslinks are among the most potent inducers of SCEs, we suggest that a DNA interstrand crosslink may be the major lesion leading to SCE formation in cells unifilarily labelled with BrdU and irradiated with UV or ionising radiation.

Supported by the Polish State Committee for Scientific Research (KBN) statutory grant for the INCT.

References

[1]. Latt S.: Ann. Rev. Genet., 15, 11-55 (1981).
[2]. Bredberg A., Lambert B.: Mutat. Res., 118, 191-204 (1983).
[3]. Kato H.: Nature, 249, 552-553 (1974).
[4]. Nejedly K., Kittner R., Pospisilova S., Kypr J.: Biochem. Biophys. Acta, 151, 365-375 (2001).
[5]. Hutchinson F.: Q. Rev. Biophys., 6, 201-246 (1973).
[6]. Zwanenburg T.S.B., van Zeeland A.A., Natarajan A.T.: Mutat. Res., 150, 283-292 (1985).
[7]. Bruckmann E., Wójcik A., Obe G.: Chrom. Res., 7, 185-189 (1999).
[8]. Bruckmann E., Wójcik A., Obe G.: Chrom. Res., 7, 277-288 (1999).
[9]. Hutchinson F., Köhnlein W.: Progr. Mol. Subcell. Biol., 7, 1-42 (1980).

ANALYSIS OF MICRONUCLEI IN PERIPHERAL LYMPHOCYTES OF PATIENTS TREATED FOR THYROID CANCER WITH IODINE-131

Sylwester Sommer[1/], Iwona Buraczewska[1/], Emil Lisiak[2/], Maksymilian Siekierzyński[2/], Eugeniusz Dziuk[2/], Marek Bilski[2/], Marek K. Janiak[2/], Andrzej Wójcik[1,3/]

[1/] Institute of Nuclear Chemistry and Technology, Warszawa, Poland
[2/] Military Hospital, Warszawa, Poland
[3/] Świętokrzyska Academy, Kielce, Poland

Micronucleus formation in cells exposed to ionizing radiation can be monitored to obtain information on the distribution and extent of the radiation-induced damage following accidental, occupational, or therapeutic exposures. Application of radioactive iodine-131 to the therapy of thyroid cancer can be associated with the induction and persistence of cytogenetic damages in healthy tissues *in vivo* [1, 2]. In the present study, we aimed to evaluate the dose-effect relationship between the radiation doses received by patients treated with I-131 and the frequency of micronuclei in circulating lymphocytes of these patients. The purpose of the present study was to verify the sensitivity of the micronuclei assay to detect a putative exposure to radioactive iodine.

Twenty nine patients with various forms of thyroid cancer who were treated with 166 MBq to 6.5 GBq of I-131 were included in the present study. From these patients blood samples were collected on day 4 following administration of the radioiodine, lymphocytes were cultured and scored for the occurrence of micronuclei. As controls, lymphocytes obtained from 34 control healthy, sex- and age-matched donors who were not treated with I-131 were used. Although a significant difference

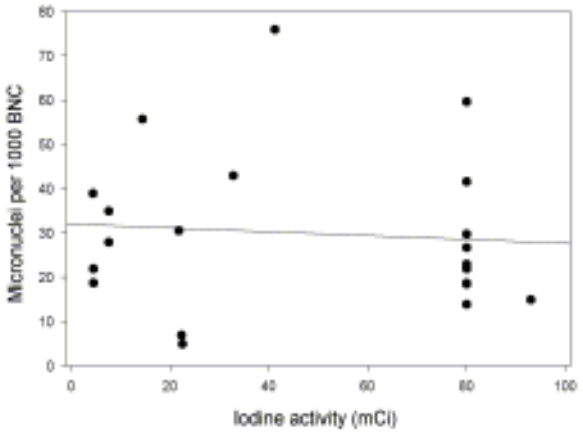

Fig. The frequencies of micronuclei in peripheral lymphocytes of patients treated with various activities of I-131. BNC: binucleated cells.

in the frequency of micronuclei was observed between the I-131-treated and control subjects, the missing dose-effect relationship (Fig.) indicates that the micronucleus assay is not sensitive enough to detect exposure to this radioisotope at doses used for the treatment of thyroid cancer.

Supported by the Polish State Committee for Scientific Research (KBN) statutory grant for the INCT.

References

[1]. Monteiro G.O., Oliveira N.G., Rodrigues A.S., Laires A., Ferreira T.C., Limbert E., Leonard A., Gerber G., Rueff J.: Mutagenesis, 15, 69-75 (2000).

[2]. Gutierrez S., Carbonell E., Galofre P., Creus A., Marcos R.: Mutat. Res., 413, 111-119 (1998).

NUCLEAR TECHNOLOGIES
AND
METHODS

PROCESS ENGINEERING

CERAMIC MEMBRANES APPLIED FOR RADIOACTIVE WASTES PROCESSING

Grażyna Zakrzewska-Trznadel, Marian Harasimowicz, Bogdan Tymiński, Andrzej G. Chmielewski

Ceramic membranes (MEMBRALOX® and CeRAM *INSIDE*®) were used for filtration of liquid radioactive wastes. The experimental runs with samples of original radioactive wastes were carried out. The waste was characterized by a relatively low salinity (<1 g/dm^3), however, the specific radioactivity was in the medium-level liquid waste range (~150 kBq/dm^3). The main activity came from radioactive cobalt and caesium, but also a significant amount of lanthanides and actinides was present. To enhance the separation, membrane filtration was combined with complexation (sole ultrafiltration gave decontamination factors in the range of 1.1-1.7). Soluble polymers like polyacrylic acid (PAA) derivatives of different average molecular weight, polyethylenimine (PEI) and cyanoferrates of transition metals were used to enhance the removal of radioactive ions [1]. Each polymer was added separately to the feed solution.

Decontamination factors calculated for the radioisotopes: Co-60, Cs-137, Eu-152, Eu-154, and Am-241 in ultrafiltration (UF)/complexation by the use of different complexing agents are shown in Fig.1. Best removal of cobalt, europium and americium was observed when chelating polymers NaPAA or PEI were applied. Complexing with polyacrylic acid of molecular weight 1200 and 8000 did not result in sufficient increase of decontamination factor. For the membrane of 15 nm pore size, which was used in experiments, the proper molecular weight of NaPAA was 15 000 or 30 000. In most of experiments the removal of Eu-154 and Am-241 was complete (specific activity below the detection limit). Binding the caesium ions with all tested polymers gave rather poor results. The best complexing agent for caesium was cobalt hexacyanoferrate, which gave decontamination factors higher than 100.

Studying the results obtained in the experiment when cobalt hexacynoferrate together with a soluble polymer (PEI) were employed one can observe a significant increase of Cs-137 removal, however the decontamination factors for other radioisotopes have decreased compared with experi-

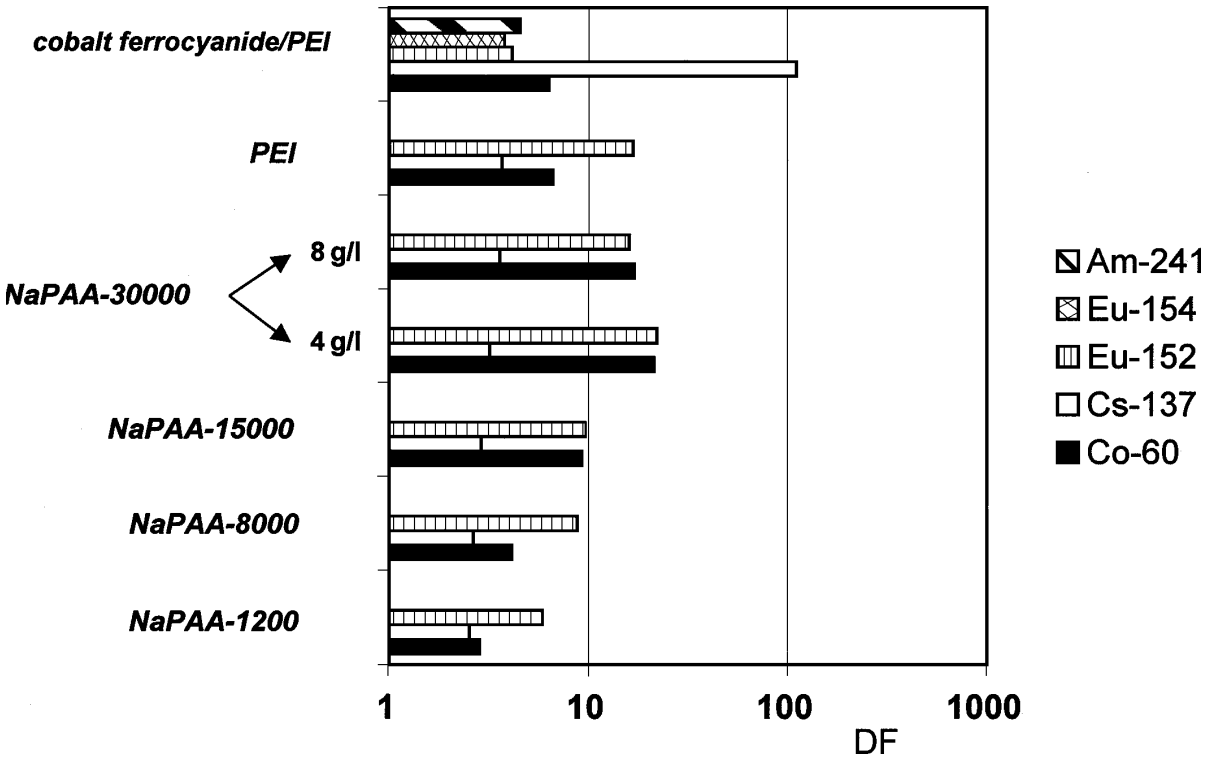

Fig.1. Decontamination of a real liquid radioactive waste in a UF/complexation process with the use of different complexing agents. A 15 nm pore size membrane was used.

ments when only chelating polymers were applied as complexing agents. The removal of isotopes by UF/complexation is efficient when a mixture of the ligands binds the ions effectively under the same conditions (the same pH, concentration of alkali--metal salts, etc.). To avoid the DF's decrease, the process was arranged in two steps. At first, a CoCF slurry was introduced into the feed solution to bind the caesium ions. After some hours, the feed was filtered with UF ceramic membranes up to 3-fold volume reduction. Sodium polyacrylate, MW 30 000 was added to the permeate and after a wait and pH adjustment the solution was ultrafiltered. The DF's for such a process arrangement are presented in Fig.2. In the first stage of filtration, a high removal of Cs-137 was reached, while other radio-

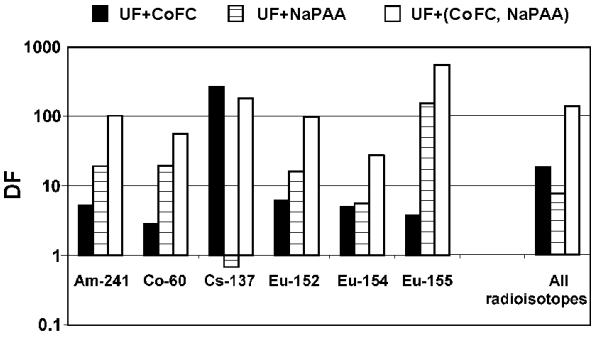

Fig.2. Decontamination factors for a 2-stage process, CeRAM *INSIDE*® 15 nm.

isotopes were rejected at a moderate rate. In the second stage, where sodium polyacrylate was employed, the decontamination factors were much higher for most of the radioisotopes present in the waste. Only for Cs-137 ultrafiltration gave DF's smaller than 1, which corresponds with a higher specific activity in the permeate. Low DF<1 shows that Cs-137 is not bound by NaPAA and passes through the membrane. Additionally, the low decontamination for caesium is caused by the low concentration of this radioisotope and generally low salinity of the effluent after the treatment in the first stage, as was earlier observed during operation of an reverse osmosis (RO) plant [2].

It was observed that the decontamination factors were higher for all the radioisotopes present in the waste sample when the cyanoferrate and chelating polymer were applied subsequently in a 2-stage process than those obtained when the complexing agents were added to the feed solution simultaneously. All these decontamination factors were higher than those obtained for the single soluble polymer (NaPAA or PEI).

Ceramic membranes, made of aluminium, titanium or zirconium oxides are expected to overcome disadvantages of polymer membranes, like limited resistance to strong chemical conditions, organic solvents or some kind of ionising radiation, as well. High temperature resistance allows the washing with warm streams and sterilisation by steam. Easy washing is very important when macromolecular complexing ligands are used to enhance the separation *via* ultrafiltration.

Ultrafiltration combined with complexation ensured satisfactory decontamination factors and volume reduction to treat a wide range of contaminated streams. The process can be alternative to RO, and in some cases when recovery of some selected components of the solution is important, more beneficial than RO.

The best conditions for UF/complexation resulted in high decontamination factors were found in the multistage arrangement, especially when radioactive wastes contained one dominant component.

References

[1]. Zakrzewska-Trznadel G., Harasimowicz M.: Removal of radionuclides by membrane permeation combined with complexation. Desalination, 144, 207-212 (2002).

[2]. Chmielewski A.G., Harasimowicz M., Tymiński B., Zakrzewska-Trznadel G.: Concentration of Low- and Medium-Level Radioactive Wastes with 3-stage Reverse Osmosis Pilot Plant. Sep. Sci. Technol., 36, 5&6, 1117-1129 (2001).

DETERMINATION OF SULFUR ISOTOPE RATIO IN COAL COMBUSTION PROCESS

Andrzej G. Chmielewski, Małgorzata Derda

Europe, including Poland, is a continent, where a great increase of social awareness for problems of environmental protection is growing in the last two decades. Production activity is usually connected with a consequence, to a certain degree, of waste production and pollutant emission. It has a visible influence on wholesomeness of the population and condition of the natural environment, which can be proved by such occurrences as acid rains, greenhouse effect, worsening conditions of forests, or destruction of ozone layer.

Very important is the evaluation of economic responsibility for emitted pollution. Therefore, scientists look for a suitable marker which could be used as environmental tracer.

Preliminary results show that sulfur in coal has a different isotopic composition (δ) and occurs in many different forms (pyrite sulfur, sulfate and organic sulfur) [1]. The separation and determination of isotope composition may provide information concerning the area and mechanism of sulfur incorporation in organic-rich sediments.

The stable isotope composition of sulfur compounds of industrial origin contained in the atmosphere, biosphere, hydrosphere, groundwater, soil, etc., may differ from natural analogues. Analysis of stable isotopes of sulfur is the only method to distinguish anthropogenic and natural sources of sulfur.

The Bełchatów Power Plant Ltd consumes yearly about 35 million Mg of lignite. The lignite deposit

is exploited in a nearly open pit or in places not very deep and that is the reason why a strip mine was built there. Situating a power station in the neighborhood of the mine allows to reduce the cost of transportation and diminish the arduousness issuing from the problem. The wastes formed in the energy production process are being utilized for reclamation of the excavation's exploited part.

The solid samples (coal, ashes, slag) were taken from the Bełchatów Power Plant Ltd to determine sulfur isotope ratio ($^{34}S/^{32}S$) in the coal combustion process. Samples of the flue gas and the product from desulfurization process were investigated as well. The product from the desulphurization process is gypsum.

Each form of sulfur has been prepared by extraction [2] of solid samples taken from the power plant and transformed into stable compounds, which can be subsequently converted to gas phase (SO_2) for mass spectrometric analysis [3] (Table 1).

Table 1. Sulfur isotope ratio $\delta^{34}S/^{32}S$ in the particular form of sulfur in different solid samples [‰].

	Coal	Slag	Ash
Organic sulfur	7.81 ± 0.03	-	-
Pyrite sulfur	-4.6 ± 0.03	1.01 ± 0.04	-
Sulfate sulfur	-6.14 ± 0.03	0.82 ± 0.04	0.59 ± 0.03

The received results ($\delta^{34}S/^{32}S$ ranged from +7.81 to -6.14‰) and suggest that the sulfur in coal originates from the sulfur bounded by plants and depleted in the isotope ^{34}S. The sulfur was probably produced in the process of sulfate bacterial reduction. $\delta^{34}S$ values in slag and ash are enriched in the heavier isotope ^{34}S in the coal combustion process.

Sulfur from the outlet gases was absorbed in a hydrogen peroxide solution [4]. The sulfate ions produced in this way were quantatively recovered as $BaSO_4$ by precipitation with a $BaCl_2$ solution [5] (Table 2).

Table 2. Sulfate sulfur in flue gas and product from desulfurization process [‰].

Inlet	Product	Outlet
1.56 ± 0.03	2.29 ± 0.03	-4.03 ± 0.03

The difference between the sulfur isotope ratio for SO_2 in the inlet and outlet gases was observed. α=0.994 obtained for this process means that the sulfur in the outlet gas is depleted in the heavier isotope ^{34}S, while the sulfur in the product is enriched in the heavier isotope ^{34}S in the desulfurization process.

This method of investigation can be used for:
- monitorig of water,
- investigation of gypsum dissolution,
- investigation of ashes leaching,
- investigation of dry and wet deposition of sulfur from gases after desulfurization process.

References

[1]. Chmielewski A.G., Wierzchnicki R., Derda M., Mikołajczuk A.: Nukleonika, 47, 69 (2002).
[2]. Westgate L.M., Anderson T.F.: Anal. Chem., 54, 2136 (1982).
[3]. Halas S., Wolacewicz W.D.: Anal. Chem., 53, 686 (1981).
[4]. Federal EPA Method. Determination of Sulfur Dioxide Emissions from Stationary Sources. 1977.
[5]. Halas S., Jasionowski M., Peryt T.M.: Przegl. Geol., 44, 10 (1996).

SEPARATION OF THE SULFUR ISOTOPES ^{34}S AND ^{32}S IN THE SYSTEM: GASEOUS SO_2 AND SO_2 ADSORBED ON SILICA GEL

Andrzej G. Chmielewski, Agnieszka Mikołajczuk

Adsorption is used in many fields related to separation and purification processes, including hazardous pollutant removal from flue gases. Sulfur dioxide is believed to be a major precursor of acidic rain, therefore the control of sulfur dioxide emissions is a significant subject for research and development, as well as industrial implementation.

Physical adsorption processes offer an alternative and promising way for emission control of sulfur dioxide since they are dry, self-contained and energy saving. The key to the success of the adsorption process for SO_2 concentration is mainly dependent on the search or development of an appropriate adsorbent that possesses ideal properties for the selective adsorption of SO_2 [1].

Silica gel is a partially dehydrated form of polymeric colloidal silica acid. The chemical composition can be expressed as $SiO_2 \cdot nH_2O$. The water content, which is present mainly in the form of chemically bounded hydroxyl groups, amounts typically to about 5 wt. % [2]. Silica gels have a different pore size. The large-pores material is used mainly for liquid-phase applications, while the small-pore material is widely used as a desiccant in the vapor-phase system.

In this work, isotope separation factor during adsorption of sulfur dioxide on silica gel was investigated. Silica gel samples of different grain size and different BET surface areas (Table 1), were packed in glass columns of 0.16 m length connected with a vacuum line. Before packing, silica gels were dried at 373 K for 1 h, then weighed and packed to columns. In each experiment, about 8 or 4 g of silica gel granules was used. Before each experiment, silica gel samples were dried at 294 K in the vacuum line for 2 h.

The adsorption isotherm models of Langmuir, Freundlich and Brunauer-Emmett-Teller were used to describe the adsorption of SO_2 on silica gel [1]. An adsorption isotherm is characterized by certain

constants, the values of which express surface properties. The Langmuir model is valid for the monolayer sorption on the surface with a finite number of identical sites [2]. The Langmuir model consid-

Table 1. Physical properties of silica gel used in experiments.

Silica gel	BET surface area [m^2/g]	Size granules [mm]
1	250-350	2-7
2	500-800	1-3
3	600	0.2-0.3
4	400	0.2-0.3

ers only the monolayer adsorption which reaches a maximum volume for chemisorption. However, physical adsorption is never single-layer, except for very low coverages. The Freundlich model does not describe the saturation behavior of the sorbent and is an empirical equation based on the sorption on a heterogeneous surface, suggesting that binding sites are not and/or independent [2]. The BET isotherm is valid mainly for physical adsorption. The BET isotherm treats this by performing, essentially, a series of Langmuir isotherms. This equation is used to determine the surface area of porous catalysts and other materials [2].

Experimental data of SO_2 adsorption [1] showed that the adsorption isotherm is described by the Freundlich isotherm (the square of correlation coefficient is 0.9818 for the Freundlich model but for the Langmuir and BET models it is 0.7998 and 0.490, respectively).

At the moment, the adsorption isotherms were determined for two silica gels No. 1 and No. 4, and are shown in Fig. In the future, the adsorption isotherm will be determined for silica gel No. 2 and No. 3.

The performed experiments on SO_2 adsorption on silica gel were focused on the determination of separation factors of sulfur isotopes. The time of SO_2 adsorption ranged from 5 min to 1 month, when the system attained equilibrium state. Sulfur isotope separation factors were low at the equilib-

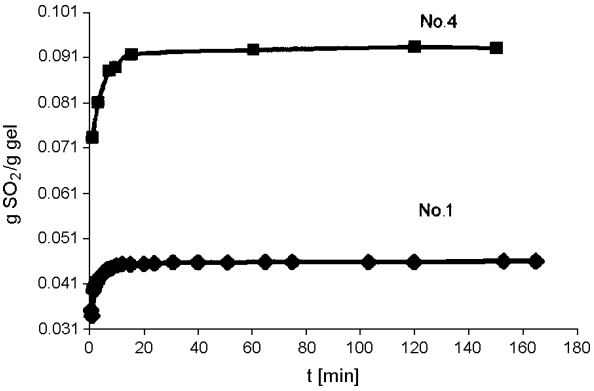

Fig. Experimental adsorption isotherms of sulfur dioxide on silica gels No. 1 and No. 4.

rium state (below 1), but when the time of adsorption was 5 min, the separation factor was higher for both samples of silica gel (Table 2) and the highest being for silica gel No. 2. Firstly, $^{32}SO_2$ was adsorbed on silica gel and the gas phase was enriched in the heavier sulfur isotope ^{34}S. When the system reached equilibrium state the gas phase was enriched in ^{32}S. For small size of silica granules (gels No. 3 and 4; 0.2-0.3 mm) the separation factors were small too. At the moment we have no information about the pore size.

The pressure/temperature kinetic process has much more advantages over the equilibrium process. Silica gels No. 1 and No. 2 may be used to the separation of sulfur isotopes.

Table 2. Sulfur separation factor for the system SO_2 gaseous and SO_2 adsorbed on silica gel at 295 K.

Adsorption time [h]	Separation factor (±0.00002)			
	Silica gel No. 1 [3]	Silica gel No. 2	Silica gel No. 3	Silica gel No. 4
0.08	1.00681	1.01132	1.00299	1.00176
~0.17	1.00545	1.09460	1.00059	1.00029
2	1.00162	1.00155		0.99954
~20	1.00067	1.00063	0.99943	0.99943
~140	0.99899	0.99971	0.99940	0.99955
~200	0.99879	0.99812	0.99948	0.99953
~600	0.99883	0.99815	0.99954	

References

[1]. Kopac T., Kocabas S.: Chem. Eng. Proces., 41, 223-230 (2002).
[2]. Ruthven D.M.: Principles of adsorption and adsorption processes. Wiley, New York 1984.
[3]. Chmielewski A.G., Miljević N., Mikołajczuk A.: Sposób rozdzielenia izotopów siarki ^{34}S i ^{32}S. Patent application P.354392.

INDUSTRIAL INSTALLATION FOR ELECTRON BEAM FLUE GAS TREATMENT – OPERATIONAL TRIALS

Andrzej Pawelec, Bogdan Tymiński, Andrzej G. Chmielewski

Although the idea of the electron beam (EB) flue gas treatment is not new it is still the only known method for simultaneous SO_2 and NO_x removal in one installation. According to classical installations with separated desulphurisation and denitrification parts, this method saves place (that is extremely important especially in old power plants) and reduces energy consumption and costs. Moreover, the process is dry and no wastes are generated because of the agricultural use of by-products. All this makes the method competitive with other applied methods.

Positive results of the tests performed on a pilot installation has led to the construction of industrial installation in the electric power station (EPS) "Pomorzany" in Szczecin [1, 2]. There is also another EB flue gas treatment installation in Chengdu (China) but it is designed mainly for SO_2 removal. In this way, the Polish installation is, in fact, the first one in the world for simultaneous flue gas desulphurisation and denitrification. After the construction had been completed, first optimization tests started in January 2001. At the beginning of the tests, high voltage supply malfunction occurred and the rest of trials were performed using only two accelerators instead of four. After repair, the nominal electron energy was lowered from 800 to 700 keV, so some modifications to the process were necessary. After that, the installation was put into operation with four accelerators in the spring of 2002. Description of the results obtained is presented in this paper.

The parameters of the installation are optimized to meet the requirements of the EPS according to the Polish law regulations. High concentration of NO_x and relatively low concentration of SO_2 in flue gas emitted from Benson boilers established specific conditions for flue gas treatment. In spite of this, the efficiency of SO_2 removal may reach 95% and the removal efficiency of NO_x may even exceed 70% in continuous operation of the installation (Fig.1). The by-product obtained fulfils all the requirements of Polish Standards for this kind of fertilizers.

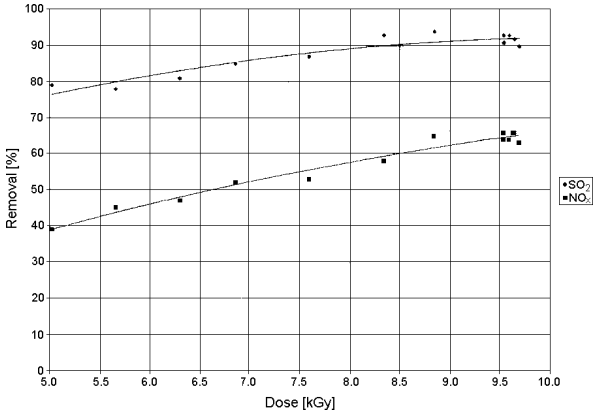

Fig.1. SO_2 and NO_x removal efficiency *vs*. dose in double stage irradiation process.

The experimental data obtained during the preliminary exploitation of the installation show good agreement with the results of pilot plant tests and theoretical calculations [3]. The most important factor for NO_x removal is the dose. Less important are the initial concentration of NO_x and ammonia stoichiometry. Although the total removal of NO_x (mg/Nm^3) increases linearly with the rise of initial concentration of NO_x, in the same time the removal efficiency (%) decreases (with the rest of the parameters remaining unchanged).

In the case of SO_2 removal, the most important parameters are temperature and ammonia stoichiometry. The cooling and humidifying of the flue gases is achieved in the process of spray drying the humidity which is correlated with a high degree with the temperature of flue gases. That is why this parameter exerts a lesser impact on the process. If this parameter was more independent of temperature (for example, by adding the steam to the cooling tower), the influence on the SO_2 removal would be more clear. As theoretically predicted the dose and impurity inlet concentration have very little impact on the process.

The previous experiments were done with a rather little range of ammonia stoichiometry variation. This set of experiments shows with no doubt that SO_2 removal depends strongly on ammonia stoichiometry, while NO_x only to a very minor degree (Fig.2). Beside the previously mentioned parameters, there was also one more parameter having impact on SO_2 removal – the way of ammonia injection. Ammonia may be injected in the gaseous form, in front of the irradiation chambers, or as ammonia water form, to the cooling tower or in both forms in various proportions. It was found that the presence of ammonia in the cooling tower increases the total efficiency of SO_2 removal.

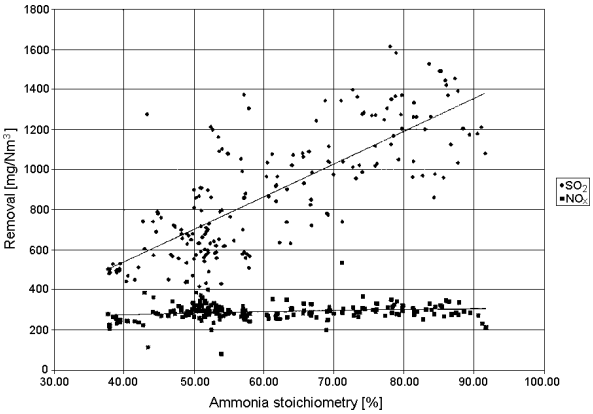

Fig.2. SO_2 and NO_x removal *vs*. ammonia stoichiometry.

Thus, it may be stated that the main goals of the installation were achieved. The full operation of the installation with four accelerators has already been in operation for over 2000 h already. The removal efficiency was found satisfactory

under various inlet flue gas parameters (flow rate, temperature, pollutants concentration etc.). The by-product obtained appeared stable and was acclaimed by the recipients as good for fertilizer production. Such good results of the biggest radiation processing facility in the world allows to hope for future development of this technology.

References

[1]. Chmielewski A.G., Iller E., Zimek Z., Licki J.: Radiat. Phys. Chem., 40, 4, 321-325 (1992).
[2]. Chmielewski A.G., Iller E., Tymiński B., Zimek Z., Licki J.: Modern Power Systems. May 2001, pp.53-54.
[3]. Chmielewski A.G., Iller E., Dobrowolski A., Tymiński B., Zimek Z., Licki J.: Radiat. Phys. Chem., 57, 527-530 (2000).

STABLE ISOTOPE COMPOSITION IN FOOD AUTHENTICITY CONTROL

Ryszard Wierzchnicki

Food products are mixtures of basic organic elements: carbon, hydrogen, oxygen and nitrogen. Stable isotope composition of these elements provides useful information for food authenticity control. Their isotopic fractionation in the environment follows complex patterns allowing to established the correlation between the food (fruits, vegetables etc.) and raw materials (water, air and soil) [1].

The aim of the study was to explore the relationship between isotope composition of different sort of foods and their geographical origin. The purpose of the study was to compare the data from different regions of Poland. The samples were received directly from the producer.

The hydrogen, oxygen, nitrogen and carbon composition was measured in many sorts of food. The obtained data give the possibility to find the relationship between the time and place of origin and isotope ratio: $^{18}O/^{16}O$, $^{13}C/^{12}C$, $^{15}N/^{14}N$ and D/H.

The composition of water present in the food was tested. Hydrogen was measured by an H/Device and oxygen isotope ratio by GasBench II (both instruments connected with a mass spectrometer) [2]. For comparison, the water samples from the region of plant growing were tested.

In this study, for measurements of carbon and nitrogen composition in food, we used our new instrument – an elemental analyzer. The Elemental Analyzer Flash 1112 NCS (Thermo Quest, Italy) for organic matter analyses is coupled with a Mass Spectrometer DELTA plus ConFloIII (Fig.). This system is a very useful research tool in many fields: environmental science, agriculture and medicine. Application of EA-IRMS to the solution of a wide variety of environmental problems is still increasing in recent years. This analytical method is most popular for studying stable isotope composition in food.

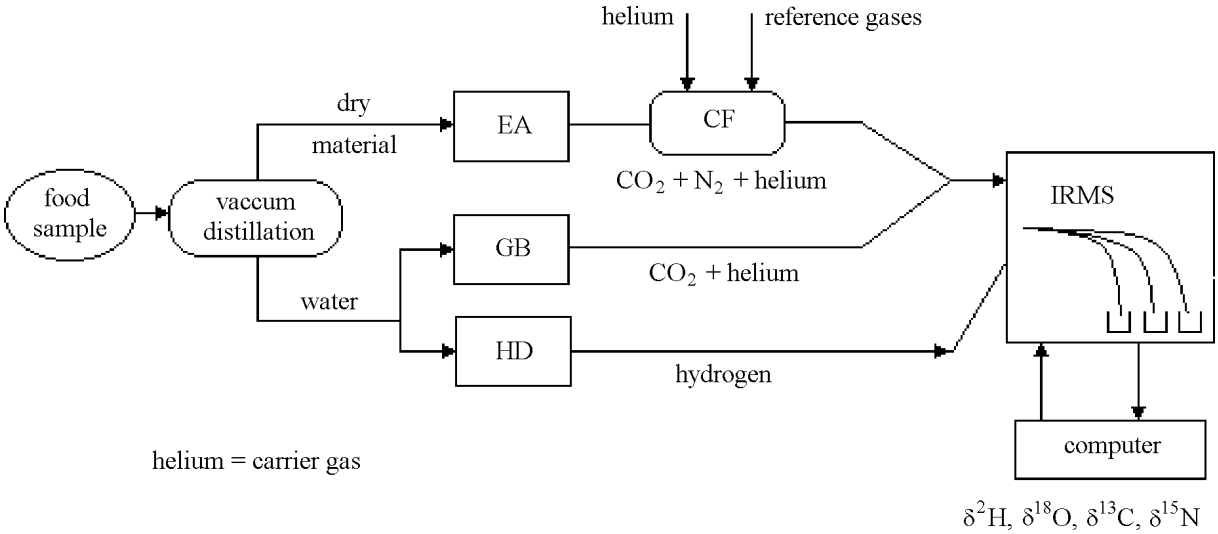

Fig. Block diagram of the sample preparation and measuring arrangement: EA – Elemental Analyzer Flash 1112 NCS, GB – GasBench II, HD – H/Device, CF – ConFloIII, IRMS – Isotope Ratio Mass Spectrometer.

Samples should be prepared in dry matter by drying raw material from food.

The measurements are fully automated and data are stored by a powerful data system.

The first testing measurements on the new instrument have been carried out recently.

The correlation between the stable isotope composition $^{18}O/^{16}O$, $^{13}C/^{12}C$, $^{15}N/^{14}N$, D/H and geographical origin of the tested food will be presented in the next work.

In the future, the study will be continued and extended to sulfur isotope composition in food and in the surrounding environment (as a pollutant).

The work is supported by the International Atomic Energy Agency (IAEA). The Elemental Analyzer Flash and ConFloIII interface was purchased in the frame of IAEA TC Project POL/2/014.

References

[1]. Rossmann A.: Food Reviews International, 17(3), 347-361 (2001).
[2]. Werner R.A., Brand W.A.: Rapid Commun. Mass Spectrom., 15, 501-519 (2001).

A STUDY OF HYDRAULIC CONTACTS AND FLOW DYNAMICS OF GROUND WATERS IN THE REGION OF SALT DOME "DĘBINA" IN THE LIGNITE STRIP MINE "BEŁCHATÓW"

Wojciech Sołtyk, Jolanta Walendziak, Andrzej Dobrowolski, Andrzej Owczarczyk

Any study of ground water usually needs determination of its flow direction and velocity.

Two well mode tracer experiments are one of the possible resolution of the problem [1, 2]. The salt dome "Dębina" has devided the "Bełchatów" liqnite deposit into two parts. The first, Bełchatów Field, which is actually being exploited, and the second – Szczerców Field just started to be prepared for future exploitation (Fig.1).

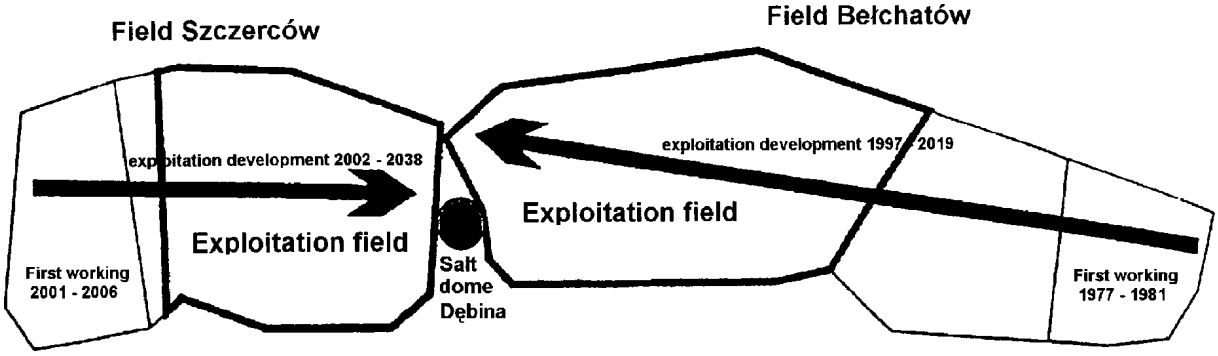

Fig.1. Scheme of strip exploitation development in mine "Bełchatów".

The salt dome drainage protection barrier consists of 40 wells (~250 m deep) localized around the salt deposit. The system has been successfully exploited since 1992. The main aim of the system is the elimination of ground water flow through the salt deposit sphere to avoid its dissolution and to prevent contamination of mine ground waters by brines.

The basic condition of the system is to keep the depression at a stable level.

The existing barrier fulfiled very well its aims during the past 10 years. At present, when simultaneously with the Bełchatów Field exploitation, preparation works of the Szczerców Field have begun, the efficiency of depression protection barrier of salt dome should to be increased (probably by a second ring of pumping wells localized outside the actually working barrier). Therefore, before starting the design process and build-up a new drainage system, an investigation on aquifer characteristics should be performed. The main problem is to determine hydrological conditions in the south-west part of the salt dome foreland as well as to estimate necessary input data for actualization of the hydrogeological model of the region.

The aqueous solution of uranine has been used as a tracer in all experiments. The injection piezometers and observation of the pumped wells have been chosen on the basis of the existing system of protection barrier around the salt dome "Dębina".

The tracer has been injected strictly to the filtrated zone of each investigated wells (175-330 m below ground level). After uranine injection, the well was filled with 0.4-2.5 m^3 of water causing the tracer to investigate the aquifer strata.

The observations of tracer appearance in the samples taken from the neighbouring wells was carried out during the period from 40 to 72 days. The obtained tracer response curves have been the basis for mathematical modelling of ground water flow. The best fitting of experimental curves have been obtained by applying one dimensional diffusion model for point injection.

The solution of the model equation has been done by Zuber [3]. The examplary tracer response curve is shown in Fig.2. The experimental curve can be well fitted by the model curve being the superposition of three curves representing the partial flows through the geological system (Fig.2 – model 1, 2, 3). This means that there are three crack systems in the aquifer, each of them can be characterized by different velocity and rate of ground water flow.

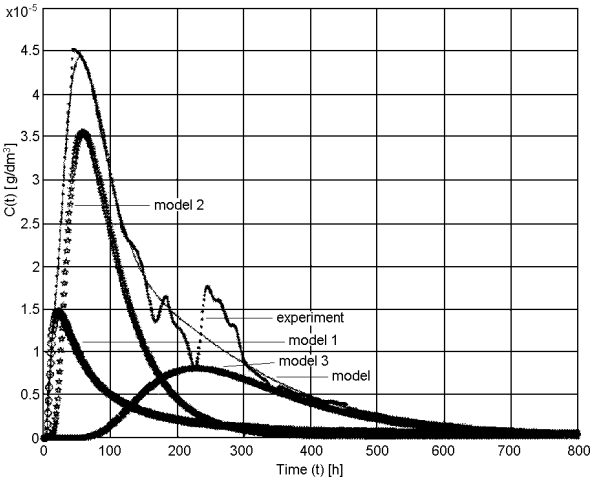

Fig.2. Concentration of tracer in water of 24 SD well: C(t) dynamic curves exp-model (exp: t_0=176.4 h, w=0.6921, k=0.992; model: t_0=175.4 h, w=0.7043, t1=263.5 h, Pe1=0.53, t2=101.6 h, Pe2=5.6, t3=317.8 h, Pe3=8.8).

So, the individual interpretation of the obtained tracer response curves enables to determine the mechanism of water transport, its velocity and direction as well as the longitudinal dispersion coefficient.

References

[1]. Knuttson G.: Graund Water Problems. Pergamon Press, Oxford 1968.
[2]. Guidebook on Nuclear Techniques in Hydrology. International Atomic Energy Agency, Vienna 1983.
[3]. Zuber A.: Dyspersja wskaźnika przy przepływach przez ośrodki porowate w aspekcie zastosowań hydrogeologicznych. Zeszyt 7 (302), AGH, Kraków 1971.

CHLORINATED HYDROCARBONS DECOMPOSITION BY USING ELECTRON BEAM TECHNOLOGY

Andrzej G. Chmielewski, Yongxia Sun, Sylwester Bułka, Zbigniew Zimek

Chlorinated organic compounds emitted into the atmosphere are very harmful to the environment and human health. These organic compounds are formed from various sources, including industrial fabrication, incineration process of coal power station and municipal waste incinerators etc. Recent research shows that chlorinated organic compounds might be precursors of dioxin's formation. Dioxins' emission into atmosphere causes very serious problem to the environment and they are categorized as the most toxic compounds by the Environmental Protection Agency.

It is very important to destruct/diminish chlorinated organic compounds formation during incineration process, therefore to minimize dioxin's formation. Different methods have been studied. They are: new model of incinerators combined with optimizing combustion process, biotechnology and electron beam (EB) technology [1-3]. Hirota and Paul studied PCDD/F destruction by using EB technology and obtained promising results.

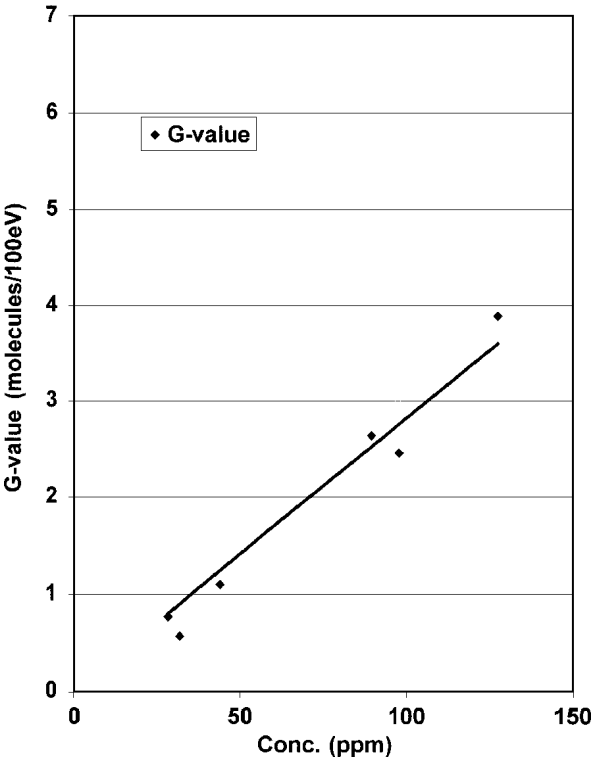

Fig.1. G-value *vs*. initial concentration of 1,4-dichlorobenzene/air at 5 kGy dose.

The aim of our work was to study chlorinated volatile organic compounds (VOCs) destruction by using EB technology. Dichloroethylene (DCE) and chlorinated dichlorobenzene were chosen as representative compounds for chlorinated aliphatic and aromatic hydrocarbons, respectively. Based on our lab experimental results and theoretical analysis, the mechanism of chlorinated VOCs decomposition will be elaborated. It will give valuable information for environmental application.

In our previous work [4], we have reported (DCE) decomposition in low-humidity air by using EB and gamma-ray irradiation. It was found that over 95% DCE was decomposed at 8 kGy absorbed dose for 300 ppm of initial concentrations of DCE. G-values (unit: molecules/100 eV) of dichloroethylene were 20~60 for 300 to 1500 ppm of initial concentrations of DCE. DCE decomposition is mainly initiated by Cl-dissociative secondary electron attachement reaction. Cl decomposition pathway contributes to DCE decomposition.

1,4-dichlorobenzene decomposition in an air mixture and a nitrogen mixture has been studied

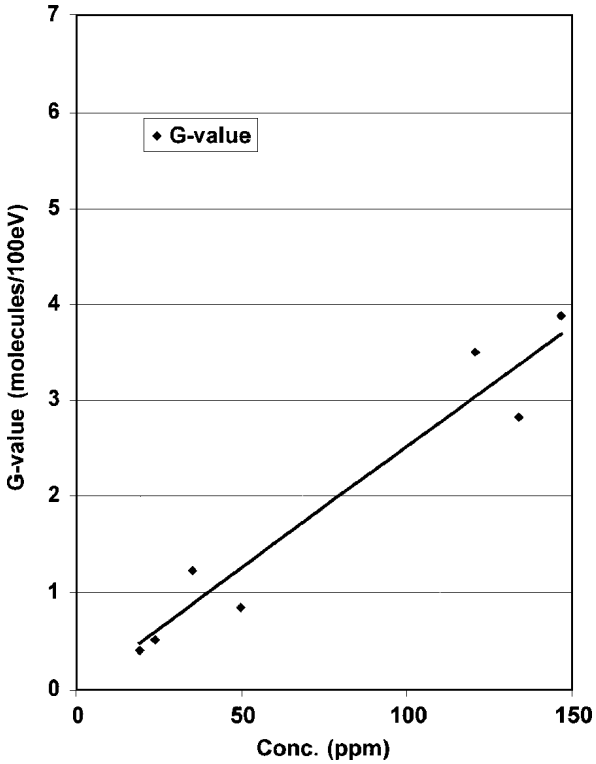

Fig.2. G-value *vs*. initial concentration of 1,4-dichlorobenzene/N_2 at 5 kGy dose.

in a "batch" system, respectively. The model gas was irradiated by an ILU-6 accelerator. Prelimi-

nary results show that the efficiency of 1,4-dichlorobenzene decomposition is much lower than that of DCE. Decomposition efficiency is below 50% at 10 kGy absorbed dose for the initial concentration of 1,4-dichlorobenzene lower than 100 ppm. G-values of 1,4-dichlorobenzene are 0.5~4.0 for 30~150 ppm of initial concentration of 1,4-dichlorobenzene in air and nitrogen mixtures, respectively. These results are shown in Figs.1 and 2, respectively. The decomposition efficiency of 1,4-dichlorobenzene is a little higher in the air mixture than that in the nitrogen mixture. The mechanism of 1,4-dichlorobenzene decomposition might be mainly caused by positive-ion charge transfer reactions; peroxyl radical decomposition pathway is not important.

References

[1]. Gordon M.: Chem. Eng. J., 86, 343-368 (2002).
[2]. Bill G.S.: http://umbbd.ahc.umn.edu/dpd/dpd_image_map.html, 2002.
[3]. Paur H.-R.: Decomposition of volatile organic compounds and polycyclic aromatic hydrocarbons in industrial off gas by electron beam – a review. International Symposium on radiation technology for conservation of the environment, Zakopane, Poland, September 1997, pp. 1-17.
[4]. Sun Y. *et al.*: Radiat. Phys. Chem., 62, 353-360 (2001).

APPLICATION OF COMPUTATIONAL FLUID DYNAMICS METHODS FOR DETERMINATION OF FLOW STRUCTURE IN WASTEWATER TREATMENT TANKS

Jacek Palige, Andrzej Dobrowolski, Andrzej Owczarczyk, Andrzej G. Chmielewski, Sylwia Ptaszek

Wastewater treatment process realized in industrial or municipal plants involves such processes as clarification, flow rate and chemical composition equalization, wastewater aeration with bubble system or aeration turbine application, sludge sedimentation and final wastewater clarification in big volume sedimentation tanks. The efficiencies of all these processes strongly depend on both the liquid and solid phase flow structure.

Many researches concerning identification and optimization of flow structure in such devices as clarifier – equalizers, aeration tanks, circular rectangular settlers and sedimentation tanks were carried out [1-4]. Using the tracer technique, experimental residence time distributions (RTD) functions for liquid phase and for sediment were determined. On the basis of these data the different multiparametric models of flow structure are proposed. Model parameters are usually obtained by optimalization procedures (minimalization for example the sum of square deviations between experimental and model curves). Unfortunately, the same experimental RTD function can be described by various models with similar accuracy.

For this reason some additional information about physics of phenomena inside the tank is necessary for validation of the model choice. One of the techniques which are used for this purpose is the computational fluid dynamics (CFD) method. For a given tank, applying numerical code, the appropriate system of three Navier-Stokes equations and continuity equation (1), boundary conditions and additional (if necessary) relations describing turbulence of flow are solved.

$$\frac{\partial u_i}{\partial t} + u_j \frac{\partial u_i}{\partial x_j} = -\frac{1}{\rho}\frac{\partial p}{\partial x_i} + \nu \frac{\partial^2 u_i}{\partial x_j^2}, \; i = 1,2,3$$
$$\frac{\partial u_i}{\partial x_i} = 0 \qquad (1)$$

As a result the velocity field that describes the flow structure in the tank is obtained. RTD function is obtained (from calculated velocity field) by the particle trajectory method or by stimulus – response numerical experiment [3].

For checking this technique, a simple laboratory model of industrial rectangular settler (in scale 1:8) was built. The scheme of tank with indication of tracer injection and output signal registration points is presented in Fig.1.

Dimensions of tank are L×W×H=4.95×1.3×0.45 m, where: L – length, W – width, H – height. For flow rate Q in the range 1÷3.8 m^3/h and for different localization of baffles inside the settler, tracer experiments were done. As tracers the radioisotopes Tc-99, Br-82 and color tracer fluoresceine were used. Comparison of the RTD functions obtained during parallel simultaneous injection of Tc-99 and fluoresceine (Fig.2) indicates that the phenomenon sorption/desorption of Tc-99 on the walls of tank is observed, so Tc-99 is not appropriate tracer for this kind of measurements. Mean residence time for Tc-99 as a tracer was obtained bigger than theoretical residence time T=V/Q, where: V – volume of tank, Q – flow rate, which is impossible from the physical point of view.

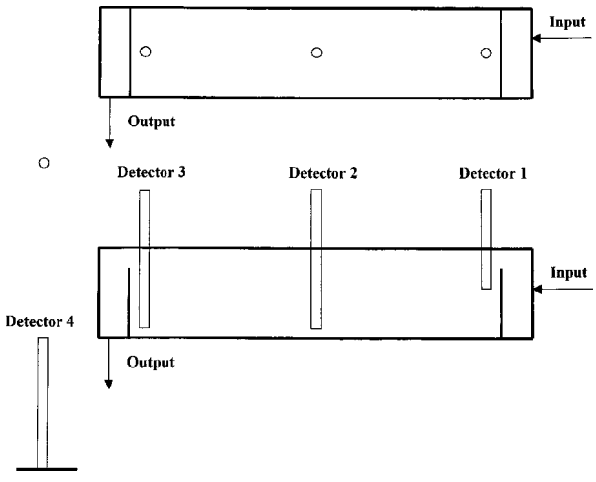

Fig.1. Scheme of the settler tank.

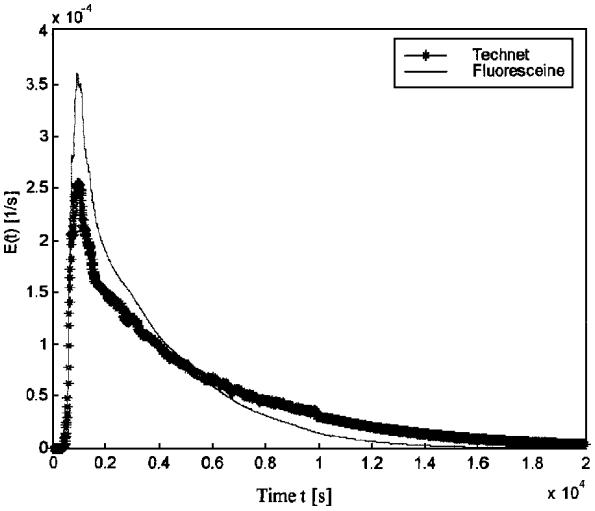

Fig.2. RTD functions obtained for fluoresceine and Tc-99 as a tracer for Q=2.86 m^3/h.

Taking into account that for Q=3 m^3/h, the velocity of water at the input of tank is about 0.13 m/s and the Reynolds number Re ≈ 3000, the standard k – ε model of turbulence was used for numerical solution of the partial differential equation system (1).

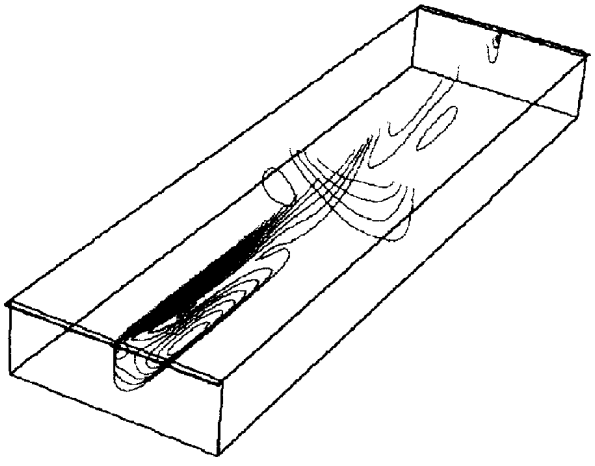

Fig.3. Calculated velocity field for empty tank in axis cross-section.

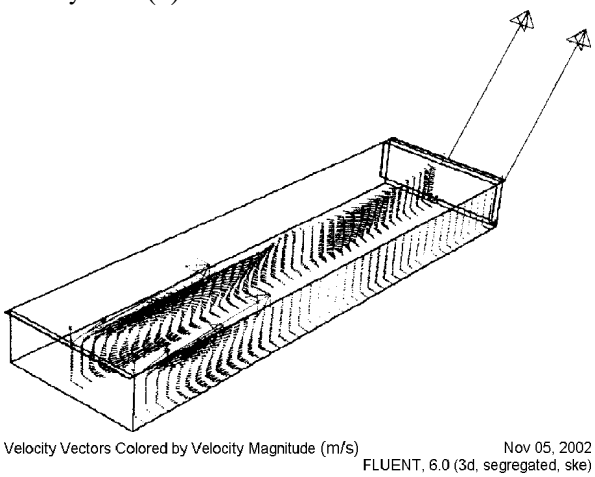

Fig.4. Calculated velocity field for tank with baffle in axis cross-section.

The obtained velocity field for empty tank and for tank with baffle, installed near the output of settler are presented in Figs.3 and 4, respectively. Using the particle trajectory method the RTD functions were calculated. Comparison of numerical and experimental curves (obtained with the Br-82 radiotracer) is presented in Figs.5 and 6. It is observed that experimental and calculated RTD curves differs for small values of residence time indicating that methodology has to be improved.

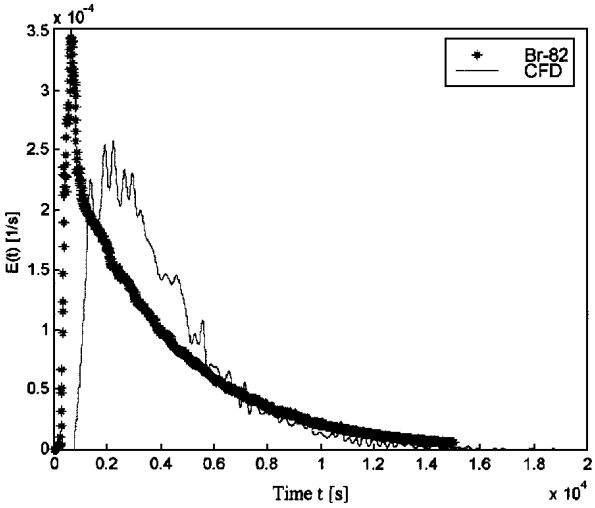

Fig.5. Comparison of calculated and experimental RTD functions (tracer Br-82, empty tank).

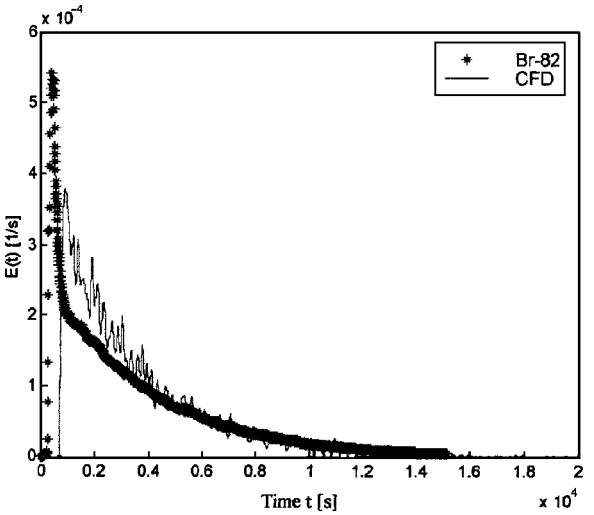

Fig.6. Comparison of calculated and experimental RTD functions (tracer Br-82, tank with baffle).

The work was supported by the Polish State Committee for Scientific Research (KBN) – grant No. 7T09C02221.

References

[1]. Chmielewski A.G., Owczarczyk A., Palige J.: Nukleonika, 43, 2, 185-194 (1998).
[2]. Farooq M. *et al*.: Inż. Ap. Chem., 3s, 40-41 (2000).
[3]. Thyn J., Zitny R.: Analysis and Diagnostics of Industrial Processes by Radiotracers and Radioisotope Sealed Sources. Part I. CVUT, Praha 2000, 329 p.
[4]. Farooq M. *et al*.: Nukleonika, 1 (2003), in print.

CATALYTIC CRACKING OF POLYETHYLENE WASTES

Andrzej G. Chmielewski, Bogdan Tymiński, Krzysztof Zwoliński

Plastics have a number of advantages in comparison to traditional materials like paper, metals, glass or wood and their application gradually increases. Among the plastics most popular are polyolefines and their production is *ca*. 70% of the whole plastics production. Similar or even larger is the polyolefine fraction in waste plastics. Waste polyolefines are very stable and during landfilling practically do not undergo degradation. Some polyolefines are recycled as components in the production of new articles. Also very small amounts of plastics are burned for heat production. Very perspective is the conversion of waste polyolefines into liquid fuels, which are most valuable among the fuels. In this field a number of works was done. Usually, the process was carried in a batch apparatus and without separation of cracking products. It seems that more perspective for industrial purpose is a continuous working installation with tubular catalytic cracking reactor and fractionation of product. Product collected without fractionation is similar to crude oil and usually is sold to rafinery where is processed together with crude oil.

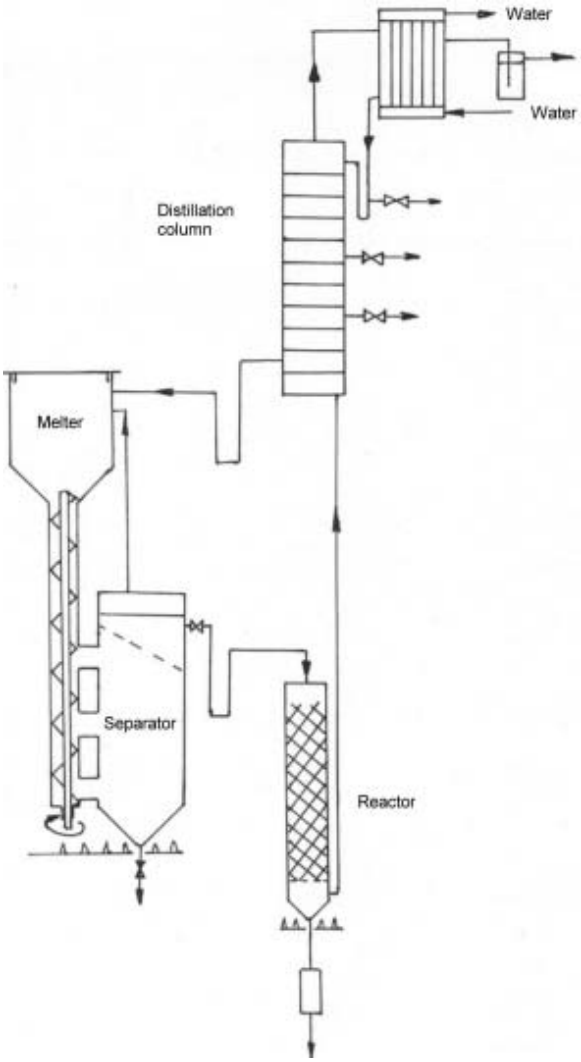

Fig.1. Scheme of installation for catalytic cracking of polyethylene wastes.

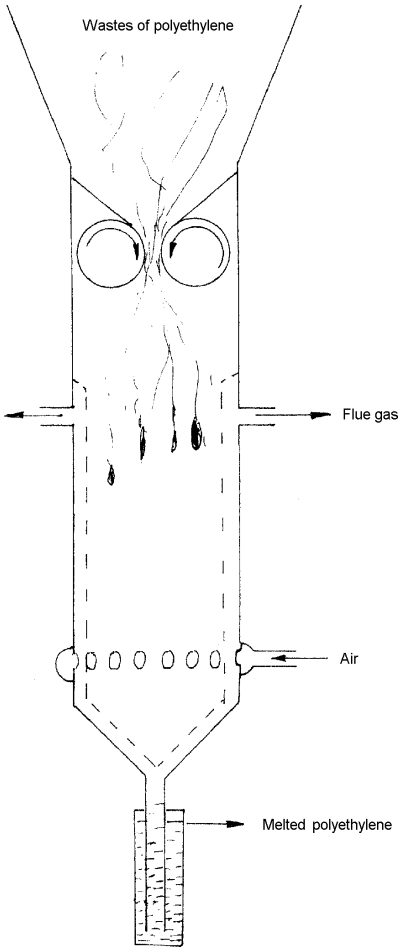

Fig.2. Melter with partial burning of polethylene wastes.

We developed a continuous process for which a patent application P.342948 was made.
A scheme of installation is presented in Fig.1. Waste polyolefines are melted in a melter and the liquid flows to a separator where it is filtrated on a net. Then the liquid polyethylene flows to a tubular catalytic reactor. Gas products of cracking flows to a distaillation column, where the products are fractionated into four fractions: gas fraction is used as a fuel for heating of installation, gasoline and oil fraction are taken out as a product and heavy oil fraction is recycled to the melter.

In this process some problems were encountered with operation of the melter, because during intro-

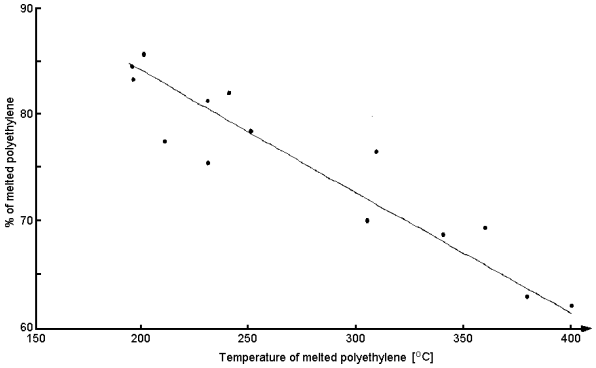

Fig.3. Fraction of melted polethylene *vs*. its temperature.

duction of the waste polyethylene some air is introduced which can ignite hydrocarbon vapours inside the melter. Some odours are also released from the melter.

In a new version of the melter, waste polyethylene is introduced by sluice and nitrogen is introduced into the separator.

Parallely, we developed a new type of melter in which waste polyethylene is partially burned and heat of combustion melts the unburned polymer. Patent application P.353434 for this solution of melter was elaborated. The scheme of the melter is presented in Fig.2. Theoretical calculations shows that combustion of about 3% of polyethylene gives enough heat for melting of the remainder 97% of polyethylene. In practice, the fraction of melted polyethylene depends on design of the melter as well as on temperature of the melted polyethylene. Results of tests for one version of the melter are presented in Fig.3.

MATERIAL ENGINEERING, STRUCTURAL STUDIES, DIAGNOSTICS

DETERMINATION OF TRACE ELEMENTS CONCENTRATIONS IN LEAD WHITE BY NEUTRON ACTIVATION ANALYSIS OF THE *JERUSALEM TRIPTYCH* DATED ABOUT 1500

Ewa Pańczyk, Justyna Olszewska-Świetlik[1/], Lech Waliś

[1/] Institute for the Study, Restoration and Conservation of Cultural Heritage, Nicolaus Copernicus University, Toruń, Poland

Material analysis plays an important role in the technological tests of easel paintings. Various methods including physical and chemical ones, are used in this area. Development and continuous improvement of ultra-sensitive instrumental techniques in the analytical chemistry make it possible to carry out more precise and detailed analyses. Nuclear methods have found a wide application in the examination of art objects [1]. One of these methods is the neutron activation analysis used to determine the trace elements in various materials. In examination of paintings, this method is mainly used to determine the trace elements in given pigments, including lead white. The lead white is regarded as one of the oldest and most widely used pigments over the centuries. Thus, it is possible to examine and compare the paintings from various ages. The purity of lead white is directly related to the development of lead production and purification methods. The significant development of this processes was not noted before the 19th century. Therefore, the determination of trace elements in the lead white is helpful in establishing the time of painting creation. Apart from the technological process used in the white lead manufacture, the trace element distribution depends on the lead ore extraction location. Due to this, the examination results yield additional information on the painting origin.

Systematic record keeping and expansion of the database relating to the trace element concentration in the lead white allows a comparison of material types used by given artists and determination of the painting school.

Table 1. The description of samples taken from the *Jerusalem Triptych* (about 1500), National Museum in Warsaw.

Sample No.	Place of sample taking
1	The *Massacre of the Innocents* – (obverse) the white from the impasto on the sleeve of grey soldier's armour in the middle distance
2	The *Massacre of the Innocents* – (obverse) the white from the highest light on left sleeve of the child's robe in the foreground
3	*Predella* – the white, impasto on the hand of the fifth apostle to the right
4	*Predella* – the white, impasto on the hand of the fifth apostle to the right
5	*Predella* – the white, impasto, the pupil of the eye of the third apostle to the right
6	*Predella* – the white from the hair of the first apostle to the right

Accordingly, it is possible to establish the interrelations or to separate the different features relating to the painting schools active in various parts of Poland and Europe.

The analyses of the lead white from West European paintings from the 15th to 19th centuries have divided the pigment into two basic types: beyond-Alpine used in North Europe and ante-Alpine present in southern painting, mostly Italian [1]. Compared to the past-Alpine white, the ante-Alpine type

Table 2. Irradiation and measurements parameters.

Neutron flux intensity	$8 \cdot 10^{13}$ n/cm^{2}s			
Irradiation time	24 h			
Cooling time	1 day	6 days	20-30 days	60 days
Measurement time	1000 s	3200 s	7200 s	10000 s

is characterized by higher concentration of copper and manganese and lower concentration of silver and antimony.

For a few years the Institute of Nuclear Chemistry and Technology in cooperation with other research institutes (including Division of Painting Technology and Techniques of the Institute of Study and Preservation of Historical Monuments, Nicolaus Copernicus University in Toruń) has been using neutron activation analysis in tests of the lead white from the table paintings dated between the 15th and 18th centuries.

This article presents the results of the examination of the *Jerusalem Triptych* from the Holy Virgin Mary Basilica in Gdańsk representing the late-Gothic painting in Northern Poland.

Table 3. Concentration of determined elements [ppm].

Specimen No. / Element	1	2	3	4	5	6
Na	1010.00	1740.00	763.00	880.00	417.00	1770.00
K	3400	4960	2620	3670	1790	5800
Sc	32.10	62.50	22.30	33.80	14.00	64.30
Cr	41.20	76.00	33.60	36.40	16.60	76.00
Mn	249.00	61.00	173.00	321.00	147.00	800.00
Fe	2640.00	4010.00	1660.00	1810.00	691.00	2300.00
Co	23.70	47.90	8.28	20.10	8.04	41.80
Cu	88.00	45.70	4.54	47.70	6.61	413.00
Zn			7.42	6.37		3.77
Ga	2.22	24.90	6.26	7.10		22.30
Ge			9.11		22.70	
As	34.70	21.30	8.59	9.73	2.87	18.40
Br	170.00	294.00	130.00	168.00	56.90	274.00
Sr			74.80			
Mo	1.05	38.00	7.68	13.60	3.81	
Ag	13.1	51.1	1.88	20.7	2.02	
Cd			7.30			
Sn	278.00	184.00		930.00	82.80	
Sb	1.31	2.23	1.57	2.07	0.687	5.36
Cs	8.72	16.10	6.46	9.02	3.13	12.00
Ba	83.30	124.00	68.20	76.50	21.60	302.00
La	1.73	2.95	1.14	2.07	0.64	3.23
Ce	1.18	2.47	0.624	3.90	0.479	3.33
Sm	0.51	0.735	0.364	0.67	0.173	0.827
Eu	0.244	0.122	1.24	0.145	0.028	
Dy				48.50		
Er		4.80	1.12			
Yb	0.128	0.307		1.54	0.050	1.49
Lu			0.043			
Ta	0.0865	0.814	0.578	0.204	0.134	0.301
W	0.255	0.439	0.168	0.766	0.14	0.737
Ir		0.11		0.587	0.079	
Au	4.33	16.1	3150	9490	2.33	210
Hg	150.00	29.30	3.36			
Th	2.01	3.38	0.796	2.77	0.518	9.02
^{238}U	2.44	0.294	10.20	32.00	0.333	2.13

The tests employing the neutron activation analysis are supposed to yield additional information

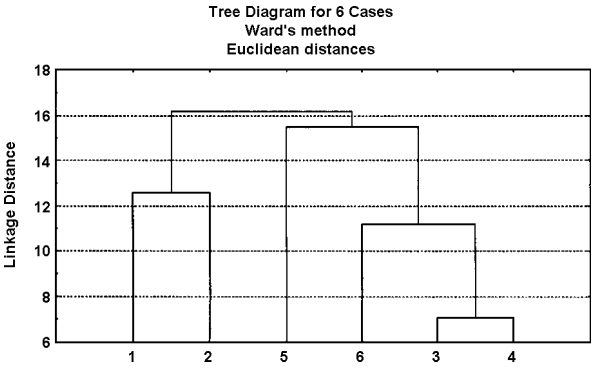

Fig.1. Clustering for 6 lead white specimens taken from the *Jerusalem Triptych,* standardized variables, number of features 33.

on the types of materials used to paint the Triptych. Moreover, the test results will help to determine the retable origin, influence of other painting schools, and attribute it to the appropriate painting workshop.

Within the research project related to the determination of painting technology and technique of the *Jerusalem Triptych*, the lead white samples have been examined by means of the neutron activation analysis.

The Triptych comes from the Holy Virgin Mary Basilica in Gdańsk [2]. Since 1945, it has been kept in the National Museum in Warsaw. The altar was most likely founded by the Holy Virgin Mary Priest Brotherhood for the Jerusalem Chapel in the Holy Virgin Basilica. The retable is an example of a simultaneous composition, where in each quarter a few various scenes are presented.

The Triptych was painted at the end of the 15th century. Till this date, precise date of its creation and the painting school have not been unequivocally determined.

The test samples have been taken from the obverse of the left wing depicting the *Massacre of the Innocents*, *Miraculous Growth of the Cereal during*

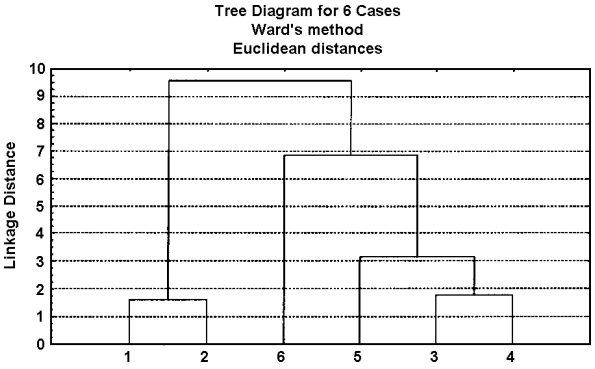

Fig.2. Clustering for 6 lead white specimens taken from the *Jerusalem Triptych,* standardized variables, number of features 4 – rare earth elements: La, Ce, Eu, Yb.

the Pursuit of the Holy Family by Herod's Soldiers, and from the *Predella*. The sample designation and their detailed description are presented in Table 1.

Samples of the mass from 0.1 to 0.5 mg have been taken from the places of maximum original-

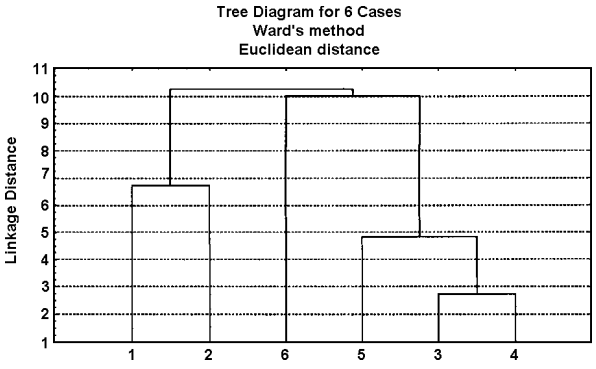

Fig.3. Clustering for 6 lead white specimens taken from the *Jerusalem Triptych,* standardized variables, number of features 9 – Ag, Cu, Zn, Mn, Fe, Cr, Co, Cd, Au.

ity not showing admixtures of other pigments and put directly to quartz ampoules.

After weighing and sinking in the quartz ampoules, the test specimens have been packed in a 7-specimen packages together with the reference specimens of 47 determined elements. Additionally, for thermal neutrons flux monitoring, Sc and Au reference specimens have been attached to each batch of specimens.

The irradiation of the specimens was performed in the MARIA reactor at Świerk, at a neutron flux of $8 \cdot 10^{13}$ n/cm^{2}s thermal neutrons flux. The specimens were irradiated for 24 h and cooled for 8 h. In order to remove the surface contaminations, the specimens taken out of the packaging were washed in a 1:1 HCl solution, and then in alcohol. The reference specimens have been washed out of the ampoules, or – in the case of Sc and Au – have been solved together with the aluminium film. Then, specified volumes (0.01-0.1 ml) have been put to glass measurement vessels and evaporated dry. The radioactivity measurements of such prepared specimens were performed with an HP class germanium detector, its active volume was 80^3, energy resolution – 1.95 keV for energy 1333 keV – ^{60}Co. The de-

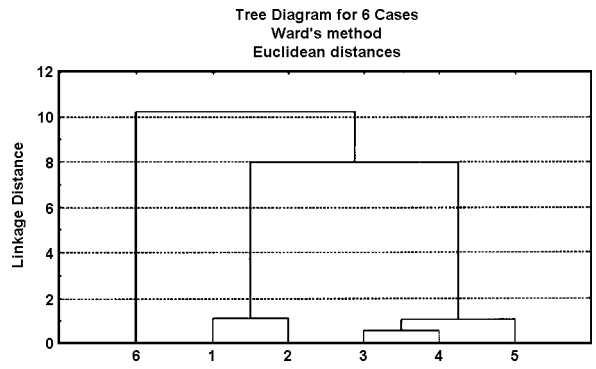

Fig.4. Clustering for 6 lead white specimens taken from the *Jerusalem Triptych,* standardized variables, number of features 4 – Ag, Cu, Zn, Mn.

tector cooperates with a Canberra's S100 analyser controlled by an IBM/PS-2 computer. The analysis of the complex gamma-ray spectra from the apparatus was performed with the use of the micro-

-SAMPO software. The parameters of irradiation in the reactor and of the spectrometric measurements are presented in Table 2. Eight measurements of each specimen have been made.

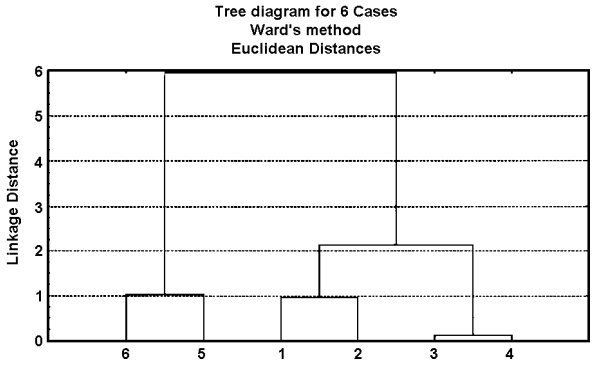

Fig.5. Clustering for 6 lead white specimens taken from the *Jerusalem Triptych,* standardized variables, number of features 2 – Sc, Cs.

Thirty six elements have been identified and determined in the tested specimens. The determination results are presented in Table 3.

In order to determine the degree of probability of the tested objects, the clustering was performed by means of the STATISTICA (StatSoft) software application. The clustering was performed for standardized variables.

The clustering in the *Jerusalem Triptych* has been presented in several versions:

- all determined elements (number of features 33), (Fig.1);
- rare-earth elements: La, Ce, Eu, Yb (number of features 4), (Fig.2);
- only Ag, Cu, Zn, Mn, Fe, Cr, Co, Cd, Au, (number of features 9), (Fig.3);
- only Ag, Cu, Zn, Mn (number of features 4), (Fig.4);

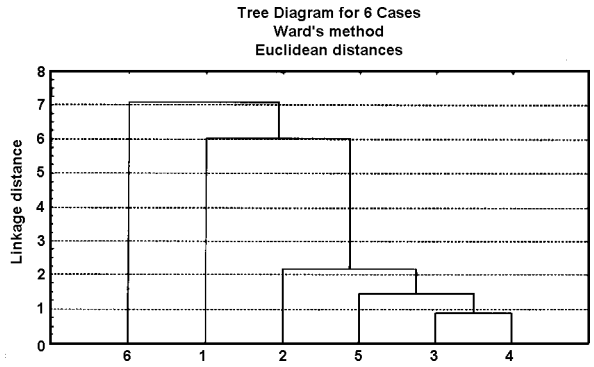

Fig.6. Clustering for 6 lead white specimens taken from the *Jerusalem Triptych,* standardized variables, number of features 2 – Th, ^{238}U.

- only Sc, Cs (number of features 2), (Fig.5);
- only Th, ^{238}U (number of features 2), (Fig.6);
- only Cu, Mn (number of features 2), (Fig.7);
- only Ag, Sb (number of features 2), (Fig.8).

The clustering of the elements from the *Jerusalem Triptych* (illustrated by examples 1 through 8)

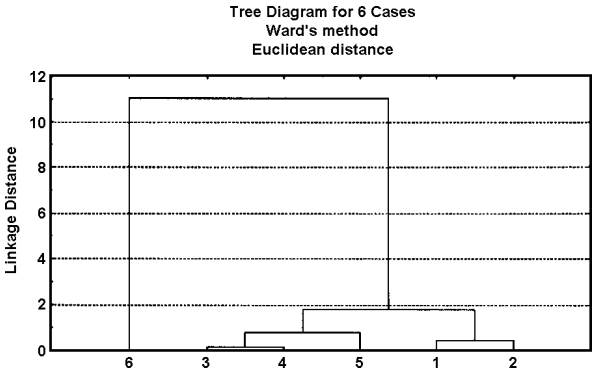

Fig.7. Clustering for 6 lead white specimens taken from the *Jerusalem Triptych,* standardized variables, number of features 2 – Cu, Mn.

has shown that all specimens are similar. The differences between the specimens from the obverse of the left wing (specimens 1 and 2) and from the *Predella* (specimens 3, 4 and 5) are insignificant. The specimen 5 from the *Predella* is slightly less similar to the other specimens.

The most common trace elements in the tested lead white samples are Fe, Mn, Cu and Cr. Additionally, the samples 1 and 2 are characterized by high concentration of Hg, and specimens 3, 4 and 6 by high concentration of Au (Table 3).

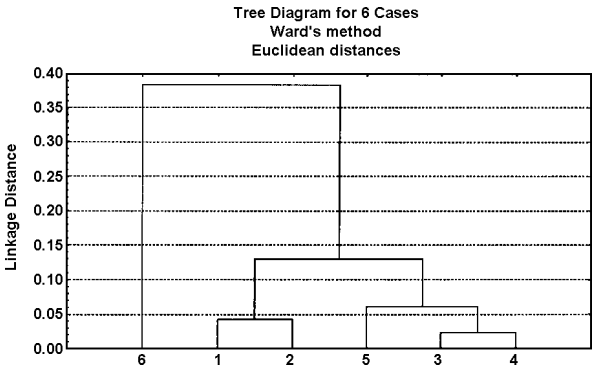

Fig.8. Clustering for 6 lead white specimens taken from the *Jerusalem Triptych,* standardized variables, number of features 2 – Ag, Sb.

The white from the 6 examined specimens from the wing and *Predella* of the *Jerusalem Triptych* may be included among the so-called beyond-Alpine white used in North Europe.

Further qualification will be possible after the database related to the examination of the white is updated, including the currently carried out examination of the paintings from the Polish Northern School in the 15th century.

References

[1]. Pańczyk E., Ligęza M., Waliś L.: J. Radioanal. Chem., 244, 3, 543-551 (2000).
[2]. Labuda A.S.: Malarstwo tablicowe w Gdańsku w 2 poł. XV w. PWN, Warszawa 1979, pp.91-104.

NEW SILICA MATERIALS WITH BIOCIDAL ACTIVITY

Andrzej Łukasiewicz, Lech Waliś, Luzja Rowińska, Dagmara Chmielewska

Silica gel (SiO_2) modified with ethanolamine (EA) was described previously as effective sorbent for heavy metals [1, 2]. In course of further investigations we have found that the sorbent SiO_2-EA binds effectively quaternary N-alkilammonium salts (QAC) such as benzalkonium chloride (Preventol, Bayer) or Bardap 26 (Lonza), giving new materials SiO_2-EA·QAC(I). We found further that SiO_2 coated with polyaminosugar Chitosan (Chit) binds also QAC to form SiO_2-Chit·QAC materials (II). SiO_2 coated with $Cu(EA)_4$ complex (Cus-cooper II salt) binds QAC to give SiO_2-Cus$(EA)_4$·QAC(III) materials. All three kinds of new materials are interesting as solids (pigments) with biocidal activity of the surface. QAC (Preventol, Bardap) are used as water soluble agents of broad biocidal activity against algae, fungi, yeasts and bacteria. Chitosan is a compound of invested biological properties, among others of fungicidal activity [3]. The

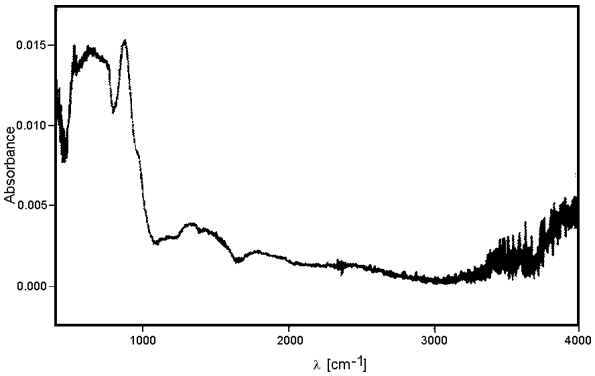

Fig.1. IR of SiO_2-EA material.

copper complexes Cus$(EA)_4$ showed some fungicidal activity in biological tests.

Replacing of aqueous solutions of QAC by solid materials I-III with biocidal active surface (biocidal silica materials – BSMs) seems to be very attractive for various applications such as destroying algae or bacteria by adding BSM to water or preserving various surfaces by adding BSM to suitable paints. Combination of QAC with Chit or Cus$(EA)_4$ on SiO_2 can be of special interest. The pigments SiO_2-Chit·QAC show high affinity for heavy metals. Binding of a metal to II material can increase its biocidal activity. Solid BSM can be used as a kind of biological filters.

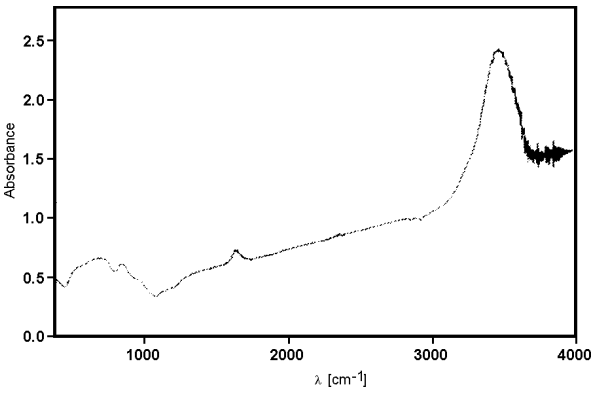

Fig.2. IR of SiO_2-EA·Pr material.

SiO_2-EA·QAC materials were prepared by stirring silica gel (Merck, grade 60, 63-200 μm) with a 5% EA solution in water, filtering off and washing with water. The SiO_2-EA material (~4% of EA) was then stirred with a 5% aqueous solution of Preventol R-80 (Pr). By using suitable proportions, complete binding of Pr to SiO_2-EA took place (lack of Pr in the filtrate). Maximal amount of Pr in I material was ~15% by weight. SiO_2-Chit·QAC(II) was obtained by stirring SiO_2 (5 g) for 5 min with 25 cm^3 of 1% solution of Chit (Aldrich, high molecular weight) in 1% CH_3COOH, 5 cm^3 of 5% NaOH in water was added and the mixture was stirred intensively. The solid SiO_2-Chit was filtered off and washed with water (it contained ~5% of Chit). SiO_2-Chit was stirred with the 5% Pr solution in water, the material was filtered off (lack of Pr in the filtrate indicated that binding of Preventol is complete). The material II contained maximally ~25% of Pr.

SiO_2-Cus$(EA)_4$·QAC was prepared as follows: to 0.02 mol of $Cu(CH_3COO)_2$ in water 0.08 mol of EA was added, to intensively blue solution of the complex Cus$(EA)_4$ formed SiO_2 was added (20 g) and stirred for 5 min. Complete discolouring of the solution and colouring of SiO_2 to blue colour occurred. The material was filtered off, washed with water and stirred with 5% Pr. Up to ~15% of Pr was bound in the material SiO_2-Cus$(EA)_4$·QAC(III).

Some structural investigations on BSMs were carried out. IR spectra showed very intense absorption in the region ~3500 cm^{-1} in SiO_2-EA·QAC and SiO_2-Cus$(EA)_4$ materials (Figs.2 and 3). In SiO_2-EA absorption intensity in this region is very low (Fig.1). Intense absorption in the region ~3500 cm^3 corresponds to streaching vibrations of OH groups. High intensity of this absorption can be caused by the influence of positively charged nitrogen of QAC and of Cus$(EA)_4$ complex (Cu-NH_2-) on OH groups of EA. Attaching of QAC to SiO_2-Cus$(EA)_4$ do not change this absorption intensity.

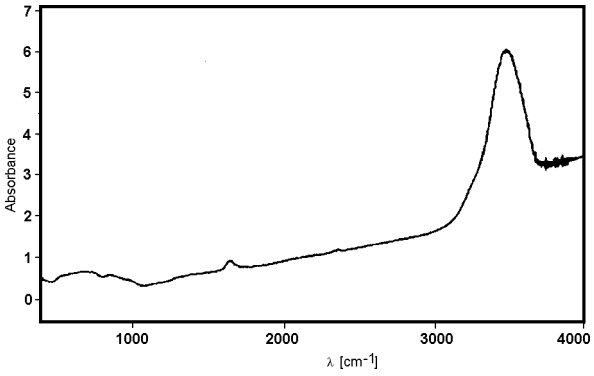

Fig.3. IR of SiO-Cus$(EA)_4$ material.

Preliminary biological tests were carried out for BSM pigments. When added to suspension of algae in water it caused discolouring of algae within a few

days. BSM added to points preserved pointed surfaces from fungi Trichoderma viride. BSMs based on water glass were prepared and are investigated [4].

References

[1]. Łukasiewicz A., Waliś L., Rowińska L.: Patent application P.3336188.
[2]. Łukasiewicz A., Waliś L., Rowińska L.: In: INCT Annul Report 1999. Institute of Nuclear Chemistry and Technology, Warszawa 2000, p.121.
[3]. Ullmans Encyclopedia of Industrial Chemistry. Vol. A6. Weinheim 1986, p.231.
[4]. Łukasiewicz A., Krajewski K., Chmielewska D., Waliś L., Rowińska L.: Patent application P.357356.

SEM OBSERVATIONS ON THE SPECIAL TYPE OF PARTICLE TRACK MEMBRANES

Bożena Sartowska, Oleg Orelovitch[1/]

[1/] Flerov Laboratory of Nuclear Reaction, Joint Institute for Nuclear Research, Dubna, Russia

The production of track membranes is well known and described in the literature [1, 2]. A new kind of membranes with specific parameters were developed and made. To understand more details of the production process we need to investigate membrane parameters and to determine their characteristic features. Using scanning electron microscopy (SEM) we can investigate membrane surfaces and fractures and characterize small objects – pores.

PET (polyethylene terephthalate) non-symmetrical track membranes made with special technology were investigated. We expected to obtain non-cylindrical channels through the membrane and very small pores on the surface. So, we need to use a non-standard preparation procedure of the samples. The surface of membrane was observed to determine main membrane parameters. The fracture of the membrane was made using the destruction of samples by UV irradiation [3] and was investigated to determine the shape of pores and to obtain more detailed data on the membrane structure. Non-conductive materials are usually being charged, heated and damaged under an electron beam. To reduce or eliminate charging, the samples were coated with a thin layer of carbon or metal [4]. The samples were fixed using a conductive glue (Quick Drying Silver Paint, Agar Scientific Ltd.). Then, they were covered with a thin (8-10 nm) layer of gold using a vacuum evaporator JEE-4X (JEOL, Japan) with high vacuum 2.5×10^{-4} Pa and a current of 50 A. A special facility inside the bell was used to diminish the influence of overheating of the membrane surface. The distance between the Au source and the sample level was 24 cm. This condition allows us to protect the sample from heat destruction and to keep real parameters of objects [5]. Observations were carried out using SEM LEO 1530 GEMINI with low accelerating voltage – 1 kV. This SEM has enough resolution to measure small morphological objects, not only register the presence of them.

Figure 1 presents surface morphology of the investigated membrane. Pore diameter measured by SEM was on the average 52.31 nm with standard deviation $\sigma = 12.42$ nm. In a majority they were in round shape. Multiple pores can be seen. Counted pore density is 3.3×10^{9} cm^{-2}.

Figure 2 shows the fracture through the membrane. Non-cylindrical pores can be clearly seen. This result is with good conformation with our expectations. Pores were in the shape like spindle with increasing diameter from the membrane surfaces to the membrane core. The diameter of inner part of pores is bigger than pores diameter on the surface and it was estimated as 90.0 nm with standard deviation $\sigma = 16.46$ nm. Pores were not parallel; their directions are not perpendicular to the surface – they were randomly oriented. Places of pores intersection can be clearly seen, too.

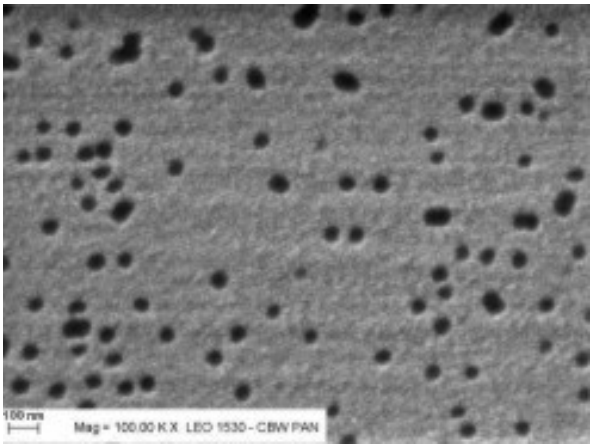

Fig.1. View of the surface of investigated particle track membrane.

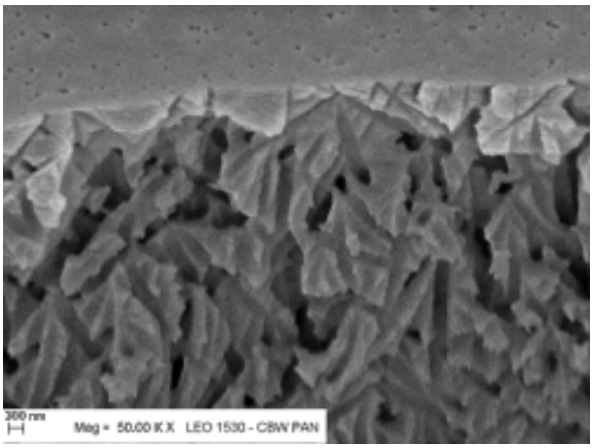

Fig.2. Fracture through the investigated particle track membrane.

Investigations of special non-symmetrical membranes using the non-standard preparing procedure and SEM observations will be continued.

Thanks to Dr. Adam Presz (Unipress, Warszawa) for his help in SEM observation.

References

[1]. Kuznietsov V.I., Didyk A.Yu., Apel P.Yu.: Rad. Meas., 19, 1-4, 919-924 (1991).
[2]. Spohr R.: Ion Tracks and Microtechnology. Principles and Applications. Vieweg, Braunschweig 1990, 272 p.
[3]. Orelovitch O.L., Apel P.Yu.: Instrum. Exp. Tech., 44, 1, 111-114 (2001).
[4]. Goldstein I.J.: Electron Microscopy and X-Ray Microanalysis. Text for Biologist, Material Scientists and Geologists. Plenum Press, New York 1992, 820 p.
[5]. Orelovitch O., Sartowska B.: Methods of Scanning Electron Microscopy in Particle Track Membrane Investigations. Proceedings of the X Conference on Electron Microscopy of Solids, Warszawa-Serock, Poland, 20-23 September 1999, pp.397-400.

INVESTIGATIONS OF PHASE CHANGES IN STEELS IRRADIATED WITH INTENSE PULSED PLASMA BEAMS

Bożena Sartowska[1/], Jerzy Piekoszewski[1,2/], Lech Waliś[1/], Michał Kopcewicz[3/], Zbigniew Werner[2/], Jacek Stanisławski[2/], Justyna Kalinowska[3/], Fridrich Prokert[4/]

[1/] Institute of Nuclear Chemistry and Technology, Warszawa, Poland
[2/] Andrzej Sołtan Institute for Nuclear Studies, Świerk, Poland
[3/] Institute of Electronic Materials Technology, Warszawa, Poland
[4/] Institut für Ionenstrahlphysik und Materialforschung, Forschungszentrum Rossendorf e.V., Dresden, Germany

It is known that transformation of martensite into austenite α' → γ can take place in the surface layer of steels treated with sufficiently intense pulses of laser, ion or plasma beams. The energy density of the pulse has to be high enough for a given pulse duration as to melt the near surface region of the substrate. It was earlier observed that in high-carbon tool steel the austenite forms after irradiations with hydrogen and nitrogen plasma pulses [1-3]. In this case high carbon concentration, melting and rapid cooling (10^7-10^8 K/s) is enough for austenitisation. In low-carbon steel austenite occurs only for nitrogen plasma. Nitrogen supplied with the plasma pulses can play the carbon role in increasing of the austenitisation processes. Two austenite phases were detected: γ-Fe with no interstitial nearest neighbours, and γ_N-Fe with nitrogen nearest neighbourhood atoms. Formation of γ-Fe and γ_N-Fe was also observed after irradiation of steel samples with intense pulses of light ion beam [4, 5].

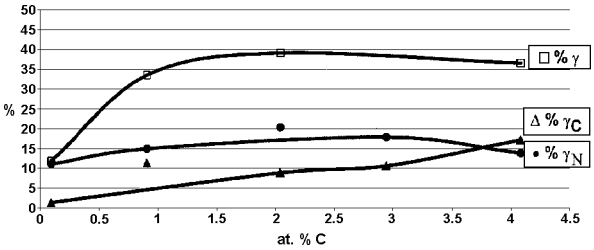

Fig.1. Share of paramagnetic phase in carbon steels after intense pulsed plasma beam modification.

Our investigations focus on the phase transformations in the near-surface layer of various types of steel irradiated with short (μs range) intense (5-6 J/cm^2) nitrogen and argon plasma pulses.

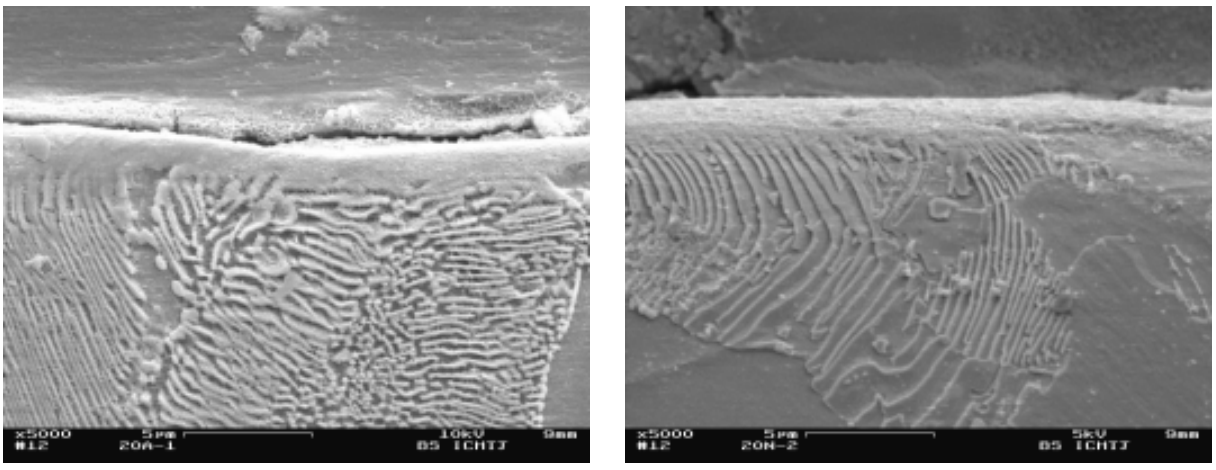

a) b)

Fig.2. Cross-section SEM images of steel 20, magnification x5000: a) modified with argon intense pulsed plasma beam, b) modified with nitrogen intense pulsed plasma beam.

Five carbon steels samples with different concentration of carbon were prepared: Armco-iron – 0.02-0.04%C, 20 – 0.17-0.24%C, 45 – 0.42-0.50%C, 65 – 0.62-0.70%C and N9 – 0.85-0.94%C. Samples were heat treated according to standard procedures predicted for these steels (PN-93/H-84019, PN-84/H-85020) and polished to $R_a < 0.35$ μm.

The plasma pulses were generated in a rod plasma injector of the RPI type described in [6] in the mode pulse implantation doping (PID). An energy density is in the 1-10 J/cm^2 range and pulse duration in the μs scale are sufficient to raise the temperature of the near-surface layer of most solids up to their melting point. When this region is melted, a rapid inward diffusion of the pulse-delivered and/or pre-deposited atoms into the liquid can occur, leading to formation of new phases, alloys or compounds. We used two kinds of plasma impulses to compare effects of thermal processes and supplying of reactive gas. The samples were irradiated with five plasma (argon or nitrogen) pulses at an energy density of about 5 J/cm^2. The cooling rate was in the range of 10^7-10^8 K/s. According to the computer simulation of heat evolution in the sample we expected that the melted layer could be about 1.5 μm thickness.

Samples were characterized by the following methods:

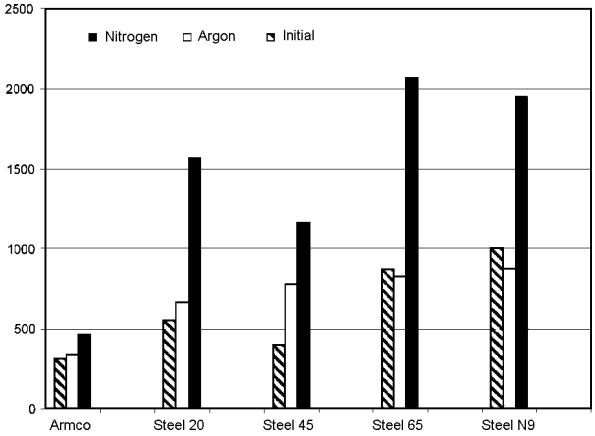

Fig.3. μHV 0.01 changes of investigated steels as a result of intense pulsed plasma modification.

- Nuclear reaction analysis (NRA) $^{14}N(d,\alpha)^{12}C$ for determination of retained nitrogen dose;
- Scanning Electron Microscopy (SEM) with DSM 942 instrument;
- XRD with grazing incidence (GXRD);
- Conversion Electron Mössbauer Spectroscopy (CEMS);
- Microhardness HV 0.01 measurements using Hanemann Mod. 932 tester;
- The wear tests using the T10 ball-on-disc Testing Machine with 3 mm diameter WC ball, 5N

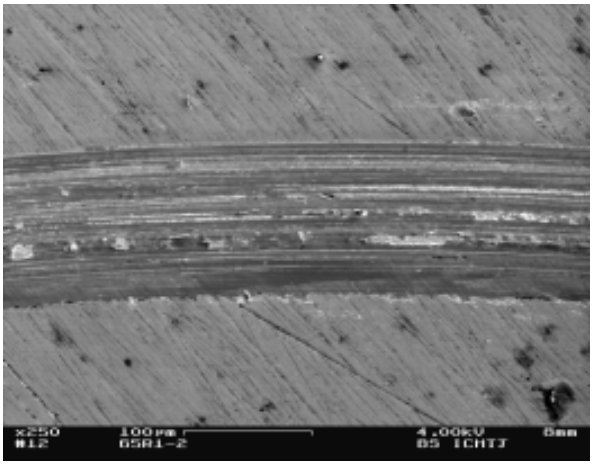

a)

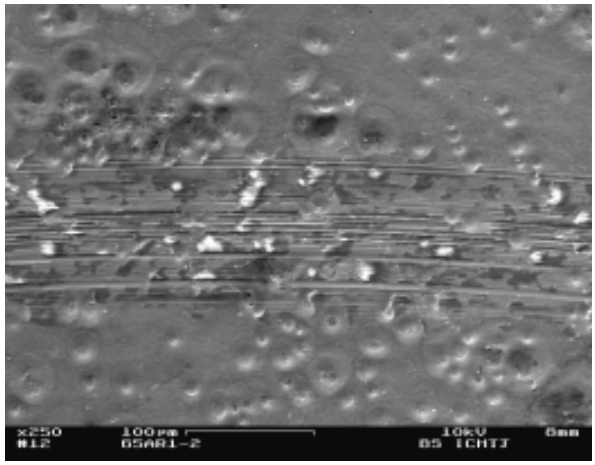

b)

c)

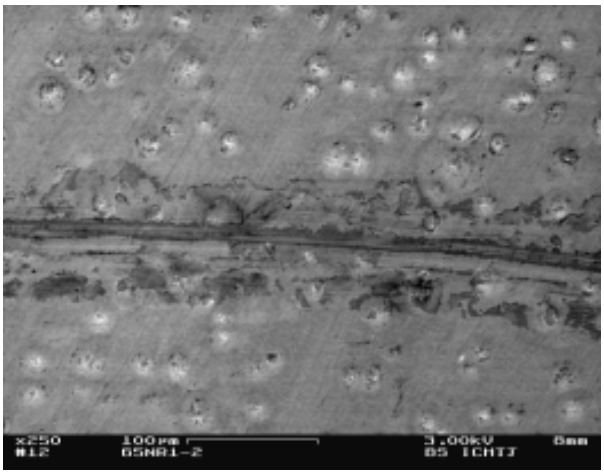

Fig.4. SEM images of the wear tracks after pin-on-disc wear tests for steel 65: a) initial, magnification x250, b) modified with argon intense pulsed plasma beam, magnification x250, c) modified with nitrogen intense pulsed plasma beam, magnification x250.

load, 200 rpm, 7 and 8 mm tracks diameter, 1000 and 2000 rotations, respectively.

Below we summarise the most important results obtained thus far.

1. Surface concentration of nitrogen supplied by the plasma pulses is 1.2×10^{17} N/cm^2 with the standard deviation 2×10^{16} N/cm^2.
2. In all steels irradiated with nitrogen plasma the γ, γ_N, γ_C and $\varepsilon = Fe_3N$ phases were found. In steels irradiated with argon, only γ and γ_C phases were found. Figure 1 shows the presence of paramagnetic phase in the modified layer of samples. It can be seen that there are more γ and γ_C phases in the material after nitrogen irradiation. This result/observation still needs explanation.
3. Figure 2 shows the cross-section of steel 20 after modification. Thickness of the changed layer is in the range of 1.2-1.6 μm. This fact is in good conformity with results form computer simulation.
4. Figure 3 presents the diagram of microhardness measurements. The increase of μHV 0.01 for all steels irradiated with nitrogen plasma can be seen. It is very interesting that the significant increase was observed for the very hard material. We suggest that the increase of μHV 0.01 is the effect of presence of γ_N and ε-Fe_3N phases in the modified layer. But for now we cannot explain which one has greater meaning. We can expect possibilities of practical use this kind of surface modification.
5. Decrease of wear tracks widths for all modified samples comparing with the virgin samples were observed (Fig.4). These results show improving the wear resistant of investigated samples.

In conclusion: the thin modified continuous layers were created in the near-surface region of carbon steels treated with intense pulsed argon or nitrogen plasma beams. The paramagnetic phases were detected in the modified surface layers. The γ_N phase was created using nitrogen intense pulsed plasma beam. Increased microhardness and wear resistance was observed for most of the studied samples. Greater increase of tribological properties occurs for nitrogen treatment, which can be explained by the presence of nitrogen phases.

Our investigations will be continued; especially we plan to determine the nitrogen and carbon distribution in modified layers.

References

[1]. Zhu J., Liu J., Chou C., Chen N.: In: Surface engineering practice processes, fundamentals and applications in corrosion and wear. Eds. K.N. Straford, P.K. Datta, J.S. Gray, E. Horwood. New York 1990, pp.168-176.

[2]. Piekoszewski J., Langner J., Nowicki L., Turos A., Waliś L., Ciurapiński A.: Mater. Lett., 14, 131-134 (1992).

[3]. Piekoszewski J., Langner J., Białoskórski J., Kozłowska B., Pochrybniak C., Werner Z., Kopcewicz M., Waliś L., Ciurapiński A.: Nucl. Instrum. Meth. Phys. Res. B., 80/81, 344-347 (1993).

[4]. Rej D.J., Davis H.A., Nastasi M., Olson J.C., Peterson E.J., Reiswig R.D., Walter K.C., Stinnett R.W., Remnev G.E., Struts V.K.: Nucl. Instrum. Meth. Phys. Res. B., 127, 987-991 (1997).

[5]. Heyden D., Müller D., Wolf G.K., Amaral L., Behar M.: Nucl. Instrum. Meth. Phys. Res. B., 175-177, 403-409 (2001).

[6]. Werner Z., Piekoszewski J., Szymczyk W.: Vacuum, 63, 701-708 (2001).

CORROSION PROPERTIES OF TITANIUM SURFACE ALLOYED WITH PALLADIUM BY IMPLANTATION AND/OR PLASMA PULSES, IN 0.1 M H_2SO_4 AT 80°C

Fernando A. Bonilla[1/], Peter Skeldon[1/], George E. Thompson[1/], Jerzy Piekoszewski[2,3/], Andrzej G. Chmielewski[3/], Jacek Stanisławski[2/], Zbigniew Werner[2/]

[1/] Corrosion and Protection Centre, University of Manchester Institute of Science and Technology, United Kingdom

[2/] Andrzej Sołtan Institute for Nuclear Studies, Świerk, Poland

[3/] Institute of Nuclear Chemistry and Technology, Warszawa, Poland

The reduction in the emission of pollutants (i.e., NO_x, SO_2, CO_2, CO and volatile organic compounds – VOC's) from the metallurgical industry and thermal power stations has been achieved successfully by the electron beam treatment of flue gases. An essential component of this technology is a window through which the electrons enter the reaction chamber. A 99.6% purity Ti foil 50 μm in thickness is currently used for the window due to its high strength to weight ratio and its generally good corrosion resistance. The current service life of windows is typically 2000 h, whereas, the programmed shut-downs of the plants are up to 10 000 h.

The degradation of Ti caused by the environment within the irradiation chamber has been simulated in a 0.1 M H_2SO_4 solution at 80°C. In order to improve the corrosion resistance of the window, Ti foil has been surface-alloyed with Pd by various processes: (i) high intensity pulsed plasma beams (HIPPB) under the deposition by pulsed erosion (DPE) mode of operation of a rod plasma injector (RPI); (ii) Pd pre-deposition onto Ti by e-gun evaporation and processing by HIPPB under the pulsed implantation doping (PID) mode; (iii) implantation of Pd into the Ti foil using a metal vapour vacuum arc (MEVVA) source followed by HIPPB under the PID mode. Nitrogen was used as the working gas for the HIPPB processes. Surface alloys with smooth depth composition profiles, with thicknesses of 30-900 nm and with average

concentrations 0.7-17 at.% were produced as assessed by Rutherford backscattered spectrometry (RBS).

The behaviours of the Ti foil and the surface alloys in the simulated environment were evaluated by measurement of the open circuit potential (OCP) during immersion tests; the average weight loss rate was calculated. The weight loss rate of Ti after 15 h immersion was ~45 $g \cdot m^{-2} \cdot d^{-1}$ and the steady OCP was -780 mV *vs*. SCE. The results of 100 h immersion tests for the surface alloys indicate a reduction of at least 2 orders of magnitude in the weight loss rate compared with that of the Ti foil. The alloys with lower Pd concentration exhibited enrichment of the alloying element in the outer 20 nm of the alloy, during immersion in the acid, as assessed by medium energy ion scattering (MEIS). For the alloys with higher Pd concentration, a crystalline Pd-rich film (as assessed by electron diffraction and energy dispersive X-ray – EDX analysis) was detached upon removal from the solution, as observed by the unaided eye and later by transmission electron microscopy. RBS and EDX indicate that the proportion of the initial deposited Pd, lost during immersion tests (13-99%) generally increased with increasing Pd concentration in the outer layers, for alloys prepared under similar conditions. Further, increasing amounts of deposited Pd did not necessarily resulted in a lower net average weight loss rate (total weight loss rate minus contribution of Pd). The net average weight loss rate for the surface alloys is about 0.14 $g \cdot m^{-2} \cdot d^{-1}$, which is equivalent to 0.4 $pm \cdot s^{-1}$ or 1.3 $\mu A \cdot cm^{-2}$ (assuming formation Ti^{4+} ions).

ABLATION OF SUBSTRATE MATERIAL INDUCED BY PULSED PLASMA BEAMS IN MW/cm² RANGE AS OBSERVED BY OPTICAL SPECTROSCOPY

Jacek Stanisławski[1/], Jarosław Baranowski[1/], Jerzy Piekoszewski[1,2/], Elżbieta Składnik-Sadowska[1/], Zbigniew Werner[1/]

[1/] Andrzej Sołtan Institute for Nuclear Studies, Świerk, Poland

[2/] Institute of Nuclear Chemistry and Technology, Warszawa, Poland

The Rod Plasma Injector (RPI) type of pulsed plasma generator, i.e. a generator with "transparent" electrodes was originally designed for the purposes of the research on controlled release of thermonuclear energy. However, in the early eighties it appeared clear that this kind of device can be successfully used for modification of the near-surface layer of engineering materials. Processing based on the use of plasma pulses has some features in common with ion implantation since a mass transport takes place, and some features of laser processing because heat transport and hence melting of the near surface layer of the processed material occurs. An energy density in the 1-10 J/cm² range and duration in μs scale are sufficient to rise the temperature of the near-surface layer of most solids up to their melting point (or above). When this region is molten, a rapid inward diffusion of the pulse-delivered and/or pre-deposited atoms into the liquid can occur, leading to the formation of new phases, alloys or compounds. For material processing, depending on the working gas conditions RPI generator can be used in two modes of operation.

In one, referred to as pulse implantation doping (PID), the pulse contains almost exclusively elements of the working gas. In the other mode, referred to as deposition by pulsed erosion (DPE) apart from the working gas plasma, there are also elements of deliberately chosen electrode material (e.g. Mg, Al, Ti, Fe, Ni, Cu etc.). They are deposited on a substrate making well adhering coatings. However, thus far the mechanism of partial erosion of some substrates is not known; whether it results from evaporation, sputtering or ablation.

The aim of the present work was to clarify this issue. DPE experiments were performed with alumina substrate, Ti electrodes and N_2 working gas. Pulse energy density was about 5 J/cm². The diagnostics has been performed by spectral measurements in the 200-800 nm wavelength range. The optical collimator was aimed to collect only those photons, which are emitted from the substrate. The time evolution of a chosen spectral line has been analyzed. The spectra contain clear Al I, Al II, Al III lines and after couple of pulses also Ti I and Ti II lines. In addition, also week lines of nitrogen could be observed. By analysis of Al III line it was possible to determine the temperature of the electrons exciting radiation as equal to about 2-3 eV. For Al an emission of line has a pulse character with FWHF equal to about 1 μs. Such surprisingly high temperature means that ablation of a part of surface region of the substrate and formation of metallic plasma take place. In the literature [1, 2] similar temperature distribution of Al ions was observed for laser ablation of Al targets when the power densities were at the level of 50-100 MW/cm². The main conclusions can be summarized as follows: (i) The pulse duration of gaseous plasma in DPE operation mode equals to about 1 μs. (ii) Gaseous plasma pulse of energy density of 5 J/cm² causes the surface ablation of Al_2O_3 (containing alloyed Ti) and forms a Al-Ti plasma plum having a temperature of 2-3 eV.

References

[1]. Lash J.S., Gilgenbach R.M., Ching C.H.: Appl. Phys. Lett., 65, 531-533 (1994).

[2]. Knudtson J.T., Green W.B., Sutton D.G.: J. Appl. Phys., 61, 4771-4780 (1987).

PHYSICAL STATE OF THE ELECTRODE MATERIAL ERODED DURING THE PLASMA DISCHARGE IN ROD PLASMA INJECTOR GENERATORS AS DETERMINED BY SPECTRAL DIAGNOSTICS

Jacek Stanisławski[1/], **Jarosław Baranowski**[1/], **Jerzy Piekoszewski**[1,2/], **Elżbieta Składnik-Sadowska**[1/]

[1/] Andrzej Sołtan Institute for Nuclear Studies, Świerk, Poland

[2/] Institute of Nuclear Chemistry and Technology, Warszawa Poland

As a result of low-pressure, high-current discharges between two concentric sets of electrodes in the Rod Plasma Injector (RPI) devices [1], high intensity pulsed plasma beams are generated. The discharge is ignited by a high voltage pulse appropriately delayed in respect to the moment of injection of a working gas into the inter-electrode space. For sufficiently short delay time there is a steep gradient of gas concentration in the inter-electrode space, and effective erosion of the metallic electrodes occurs. In this case a pulse of vapor and low energy ions of the electrode material is produced apart from the pulse of the working gas plasma.

Spectral measurements were performed with the J-046 device operated at 16.8 kJ/29 kV level, with titanium electrodes and nitrogen as the working gas. Photons emitted by plasma beams within the 200-800 nm wavelength range were analyzed by means of an optical spectrometer. Measurements were done perpendicularly to the symmetry axis of the RPI device at two distances: 9.5 and 27.5 cm from the electrode ends. The collected data were used in the time-of-flight calculations.

The spectra contained lines characteristic for singly and doubly ionized nitrogen atoms and singly ionized titanium atoms. Particular attention was paid to time evolution of the titanium Ti II lines (375.93, 376.13, 430.00, 439.5 and 444.38 nm). Energies of titanium ions were estimated at the level of 200-500 eV by the time-of-flight method. Comparing the observed discharge voltage waveform and the measured time-of-flight data for titanium lines, it was possible to conclude that metallic ions are not generated before the over-voltage between the generator electrodes.

The present results are in agreement with our previous observation [2] that metallic ions from electrodes are not accelerated to energies of several keV during the discharge as it is the case for the working gas ions. Energies in the range of few hundred eV correspond well to energies observed for vacuum plasma arcs [3]. Therefore, we confirm our previous conclusion that electrode erosion in the RPI plasma generators occurs *via* vacuum arc mechanism.

References

[1]. Piekoszewski J., Langner J.: Nucl. Instrum. Meth. Phys. Res. B, 53, 148-160 (1991).

[2]. Piekoszewski J., Stanisławski J., Jagielski J., Szymczyk W., Grötzschel R., Matz W.: Nukleonika, 47, 3, 113-117 (2000).

[3]. Witke T., Ziegele H.: Surf. Coat. Technol., 97, 414-419 (1997).

NUCLEONIC CONTROL SYSTEMS AND ACCELERATORS

AUTOMATIC GAIN CONTROL CIRCUIT FOR A SCINTILLATION DETECTOR

Bronisław Machaj, Jan Mirowicz, Jakub Bartak, Edward Świstowski

A modified version of an automatic gain control circuit (AGC) used in [1] was developed. Block diagram of the AGC of scintillation probe for measurement of ^{131}I is shown in Fig. Green LED (light emitting diode) light pulse is used as reference signal whose amplitude is kept constant by the AGC. A three-terminal adjustable current source LM334 (National Semiconductor) was employed to supply L-2060GD green LED (Kingbright). Constant current from LM334 is short-circuited periodically by MOSFET BS108 that is connected parallel to the LED and is triggered from a microprocessor (not shown in Fig.). In such a manner the reference light pulse is produced. The pulse (LEDP) of LED light pulse from A1 amplifier is fed to pulse discriminator (E) and to monovibrator (MV). The width of the MV pulse ensures that at half of the LEDP frequency the MV output takes logic 1 at which the photo-multiplier tube (PMT) gain is correct. The MV output is detected by the microprocessor. The PMT HV (high voltage) is increased or decreased by the microprocessor through D/A (digit to analog) converter as to get proper LEDP amplitude in 0.5 V steps (approx. 0.5% gain variation). The pulses from the single channel analyzer (SCA) counted by a programmable counter under measuring cycles under control of the microprocessor.

To ensure stability of the reference pulse, before use the LEDs were kept at an elevated temperature of 75°C within 100 h. To ensure good stability of the light output against temperature variation, a thermal coefficient of LED was compensated by adjusting the temperature coefficient of LM334. A similar solution of automatic gain control of PMT was adopted for gain stabilization of scintillation probe of gamma counter for radioimmunoassay (RIA) and immunoradiometric assay (IRMA) employing the ^{125}I isotope.

When measuring ^{125}I radiation, no frequent gain correction is necessary as the count rate from the SCA very little depends on the gain variation. Laboratory measurements of 4 measuring channels showed that in a 5 h period the count rate variation in the worst case was less than 1%. In the measurements of ^{131}I radiation the valley between the photo-peak and the rest of the spectrum is less distinct than in the ^{125}I radiation spectrum and gain correction is carried out every 10 s. Laboratory investigations show that the PMT thermal coefficient of gain variation is 1%/10°C and count rate stability from ^{131}I radiation is not worse than 1%/10°C.

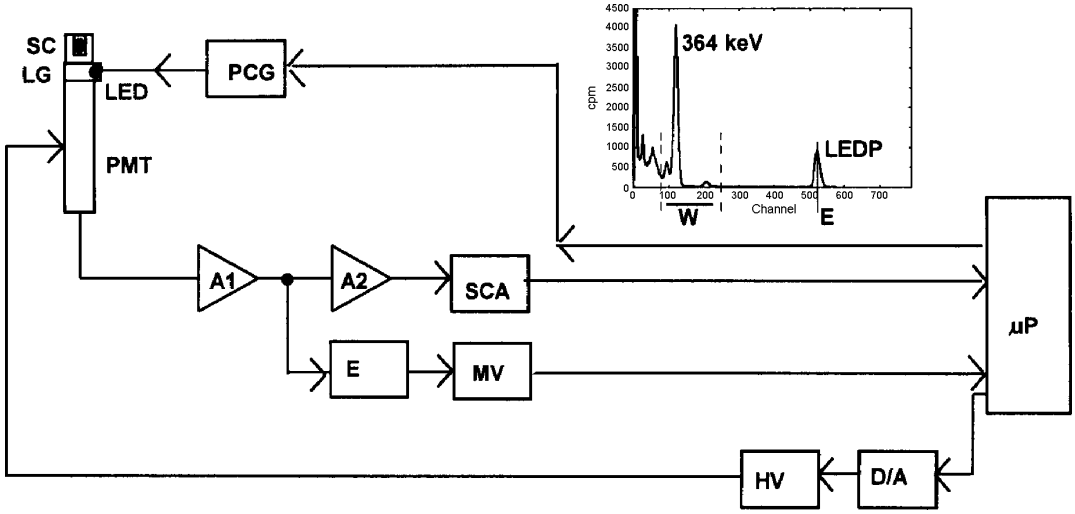

Fig. Block diagram of a gauge for measurement of ^{131}I activity with an AGC: SC – NaI(Tl) scintillator; LG – light guide; LED – green LED; PCG – pulse current generator; A1, A2 – pulse amplifier; SCA – single channel analyzer; W – SCA window width; E – LEDP discriminator; MV – monovibrator; D/A – digit to analog converter; PTM – photo-multiplier tube; HV – PMT high voltage; μP – microprocesor.

microprocessor control are the measure of radiation intensity from the investigated isotope. Automatic gain control is carried out between the

References

[1]. Machaj B., Świstowski E., Hoang C. Doo, Bilski P., Olko P.: Nukleonika, 47, 3, 107-111 (2002).

DETECTING DISTORTIONS OF THE SMOOTHED SPECTRA USING AUTOCORRELATION FUNCTION

Piotr Urbański, Ewa Kowalska

Every procedure of smoothing leads to some distortions of the smoothed spectra. However, it is difficult to find an objective measure of the degree to which the smoothed spectrum was distorted, because the shape of "ideal" spectrum is unknown. Most of the smoothing and denoising procedures are based on the assumption of the additive noise model [1]:

$$\mathbf{w} = \mathbf{w}_p - \mathbf{v} \quad (1)$$

where: $\mathbf{w}$, $\mathbf{w}_p$ – vectors of the raw and "ideal" spectrum, respectively; $\mathbf{v}$ – vector of noise. In practice, if a smoothing procedure is applied to a spectrum, the experimentator knows, beside the raw spectrum, the smoothed spectrum only (vectors of $\mathbf{w}$ and $\mathbf{w}_s$), and can compute the vector of removed part assuming the linear model:

$$\mathbf{v}_s = \mathbf{w} - \mathbf{w}_s \quad (2)$$

The aim of this work is to find a qualitative parameter, which could be used, as a figure of merit for detecting distortion of the smoothed spectra, based on the above linear model.

It is assumed that as long as the part of the raw spectrum removed by the smoothing procedure ($\mathbf{v}_s$) will be of stochastic nature, the smoothed spectrum can be considered as undistorted. To detect the random nature of the $\mathbf{v}_s$ one can use its autocorrelation function $\mathbf{r}_{vs}$ [2]:

$$\mathbf{r}_{vs} = \frac{\mathrm{cov}\left[\mathbf{v}_s(i),\ \mathbf{v}_s(i+p)\right]}{\sigma^2(\mathbf{v}_s)} \quad (3)$$

$$rms(\mathbf{r}_{vs}) = \sqrt{\frac{1}{p}\sum_{i}^{p}\left[\mathbf{r}_{vs}(i)\right]^2} \quad (4)$$

where: $i = 1...k$, k – number of channels, p – shift (lag), $\sigma^2(\mathbf{v}_s)$ – variance of removal noise.

If the vectors $\mathbf{v}_s$ is of random nature (e.g. white noise) its autocorrelation function has a zero value at all lags except the value of unity at lag zero, to indicate that the removed noise is completely uncorrelated. A correlated noise, on the other hand, will produce non-zero values at lags other than zero to indicate a correlation between different lagged observation [3]. Thanks to this feature of the autocorrelation function drifts of the mean value in the removed noise $\mathbf{v}_s$ as well as its periodicity can be more easily detected from the autocorrelogram than from the original data [4]. As a measure of the random nature of the removed noise, the root mean square value of the correlation function $rms(\mathbf{r}_{vs})$ was used:

The above considerations were checked on simulated spectra consisting of k channels and corrupted with Poisson distributed noise and then smoothed with the Savitsky-Golay procedure using the second order polynomial and variable filter width dw [5]. As a measure of the smoothing quality, the ratio of the mean square error (MSE) of the total counts for the smoothed and raw spectra $s(N_s)/s(N)$ was applied [6]. The $s^*(N_s)/s(N)$ ratio was computed using the bootstrap method for a single spectrum. The both ratios and $rms(\mathbf{r}_{vs})$ *vs.* filter width dw were plotted and are shown in Fig. It is seen that with increasing filter width dw, the

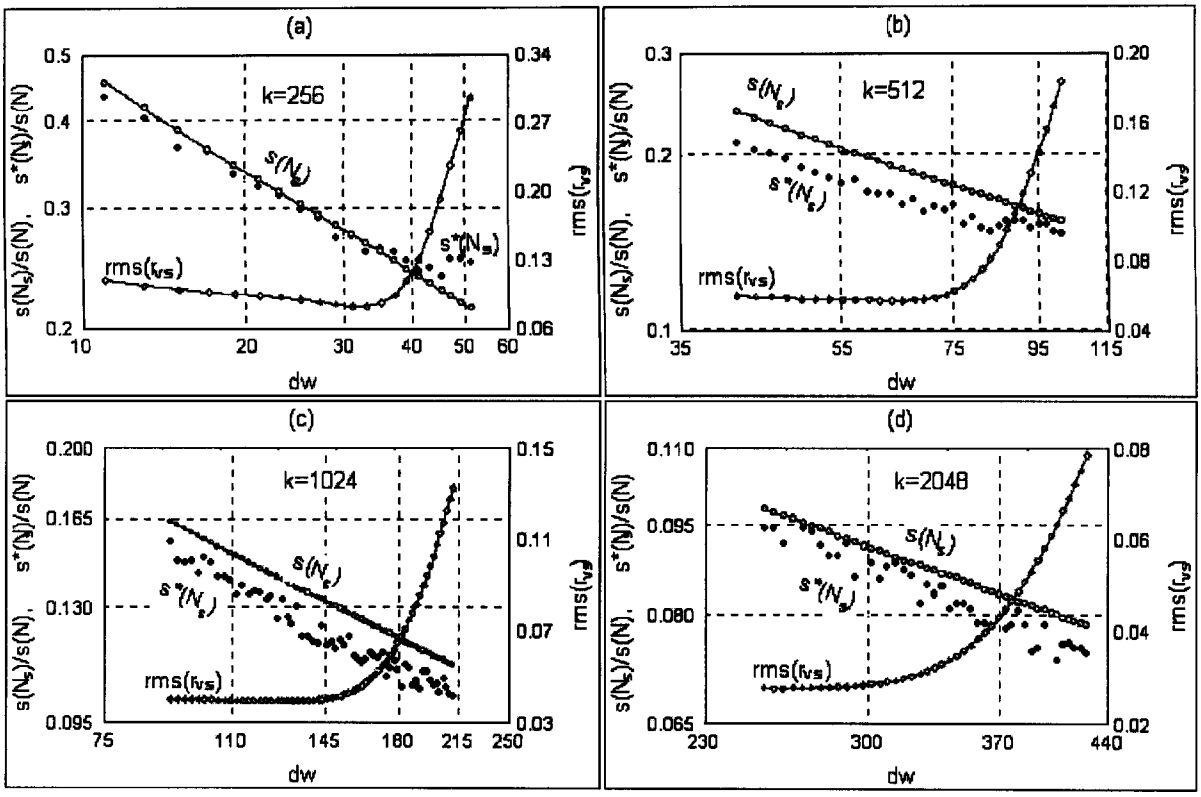

Fig. MSE of total counts and *rms* of the autocorrelation function of the removed noise *vs.* filter width for simulated spectra smoothed with the Savitsky-Golay procedure.

quality of the smoothing also increases (MSE ratio is lower), however, beginning from a certain channel, the $rms(\mathbf{r}_{vs})$ also increases sharply indicating that in the removed noise some non-random component appears. If the goal of the optimization is to minimise distortion and maximise smoothing quality, the filter width should be chosen for the $rms(\mathbf{r}_{vs})$ lying on the flat part of the plot and in "safe" distance left from the observed knee of the plot.

The presented results have shown that the *rms* value of the autocorrelation function of the noise removed from the spectra during the smoothing procedure can be used for detection of its distortion. Although this possibility has been shown on an example of the Golay-Savitsky smoothing procedure, it can be used for other denoising methods as well.

References

[1]. Larivee R.J., Brown S.D.: Anal. Chem., 64, 2057-2066 (1992).
[2]. Vandeginste B.G.M. *et al.*: Handbook of Chemometrics and Qualimetrics. Part B. Elsevier, Amsterdam 1998.
[3]. Nounou M.N., Bakshi B.R.: Multiscale Methods for Denoising and Compression. In: Wavelets in Chemistry. Ed. B. Walczak. Elsevier, Amsterdam 2000.
[4]. Massart D.L. *et al.*: Handbook of Chemmometrics. Part A. Elsevier, Amsterdam 1998.
[5]. PLS Toolbox 2.0 for use with MATLAB. Eigenvector 1998.
[6]. Urbański P., Kowalska E.: Odszumianie widm promieniowania jonizującego. In: Technika jądrowa w przemyśle, medycynie, rolnictwie i ochronie środowiska. T.2. Instytut Chemii i Techniki Jądrowej, Warszawa 2002, pp.491-497. Raporty IChTJ. Seria A nr 2/2002.

APPLICATION OF A FIELD AND INDUSTRIAL RADIOMETER TYPE FIR-1 FOR RADIOTRACER AND RADIOMETRIC MEASUREMENTS

Jacek Palige, Andrzej Owczarczyk, Andrzej Dobrowolski, Sylwia Ptaszek, Jan Pieńkos, Edward Świstowski

The Field and Industrial Radiometer FIR-1 developed in the Institute of Nuclear Chemistry and Technology (INCT) is an up to date instrument designed for radiometric measurements [1, 2] and for registration of ionizing radiation from radiometric tracers introduced into the investigated object.

In the Department of Nuclear Methods of Process Engineering (INCT) practical tests of radiotracer experiments with the use of an FIR instrument with scintillation probes were carried out. Comparison was made of measured results describing the flow dynamics in a model tank obtained with classic radiotracer techniques and with computations of Computational Fluid Dynamics (CFD). The model tank was an equivalent of a secondary settling tank for a biological deposit of flow refinery of petrochemical sewage. Optimization of the comparison was done by selecting computation parameters as to get fine matching between the experimental curve of stay time distribution (STD) with the computed curve of the CFD method. The experiments were carried out in a flow channel with main dimensions 4.95x1.3x0.5 m.

Water supply of the channel was made through an inlet overflow and could be controlled in the range 0-5 m^3/h. Water supply was forced with a submerse pump. Outflow of water took place along the whole cross-section of the channel through an overflow. Above the inlet overflow a cradle was installed dosing the radiotracers ensuring dose homogeneity along the whole inlet overflow. Inside the channel three submersible scintillation probes were placed. The fourth detector probe registered radiation at the outlet. The probes were connected to the FIR-1 instrument collecting data concerning stay time distribution of radioactive marker in three cross-sections and at the model outlet. Registered data from each detector output (proportional to the STD) were transmitted to a computer where they are stored and statistically processed.

Two radiotracers used were Tc-99 and Br-82. Additionally, a fluorescent coloring substance (fluoresceine) was used as a verification marker of the radiotracers. It is known from earlier laboratory investigations that fluoresceine is not absorbed on the construction materials and by sand covering the channel bottom.

Proper radiotracers were selected by comparison of the STD curves at the outlet of the model for jointly dosed pairs Tc-99+fluoresceine and Br-82+fluoresceine (Figs.1 and 2).

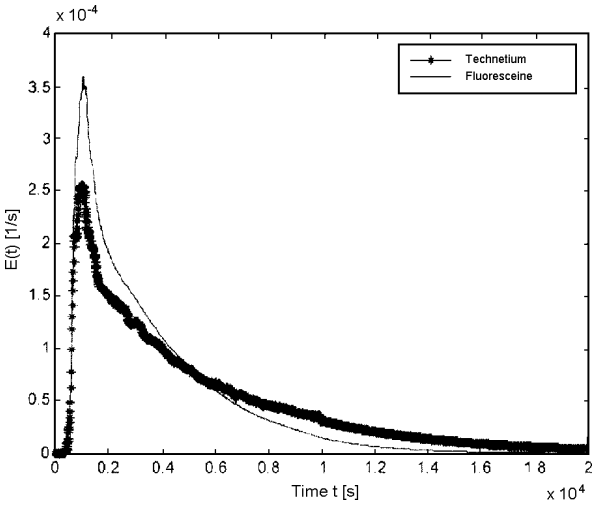

Fig.1. Output signal at the outlet of the model. Radiotracer Tc-99, Q=2.86 m^3/h.

On inspecting the diagrams, it was found that the Tc-99 generator, very convenient in use, has to be abandoned due to considerable sorption re-

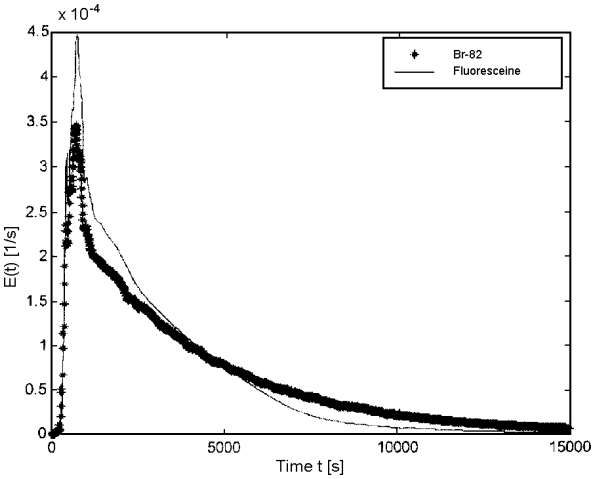

Fig.2. Output signal at the outlet of the model. Radiotracer Br-82, Q=2.91 m^3/h.

sulting in false measuring results. Such effect was not found in the case of Br-22 and this radiotracer was used in further investigations. A series of experiments was carried out at different flow rate:

- flow Q=2.86 m^3/h, without partition;
- flow Q=2.91 m^3/h, without partition;
- flow Q=2.96 m^3/h., with partition.

The flow was controlled by variation of the pump choke. The flow geometry was varied inserting an additional partition at the end of the flow channel. To each achieved (measured) STD curve the CFD computer simulation curve was fitted by selection (optimization) of computing parameters.

The Field and Industrial Radiometer FIR-1 equipped with a set of scintillation probes (original development of the Department of Radioisotope Instruments and Methods) for which the investigations were carried out is a practical test operating without any restrictions and proved to be a fully useful tool in radiotracer investigations of large objects. It is the more so important as in the year 2003 investigations of a large sewage tank in the ORLEN S.A. petrol company is foreseen, where 8 scintillation probes will be employed at the same time.

Proposed method of optimization of CFD curve based on radiotracer experimental curves seems to be the necessary step in application of the above method in investigation of large industrial objects.

References

[1]. Iller E., Thys J.: Metody radioznacznikowe w praktyce przemysłowej. WNT, Warszawa 1994.
[2]. Iller E.: Badania znacznikowe w inżynierii procesowej. WNT, Warszawa 1992.

APPLICATION OF THE MORPHOLOGICAL IMAGE ANALYSIS FOR IDENTIFICATION OF THE STEEL SURFACES IRRADIATION WITH PLASMA PULSES

Adrian Jakowiuk

The aim of this work was to find a quantitative measure which could characterize and/or identify an image of the steel surface modified with argon and nitrogen plasma pulses. The investigations were carried on the images of the steel 45 obtained from an electron microscope of magnification x100 [1]. Surface images of the steel modified with the argon and nitrogen plasma are shown in Fig.1. To solve the above problem, morphological analysis based on the Minkowski functionals is proposed [2, 3].

Morphological analysis with application of the Minkowski functionals [3] is based on investigation of the relation between particular elements of the image, i.e. their shape and position (influence on the neighboring elements). The relations can be identified using three variables: n_0 – shows mutual influence of the investigated elements on each other, n_1 – represents mutual influence of the image elements in the axes X and Y, n_2 – contains information concerning dimension of the region occupied by the investigated elements.

After calculation of the above parameters the Minkowski functionals (A, L, X) can be computed. They explicit determine the image to be investigated [1].

$$A = a^2 n_2 \quad (1)$$

$$L = -4an_2 + 2an_1 \quad (2)$$

$$X = n_2 - n_1 + n_0 \quad (3)$$

where: $a = 2r + 1$, r – radius change of a pixel.

The computed parameters are normalized with respect to the total number of the image elements.

Prior to the morphological analysis, the image has to be normalized (to become independent of the conditions of its processing) and should be converted to 1-bit image (at the beginning it was 265-bit image).

Since a limited number of picture was available for the experiment, each image was divided into 1, 4 or 9 parts. For each part the Minkowski functionals were computed separately and then averaged. Thanks to this it was possible to observe variability of the computed parameters for different parts of the image.

As it was mentioned above, the aim of the work was to find a single value for each image, whereas the computed parameters A, L and X are the functions. It was found that the combination of those variables (LX/A) at $r=1$ could be used as the required parameter.

From Fig.2 it can be screen, that at the point $r=1$ the difference between the curves obtained for both the investigated images is the most significant. The mean of the product LX/A for the steel 45a is -1.42, whereas for the steel 45n is -1.92. The difference (-0.46) is close to 25% of the product value for the steel 45n.

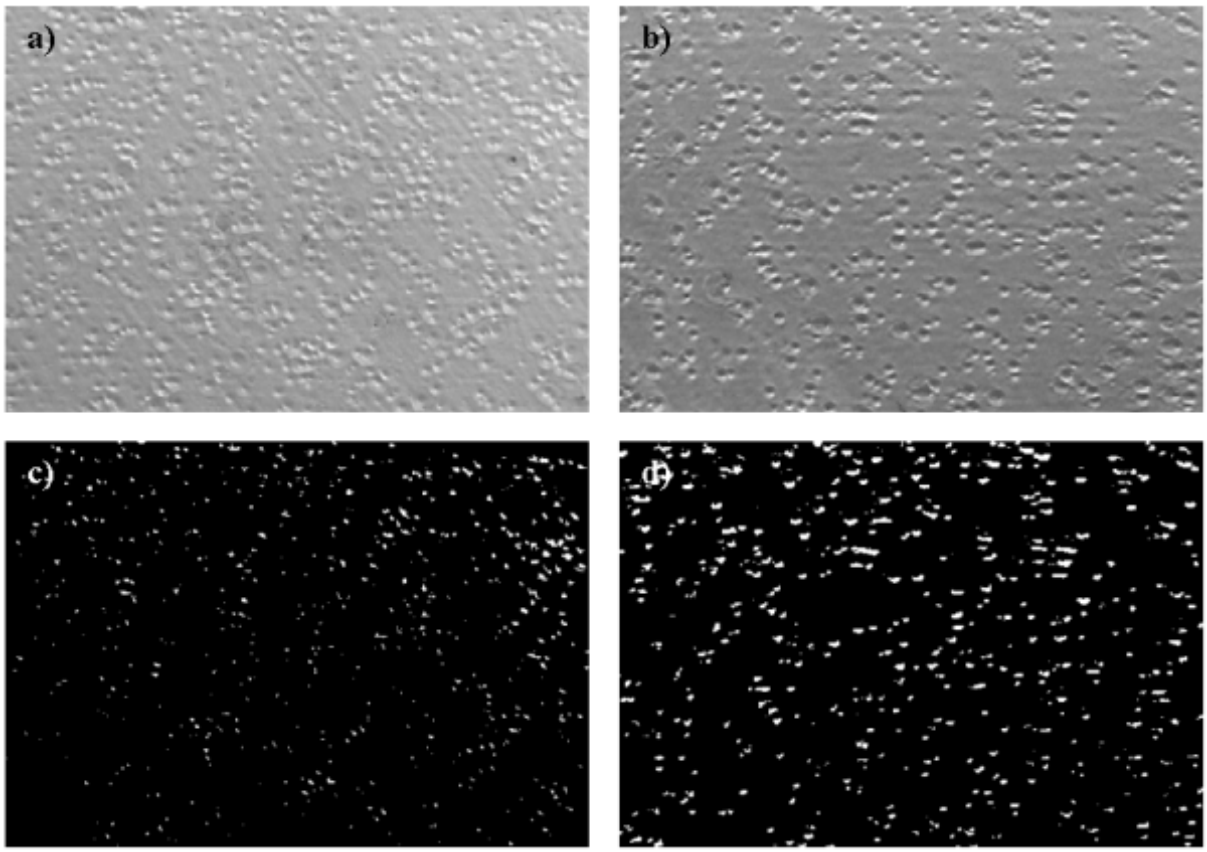

Fig.1. Images of the modified surfaces, a) steel 45a, b) steel 45n, c) 1-bit image of 45a, d) 1-bit image of 45n.

Analysis of the images of the steel surfaces irradiated with argon and nitrogen plasma pulses has shown that the proposed method can be used for identification of the modification type applied to the steel surface.

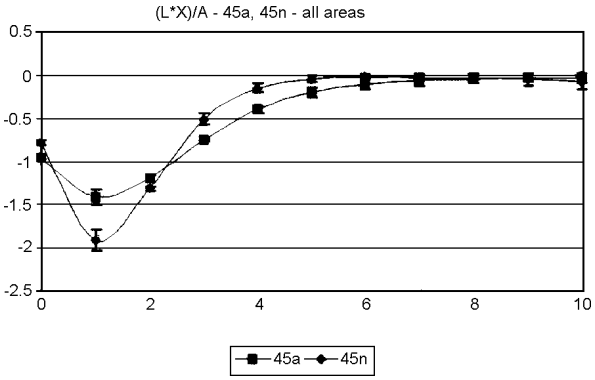

Fig.2. Plot of the mean value of the product *LX/A vs*. *r* for the both types of modifications.

To obtain satisfactory results, an effort has to be made to assure uniform illumination of the image. The magnitude of contrast and brightness of the image are not very important because prior to the morphological analysis it is normalized to 1-bit image.

References

[1]. Sartowska B., Piekoszewski J., Waliś L., Stanisławski J.: Zmiany morfologii powierzchni i niektórych własności mechanicznych wybranych gatunków stali po modyfikacji intensywnymi impulsami plazmowymi. In: Technika jądrowa w przemyśle, medycynie rolnictwie i ochronie środowiska. T.1. Instytut Chemii i Techniki Jądrowej, Warszawa 2002, pp.110-116. Raporty IChTJ. Seria A nr 1/2002.

[2]. Michielsen K., De Raedt H.: Comput. Phys. Commun., 132, 94-103 (2000).

[3]. Michielsen K., De Raedt H.: Phys. Rep., 347, 461-538 (2001).

THE INCT PUBLICATIONS IN 2002

ARTICLES

1. **Adach A., Wroński S., Buczkowski M., Starosta W., Sartowska B.**
   Mechanism of microfiltration on the rotating track membrane.
   Separation and Purification Technology, 26, 33-41 (2002).

2. **Ambroż H.B., Kemp T.J., Kornacka E., Przybytniak G.**
   The influence of dithiothreitol on DNA radiolysis in frozen aqueous solution: an EPR study.
   Radiation Physics and Chemistry, 64, 107-113 (2002).

3. **Ambroż H.B., Kornacka E.M., Marciniec B., Przybytniak G.**
   Radical decay in irradiated drugs: flutamide, ifosfamide and aminoglutethimide.
   Journal of Radioanalytical and Nuclear Chemistry, 254, 2, 293-298 (2002).

4. **Autschbach J., Siekierski S., Seth M., Schwerdtfeger P., Schwarz W.H.E.**
   Dependence of relativistic effects on electronic configuration in the neutral atoms of d- and f-block elements.
   Journal of Computational Chemistry, 23, 804-813 (2002).

5. **Bigolas A., Kuliński S., Maciszewski W., Pachan M., Pławski E., Zimek Z.**
   Current approach to design of high-power electron accelerators to match actual requirements of radiation technology in Poland.
   Radiation Physics and Chemistry, 63, 3-6, 595-599 (2002).

6. **Bilewicz A.**
   The ionic radius of No^{3+}.
   Journal of Nuclear and Radiochemical Sciences, 3, 1, 147-149 (2002).

7. **Chmielewski A.G., Derda M., Wierzchnicki R., Mikołajczuk A.**
   Sulfur isotope effects for the $SO_{2(g)}$-$SO_{2(aq)}$ system.
   Nukleonika, 47, Supplement 1, S69-S70 (2002).

8. **Chmielewski A.G., Harasimowicz M., Tymiński B., Zakrzewska-Trznadel G., Tomczak W., Cholerzyński A.**
   Oczyszczanie ciekłych odpadów promieniotwórczych za pomocą 3-stopniowej instalacji pilotowej JP3RO (Purification of liquid radioactive wastes using 3-stage pilot plant JP3RO).
   Zeszyty Naukowe Politechniki Śląskiej. Seria: Inżynieria Środowiska, 47, 169-175 (2002).

9. **Chmielewski A.G., Ostapczuk A., Zimek Z., Licki J., Kubica K.**
   Reduction of VOCs in flue gas from coal combustion by electron beam treatment.
   Radiation Physics and Chemistry, 63, 3-6, 653-655 (2002).

10. **Chmielewski A.G., Sun Y., Zimek Z., Bułka S., Licki J.**
    Mechanism of NO_x removal by electron beam process in the presence of scavengers.
    Radiation Physics and Chemistry, 65, 4-5, 397-403 (2002).

11. **Chmielewski A.G., Tymiński B., Pawelec A., Zimek Z., Licki J.**
    Przemysłowa instalacja do jednoczesnego usuwania SO_2, NO_x przy użyciu wiązki elektronów (Industrial installation for simultaneous removal of SO_2, NO_x using electron beam irradiation).
    Monografie Komitetu Inżynierii Środowiska Polskiej Akademii Nauk, 11, 33-40 (2002).

12. **Chmielewski A.G., Wierzchnicki R., Derda M., Mikołajczuk A.**
    Sulfur isotope composition of selected Polish coals.
    Nukleonika, 47, Supplement 1, S67-S68 (2002).

13. Ciesielski B., Schultka K., Kobierska A., Nowak R., Stuglik Z.
Dozymetria *in vivo* metodą spektroskopii EPR w L-alaninie (*In vivo* dosimetry by means of L-alanine EPR spectroscopy).
Nowotwory, 53, Supplement 4, 41-42 (2002).

14. Ciesielski B., Schultka K., Stuglik Z., Kobierska A., Nowak R.
Dozymetria alaninowa EPR *in vivo* – podstawy metodyczne (*In vivo* alanine/EPR dosimetry – basic methodology).
Annales Academiae Medicae Gedanensis, 32, 243-252 (2002).

15. Cieśla K., Eliasson A.-C.
Influence of gamma radiation on potato starch gelatinization studied by differential scanning calorimetry.
Radiation Physics and Chemistry, 64, 137-148 (2002).

16. Croce F., D' Epifanio A., Hassoun J., Deptuła A., Olczak T., Scrosati B.
A novel concept for the synthesis of an improved $LiFePO_4$ lithium battery cathode.
Electrochemical and Solid-State Letters, 5, 3, A47-A50 (2002).

17. Deptuła A., Olczak T., Łada W., Sartowska B., Chmielewski A.G., Alvani C., Carconi P.L., Di Bartolomeo A., Pierdominici F., Casadio S.
Fabrication of Li_2TiO_3 spherical microparticles from $TiCl_4$ by a classical, inorganic sol-gel route; characteristics and tritium release properties.
Journal of Materials Science, 27, 2549-2556 (2002).

18. Deptuła A., Olczak T., Łada W., Sartowska B., Chmielewski A.G., Alvani C., Carconi P.L., Di Bartolomeo A., Pierdominici F., Casadio S.
Inorganic sol-gel preparation od medium sized microparticles of Li_2TiO_3 from $TiCl_4$ as tritium breeding material for fusion reactors.
Journal of Sol-Gel Science and Technology, 26, 207-212 (2002).

19. Deptuła A., Olczak T., Łada W., Sartowska B., Croce F., Giorgi L., Di Bartolomeo A., Brignocchi A.
Thermal conversion of gels prepared by the complex sol-gel process (CSGP) from Li^+-Me^{2+}-CH_3COO^- ascorbic acid (ASC)-NH_4^+-OH-H_2O systems to $LiMn_2O_4$ and $LiNi_xCo_{1-x}O_2$.
Journal of Sol-Gel Science and Technology, 26, 201-206 (2002).

20. Drzewicz P., Bojanowska-Czajka A., Nałęcz-Jawecki G., Sawicki J., Trojanowicz M.
Zastosowanie promieniowania jonizującego do degradacji zanieczyszczeń organicznych w wodach i ściekach (Application of ionizing radiation for degradation of organic pollutants in waters and wastes).
Postępy Techniki Jądrowej, 45, 1, 27-32 (2002).

21. Dybczyński R.
Considerations on the accuracy of determination of some essential and/or toxic trace elements in biological materials.
Chemia Analityczna, 47, 325-334 (2002).

22. Dybczyński R.
Preparation and use of reference materials for quality assurance in inorganic trace analysis.
Food Additives and Contaminants, 19, 10, 928-938 (2002).

23. Dźwigalski Z., Zimek Z.
Pomiary ładunku nanosekundowych impulsów elektronów akceleratora LAE 10 (Charge of nanosecond pulses measurements in LAE 10 electron accelerator).
Elektronika, 43, 2, 11-13 (2002).

24. Gackowski D., Kruszewski M., Banaszkiewicz Z., Jawień A., Oliński R.
Lymphocyte labile iron pool, plasma iron, transferrin saturation and ferritin levels in colon cancer patients.
Acta Biochimica Polonica, 49, 1, 269-272 (2002).

25. Gackowski D., Kruszewski M., Bartłomiejczyk T., Jawień A., Ciecierski M., Oliński R.
The level of 8-oxo-7,8-dihydro-2'-deoxyguanosine is positively correlated with the size of the labile iron pool in human lymphocytes.
Journal of Biological Inorganic Chemistry, 7, 548-550 (2002).

26. Głuszewski W.
Przyszłość technik radiacyjnych (The future of radiation techniques).
Postępy Techniki Jądrowej, 45, 4, 14-15 (2002).

27. Gniazdowska E., Narbutt J.
Thermodynamics of liquid-liquid partition and hydration of aliphatic ethers.
Polish Journal of Chemistry, 76, 111-116 (2002).

28. Grigoriew H., Wolińska-Grabczyk A., Bernstorff S.
Solvent-influenced mesostructures in polyurethane-based membranes of different transport using SAXS synchrotron method.
Journal of Materials Science Letters, 21, 113-116 (2002).

29. Grigoriew H., Wolińska-Grabczyk A., Płusa M., Bernstorff S.
Kinetics of the structural changes in polyurethanes saturated with benzene during the desorption process.
Journal of the Materials Science Letters, 21, 1179-1182 (2002).

30. Grodkowski J., Neta P.
Formation and reaction of radicals in the ionic liquid methyltributylammonium bis(trifluoromethylsulfonyl)imide and in other solvents.
Journal of Physical Chemistry A, 106, 46, 11130-11134 (2002).

31. Grodkowski J., Neta P., Fujita E., Mahammed A., Simkhovich L., Gross Z.
Reduction of cobalt and iron corroles and catalyzed reduction of CO_2.
Journal of Physical Chemistry A, 106, 4772-4778 (2002).

32. Iller E., Kukiełka A., Stupińska H., Mikołajczyk W.
Electron beam stimulation of the reactivity of cellulose pulps for production of derivatives.
Radiation Physics and Chemistry, 63, 3-6, 253-257 (2002).

$Br_2^{\bullet-}$

33. Jaworska A., Wojewódzka M., De Angelis P.
Radiation sensitivity and the status of some radiation sensitivity markers in relatively sensitive lymphoid cells.
Radiacionnaja Biologija. Radioekologija, 42, 6, 595-599 (2002).

34. Jaworska-Gołąb T., Gondek A., Szytuła A., Zygmunt A., Penc B., Leciejewicz J., Baran S., Stüsser N.
Neutron diffraction and magnetization studies of pseudoternary $HoRh_{2-x}Pg_xSi_2$ solid solutions ($0 \quad x<2$).
Journal of Physics, Condensed Matter, 14, 5315-5323 (2002).

35. Kierzek J., Kunicki-Goldfinger J.
Determination of potassium content in the B, C and D corning reference glasses using gamma-ray spectrometry.
Glass, Science and Technology, 75, 3, 158-159 (2002).

36. Kleczkowska H.E., Malanga M., Szumiel I., Althaus F.R.
Poly ADP-ribosylation in two L5178Y murine lymphoma sublines differentially sensitive to DNA-damaging agents.
International Journal of Radiation Biology, 78, 6, 527-534 (2002).

37. Kolenda M., Hofmann M., Leciejewicz J., Penc B., Szytuła A.
Neutron-diffraction studies of $R_5Rh_4Ge_{10}$ (R=Tb, Ho, Er) compounds.
Applied Physics A, 74, Supplement, S769-S771 (2002).

38. Korzeniowska-Sobczuk A., Hug G.L., Carmichael I., Bobrowski K.
Spectral, kinetics and theoretical studies of radical cations derived from thioanisole and its carboxylic derivative.
Journal of Physical Chemistry A, 106, 40, 9251-9260 (2002).

39. Kruszewski M., Kruszewska H., Mori M., Eguchi-Kasai K., Inaba H., Zakierska I., Hayata I.
Low frequency of spontaneous rearragements during plasmid incorporation in CHO-KI mutant cells defective in DNA repair.
Nukleonika, 47, 1, 7-11 (2002).

40. Kruszewski M., Starzyński R., Bartłomiejczyk T., Drapier J.-C., Smuda E., Lipiński P.
Modulation of IRP1 by no: an unexpected correlation between RNA-binding activity of IRP1 and labile iron pool.
Free Radical Biology and Medicine, 39, Supplement 2, S378 (2002).

41. Kunicki-Goldfinger J., Kierzek J.
Ultraviolet blue fluorescence of the 18th century Central European glass: an auxiliary indicator for curators and conservators.
Glass Technology, 43C, 111-113 (2002).

42. Kunicki-Goldfinger J., Kierzek J., Małożewska-Bućko B., Kasprzak A.J.
Some observations on crizzled glass (preliminary results of a survey of 18th century central European tableware).
Glass Technology, 43C, 364-368 (2002).

43. Lewandowska H., Szumiel I.
Histone H2AX in DNA repair.
Nukleonika, 47, 4, 127-131 (2002).

44. Lewandowski W., Dasiewicz B., Koczoń P., Skierski S., Dobrosz-Teperek K., Świsłocka R., Fuks L., Priebe W., Mazurek A.P.
Vibrational study of alkaline metal nicotinates, benzoates and salicylates.
Journal of Molecular Structure, 604, 189-193 (2002).

45. Licki J., Chmielewski A.G., Zimek Z., Tymiński B., Bułka S.
Electron beam process for SO_2 removal from flue gases with high SO_2 content.
Radiation Physics and Chemistry, 63, 3-6, 637-639 (2002).

46. Lisowska H., Lankoff A., Banasik A., Wieczorek A., Kuszewski T., Góźdź S., Wójcik A.
Analiza aberracji chromosomowych na limfocytach krwi jako test predykcyjny dla pacjentów z nowotworami krtani poddawanych radioterapii (Analysis of chromosomal aberrations in lymphocytes as predictive assay for patients with larynx cancer after radiotherapy).
Nowotwory, 53, Supplement 4, 53 (2002).

47. Machaj B., Świstowski E., Do Hoang Cuong, Bilski P., Olko P.
A gauge for measuring the dose rate and activity of ophthalmic applicators.
Nukleonika, 47, 3, 107-111 (2002).

48. Machaj B., Urbański P.
Principal component data processing in radon metrology.
Nukleonika, 47, 1, 39-42 (2002).

49. Majerz I., Pawlukojć A., Sobczyk L., Grech E., Nowicka-Scheibe J.
Dimerization of 1,8-diaminonaphthalene. DFT theoretical, infra-red, Raman and inelastic neutron scattering studies.
Polish Journal of Chemistry, 76, 409-417 (2002).

50. Michalik J., Sadło J., Danilczuk M., Perlińska J., Yamada H.
Cationic silver clusters in zeolite rho and sodalite.
Studies in Surface Science and Catalysis, 142, 311-318 (2002).

51. Migdał W., Owczarczyk H.B.
Radiation decontamination of meat lyophilized products.
Radiation Physics and Chemistry, 63, 3-6, 371-373 (2002).

52. Nichipor H., Dashouk E., Yacko S., Chmielewski A.G., Zimek Z., Sun Y.
Chlorinated hydrocarbons and PAH decomposition in dry and humid air by electron beam irradiation.
Radiation Physics and Chemistry, 65, 4-5, 423-427 (2002).

53. Owczarczyk H.B., Migdał W., Stachowicz W.
Electron beam calibration for 10 MeV linear accelerator.
Radiation Physics and Chemistry, 63, 3-6, 803-805 (2002).

54. Paluchowska B., Maurin J.K., Leciejewicz J.
The crystal and molecular structures of Pb(II) complexes with furan-2-carboxylate and furan-3-carboxylate ligands.
Journal of Coordination Chemistry, 55, 7, 771-779 (2002).

55. Pańczyk E., Waliś L., Flik J., Olszewska-Świetlik J.
Badania bieli ołowiowej w wybranych obrazach Szkoły Śląskiej z 2 poł. XV wieku metodą neutronowej analizy aktywacyjnej (The examination of ceruse in selected paintings of the Silesian School from the second half of the 15th century by means of neutron activation analysis method).
Acta Universitatis Nicolai Copernici, Zabytkoznawstwo i Konserwatorstwo, XXXII, 344 (2002).

56. Pawlukojć A., Leciejewicz J., Tomkinson J., Parker S.F.
Neutron spectroscopic study of hydrogen bonding dynamics in L-serine.
Spectrochimica Acta, Part A, 58, 2897-2904 (2002).

57. Piekoszewski J., Stanisławski J., Grötzschel R., Matz W., Jagielski J., Szymczyk W.
Electrode erosion mechanism in the rod plasma injector type of generator as deduced from the structure of irradiated substrates.
Nukleonika, 47, 3, 113-117 (2002).

58. Pogocki D., Schöneich C.
Computational characterization of sulfur-oxygen-bonded sulfuranyl radicals derived from alkyl- and (carboxyalkyl)thiopropionic acids: Evidence for σ^*-type radicals.
Journal of Organic Chemistry, 67, 1526-1535 (2002).

59. Pogocki D., Schöneich C.
Redox properties of Met^{35} in neurotoxic β-amyloid peptide. A molecular modeling study.
Chemical Research Toxicology, 15, 408-418 (2002).

60. Polkowska-Motrenko H.
Certyfikowane materiały odniesienia opracowane w Instytucie Chemii i Techniki Jądrowej (Certified reference materials prepared in the Institute of Nuclear Chemistry and Technology).
Postępy Techniki Jądrowej, 45, 4, 26-36 (2002).

61. Przybytniak G.
Czy DNA jest przewodnikiem? (Is DNA the wire?)
Postępy Techniki Jądrowej, 45, 2, 19-21 (2002).

62. Romaka L., Penc B., Baran S., Leciejewicz J., Szytuła A., Stüsser N., Hernandez-Velasco J., Zygmunt A.
Magnetic structures of $RNiSn_2$ (R=Tb, Dy, Ho) compounds.
Journal of Alloys and Compounds, 343, 66-70 (2002).

63. Rudawska K., Ptasiewicz-Bąk H., Siekierski S.
The crystal structure of tetra-n-butylammonium tetraiodoindate(III).
Journal of Coordination Chemistry, 55, 4, 403-409 (2002).

64. Samczyński Z., Dybczyński R.
The use of retardion 11A8 amphoteric ion exchange resin for the separation and determination of cadmium and zinc in geological and environmental materials by neutron activation analysis.
Journal of Radioanalytical and Nuclear Chemistry, 254, 2, 335-341 (2002).

65. Sayed Aly M., Wójcik A., Schunck C., Obe G.
Correlation of chromosomal aberrations and sister chromatid exchanges in individual CHO cells pre-labelled with BrdU and treated with DNaseI or X-rays.
International Journal of Radiation Biology, 78, 11, 1037-1044 (2002).

66. Skopińska-Różewska E., Rogala E., Sommer E., Borowska A., Skopiński P., Demkow U., Załęska J., Dziedzic D., Langfort R., Sommer S., Orłowski T.
Aktywność angiogenna i poziom enzymu konwertującego angiotensynę (ACE) w surowicach chorych na niedrobnokomórkowego raka płuca (Angiogenic activity and level of angiotensin converting enzyme (ACE) in serum of patients with non-small cell lung cancer).
Nowotwory, 53, Supplement 4, 122-123 (2002).

67. Sommer E., Krotkiewski M., Filewska M., Białas B., Sommer S., Skopińska-Różewska E.
Wpływ sprzężonych izomerów kwasu linolowego na angiogenezę i wzrost guzów Sarcoma L-1 u myszy (Effects of linoleic acid on cutaneous angiogenesis and tumour growth induced in mice by L-1 Sarcoma cells).
Nowotwory, 53, Supplement 4, 123 (2002).

68. Sommer E., Krotkiewski M., Sommer S., Skopińska-Różewska E.
Different effect of linoleic acid and conjugated linoleic acid on cutaneous angiogenesis induced in mice by L-1 Sarcoma cells.
Central European Journal of Immunology, 27, Supplement I, 118 (2002).

69. Sommer E., Sommer S., Skopińska-Różewska E.
Nienasycone kwasy tłuszczowe a nowotworzenie (Unsaturated fatty acid and cancer).
Współczesna Onkologia, 6, 2, 60-63 (2002).

70. Stachowicz W., Malec-Czechowska K., Dancewicz A.M., Szot Z., Chmielewski A.G.
Accredited laboratory for detection of irradiated foods in Poland.
Radiation Physics and Chemistry, 63, 3-6, 427-429 (2002).

71. Stanisławski J., Piekoszewski J., Richter E., Werner Z.
An apparatus for sequential pulsed plasma beam treatment in combination with Arc PVD deposition.
Nukleonika, 47, 3, 119-122 (2002).

72. Starosta W., Ptasiewicz-Bąk H., Leciejewicz J.
The crystal and molecular structure of a new calcium(II) complex with pyridine-2,6-dicarboxylate, water and nitrate ligands.
Journal of Coordination Chemistry, 55, 10, 1147-1153 (2002).

73. Starosta W., Ptasiewicz-Bąk H., Leciejewicz J.
The crystal structures of two polymorphic forms of a calcium(II) complex with pyridine-2,6-dicarboxylate, water and nitrate ligands.
Journal of Coordination Chemistry, 55, 8, 873-881 (2002).

74. Starosta W., Ptasiewicz-Bąk H., Leciejewicz J.
Dimeric molecules in the crystals of calcium complex with pyridine-3,5-dicarboxylate ligand.
Journal of Coordination Chemistry, 55, 1, 1-9 (2002).

75. Starosta W., Ptasiewicz-Bąk H., Leciejewicz J.
Dimeric molecules in the crystals of a calcium(II) complex with pyridine-2,6- dicarboxylate and water ligands.
Journal of Coordination Chemistry, 55, 4, 469-478 (2002).

76. Starosta W., Ptasiewicz-Bąk H., Leciejewicz J.
Molecular chains in the crystals of a calcium(II) complex with pyridine-3,5-dicarboxylate (dinicotinate) and water ligands.
Journal of Coordination Chemistry, 55, 9, 985-990 (2002).

77. Starzyński R.R., Drapier J.C., Kruszewski M., Lipiński P.
The modulation of iron regulatory protein I (IRPI) by nitric oxide (NO) in a pair lymphoma cell lines L5178Y displaying different control of iron metabolism.
Cellular & Molecular Biology Letters, 7, Supplement, 105 (2002).

78. Stoilov L., Wójcik A., Giri A.K., Obe G.
SCE formation after exposure of CHO cells prelabelled with BrdU or biotin-dUTP to various DNA-damaging agents.
Mutagenesis, 17, 5, 399-403 (2002).

79. Szumiel I.
Punkty kontrolne w cyklu komórkowym (Checkpoints in cell cycle).
Postępy Biologii Komórki, 29, Supplement 19, 3-4 (2002).

80. Szymczyk W., Piekoszewski J., Werner Z., Szyszko W.
Thermal evolution of solid targets irradiated by pulsed plasma beams.
Nukleonika, 47, 4, 163-166 (2002).

81. Trojanowicz M., Drzewicz P., Panta P., Głuszewski W., Nałęcz-Jawecki G., Sawicki J., Sampa M.H.O., Oikawa H., Borrely S.I., Czaplicka M., Szewczyńska M.
Radiolytic degradation and toxicity changes in γ-irradiated solutions of 2,4-dichlorophenol.
Radiation Physics and Chemistry, 65, 4-5, 357-366 (2002).

82. Vanhaelewyn G.C.A.M., Sadło J., Matthys P.F.A.E., Callens F.J.
Comparative X- and Q-band EPR study of radiation-induced radicals in tooth enamel.
Radiation Research, 158, 615-625 (2002).

83. Voisin P., Barquinero F., Blakely B., Lindholm C., Lloyd D., Luccioni C., Miller S., Palitti F., Prasanna P.G.S., Stepham G., Thierens H., Turai I., Wilkinson D., Wójcik A.
Towards a standardization of biological dosimetry by cytogenetics.
Cellular and Molecular Biology, 48, 5, 501-504 (2002).

84. Warchoł S., Rzewuski H., Krynicki J., Grötzschel R.
Angular dependence of post-implantation damage recovery under 1 MeV electron irradiation in GaAs.
Nukleonika, 47, 1, 19-21 (2002).

85. Wiśniowski P., Carmichael I., Fessenden R.W., Hug G.L.
Evidence for β scission in the oxidation of amino acids.
Journal of Physical Chemistry A, 106, 4573-4580 (2002).

86. Wojewódzka M., Buraczewska I., Kruszewski M.
A modified neutral comet assay: elimination of lysis at high temperature and validation of the assay with anti-single-stranded DNA antibody.
Mutation Research, Genetic Toxicology and Environmental Mutagenesis, 518, 9-20 (2002).

87. Wojewódzka M., Grądzka I., Buraczewska I.
Modified neutral comet assay for human lymphocytes.
Nukleonika, 47, 1, 1-5 (2002).

88. Wójcik A.
Cez, chromosomy i wypadki radiacyjne (Caesium, chromosomes and radiation accidents).
Postępy Techniki Jądrowej, 45, 2, 22-25 (2002).

89. Wójcik A.
Training and studying opportunities in the Institute of Nuclear Chemistry and Technology (INCT).
Newsletter, 12, 28 (2002).

90. Wójcik A., Sommer S., Buraczewska I., Lisiak E., Siekierzyński S., Dziuk E., Bilski M., Janiak M.K.
Analiza częstości mikrojąder w limfocytach u osób z rakiem tarczycy leczonych jodem-131 (Analysis of micronuclei in peripheral lymphocytes of patients with thyroid cancer treated with iodine-131).
Nowotwory, 53, Supplement 4, 70-71 (2002).

91. Wójcik A., Stephan G., Sommer S., Buraczewska I., Kuszewski T., Wieczorek A., Góźdź S.
Aberracje chromosomowe i mikrojądra w limfocytach krwi obwodowej pacjentek z nowotworami piersi napromienionych na skutek awarii akceleratora NEPTUN 10p (Biological dosimetry for the reconstruction of doses absorbed during accidents in radiotherapy).
Nowotwory, 53, Supplement 4, 122-123 (2002).

92. Zagórski Z.P.
Modification, degradation and stabilization of polymers in view of the classification of radiation spurs.
Radiation Physics and Chemistry, 63, 9-19 (2002).

93. Zagórski Z.P.
Niebezpieczne asteroidy i broń jądrowa (Dangerous asteroids and nuclear weapons).
Postępy Techniki Jądrowej, 45, 3, 33-35 (2002).

94. Zagórski Z.P.
Potencjalne źródło materiału na brudną bombę (Possible raw material for a dirty atomic bomb).
Postępy Techniki Jądrowej, 45, 2, 30-32 (2002).

95. Zagórski Z.P.
Profesor Kemula – niezwykły Profesor trudnych czasów (Professor W. Kemula – unusual Professor in difficult times).
Kwartalnik Historii Nauki i Techniki, 47, 1, 79-82 (2002).

96. Zagórski Z.P.
Rozterki fizyków – chemik pociesza (Physicist at a loss – a chemist's offers consolation).
Orbital. Wiadomości i informacje, 5, 214-216 (2002).

97. Zagórski Z.P.
Sekrety atomowe. Utajniać, odtajniać? (Atomic secrets, to classify and declassify?)
Postępy Techniki Jądrowej, 45, 3, 23-32 (2002).

98. Zagórski Z.P., Głuszewski W., Rzymski W.M.
Radiacyjna modyfikacja polimerów (Modification of polymers by ionizing radiation).
Plastics Review, 7(20), 23-28 (2002).

99. Zakrzewska-Trznadel G., Harasimowicz M.
Removal of radionuclides by membrane permeation combined with complexation.
Desalination, 144, 207-212 (2002)

100. Zakrzewska-Trznadel G., Harasimowicz M., Tymiński B., Chmielewski A.G.
Oczyszczanie roztworów promieniotwórczych za pomocą membran ceramicznych (Purification of radioactive solutions with ceramic membranes).
Zeszyty Naukowe Politechniki Śląskiej. Seria: Inżynieria Środowiska, 46, 229-236 (2002).

101. Ziaie F., Zimek Z., Bułka S., Afarideh H., Hadji-Saeid S.M.
Calculated and measured dose distribution in electron and X-ray irradiated water phantom.
Radiation Physics and Chemistry, 63, 177-183 (2002).

102. Zimek Z., Kałuska I.
Sterilization dose auditing for various types of medical products.
Radiation Physics and Chemistry, 63, 3-6, 673-674 (2002).

BOOKS

1. Siekierski S., Burgess J.
Concise chemistry of the elements.
Horwood Publishing, Chichester 2002, 198 p.

CHAPTERS IN BOOKS

1. Bartak J., Machaj B., Pieńkos J.P.
Aparatura do pomiaru stężenia radonu w powietrzu (Radiometers for radon concentration in air).
In: Technika jądrowa w przemyśle, medycynie, rolnictwie i ochronie środowiska. T.2. Instytut Chemii i Techniki Jądrowej, Warszawa 2002, pp. 303-311. Raporty IChTJ. Seria A nr 2/2002.

2. Bik J., Smejda A., Wolska B., Rzymski W.M., Głuszewski W., Zagórski Z.P.
Radiacyjne sieciowanie uwodornionego kauczuku butadienowo-akrylonitrylowego (Radiation crosslinking of hydrogenated butadiene-nitrile rubber).
In: Postęp w przetwórstwie materiałów polimerowych. Pod red. Józefa Koszkula. Wydawnictwo Politechniki Częstochowskiej, Częstochowa 2002, pp. 298-306.

3. Bryl-Sandelewska T., Panta P.P.
Dozymetria dawek mniejszych i większych od dawek sterylizacyjnych (Dose measurements below and above the sterilization doses).
In: Technika jądrowa w przemyśle, medycynie, rolnictwie i ochronie środowiska. T.1. Instytut Chemii i Techniki Jądrowej, Warszawa 2002, pp. 103-109. Raporty IChTJ. Seria A nr 1/2002.

4. Bułka S., Zimek Z., Roman K., Mirkowski J.

Układ do pomiaru charakterystyki widmowej wiązki elektronów (Secondary electrons monitor for continuous electron energy measurements in UHF linac).

In: Technika jądrowa w przemyśle, medycynie, rolnictwie i ochronie środowiska. T.2. Instytut Chemii i Techniki Jądrowej, Warszawa 2002, pp. 564-568. Raporty IChTJ. Seria A nr 2/2002.

5. Chmielewski A.G., Sun Y.-X., Ostapczuk A., Licki J., Zimek Z., Bułka S.

Electron beam removal of gaseous organic pollutants.

In: Technika jądrowa w przemyśle, medycynie, rolnictwie i ochronie środowiska. T.1. Instytut Chemii i Techniki Jądrowej, Warszawa 2002, pp. 66-70. Raporty IChTJ. Seria A nr 1/2002.

6. Chmielewski A.G., Tymiński B., Iller E., Zimek Z., Licki J., Kostrzewski R., Sobolewski L., Cybulski J.

Instalacja przemysłowa do oczyszczania gazów spalinowych za pomocą wiązki elektronów w EC „Pomorzany" (Industrial plant for flue gas cleaning with use of electron beam at the "Pomorzany" power plant).

In: Technika jądrowa w przemyśle, medycynie, rolnictwie i ochronie środowiska. T.1. Instytut Chemii i Techniki Jądrowej, Warszawa 2002, pp. 5-10. Raporty IChTJ. Seria A nr 1/2002.

7. Drzewicz P., Bojanowska-Czajka A., Panta P.P., Głuszewski W., Nałęcz-Jawecki G., Sawicki J., Trojanowicz M.

Zastosowanie promieniowania jonizującego do degradacji zanieczyszczeń organicznych w wodach i ściekach (Application of ionizing radiation for degradation of organic pollutants in waters and wastes).

In: Technika jądrowa w przemyśle, medycynie, rolnictwie i ochronie środowiska. T.1. Instytut Chemii i Techniki Jądrowej, Warszawa 2002, pp. 71-77. Raporty IChTJ. Seria A nr 1/2002.

8. Dybczyński R., Danko B., Polkowska-Motrenko H.

A study on homogeneity of the IAEA candidate reference materials for microanalysis and analytical support in the certification of these materials.

In: Reference materials for microanalytical nuclear techniques. Final report of a co-ordinated research project 1994-1999 (IAEA-TECDOC-1295). International Atomic Energy Agency, Vienna 2002, pp. 65-70.

9. Dziedzic-Gocławska A., Stachowicz W.

Sterylizacja radiacyjna przeszczepów tkankowych (Radiation sterilisation of tissue allografts).

In: Biocybernetyka i inżynieria biomedyczna 2000. Pod red. Macieja Nałęcza. T.9. Fizyka Medyczna. Akademicka Oficyna Wydawnicza EXIT, Warszawa 2002, pp. 329-362.

10. Dźwigalski Z., Zimek Z.

Formowanie krótkich impulsów w akceleratorze liniowym elektronów (Short pulse shaping in linear electron accelerator).

In: Technika jądrowa w przemyśle, medycynie, rolnictwie i ochronie środowiska. T.2. Instytut Chemii i Techniki Jądrowej, Warszawa 2002, pp. 557-563. Raporty IChTJ. Seria A nr 2/2002.

11. Flik J., Olszewska-Świetlik J., Waliś L., Pańczyk E.

Śląski warsztat malarski tzw. Mistrza lat 1486/87 w świetle badań bieli ołowiowej metodą neutronowej analizy aktywacyjnej (Silesian workshop of Master Painter 1486-87 in the light of studies on lead white by means of neutron activation analysis).

In: Technika jądrowa w przemyśle, medycynie, rolnictwie i ochronie środowiska. T.2. Instytut Chemii i Techniki Jądrowej, Warszawa 2002, pp. 383-389. Raporty IChTJ. Seria A nr 2/2002.

12. Głuszewski W., Zagórski Z.P.

Obróbka radiacyjna jako unikatowa metoda modyfikacji właściwości polimerów (Radiation processing as an unique method of modification of properties of polymers).

In: Technika jądrowa w przemyśle, medycynie, rolnictwie i ochronie środowiska. T.1. Instytut Chemii i Techniki Jądrowej, Warszawa 2002, pp. 91-95. Raporty IChTJ. Seria A nr 1/2002.

13. Iller E., Kukiełka A., Mikołajczyk W., Stupińska H., Starostka P.

Radiacyjna stymulacja reaktywności różnych rodzajów masy celulozowej z przeznaczeniem do wytwarzania pochodnych (Electron beam processing technology for modification of different types of cellulose pulps for production of derivatives).

In: Technika jądrowa w przemyśle, medycynie, rolnictwie i ochronie środowiska. T.1. Instytut Chemii i Techniki Jądrowej, Warszawa 2002, pp. 46-53. Raporty IChTJ. Seria A nr 1/2002.

14. Jakowiuk A.

Wizualizacja danych pomiarowych miernika zapylenia powietrza AMIZ-2000 przy użyciu programu

LabVIEW (Application of the LabVIEW package for representation of measurement data from airborne dust monitor AMIZ 2000).

In: Technika jądrowa w przemyśle, medycynie, rolnictwie i ochronie środowiska. T.2. Instytut Chemii i Techniki Jądrowej, Warszawa 2002, pp. 525-532. Raporty IChTJ. Seria A nr 2/2002.

15. Kierzek J., Kunicki-Goldfinger J.

Wielowymiarowa analiza statystyczna i rentgenowska analiza fluorescencyjna w badaniach nowożytnych szkieł (The studies of post-medieval glass by multivariate and X-ray fluorescence analysis).

In: Technika jądrowa w przemyśle, medycynie, rolnictwie i ochronie środowiska. T.2. Instytut Chemii i Techniki Jądrowej, Warszawa 2002, pp. 395-404. Raporty IChTJ. Seria A nr 2/2002.

16. Kraś J., Waliś L., Myczkowski S.

Doświadczenia z izotopowej kontroli szczelności obiektów technologicznych – aspekty techniczne i ekonomiczne (Experience in isotope leak-proof control of engineering objects – technical and economical aspects).

In: Technika jądrowa w przemyśle, medycynie, rolnictwie i ochronie środowiska. T.2. Instytut Chemii i Techniki Jądrowej, Warszawa 2002, pp. 373-379. Raporty IChTJ. Seria A nr 2/2002.

17. Legocka I., Zimek Z., Woźniak A., Mirkowski K., Nowicki A.

Optymalizacja parametrów technicznych i ekonomicznych sieciowanych radiacyjnie, polietylenowych wyrobów termokurczliwych (Optimization of technical and economical parameters of thermoshrinkable products made of polyethylene modified by radiation).

In: Technika jądrowa w przemyśle, medycynie, rolnictwie i ochronie środowiska. T.1. Instytut Chemii i Techniki Jądrowej, Warszawa 2002, pp. 37-45. Raporty IChTJ. Seria A nr 1/2002.

18. Licki J., Chmielewski A.G., Iller E., Tymiński B., Mazurek J., Sobolewski L.

Systemy monitoringu i sterowania przemysłową instalacją odsiarczania i odazotowania spalin przy użyciu wiązki elektronów z akceleratora (Monitoring and control system of industrial installation for desulphurisation and denitrification of flue gas using the electron beam from accelerator).

In: Technika jądrowa w przemyśle, medycynie, rolnictwie i ochronie środowiska. T.1. Instytut Chemii i Techniki Jądrowej, Warszawa 2002, pp. 11-19. Raporty IChTJ. Seria A nr 1/2002.

19. Machaj B., Świstowski E., Do Hoang Cuong

Miernik mocy dawki promieniowania ^{106}Ru oraz ^{125}I (^{106}Ru and ^{125}I radiation dose rate gauge).

In: Technika jądrowa w przemyśle, medycynie, rolnictwie i ochronie środowiska. T.2. Instytut Chemii i Techniki Jądrowej, Warszawa 2002, pp. 505-511. Raporty IChTJ. Seria A nr 2/2002.

20. Malec-Czechowska K., Stachowicz W.

Wykrywanie napromieniowania składników przyprawowych zawartych w niektórych produktach żywnościowych (Detection of radiation treatment in spices, the components of foodstuffs).

In: Technika jądrowa w przemyśle, medycynie, rolnictwie i ochronie środowiska. T.1. Instytut Chemii i Techniki Jądrowej, Warszawa 2002, pp. 54-61. Raporty IChTJ. Seria A nr 1/2002.

21. Migdał W., Owczarczyk H.B.

Prognozowanie skutków sanitarnych zastosowania przypraw niedekontaminowanych i dekontaminowanych radiacyjnie w artykułach spożywczych (Prognosis of the application spices, non-decontaminated and decontaminated by irradiation on the sanitary effect foodstuffs).

In: Technika jądrowa w przemyśle, medycynie, rolnictwie i ochronie środowiska. T.1. Instytut Chemii i Techniki Jądrowej, Warszawa 2002, pp. 20-27. Raporty IChTJ. Seria A nr 1/2002.

22. Mirowicz J., Owczarczyk A., Pieńkos J.P., Świstowski E., Urbański P.

Urządzenie do zbierania i przetwarzania wyników pomiarów radiometrycznych realizowanych w warunkach przemysłowych i terenowych (An instrument for collecting and processing data for radiometric experiments carried out in field and industrial conditions).

In: Technika jądrowa w przemyśle, medycynie, rolnictwie i ochronie środowiska. T.2. Instytut Chemii i Techniki Jądrowej, Warszawa 2002, pp. 533-538. Raporty IChTJ. Seria A nr 2/2002.

23. Narbutt J., Zasępa M., Gniazdowska E.

Tricarbonyl ^{99m}technetium(I) complexes with lipophilic bidentate ligands in solution.

In: Technetium, Rhenium and Other Metals in Chemistry and Nuclear Medicine. Vol. 6. Eds. M. Nicolini and U. Mazzi. SG Editoriali, Padova 2002, pp. 147-149.

24. Narbutt J., Zasępa M., Gniazdowska E.

Tricarbonyl ^{99m}technetium(I) complexes with lipophilic bidentate ligands in solution.

In: Technetium, Rhenium and Other Metals in Chemistry and Nuclear Medicine. Vol. 6. Eds. M. Nicolini and U. Mazzi. SG Editoriali, Padova 2002, p. 14.

25. Owczarczyk A., Dobrowolski A.

Badanie rozpływu zanieczyszczeń w rzekach meandrujących o nieuregulowanym korycie (Study of effluent transport in meandring rivers with unregulated bed).

In: Technika jądrowa w przemyśle, medycynie, rolnictwie i ochronie środowiska. T.1. Instytut Chemii i Techniki Jądrowej, Warszawa 2002, pp. 197-204. Raporty IChTJ. Seria A nr 1/2002.

26. Owczarczyk H.B., Migdał W.

Radiacyjne utrwalanie liofilizatów mięsnych (Radiation decontamination of meat lyophilized products).

In: Technika jądrowa w przemyśle, medycynie, rolnictwie i ochronie środowiska. T.1. Instytut Chemii i Techniki Jądrowej, Warszawa 2002, pp. 62-65. Raporty IChTJ. Seria A nr 1/2002.

27. Palige J., Dobrowolski A., Chmielewski A.G.

Wykorzystanie technik komputerowej symulacji przepływu plynów w opracowaniu wyników eksperymentów radioznacznikowych (Application of computational fluid dynamics technique for radiotracer experiments data treatment).

In: Technika jądrowa w przemyśle, medycynie, rolnictwie i ochronie środowiska. T.2. Instytut Chemii i Techniki Jądrowej, Warszawa 2002, pp. 498-502. Raporty IChTJ. Seria A nr 2/2002.

28. Panta P.P., Głuszewski W.

Radiacyjna modyfikacja właściwości materiałów (Radiation modification of materials properties).

In: Technika jądrowa w przemyśle, medycynie, rolnictwie i ochronie środowiska. T.1. Instytut Chemii i Techniki Jądrowej, Warszawa 2002, pp. 96-102. Raporty IChTJ. Seria A nr 1/2002.

29. Peimel-Stuglik Z., Fabisiak S.

EPR-dozymetria w radiacyjnej obróbce żywności (EPR-dosimetry for radiation processing of food).

In: Technika jądrowa w przemyśle, medycynie, rolnictwie i ochronie środowiska. T.1. Instytut Chemii i Techniki Jądrowej, Warszawa 2002, pp. 117-123. Raporty IChTJ. Seria A nr 1/2002.

30. Peimel-Stuglik Z., Sartowska B., Fabisiak S.

Wykorzystanie mikroskopii elektronowej do badania wewnętrznej struktury dozymetrów alaninowo-polimerowych (The use of electron microscopy to study alanine-polymer dosimeter microstructure).

In: Technika jądrowa w przemyśle, medycynie, rolnictwie i ochronie środowiska. T.1. Instytut Chemii i Techniki Jądrowej, Warszawa 2002, pp. 124-129. Raporty IChTJ. Seria A nr 1/2002.

31. Sartowska B., Piekoszewski J., Waliś L., Stanisławski J.

Zmiany morfologii powierzchni i niektórych własności mechanicznych wybranych gatunków stali po modyfikacji intensywnymi impulsami plazmowymi (High intensity pulsed plasma beams modification of surface morphology and mechanical properties of steels).

In: Technika jądrowa w przemyśle, medycynie, rolnictwie i ochronie środowiska. T.1. Instytut Chemii i Techniki Jądrowej, Warszawa 2002, pp. 110-116. Raporty IChTJ. Seria A nr 1/2002.

32. Sołtyk W., Walendziak J., Owczarczyk A.

Wykorzystanie badań hydrochemicznych, pomiarów trytu i izotopów stabilnych do oceny wpływu kopalni odkrywkowej na środowisko wodne (Application of hydrochemical and tritium content measurements as well as stable isotope ratios for assessment of strip mine impact on the environment).

In: Technika jądrowa w przemyśle, medycynie, rolnictwie i ochronie środowiska. T.1. Instytut Chemii i Techniki Jądrowej, Warszawa 2002, pp. 267-273. Raporty IChTJ. Seria A nr 1/2002.

33. Sommer S., Wojewódzka M., Buraczewska I., Kobiałko G., Pontek J., Szumiel I., Wójcik A.

Malowanie chromosomów i przedwczesna kondensacja chromatyny – nowe metody dozymetrii biologicznej (Chromosome painting and prematurely condensed chromosomes (PCC) – new methods of biological dosimetry).

In: Technika jądrowa w przemyśle, medycynie, rolnictwie i ochronie środowiska. T.2. Instytut Chemii i Techniki Jądrowej, Warszawa 2002, pp. 333-340. Raporty IChTJ. Seria A nr 2/2002.

34. Stachowicz W., Malec-Czechowska K., Dancewicz A.M., Szot Z., Strzelczak G., Lehner K.

Metody wykrywania napromieniowania żywności rozwijane w IChTJ (Detection methods for irradiated foods developed in the INCT).

In: Technika jądrowa w przemyśle, medycynie, rolnictwie i ochronie środowiska. T.1. Instytut Chemii i Techniki Jądrowej, Warszawa 2002, pp. 28-36. Raporty IChTJ. Seria A nr 1/2002.

35. Szumiel I.

Forty years of the L5178Y model: in pursuit of factors that determine the cellular sensitivity to DNA damaging agents.

In: Ganzkörperbestrahlung Strahlenschutzsubstanzen Strahlenexposition in der Diagnostik. Herausgegeben von D. Gottschild und Chr. Reiners. Urban & Fischer, München 2002, pp. 7-10.

36. Urbański P., Kowalska E.

Odszumianie widm promieniowania jonizującego (Denoising of the ionising radiation spectra).

In: Technika jądrowa w przemyśle, medycynie, rolnictwie i ochronie środowiska. T.2. Instytut Chemii i Techniki Jądrowej, Warszawa 2002, pp. 491-497. Raporty IChTJ. Seria A nr 2/2002.

37. Wawszczak D., Buczkowski M., Sartowska B., Starosta W.

Trawienie chemiczne wybranych folii polimerowych naświetlanych wiązką ciężkich jonów i wiązką wysokoenergetycznych elektronów (Chemical etching of some polymeric films irradiated with heavy ion beam and high-energy electron beam).

In: Technika jądrowa w przemyśle, medycynie, rolnictwie i ochronie środowiska. T.1. Instytut Chemii i Techniki Jądrowej, Warszawa 2002, pp. 78-85. Raporty IChTJ. Seria A nr 1/2002.

38. Wierzchnicki R.

Kontrola pochodzenia żywności na podstawie izotopów stabilnych wybranych pierwiastków (The use of stable isotope compositions of selected elements in food origin control).

In: Technika jądrowa w przemyśle, medycynie, rolnictwie i ochronie środowiska. T.2. Instytut Chemii i Techniki Jądrowej, Warszawa 2002, pp. 430-436. Raporty IChTJ. Seria A nr 2/2002.

39. Wójcik A.

Ryzyko zdrowotne promieniowania jonizującego (Health risk of ionising radiation).

In: Bezpieczeństwo człowieka we współczesnym świecie. Instytut Problemów Współczesnej Cywilizacji, Warszawa 2002, pp. 33-42.

40. Wójcik Z., Stephan G., Sommer S., Urbanik W., Kukołowicz P., Kuszewski T., Góźdź S.

Dozymetria biologiczna do rekonstrukcji dawek pochłoniętych w wypadkach radiacyjnych w radioterapii (Biological dosimetry for the reconstruction of doses absorbed during accidents in radiotherapy).

In: Technika jądrowa w przemyśle, medycynie, rolnictwie i ochronie środowiska. T.2. Instytut Chemii i Techniki Jądrowej, Warszawa 2002, pp. 327-332. Raporty IChTJ. Seria A nr 2/2002.

41. Zagórski Z.P., Głuszewski W., Rzymski W.M.

Radiacyjna modyfikacja polimerów (Modification of polymers by ionizing radiation).

In: Postęp w przetwórstwie materiałów polimerowych. Pod red. Józefa Koszkula. Wydawnictwo Politechniki Częstochowskiej, Częstochowa 2002, pp. 310-314.

42. Zakrzewska-Trznadel G.

Wykorzystanie membran ceramicznych do oczyszczania roztworów promieniotwórczych (The use of ceramic membranes for radioactive solutions purification).

In: Technika jądrowa w przemyśle, medycynie, rolnictwie i ochronie środowiska. T.1. Instytut Chemii i Techniki Jądrowej, Warszawa 2002, pp. 261-266. Raporty IChTJ. Seria A nr 1/2002.

43. Zimek Z., Kałuska I.

Walidacja procesu napromieniowania w stacji sterylizacji radiacyjnej sprzętu medycznego i przeszczepów (Validation of sterilization by irradiation at the pilot plant of radiation sterilization of medical devices and allografts).

In: Technika jądrowa w przemyśle, medycynie, rolnictwie i ochronie środowiska. T.1. Instytut Chemii i Techniki Jądrowej, Warszawa 2002, pp. 86-90. Raporty IChTJ. Seria A nr 1/2002.

THE INCT REPORTS

1. INCT Annual Report 2001.

Institute of Nuclear Chemistry and Technology, Warszawa 2002, 214 p.

2. Technika jądrowa w przemyśle, medycynie, rolnictwie i ochronie środowiska. T.1. (Nuclear technique in industry, medicine, agriculture and environmental protection. T.1).

Instytut Chemii i Techniki Jądrowej, Warszawa 2002. Raporty IChTJ. Seria A nr 1/2002, 274+X p.

3. Technika jądrowa w przemyśle, medycynie, rolnictwie i ochronie środowiska. T.2. (Nuclear technique in industry, medicine, agriculture and environmental protection. T.2).

Instytut Chemii i Techniki Jądrowej, Warszawa 2002. Raporty IChTJ. Seria A nr 2/2002, 294+X p.

4. Dybczyński R., Danko B., Kulisa K., Maleszewska E., Polkowska-Motrenko H., Samczyński Z., Szopa Z.

Preparation and certification of the Polish reference material: Tea Leaves (INCT-TL-1) for inorganic trace analysis.

Institute of Nuclear Chemistry and Technology, Warszawa 2002. Raporty IChTJ. Seria A nr 3/2002, 56 p.

5. Dybczyński R., Danko B., Kulisa K., Maleszewska E., Polkowska-Motrenko H., Samczyński Z., Szopa Z.

Preparation and certification of the Polish reference material: Mixed Polish Herbs (INCT-MPH-2) for inorganic trace analysis.

Institute of Nuclear Chemistry and Technology, Warszawa 2002. Raporty IChTJ. Seria A nr 4/2002, 56 p.

6. Iller E., Chmielewska D.K., Koczy B., Ryguła Cz.

Badania parametrów pracy małogabarytowego elektrofiltru do usuwania aerozoli higroskopijnych soli amonowych z gazów odlotowych (Testing of compact electrostatic precipitator for removal of hygroscopic ammonium salts from flue gases).

Instytut Chemii i Techniki Jądrowej, Warszawa 2002. Raporty IChTJ. Seria A nr 5/2002, 52 p.

7. Bryl-Sandelewska T., Panta P.P.

Ocena przydatności niektórych polimerów, produkowanych masowo, do pomiaru dawek technologicznych w napromieniowaniach akceleratorowych (Evaluation of some commercial grade polymers as possible dosimeters for technological irradiations in electron accelerators).

Instytut Chemii i Techniki Jądrowej, Warszawa 2002. Raporty IChTJ. Seria B nr 1/2002, 16 p.

8. Dybczyński R., Chajduk-Maleszewska E., Danko B., Kulisa K., Polkowska-Motrenko H., Samczyński Z., Szopa Z.

Collaborative study of the determination of trace elements in two candidate reference materials: Tea Leaves (INCT-TL-1) and Mixed Polish Herbs (INCT-MPH-2). Perliminary report.

Institute of Nuclear Chemistry and Technology, Warszawa 2002. Raporty IChTJ. Seria A nr 2/2002, 36 p.

CONFERENCE PROCEEDINGS

1. Chmielewski A.G.

Praktyczne możliwości wykorzystania odnawialnych źródeł energii (Practical possibilities of renewable energy sources).

„Wytwarzanie energii elektrycznej i cieplnej z biomasy szansą dla rolniczej Lubelszczyzny". Konferencja. Materiały. Lublin, Poland, 24.09.2002, pp. [1-6].

2. Chmielewski A.G.

Spalanie paliw kopalnych a zrównoważony rozwój (Combustion of fossil fuel and sustainable progress).

I Ogólnopolski Kongres Inżynierii Środowiska. Głosy w dyskusji. Lublin, Poland, 23-25.09.2002, pp. 9-12.

3. Chmielewski A.G., Ostapczuk A., Licki J., Sun Y., Kubica K.

VOCs emission from coal – fired power station boiler.

International Conference on Air Quality. Mercury, Trace Elements and Particulate Matter. Proceedings. Arlington, Virginia, USA, 9-12.09.2002, pp. 1-8.

4. Chmielewski A.G., Tymiński B., Pawelec A.

Jednoczesne usuwanie SO_2, NO_x i LZO przy użyciu wiązki elektronów (Simultaneous removal of SO_2, NO_x and VOCs using electron beam irradiation).

Dla miasta i środowiska. Konferencja: Problemy spalania odpadów komunalnych. Materiały konferencyjne. Warszawa, Poland, 28.11.2002, pp. 51-54.

5. Chmielewski A.G., Tymiński B., Zimek Z., Pawelec A., Licki J.

Industrial plant for flue gas treatment with high power electron accelerators.

17th International Conference on the Application of Accelerators in Research and Industry. Proceedings. Denton, Texas, USA, 12-16.11.2002, pp. [1-5].

6. **Chmielewski A.G., Zimek Z., Ostapczuk A., Licki J., Sun Y., Kubica K., Bułka S.**
   Electron beam process for destruction of VOCs emitted from coal – fired boiler.
   International Conference on Air Quality. Mercury, Trace Elements and Particulate Matter. Proceedings. Arlington, Virginia, USA, 9-12.09.2002, pp. 1-7.

7. **Dźwigalski Z., Zimek Z.**
   LAE-10 electron accelerator charge monitor.
   Proceedings of European Particle Accelerator Conference 2002. Paris, France, 3-7.06.2002, pp. 1879-1881.

8. **Dźwigalski Z., Zimek Z.**
   Performances of LAE-10 accelerator with a three electrode electron gun.
   Proceedings of European Particle Accelerator Conference 2002. Paris, France, 3-7.06.2002, pp. 2786-2788.

9. **Ostapczuk A., Chmielewski A.G.**
   Metody analizy LZO i WWA w próbkach gazowych (Methods of analysis of VOCs and PAH in gaseous samples).
   Dla miasta i środowiska. Konferencja: Problemy spalania odpadów komunalnych. Materiały konferencyjne. Warszawa, Poland, 28.11.2002, pp. 47-50.

10. **Paviet-Hartmann P., Dziewiński J., Hartmann T., Marczak S., Lu N., Walthall M., Rafalski A., Zagórski Z.P.**
    Spectroscopic investigation of the formation of radiolysis by-products by 13/9 linear accelerator of electrons (LAE) in salt solutions.
    Waste Management'02 Conference. Proceedings. Tucson, Arizona, USA, 24-28.02.2002, pp. 1-10.

12. **Tymiński B., Chmielewski A.G., Zwoliński K.**
    Recykling odpadów polietylenowych metodą krakingu katalitycznego (Catalytic cracking of the polyethylene wastes).
    Dla miasta i środowiska. Konferencja: Problemy spalania odpadów komunalnych. Materiały konferencyjne. Warszawa, Poland, 28.11.2002, pp. 64-68.

CONFERENCE ABSTRACTS

1. **Bartoś B., Bilewicz A.**
   Effect of crown ethers on the Sr^{2+}, Ba^{2+} and Ra^{2+} uptake on tunnel structure ion exchangers.
   Proceedings of the XVIIth International Symposium on Physico-Chemical Methods of the Mixtures Separation "Ars Separatoria 2002". Borówno n. Bydgoszcz, Poland, 17-20.06.2002, p. 125.

2. **Bik J., Głuszewski W., Rzymski M., Zagórski Z.P.**
   EB radiation crosslinking of elastomers.
   10th "Tihany" Symposium on Radiation Chemistry. Program and Abstracts. Sopron, Hungary, 31.08.-05.09.2002, p. P-54.

3. **Bobrowski K., Marciniak B., Korzeniowska-Sobczuk A., Filipiak P., Strzelczak G., Kozubek H., Mirkowski J., Wiśniowski P.**
   Indukowane radiacyjnie i fotochemicznie procesy rodnikowe w aromatycznych kwasach karboksylowych zawierających grupę tioeterową (Radiation and photochemically induced radical processes in aromatic carboxylic acids containing thioether group).
   XLV Zjazd Naukowy Polskiego Towarzystwa Chemicznego. Tom I. Streszczenia prezentacji. Kraków, Poland, 9-13.09.2002, p. 1171.

4. **Bobrowski K., Wiśniowski P., Pogocki D., Hug G.L., Schöneich C.**
   Mechanistic studies of the -induced oxidation of model organic sulfides.
   20th International Symposium on the Organic Chemistry of Sulfur. Book of Abstracts. Flagstaff, Arizona, USA, 14-19.07.2002, p. OA9.

5. **Chmielewski A.G.**
   Chronić środowisko i miejsca pracy (Protect environment and place of work).
   Ogólnopolski Kongres Inżynierii Środowiska. Głosy w dyskusji. Lublin, Poland, 23-25.09.2002, pp. 7-8.

6. Chmielewski A.G., Tymiński B., Iller E., Zimek Z., Pawelec A., Sun Y., Ostapczuk A., Licki J., Getoff N.

Advanced technology for SO_2, NO_x and VOC removal from industrial off-gases.

Ecology and ECO-Technologies. Review Conference on scientific cooperation between Austria and Poland. Abstracts. Vienna, Austria, 24-28.02.2002, p. [1].

7. Chwastowska J., Skwara W., Sterlińska E., Dąbrowska M., Pszonicki L.

Wstępne wzbogacanie i oznaczanie platyny i palladu w próbkach środowiskowych metodą absorpcyjnej spektrometrii atomowej z elektrotermiczną atomizacją (Preconcentration and determination of platinum and palladium in environmental samples by graphite furnace atomic absorption spectrometry).

Nowoczesne metody przygotowania próbek i oznaczania śladowych ilości pierwiastków. Materiały XI Poznańskiego Konwersatorium Analitycznego. Materiały Szkoły Naukowej „Analityka wód, ścieków i gleb". Poznań, Poland, 4-5.04.2002, p. 66.

8. Chwastowska J., Skwara W., Sterlińska E., Dudek J., Pszonicki L.

Zastosowanie sorbentów chelatujących z grupami tiolowymi do wydzielania i zagęszczania rtęci nieorganicznej i alkilorteci z wód naturalnych (Application of a chelating sorbents to the separation and preconcentration of inorganic and alkylmercury species in natural waters).

Nowoczesne metody przygotowania próbek i oznaczania śladowych ilości pierwiastków. Materiały XI Poznańskiego Konwersatorium Analitycznego. Materiały Szkoły Naukowej „Analityka wód, ścieków i gleb". Poznań, Poland, 4-5.04.2002, p. 67.

9. Ciesielski B., Schultka K., Stuglik Z., Kobierska A.

Dozymetria alaninowa *in vitro* w radioterapii – ocena dokładności, perspektywy zastosowań klinicznych (*In vitro* alanine-dosimetry in radiotherapy – evaluation of accuracy and usefulness to clinical applications).

XIX Szkoła Jesienna „Promieniowanie jonizujące w medycynie. Narażenie i ochrona pacjenta, kontrola jakości, przepisy prawne". Materiały konferencyjne. Zakopane, Poland, 14-18.10.2002, p. [1].

10. Danilczuk M., Sadło J., Michalik J.

Badania EPR rodników metylowych w napromienionym zeolicie A (EPR study of radiation-induced methyl radicals in zeolite A).

Szkoła Fizykochemii Organicznej „Nowe metody w spektroskopii molekularnej". Abstrakty. Karpacz, Poland, 10-15.06.2002, p. P3.

11. Danko B., Polkowska-Motrenko H., Dybczyński R.

Korzyści płynące z zastosowania techniki mikrofalowej do roztwarzania próbek analizowanych na zawartość Co, Mo i U za pomocą NAA (Benefits from microwave digestion for the determination of Co, Mo and U by NAA).

Nowoczesne metody przygotowania próbek i oznaczania śladowych ilości pierwiastków. Materiały XI Poznańskiego Konwersatorium Analitycznego. Materiały Szkoły Naukowej „Analityka wód, ścieków i gleb". Poznań, Poland, 4-5.04.2002, p. 133.

12. Dybczyński R., Danko B., Kulisa K., Maleszewska E., Polkowska-Motrenko H., Samczyński Z., Szopa Z.

Wstępna ocena wkładu poszczególnych technik analitycznych w dzieło atestacji dwóch nowych polskich materiałów odniesienia (Preliminary assessment of analytical methods used in the certification process of two new Polish CRMs).

Nowoczesne metody przygotowania próbek i oznaczania śladowych ilości pierwiastków. Materiały XI Poznańskiego Konwersatorium Analitycznego. Materiały Szkoły Naukowej „Analityka wód, ścieków i gleb". Poznań, Poland, 4-5.04.2002, p. 47.

13. Dziewinski J., Paviet-Hartmann P., Zagórski Z.P.

Radiation chemistry in the management of radioactive waste (selected topics).

14th Radiochemical Conference. Booklet of Abstracts. Conference Programme. Marianske Lazne, Czech Republic, 14-19,04.2002, p. 317.

14. Dziewinski J., Zagórski Z.P.

Radiation chemistry of polymeric components of radioactive waste.

5th International Symposium on Ionizing Radiation and Polymers "IRaP 2002". Final Program and Abstracts. Sainte-Adele Quebec, Canada, 21-26.09.2002, p. 183.

15. Dźwigalski Z., Zimek Z.

Pomiar dawki ekspozycyjnej w eksperymentach z akceleratorem LAE 10 (Measurement of the exposure dose in experiments with LAE 10 accelerator).

VI Krajowa Konferencja Techniki Próżni i VII Polsko-Białoruskie Sympozjum Technologii Próżniowych. Materiały konferencyjne. Korbielów, Poland, 23-25.09.2002, p. 40.

16. Grądzka I., Buraczewska I., Szumiel I., Romaniewska A., Kuduk-Jaworska J.

Radiosensitising properties of novel hydroxydicarboxylato platinum (II) complexes: two modes of action.

XLV Zjazd Naukowy Polskiego Towarzystwa Chemicznego. Tom II. Streszczenia prezentacji. Kraków, Poland, 9-13.09.2002, p. 841.

17. Grądzka I., Buraczewska I., Szumiel I., Romaniewska A., Kuduk-Jaworska J.

Radiosensitising properties of novel hydroxydicarboxylato platinum (II) complexes with high or low reactivity with thiols: two modes of action.

The Third Multidisciplinary Conference on Drug Research. Book of Abstracts. Piła, Poland, 13-16.05.2002, p. [1].

18. Jaworska A., Wojewódzka M., De Angelis P.

Radiation sensitivity and the status of some radiation sensitivity markers in relatively sensitive lymphoid cells.

International Conference "Genetic Consequences of Emergency Radiation Situations". Abstracts. Moscow, Russian Federation, 10-13.06.2002, pp. 174-175.

19. Korzeniowska-Sobczuk A., Bobrowski K.

Radioliza impulsowa wybranych aromatycznych kwasów karboksylowych zawierających grupę tioeterową (Pulse radiolysis of selected aromatic carboxylic acids containing thioether group).

Szkoła Fizykochemii Organicznej „Nowe metody w spektroskopii molekularnej". Abstrakty. Karpacz, Poland, 10-15.06.2002, p. L32.

20. Kruszewski M., Iwaneńko T., Lipiński P.

Formation of oxidative DNA damage in mammalian cells depends on labile iron pool level.

32nd Annual Meeting of European Environmental Mutagen Society "DNA Damage and Repair Fundamental Aspects and Contribution to Human Disorders". Book of Abstracts. Warszawa, Poland, 3-7.09.2002, p. 211.

21. Legocka I., Bojarski J., Zimek Z., Sadło J., Cieśla K., Mirkowski K., Nowicki A.

Influence of nucleating agent on physical properties of polypropylene and its blends.

5th International Symposium on Ionising Radiation and Polymers (IRaP 2002). Final Program and Abstracts. Sainte Adele, Quebec, Canada, 21-26.09.2002, p. 187(P-165).

22. Legocka I., Zimek Z., Bartczak Z., Borycki J.

Radiation modification of polypropylene with selected oligomeric resins.

II Ukrajins'ko-Pol's'ka Naukova Konferencjhja –$[PSA]_n$- "Polimeri special'nogo priznaèennja. Tezi dopovidej. Dninpopetrovs'k, Ukraine, 27-31.05.2002, pp. 92-93.

23. Lehner K., Stachowicz W.

Detection of irradiated chicken carcasses with the use of gas chromatography.

European Society for New Methods in Agricultural Research XXXII Annual Meeting and International Union of Radioecology (IUR). Book of Abstracts and Plenary Lectures. Warszawa, Poland, 10-14.09.2002, p. 28.

24. Malec-Czechowska K., Stachowicz W.

Detection of radiation treatment in spices, the components of non irradiated foodstuffs.

European Society for New Methods in Agricultural Research XXXII Annual Meeting and International Union of Radioecology (IUR). Book of Abstracts and Plenary Lectures. Warszawa, Poland, 10-14.09.2002, p. 29.

25. Michalik J., Sadło J., Danilczuk M., Perlińska J.

Silver clusters in molecular sieves.

35th Annual International Meeting: Advanced Techniques and Applications of EPR. Abstracts. Aberdeen, Scotland, 7-11.04.2002, p. L26.

26. Michalik J., Sadło J., Danilczuk M., Perlińska J., Yamada H.

Cationic silver clusters in zeolite rho and sodalite.

[2]FEZA Conference "Impact of zeolites and other porous materials on the new technologies at the beginning of the new millennium". Book of Abstracts and Recent Research Reports.Taormina, Italy, 1-5.09.2002, p. [1].

27. Narbutt J.

Coordination number of metal ion and amphiphilicity of the metal complex – fundamental properties of metal-essential radiopharmaceuticals.

14th Radiochemical Conference. Radiochemie. Conference Programme. Book of Abstracts. Marianske Lazne, Czech Republic, 14-19.04.2002, p. 354.

28. Paviet-Hartmann P., Dziewinski J., Marczak S., Hartmann T., Rafalski A., Zagórski Z.P.

Spectroscopic investigation of the formation of radiolysis by-products by 10 MeV linear accelerator electron in salt solutions.

14th Radiochemical Conference. Booklet of Abstracts. Conference Programme. Marianske Lazne, Czech Republic, 14-19,04.2002, p. 206.

29. Pogocki D.

Własności Redox Met_{35} w neurotoksycznym β-peptydzie Alzheimera (Redox properties of Met^{35} in neurotoxic Alzheimer β-peptide).

Szkoła Fizykochemii Organicznej „Nowe metody w spektroskopii molekularnej". Abstrakty. Karpacz, Poland, 10-15.06.2002, p. L10.

30. Stachowicz W., Malec-Czechowska K., Dancewicz A.M., Szot Z., Lehner K., Strzelczak G.

Analytical methods adapted for the detection of irradiated foods in Poland.

European Society for New Methods in Agricultural Research XXXII Annual Meeting and International Union of Radioecology (IUR). Book of Abstracts and Plenary Lectures. Warszawa, Poland, 10-14.09.2002, p. 35.

31. Strzelczak G., Korzeniowska-Sobczuk A., Bobrowski K.

Rodniki w aromatycznych kwasach karboksylowych z grupą tioeterową. Badania metodą EPR (Radicals in aromatic carboxylic acids with tioether groups. EPR studies).

XLV Zjazd Naukowy Polskiego Towarzystwa Chemicznego. Tom I. Streszczenia prezentacji. Kraków, Poland, 9-13.09.2002, p. 415.

32. Szydłowski A., Sadowski M., Banaszak A., Jaskóła M., Korman A., Fijal I., Zimek Z.

Influence of intense electromagnetic radiation on tracks formation in PM-355 detectors.

21st International Conference on Nuclear Tracks in Solids (ICNTS 21). Book of Abstracts. New Delhi, India, 21-25.10.2002, p. 47.

33. Wojewódzka M., Buraczewska I., Kruszewski M.

Validation of the neutral comet assay.

32nd Annual Meeting of European Environmental Mutagen Society "DNA Damage and Repair Fundamental Aspects and Contribution to Human Disorders". Book of Abstracts. Warszawa, Poland, 3-7.09.2002, p. 209.

34. Woźniak G., Sochanowicz B., Grądzka I., Szumiel I.

The influence of X-radiation on the expression of DNA-PK subunits in two L5178Y sublines differing in radiosensitivity.

32nd Annual Meeting of European Environmental Mutagen Society "DNA Damage and Repair Fundamental Aspects and Contribution to Human Disorders". Book of Abstracts. Warszawa, Poland, 3-7.09.2002, p. 97.

35. Zagórski Z.P.

Radiation chemistry and origins of life on earth.

10th "Tihany" Symposium on Radiation Chemistry. Program and Abstracts. Sopron, Hungary, 31.08.-05.09.2002, p. O-6.

36. Zasępa M., Gniazdowska E., Narbutt J.

Lipophilic mixed-ligand tricarbonyl technetium(I) complexes in solution.

14th Radiochemical Conference. Radiochemie. Conference Programme. Book of Abstracts. Marianske Lazne, Czech Republic, 14-19.04.2002, p. 376.

37. Zimek Z., Głuszewski W.

Niewidzialne ale pracowite (Invisible but laborious).

Piąte Spotkanie Inspektorów Ochrony Radiologicznej. Streszczenia referatów oraz materiały konferencyjne. Dymaczewo Nowe, Poland, 4-7.06.2002, p. [1].

SUPPLEMENT LIST OF THE INCT PUBLICATIONS IN 2001

ARTICLES

1. Liu W., Shiotani M., Michalik J., Lund A.

Cage effect on stability and molecular dynamics of $[(CH_3)_3N]^{\cdot+}$ and $[(CH_3)_3NCH_2]^{\cdot+}$ generated in γ-irradiated zeolites.

Physical Chemistry Chemical Physics, 3, 3532-3535 (2001).

2. Szytuła A., Hofmann M., Leciejewicz J., Kolenda M., Penc B.

Neutron diffraction study of the magnetic structures of some RT_2X_2 compounds.

Materials Science Forum, 378-381, 408-413 (2001).

3. Trojanowicz M., Biesaga M., Orska-Gawryś J.

Chromatographic applications of porphyrins.

Analytical Sciences, 17, Supplement, i587-i590 (2001).

CHAPTERS IN BOOKS

1. Berne P., BjØrnstad T., Chmielewski A.G. *et al*.

Radiotracer investigations of wastewater treatment plant.

In: Radiotracer technology as applied to industry. Final report of a co-ordinated research project 1997-2000 (IAEA-TECDOC-1262). International Atomic Energy Agency, Vienna 2001, pp. 45-52.

NUKLEONIKA
THE INTERNATIONAL JOURNAL OF NUCLEAR RESEARCH

CONTENTS OF No. 1/2002

SUPPLEMENT No. 1/2002

Proceedings of the International Conference "2001 an Isotope Odyssey: New Application for a New Millenium", 24-29 June 2001, Zakopane, Poland

CONTENTS OF No. 2/2002

Proceedings of the Third National Conference on Radiochemistry and Nuclear Chemistry, 6-9 May 2001, Kazimierz Dolny, Poland

CONTENTS OF No. 3/2002

CONTENTS OF No. 4/2002

Information

INSTITUTE OF NUCLEAR CHEMISTRY AND TECHNOLOGY
NUKLEONIKA
Dorodna 16, 03-195 Warszawa, Poland
phone: (+4822) 811-30-21 or 811-00-81 int. 14-91; fax: (+4822) 811-15-32;
e-mail: nukleon@orange.ichtj.waw.pl
Abstracts are available on-line at http://www.euronuclear.org/publications/nukleonika/index.html

THE INCT PATENTS AND PATENT APPLICATIONS IN 2002

PATENTS

1. A process for removal of SO_2 and NO_x from combustion flue gases and an apparatus used therefor
   N. Frank, G. Lysov, Z. Zimek, I. Artiuch, A.G. Chmielewski
   Canadian patent No. 2,087,833
2. A process for removal of SO_2 and NO_x from combustion flue gases and an apparatus used therefor
   Z. Zimek, A.G. Chmielewski, I. Artiuch, G. Lysov, N. Frank
   Japanese patent No. 3329386

PATENT APPLICATIONS

1. Sposób selektywnego wyodrębniania złota i srebra z rozcieńczonych roztworów wodnych (Method for selective separation of gold and silver from dilute aqueous solutions)
   A. Łukasiewicz, L. Rowińska, L. Waliś
   P. 352619
2. Sposób topienia termoplastycznych tworzyw sztucznych i urządzenie do realizacji tego sposobu (Method for thermoplastic melting of plastics and a device to apply the method)
   A.G. Chmielewski, B. Tymiński, K. Zwoliński
   P. 353434
3. Sposób rozdzielenia izotopów siarki ^{34}S i ^{32}S (Method for separation of sulphur isotopes ^{34}S and ^{32}S)
   A.G. Chmielewski, A. Mikołajczuk, N. Miljević
   P. 354392
4. Sposób otrzymywania radionuklidów aktynu-225 i aktynu-228 (Method for obtaining radionuclides actinium-225 and actinium-228)
   B. Bartoś, A. Bilewicz, B. Włodzimirska
   P. 355940
5. Sposób otrzymywania nowych materiałów aktywnych biocydowo (Method for obtaining new materials active as biocides)
   A. Łukasiewicz, K. Krajewski, L. Waliś, D. Chmielewska, L. Rowińska
   P. 357356
6. Sposób otrzymywania katod Ni/NiO (Method for obtaining Ni/NiO cathods)
   W. Łada, A. Deptuła, T. Olczak, A.G. Chmielewski, A. Moreno
   P. 357688

CONFERENCES ORGANIZED AND CO-ORGANIZED BY THE INCT IN 2002

1. KRAJOWE SYMPOZJUM "TECHNIKA JĄDROWA W PRZEMYŚLE, MEDYCYNIE, ROLNICTWIE I OCHRONIE ŚRODOWISKA" (NATIONAL SYMPOSIUM ON NUCLEAR TECHNIQUE IN INDUSTRY, MEDICINE, AGRICULTURE AND ENVIRONMENTAL PROTECTION), 17-19 APRIL 2002, WARSZAWA, POLAND

Organized by the Institute of Nuclear Chemistry and Technology

Organizing Committee: G. Zakrzewska-Trznadel (Chairman), K. Malec-Czachowska, W. Głuszewski, A. Jakowiuk, A. Owczarczyk, J.P. Pieńkos, S. Ptaszek, B. Sartowska, Z. Stęgowski

Scientific Committee: P. Urbański (Chairman), A.G. Chmielewski, E. Iller, R. Jabłoński, J. Liniecki, J. Michalik, K. Przewłocki, W. Reimschüssel, K. Różański, T. Sikora, M. Wasilewska-Radwańska

PLENARY LECTURES

- Technologie jądrowe – korzyści i zagrożenia (Nuclear technology – advantages and threats)
  J. Niewodniczański (State Atomic Agency, Warszawa, Poland)
- Pozytonowa tomografia emisyjna (Positon emission tomography)
  A. Hrynkiewicz (H. Niewodniczański Institute of Nuclear Physics, Kraków, Poland)
- Aktualny stan i tendencje rozwojowe medycyny nuklearnej (The state-of-arts and future trands of nuclear medicine)
  J. Liniecki (Medical Academy of Łódź, Poland)
- Techniki jądrowe w ochronie środowiska (Nuclear techniques in environmental protection)
  A.G. Chmielewski (Institute of Nuclear Chemistry and Technology, Warszawa, Poland)
- Nowe trendy w technologiach radiacyjnych (New trends in radiation technologies)
  J. Rosiak (Technical University of Łódź, Poland)

LECTURES

Section: METODY RADIOANALITYCZNE (RADIOANALYTICAL METHODS)

- Wybrane zastosowania rentgenowskiej mikroanalizy fluorescencyjnej (Some applications of XRF micro-analysis)
  M. Lankoza (Academy of Mining and Metallurgy, Kraków, Poland)
- Zastosowanie neutronowej analizy aktywacyjnej do badania składu chemicznego meteorytów (Application of NAA for elemental analysis of meteorites)
  H. Polkowska-Motrenko (Institute of Nuclear Chemistry and Technology, Warszawa, Poland), B. Danko (Institute of Nuclear Chemistry and Technology, Warszawa, Poland), R. Dybczyński (Institute of Nuclear Chemistry and Technology, Warszawa, Poland), K. Kulisa (Institute of Nuclear Chemistry and Technology, Warszawa, Poland), Z. Samczyński (Institute of Nuclear Chemistry and Technology, Warszawa, Poland), Z. Szopa (Institute of Nuclear Chemistry and Technology, Warszawa, Poland)
- Zastosowanie INAA w badaniach emisji pierwiastków w procesie spopielania polskiego węgla brunatnego (Use of INAA for investigation of emission of elements in combustion of Polish lignite)
  J. Janczyszyn (Academy of Mining and Metallurgy, Kraków, Poland), L. Loska (Academy of Mining and Metallurgy, Kraków, Poland), W. Pohorecki (Academy of Mining and Metallurgy, Kraków, Poland), M. Wagner (Academy of Mining and Metallurgy, Kraków, Poland)
- Oznaczanie izotopów naturalnie promieniotwórczych w wodach podziemnych i powierzchniowych techniką spektrometrii α/β z ciekłym scyntylatorem (Determination of natural radioactivity of isotopes in the surface and ground water by techniques of liquid scintillation α/β spectrometry)
  E. Chruściel (Academy of Mining and Metallurgy, Kraków, Poland), Nguyen Dinh Chau (Academy of Mining and Metallurgy, Kraków, Poland)
- Kontrola pochodzenia żywności na podstawie składu izotopów stabilnych wybranych pierwiastków (The use of stable isotope compositions of selected elements in food origin control)
  R. Wierzchnicki (Institute of Nuclear Chemistry and Technology, Warszawa, Poland)

Section: RADON W ŚRODOWISKU (RADON IN THE ENVIRONMENT)

- Wykorzystanie przenośnego licznika ciekłoscyntylacyjnego do pomiarów stężenia produktów rozpadu radonu w powietrzu (Application of the portable liquid scintillation counter for measurements of radon progeny concentration in air)
  S. Chałupnik (Central Mining Institute, Katowice, Poland), A. Kies (Centre Universitaire, Luxembourg)
- Porównanie kosztów prewencji i ryzyka radonowego w polskich kopalniach (Comparison of costs of prevention and radon hazard in Polish mines)
  J. Skowronek (Central Mining Institute, Katowice, Poland)
- Wpływ geologicznej struktury podłoża na stężenie radonu w budynkach mieszkalnych dla wybranego rejonu Krakowa (Influence of geological structure on radon content in houses in some chosen region of Kraków)
  J. Bogacz (H. Niewodniczański Institute of Nuclear Physics, Kraków, Poland), T. Horwacik (H. Niewodniczański Institute of Nuclear Physics, Kraków, Poland), K. Kozak (H. Niewodniczański Institute of Nuclear Physics, Kraków, Poland), J. Swakoń (H. Niewodniczański Institute of Nuclear Physics, Kraków, Poland), J. Łoskiewicz (H. Niewodniczański Institute of Nuclear Physics, Kraków, Poland), J. Mazur (H. Niewodniczański Institute of Nuclear Physics, Kraków, Poland), M. Paszkowski (H. Niewodniczański Institute of Nuclear Physics, Kraków, Poland), M. Janik (H. Niewodniczański Institute of Nuclear Physics, Kraków, Poland)
- Zastosowanie wyników badań wymywania izotopów radu z osadników kopalnianych do projektowania procesów rekultywacji (Leaching of radium from mine deposits – application for planning of ground reclamation)
  S. Chałupnik (Central Mining Institute, Katowice, Poland)
- Pomiar krótkotrwałych pochodnych radonu w Radonowym Stanowisku Wzorcowym CLOR (Measurement of radon progeny at the radon reference chamber of CLOR)
  K. Mamont-Cieśla (Central Laboratory of Radiation Protection, Warszawa, Poland), M. Kusyk (Central Laboratory of Radiation Protection, Warszawa, Poland)

Section: PRODUKCJA I METROLOGIA ŹRÓDEŁ PROMIENIOWANIA (PRODUCTION AND METROLOGY OF RADIATION SOURCES)

- Aplikatory oftalmiczne jodu-125 z monolitycznym rdzeniem aktywnym (Iodine-125 ophthalmic applicators with monolithic active insert)
  I. Puchalska (Radioisotope Centre POLATOM, Świerk, Poland), A. Piasecki (Radioisotope Centre POLATOM, Świerk, Poland), T. Barcikowski (Radioisotope Centre POLATOM, Świerk, Poland), M. Mielcarski (Radioisotope Centre POLATOM, Świerk, Poland)
- Otrzymywanie izotopów promieniotwórczych w cyklotronie AIC-144 w Krakowie (Obtaining of radiactive isotopes in the AIC-144 cyclotron in Kraków)
  M. Bartyzel (H. Niewodniczański Institute of Nuclear Physics, Kraków, Poland), R. Misiak (H. Niewodniczański Institute of Nuclear Physics, Kraków, Poland), E. Ochab (H. Niewodniczański Institute of Nuclear Physics, Kraków, Poland), B. Petelenz (H. Niewodniczański Institute of Nuclear Physics, Kraków, Poland), B. Wąs (H. Niewodniczański Institute of Nuclear Physics, Kraków, Poland)
- Badania produkcji radionuklidów w otoczeniu spallacyjnego źródła neutronów (Experimental assessment of radionuclide production in materials irradiated near to the spallation target)
  W. Pohorecki (Academy of Mining and Metallurgy, Kraków, Poland), J. Janczyszyn (Academy of Mining and Metallurgy, Kraków, Poland), S. Taczanowski (Academy of Mining and Metallurgy, Kraków, Poland), G. Domański (Academy of Mining and Metallurgy, Kraków, Poland)
- Nowa generacja metod standaryzacji radionuklidów ^{22}Na, ^{99}Mo, ^{65}Zn i ^{169}Yb (New generation methods of ^{22}Na, ^{99}Mo, ^{65}Zn and ^{169}Yb radionuclides standardization)
  A. Chyliński (Radioisotope Centre POLATOM, Świerk, Poland), T. Radoszewski (Radioisotope Centre POLATOM, Świerk, Poland), T. Terlikowska (Radioisotope Centre POLATOM, Świerk, Poland)

Section: AKWIZYCJA I PRZETWARZANIE DANYCH (DATA ACQUISITION AND PROCESSING)

- Analiza radioaktywności ^{7}Be za pomocą sieci neuronowych (Analysis of the atmospheric ^{7}Be radioactivity by neural network)
  Z. Moroz (Andrzej Sołtan Institute for Nuclear Studies, Świerk, Poland; Białystok Technical University, Poland), C. Kownacka (Białystok Technical University, Poland), B. Mysłek-Laurikainen (Andrzej Sołtan Institute for Nuclear Studies, Świerk, Poland), M. Matul (Andrzej Sołtan Institute for Nuclear Studies, Świerk, Poland), S. Mikołajewski (Andrzej Sołtan Institute for Nuclear Studies, Świerk, Poland), Z. Preibisz (Andrzej Sołtan Institute for Nuclear Studies, Świerk, Poland), H. Trzaskowska (Andrzej Sołtan Institute for Nuclear Studies, Świerk, Poland)
- Spektrometryczna analiza widma z detektora scyntylacyjnego z zastosowaniem sieci neuronowych (Artificial neural networks application for analysis of gamma-ray spectrum obtains from the scintillation detectors)
  Z. Stęgowski (Academy of Mining and Metallurgy, Kraków, Poland)

- Odszumianie widm promieniowania jonizującego (Denoising of the ionising radiation spectra)
  P. Urbański (Institute of Nuclear Chemistry and Technology, Warszawa, Poland), E. Kowalska (Institute of Nuclear Chemistry and Technology, Warszawa, Poland)
- Wielowymiarowa analiza statystyczna i rentgenowska analiza fluorescencyjna w badaniach nowożytnych szkieł (The studies of post-medieval glass by multivariate and X-ray fluorescence analysis)
  J. Kierzek (Institute of Nuclear Chemistry and Technology, Warszawa, Poland), J. Kunicki-Goldfinger (Institute of Nuclear Chemistry and Technology, Warszawa, Poland)
- Wykorzystanie technik komputerowej symulacji przepływu płynów w opracowaniu wyników eksperymentów radioznacznikowych (Application of computational fluid dynamic technique for radiotracer experiments data treatment)
  J. Palige (Institute of Nuclear Chemistry and Technology, Warszawa, Poland), A. Dobrowolski (Institute of Nuclear Chemistry and Technology, Warszawa, Poland), A.G. Chmielewski (Institute of Nuclear Chemistry and Technology, Warszawa, Poland)

Section: OCHRONA PRZED PROMIENIOWANIEM (RADIATION PROTECTION)

- Narażenie na promieniowanie jonizujące w Polsce – ocena za 2001 r. (Exposure to the ionizing radiation in Poland in 2001)
  J. Henschke (Central Laboratory of Radiation Protection, Warszawa, Poland), M. Biernacka (Central Laboratory of Radiation Protection, Warszawa, Poland), K. Florowska (Central Laboratory of Radiation Protection, Warszawa, Poland), D. Grabowski (Central Laboratory of Radiation Protection, Warszawa, Poland), B. Rubel (Central Laboratory of Radiation Protection, Warszawa, Poland), A. Sosińska (Central Laboratory of Radiation Protection, Warszawa, Poland)
- Zagrożenie radiacyjne w kopalniach i wokół kopalń rud miedzi KGHM Polska Miedź S.A. (Radiological hazard in site and around copper ore mines in Poland)
  E. Chruściel (Academy of Mining and Metallurgy, Kraków, Poland), M. Waligórski (H. Niewodniczański Institute of Nuclear Physics, Kraków, Poland), P. Jodłowski (Academy of Mining and Metallurgy, Kraków, Poland), S.J. Kalita (Academy of Mining and Metallurgy, Kraków, Poland), Nguyen Dinh Chau (Academy of Mining and Metallurgy, Kraków, Poland), P. Bilski (H. Niewodniczański Institute of Nuclear Physics, Kraków, Poland), M. Budzanowski (H. Niewodniczański Institute of Nuclear Physics, Kraków, Poland), A. Maksymowicz (KGHM Polska Miedź S.A., Lublin, Poland)
- Właściwości radiologiczne terenu zrekultywowanego przy użyciu mieszaniny popiołowo-żużlowej z energetycznego spalania węgla (Radiological characteristics of an area reclaimed by means of an ash-gravel power plant wastes)
  A. Żak (Central Laboratory of Radiation Protection, Warszawa, Poland), M. Biernacka (Central Laboratory of Radiation Protection, Warszawa, Poland), M. Kusyk (Central Laboratory of Radiation Protection, Warszawa, Poland), K. Mamont-Cieśla (Central Laboratory of Radiation Protection, Warszawa, Poland), K. Florowska (Central Laboratory of Radiation Protection, Warszawa, Poland)
- Retrospektywna ocena depozycji jodu-131 na terytorium Polski po awarii czarnobylskiej (Retrospective evaluation of I-131 deposition in Poland after the Chernobyl accident)
  Z. Pietrzak-Flis (Central Laboratory of Radiation Protection, Warszawa, Poland), P. Krajewski (Central Laboratory of Radiation Protection, Warszawa, Poland), I. Radwan (Central Laboratory of Radiation Protection, Warszawa, Poland)
- Zastosowanie obliczeń modelowych programu „SAVEC" dla przechodzenia Cs-137 z gleby do żywności konsumowanej przez ludność Polski (SAVEC application for Cs-137 transfer from soil to food products consumed by Polish population)
  P. Krajewski (Central Laboratory of Radiation Protection, Warszawa, Poland)

Section: ZASTOSOWANIE TECHNIK JĄDROWYCH W OCHRONIE ŚRODOWISKA I NAUKACH O ZIEMI (APPLICATION OF NUCLEAR TECHNIQUES IN ENVIRONMENTAL PROTECTION AND EARTH SCIENCE)

- Zastosowanie spektrometrii alfa w badaniach środowiska (Application of alpha spectrometry in environmental studies)
  B. Skwarzec (University of Gdańsk, Poland)
- Pomiar składu izotopowego strumienia glebowego dwutlenku węgla do atmosfery (Measurements of flux and isotopic composition of soil carbon dioxide)
  Z. Gorczyca (Academy of Mining and Metallurgy, Kraków, Poland), K. Różański (Academy of Mining and Metallurgy, Kraków, Poland), T. Kuc (Academy of Mining and Metallurgy, Kraków, Poland)
- Zastosowanie technologii oczyszczania wód kopalnianych w wyrobiskach podziemnych na przykładzie KWK „Piast" (Application of the underground treatment of mine waters in underground galleries in "Piast" mine)
  S. Chałupnik (Central Mining Institute, Katowice, Poland), M. Wysocka (Central Mining Institute, Katowice, Poland)
- Wykorzystanie membran ceramicznych do oczyszczania roztworów promieniotwórczych (The use of ceramic membranes for radioactive solution purification)

G. Zakrzewska-Trznadel (Institute of Nuclear Chemistry and Technology, Warszawa, Poland)

- Badanie rozpływu zanieczyszczeń w rzekach meandrujących o nieuregulowanym korycie (Study of effluent transport in meandring rivers with unregulated bed)
  A. Owczarczyk (Institute of Nuclear Chemistry and Technology, Warszawa, Poland), A. Dobrowolski (Institute of Nuclear Chemistry and Technology, Warszawa, Poland)
- Skład izotopowy głównych gazów cieplarnianych (CH_4, CO_2) w atmosferze Polski południowej (Isotopic composition of the major greenhouse gases (CH_4, CO_2) in the atmosphere of southern Poland)
  T. Kuc (Academy of Mining and Metallurgy, Kraków, Poland), J.M. Nęcki (Academy of Mining and Metallurgy, Kraków, Poland), M. Zimnoch (Academy of Mining and Metallurgy, Kraków, Poland)

Section: DETEKTORY I APARATURA POMIAROWA (DETECTORS AND MEASURING DEVICES)

- Miernik mocy dawki promieniowania ^{106}Ru oraz ^{125}I (^{106}Ru oraz ^{125}I radiation doserate gauge)
  B. Machaj (Institute of Nuclear Chemistry and Technology, Warszawa, Poland), E. Świstowski (Institute of Nuclear Chemistry and Technology, Warszawa, Poland), Do Hoang Cuong (Institute of Nuclear Chemistry and Technology, Warszawa, Poland)
- Oznaczanie zawartości popiołu w węglu metodą rozpraszania w przód niskoenergetycznego promieniowania gamma (Determination of ash content in coal by the forward-scattering method of low-energy gamma radiation)
  B. Czerw (Research and Development for Electrical Engineering and Automation in Mining EMAG, Katowice, Poland), T. Sikora (Research and Development for Electrical Engineering and Automation in Mining EMAG, Katowice, Poland)
- Fluorescencja rentgenowska w zastosowaniu przemysłowym (Some industrial applications of XRF spectrometry)
  R. Jabłoński (Technical Servis Works Ltd, Milanówek, Poland)
- Lampa rentgenowska ze strumieniem 4π (X-ray tube with 4π flux)
  M. Traczyk (Andrzej Sołtan Institute for Nuclear Studies, Świerk, Poland), W. Straś (Andrzej Sołtan Institute for Nuclear Studies, Świerk, Poland), M. Słapa (Andrzej Sołtan Institute for Nuclear Studies, Świerk, Poland)
- Ruchome Laboratorium Spektrometryczne (Mobile spectrometric laboratory)
  K. Isajenko (Central Laboratory of Radiation Protection, Warszawa, Poland), P. Lipiński (Central Laboratory of Radiation Protection, Warszawa, Poland), W. Bekiert (Central Laboratory of Radiation Protection, Warszawa, Poland)

Section: TECHNOLOGIE RADIACYJNE (RADIATION TECHNOLOGIES)

- Instalacja przemysłowa do czyszczenia gazów spalinowych przy pomocy wiązki elektronów w EC POMORZANY (Industrial plant for flue gas cleaning with use of electron beam at the POMORZANY power plant)
  A.G. Chmielewski (Institute of Nuclear Chemistry and Technology, Warszawa, Poland), B. Tymiński (Institute of Nuclear Chemistry and Technology, Warszawa, Poland), E. Iller (Institute of Nuclear Chemistry and Technology, Warszawa, Poland), Z. Zimek (Institute of Nuclear Chemistry and Technology, Warszawa, Poland), J. Licki (Institute of Atomic Energy, Świerk, Poland), R. Kostrzewski (Power Station DOLNA ODRA, Poland), L. Sobolewski (Power Plant POMORZANY, Szczecin, Poland), J. Cybulski (Energomontaż, Opole, Poland)
- System monitoringu i sterowania przemysłową instalacją odsiarczania i odazotowania spalin przy użyciu wiązki elektronów z akceleratora (Monitoring and control system of industrial installation for desulphurisation and denitrification of flue gas using the electron beam from accelerator)
  J. Licki (Institute of Atomic Energy, Świerk, Poland), A.G. Chmielewski (Institute of Nuclear Chemistry and Technology, Warszawa, Poland), E Iller (Institute of Nuclear Chemistry and Technology, Warszawa, Poland), B. Tymiński (Institute of Nuclear Chemistry and Technology, Warszawa, Poland), J. Mazurek (Institute of Nuclear Chemistry and Technology, Warszawa, Poland), L. Sobolewski (Power Plant POMORZANY, Szczecin, Poland)
- Prognozowanie skutków sanitarnych zastosowania przypraw niedekontaminowanych i dekontaminowanych radiacyjnie w artykułach spożywczych (Prognosis of the application spices, non-decontaminated and decontaminated by irradiation on the sanitary effect foodstuffs)
  W. Migdał (Institute of Nuclear Chemistry and Technology, Warszawa, Poland), H.B. Owczarczyk, (Institute of Nuclear Chemistry and Technology, Warszawa, Poland)
- Metody wykrywania napromieniowania żywności rozwijane w IChTJ (Detection methods for irradiated foods developed in the INCT)
  W. Stachowicz (Institute of Nuclear Chemistry and Technology, Warszawa, Poland), K. Malec-Czechowska (Institute of Nuclear Chemistry and Technology, Warszawa, Poland), A.M. Dancewicz (Institute of Nuclear Chemistry and Technology, Warszawa, Poland), Z. Szot (Institute of Nuclear Chemistry and Technology, Warszawa, Poland), G. Strzelczak (Institute of Nuclear Chemistry and Technology, Warszawa, Poland), K. Lehner (Institute of Nuclear Chemistry and Technology, Warszawa, Poland)

- Trawienie chemiczne wybranych folii polimerowych naświetlanych wiązką ciężkich jonów i wiązką wysokoenergetycznych elektronów (Chemical etching of some polymeric films irradiated with heavy ion beam and high-energy electron beam)

  D. Wawszczak (Institute of Nuclear Chemistry and Technology, Warszawa, Poland), M. Buczkowski (Institute of Nuclear Chemistry and Technology, Warszawa, Poland), B. Sartowska (Institute of Nuclear Chemistry and Technology, Warszawa, Poland), W. Starosta (Institute of Nuclear Chemistry and Technology, Warszawa, Poland)

- Optymalizacja parametrów technicznych i ekonomicznych sieciowanych radiacyjnie polietylenowych wyrobów termokurczliwych (Optimization of technical and economical parameters of thermoshrinkable products made of polyethylene modified by radiation)

  I. Legocka (Institute of Nuclear Chemistry and Technology, Warszawa, Poland), Z. Zimek (Institute of Nuclear Chemistry and Technology, Warszawa, Poland), A. Woźniak (Institute of Nuclear Chemistry and Technology, Warszawa, Poland), K. Mirkowski (Institute of Nuclear Chemistry and Technology, Warszawa, Poland), A. Nowicki (Institute of Nuclear Chemistry and Technology, Warszawa, Poland)

Section: ZASTOSOWANIE TECHNIK JĄDROWYCH W BIOLOGII I MEDYCYNIE (APPLICATION OF NUCLEAR TECHNIQUES IN BIOLOGY AND MEDICINE)

- Ocena dawki pochłoniętej w diagnostyce medycznej radioizotopowej i rentgenowskiej (Estimation of absorbed dose in medical diagnostics with use of radioisotope and X-rays)

  M. Wasilewska-Radwańska (Academy of Mining and Metallurgy, Kraków, Poland), A. Stępień (Military Clinic Hospital, Kraków, Poland)

- Rentgenowska analiza fluorescencyjna w badaniach tkanki mózgu i płynów ustrojowych człowieka (X-ray fluorescence analysis in application for study of human brain tissue and body fluids)

  M. Boruchowska (Academy of Mining and Metallurgy, Kraków, Poland), M. Lankosz (Academy of Mining and Metallurgy, Kraków, Poland), D. Adamek (Jagiellonian University Medical College, Kraków, Poland), B. Ostachowicz (Academy of Mining and Metallurgy, Kraków, Poland), J. Ostachowicz (Academy of Mining and Metallurgy, Kraków, Poland), B. Tomik (Jagiellonian University Medical College, Kraków, Poland)

- Dozymetria biologiczna do rekonstrukcji dawek pochłoniętych w wypadkach radiacyjnych w radioterapii (Biological dosimetry for the reconstruction of doses absorbed during accidents in radiotherapy)

  A. Wójcik (Institute of Nuclear Chemistry and Technology, Warszawa, Poland; Świętokrzyska Academy, Kielce, Poland), G. Stephan (Bundesampt fuer Strahlenschutz, Monachium, Niemcy), S. Sommer (Institute of Nuclear Chemistry and Technology, Warszawa, Poland), W. Urbanik (Wrocław University of Economics, Poland), P. Kukołowicz (Holycross Cancer Center, Kielce, Poland) T. Kuszewski (Holycross Cancer Center, Kielce, Poland), S. Góźdź (Holycross Cancer Center, Kielce, Poland)

- Malowanie chromosomów i przedwczesna kondensacja chromatyny – nowe metody dozymetrii biologicznej (Chromosome painting and prematurely condensed chromosomes (PCC) – new methods of biological dosimetry)

  S. Sommer (Institute of Nuclear Chemistry and Technology, Warszawa, Poland), M. Wojewódzka (Institute of Nuclear Chemistry and Technology, Warszawa, Poland), I. Buraczewska (Institute of Nuclear Chemistry and Technology, Warszawa, Poland), G. Kobiałko (Institute of Nuclear Chemistry and Technology, Warszawa, Poland), J. Pontek (Institute of Nuclear Chemistry and Technology, Warszawa, Poland), I. Szumiel (Institute of Nuclear Chemistry and Technology, Warszawa, Poland), A. Wójcik (Institute of Nuclear Chemistry and Technology, Warszawa, Poland)

Section: ZASTOSOWANIE ZNACZNIKÓW PROMIENIOTWÓRCZYCH (APPLICATION OF RADIOTRACERS)

- Planowanie pomiaru prędkości przepływu mieszanin wielofazowych w rurociągach (Design of multiphase flow velocity measurement in pipes)

  E. Nowak (Academy of Mining and Metallurgy, Kraków, Poland), L. Petryka (Academy of Mining and Metallurgy, Kraków, Poland)

- Badania przepływów wielofazowych z zastosowaniem znaczników promieniotwórczych (Radiotracer applications for analysis of multiphase flows)

  R. Kębłowski (Academy of Mining and Metallurgy, Kraków, Poland), L. Petryka (Academy of Mining and Metallurgy, Kraków, Poland)

- Doświadczenia z izotopowej kontroli szczelności obiektów technologicznych – techniczne i ekonomiczne uzasadnienie jej stosowania (Experience in isotope leak-proof control of engineering objects – technical and economical aspects)

  J. Kraś (Institute of Nuclear Chemistry and Technology, Warszawa, Poland), L. Waliś (Institute of Nuclear Chemistry and Technology, Warszawa, Poland), S. Myczkowski (Institute of Nuclear Chemistry and Technology, Warszawa, Poland), A. Kalicki (Institute of Nuclear Chemistry and Technology, Warszawa, Poland)

POSTER SESSION

TECHNOLOGIE RADIACYJNE (RADIATION TECHNOLOGIES)

- Wykrywanie napromieniowania składników przyprawowych zawartych w niektórych produktach żywnościowych (Detection of radiation treatment in spices, the components of some foodstuffs)
  K. Malec-Czechowska (Institute of Nuclear Chemistry and Technology, Warszawa, Poland), W. Stachowicz (Institute of Nuclear Chemistry and Technology, Warszawa, Poland)
- Radiacyjna pasteryzacja liofilizatów roślinnych i zwierzęcych (Radiation decontamination of meat lyophilized products)
  W. Migdał (Institute of Nuclear Chemistry and Technology, Warszawa, Poland), H.B. Owczarczyk (Institute of Nuclear Chemistry and Technology, Warszawa, Poland)
- Usuwanie organicznych zanieczyszczeń gazowych przy użyciu wiązki elektronów (Electron beam removal of gaseous organic pollutants)
  A.G. Chmielewski (Institute of Nuclear Chemistry and Technology, Warszawa, Poland), Y. Sun (Institute of Nuclear Chemistry and Technology, Warszawa, Poland), A. Ostapczuk (Institute of Nuclear Chemistry and Technology, Warszawa, Poland), J. Licki (Institute of Atomic Energy, Świerk, Poland), Z. Zimek (Institute of Nuclear Chemistry and Technology, Warszawa, Poland), S. Bułka (Institute of Nuclear Chemistry and Technology, Warszawa, Poland)
- Zastosowanie promieniowania jonizującego do degradacji zanieczyszczeń organicznych w wodach i ściekach (Application of ionizing radiation for degradation of organic pollutants in waters and wastes)
  P. Drzewicz (Institute of Nuclear Chemistry and Technology, Warszawa, Poland), A. Bojanowska-Czajka (Institute of Nuclear Chemistry and Technology, Warszawa, Poland), P. Panta (Institute of Nuclear Chemistry and Technology, Warszawa, Poland), W. Głuszewski (Institute of Nuclear Chemistry and Technology, Warszawa, Poland), G. Nałęcz-Jawecki (Medical University of Warsaw, Poland), J. Sawicki (Medical University of Warsaw, Poland), M. Trojanowicz (Institute of Nuclear Chemistry and Technology, Warszawa, Poland)
- Radiacyjna intensyfikacja sektora rolno-spożywczego (Radiative intensification of agricultural-alimentary sector)
  S. Bachman (Technical University of Łódź, Poland), M. Pietrzak (Technical University of Łódź, Poland), A. Żegota (Technical University of Łódź, Poland)
- Walidacja procesu napromienienia w stacji sterylizacji radiacyjnej sprzętu medycznego i przeszczepów (Validation of sterilization by irradiation at the pilot plant of radiation sterilization of medical devices allografts)
  Z. Zimek (Institute of Nuclear Chemistry and Technology, Warszawa, Poland), I. Kałuska (Institute of Nuclear Chemistry and Technology, Warszawa, Poland)
- Obróbka radiacyjna jako unikatowa metoda modyfikacji polimerów (Radiation processing as an unique method of modification of properties of polymers)
  W. Głuszewski (Institute of Nuclear Chemistry and Technology, Warszawa, Poland), Z.P. Zagórski (Institute of Nuclear Chemistry and Technology, Warszawa, Poland)
- Radiacyjna modyfikacja właściwości materiałów (Radiation modification of materials properties)
  P. Panta (Institute of Nuclear Chemistry and Technology, Warszawa, Poland), W. Głuszewski (Institute of Nuclear Chemistry and Technology, Warszawa, Poland)
- Dozymetria dawek mniejszych i większych od dawek sterylizacyjnych (Dose measurements below and above the sterilization doses)
  T. Bryl-Sandelewska (Institute of Nuclear Chemistry and Technology, Warszawa, Poland), P. Panta (Institute of Nuclear Chemistry and Technology, Warszawa, Poland)
- Zmiany morfologii i niektórych właściwości mechanicznych wybranych gatunków stali po modyfikacji intensywnymi impulsami plazmowymi (High intensity pulsed plasma beams modification of surface morphology and mechanical properties of steels)
  B. Sartowska (Institute of Nuclear Chemistry and Technology, Warszawa, Poland), J. Piekoszewski (Institute of Nuclear Chemistry and Technology, Warszawa, Poland), L. Waliś (Institute of Nuclear Chemistry and Technology, Warszawa, Poland), J. Stanisławski (Andrzej Sołtan Institute for Nuclear Studies, Świerk, Poland)
- EPR-dozymetria w radiacyjnej obróbce żywności (EPR-dosimetry for radiation processing of food)
  Z. Peimel-Stuglik (Institute of Nuclear Chemistry and Technology, Warszawa, Poland), S. Fabisiak (Institute of Nuclear Chemistry and Technology, Warszawa, Poland)
- Wykorzystanie mikroskopii elektronowej do badania wewnętrznej struktury dozymetrów alaninowo-polimerowych (The use of electron microscopy to study alanine-polymer dosimeter microstructure)
  Z. Peimel-Stuglik (Institute of Nuclear Chemistry and Technology, Warszawa, Poland), S. Fabisiak (Institute of Nuclear Chemistry and Technology, Warszawa, Poland)
- Radiacyjna degradacja różnych rodzajów mas celulozowych z przeznaczeniem do wytwarzania pochodnych (Electron beam processing technology for modification of different types of cellulose pulps for production of derivaties)

A. Kukiełka (Institute of Nuclear Chemistry and Technology, Warszawa, Poland), E. Iller (Institute of Nuclear Chemistry and Technology, Warszawa, Poland), H. Stupińska (Pulp and Paper Research Institute, Łódź, Poland), W. Mikołajczyk (Institute of Chemical Fibres, Łódź, Poland), P. Starostka (Institute of Chemical Fibres, Łódź, Poland)

- Radiation-induced crosslinking of cellulose ethers
  R.A. Wach (Gunma University, Japan), H. Mitomo (Gunma University, Japan), F. Yoshii (Takasaki Radiation Chemistry Research Establishment, JAERI, Japan), T. Kume (Gunma University, Japan)

RADON W ŚRODOWISKU (RADON IN ENVIRONMENT)

- Kalibracyjne komory radonowe w Instytucie Fizyki Jądrowej im. Henryka Niewodniczańskiego (Calibration radon chambers in H. Niewodniczański Institute of Nuclear Physics)
  K. Kozak (H. Niewodniczański Institute of Nuclear Physics, Kraków, Poland), J. Łoskiewicz (H. Niewodniczański Institute of Nuclear Physics, Kraków, Poland), J. Bogacz (H. Niewodniczański Institute of Nuclear Physics, Kraków, Poland), J. Swakoń (H. Niewodniczański Institute of Nuclear Physics, Kraków, Poland), J. Mazur (H. Niewodniczański Institute of Nuclear Physics, Kraków, Poland), P. Olko (H. Niewodniczański Institute of Nuclear Physics, Kraków, Poland), M. Janik (H. Niewodniczański Institute of Nuclear Physics, Kraków, Poland), T. Zdziarski (H. Niewodniczański Institute of Nuclear Physics, Kraków, Poland), R. Haber (H. Niewodniczański Institute of Nuclear Physics, Kraków, Poland)
- Wpływ parametrów gleby na transport radonu z gleby do budynku (Influence of the soil parameters on radon transport from soil to house)
  M. Janik (H. Niewodniczański Institute of Nuclear Physics, Kraków, Poland)
- Aparatura do pomiaru stężenia radonu w powietrzu (Radiometers for radon concentration on air)
  J. Bartak (Institute of Nuclear Chemistry and Technology, Warszawa, Poland), B. Machaj (Institute of Nuclear Chemistry and Technology, Warszawa, Poland), J.P. Pieńkos (Institute of Nuclear Chemistry and Technology, Warszawa, Poland)

ZASTOSOWANIE TECHNOLOGII JĄDROWYCH W OCHRONIE ŚRODOWISKA I NAUKACH O ZIEMII (APPLICATION OF NUCLEAR TECHNIQUES IN ENVIRONMENTAL PROTECTION AND EARTH SCIENCE)

- Rutynowe monitorowanie zanieczyszczeń atmosferycznych za pomocą INAA (Routine monitoring of the air pollution with INAA)
  Z. Szopa (Institute of Nuclear Chemistry and Technology, Warszawa, Poland), K. Kulisa (Institute of Nuclear Chemistry and Technology, Warszawa, Poland), R. Dybczyński (Institute of Nuclear Chemistry and Technology, Warszawa, Poland)
- Stężenie i skład izotopowy metanu atmosferycznego w Wałbrzyskim Okręgu Węglowym (Concentration and isotope composition of atmospheric methane in the Wałbrzych coal district)
  A. Korus (Academy of Mining and Metallurgy, Kraków, Poland), M. Kotarba (Academy of Mining and Metallurgy, Kraków, Poland), J. Nęcki (Academy of Mining and Metallurgy, Kraków, Poland)
- Badanie sorpcji wybranych znaczników promieniotwórczych na iłach i iłowcach solnych (Study of selected radiotracer sorption on clays and salt claystones)
  J. Banaszczuk (Academy of Mining and Metallurgy, Kraków, Poland), A. Ochoński (Academy of Mining and Metallurgy, Kraków, Poland)
- Izotopy uranu ^{234}U i ^{238}U w środowisku południowego Bałtyku (Uranium ^{234}U and ^{138}U isotopes in the southern Baltic environment)
  A. Boryło (University of Gdańsk, Poland), B. Skwarzec (University of Gdańsk, Poland)
- Radioaktywne papierosy (The radioactive cigarettes)
  J. Ulatowski (University of Gdańsk, Poland), B. Skwarzec (University of Gdańsk, Poland)
- Bilans plutonu $^{239+240}Pu$ w Zatoce Gdańskiej i Basenie Gdańskim (Plutonium $^{239+240}Pu$ inventories in the Gdańsk bay and Gdańsk basin)
  D. Strumińska (University of Gdańsk, Poland), M. Prucnal (University of Gdańsk, Poland), B. Skwarzec (University of Gdańsk, Poland)
- Wykorzystanie badań hydrochemicznych, pomiarów trytu i izotopów stabilnych do oceny wpływu kopalni odkrywkowej na środowisko (Application of hydrochemical and tritium content measurements as well as stable isotope ratios for assessment of strip mine impact on the environment)
  W. Sołtyk (Institute of Nuclear Chemistry and Technology, Warszawa, Poland), J. Walendziak (Institute of Nuclear Chemistry and Technology, Warszawa, Poland), A. Owczarczyk (Institute of Nuclear Chemistry and Technology, Warszawa, Poland)

DETEKTORY I APARATURA (DETECTORS AND MEASURING DEVICES)

- Wizualizacja danych pomiarowych przy użyciu programu LabVIEW miernika zapylenia powietrza AMIZ 2000 (Application of the LabView package for representation of measurement data from airborne dust monitor AMIZ 2000)
  A. Jakowiuk (Institute of Nuclear Chemistry and Technology, Warszawa, Poland)

- Zestaw do radioterapii igłą fotonową (A set radiotherapy with foton needle)
  M. Słapa (Andrzej Sołtan Institute for Nuclear Studies, Świerk, Poland), J. Dora (Andrzej Sołtan Institute for Nuclear Studies, Świerk, Poland), M. Harat (Andrzej Sołtan Institute for Nuclear Studies, Świerk, Poland), P. Sokal (Andrzej Sołtan Institute for Nuclear Studies, Świerk, Poland), W. Straś (Andrzej Sołtan Institute for Nuclear Studies, Świerk, Poland), M. Traczyk (Andrzej Sołtan Institute for Nuclear Studies, Świerk, Poland)
- Urządzenie do zbierania i przetwarzania wyników pomiarów radiometrycznych realizowanych w warunkach przemysłowych i terenowych (An instrument for collecting and processing data from radiometric experiments carried out in field and industrial conditions)
  J. Mirowicz (Institute of Nuclear Chemistry and Technology, Warszawa, Poland), A. Owczarczyk (Institute of Nuclear Chemistry and Technology, Warszawa, Poland), J. Pieńkos (Institute of Nuclear Chemistry and Technology, Warszawa, Poland), E. Świstowski (Institute of Nuclear Chemistry and Technology, Warszawa, Poland), P. Urbański (Institute of Nuclear Chemistry and Technology, Warszawa, Poland)

ZASTOSOWANIE TECHNIK RADIACYJNYCH W BIOLOGII I MEDYCYNIE (APPLICATION OF NUCLEAR TECHNIQUES IN BIOLOGY AND MEDICINE)

- Badania porównawcze technik XRF i PIXE w zastosowaniu do analizy materiałów organicznych (Comparative study of XRF and PIXE techniques in application for analysis of organic materials)
  M. Boruchowska (Academy of Mining and Metallurgy, Kraków, Poland), M. Lankosz (Academy of Mining and Metallurgy, Kraków, Poland), J. Ostachowicz (Academy of Mining and Metallurgy, Kraków, Poland), M. Jaskóła (Andrzej Sołtan Institute for Nuclear Studies, Świerk, Poland), A. Korman (Andrzej Sołtan Institute for Nuclear Studies, Świerk, Poland), D. Adamek (Jagiellonian University Medical College, Kraków, Poland)
- Badania nad radiofarmaceutykiem do diagnozowania stanów zapalnych z wykorzystaniem peptydu antybakteryjnego znakowanego technetem-99m (Investigation of technetium-99m labelled infection imaging radiopharmaceutical based on antibacterial peptide)
  E. Zakrzewska (Radioisotope Centre POLATOM, Świerk, Poland), R. Mikołajczak (Radioisotope Centre POLATOM, Świerk, Poland), A. Markiewicz (Radioisotope Centre POLATOM, Świerk, Poland), W. Zulczyk (Radioisotope Centre POLATOM, Świerk, Poland), B. Górska (Radioisotope Centre POLATOM, Świerk, Poland), E. Byszewska-Szpocińska (Radioisotope Centre POLATOM, Świerk, Poland)
- Zastosowanie sorbentów naturalnych i półsyntetycznych do dekontaminacji mięsa pochodzącego od zwierząt skażonych Cs-137 (Application of natural and semi-synthetic sorbents for decontamination of meat from animals contaminated by Cs-137)
  J. Gaweł (Military Institute of Hygiene and Epidemiology, Puławy, Poland), B. Osiak (Military Institute of Hygiene and Epidemiology, Puławy, Poland), M. Niemcewicz (Military Institute of Hygiene and Epidemiology, Puławy, Poland)
- Badania nad otrzymaniem znaczników ^{125}I – gastryna i ^{125}I – minigastryna do zastosowania w diagnostyce medycznej (The preparation of ^{125}I – gastrin and ^{125}I – minigastrin for medical diagnostics)
  E. Byszewska-Szpocińska (Radioisotope Centre POLATOM, Świerk, Poland), A. Markiewicz (Radioisotope Centre POLATOM, Świerk, Poland)

TECHNIKI JĄDROWE W BADANIACH ZABYTKÓW (NUCLEAR TECHNIQUES IN CULTURAL HERITAGE STUDIES)

- Techniki jądrowe przed konserwacją obrazów (Nuclear techniques before conservation of paintings)
  E. Pańczyk (Institute of Nuclear Chemistry and Technology, Warszawa, Poland), L. Waliś (Institute of Nuclear Chemistry and Technology, Warszawa, Poland), A. Kalicki (Institute of Nuclear Chemistry and Technology, Warszawa, Poland), L. Rowińska (Institute of Nuclear Chemistry and Technology, Warszawa, Poland)
- Śląski warsztat malarski tzw. Mistrza lat 1486/87 w świetle badań bieli ołowianej metodą neutronowej analizy aktywacyjnej (Silesian workshop of master painter 1486/87 in the light of studies on lead white by means of neutron activation analysis)
  J. Flik (Nicolaus Copernicus University, Toruń, Poland), J. Olszewska-Świetlik (Nicolaus Copernicus University, Toruń, Poland) L. Waliś (Institute of Nuclear Chemistry and Technology, Warszawa, Poland), E. Pańczyk (Institute of Nuclear Chemistry and Technology, Warszawa, Poland)
- Wykorzystanie promieniowania Am-241 w diagnostyce zachowania podobrazi drewnianych (Assessment of the painting support based on irradiation Am-241)
  P. Mańkowski (Warsaw Agricultural University, Warszawa, Poland), S. Krzosek (Warsaw Agricultural University, Warszawa, Poland), W. Dzbeński (Warsaw Agricultural University, Warszawa, Poland)
- Technika radiacyjna w konserwacji obiektów zabytkowych – osiągnięcia w Polsce (Radiation technique in conservation of antique objects – achievement in Poland)
  J. Perkowski (Technical University of Łódź, Poland)

AKCELERATORY (ACCELERATORS)

- Kolimator akceleratora 6/15 MeV (Collimator for 6/15 accelerator)
  K. Gryn (Andrzej Sołtan Institute for Nuclear Studies, Świerk, Poland), R. Hornung (Andrzej Sołtan Institute for Nuclear Studies, Świerk, Poland), L. Kotulski (Andrzej Sołtan Institute for Nuclear Studies, Świerk, Poland), J. Olszewski (Andrzej Sołtan Institute for Nuclear Studies, Świerk, Poland)
- Koncepcja programu sterowania akceleratora 6/15 MeV (Concept of control system of a 6/15 accelerator)
  J. Pracz (Andrzej Sołtan Institute for Nuclear Studies, Świerk, Poland), R. Hornung (Andrzej Sołtan Institute for Nuclear Studies, Świerk, Poland), E. Jankowski (Andrzej Sołtan Institute for Nuclear Studies, Świerk, Poland)
- Zespół grupująco-przyspieszający intensywnej wiązki elektronów o energii 2 MeV jako iniektor akceleratora wysokiej mocy (2 MeV bunching section of intensive electron beam as an injector for high power electron accelerator)
  M. Pachan (Andrzej Sołtan Institute for Nuclear Studies, Świerk, Poland), W. Maciszewski (Andrzej Sołtan Institute for Nuclear Studies, Świerk, Poland), S. Kuliński (Andrzej Sołtan Institute for Nuclear Studies, Świerk, Poland), J. Bigolas (Andrzej Sołtan Institute for Nuclear Studies, Świerk, Poland), A. Kucharczyk (Andrzej Sołtan Institute for Nuclear Studies, Świerk, Poland), E. Pławski (Andrzej Sołtan Institute for Nuclear Studies, Świerk, Poland)
- Formowanie krótkich impulsów w akceleratorze liniowym elektronów (Short pulse shaping in linear electron accelerator)
  Z. Dźwigalski (Institute of Nuclear Chemistry and Technology, Warszawa, Poland), Z. Zimek (Institute of Nuclear Chemistry and Technology, Warszawa, Poland)
- Układ do pomiaru charakterystyki widmowej wiązki elektronów (Secondary electrons monitor for continuous electron energy measurements in UHF linac)
  S. Bułka (Institute of Nuclear Chemistry and Technology, Warszawa, Poland), J. Mirkowski (Institute of Nuclear Chemistry and Technology, Warszawa, Poland), K. Roman (Institute of Nuclear Chemistry and Technology, Warszawa, Poland), Z. Zimek (Institute of Nuclear Chemistry and Technology, Warszawa, Poland)

2. ACCELERATORS FOR RADIATION PROCESSING – TECHNICAL MEETING, 15-18 SEPTEMBER 2002, WARSZAWA, POLAND

Organized by the Institute of Nuclear Chemistry and Technology

Organizing Committee: Prof. A.G. Chmielewski, Ph.D., D.Sc., Z. Zimek, Ph.D., S. Bułka, M.Sc.

SCIENTIFIC PART

- General design of the facility for flue gas treatment
  A.G. Chmielewski (Institute of Nuclear Chemistry and Technology, Warszawa, Poland)
- Accelerators for radiation processing (design, installation, exploitation)
  Z. Zimek (Institute of Nuclear Chemistry and Technology, Warszawa, Poland)
- Program on the development of a Laboratory Scale Electron Beam Machine (EBM) facility
  R.H. Razali (Malaysian Institute for Nuclear Technology Research, Bangi, Malaysia)
- Accelerators installed in the INCT laboratory, pilot plant, industrial facilities
  Z. Zimek (Institute of Nuclear Chemistry and Technology, Warszawa, Poland)

PRACTICAL PART

- The INCT accelerator facilities demonstration: LAE 13/9, LAE 10, ELEKTRONIKA 10/10, AS 2000, IŁU-6
- Visiting of the pilot plant facility at the Warsaw Electro-Power Station "Kawęczyn"
- Visiting of the accelerators manufacturer in Świerk (HF accelerator, HV accelerator, accelerator components)

3. THE FINAL REGIONAL WORKSHOP OF IAEA TC PROJECT RER/2/004 "QUALITY ASSURANCE AND QUALITY CONTROL OF NUCLEAR ANALYTICAL TECHNIQUES", 18-22 NOVEMBER 2002, WARSZAWA, POLAND

Organized by the Institute of Nuclear Chemistry and Technology and the International Atomic Energy Agency

Organizer: Halina Polkowska-Motrenko, Ph.D.

SCIENTIFIC PART – lectures

- The "Main Group Elements" of marketing
  R. Jakobi (MBA, Zurich, Switzerland)
- Traditional cost analysis
  P. Vermaercke (SCK-CEN, the Belgium Nuclear Research Centre, Mol, Belgium)
- Quality policy deployment
  P. Vermaercke (SCK-CEN, the Belgium Nuclear Research Centre, Mol, Belgium)
- Towards a Total Quality Management and EFQM
  P. Vermaercke (SCK-CEN, the Belgium Nuclear Research Centre, Mol, Belgium)
- Preparation of PR material for clients
  A. Bourykine (International Atomic Energy Agency, Vienna, Austria)
- Creating a Web Page, demonstration and group training
  A. Bourykine (International Atomic Energy Agency, Vienna, Austria)

REPORTING A WORK DONE IN THE FRAME OF PROJECT – Individual reports of the participants from: Belarus, Croatia, Estonia, Latvia, Hungary, Poland, Romania, Slovakia, Slovenia, Turkey

4. KONFERENCJA „PROBLEMY SPALANIA ODPADÓW KOMUNALNYCH" (CONFERENCE ON PROBLEMS OF INCINERATION OF MUNICIPAL WASTES), 28 NOVEMBER 2002, WARSZAWA, POLAND

Organized by the Warsaw University of Technology, Plant for Utilization of Solid Municipal Wastes (Warszawa), Technical University of Łódź, Institute of Nuclear Chemistry and Technology

Organizing Committee: M. Obrębska, Ph.D. (Chairman), A. Ostapczuk, M.Sc.

LECTURES

Session I

Chairman: Prof. A.G. Chmielewski, Ph.D., D.Sc. (Institute of Nuclear Chemistry and Technology, Warszawa, Poland; Warsaw University of Technology, Poland)

- ZUSOK jako element warszawskiego systemu gospodarki odpadami (Plant for Utilization of Solid Municipal Wastes as an element of Warsaw management system of wastes)
  J. Kaznowski (Plant for Utilization of Solid Municipal Wastes, Warszawa, Poland)
- Procedury prowadzenia procesu spalania w instalacjach ZUSOK na tle prawa środowiskowego (Procedures for conducting incineration process in the installations of Plant for Utilization of Solid Municipal Wastes in relation to the environmental law)
  J. Naumienko (Plant for Utilization of Solid Municipal Wastes, Warszawa, Poland)
- Instalacje oczyszczania gazów spalinowych ZUSOK a obowiązujące przepisy emisyjne (Plant for Utilization of Solid Municipal Wastes installations for the purification of flue gases in relation to the obligatory emission regulations)
  S. Sochan (Plant for Utilization of Solid Municipal Wastes, Warszawa, Poland)
- Usuwanie dioksyn i furanów – adsorber przeciwprądowy WKV (Removal of dioxins and furans – WKV countercurrent absorber)
  T. Wadas (Plant for Utilization of Solid Municipal Wastes, Warszawa, Poland)
- Zapobieganie odoryzacji powietrza na tle doświadczeń ZUSOK (Prevention of air odorization against the Plant for Utilization of Solid Municipal Wastes experience)
  J. Stępień (Plant for Utilization of Solid Municipal Wastes, Warszawa, Poland)

Session II

Chairman: J. Kaznowski, M.Sc. (Plant for Utilization of Solid Municipal Wastes, Warszawa, Poland)

- Trendy rozwojowe w konstrukcji spalarni odpadów komunalnych (Development trends in the construction of incinerating plants of municipal wastes)
  R. Zarzycki (Technical University of Łódź, Poland)
- Technologie oczyszczania gazów z SO_2, NO_x i HCl (Technologies for purification of gases from SO_2, NO_x and HCl)
  J. Warych (Warsaw University of Technology, Poland)
- Metody usuwania pyłów z gazów spalinowych (Methods for removal of dusts from flue gases)
  L. Gradoń (Warsaw University of Technology, Poland), P. Grzybowski (Warsaw University of Technology, Poland)

- Możliwości zastosowania sieci neuronowych do modelowania i sterowania procesami oczyszczania ścieków i odpadów (The possibility of application of neuron nets to the modelling and controlling of purification processes of sewages and wastes)
  E. Molga (Warsaw University of Technology, Poland)
- Powstawanie i metody ograniczania emisji dioksyn podczas spalania odpadów (Formation of dioxins during incineration of wastes and methods for their limitation)
  G. Wielgosiński (Technical University of Łódź, Poland)

Session III

Chairman: Prof. R. Zarzycki, Ph.D., D.Sc. (Technical University of Łódź, Poland)

- Metody analizy LZO i WWA w próbkach gazowych (Methods of analysis of VOCs and PAH in gaseous samples)
  A. Ostapczuk (Institute of Nuclear Chemistry and Technology, Warszawa, Poland)
- Jednoczesne usuwanie SO_2, NO_x i LZO przy użyciu wiązki elektronów (Simultaneous removal of SO_2, NO_x and VOCs using electron beam irradiation)
  A.G. Chmielewski (Institute of Nuclear Chemistry and Technology, Warszawa, Poland; Warsaw University of Technology, Poland)
- Utylizacja stałych odpadów komunalnych w świetle uregulowań prawnych w Unii Europejskiej (Utilization of solid municipal wastes in relation to the legal regulation in the European Union)
  M. Obrębska (Warsaw University of Technology, Poland)
- Wykorzystanie CFD do analizy procesu spalania w piecach do utylizacji odpadów (Use of CFD to the analysis of combustion process in incinerators for utilization of wastes)
  L. Rudniak (Warsaw University of Technology, Poland)
- Recykling odpadów polietylenowych metodą krakingu katalitycznego (Catalytic cracking of the polyethylene wastes)
  B. Tymiński (Institute of Nuclear Chemistry and Technology, Warszawa, Poland)

VISIT TO THE INSTALLATION FOR INCINERATION OF SOLID MUNICIPAL WASTES (PLANT FOR UTILIZATION OF SOLID MUNICIPAL WASTES) IN WARSAW

Ph.D./D.Sc. THESES IN 2002

Ph.D. THESES

Jakub Dudek, M.Sc.
Badanie mechanizmu działania modyfikatorów palladowego i palladowo-magnezowego stosowanego w atomowej spektroskopii absorpcyjnej z atomizacją w piecu grafitowym (Mechanism of the action of the palladium and palladium-magnesium modifiers in the graphite furnace atomic absorption spectrometry)
supervisor: Prof. Leon Pszonicki, Ph.D., D.Sc.
Institute of Nuclear Chemistry and Technology, 12.12.2002

EDUCATION

Ph.D. PROGRAMME IN CHEMISTRY

The Institute of Nuclear Chemistry and Technology holds a four-year Ph.D. degree programme to graduates of chemical, physical and biological departments of universities, to graduates of medical universities and to engineers in chemical technology and material science.

The main areas of the programme are:

- radiation chemistry and biochemistry,
- chemistry of radioelements,
- isotopic effects,
- radiopharmaceutical chemistry,
- analytical methods,
- chemistry of radicals,
- application of nuclear methods in chemical and environmental research, material science and protection of historical heritage.

The candidates accepted for the forementioned programme can be employed in the Institute. The candidates can apply for a doctorial scholarship. The INCT offers accommodation in 10 rooms in the guesthouse for Ph.D. students not living in Warsaw.

During the four-year Ph.D. programme the students participate in lectures given by senior staff from the INCT, Warsaw University and the Polish Academy of Sciences. In the second year, the Ph.D. students have teaching practice in the Chemistry Department of Warsaw University. Each year the Ph.D. students are obliged to deliver a lecture on topic of his/her dissertation at a seminar. The final requirements for the Ph.D. programme graduates, consistent with the regulation of the Ministry of National Education, are:

- submission of a formal dissertation, summarizing original research contributions suitable for publication;
- final examination and public defense of the dissertation thesis.

In 2002 the following lecture series were organized:

- "Chemistry of Radicals" – Prof. Krzysztof Bobrowski, Ph.D., D.Sc. (Institute of Nuclear Chemistry and Technology);
- "Chemometrics" – Prof. Piotr Urbański, Ph.D., D.Sc. (Institute of Nuclear Chemistry and Technology);
- "Biological Effects of Radiation" – Assoc. Prof. Andrzej Wójcik, Ph.D., D.Sc. (Institute of Nuclear Chemistry and Technology);
- "Radiation and Radical Chemistry" – Prof. Klaus-Dieter Asmus (Notre Dame University, USA and Wiadrina University, Frankfurt/Oder, Germany);
- "Chemistry of Elements" – Prof. Sławomir Siekierski, Ph.D., D.Sc. (Institute of Nuclear Chemistry and Technology)

Most of the students expand their knowledge during a short or long training in numerous renowned European research centres, e.g. European Institute of Transuranium Elements (Karlsruhe, Germany), Philips Cyclotron in Paul Scherrer Institute (Switzerland), Gent University (Belgium), Orsay University (France), Mainz University (Germany), etc.

The qualification interview for the Ph.D. programme takes place in the mid of October. Detailed information can be obtained from:

- Head: Assoc. Prof. Aleksander Bilewicz, Ph.D., D.Sc.
  (phone: (+4822) 811-30-21 ext. 15-98, e-mail: abilewic@orange.ichtj.waw.pl);
- Secretary: Dr. Ewa Gniazdowska
  (phone: (+4822) 811-30-21 ext. 15-96, e-mail: studium@orange.ichtj.waw.pl).

TRAINING OF STUDENTS

Institution	Country	Number of participants	Period
International Atomic Energy Agency	Syria	2	3 months

Institution	Country	Number of participants	Period
International Atomic Energy Agency	Libya	1	1 month
International Atomic Energy Agency	Croatia	1	2 months
International Atomic Energy Agency	Egypt	1	2 months
International Atomic Energy Agency	Kazakhstan	1	3 months
Technical School of Chemistry	Poland (Warszawa)	2	1 month
Academy of Mining and Metallurgy	Poland	6	2 weeks
Warsaw University of Technology, Faculty of Materials Science and Engineering	Poland	4	1 month
Warsaw University of Technology, Faculty of Chemical and Process Engineering	Poland	1	four-day practice
Warsaw University of Technology, Faculty of Electrical Engineering	Poland	2	1 month
Warsaw University of Technology, Faculty of Physics	Poland	14	one-day practice

RESEARCH PROJECTS AND CONTRACTS

RESEARCH PROJECTS GRANTED BY THE POLISH STATE COMMITTEE FOR SCIENTIFIC RESEARCH IN 2002 AND IN CONTINUATION

1. **Investigations in the range of functionalization technology of particle track-etched membranes and their application.**
   supervisor: Assoc. Prof. Tadeusz Żółtowski, Ph.D., D.Sc.
2. **Radiation and photochemically induced radical processes in aromatic carboxylic acids containing thioether group.**
   supervisor: Prof. Krzysztof Bobrowski, Ph.D., D.Sc.
3. **Application of ceramic membranes for liquid low- and medium-level radioactive waste processing.**
   supervisor: Grażyna Zakrzewska-Trznadel, Ph.D.
4. **Decomposition of organic compounds emitted during coal burning with the use of electron beam.**
   supervisor: Prof. Andrzej G. Chmielewski, Ph.D., D.Sc.
5. **Detection of irradiated additives (spices) in foodstuffs.**
   supervisor: Kazimiera Malec-Czechowska, M.Sc.
6. **Multiphase flow dynamics determination by radiotracer and computational fluid dynamics (CFD) methods.**
   supervisor: Jacek Palige, Ph.D.
7. **Estimation of post-irradiation chromosomal translocations in human blood lymphocytes for biological dosimetry purposes with the use of chromosome painting and PCC.**
   supervisor: Prof. Irena Szumiel, Ph.D., D.Sc.
8. **Factors that define sensitivity to oxygen stress: characteristics of new mutants of V79 Chinese hamster cells susceptible to reactive oxygen species.**
   supervisor: Assoc. Prof. Marcin Kruszewski, Ph.D., D.Sc.
9. **Influence of relativistic effect on hydrolytic properties, stabilization of lower oxidation states and $6s^2$ and $6p_{1/2}^2$ lone pair character of the heaviest elements.**
   supervisor: Assoc. Prof. Aleksander Bilewicz, Ph.D., D.Sc.
10. **Catalytic tubular reactor for olefine polymers cracking with distillation products of decomposition.**
    supervisor: Bogdan Tymiński, Ph.D.
11. **Tricarbonyl technetium(I) and rhenium(I) complexes with chelating ligands as radiopharmaceutical precursors.**
    supervisor: Prof. Jerzy Narbutt, Ph.D., D.Sc.
12. **Investigation of the mechanism of human glioma MO59 cells radiosensitisation by inhibitors of signal transduction pathways which are growth factors dependent: influence on DNA double-strand break rejoning and apoptosis.**
    supervisor: Iwona Grądzka, Ph.D.

IMPLEMENTATION PROJECTS GRANTED BY THE POLISH STATE COMMITTEE FOR SCIENTIFIC RESEARCH IN 2002 AND IN CONTINUATION

1. **New Polish certified reference materials of biological origin for inorganic trace analysis: Tea Leaves and Mixture of Polish Herbs.**
   3 T09A 001 99 C/4265
   supervisor: Halina Polkowska-Motrenko, Ph.D.
2. **The Christian art in Egypt. Studies and conservation of Coptic art in the collection of the National Museum in Warsaw.**

1 H01E 002 99 C/4402
supervisor: Prof. Marek Trojanowicz, Ph.D., D.Sc.

3. **An instrument for collecting and processing data from radiometric experiments carried out in field and industrial conditions.**
8 T10 C 061 2000 C/5050
supervisor: Prof. Piotr Urbański, Ph.D., D.Sc.

4. **Manufacturing technology of joints of preisolated pipes for heat transportation.**
7 T08 E 678 2000 C/5023
supervisor: Zbigniew Zimek, Ph.D.

IAEA RESEARCH CONTRACTS IN 2002

1. **Decontamination of herbal raw materials and herbal drugs by irradiation.**
10355/Regular Budget Fund
principal investigator: Assoc. Prof. Wojciech Migdał, Ph.D., D.Sc.

2. **Electron beam treatment of gaseous organic compounds emitted from fossil fuel combustion.**
11093/RO
principal investigator: Prof. Andrzej G. Chmielewski, Ph.D., D.Sc.

3. **Application of ionizing radiation for removal of pesticides from ground waters and wastes.**
12016/Regular Budget Fund
principal investigator: Prof. Marek Trojanowicz, Ph.D., D.Sc.

IAEA TECHNICAL CONTRACTS IN 2002

1. **Industrial scale demonstration plant for electron beam purification of flue gases.**
POL/8/014

2. **Accredited laboratory for the use of nuclear and nuclear-related analytical techniques.**
POL/2/014

EUROPEAN COMMISSION RESEARCH PROJECTS IN 2002

1. **Electron beam for processing of flue gases, emitted in metallurgical processes, for volatile organic compounds removal.**
supervisor: Prof. Andrzej G. Chmielewski, Ph.D., D.Sc.
Programme coordinated by the INCT

2. **Research Training Network: Sulphur radical chemistry of biological significance: the protective and damaging roles of the thiol and thioether radicals.**
principal investigator: Prof. Krzysztof Bobrowski, Ph.D., D.Sc.

OTHER FOREIGN CONTRACTS IN 2002

1. **Analytical and scientific services in support of LANL Actinide Chemistry and Repository Science Program**
Contract with Los Alamos National Laboratory, USA
principal investigator: Prof. Zbigniew Zagórski, Ph.D., D.Sc.

LIST OF VISITORS TO THE INCT IN 2002

1. **Aizava Shiro**, National Institute of Radiation Sciences, Japan, *28.09.-05.10.*
2. **Ali Zakaria**, National Center for Radiation Research and Technology (NCRRT), Cairo, Egypt, *01.07.-27.09.*
3. **Armstrong David**, Department of Chemistry, University of Calgary, Canada, *26-31.08.*
4. **Asmus Klaus-Dieter**, University of Notre Dame, USA, *01-03.03, 19-25.04.*
5. **Bakar Van Ab. Hadi Abu**, Malaysian Institute for Nuclear Technology Research (MINT), Bangi, Malaysia, *15-18.09.*
6. **Baresic Jadranka**, Institute R. Boskovic, Zagreb, Croatia, *04-09.06.*
7. **Bexultanov Zhomart**, Institute of Nuclear Physics, Almaty, Kazakhstan, *08.04.-06.07.*
8. **Cobalt Atlantis**, Institute R. Boskovic, Zagreb, Croatia, *15.09.-14.11.*
9. **Dashouk Elena**, Institute of Radiation Physical and Chemical Problems, Academy of Science of Belarus, Belarus, *12-28.10*
10. **Dermawan Rosli**, Malaysian Institute for Nuclear Technology Research (MINT), Bangi, Malaysia, *15-18.09.*
11. **Dziewinski Jacek**, Los Alamos National Laboratory, University of California, USA, *27.05.-11.06.*
12. **El-Naggar Abdel Wahab**, National Center for Radiation Research and Technology (NCRRT), Cairo, Egypt, *03-06.11.*
13. **Eswayah Abdurrahman**, Tajoura Nuclear Research Center, Libya, *14.01.-17.09.*
14. **Fainchtein Aleksander**, Research and Design Institute ENERGOSTAL, Ukraine, *23.10.-10.11.*
15. **Feng Chunyang**, Institute of Environmental Protection Engineering, China Academy of Engineering Physics, China, *27.11.-26.12.*
16. **Frank Norman**, International Business Consultants, USA, *16-29.11.*
17. **Garcia-Heras Manuel**, Spanish Council for Scientific Research (CSiC), Spain, *21-22.05.*
18. **Ghazaki Zulłafli**, Malaysian Institute for Nuclear Technology Research (MINT), Bangi, Malaysia, *15-18.09.*
19. **Ghazali Abu Bakar Mhd**, Malaysian Institute for Nuclear Technology Research (MINT), Bangi, Malaysia, *15-18.09.*
20. **Goovaerts Etienne**, Ghent University, Belgium, *11-12.04.*
21. **Gryzlov Anatolij**, State Research and Production Corporation TORIJ, Russia, *31.10.-19.11.*
22. **Hashim Siti A'Aisah**, Malaysian Institute for Nuclear Technology Research (MINT), Bangi, Malaysia, *15-18.09.*
23. **Hug Gordon**, University of Notre Dame, USA, *20.02.-03.03.*
24. **Ibrahim Sahab**, Atomic Energy Commission, Damascus, Syria, *13.01.-06.04.*
25. **Ionita Gheorghe**, National Institute of Cryogenics and Isotopic Separation, Rm-Valcea, Romania, *15-20.10.*
26. **Kasztovszky Zsolt**, Department of Nuclear Research, Institute of Isotope and Surface Chemistry, Hungary, *23.09.-05.10.*
27. **Kemp Terence J.**, University of Warwick, Great Britain, *18-22.03.*
28. **Kokubo Tadashi**, Graduate School of Engineering, Kyoto University, Japan, *22-23.07.*
29. **Lazurik Vladymir**, Kharkiv National University, Ukraine, *04-09.02.*
30. **Lyssukhin Sergey**, Institute of Nuclear Physics, Almaty, Kazakhstan, *02-08.06.*
31. **Matar Mohammad Jamal**, Syrian Atomic Energy Commission, Damascus, Syria, *13.05.-12.08.*
32. **Mori Masahiko**, National Institute of Radiation Sciences, Japan, *28.09.-05.10.*
33. **Nichipor Henrieta**, Institute of Radiation Physical and Chemical Problems, Academy of Science of Belarus, Belarus, *10-22.02., 27-28.05, 01-13.12.*
34. **Orelovitch Oleg**, Joint Institute for Nuclear Research, Russia, *12-19.05, 22-26.05.*
35. **Paraskevopoulos Konstantinos**, Solid State Section, Physics Department, Aristotle University of Thessaloniki, Greece, *14-18.09.*
36. **Politovskij Fiodor**, State Research and Production Corporation TORIJ, Russia, *31.10.-19.11.*

37. **Polychroniadis Eustatius**, Solid State Section, Physics Department, Aristotle University of Thessaloniki, Greece, *14-18.09.*
38. **Popov Genadij**, Kharkiv National University, Ukraine, *04-09.02.*
39. **Razali Hamzah**, Malaysian Institute for Nuclear Technology Research (MINT), Bangi, Malaysia, *15-18.09.*
40. **Samiei Mossoud**, International Atomic Energy Agency, United Nations, *16.11.*
41. **Villegas Maria-Angeles**, Spanish Council for Scientific Research (CSiC), Spain, *21-22.05.*
42. **Yamada Hirohisa**, National Institute of Material Science, Japan, *17-22.03.*
43. **Yang Ruizhuang**, Institute of Environmental Protection Engineering, China Academy of Engineering Physics, China, *27.11.-28.12.*
44. **Yatsko Svetlana**, Institute of Radiation Physical and Chemical Problems, Academy of Science of Belarus, Belarus, *12-28.10.*

THE INCT SEMINARS IN 2002

1. Prof. David A. Armstrong (Department of Chemistry, University of Calgary, Canada)
   H atom transfer between carbon-centered and sulfur-centered radicals
2. Marek Danilczuk, M.Sc. (Institute of Nuclear Chemistry and Technology, Warszawa, Poland)
   Badania EPR centrów paramagnetycznych stabilizowanych w zeolitach; małe rodniki i cząstki metaliczne (EPR study of paramagnetic centers in zeolites; small radicals and metallic particles)
3. Małgorzata Derda, M.Sc. (Institute of Nuclear Chemistry and Technology, Warszawa, Poland)
   Oznaczanie stosunków izotopowych siarki w procesie spalania węgla (Determination of sulphur isotope ratio in coal combustion process)
4. Dr. Jan Grodkowski (Institute of Nuclear Chemistry and Technology, Warszawa, Poland)
   Ciecze jonowe – nowy alternatywny rozpuszczalnik w zastosowaniach i badaniach chemicznych (Anionic liquids – new alternative solvent for chemical studies and applications)
5. Dr. Gheorghe Ionita (National Institute of Cryogenics and Isotopic Separation, Rm-Valcea, Romania)
   The assessment of application of hydrophobic catalysts in nuclear and environmental field
6. Prof. Marek Janiak, Ph.D., D.Sc. (Military Institute of Hygiene and Epidemiology, Warszawa, Poland)
   Współczesne zagrożenia bronią jądrową i radiologiczną (Contemporary threat of nuclear and radiologic weapons)
7. Dr. Zsolt Kasztovszky (Institute of Isotope and Surface Chemistry, Hungary Academy of Sciences, Hungary)
   Prompt gamma activation analysis and its applications in archaeometry
8. Prof. Tadashi Kokubo (Department of Material Chemistry, Kyoto University, Japan)
   Novel inorganic materials for biomedical applications
9. Prof. Wacław Kołodziejski, Ph.D., D.Sc. (Faculty of Inorganic Chemistry, Medical Academy in Warsaw, Poland)
   Spektroskopia NMR wysokiej zdolności rozdzielczej w ciele stałym w wybranych zagadnieniach chemii, biologii i medycyny (NMR spectroscopy of high resolution in the solid state in selected fields of chemistry, biology and medicine)
10. Dr. Robert Kołos (Institute of Physical Chemistry, Polish Academy of Sciences, Warszawa, Poland)
    W kosmosie, eksperymentach i obliczeniach nienasycone łańcuchy węglowo-azotowe (Unsaturated carbon-nitrogen chains in the universe, experiments and calculations)
11. Assoc. Prof. Izabela Legocka, Ph.D., D.Sc. (Institute of Nuclear Chemistry and Technology, Warszawa, Poland)
    Zmiany właściwości fizycznych polimerów semi-krystalicznych wywołane promieniowaniem elektronowym (Changes in physical properties of semicrystalline polymers under the influence of electron radiation)
12. Agnieszka Mikołajczuk, M.Sc. (Institute of Nuclear Chemistry and Technology, Warszawa, Poland)
    Równowagowe efekty izotopowe siarki ($^{34}S/^{32}S$) w wybranych układach dwufazowych zawierających SO_2 (Equilibrium sulphur isotope effects in select systems which contain SO_2)
13. Anna Ostapczuk, M.Sc. (Institute of Nuclear Chemistry and Technology, Warszawa, Poland)
    Degradacja wybranych węglowodorów aromatycznych w mieszaninach gazowych pod wpływem wiązki elektronów (Degradation of various aromatic compounds in gaseous mixtures under electron beam)
14. Assoc. Prof. Konstantinos M. Paraskevopoulos (Aristotle University of Thessaloniki, Greece)
    Infrared spectroscopy in the study of wall paintings: the case of two Xth century churches
15. Dariusz Pawlak, M.Sc. (Radioisotope Centre POLATOM, Świerk, Poland)
    Badanie wiązania fosfonowych kompleksów wybranych radionuklidów na hydroapatytach (Bond studies of phosphonic complexes of selected radionuclides fixed on hydroapatites)
16. Joanna B. Perlińska, M.Sc. (Institute of Nuclear Chemistry and Technology, Warszawa, Poland)
    Nanocząsteczki metaliczne w sodalitach: stabilizacja i oddziaływania (Study of small metal particles stabilised in sodalites)

17. Izabela Puchalska, M.Sc. (Radioisotope Centre POLATOM, Świerk, Poland)
    Elektrochemiczne procesy utrwalania radionuklidów stosowanych w źródłach promieniotwórczych do brachyterapii (Electrochemical fixation processes of radionuclides applied in radioactive sources to brachyterapy)
18. Kinga Rudawska, M.Sc. (Institute of Nuclear Chemistry and Technology, Warszawa, Poland)
    Struktury krystalograficzne soli tetra-n-butyloamoniowych z anionami $[MX_4]^-$, gdzie M=Al, Ga, In, Tl, a X=Cl, Br, I (Crystallographic structures of tetra-n-butylammonium salts with MX_4 anions, where M=Al, Ga, In, Tl and X=Cl, Br, I)
19. Wojciech Starosta, M.Sc. (Institute of Nuclear Chemistry and Technology, Warszawa, Poland)
    Krystalochemia związków koordynacyjnych jonów wapnia z ligandami w postaci molekuł niektórych dwukarboksylowych kwasów pirydyny i pirazyny (Crystal chemistry of calcium coordination compounds with some pyridine and pyrazine dicarboxylation ligands)
20. Dr. Marek Strzelec (Institute of Optoelectronics, Military University of Technology, Warszawa, Poland)
    Laserowa renowacja zabytków i dzieł sztuki – udział Instytutu Optoelektroniki WAT w programach europejskich (Laser renovation of monuments of art and art objects – contribution from the Institute of Optoelectronics, Military University of Technology, in European scientific programmes)
21. Yongxia Sun, M.Sc. (Institute of Nuclear Chemistry and Technology, Warszawa, Poland)
    Radiation induced decomposition of selected chlorinated hydrocarbons in gaseous phase
22. Prof. Piotr Urbański, Ph.D., D.Sc. (Institute of Nuclear Chemistry and Technology, Warszawa, Poland)
    6 Program Ramowy Unii Europejskiej (The Sixth Frame Programme of the European Union)
23. Barbara Włodzimirska, M.Sc. (Institute of Nuclear Chemistry and Technology, Warszawa, Poland)
    Wpływ efektu relatywistycznego na własności hydrolityczne kationów ciężkich pierwiastków (Influence of relativistic effect on the hydrolitic properties of the cations of heavy elements)

SEMINARS DELIVERED OUT OF THE INCT IN 2002

1. **Bilewicz Aleksander**

   Badania wpływu efektu relatywistycznego na liczbę koordynacyjną transaktynowców (Influence of relativistic effect on coordination number of transactinides).

   Joint Institute of Nuclear Research, Dubna, Russia, 17.12.2002.

2. **Bilewicz Aleksander**

   Radiopierwiastki i ich niektóre zastosowania (Application of radioelements).

   Polish Nuclear Society, Warsaw University of Technology, Institute of Heat Engineering, Warszawa, Poland, 03.04.2002.

3. **Chmielewski Andrzej Grzegorz**

   Specjalne zastosowania procesów membranowych (Special applications of membrane processes).

   Warsaw University of Technology, Faculty of Chemical and Process Engineering, Warszawa, Poland, 21.05.2002.

4. **Chmielewski Andrzej Grzegorz**

   Wykorzystanie analizy śladowej w badaniach procesów ochrony środowiska (The use of trace analysis for studies of environment protection processes).

   Warsaw University of Technology, Faculty of Chemical and Process Engineering, Warszawa, Poland, 03.12.2002.

5. **Dembiński Wojciech**

   Rynek uranu i paliw jądrowych a cykl paliwowy (The market of uranium and nuclear fuels *vs*. fuel cycles).

   Polish Nuclear Society, Warsaw University of Technology, Institute of Heat Engineering, Warszawa, Poland, 20.03.2002.

6. **Kałuska Iwona**

   Metody obniżania poziomu zanieczyszczeń mikrobiologicznych w surowcach i materiałach pochodzenia naturalnego – metoda radiacyjna (Microbiological decontamination methods of botanical raw materials – radiation method).

   POLFA Scientific Information Centre, Mądralin n. Otwock, Poland, 15.02.2002.

7. **Kałuska Iwona**

   Metody obniżania poziomu zanieczyszczeń mikrobiologicznych w surowcach i materiałach pochodzenia naturalnego – metoda radiacyjna (Microbiological decontamination methods of botanical raw materials – radiation method).

   POLFA Scientific Information Centre, Zakopane, Poland, 09.10.2002.

8. **Kulisa Krzysztof**

   Oznaczanie zawartości SO_2 i NO_x w gazach spalinowych i analiza ekstraktów z popiołów i produktów pochodzących z elektrowni opalanych węglem (Determination of SO_2 and NO_x content in flue gases and analysis of extracts from ashes and products originating from coal combustion power stations).

   Dionex A.G.A. Analytical, Warszawa, Poland, 07.03.2002.

9. **Narbutt Jerzy**

   Hydratacja chelatów metali a równowagi ekstrakcyjne (Hydration of metal chelates and solvent extraction equilibria).

   Poznań University of Technology, Institute of Technology and Chemical Engineering, Poznań, Poland, 13.06.2002.

10. **Narbutt Jerzy**

    Nieorganiczne wymieniacze jonów jako bariery inżynierskie w składowiskach odpadów promieniotwórczych (Inorganic ion exchangers as engineered barriers in nuclear waste repositories).

    Polish Nuclear Society, Warsaw University of Technology, Institute of Heat Engineering, Warszawa, Poland, 10.04.2002.

11. Pogocki Dariusz

Własności redox Met^{35} w neurotoksycznym β-peptydzie Alzheimera. Badania metodami modelowania molekularnego (Redox properties of Met^{35} in neurotoxic Alzheimer β-peptide. Investigations by molecular modeling methods).

Pedagogical University, Institute of Chemistry and Environmental Protection, Częstochowa, Poland, 23.10.2002.

12. Przybytniak Grażyna

Rodniki generowane przez promieniowanie jonizujące w nukleotydach i DNA (Radicals induced by ionising radiation in nucleotides and DNA).

Maria Skłodowska-Curie Polish Radiation Research Society, Łódź Division, Poland, 21.05.2002.

13. Szumiel Irena

Punkty kontrolne (checkpoints) w cyklu komórkowym (Checkpoints in the cell cycle).

Polish Society of Cell Biology, Warszawa, Poland, 09.11.2002.

14. Szumiel Irena

Uszkodzenia DNA i ich naprawa (DNA damage and its repair).

International Institute of Molecular Biology, Warszawa, Poland, 11.12.2002.

15. Urbański Piotr

Radioizotopowa aparatura przemysłowa (Nucleonic control systems).

Polish Nuclear Society, Warsaw University of Technology, Institute of Heat Engineering, Warszawa, Poland, 27.02.2002.

16. Wójcik Andrzej

Radium, radon and healing water – or how did we learn to deal with radiation.

Essen University, Germany, 12.11.2002.

17. Wójcik Andrzej

Role of 5'-bromo-2'-deoxyuridine in the formation of radiation-induced sister chromatid exchanges.

University Clinics, Institute for Medical Radiobiology, Essen, Germany, 28.11.2002.

18. Wójcik Andrzej

Ryzyko promieniowania jonizującego (The risk of ionising radiation).

Institute of Modern Civilization Problems, Warszawa, Poland, 22.03.2002.

19. Wójcik Andrzej

Strahleninduzierte chromosomale Aberrationen und biologische Dosimetrie (Radiation-induced chromosomal aberrations and biological dosimetry).

Essen University, Germany, 05.12.2002.

20. Zagórski Zbigniew Paweł

Los Alamos National Laboratory, New Mexico, USA.

Warsaw University of Technology, Institute of Heat Engineering, Warszawa, Poland, 13.03.2002.

AWARDS IN 2002

1. State Committee for Scientific Research, Diploma
   for invention "Method for preparing of calcium phosphates layers, especially hydroxyapatite"
   Institute of Nuclear Chemistry and Technology (Andrzej Deptuła, Wiesława Łada, Tadeusz Olczak)
2. World Intellectual Property Organization Certificate of Merit on the occasion of the 2th Competition – Plebiscite for "Woman Inventor" – 2001, organized by the Association of Polish Inventors and Rationalizers (SPWIR), in cooperation with the "Przegląd Techniczny" magazine and the Society for Technical Culture in Poland
   Wiesława Łada

INSTRUMENTAL LABORATORIES AND TECHNOLOGICAL PILOT PLANTS

I. DEPARTMENT OF NUCLEAR METHODS OF MATERIAL ENGINEERING

Laboratory of Materials Research

Activity profile: Studies of the structure and properties of materials and historical art objects.

- Scanning electron microscope

DSM 942, LEO-Zeiss (Germany)
Technical data: spatial resolution – 4 nm at 30 kV, and 25 nm at 1 kV; acceleration voltage – up to 30 kV; chamber capacity – 250x150 mm.
Application: SEM observation of various materials such as metals, polymers, ceramics and glasses. Determination of characteristic parameters such as molecule and grain size.

- Scanning electron microscope equipped with the attachment for fluorescent microanalysis

BS-340 and NL-2001, TESLA (Czech Republic)
Application: Observation of surface morphology and elemental analysis of various materials.

- Vacuum evaporator

JEE-4X, JEOL (Japan)
Application: Preparation of thin film coatings of metals or carbon.

- Gamma radiation spectrometer

HP-Ge, model GS 6020; Canberra-Packard (USA)
Technical data: detection efficiency for gamma radiation – 60.2%, polarization voltage – 4000 V, energy resolution (for Co-60) – 1.9 keV, analytical program „GENIE 2000".
Application: Neutron activation analysis, measurements of natural radiation of materials.

II. DEPARTMENT OF STRUCTURAL RESEARCH

1. Track-Etched Membranes Studies and Application Laboratory

Activity profile: Studies on structural defects in polymers created under influence of heavy ion beam irradiation. Manufacturing and determination of physical and structural parameters of TEM (Track-Etched Membranes) – modern filtration materials, obtained by chemical etching of latent heavy ions tracks in polymer films. Modification of TEM surface properties by physical methods. Research and developments on application of TEM in the field of sterilization, filtration and as microbiological barrier.

- Coulter Porometer II

Coulter Electronics Ltd (Great Britain)
Application: Pore size analysis in porous media.

- Vacuum chamber for plasma research

POLVAC Technika Próżniowa
Technical data: dimensions – 300x300 mm; high voltage and current connectors, diagnostic windows.
Application: Studies on plasma discharges influence on physicochemical surface properties of polymer films, particularly TEM.

2. Laboratory of Diffractional Structural Research

Activity profile: Studies on magnetic properties of new materials using neutron diffraction method. X-ray diffraction structural studies on metal-organic compounds originating as degradation products of substances naturally occurring in the environment. Röntgenostructural phase analysis of materials. Studies on interactions in a penetrant-polymer membrane system using small angle scattering of X-rays, synchrotron and neutron radiation. Studies of structural changes occurring in natural and synthetic polymers under influence of ionising radiation applying X-ray diffraction and differential scanning calorimetry.

- KM-4 X-ray diffractometer

KUMA DIFFRACTION (Poland)
Application: 4-cycle diffractometer for monocrystal studies.

- CRYOJET - Liquid Nitrogen Cooling System

Oxford Instruments

Application: Liquid nitrogen cooling system for KM-4 single crystal diffractometer.

- HZG4 X-ray diffractometer

Freiberger Präzisionsmechanik (Germany)

Application: Powder diffractometers for studies of polycrystalline, semicrystalline and amorphous materials.

- URD 6 X-ray diffractometer

Freiberger Präzisionsmechanik (Germany)

Application: Powder diffractometers for studies of polycrystalline, semicrystalline and amorphous materials.

3. Heavy Metal and Radioactive Isotopes Environment Pollution Studies Laboratory

Activity profile: Determination of elemental content of environmental and geological samples, industrial waste materials, historic glass objects and other materials by Energy Dispersive X-ray Fluorescence Spectrometry using a radioisotope excitation source as well as a low power X-ray tube and using 2 kW X-ray tube in total reflection geometry. Determination of radioactive isotopes content in environmental samples and historic glass objects by gamma spectrometry.

- Gamma spectrometer in low-background laboratory

EGG ORTEC

Technical data: HPGe detector with passive shield; FWHM – 1.9 keV at 1333 keV, relative efficiency – 92%.

- Total reflection X-ray spectrometer

Pico TAX, Institute for Environmental Technologies (Berlin, Germany)

Technical data: Mo X-ray tube, 2000 W; Si(Li) detector with FHWM 180 eV for 5.9 keV line; analysed elements: from sulphur to uranium; detection limits – 10 ppb for optimal range of analysed elements, 100 ppb for the others.

Application: XRF analysis in total reflection geometry. Analysis of minor elements in water (tap, river, waste and rain water); analysis of soil, metals, raw materials, fly ash, pigments, biological samples.

- X-ray spectrometer

SLP-10180-S, ORTEC (USA)

Technical data: FWHM – 175 eV for 5.9 keV line, diameter of active part – 10 mm, thickness of active part of detector – 5.67 mm.

Application: X-ray fluorescence analysis.

4. Sol-Gel Laboratory of Modern Materials

Activity profile: The research and production of adavanced ceramic materials in the shape of powders, monoliths, fibres and coatings by classic sol-gel methods with modifications – IChTJ Process or by CSGP (Complex Sol-Gel Method) are carried. Materials obtained by this method are the following powders: alumina and its homogeneous mixtures with Cr_2O_3, TiO_3, Fe_2O_3, $MgO+Y_2O_3$, MoO_3, Fe, Mo, Ni and CaO, CeO_2, Y_2O_3 stabilized zirconia, β and β'' aluminas, ferrites, $SrZrO_3$, ceramic superconductors, type YBCO (phases 123, 124), BSCCO (phases 2212, 2223), $NdBa_2Cu_3O_x$, their nanocomposites, Li-Ni-Co-O spinels as cathodic materials for Li rechargeable batteries and fuel cells MCFC, $BaTiO_3$, $LiPO_4$, Li titanates: spherical for fusion technology, irregularly shaped as superconductors and cathodic materials, Pt/WO_3 catalyst. Many of the mentioned above systems, as well as sensors, type SnO_2, were prepared as coatings on metallic substrates. Bioceramic materials based on calcium phosphates (e.g. hydroxyapatite) were synthesized in the form of powders, monoliths and fibres.

- DTA and TGA thermal analyser

OD-102 Paulik-Paulik-Erdey, MOM (Hungary)

Technical data: balance fundamental sensitivity – 20-0.2 mg/100 scale divisions, weight range – 0-9.990 g, galvanometer sensitivity – $1x10^{-10}$ A/mm/m, maximum temperature – 1050°C.

Application: Thermogravimetric studies of materials up to 1050°C.

- DTA and TGA thermal analyser 1500

MOM (Hungary)

Technical data: temperature range – 20-1500°C; power requirements – 220 V, 50 Hz.

Application: Thermal analysis of solids in the temperature range 20-1500°C.

- Research general-purpose microscope

Carl Zeiss Jena (Germany)

Technical data: General purpose microscope, enlargement from 25 to 2500 times, illumination of sample from top or bottom side.

- Metallographic microscope

EPITYP-2, Carl-Zeiss Jena (Germany)
Technical data: enlargement from 40 to 1250 times.
Application: Metallographic microscope for studies in polarized light illumination and hardness measurements.

- Laboratory furnace

CSF 12/13, CARBOLITE (Great Britain)
Application: Temperature treatment of samples in controlled atmosphere up to 1500°C with automatic adjustment of final temperature, heating and cooling rate.

III. DEPARTMENT OF RADIOISOTOPE INSTRUMENTS AND METHODS

Laboratory of Industrial Radiometry

Activity profile: Research and development of non-destructive methods and measuring instruments utilizing physical phenomena connected with the interaction of radiation with matter: development of new methods and industrial instruments for measurement of physical quantities and analysis of chemical composition; development of measuring instruments for environmental protection purpose (dust monitors, radon meters); implementation of new methods of calibration and signal processing (multivariate models, artificial neural networks); designing, construction and manufacturing of measuring instruments and systems; testing of industrial and laboratory instruments.

- Multichannel analyser board with software for X and γ-ray spectrometry

Canberra

- Function generator

FG-513, American Reliace INC

IV. DEPARTMENT OF RADIOCHEMISTRY

1. Laboratory of Coordination and Radiopharmaceutical Chemistry

Activity profile: Preparation of novel complexes, potential radiopharmaceuticals, e.g. derivatives of tricarbonyltechnetium(I) (^{99m}Tc) with chelating ligands mono- and bifunctional. Studying of their hydrophilic-lipophilic properties, structure and their interactions with peptides. Also rhenium(VI) complexes with dendrimeric ligands are synthesised and studied. Novel platinum and palladium complexes with organic ligands, analogs of *cis*platin, are synthesised and studied as potential anti-tumor agents. Studies in the field of isotope chemistry of middle and heavy elements in order to find correlations between isotope separation factor and the structure of species which exchange isotopes in chemical systems, as well as to select the methods suitable for isotope enrichment.

- Two radiometric sets

ZM 701, ZZUJ POLON (Poland)
Application: Measurements of radioactivity of radiotracers and radioelements.

- Spectrometric set

ORTEC
Multichannel analyser, type 7150, semiconductor detector
Application: Measurements and identification of γ- and α-radioactive nuclides.

- Spectrometric set

TUKAN, IPJ (Świerk, Poland)
Multichannel analyser, type SILENA with a PC card type TUKAN
Application: Measurements and identification of γ-radioactive nuclides.

- Gamma radiation counter

ZR-11, ZZUJ POLON (Poland)
Application: Measurements of γ-radioactive samples, the volume of samples up to 5 ml.

- Counter of low activities

ZR-16, ZZUJ POLON (Poland)
Application: Measurements of low activities of α- and β-radioactive nuclides, also of low energies.

- Gas chromatograph

610, UNICAM (England)
Application: Analysis of the composition of mixtures of organic substances in the gas and liquid state.

- High Performance Liquid Chromatography system

Gradient HPLC pump L-7100, Merck (Germany) with γ-radiation detector, INCT (Poland)
Application: Analytical and preparative separations of radionuclides and/or various chemical forms of radionuclides.

- UV-VIS spectrophotometer

DU 68, Beckman (Austria)

Application: Recording of electronic spectra of metal complexes and organic compounds in solution. Analytical determination of the concentration of these compounds.

- FT-IR spectrophotometer

EQUINOX 55, Bruker (Germany)

Application: Measurements of the IR spectra of metal complexes and other species in the solid state and in solution.

2. Laboratory of Heavy Elements

Activity profile: Studies on chemical properties of the heaviest elements: nobelium, rutherfordium, dubnium, element 112. Studies on the influence of relativistic effects on the chemical properties (oxidation state, hydrolytic properties etc.) Elaboration of new analytical techniques for the determination of radium isotopes in natural waters.

V. DEPARTMENT OF NUCLEAR METHODS OF PROCESS ENGINEERING

1. Pilot Plant for Flue Gases Treatment

Activity profile: Pilot plant was installed for basic and industrial research on radiation processing application for flue gases treatment at the Electric-Power Station KAWĘCZYN.

- Two accelerator ELW-3A

Technical data: 50 kW power, 800 kV

- Analyser of gases

Model 17, Thermo Instrument (USA)

Application: Measurement of NO, NO_2, NO_x, NH_3 concentrations.

- Analyser 10AR (Shimadzu, Japan) with analysers NOA-305A for NO concentration determination and URA-107 for SO_2 determination
- Analysers CO/CO_2, O_2

2. Laboratory for Flue Gases Analysis

Activity profile: Experimental research connected with elaboration of technology for SO_2 and NO_x and other hazardous pollutants removal from flue gases.

- Ultrasonic generator of aerosols

TYTAN XLG

- Gas chromatograph

Perkin-Elmer (USA)

- Gas analyser LAND

Application: Determination of SO_2, NO_x, O_2, hydrocarbons, and CO_2 concentrations.

- Impactor MARK III

Andersen (USA)

Application: Measurement of aerosol particle diameter and particle diameter distribution.

3. Laboratory of Stable Isotope Ratio Mass Spectrometry

Activity profile: study of isotope ratios of stable isotopes in hydrogeological, environmental, medical and food samples.

- Mass spectrometer DELTA^{plus}

Finnigan MAT (Bremen, Germany)

Technical data: DELTA^{plus} can perform gas isotope ratio measurements of H/D, $^{13}C/^{12}C$, $^{15}N/^{14}N$, $^{18}O/^{16}O$, $^{34}S/^{32}S$.

Application: For measurements of hydrogen (H/D) and oxygen ($^{18}O/^{16}O$) in water samples with two automatic systems: H/Device and GasBench II. The system is fully computerized and controlled by the software ISODAT operating in multiscan mode (realtime). The H/Device is a preparation system for hydrogen from water and volatile organic compounds determination. Precision of hydrogen isotope ratio determination is about 0.5• for water. The GasBench II is a unit for on-line oxygen isotope ratio measurements in water samples by “continuous flow” techniques. With GasBench II, water samples (0.5 ml) can be routinely analyzed with a precision and accuracy of 0.05 . The total volume of water sample for oxygen and hydrogen determination is about 2 ml.

- Elemental Analyzer Flash 1112 NCS

Thermo Finnigan (Italy)

Application: For measurement of carbon, nitrogen and sulfur contents and their isotope composition in organic matter (foodstuff and environmental samples).

4. Radiotracers Laboratory

Activity profile: Radiotracer research in the field of: environment protection, hydrology, underground water flow, sewage transport and dispersion in rivers and sea, dynamic characteristics of industrial installations and wastewater treatment stations studies.

- Heavy lead chamber (10 cm Pb wall thickness) for up to 1 Ci radiotracer activity preparations in liquid or solid forms
- Field radiometers for radioactivity measurements
- Apparatus for liquid sampling
- Liquid chromatograph Perkin-Elmer
- Turner fluorimeters for dye tracer concentration measurements
- Automatic devices for liquid tracers injection
- Liquid-scintillation counter

Model 1414-003 „Guardian", Wallac-Oy (Finland)

Application: Extra-low level measurements of α and β radionuclides concentration, especially for H-3, Ra-226, Rn-222 in environmental materials e.g. underground waters surface natural waters; in other liquid samples as waste waters biological materials, mine waters etc.

5. Membrane Laboratory

Activity profile: Research in the field of application of membranes for radioactive waste processing and separation of isotopes.

- Membrane distillation plant for concentration of solutions

Technical data: output ~0.05 m^3/h, equipped with spiral-wound PTFE module G-4.0-6-7 (SEP GmbH) with heat recovery in two heat-exchangers.

- Multi-stage MD unit (PROATOM) with 4 chambers equipped with flat sheet membranes for isotope separations research
- US 150 laboratory stand (Alamo Water) for reverse osmosis tests

Technical data: working pressure – up to 15 bar, flow rate – 200 dm^3/h, equipped with two RO modules.

- Laboratory stand with 5 different RP spiral wound modules and ceramic replaceable tubular modules
- Laboratory set-up for small capillary and frame-and-plate microfiltration and ultrafiltration modules examination (capillary EuroSep, pore diameter 0.2 μm and frame-and-plate the INCT modules)
- The system for industrial waste water pretreatment

Technical data: pressure – up to 0.3 MPa; equipped with ceramic filters, bed Alamo Water filters with replaceable cartridge (ceramic carbon, polypropylene, porous or fibrous) and frame-and-plate microfiltration module.

- The set-up for chemically agressive solutions (pH 0-14), high-saline solutions ~50 g/l) in the whole pH range, and radioactive solutions treatment

Technical data: equipped with TONKAFLO high pressure pump, up to 7 MPa, chemically resistant Kiryat Weizmann module (cut-off 400 MW), and high-pressure RO module.

VI. DEPARTMENT OF RADIATION CHEMISTRY AND TECHNOLOGY

1. Pilot Installation for Radiation Processing of Polymers

Activity profile: The research is being performed in the field of polymer materials development particularly in relation with medical quality polypropylene suitable for radiation sterilization, thermomeltable glue and PE based composites for thermoshrinkable products applications.

- Accelerator ILU-6

INP (Novosibirsk, Russia)

Technical data: beam power – 20 kW, electron energy – 0.7-2 MeV.

Application: Radiation processing.

- Extruder

PLV-151, BRABENDER-DISBURG (Germany)

Technical data: Plasti-Corder consists of: driving motor, temperature adjustment panel, thermostat, crusher, mixer, extruder with set of extrusion heads, (for foils, rods, sleevs, tubes) cooling tank, pelleting machine, collecting device.

Application: Preparation of polymer samples.

- Equipment for mechanical testing of polymer samples

INSTRON 5565, Instron Co. (England)

Technical data: High performance load frame with computer control device, equipped with Digital

Signal Processing and MERLIN testing software; max. load of frame is 5000 N with accuracy below 0.4% in full range; max. speed of testing 1000 mm/min in full range of load; total crosshead travel – 1135 mm; space between column – 420 mm; the environmental chamber 319-409 (internal dimensions 660x230x240 mm; temperature range from -70°C to 250°C).
Application: The unit is designed for testing of polymer materials (extension testing, tension, flexure, peel strength, cyclic test and other with capability to test samples at low and high temperatures).

2. Radiation Sterilization Pilot Plant of Medical Devices and Tissue Grafts

Activity profile: Research and development studies concerning new materials for manufacturing single use medical devices (resistant to radiation up to sterilization doses). Elaboration of monitoring systems and dosimetric systems concerning radiation sterilization processing. Introducing specific procedures based on national and international recommendations of ISO 9000 and PN-EN 552 standards. Sterilization of medical utensils, approx. 70 million pieces per year.

- Electron beam accelerator

UELW-10-10, NPO TORIJ (Moscow, Russia)
Technical data: beam energy – 10 MeV, beam power – 10 kW, supply power – 130 kVA.
Application: Radiation sterilization of medical devices and tissue grafts.

- Spectrophotometer UV-VIS

Model U-1100, Hitachi
Technical data: wavelength range – 200-1100 nm; radiation source – deuterium discharge (D_2) lamp, and tungsten-iodine lamp.

- Dose reading apparatus

CD-96, INCT
Technical data: wavelength range – 300-720 nm.
Application: Only for measurements of dosimetric foils.

- Bacteriological and culture oven with temperature and time control and digital reading

Incudigit 80L
Technical data: maximum temperature – 80°C, homogeneity – ±2%, stability – ±0.25% °C, thermometer error – ±2%, resolution – 0.1°C.

3. Laboratory of Radiation Microwave Cryotechnique

Activity profile: Radiation processes in solids of catalytic and biological importance: stabilization of cationic metal clusters in zeolites, radical reactions in polycrystalline polypeptides, magnetic properties of transition metals in unusual oxidation states; radical intermediates in heterogeneous catalysis.

- Electron spin resonance X-band spectrometer (ESR)

Bruker ESP-300, equipped with: microwave power meter HP 436A, continuous flow helium cryostat Oxford Instruments ESR 900, continuous flow nitrogen cryostat Bruker ER 4111VT, ENDOR-TRIPLE unit Bruker ESP-351.
Application: Studies of free radicals, paramagnetic cations, atoms and metal nanoclusters as well as stable paramagnetic centers.

- Spectrophotometer UV-VIS

LAMBDA-9, Perkin-Elmer
Technical data: wavelength range – 185-3200 nm, equipped with 60 nm integrating sphere.

4. Pulse Radiolysis Laboratory

Activity profile: Studies of charge and radical centres transfer processes in thioether model compounds of biological relevance in liquid phase by means of time-resolved techniques (pulse radiolysis and laser flash photolysis) and steady-state α-radiolysis.
The influence of nuclear radiation (electrons, ions) on solid state, especially on semiconductor materials. Radiation lattice defects. The distribution of dose radiation in gaseous media.

- Accelerator LAE 10 (nanosecond electron linear accelerator)

INCT (Warszawa, Poland)
Technical data: beam power – 0.2 kW, electron energy – 10 MeV, pulse duration – 7-10 ns and about 100 ns, repetition rate – 1, 12.5, 25 Hz and single pulse, pulse current – 0.5-1 A, year of installation 1999.
Application: Research in the field of pulse radiolysis.

- Gas chromatograph

GC-14B, Shimadzu (Japan)
Specifications: two detectors: thermal conductivity detectors (TCD) and flame ionization detector (FID). Column oven enables installation of stainless steel columns, glass columns and capillary columns. Range of temperature settings for column oven: room temperature to 399°C (in 1°C steps),

rate of temperature rise varies from 0 to 40°C/min (in 0.1°C steps). Dual injection port unit with two lines for simultaneous installation of two columns.
Application: Multifunctional instrument for analysis of final products formed during radiolysis of sulphur and porphyrin compounds and for analysis of gaseous products of catalytic reactions in zeolites.

- Dionex DX500 chromatograph system

Dionex Corporation
Specifications: The ED40 electrochemical detector provides three major forms of electrochemical detection: conductivity, DC amperometry and integrated and pulsed amperometry. The AD20 absorbance detector is a dual-beam, variable wavelength photometer, full spectral capability is provided by two light sources: a deuterium lamp for UV detection (from 190 nm) and a tungsten lamp for VIS wavelength operation (up to 800 nm). The GP40 gradient pump with a delivery system designed to blend and pump mixtures of up to four different mobile phases at precisely controlled flow rates. The system can be adapted to a wide range of analytical needs by choice of the chromatography columns: AS11 (anion exchange), CS14 (cation exchange) and AS1 (ion exclusion).
Application: The state-of-the-art analytical system for ion chromatography (IC) and high-performance liquid chromatography (HPLC) applications. Analysis of final ionic and light-absorbed products formed during radiolysis of sulphur compounds. The system and data acquisition are controlled by a Pentium 100 PC computer.

- Digital storage oscilloscope

9354AL, LeCroy
Specifications: Bandwidth DC to 500 MHz; sample rate – 500 Ms/s up to 2 Gs/s (by combining 4 channels); acquisition memory – up to 8 Mpt with 2 Mpt per channel; time/div range – 1 ns/div to 1000 s/div; sensitivity – 2 mV/div to 5 V/div; fully variable, fully programmable *via* GPIB and RS-232C.
Application: Digital storage osciloscope (DSO) with high speed and long memory controls pulse radiolysis system dedicated to the nanosecond electron linear accelerator (LAE 10). The multiple time scales can be generated by a computer from a single kinetic trace originating from DSO since the oscilloscope produces a sufficient number of time points (up to 8 M points record length).

- Digital storage oscilloscope

9304C, LeCroy
Specifications: Bandwidth DC to 200 MHz; sample rate – 100 Ms/s up to 2 Gs/s (by combining 4 channels); acquisition memory – up to 200 kpt per channel; time/div range – 1 ns/div to 1000 s/div; sensitivity – 2 mV/div to 5 V/div; fully variable.
Application: Digital osciloscope (DO) is used in pulse radiolysis system dedicated to the nanosecond electron linear accelerator (LAE 10).

- Nd:YAG laser

Surelite II-10, Continuum (USA)
Specifications: energy (mJ) at 1064 nm (650), 532 nm (300), 355 nm (160) and 266 nm (80); pulse width – 5-7 ns (at 1064 nm) and 4-6 ns (at 532, 355 and 266 nm); energy stability – 2.5-7%; can be operated either locally or remotely through the RS-232 or TTL interface.
Application: A source of excitation in the nanosecond laser flash photolysis system being currently under construction in the Department.

- Electron accelerator

AS-2000 (Holland)
Technical data: energy – 0.1-2 MeV, max. beam current – 100 μA.
Application: Irradiation of materials.

- Spectrometer

DLS-82E, SEMITRAP (Hungary)
Application: Research in radiation physics of semiconductors.

- Argon laser

ILA-120, Carl Zeiss (Jena, Germany)
Application: Measurements of optical properties.

- Spectrometer

DLS-81 (Hungary)
Application: Measurements of semiconductor properties.

- Argon laser

LGN-503 (Russia)
Application: Measurements of optical properties.

5. Research Accelerator Laboratory

Activity profile: Laboratory is equipped with accelerators providing electron beams which make capable to perform the irradiation of investigated objects within wide range of electron energy from

100 keV to 13 MeV and average beam power from 0.1 W do 20 kW, as well as with gamma sources Co-60 with activity $3.7x10^{13}$ to $1.71x10^{14}$ Bq and dose rate from 0.03 to 1 kGy/h. The described above irradiators are completed in a unique in the world scale set of equipment which can be applied in wide range of electron beam and gamma-ray research and radiation processing.

- Linear electron accelerator

LAE 13/9, Institute of Electro-Physical Equipment (Russia)
Technical data: electron energy – 10-13 MeV; electron beam power – 9 kW.
Application: Radiation processing.

- Cobalt source I

"Spectrophotometric", INCT (Warszawa, Poland)
Technical data: provided for the optical, periscopic access to the irradiation chamber surrounded with Co-60 rods. 6 rods – loaded initially to $3.7x10^{13}$ Bq, after many reloadings actual activity is $1.9x10^{10}$ Bq.
Application: Radiation research.

- Cobalt source II

Issledovatel (Russia)
Technical data: 32 sources with an actual activity of $1.71x10^{14}$ Bq.
Application: Radiation research.

- Cobalt source III

Mineza, INR (Świerk, Poland)
Technical data: 6 rods with an initial activity of $2.66x10^{13}$ Bq; an actual activity is $1.9x10^{10}$ Bq.
Application: Radiation research.

- Transiluminator UV

STS-20M, JENCONS (United Kingdom)
Technical information: six 15 W bulbs, emitted 312 nm wavelength, which corresponds to the fluorescence excitation maximum of ethidium bromide. Product description: For visualisation of ethidium bromide – stained nucleic acids fluorescence detection systems. Fluorescence intensity is enhanced, while photobleaching and photonicking of stained nucleic acids are reduced.

VII. DEPARTMENT OF ANALYTICAL CHEMISTRY

1. Laboratory of Spectral Atomic Analysis

Activity profile: atomic absorption and emission spectroscopy, studies on interference mechanisms, interpretation of analytical signals, service analysis.

- Atomic absorption spectrometer

SH-4000, Thermo Jarrell Ash (USA); equipped with a 188 Controlled Furnace Atomizer (CTF 188), Smith-Heftie background correction system and atomic vapor (AVA-440) accessory.
Application: For analyses of samples by flame and furnace AAS.

- Atomic absorption spectrometer

SP9-800, Pye Unicam (England); equipped with SP-9 Furnace Power Supply, PU-9095 data graphics system, PU-9095 video furnace programmer and SP-9 furnace autosampler.
Application: For analyses of samples by flame and furnace AAS.

2. Laboratory of Neutron Activation Analysis

Activity profile: The sole laboratory in Poland engaged for 40 years in theory and practice of neutron activation analysis in which the following methods are being developed: reactor neutron activation analysis (the unique analytical method of special importance in inorganic trace analysis), radiochemical separation methods, ion chromatography.

- Laminar box

HV mini 3, Holten (Denmark)
Technical data: air flow rate 300 m^3/h.
Application: Protection of analytical samples against contamination.

- Ion chromatograph

2000i/SP, Dionex (USA)
Technical data: calculating program AI-450, conductivity detector, UV/VIS detector.
Application: Analyses of water solutions, determination of SO_2, SO_3 and NO_x in flue gases and air.

- Well HPGe detector

CGW-3223, Canberra, coupled with analog line (ORTEC) and multichannel gamma-ray analyzer TUKAN
Application: Instrumental and radiochemical activation analysis.

- Coaxial HPGe detector

POP-TOP, ORTEC (USA), coupled with analog line (ORTEC) and multichannel gamma-ray analyzer TUKAN
Application: Instrumental and radiochemical activation analysis.

- Well HPGe detector

CGW-5524, Canberra, coupled with multichannel gamma-ray analyzer (hardware and software) Canberra

- HPLC

Shimadzu, LC-10ATVp pump, diode detector SPD-M10AVp
Application: Analyses of natural dyes, water and waste water samples.

VIII. DEPARTMENT OF RADIOBIOLOGY AND HEALTH PROTECTION

Laboratory of Cellular Microbiology

Activity profile: The laboratory serves for production of plasmid DNA, subsequently used for studies on DNA recombination repair, determination of topoisomerase I activity and for EPR studies.

- Equipment for electrophoretic analysis of DNA

CHEF III, BIO-RAD (Austria)
Application: Analysis of DNA fragmentation as a result of damage by various physical and chemical agents.

- Microplate reader

ELISA, ORGANON TEKNICA (Belgium)
Application: For measurement of optical density of solutions in microplates.

- Hybridisation oven

OS-91, BIOMETRA (Germany)
Technical data: work temperatures from 0°C to 80°C; exchangeable test tubes for hybridisation.
Application: For polymerase chain reaction (PCR).

- Spectrofluorimeter

RF-5000, Shimadzu (Japan)
Application: For fluorimetric determinations.

- Transilluminator for electrophoretic gels

Biodoc, BIOMETRA (Great Britain)
Application: For analysis of electrophoretic gels.

- Laminar flow cabinet

1446, GV 1920
Application: For work under sterile conditions.

- Liquid scintillation counter

LS 6000LL, BECKMAN (USA)
Application: For determinations of radioactivity in solutions.

- Research microscope universal

NU, Carl Zeiss Jena (Germany)
Application: For examination of cytological preparations.
Comments: Universal microscope for transmission and reflected light/polarised light. Magnification from 25x to 2500x. Possibility to apply phase contrast.

- Incubator

T-303 GF, ASSAB (Sweden)
Technical data: 220 V, temperature range – 25-75°C.
Application: For cell cultures under 5% carbon dioxide.

- Laminar flow cabinet

V-4, ASSAB (Sweden)
Application: For work under sterile conditions.

- Image analysis system

Komet 3.1, Kinetic Imaging (Great Britain)
Application: For comet (single cell gel electrophoresis) analysis.

- ISIS 3

Metasystem (Germany)
Application: Microscopic image analysis system for chromosomal aberrations (bright field and fluorescence microscopy).

IX. LABORATORY FOR DETECTION OF IRRADIATED FOODS

Activity profile: Detection (identification) of irradiated foods. The analytical methods routinely used are based on electron paramagnetic resonance spectroscopy (EPR) and thermoluminescence measurements (TL). The research work is focused on the development of both methods and on validation and implementation of such detection methods as gas chromatographic determination of volatile hydrocarbons in fats, DNA comet assay (decomposition of single cells), statistical germination study. The quality assurance system is adapted in the Laboratory in agreement with the PN-EN 150/IEC 17025:2001 standard. Laboratory has full documentation of the adapted quality assurance system. Laboratory obtained Certificate of Testing Laboratory Accreditation NR L 262/I/99 issued by the Polish Centre for Testing and Accreditation and Accreditation Certificate for Testing Laboratory issued by the Polish Centre for Accreditation valid from 25.10.2002 to 25.10.2006.

- Thermoluminescence reader

TL-DA-15 Automated, Risoe National Laboratory (Denmark)

Technical data: 24 samples turntable, heating range – 50-500°C, heating speed – 0.5-10.0°C/s, optical stimulated luminescence (OSL) system.

Application: Detection of irradiated foods, research work on irradiated foods, thermoluminescence dosimetry.

- Fluorescence microscope

OPTIPHOT Model X-2, NIKON (Japan)

Technical data: halogen lamp 12 V-100 W LL; mercury lamp 100 W/102 DH; lenses (objectives) CF E Plan Achromat 4x, CF E Plan Achromat 40x; CF FLUOR 20x.

Application: Detection of irradiated foods by the DNA comet assay, research work on apoptosis in mammalian cells, biological dosimetry, analysis of DNA damage in mammalian cells.

- Compact EPR spectrometer

EPR 10-MINI, St. Petersburg Instruments Ltd. (Russia)

Technical data: sensitivity $3x10^{10}$, operating frequency (X band) – 9.0-9.6 GHz, max. microwave power – 80 mW, magnetic field range – 30-500 mT, frequency modulation – 100 kHz.

Application: Detection of irradiated foods, bone and alanine dosimetry, research work on irradiated foods and bone tissues.

X. EXPERIMENTAL PLANT FOR FOOD IRRADIATION

1. Microbiological Laboratory

Activity profile: optimization of food irradiation process by microbiological analysis.

- Sterilizer

ASUE, SMS (Warszawa, Poland)

Application: Autoclaving of laboratory glass, equipment, and microbiological cultures.

- Fluorescence microscope

BX, Olimpus (Germany)

Application: Quantitative and qualitative microbiological analysis.

2. Experimental Plant for Food Irradiation

Activity profile: Development of new radiation technologies for the preservation and hygienization of food products and feeds. Development and standarization of the control system for electron beam processing of food and feeds. Development of analytical methods for the detection of irradiated food. Organization of consumer tests with radiation treated food products.

- Accelerator ELEKTRONIKA (10 MeV, 10 kW)

UELW-10-10, NPO TORIJ (Moscow, Russia)

Application: Food irradiation.

INDEX OF THE AUTHORS

X

Z